CHAPTER FIVE

URANIUM*

Ingmar Grenthe, Janusz Drożdżyński, Takeo Fujino, Edgar C. Buck, Thomas E. Albrecht-Schmitt, and Stephen F. Wolf

5.1 HISTORICAL

Uranium compounds have been used as colorants since Roman times (Caley, 1948). Uranium was discovered as a chemical element in a pitchblende specimen by Martin Heinrich Klaproth, who published the results of his work in 1789. Pitchblende is an *impure* uranium oxide, consisting partly of the most reduced oxide uraninite (UO_2) and partly of U_3O_8. Earlier mineralogists had considered this mineral to be a complex oxide of iron and tungsten or of iron and zinc, but Klaproth showed by dissolving it partially in strong acid that the solutions yielded precipitates that were different from those of known elements. Therefore he concluded that it contained a new element (Mellor, 1932); he named it after the planet Uranus, which had been discovered in 1781 by William Herschel, who named it after the ancient Greek deity of the Heavens.

* Part of this chapter is based on Chapter 5 in the previous edition authored by the late Fritz Weigel.

The name 'Uranus' was first proposed by Johann Elert Bode in conformity with the other planetary names from classical mythology, but this name for the planet did not come into common use until 1850. However, uranium was accepted as the name for the chemical element.

The pure oxide UO_2 isolated by Klaproth by reduction was believed to be the elemental form until 1841, when Eugène-Melchior Péligot (1841a,b) showed that Klaproth's 'partially metallic' substance was in reality the oxide UO_2. Péligot (1841b, 1842, 1844) succeeded in preparing metallic uranium by reducing the tetrachloride with potassium. Péligot may thus properly be considered the founder of modern uranium chemistry; he was the first to use the word 'uranyl' to designate the yellow salts of uranium.

In the elaboration of the periodic table, Mendeleev assigned in 1872 an atomic weight of 240 and a highest valence of six to uranium, rather than the value of 120 that was then commonly used based on the assumption that uranium was trivalent. Mendeleev's reason was that he could not place an element with atomic weight 120 in group III of the periodic table; thus he conferred upon uranium the distinction of having the highest atomic weight in the periodic table. An atomic weight of nearly 240 was firmly established by Zimmerman (1882) by determining the mass ratios of several oxides and sodium uranyl acetate. The valence and atomic weight were confirmed by determination of the vapor density of UCl_4 and later of UF_6 and the atomic number 92 was established (Hahn, 1925) from nuclear decay systematics.

The principal use of uranium during the first century after its discovery (and for the previous two millenia) was as a colorant for ceramics and glasses. The obscurity surrounding the element was permanently dissipated by the discovery of Henri Becquerel (1896) that uranium emits penetrating rays. In connection with investigations of the fluorescence and phosphorescence of uranium salts that had been undertaken by generations of Becquerels (Zhang and Pitzer, 1999), H. Becquerel placed photographic plates that were covered with black paper near any salt or other material containing uranium. Whether the material was phosphorescent or not, he found that the emulsion was blackened by emanations that passed through the paper. He compared this phenomenon to that of X-rays, which had been announced only a few weeks earlier by Roentgen. Later Becquerel showed that the penetrating rays could discharge an electroscope. Shortly thereafter, Marie Curie developed quantitative techniques for measuring the radioactivity of uranium. She and others also found thorium to be radioactive and discovered by chemical separations that there were other elements present at trace levels in the uranium ore. Working with her husband Pierre, she discovered and named polonium and radium and described this property of these heavy elements as 'radioactivity'.

Because the Curies recognized that ores of uranium and thorium are much more radioactive than purified compounds of these elements, they and other radiochemists (e.g. Rutherford, Fajans, and Soddy) separated other radioelements and identified their chemical and nuclear transformations. The

luminescent and medical properties of radium created a market for uranium ores and the processed radium that far exceeded the use of uranium as a colorant for glasses.

By 1911, the atomic weight of uranium had been refined to 238.5 (Gmelin, vol. A2, 1980a). The natural isotope ^{235}U was discovered in 1935 by mass spectrometry. The artificial isotope ^{239}U, which is the precursor of ^{239}Np and ^{239}Pu, was postulated and identified by Hahn and coworkers (Hahn *et al*., 1937; Meitner *et al*., 1937) as a 23 min half-life intermediate to transuranium elements that were not identified until the famous studies of Seaborg and coworkers 3 years later.

Despite these important discoveries, the crucial importance of uranium was not established until Hahn and Strassman (1939) discovered nuclear fission in late 1938. Since then, the chemistry, materials science, and nuclear properties of uranium have occupied a central position in the field of nuclear energy. Most schemes so far proposed for the release of nuclear energy involve the naturally occurring fissionable ^{235}U, fertile ^{238}U, or the artificial fissionable ^{233}U in one way or another, so that the chemistry and technology of uranium have become of great scientific and technical importance. For these reasons many reviews dealing with uranium chemistry, technology, and metallurgy have been published. The main volume on uranium of the *Gmelin Handbook of Inorganic Chemistry* (Gmelin, 1936) and a chapter by Mellor (1932) are the earliest comprehensive reviews of uranium chemistry prior to the discovery of fission. The Manhattan Project work was summarized in a number of volumes of the National Nuclear Energy Series (Katz and Rabinowitch, 1951, 1958; Seaborg and Katzin, 1951; Vance and Warner, 1951; Katzin, 1952; Warner, 1953; Wilkinson, 1962). These volumes deal with the chemistry of uranium and its compounds, ^{233}U, metallurgy, and technology of uranium, respectively. The most recent monograph on the chemistry of uranium is that by Cordfunke (1969). The most comprehensive treatment of all phases of uranium chemistry is the multi-volume uranium supplement to the *Gmelin Handbook of Inorganic Chemistry* (1975–1996).

5.2 NUCLEAR PROPERTIES

Uranium, as it occurs in nature, consists of a mixture of the three isotopes ^{238}U, ^{235}U, and ^{234}U. The relative abundances of ^{238}U, ^{235}U, and ^{234}U have been measured by various investigators, and 'best values' for the ^{238}U, ^{235}U, and ^{234}U relative abundances have been chosen through a review of the literature by Holden (1977). We have accepted these values and they are listed in Table 5.1. One has to keep in mind, however, that the isotopic ratio of the uranium isotopes in nature may vary as much as 0.1%. By utilizing mass spectrometric and nuclear disintegration data, the (chemical) atomic weight of natural uranium is calculated to be (238.0289 ± 0.0001). The isotope ^{238}U is the parent of the

Table 5.1 *Natural abundance of the uranium isotopes* (*Holden*, 1977).

Abundance (*at%*)		
Mass number	*Range*	*'Best' value*
234	0.0059–0.0050	0.005 ± 0.001
235	0.7202–0.7198	0.720 ± 0.001
238	99.2752–99.2739	99.275 ± 0.002

natural $4n + 2$ radioactive series, and the isotope ^{235}U is the parent of the natural $4n + 3$ radioactive series. ^{234}U arises from ^{238}U by radioactive decay and these two isotopes are thus linked to each other, but ^{235}U appears to be of independent origin.

The isotope ^{235}U, which exists in nature to the extent of 0.72%, and was identified by Dempster (1935) using mass spectrometry. This isotope is of special importance since it undergoes fission with slow neutrons.

Complete fission of ^{235}U gives rise to an energy equivalent of about 2×10^7 kWh kg^{-1} (corresponding to about 200 MeV per fission). Advantage can be taken of the fissionability of ^{235}U not only to generate large amounts of power but also to synthesize other important actinide elements. Uranium with its natural isotopic composition can be used in nuclear reactors to generate neutrons. The chain reaction is sustained by the excess neutrons produced by the fission of ^{235}U, while neutrons in excess of those required to propagate the chain reaction can be captured by the other natural isotope to produce plutonium:

$$^{235}U + n \rightarrow \text{fission products} + \text{energy} + 2.5\,\text{neutrons}$$

$$^{238}U + n \rightarrow {}^{239}U$$

$$^{239}U \xrightarrow{\beta^-} {}^{239}Np \xrightarrow{\beta^-} {}^{239}Pu$$

The abundant isotope ^{238}U can in this way be converted to plutonium-239, which, like ^{235}U, is also fissionable with slow neutrons.

A large number of synthetic isotopes of uranium have been prepared. The isotope ^{233}U, which was discovered by Seaborg, Gofman, and Stoughton (Katzin, 1952, paper 1.1), is particularly noteworthy, because it also undergoes fission with slow neutrons. Separation of this isotope from neutron-irradiated ^{232}Th is discussed (Thorex Process) in Chapter 24. Some of the other synthetic isotopes have particular utility as tracers for uranium. This is the case for beta-emitting ^{237}U and alpha-emitting ^{232}U, both of which have found extensive use in chemical and physical studies. The isotope ^{232}U is formed by alpha bombardment on ^{232}Th, or in the decay of the short-lived ^{232}Pa, which in turn may be obtained by neutron irradiation of ^{231}Pa. Procedures for the isolation of ^{232}U from this source have been described (Leuze *et al.*, 1962, 1963; Chilton, 1963).

The naturally occurring ^{234}U appears also in the α decay of ^{238}Pu (87.7 years). Separation of this ^{234}U from its parent furnishes a simple way to obtain isotopically pure ^{234}U (Figgins and Bernardinelli, 1966).

The various isotopes of uranium are listed in Table 5.2.

5.3 OCCURRENCE IN NATURE

The most important oxidation states of uranium in natural environments are 4+ and 6+. Compounds containing tetravalent uranium are insoluble in mildly acidic to alkaline conditions, whereas, those containing the linear uranyl moiety $(O{=}U{=}O)^{2+}$ are highly soluble and mobile. In solution, UO_2^{2+} forms soluble complexes with carbonate, oxalate, and hydroxide; UO_2^{2+} is also highly susceptible to adsorption either by organic matter, Fe oxyhydroxides, or by precipitation with various anions, such as hydroxide, silicate, vanadate, arsenate, and phosphate. In groundwater systems U(VI) is reduced to U(IV) if an effective reductant is present, such as H_2S. Other reducing agents may be fossil plants, methane, and transported humic material. Uranium minerals display an extraordinary wide structural and chemical variability, resulting from the different chemical conditions under which U minerals are formed.

Elucidation of the mechanisms of uranium sorption by mineral surfaces, refinements of complex U-mineral structures, and chemical bonding are needed to improve current models from uranium cycling in the aquo- and geospheres in order to describe the behavior of uranium in the environment. In past years, uranium mineralogy was more concerned with the economic quality of U-deposits; however, today we are equally concerned with the hazard presented by former uranium mines and nuclear waste sites to the local environment and population. This has placed greater emphasis on understanding the role of uranium sorption and for developing accurate thermodynamic and kinetic models for uranium attenuation. There are $\sim$200 minerals that contain uranium as an essential component (Burns, 1999a; Finch and Murakami, 1999). Of these, the U(VI) minerals constitute the largest portion. Burns and coworkers have developed a novel approach for describing and classifying the uranyl phases, based on polymerization of coordination polyhedra of higher bond valence, which permits easy visualization of these extremely complex structures (Burns *et al.*, 1996; Burns, 1999a). Mineral descriptions are divided according to the major anionic component and structural similarities. In Table 5.3 a list of uranium minerals with the current information on composition, space group, and lattice parameters has been provided. Hill (1999) provided a similar list of uranium minerals and related synthetic phases; recent studies have identified new phases and errors in the previous entries.

Improved understanding of uranium mineralogy gives insight into the evolution of uranium deposits, possible mechanisms for uranium and radionuclide retardation following the weathering of nuclear waste materials, and the fate of

Table 5.2 *Nuclear properties of uranium isotopes.*[a]

Mass number	*Half-life*	*Mode of decay*	*Main radiations* (MeV)	*Method of production*
217	16 ms	α	α 8.005	^{182}W(^{46}Ar,5n)
218	1.5 ms	α	α 8.625	^{197}Au(^{27}Al,6n)
219	42 μs	α	α 8.680	^{197}Au(^{27}Al,x)
222	1.0 μs	α	α 9.500	W(^{40}Ar,xn)
223	18 μs	α	α 8.780	^{208}Pb(^{20}Ne,5n)
224	0.9 ms	α	α 8.470	^{208}Pb(^{20}Ne,4n)
225	59 ms	α	α 7.879	^{208}Pb(^{22}Ne,5n)
226	0.35 s	α	α 7.430	^{232}Th(α,10n)
227	1.1 min	α	α 6.87	^{232}Th(α,9n) ^{208}Pb(^{22}Ne,3n)
228	9.1 min	α ≥ 95% EC ≤ 5%	α 6.68 (70%) 6.60 (29%) γ 0.152	^{232}Th(α,8n)
229	58 min	EC ∼ 80% α ∼ 20%	α 6.360 (64%) 6.332 (20%) γ 0.123	^{230}Th(^{3}He,4n) ^{232}Th(α,7n)
230	20.8 d	α	α 5.888 (67.5%) 5.818 (31.9%) γ 0.072	^{230}Pa daughter ^{231}Pa(d,3n)
231	4.2 d	EC > 99% α 5.5×10^{-3}%	α 5.46 γ 0.084	^{230}Th(α,3n) ^{231}Pa(d,2n)
232	68.9 yr ≈ 8×10^{13} yr	α SF	α 5.320 (68.6%) 5.264 (31.2%) γ 0.058	^{232}Th(α,4n)
233	1.592×10^{5} yr 1.2×10^{17} yr	α SF	α 4.824 (82.7%) 4.783 (14.9%) γ 0.097	^{233}Pa daughter
234	2.455×10^{5} yr 2×10^{16} yr	α SF	α 4.777 (72%) 4.723 (28%)	nature
235	7.038×10^{8} yr 3.5×10^{17} yr	α SF	α 4.397 (57%) 4.367 (18%) γ 0.186	nature
235 m	25 min	IT		^{239}Pu daughter
236	2.3415×10^{7} yr 2.43×10^{16} yr	α SF	α 4.494 (74%) 4.445 (26%)	^{235}U(n,γ)
237	6.75 d	β$^-$	β$^-$ 0.519 γ 0.60	^{236}U(n,γ) ^{241}Pu daughter
238	4.468×10^{9} yr 8.30×10^{15} yr	α SF	α 4.196(77%) 4.149 (23%)	nature
239	23.45 min	β$^-$	β$^-$ 1.29 γ 0.075	^{238}U(n,γ)
240	14.1 h	β$^-$	β$^-$ 0.36 γ 0.044	^{244}Pu daughter
242	16.8 min	β$^-$	β$^-$ 1.2 γ 0.068	^{244}Pu(n,2pn)

[a] Appendix II.

Table 5.3 *List of natural minerals with uranium as an essential component.*

Mineral	*Formula*	*Space group*	*a* (Å)	*b* (Å)	*c* (Å)	*Angle* (°)	*References*
uranium oxide	UO_2	*Fm*3*m*	5.4682				Roberts *et al.* (1990)
natural uraninite	$[U^{4+}_{1-x-y-z-u}U^{6+}_{x}(Th^{4+})_{u}REE^{3+}_{y}M^{z+}_{z}]O_{2+x-(0.5y)-z}$	*Fm*3*m*	5.470–5.443				Janeczek and Ewing (1992)
uranyl oxide hydrates							
dehydrated schoepite	$(UO_2)_4O(OH)_6 \cdot H_2O$		6.86	4.26	10.20		Finch *et al.* (1998)
ianthinite	$[U^{4+}_2(UO_2)_4O_6(OH)_4(H_2O)_4](H_2O)_5$	$P2_1cn$	7.178	11.473	30.39		Burns *et al.* (1997a)
meta-schoepite	$(UO_2)_4O(OH)_6 \cdot 5H_2O$	*Pbcn*	14.6861	13.9799	16.7063		Weller *et al.* (2000)
schoepite	$[(UO_2)_8O_2(OH)_{12}](H_2O)_{12}$	$P2_1ca$	14.337	16.813	14.731		Finch *et al.* (1996a)
wyartite	$Ca[U^{5+}(UO_2)_2(CO_3)O_4(OH)](H_2O)_7$	$P2_12_12_1$	11.2706	7.1055	20.807		Burns and Finch (1999)
peroxides							
meta-studtite	$(UO_2)O_2(H_2O)_2$		6.50	8.78	4.21		Deliens and Piret (1983a)
studtite	$[(UO_2)(O_2)(H_2O)_2](H_2O)_2$	C2/c	14.068	6.721	8.428	$\beta = 123.356$	Burns and Hughes (2003)
metal uranyl oxyhydroxides							
agrinierite	$K_2(Ca_{0.65}Sr_{0.35})[(UO_2)_3O_3(OH)_2]_2 \cdot 5H_2O$	*F*2*mm*	14.094	14.127	24.106		Cahill and Burns (2000)
bauranoite	$BaU_2O_7 \cdot 4.5H_2O$	No unit cell data					Rogova *et al.* (1973)
becquerelite	$Ca[(UO_2)_3O_2(OH)_3]_2(H_2O)_8$	$Pn2_1a$	13.8378	12.3781	14.9238		Burns and Li (2002)
billietite	$Ba[(UO_2)_3O_2(OH)_3]_2(H_2O)_4$	$Pbn2_1$	12.0720	30.167	7.1455		Pagoaga *et al.* (1987)
compreignacite	$K_2[(UO_2)_3O_2(OH)_3]_2(H_2O)_7$	*Pmmn*	14.8591	7.1747	12.1871		Burns (1998c)
protasite	$Ba[(UO_2)_3O_3(OH)_2](H_2O)_3$	*Pn*	12.2949	7.2206	6.9558	$\beta = 90.401$	Pagoaga *et al.* (1987)
rameauite	$K_2CaU_6O_{20} \cdot 9H_2O$	*C*2/*c*	13.97	14.26	14.22	$\beta = 121.02$	Gaines *et al.* (1997)
uranosphaerite	$Bi(UO_2)O_2OH$	$P2_1/n$	7.559	7.811	7.693	$\beta = 92.88$	Hughes *et al.* (2003)
vandenbrandeite	$(UO_2)Cu(OH)_4$	$P\bar{1}$	7.855	5.449	6.089	$\alpha = 91.44$ $\beta = 101.90$ $\gamma = 89.2$	Rosenzweig and Ryan (1977)

Table 5.3 (*Contd.*)

Mineral	*Formula*	*Space group*	*a* (Å)	*b* (Å)	*c* (Å)	*Angle* (°)	*References*
Pb–uranyl oxyhydroxides							
calciouranoite	$(Ca,Ba,Pb)U_2O_7 \cdot 5H_2O$	No data					
clarkeite	$(NaCa_{0.5}Pb_{0.5})[(UO_2)O(OH)](H_2O)_{0-1}$	*R*-3*m*	3.954		17.73		Finch and Ewing (1997)
curite	$Pb_{3+x}(H_2O)_2[((UO_2)_4O_{4+x}(OH)_{3-x}]_2$	*Pnam*	12.551 (12.53–12.58)	13.003 (13.01–13.03)	8.390 (8.39–8.40)		Taylor *et al.* (1981)
fourmarierite	$Pb_{1-x}[(UO_2)_4O_{3-2x}(OH)_{4+2x}](H_2O)_4$	*Bb*2$_1$*m*	13.986 (14.00–14.03)	16.400 (16.40–16.48)	14.293 (14.32–14.38)		Piret (1985)
masuyite	$Pb[(UO_2)_3O_3(OH)_2](H_2O)_3$	*Pn*	12.241	7.008	6.983	$\beta = 90.40$	Burns and Hanchar (1999)
meta-calciouranoite	$(Ca,Ba,Pb,K,Na)O \cdot UO_3 \cdot 5H_2O$	No data					
meta-vandendriesscheite	$PbU_7O_{22} \cdot nH_2O \quad n < 12$	*Pmma*	14.07	41.31	43.33		Roberts *et al.* (1990)
richetite	$M_xPb_{8.57}[(UO_2)_{18}(OH)_{12}]_2(H_2O)_{41}$	*P*1	20.9391	12.1000	16.3450	$\alpha = 103.87$ $\beta = 115.37$ $\gamma = 90.27$	Burns (1998b)
sayite	$Pb_2[(UO_2)_5O_6(OH)_2](H_2O)_4$	*P*2$_1$/*c*	10.704	6.960	14.533	$\beta = 116.81$	Piret *et al.* (1983)
spriggite	$Pb_3[(UO_2)_6O_8(OH)_2](H_2O)_3$	*C*2/*c*	28.355	11.990	13.998	$\beta = 104.248$	Brugger *et al.* (2004)
vandendriesscheite	$Pb_{1.57}[(UO_2)_{10}O_6(OH)_{11}](H_2O)_{11}$	*Pbca*	14.1165	41.478	14.5347		Burns (1997)
wölsendorfite	$Pb_{6.2}Ba_{0.4}[(UO_2)_{14}O_{19}(OH)_4](H_2O)_{12}$	*Cmcm*	14.131	13.885	55.969		Burns (1999b)
uranyl silicates							
haiweeite group (*U:Si = 1:3*)							
coutinhoite	$Th_xBa_{(1-2x)}(H_2O)_y(UO_2)_2Si_5O_{13} \cdot H_2O$ With $0 \leq x \leq 0.5$ and $0 \leq y \leq (2+x)$	*Cmmb*	14.1676	14.1935	35.754		Atencio *et al.* (2004)
haiweeite	$Ca[(UO_2)_2Si_5O_{12}(OH)_2](H_2O)_3$	*Cmcm*	7.125	17.937	18.342		Burns (2001b)
weeksite	$K_{1.26}Ba_{0.25}Ca_{0.12}[(UO_2)_2(Si_5O_{13})]H_2O$	*Cmmb*	14.209	14.248	35.869		Jackson and Burns (2001)

uranophane group (*U:Si = 1:1*)							
boltwoodite	$K_{0.56}Na_{0.42}[(UO_2)(SiO_3OH)](H_2O)_{1.5}$	$P2_1/m$	7.0772	7.0597	6.6479	$\beta = 104.982$	Burns (1998d)
cuprosklodowskite	$Cu(UO_2)_2(SiO_3OH)_2 \cdot 6H_2O$	$P\bar{1}$	7.052	9.267	6.655	$\alpha = 109.23$ $\beta = 89.84$ $\gamma = 110.01$	Rosenzweig and Ryan (1975)
kasolite	$Pb[(UO_2)(SiO_4)](H_2O)$	$P2_1/c$	6.704	6.932	13.252	$\beta = 104.22$	Ryan and Rosenzweig (1977)
oursinite	$(Co_{0.86}Mg_{0.10}Ni_{0.04}) \cdot O_2 \cdot UO_2 \cdot 2SiO_2 \cdot 6H_2O$	*Aba*2 *or Abam*	12.74	17.55	7.050		Deliens and Piret (1983b)
sklodowskite	$Mg(H_3O)_2[(UO_2)(SiO_4)]_2 \cdot 4H_2O$	*C2/m*	17.382	7.047	6.610	$\beta = 105.9$	Ryan and Rosenzweig (1977)
sodium boltwoodite	$(Na,K)(H_3O)[(UO_2)(SiO_4)] \cdot H_2O$	$P2_12_12_1$	27.2	7.02	6.65		Stohl and Smith (1981)
swamboite	$(UO_2)_{0.33}[(UO_2)(SiO_4)]_2 \cdot 6H_2O$	$P2_1/a$	17.64	21.00	20.12	$\gamma = 103.4$	Deliens and Piret (1981)
α-uranophane	$Ca(UO_2)_2(SiO_3OH)_2(H_2O)_5$	$P2_1$	15.909	7.002	6.665	$\beta = 97.27$	Ginderow (1988)
β-uranophane	$Ca(UO_2)_2(SiO_3OH)_2(H_2O)_5$	$P2_1/a$	13.966	15.443	6.632	$\gamma = 91.38$	Viswanathan and Harnett (1986)
other U silicates							
arapovite	$U(Ca,Na)_2(K_{1-x}\square_x)(Si_8O_{20})$, $x \sim 0.5$	*P4/mcc*	7.5505		14.7104		Uvarova *et al.* (2004)
ciprianiite	$Ca_4[(Th,U)(REE)]Al_2(Si_4B_4O_{22})(OH, F)_2]$	*P2/a*	19.032	4.746	10.248	$\gamma = 110.97$	della Ventura *et al.* (2002)
lepersonnite-Gd	$CaO(Gd,Dy)_2O_3 \cdot 24UO_3 \cdot 8CO_2 \cdot 4SiO_2 \cdot 60H_2O$	*Pnnm or Pnn*2	16.23	38.74	11.73		Deliens and Piret (1982)
soddyite	$(UO_2)_2[SiO_4](H_2O)_2$	*Fddd*	8.334	11.212	18.688		Demartin *et al.* (1992)
uranosilite	$(Mg,Ca)_4(UO_2)_4(Si_2O_5)_{5.5}(OH)_5 \cdot 13H_2O$	*Pmmb or Pmcb*	11.60	14.68	12.83		Walenta (1983)
orthosilicates							
coffinite	$U(SiO_4)_{1-x}(OH)_{4x}$	$I4_1/amd$	6.979		6.252		Fuchs and Gebert (1958)
uranyl carbonates							
albrechtschraufite	$Ca_4Mg(UO_2)_2(CO_3)_6F_2 \cdot 17H_2O$	$P\bar{1}$	13.562	13.406	11.636	$\alpha = 115.72$ $\beta = 107.66$ $\gamma = 92.86$	Mereiter (1984)

Table 5.3 (*Contd.*)

Mineral	*Formula*	*Space group*	*a* (Å)	*b* (Å)	*c* (Å)	*Angle* (°)	*References*
andersonite	$Na_2Ca[(UO_2)(CO_3)_3](H_2O)_5$	*R*-3*m*	17.904		23.753		Mereiter (1986)
astrocyanite-Ce	$Cu_2(Ce,Nd,La)_2UO_2(CO_3)_5(OH)_2 \cdot 1.5H_2O$	*P6/mmm*	14.96		26.86		Deliens and Piret (1990b)
bayleyite	$Mg_2[(UO_2)(CO_3)_3](H_2O)_{18}$	$P2_1/a$	26.560	15.256	6.505	$\gamma = 92.90$	Mayer and Mereiter (1986)
bijvoetite-Y	$[M_8^{3+}(H_2O)_{25}(UO_2)_6O_8(OH)_8(CO_3)_{16}](H_2O)_{14}$	$B12_11$	21.234	12.958	44.911	$\beta = 90.00$	Li et *al.* (2000)
blatonite	$UO_2CO_3 \cdot H_2O$		15.79		23.93		Vochten and Deliens (1998)
čejkaite	$Na_4(UO_2)(CO_3)_3$	*P*1 *or* $P\bar{1}$	9.291	9.292	12.895	$\alpha = 90.73$ $\beta = 90.82$ $\gamma = 120$	Ondruš *et al.* (2003)
fontanite	$Ca[(UO_2)_3(CO_3)_2O_2](H_2O)_6$	$P2_1/n$	6.968	17.276	15.377	$\beta = 90.064$	Hughes and Burns (2003)
grimselite	$K_3Na[(UO_2)(CO_3)_3](H_2O)$	*P*-62*c*	9.302		8.260		Li and Burns (2001b)
joliotite	$UO_2CO_3 \cdot nH_2O \quad n = 1.5–2.0$	*P*222	8.16	10.35	6.32		Walenta (1976)
kamotoite-Y	$Y_2O_4(UO_2)_4(CO_3)_3 \cdot 14H_2O$	$P2_1/a$	21.22	12.93	12.39	$\gamma = 115.3$	Gaines *et al.* (1997)
liebigite	$Ca_2UO_2(CO_3)_3 \cdot 11H_2O$	*Bba*2	16.699	17.557	13.697		Mereiter (1982a)
mckelveyite-Y	$Ba_3Na(Ca,U)Y(CO_3)_6 \cdot 3H_2O$	$P\bar{1}$	9.142	9.141	7	$\alpha = 102.51$ $\beta = 115.67$ $\gamma = 59.99$	Roberts *et al.* (1990)
meta-zellerite	$CaUO_2(CO_3)_2 \cdot 3H_2O$	*Pbnm*	9.718	18.226	4.965		Roberts *et al.* (1990)
oswaldpeetersite	$(UO_2)_2CO_3(OH)_2 \cdot 4H_2O$	$P2_1/c$	4.1425	14.098	18.374	$\beta = 103.62$	Vochten *et al.* (2001)
rabbittite	$Ca_3Mg_3(UO_2)_2(CO_3)_6(OH)_4 \cdot 18H_2O$		32.6	23.8	9.45	$\beta = 90$	Gaines *et al.* (1997)
roubaultite	$Cu_2[(UO_2)_3(CO_3)_2O_2(OH)_2](H_2O)_4$	$P\bar{1}$	7.767	6.924	7.850	$\alpha = 92.16$ $\beta = 90.89$ $\gamma = 93.48$	Ginderow and Cesbron (1985)
rutherfordine	UO_2CO_3	*Pmmn*	4.845	9.205	4.296		Finch *et al.* (1999b)
schröckingerite	(*listed under uranyl sulfates*)						
shabaite-Nd	$Ca(Nd,Sm,Y)_2UO_2(CO_3)_4(OH)_2 \cdot 6H_2O$	*P*2, *Pm*, *or* $P2_1/m$	9.208	32.09	8.335	$\beta = 90.3$	Deliens and Piret (1990a)
sharpite	$Ca(UO_2)_6(CO_3)_5(OH)_4 \cdot 6H_2O$		21.99	15.63	4.48		Gaines *et al.* (1997)
swartzite	$CaMgUO_2(CO_3)_3 \cdot 12H_2O$	$P2_1/m$	11.080	14.634	6.439	$\beta = 99.43$	Mereiter (1986)

urancalcarite	$Ca(UO_2)_3CO_3(OH)_6 \cdot 3H_2O$	*Pmcm* or $P2_1cn$	15.42	6.97	16.08		Deliens and Piret (1984a)
voglite	$Ca_2CuUO_2(CO_3)_4 \cdot 6H_2O$	$P2_1$	25.97	24.5	10.7	$\beta = 104$	Gaines *et al.* (1997)
widenmannite	$Pb_2UO_2(CO_3)_3$		8.99	9.36	4.95		Walenta (1976)
zellerite	$Ca(UO_2)(CO_3)_2(H_2O)_5$	*Pbnm*	11.22	19.25	4.93		Roberts *et al.* (1990)
znucalite	$CaZn_{11}(UO_2)(CO_3)_3(OH)_{20}(H_2O)_4$	$P\bar{1}$	12.692	25.096	11.85	$\alpha = 89.08$ $\beta = 91.79$ $\gamma = 90.37$	Ondruš *et al.* (1990)
uranyl phosphates							
althupite	$ThAl(UO_2)[(UO_2)_3(PO_4)_2O(OH)]_2(OH)_3(H_2O)_{15}$	$P\bar{1}$	10.953	18.567	13.504	$\alpha = 72.64$ $\beta = 68.20$ $\gamma = 84.21$	Piret and Deliens (1987)
ankoleite	$K_2(UO_2)_2(PO_4)_2 \cdot 6H_2O$	*P4/nmm*	6.993		8.891		Gaines *et al.* (1997)
asselbornite	$(Pb,Ba)(UO_2)_6(BiO)_4[(As,P)O_4]_2(OH)_{12} \cdot 3H_2O$	*Im3m*	15.66				Gaines *et al.* (1997)
autunite	$Ca[(UO_2)(PO_4)]_2 \cdot 11H_2O$	14*/mmm*	7.00		20.67		Locock and Burns (2003a)
bassetite	$Fe^{2+}(UO_2)_2(PO_4)_2 \cdot 8H_2O$	$P2_1/m$	6.98	17.07	7.01	$\beta = 90.32$	Roberts *et al.* (1990)
bergenite	$Ca_2Ba_4[(UO_2)_3O_2(PO_4)_2]_3(H_2O)_{16}$	$P2_1/c$	10.092	17.245	17.355	$\beta = 113.678$	Locock and Burns (2003c)
chernikovite	$(H_3O)_2(UO_2)(PO_4)_2 \cdot 6H_2O$	*P4/nmm*	7.02		9.043		Gaines *et al.* (1997)
coconinoite	$Fe_2Al_2(UO_2)_2(PO_4)_4SO_4(OH)_2 \cdot 20H_2O$	*C2/c*	12.5	12.97	23	$\beta = 106.6$	Young *et al.* (1966)
dewindtite	$Pb(UO_2)_3(PO_4)_2(OH)_2 \cdot 3H_2O$	*Bmmb*	16.031	17.264	13.605		Piret *et al.* (1990)
dumontite	$Pb_2[(UO_2)_3(PO_4)_2(OH)_4](H_2O)_5$	$P2_1/m$	8.118	16.819	6.983	$\beta = 109.03$	Locock and Burns (2003b)
françoisite-Nd	$Nd[(UO_2)_3(PO_4)_2O(OH)](H_2O)_6$	$P2_1/c$	9.298	15.605	13.668	$\beta = 112.77$	Piret *et al.* (1988)
furongite	$Al_2UO_2(PO_4)_2 \cdot 8H_2O$	$P\bar{1}$	17.87	14.18	12.18	$\alpha = 67.8$ $\beta = 77.5$ $\gamma = 79.9$	Shen and Peny (1981)
kamitugaite	$PbAl(UO_2)_5[(P,As)O_4]2(OH)_9 \cdot 5H_2O$	$P\bar{1}$	10.98	15.96	9.068	$\alpha = 95.1$ $\beta = 96.1$ $\gamma = 80$	Deliens and Piret (1984b)
lehnerite	$Mn(UO_2)_2(PO_4)_2 \cdot 8H_2O$	$P2_1/n$					Gaines *et al.* (1997)
lermontovite	$U^{4+}PO_4 \cdot OH \cdot H_2O$		9.74	19	10.01		Gaines *et al.* (1997)
meta-autunite	$Ca[(UO_2)(PO_4)]_2 \cdot 6H_2O$	*P4/nmm*	6.96		8.40		Gaines *et al.* (1997)

Table 5.3 (*Contd.*)

Mineral	*Formula*	*Space group*	*a* (Å)	*b* (Å)	*c* (Å)	*Angle* (°)	*References*
meta-torbenite	$Cu[(UO_2)(PO_4)]_2(H_2O)_8$	*P4/n*	6.9756		17.349		Locock and Burns (2003d)
meta-uranocircite-I	$Ba[(UO_2)(PO_4)]_2(H_2O)_7$	$P2_1$	6.943	17.634	6.952	$\beta = 89.95$	Locock *et al.* (2005b)
meta-vanmeersscheite	$U(UO_2)_3(PO_4)_2(OH)_6 \cdot 2H_2O$		34.18	33.88	14.07		Piret and Deliens (1982)
mundite	$Al(UO_2)_3(PO_4)_2(OH)_3 \cdot 5.5H_2O$		17.08	30.98	13.76		Gaines *et al.* (1997)
ningyoite	$(U^{4+},Ca,Ce)_2[PO_4]_2 \cdot 1–2H_2O$		6.8040	12.0117	6.3504		Gaines *et al.* (1997)
parsonsite	$Pb_2[(UO_2)(PO_4)_2](H_2O)n$, where $0 \leq n \leq 0.5$	$P\bar{1}$	6.842	10.383	6.670	$\alpha = 101.5$ $\beta = 110.84$ $\gamma = 88.09$	Sejkora *et al.* (2002)
phosphatian walpurgite	$(UO_2)Bi_4O_4[(As,P)O_4]_2 \cdot 2H_2O$	$P\bar{1}$	7.124	10.392	5.492	$\alpha = 101.22$ $\beta = 109.93$ $\gamma = 87.93$	Sejkora *et al.* (2004)
phosphuranylite	$KCa(H_3O)_3(UO_2)[(UO_2)_3(PO_4)_2O_2]_2(H_2O)_8$	*Cmcm*	15.899	13.740	17.300		Demartin *et al.* (1991)
phuralumite	$Al_2(UO_2)_3(PO_4)_3(OH)_2 \cdot 13H_2O$	$P2_1/a$	13.836	20.918	9.428		Piret *et al.* (1979)
phurcalite	$Ca_2(UO_2)_3O_2(PO_4)_2 \cdot 7H_2O$	*Pbca*	17.415	16.035	13.598		Atencio *et al.* (1991)
przhevalskite	$Pb_2(UO_2)_3(PO_4)_2(OH)_4 \cdot 3H_2O$	*Cmmm*	8.57	11.01	6.93		Gmelin (1981d)
ranunculite	$HAlUO_2PO_4(OH)_3 \cdot 4H_2O$		11.1	17.7	18.0	$\beta = 90$	Gaines *et al.* (1997)
renardite	(not a mineral species possible mixture of dewindtite and phosphuranylite (Čejka, 1999)						
sabugalite	$HAl(UO_2)_4(PO_4)_4 \cdot 16H_2O$		6.96		19.3		Frondel (1951a)
saléeite	$Mg[(UO_2)(PO_4)]_2 \cdot 10H_2O$	$P2_1/c$	6.951	19.947	9.896	$\beta = 135.17$	Miller and Taylor (1986)
threadgoldite	$Al(UO_2)_2(PO_4)_2OH \cdot 8H_2O$	*C2/c*	20.168	9.847	19.719		Khosrawan-Sazedj (1982b)
torbernite	$Cu[(UO_2)(PO_4)]_2(H_2O)_{12}$	*P4/nnc*	7.0267		20.807		Locock and Burns (2003d)
triangulite	$Al_3(UO_2)_4(PO_4)_4(OH)_5 \cdot 5H_2O$		10.39	10.56	10.6	$\alpha = 116.4$ $\beta = 107.8$ $\gamma = 113.4$	Gaines *et al.* (1997)

tristramite	*listed under uranyl sulfates*						
ulrichite	$Cu[Ca(H_2O)_2(UO_2)(PO_4)_2](H_2O)_2$	$P2_1/c$	12.84	6.996	13.007	$\beta = 91.92$	Kolitsch and Giester (2001)
upalite	$Al(UO_2)_3(PO_4)_2O(OH) \cdot 7H_2O$	$P2_1/a$	13.704	16.82	9.332	$\gamma = 111.5$	Piret and Declercq (1983)
uramphite	$NH_4UO_2PO_4 \cdot 3H_2O$		7.01		9.05		Gmelin (1981d)
uranocircite	$Ba[(UO_2)(PO_4)]_2(H_2O)_{10}$	$P2/c$	7.01	6.99	21.2	$\beta = 103.7$	Locock *et al.* (2005b)
uranospathite	$Al_{1-x}\square_x[(UO_2)(PO_4)]_2(H_2O)_{20+3x}F_{1-3x}$, $0 < x < 0.33$	$Pmn2$	30.020	7.0084	7.0492		Locock *et al.* (2005c)
vochtenite	$(Fe,Mg)Fe[(UO_2)(PO_4)]_2 \cdot 8H_2O$		12.606	19.99	9.99	$\beta = 102.52$	Gaines *et al.* (1997)
vanmeersscheite	$U(OH)_4[(UO_2)_3(PO_4)_2(OH)_2](H_2O)_4$	$P2_1mn$	17.06	16.76	7.023		Piret and Deliens (1982)
vyacheslavite	$UPO_4(OH) \cdot nH_2O$		6.96	9.1	12.38		Gaines *et al.* (1997)
xiangjiangite	$(Fe,Al)(UO_2)_4(PO_4)_2(SO_4)_2OH \cdot 22H_2O$	$C2/c$	12.54	12.98	23.8	$\beta = 108.6$	Zhang *et al.* (1992)
yingjiangite	$(K_{1-x}Ca_x)(UO_2)_3(PO_4)_2(OH)_{1+x} \cdot 4H_2O \quad x = 0.35$	$Bmmb$	15.707	17.424	13.692		Zhangru *et al.* (1986)
uranyl arsenates							
arsenuranospathite	$HAl(UO_2)_4(AsO_4)_4 \cdot 40H_2O$	$P4_2/n$	7.16		30.37		Gaines *et al.* (1997)
arsenuranylite	$Ca(UO_2)_4(AsO_4)_2(OH)_4 \cdot 6H_2O$		15.4	17.4	13.77		Gaines *et al.* (19970
asselbornite	$(Pb,Ba)(UO_2)_6(BiO)_4(AsO_4)_2(OH)_{12} \cdot 3(H_2O)$	$Im3m$	15.66				Sarp *et al.* (1983)
abernathyite	$K[(UO_2)(AsO_4)]_2(H_2O)_3$	$P4/ncc$	7.176		18.126		Ross and Evans (1964)
chadwickite	$(UO_2)H(AsO_3)$		11		15.96		Walenta (1998)
hallimondite	$Pb_2[(UO_2)(AsO_4)_2](H_2O)_n$, where $0 \leq n \leq 0.5$	$P\bar{1}$	7.123	10.469	6.844	$\alpha = 100.57$ $\beta = 94.80$ $\gamma = 91.27$	Walenta (1965)
heinrichite	$Ba[(UO_2)_2(AsO_4)]_2(H_2O)_{10}$	$P2/c$	7.1548	7.1340	21.290	$\beta = 104.171$	Locock *et al.* (2005b)
hügelite	$Pb_2[(UO_2)_3O_2(AsO_4)_2](H_2O)_5$	$P2_1/m$	31.066	17.303	7.043	$\beta = 96.492$	Locock and Burns (2003b)
kahlerite	$Fe(UO_2)_2(AsO_4)_2 \cdot 12H_2O$	$P4_2/n$	14.3		21.97		Gaines *et al.* (1997)
meta-heinrichite	$Ba[(UO_2)(AsO_4)]_2(H_2O)_7$	$P2_1$	7.08	17.7	7.09	$\beta = 90.02$	Locock *et al.* (2005b)
meta-kahlerite	$Fe(UO_2)_2(AsO_4)_2 \cdot 8H_2O$	$P4/mmm$	7.16		8.62		Gaines *et al.* (1997)
meta-kirchheimerite	$Co(UO_2)_2(AsO_4)_2 \cdot 8H_2O$	$P4/mmm$	7.16		8.60		Gaines *et al.* (1997)
meta-lodevite	$Zn(UO_2)_2(AsO_4)_2 \cdot 10H_2O$	$P4_2/m$	7.16		17.20		
meta-novácekite	$Mg(UO_2)_2(AsO_4)_2 \cdot 4–8H_2O$	$P4/n$	7.16		8.58		Roberts *et al.* (1990)

Table 5.3 (*Contd.*)

Mineral	*Formula*	*Space group*	*a* (Å)	*b* (Å)	*c* (Å)	*Angle* (°)	*References*
meta-zeunerite	$Cu[(UO_2)(AsO_4)]_2(H_2O)_8$	*P4/n*	7.1094		17.416		Locock and Burns (2003d)
novacekite	$Mg(UO_2)_2(AsO_4)_2 \cdot 12H_2O$	$P4_1/n$	7.16		20.19		Frondel (1951b)
orthowalpurgite	$(UO_2)Bi_4O_4(AsO_4)_2 \cdot 2H_2O$	*Pbcm*	5.492	13.324	20.685		Krause *et al.* (1995)
séelite	$Mg(UO_2)(AsO_3)_{0.7}(AsO_4)_{0.3} \cdot 7\beta\beta H_2O$	*C2/m*	18.207	7.062	6.661	$\beta = 99.65$	Frondel (1951b)
trögerite	$(UO_2)_3(AsO_4)_2 \cdot 12H_2O$	*P4/mmm*	7.16		8.8		Gaines *et al.* (1997)
uranospinite	$Ca[(UO_2)(AsO_4)]_2(H_2O)_{11}$	*Pnma*	14.35	20.66	7.17		Lockock *et al.* (2005b)
walpurgite	$(UO_2)Bi_4O_4(AsO_4)_2 \cdot 2H_2O$	$P\bar{1}$	7.135	10.426	5.494	$\alpha = 101.47$ $\beta = 110.82$ $\gamma = 88.20$	Mereiter (1982b)
zeunerite	$Cu[(UO_2)(AsO_4)]_2(H_2O)_{12}$	*P4/nnc*	7.1797		20.857		Locock and Burns (2003d)
uranyl molybdates							
calcurmolite	$Ca(UO_2)_3(MoO_4)_3(OH)_2(H_2O)_{11}$						Gaines *et al.* (1997)
deloryite	$Cu_4(UO_2)(MoO_4)_2(OH)_6$	*C2/m*	19.94	6.116	5.52	$\beta = 104.2$	Pushcharovsky *et al.* (1996)
iriginite	$[(UO_2)Mo_2O_7(H_2O)_2](H_2O)$	*Pbcm*	6.705	12.731	11.524		Krivovichev and Burns (2000)
moluranite	$U^{4+}(UO_2)_2Mo_5O_{19} \cdot 12H_2O$	*amorphous*					Roberts *et al.* (1990)
mourite	$U^{4+}Mo_5O_{12}(OH)_{10}$	*P2/c*	24.443	7.182	9.901	$\beta = 102.22$	Gaines *et al.* (1997)
tengchongite	$CaO_6UO_3 \cdot 2MoO_3 \cdot 12H_2O$		15.616	13.043	17.716		Chen *et al.* (1986)
sedovite	$U(MoO_4)_2$		3.36	11.08	6.42		Roberts *et al.* (1990)
umohoite	$[(UO_2)MoO_4(H_2O)](H_2O)$	$P2_1/c$	6.3748	7.5287	14.628	$\alpha = 82.64$ $\beta = 85.95$ $\gamma = 89.91$	Krivovichev and Burns (2000b)
uranyl vanadates							
carnotite	$[K_2(UO_2)_2(VO_4)_2 \cdot 1\text{–}3H_2O]$	*P21/a*	10.51	8.45	7.32	$\gamma = 106.08$	Appleman and Evans (1965)
curienite	$Pb[(UO_2)_2(V_2O_8)](H_2O)_5$	*Pcan*	10.40	8.45	16.34		Borène and Cesbron (1971)

francevillite	$Ba_{0.96}Pb_{0.04}[(UO_2)_2(V_2O_8)](H_2O)_5$	*Pcan*	10.419	8.510	16.763		Mereiter (1986)
fritzscheite	$Mn(UO_2)_2(PO_4,VO_4)_2 \cdot 10H_2O$	*Pnam*	10.59	8.25	15.54		Roberts *et al.* (1990)
margaritasite	$(Cs,K,H_3O)_2(UO_2)_2(VO_4)_2 \cdot H_2O$	$P2_1/a$	10.514	8.425	7.25	$\gamma = 106.01$	Roberts *et al.* (1990)
meta-tyuyamunite	$Ca(UO_2)_2(VO_4)_2 \cdot 3–5H_2O$	*Pnam*	10.54	8.49	17.34		Roberts *et al.* (1990)
meta-vanuralite	$Al(UO_2)_2(VO_4)_2OH \cdot 8H_2O$	*P*1	10.46	8.44	10.43	$\alpha = 75.88$ $\beta = 102.83$ $\gamma = 90$	Roberts *et al.* (1990)
rauvite	$Ca(UO_2)_2V_{10}O_{28} \cdot 16H_2O$	(*no unit cell data*)					
sengierite	$Cu_2[(UO_2)_2(V_2O_8)](OH)_2(H_2O)_6$	$P2_1/a$	10.599	8.093	10.085	$\gamma = 103.42$	Piret *et al.* (1980)
strelkinite	$NaUO_2VO_4 \cdot 3H_2O$	*Pnmm*	10.64	8.36	32.72		Gaines *et al.* (1997)
tyuyamunite	$Ca(UO_2)_2(VO_4)_2 \cdot 5–8H_2O$	*Pnan*	10.36	8.36	20.4		Roberts *et al.* (1990)
uvanite	$U_2V_6O_{21} \cdot 15H_2O$	(*no unit cell data*)					
vanuralite	$Al(UO_2)_2(V^{5+}O_4)_2(OH) \cdot 11H_2O$		10.55	8.44	24.52	$\beta = 103$	Roberts *et al.* (1990)
vanuranylite	$(H_3O,Ba,Ca,K)_{1.6}(UO_2)_2(VO_4)_2 \cdot 4H_2O$	*C*2/*c*	10.49	8.37	20.2	$\beta = 90$	Roberts *et al.* (1990)
uranyl tungstates							
uranotungstite	$(Fe^{2+},Ba,Pb)(UO_2)_2WO_4(OH)_4(H_2O)_{12}$		9.22	13.81	7.17		Walenta (1985)
uranyl sulfates							
deliensite	$Fe(UO_2)_2(SO_4)_2(OH)_2 \cdot 3H_2O$	*Pnnm or Pnn*2	15.908	16.274	6.903		Vochten *et al.* (1997)
Co-zippeite	$Co(H_2O)_{3.5}[(UO_2)_2(SO_4)O_2]$	*C*2/*m*	8.650	14.252	17.742	$\beta = 104.092$	Burns *et al.* (2003)
coconinoite	$Fe_2Al_2(UO_2)_2(PO_4)_4SO_4(OH)_2 \cdot 20H_2O$		12.5	12.97	23	$\beta = 106.6$	Young *et al.* (1966)
jáchymovite	$(UO_2)_8(SO_4)(OH)_{14} \cdot 13H_2O$	(*no unit cell data*)					Brugger *et al.* (2003)
johannite	$Cu(UO_2)_2(SO_4)_2(OH)_2 \cdot 8H_2O$	$P\bar{1}$	8.903	9.499	6.812	$\alpha = 109.87$ $\beta = 112.01$ $\gamma = 100.40$	Mereiter (1982c)
marecottite	$Mg_3(H_2O)_{18}[(UO_2)_4O_3(OH)(SO_4)_2]_2(H_2O)_{10}$	$P\bar{1}$	10.815	11.249	13.851	$\alpha = 66.224$ $\beta = 72.412$ $\gamma = 69.95$	Brugger *et al.* (2003)
Mg-zippeite	$Mg_2(H_2O)_{11}[(UO_2)_2(SO_4)O_2]_2$	$P2_1/c$	8.6457	17.2004	18.4642	$\beta = 102.119$	Burns *et al.* (2003)
meta-uranopilite	$(UO_2)_6SO_4(OH)_{10} \cdot 5H_2O$	no unit cell data					Roberts *et al.* (1990)
Ni-zippeite	$Ni_2(UO_2)_6(SO_4)_3(OH)_{10} \cdot 16H_2O$	no unit cell data					Roberts *et al.* (1990)

Table 5.3 (*Contd.*)

Mineral	*Formula*	*Space group*	*a* (Å)	*b* (Å)	*c* (Å)	*Angle* (°)	*References*
rabejacite	$Ca(UO_2)_4(SO_5)_2(OH)_6 \cdot 6H_2O$		8.73	17.09	15.72		Deliens and Piret (1993)
schröckingerite	$NaCa_3(UO_2)(CO_3)_3(SO_4)F \cdot 10H_2O$		9.341		12.824		Li *et al.* (2001a)
Na-zippeite	$Na_5(H_2O)_{12}[(UO_2)_8(SO_4)_4O]_5(OH)_3$	$P2_1/n$	17.6425	14.6272	17.6922	$\beta = 104.461$	Burns *et al.* (2003)
tristramite	$(Ca,U^{4+},Fe^{3+})(PO_4,SO_4) \cdot 2H_2O$	$P6_222$	6.919		6.422		Gaines *et al.* (1997)
uranopilite	$(UO_2)_6[(SO_4)O_2(OH)_6(H_2O)]_6(H_2O)_8$	$P\bar{1}$	8.896	14.029	14.33	$\alpha = 96.610$ $\beta = 98.472$ $\gamma = 99.802$	Burns (2001a)
Zn-zippeite	$Zn(H_2O)_{3.5}[(UO_2)_2(SO_4)O_2]$	$C2/m$	8.6437	14.1664	17.701	$\beta = 104.041$	Burns *et al.* (2003)
zippeite	$K_3(H_2O)_3[(UO_2)_4(SO_4)_2O_3(OH)]$	$C2$	8.7524	13.9197	17.6972	$\beta = 104.178$	Burns *et al.* (2003)
uranyl selenites and tellurites							
cliffordite	$UO_2(Te_3O_7)$	$Pa\bar{3}$	11.335				Branstätter (1981)
derriksite	$Cu_4[(UO_2)(SeO_3)_2](OH)_6$	$Pn2_1m$	5.570	19.088	5.965		Ginderow and Cesbron (1983a)
demesmaekerite	$Cu_5Pb_2(UO_2)_2(SeO_3)_6(OH)_6(H_2O)_2$	$P\bar{1}$	11.955	10.039	5.639	$\alpha = 89.78$ $\beta = 100.36$ $\gamma = 91.34$	Ginderow and Cesbron (1983b)
guilleminite	$Ba[UO_2)_3(SeO_3)_2O_2](H_2O)_3$	$P2_1nm$	7.084	7.293	16.881		Cooper and Hawthorne (1995)
haynesite	$(UO_2)_3(OH)_2(SeO_3)_2 \cdot 5H_2O$	$Pncm$	8.025	17.43	6.953		Gaines *et al.* (1997)
larisaite	$Na(H_3O)(UO_2)_3(SeO_3)_2O_2 \cdot 4H_2O$	$P11m$	6.9806	7.646	17.249	$\beta = 90.039$	Chukanov *et al.* (2004)
marthozite	$Cu^{2+}[(UO_2)_3(SeO_3)_2O_2](H_2O)_8$	$Pbn2_1$	6.9879	16.4537	17.2229		Cooper and Hawthorne (2001)
moctezumite	$PbUO_2(TeO_3)_2$	$P2_1/c$	7.813	7.061	13.775	$\beta = 93.71$	Swihart *et al.* (1993)
piretite	$Ca(UO_2)_3(SeO_3)_2(OH)_4 \cdot 4(H_2O)$	$Pmnm$	7.01	17.135	17.606		Vochten *et al.* (1996)
schmitterite	UO_2TeO_3	$Pca2_1$	10.161	5.363	7.862		Meunier and Galy (1973)

euxenite–pyrochlore (mineral structures obtained by heating)							
betafite	$(Ca,Na,U)_2(Ti,Nb,Ta)_2O_6(OH)$	*Fd*$\bar{3}$*m*	10.31				Gaines *et al.* (1997)
calciobetafite	$(Ca,RE,Th,U)_2(Nb,Ta,Ti)_2O_7$	*Fd*$\bar{3}$*m*	10.2978				Mazzi and Munno (1983)
calciosamarskite	$(Ca,Fe^{3+},U,Y)NbO_4$	Metamict					Hanson *et al.* (1999)
euxenite-y	$(Y,Ca,Ce,U,Th)(Nb,Ta,Ti)_2O_6$	*Pcan*	5.52	14.57	5.166		Gaines *et al.* (1997)
ishikawaite	$(U,Fe,Y,Ce)(Nb,Ta)O_4$	Metamict					Hanson *et al.* (1999)
kobeite-y	$(Y,U)(Ti,Nb)_2(O,OH)_6$		5.021				Gaines *et al.* (1997)
liandratite	$U^{6+}(Nb,Ta)_2O_8$	*P*$\bar{3}$1*m*	6.36		4.01		Mucke and Strunz (1978)
petscheckite	$U^{4+}Fe^{2+}(Nb,Ta)_2O_8$	*P*$\bar{3}$1*m*	6.42		4.02		Mucke and Strunz (1978)
samarskite	$(Fe,Y,Ce,U)(Nb,Ta,Ti)O_4$	*Pbcn*	5.498	14.34	5.12		Warner and Ewing (1993)
uranopyrochlore	$(U,Ca,Ce)_2(Nb,Ta)_2O_6(OH,F)$	*Fd*$\bar{3}$*m*	10.44				Gaines *et al.* (1997)
uranmicrolite	$(U,Ca,Ce)_2(Ta,Nb)_2O_6(OH,F)$	*Fd*$\bar{3}$*m*	10.4				Gaines *et al.* (1997)
uranopolycrase	$(U,Y)(Ti,Nb)_2O_6$	*Pbcn*	14.51	5.558	5.173		Gaines *et al.* (1997)
brannerites							
brannerite	$(U,Ca,Y,Ce)(Ti,Fe)_2O_6$	*C*2/*m*	9.79	3.72	6.87	$\beta = 118.25$	Pabst (1954)
thorutite	$(Th,U,Ca)Ti_2(O,OH)_6$	*C*2/*m*	9.822	3.824	7.036	$\beta = 118.83$	Roberts *et al.* (1990)
Fe–Ti oxides							
davidite-la	$(La,Ce)(Y,U,Fe)(Ti,Fe)_{20}(O,OH)_{38}$	*R*$\bar{3}$	10.375		20.909		Gatehouse *et al.* (1979)
dessauite	$(Sr,Pb)(Y,U)(Ti,Fe^{3+})_{20}O_{38}$	*R*$\bar{3}$	9.197			$\alpha = 68.75$	Orlandi *et al.* (1997)

other anthropogenic sources of uranium of environmental concern. The long-term behavior of nuclear waste materials such as high-level waste (HLW) glass, spent UO_2 nuclear fuel (SNF), and U-bearing waste forms, can be predicted, in part, by understanding the geochemical behavior of uranium. Other forms of uranium contamination of immediate concern are located at uranium production facilities, mines, and, more recently, battlefields where depleted uranium weapons have been used. Concerns about the fate of uranium in the environment have been addressed by employing several micro-analytical techniques to identify and characterize the nature of the contaminants (Bertsch *et al.*, 1994; Buck *et al.*, 1996; Morris *et al.*, 1996; Duff *et al.*, 1997, 2002).

Burns *et al.* (1997a) have theorized that many of the alteration phases that form during waste form corrosion may be capable of incorporating key radionuclides, including Np, Tc, and Pu. The potential for uranium secondary phases to incorporate radionuclides and thus curtail their migration is of significant scientific interest (Buck *et al.*, 1997; Chen *et al.*, 1999, 2000; Li and Burns, 2001a; Burns *et al.*, 2004a). A key to predicting the thermodynamic properties of these complex U(VI) minerals is to understand the nature of the connectivity between uranium polyhedra. Finch and Murakami (1999) have reported measured and estimated thermodynamic data for 14 uranyl silicate and carbonate minerals. Additional data is published elsewhere on uranium phases (Grenthe *et al.*, 1995), studtite (Hughes-Kubatko *et al.*, 2003), and new experimental thermodynamic measurements have now been obtained from the uranyl carbonates, uranophane, and uranyl phosphates (Hughes-Kubatko *et al.*, 2005). In addition to the natural U-minerals, a wealth of complex synthetic U(VI) phases have now been explored as potential, mesoporous materials, catalysts, and waste forms.

5.3.1 Mineralogy and classification of uranium deposits

Extensive reviews of uranium mineralogy and the origin of uranium deposits have been made by Finch and Murakami (1999) and Plant *et al.* (1999), respectively. Uranium deposits can be classified into 14 groups. These are: unconformity related, sandstone, quartz–pebble conglomerate, veins, breccia complex, intrusive, phosphorite, collapse breccia, volcanic, surficial, metasomatite, metamorphic, lignite, and black shale. Uranium is precipitated in reducing environments, sandstones rich in organic matter or iron sulfides, phosphate-rich sediments, shales where uranium is concentrated in organic matter, and lignite and coals. Enrichment of uranium in lignite or coal can create environmental problems when these sources are burned. Uranium undergoes a series of complex fractionation events, resulting in highly variable levels in different rock types. Owing to its relatively large size (the ionic radius of U^{4+} is 0.940 Å) in eight-fold coordination with oxygen (Farges *et al.*, 1992), tetravalent uranium is incompatible in silicate melts, depending on alkali content and the presence of nonbonding oxygens. Uranium is preferentially partitioned into small volume,

low-temperature melts, and becomes progressively more concentrated, so that certain types of highly evolved granite, rhyolite,[1] and alkaline complexes contain significant quantities of uranium (Plant *et al.*, 1999). Uranium is usually present in accessory minerals such as zircon ($ZrSiO_4$), monazite {(Ce, La, Nd, Th)PO_4}, and pyrochlore (general formula AB_2O_7), many of which are also observed in synthetic ceramic HLW forms (Ewing, 1999). Although the levels of Th and U in terrestrial igneous rocks are variable, the Th/U ratio is relatively constant at about 3.8 (Taylor and McLennan, 1985). Although the most important uranium oxidation states of environmental and geological significance are considered to be U(IV) and U(VI), there is increasing evidence for the role of U(V) in uranium minerals (Burns and Finch, 1999; Colella *et al.*, 2005).

There are numerous U-deposits worldwide and some of these have been studied in great detail, some owing to their relevance to HLW disposal and the environmental fate of uranium, as well as being sources for unique uranium minerals. Understanding the geochemical behavior of uranium at these sites provides the basis for predictive modeling of uranium in the environment and also helps build confidence in the feasibility of geological waste isolation. Uranium deposits at Oklo, Peña Blanca, Shinkolobwe, and Koongarra will be described briefly below.

(a) Oklo, Gabon (Sandstone deposit)

The geochemical behavior of the natural fission reactors at Oklélobondo and Bangombé (Oklo), located in a Precambrian[2] sedimentary basin in Gabon (Africa) have been discussed by Brookins (1990), Hidaka and Holliger (1998), and Janeczek (1999). The Bamgombé site in the Oklo region is of particular interest as it is located at shallow depths. Furthermore, as full-scale mining was never commenced, the ore deposit has been left almost intact. Electron microprobe analysis (EMPA) of uraninite in contact with U(VI) phases indicates that the alteration resulted in increased concentrations of Si, P, S, Zr, Ce, and Nd. The dissolution of accessory apatite {$Ca_5(PO_4)_3(OH,Cl,F)$}, monazite and sulfides resulted in the retardation of uranium through the formation of secondary minerals, including phosphatian coffinites and iron–uranyl phosphate hydroxide hydrates (i.e. bassetite {$Fe^{2+}(UO_2)_2(PO_4)_2 \cdot 8H_2O$}). Jensen *et al.* (2002) investigated the mineralogy of the uranium deposits at Bamgombé and compared their experimental observations with thermodynamic predictions based on groundwater conditions. The primary U-minerals at Bamgombé are uraninite and minor coffinite [$U(SiO_4)_{4-x}(OH)_{4x}$]. The uranyl minerals include fourmarierite {$Pb_{1-x}[(UO_2)_4O_{3-2x}(OH)_{4+2x}] \cdot 4H_2O$}, bassetite possibly associated with {$U(HPO_4)_2 \cdot 2H_2O$} or chernikovite {$(H_3O)_2[(UO_2)(PO_4)]_2 \cdot 6H_2O$},

[1] Derived from the rapid cooling of a very viscous granitic magma.
[2] Between 2.5 and 1.8 billion years ago.

torbernite $\{Cu[(UO_2)(PO_4)]_2 \cdot 8–12H_2O\}$, Ce-rich françoisite $\{(Nd,Y,Sm,Ce)(UO_2)_3(PO_4)_2O(OH)(H_2O)_6\}$, and uranopilite $\{(UO_2)_6(SO_4)O_2(OH)_6(H_2O)_6 \cdot 8H_2O\}$. Autunite $\{Ca[(UO_2)(PO_4)]_2 \cdot 11H_2O\}$ has also been reported. Eh–pH diagrams predict that coffinite, $U(HPO_4)_2 \cdot H_2O$, and $UOF_2 \cdot H_2O$ are the only stable U(IV) phases and that uranopilite, torbernite, and bassetite will become stable during oxidative alteration.

(b) Peña Blanca, Chichuhua District, Mexico (Breccia Pipe)

The Sierra de Peña Blanca District, Chihuahua, Mexico consists of a gently dipping Tertiary[3] volcanic pile that covers a calcareous basement of Cretaceous age[4] (Cesbron *et al*., 1993; Pearcy *et al*., 1994). Peña Blanca is part of a much more extensive range of volcanic uranium deposits that extend from the McDermitt caldera at the Oregon–Nevada border through the Marysvale district of Utah and Date Creek Basin in Arizona and south into the Peña Blanca (Finch, 1996). In the Nopal I deposit, the ignimbritic tuffs[5] have been hydrothermally altered and U-mineralization is located within a breccia pipe structure at the intersection of several faults. The uraninite deposition under reducing conditions (8 ± 5) Ma ago has precluded the accumulation of significant amounts of lead. Later tectonic forces elevated the deposit above the local water table, exposing it to oxidizing conditions. The site is a convincing geochemical analog of the proposed HLW repository at Yucca Mountain, Nevada. The initial corrosion products from the oxidative dissolution of uraninite are uranyl oxide hydrates, including ianthinite $\{[U_2^{4+}(UO_2)_4O_6(OH)_4(H_2O)_4](H_2O)_5\}$ (Burns *et al*., 1997b), schoepite $\{[(UO_2)_8O_2(OH)_{12}](H_2O)_{12}\}$, and dehydrated schoepite $\{(UO_2)_4O(OH)_6 \cdot H_2O\}$ (Leslie *et al*., 1993). Ianthinite is unusual in that it contains both U^{6+} and U^{4+}. The phase has a narrow stability range and will easily degrade. It will form in oxygen-deficient environments, such as under localized reducing environments at Shinkolobwe (Finch and Ewing, 1992).

Uranyl silicates, uranophane $\{Ca(UO_2)_2(SiO_3OH)_2(H_2O)_5\}$, are the predominant U-phases at Nopal I, comprising more than 95% of all U-bearing minerals. They either replace earlier formed U-phases or form euhedral[6] crystals within open voids and fractures. The uranophanes at Nopal I have been dated at 3.2 Ma, suggesting that alteration of the initial uraninite took millions of years under the oxidizing environment. The paragenesis[7] of U-phases was similar to that observed in laboratory tests by Wronkiewicz *et al*. (1992) on synthetic UO_2 apart from the occurrence of the mixed uranium valence phase,

[3] ~5–45 million years ago.
[4] ~65–130 million years ago.
[5] Deposits of hot incandescently glowing ash (tuff) from volcanic activity.
[6] Well-formed crystal with regular shape.
[7] Refers to the order of mineral formation.

ianthinite that has not been observed in corrosion tests with UO_2 (Wronkiewicz *et al.*, 1996) or SNF (Finch *et al.*, 1999a; Wronkiewicz and Buck, 1999).

(c) Shinkolobwe (Sandstone U-deposit)

Uranium minerals from the 1.8-Ga-old Shinkolobwe deposit, located in the Katanga District of the Democratic Republic of the Congo, have been extensively described and discussed by Finch and Ewing (1992) and in references therein. The deposit has been exposed since Tertiary times and extensive weathering has significantly altered or replaced uraninite. Uranium mineralization occurs along fracture zones where meteoric[8] waters have penetrated. The uranyl silicates, uranophane and cuprosklodowskite $\{Cu(UO_2)_2(SiO_3OH)_2 \cdot 6H_2O\}$, are ubiquitous and replace becquerelite, compreignacite $\{K_2[(UO_2)_3O_2(OH)_3]_2(H_2O)_7\}$, vandendriesscheite $\{Pb_{1.57}[(UO_2)_{10}O_6(OH)_{11}](H_2O)_{11}\}$, fourmarierite, billietite $\{Ba[(UO_2)_3O_2(OH)_3]_2(H_2O)_4\}$ and schoepite by reaction with the silica-rich groundwater. As the groundwater interacts with the host rocks, it becomes increasingly more enriched in silica, resulting in the precipitation of uranophane. Finch *et al.* (1995) argued that the cyclical weather pattern explained the simultaneous occurrence of both becquerelite and uranophane. Becquerelite has been estimated to be 10^5 to 10^6 years old based on the $^{230}Th/^{234}U$ ratios being close to 1.0 in these minerals (Finch *et al.*, 1996b).

(d) Koongarra

Koongarra is located in a tropical monsoon climate with long dry seasons (Edghill, 1991). The host rock is quartz-rich schist[9] and the primary uranium mineral, uraninite, has been subjected to weathering for more than 1 million years. The alteration of chlorite produces Fe^{3+} minerals that become associated with some uranium. In the primary ore deposit uraninite has been altered to curite $\{Pb_3[(UO_2)_8O_8(OH)_6] \cdot 3H_2O\}$, and sklodowskite $\{Mg(H_3O)_2[(UO_2)(SiO_4)]_2 \cdot 4H_2O\}$. However, Murakami *et al.* (1997) have shown that upstream from the deposit, saléeite $\{Mg[(UO_2)(PO_4)]_2 \cdot 10H_2O\}$, has replaced sklodowskite and granular apatite and is the predominant mechanism for fixing uranium. In a transmission electron microscopy (TEM) study by Lumpkin *et al.* (1999) on Koongarra mineral substrates, uranium was observed to preferentially sorb to the iron oxide minerals (goethite, α-FeOOH, and possibly ferrihydrite) rather than the clay minerals.

[8] Groundwater of atmospheric origin (i.e. rain, snow, etc.).
[9] A thinly layered crystalline rock.

5.3.2 Reduced uranium phases

Uraninite is a common accessory mineral in pegmatites and peraluminous granites and is the most important source of dissolved uranium in groundwaters emanating from weathered granite terrains. Uraninite possesses the fluorite structure, nominally UO_{2+x}. U(IV) is coordinated by eight O atoms in a cubic arrangement, and each O atom bonds to four U^{4+} ions. Stoichiometric UO_2 is unknown in nature and is always partially oxidized in addition to containing radiogenic lead and commonly thorium, calcium, and lanthanides. Stoichiometric UO_2 ($a = 5.47$ Å) forms a complete solid solution with ThO_2 ($a = 5.6$ Å) following Végard's Law. Janeczek and Ewing (1992) proposed the formula $\{(U^{4+}_{1-x-y-z}U^{6+}_{x}Ln^{3+}_{y}M^{2+}_{z}\square_{v})O_{2-x-0.5y-z-2v}\}$ (where $\square$ denotes a vacancy).

It is possibly inappropriate to term uraninite (as well as coffinite and brannerite), as a primary uranium mineral as it can precipitate from aqueous solutions under reducing conditions or through microbial processes (e.g. sulfur-reducing bacteria (Spirakis, 1996; Fredrickson *et al*., 2002)). Primary reduced uranium minerals are usually coarse grained and present in granites and pegmatites. They have high Th and consequently larger unit cells. Hydrothermal vein[10] uraninites typically have minor lanthanides, Y, Ca, and Th absent. Low-temperature sedimentary uraninites are devoid of lanthanides and Th, but may contain Ca, Si, and P. Grandstaff (1976) observed a correlation between dissolution rate and the mole fraction of impurity cations (Pb and Th). The decrease was attributed to the buildup of low-solubility impurities in the surface as U was preferentially leached. Similar processes have been observed in corroded SNF (Buck *et al*., 2004).

The most common U-ore is fine grained uraninite, sometimes termed pitchblende, similar to the term used for fine-grained quartz (chalcedony); pitchblende is not a mineral name but a textural term. The name 'pitch' does not come from its black, resinous appearance, and botyroidal habit[11] but from the german word 'pech' meaning bad luck (Piekarski and Morfeld, 1997). Radiogenic lead can reach levels of 15–20 wt.% in ancient uraninites. Janeczek and Ewing (1991) observed lead contents of 14 wt.% in an 1800-Ma-old uraninite specimen from the Eldorado mine in Canada. The presence of lead in uraninite results in auto-oxidation and can lead to high U(VI)/U(IV) ratios in uraninite. Auto-oxidation at the uraninite deposit at Cigar Lake has led to U (VI)/U(IV) ratios from 0.02 to as high as ~0.75 according to X-ray photoelectron spectroscopy (XPS) studies by Sunder *et al*. (1996), despite the highly anoxic conditions prevalent in the deposit. Sunder and coworkers also examined uraninites from Oklo and found a similar range of ratios for uraninites.

[10] A vein formed by the crystallization of minerals from predominantly hot water solutions of igneous origin.
[11] A globular growth of minerals.

Oxidation of uraninite results in a decrease of the unit cell parameter, whereas α-decay damage has the opposite effect through the formation of defects and voids. Uraninites typically experience more than 10 displacements per atom over periods of millions of years; yet, the high rate of self-annealing prevents metamictization[12] of the uraninite. Cationic substitutions (radiogenic Pb, Th, Ca, and Ln) increase the unit cell parameter (Janeczek and Ewing, 1991). The large ionic radius of Pb^{2+} results in a substantial increase in the unit cell with increasing age of the uraninite. The presence of silicium and phosphorus in partly altered uraninite is due most likely due to the precipitation of phosphatian coffinite.

(a) U(IV) phosphates and molybdates

The UO_2–P_2O_5 system includes uranium meta-phosphate $U(PO_3)_4$, uranium diphosphate UP_2O_7, uranium oxide phosphate $(UO)_3(PO_4)_2$, and uranium oxide diphosphate $(UO)_2P_2O_7$. Douglass (1962) first characterized both orthorhombic $U(PO_3)_4$ and its isostructural plutonium analog. Brandel *et al.* (1996) synthesized two additional phosphates, uranium uranyl phosphate $U(UO_2)(PO_4)_2$, that formed in air at 1000–1200°C, which may be the only mixed valence uranium phosphate known, and diuranium oxide phosphate $U_2O(PO_4)_2$ that was formed at 1350°C in an inert atmosphere. Attempts by Brandel *et al.* (1996) to produce uranium orthophosphate, $U_3(PO_4)_4$, were unsuccessful confirming earlier data, indicating that this phase does not exist (Gmelin, 1981d).

A number of hydrous U(IV) phosphates exist in nature and some of these have been observed in secondary alteration phases formed during laboratory corrosion tests on HLW glass (Bates *et al.*, 1992). These phases have been described as brockite- and rhabdophane-related phases and contain U, Th, Ln, and Pu (Buck and Bates, 1999). Ningyoite, $\{(U^{4+},Ca,Ce)_2[PO_4]_2 \cdot 1\text{–}2H_2O\}$, is a member of the rhabdophane group of phosphates (Gaines *et al.*, 1997). Ningyoite is a translucent brown to greenish mineral observed at the Ningyo-Toge mine, Japan. The phase may form a solid solution with U-bearing brockite, $\{Ca_{z-y}(U^{4+}_{1-x}Th^{4+}_{x})_{y/2}(PO_4)_2 \cdot nH_2O\}$; in addition CO_3 and SO_4 may substitute for PO_4.

Lermontovite $\{U^{4+}(PO_4)OH\}$ and vyacheslavite $\{U^{4+}(PO_4)(OH) \cdot 2.5H_2O\}$ form under reduced conditions in hydrothermal deposits associated with sulfides.

(b) Uranium orthosilicate

Coffinite and the thorium orthosilicate, thorite, $(Th,U)SiO_4$, are widespread in igneous and metamorphic rocks and are important ore minerals in some uranium and thorium deposits (Speer, 1982). These silicates are tetragonal and

[12] Process of alteration of crystalline to non-crystalline structure through radioactive decay.

isostructural with zircon (Fuchs and Gebert, 1958). Because they can be primary in origin, they have been used in geochronological studies. Coffinite occurs as a primary uranium ore mineral in unoxidized, uranium–vanadium ores of the Colorado Plateau, USA; however, it is also found in hydrothermal, vein deposits with pitchblende, with variable composition where $(OH)^-$ substitutes for $(SiO_4)^{4-}$. Some studies have suggested that the ubiquitous occurrence of organic matter with secondary coffinite indicates a possible biogenic origin (Spirakis, 1996).

(c) Uranium in silicate melts and glasses

The partitioning of uranium into silicate melts depends on the oxygen fugacity, melt composition, and redox conditions. Under mildly reducing conditions, U(V) is present as an octahedrally coordinated species. Under very reducing conditions, such as that prevailing in silicate magmatic melts, U(IV) is the dominant uranium species. Data obtained by Farges *et al.* (1992) with extended X-ray absorption fine structure analysis (EXAFS) indicated that U(IV) is present in six coordinated sites in silicate glasses with a mean U–O distance of $\approx$ 2.26–2.29 Å. Uranium(IV) is expected to occupy similar sites in the melt. The solubility of uranium in silicate liquids is enhanced by high alkali content and the presence of nonbonding oxygens (NBO)[13] and non-framework oxygens (NFO).[14] There is a strong correlation between uranium solubility and the NBO/T ratio (where T is the number of tetrahedral cations). Up to 18 wt% U(IV) can be dissolved in sodium trisilicate glass; whereas less than 1 wt% of U(IV) will dissolve in a glass with albite (Na alumino-silicate) composition. The formation of bonds between NBO and NFO is favored because these oxygens have lower bond strength. The solubility of actinides in alkali silicate glasses decreases in the order Th > U > Np > Pu owing to decreasing ionic size and increasing actinide–oxygen bond strength. The solubilities of U(V) and U(IV) are also affected by alkali content due to variation in bond strength. Uranium(IV) and U(V) are generally incompatible with magmatic systems and tend to partition strongly into late stage formed minerals, such as zircon, titanite, or apatite. Farges *et al.* (1992) suggest that if melts have a heterogeneous distribution of bonding oxygens (BO) and NBO, uranium will become enriched in the NBO-enriched regions. With increasing magmatic differentiation,[15] the BO content of the melt increases, as a consequence U(IV) will partition to late crystallizing minerals, such as pyrochlore or zircon.

Farges *et al.* (1992) determined the U–O bond lengths in U(VI)-containing silicate glasses as $U–O_{ax} \approx 1.77–1.85$ Å and $U–O_{eq} \approx 2.18–2.25$ Å, characteristic

[13] Oxygen bonded to one Si^{4+} and an indeterminate number of other cations (Ellison *et al.*, 1994).
[14] Oxygen bonded exclusively to cations other than Si^{4+}.
[15] The process of chemical and mechanical evolution of a magma in the course of its crystallization such that different rock types are formed from the same original magma.

of the uranyl species. U(VI) is the dominant oxidation state observed in radioactive borosilicate waste glasses. XPS measurements performed on SON68-type borosilicate waste glass by Ollier *et al.* (2003) revealed two oxidation states in the glass: about 20% U(IV) and 80% U(VI) present in two different environments, uranate- and uranyl-sites, respectively. As a consequence of bond strength considerations, U(VI) also bonds primarily to NBO and NFO in both crystalline and amorphous silicates. U(V) is six-coordinated with a mean U–O bond distance of 2.19–2.24 Å (Farges *et al.*, 1992).

Karabulut *et al.* (2000) have investigated the local structure of uranium in a series of iron phosphate glasses with EXAFS and determined that the all uranium was present as U(IV).

(d) Uranium niobates, tantalates, and titanates

There are a number of complex tantalum, niobium, and titanium oxides that may contain uranium as an essential element. These phases are mainly observed in granitic rocks and granite pegmatites[16] and have been difficult to characterize as they commonly occur in the aperiodic metamict state owing to their age and radionuclide content. A common feature of these minerals is that niobium, tantalum, and titanium atoms occupy octahedral sites, and a structural framework that is formed by octahedral corner or edge sharing (Finch and Murakami, 1999).

The structures of the ixiolite, samarskite, and columbite groups, ideally $A^{3+}B^{5+}O_4$, are all derivatives of the α-PbO_2 structure. Ishikawaite $\{(U^{4+},Fe,Y,Ce)(Nb,Ta)O_4\}$ is the U-rich variety of samarskite and calciosamarskite is the Ca-rich variety. Because these minerals are chemically complex, metamict, and pervasively altered, their crystal chemistry and structure are poorly understood (Hanson *et al.*, 1999). Many of these phases are of interest because of their occurrence in designer crystalline ceramic waste forms for immobilization of actinides (Gieré *et al.*, 1998; Ewing, 1999). In particular, zirconolites, pyrochlores, and brannerites have been proposed for immobilizing transuranics. These phases will be discussed in more detail.

(*i*) *Zirconolite*

Zirconolite is an accessory mineral crystallizing under different geological conditions and in a wide range of generally SiO_2-poor rock types (Gieré *et al.*, 1998). Zirconolite has been found in mesostasis areas of ultrabasic cumulates, in granitic pegmatites, in carbonatites,[17] in nepheline syenites, and in other igneous formations. Zirconolite has been observed commonly in lunar late-stage

[16] Late stage crystallization from an igneous intrusion.
[17] Rock consisting of >50% carbonate minerals.

mesostasis areas of lunar basalts.[18] It is also a common constituent of designer titanate ceramic waste forms (Gieré *et al*., 1998; Ewing, 1999). Natural zirconolite is a reddish-brown mineral with an appearance similar to that of ilmenite; however, the grains are typically anhedral and <0.1 mm in diameter, and easily overlooked.

Zirconolite, $CaZrTi_2O_7$, belongs to a group of anion-deficient superstructures of the fluorite-type, which have been found to be the most versatile phases for the incorporation of HLW elements. Zirconolite is termed the aristotype of the group (i.e. the structurally simplest member of the series). All have the general formula $[A_2B_2X_7]$ (A = Ca, Na, Ln, U, Th, Zr, Ti; B = Ti, Nb, Ta, Al, Fe; X = O, F) (Mazzi and Munno, 1983; Bayliss *et al*., 1989). Zirconolite does not appear to incorporate uranium and lanthanides by isomorphic substitution; rather, distinct phases form depending on the particular elements present in the mineral. Elements may not be distributed uniformly throughout the zirconolite but concentrated in extended defects, which can lead to the formation of zirconolite polytypes (White, 1984). These are constructed by stacking modular units in a variety of orientations with respect to the arrangement of the interlayer cations. Each module consists of two hexagonal tungsten bronze layers and interposed cations. The zirconolite-type phases have been described in the literature as zirconolite, zirkelite, pyrochlore, and polymignyte. The three natural zirconolites are orthorhombic zirconolite, known as zirconolite-3O, trigonal zirconolite, known as as zirconolite-3T, and the more common monoclinic zirconolite called zirconolite-2M. The cubic form is termed zirkelite and for metamict minerals, the name polymignyte is used.

Geochemical studies by Lumpkin and coworkers (Lumpkin *et al*., 1988, 1995; Lumpkin and Ewing, 1995) have shown that zirconolite is highly durable in the presence of hydrothermal fluids and low-temperature groundwaters. Uranium in zirconolite is mobilized only under conditions of high temperature and pressure in hydrothermal fluids. At lower temperatures alteration takes place because previous radiation induced damage; this may result in the release of radiogenic lead. However, uranium remains relatively unaffected by the alteration process.

(*ii*) *Pyrochlore*

Minerals of the pyrochlore group have the general formula $A_{1-2}B_2O_6X_{0-1}$ (Greegor *et al*., 1989). Three subgroups are defined on the basis of the major B-site cations. The B-site is occupied by Ti, Nb, or Ta; however, Al, Fe^{3+}, Zr, Sn, and W may also be possible. Microlite and natural pyrochlore both contain more niobium and tantalum than titanium (see Fig. 5.1a). The H_2O content in

[18] Zirconolite was reported in rocks collected on Apollo 10 (mare basalt) and Apollo 14 (recrystallized breccia) moon missions.

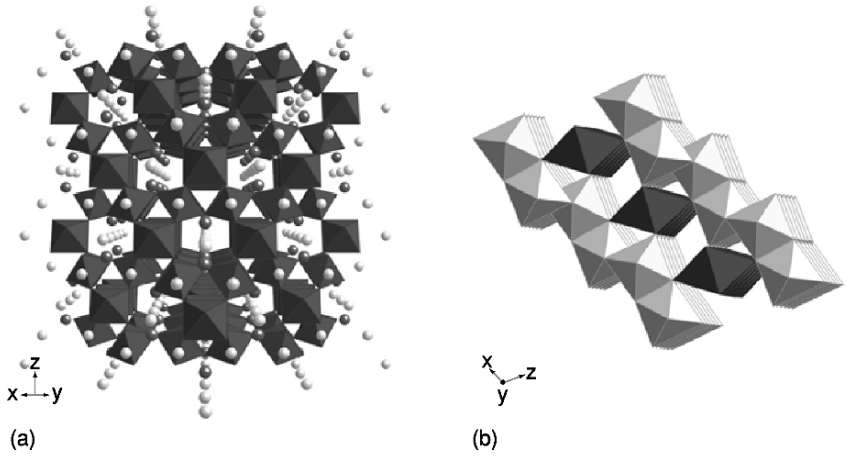

Fig. 5.1 *Structure of* (*a*) *pyrochlore* (*diagram displays grey circles = A site, dark circles = B site, and* TiO_6 *octahedra*) *and* (*b*) *brannerite* (*diagram shows uranium as dark-colored polyhedra and* TiO_6 *octahedra as gray*) (*courtesy of Prof. R. Gieré, University of Freiberg, Germany*).

the natural minerals ranges from 10 to 15 wt%, but will increase if the mineral has undergone alteration. These groups can be further subdivided based on the A-site occupation which can be Na, Ca, Mn, Fe^{2+}, Sr, Sb, Cs, Ba, rare earths, Pb, Bi, Th, and U. Natural pyrochlore minerals occur predominantly in three host rock categories: carbonatites, nepheline syenites, and granitic pegmatites.

(*iii*) *Evidence for U*(*v*) *in pyrochlores and zirconolite*

Fortner *et al.* (2002) used X-ray absorption spectroscopy near-edge structure (XANES) analysis to suggest that U(v) is present in a synthetic pyrochlore ceramic produced under reducing (Ar/H_2) conditions. The authors argue that uranium substitutes for titanium on the B-site in pyrochlore and suggest that this will also occur in natural pyrochlore-type minerals. This result is partially supported by findings by Vance *et al.* (2001) who determined that zirconolite, ($CaU_xZr_{1-x}Ti_2O_7$) oxidized at 1400°C in air, formed U(v) at the expense of U(IV) and that zirconolites with available charge-compensating lanthanides, also resulted in U(IV) to U(v) oxidation, even when sintered in an argon gas environment. The oxidation of U(IV) to U(v) is accompanied by a significant decrease in ionic size, suggesting that uranium is unlikely to enter the calcium site, but rather prefers the zirconium site. Although the presence of significant amounts of U(v) in these titanate phases has not been established by quantitative EMPA data on synthetic (Gieré *et al.*, 2002) and natural zirconolites and pyrochlores (Gieré *et al.*, 1998), the strong observed correlation between Ca and U in natural zirconolites, indicates substitution on the A-site rather than the B-site.

(*iv*) *Brannerite*

After uraninite and coffinite, brannerite is the most important uranium ore mineral. At the large uranium deposit of the El'kon District of the Aldan Shield, Siberia, brannerite is the dominant uranium phase (Miguta, 1997). Ifill *et al.* (1996) report that brannerite at the Elliot lake U-deposit in Canada formed mainly by replacement of uranium in TiO_2-rich relicts of magnetite–ilmenite intergrowths. The uranium was derived from diagenetic dissolution of uraninite. Brannerite, ideally $\{(U,Th)_{1-x}Ti_{2+x}O_6\}$, is a monoclinic accessory phase that is completely metamict (amorphous) as a result of the α-decay damage from the constituents uranium and thorium. As with many of these metamict U-minerals, the structure can be recrystallized on heating. Many cation substitutions have been identified for both uranium (Pb, Ca, Th, Y and Ce) and titanium (Si, Al, Fe) in natural brannerites (Vance *et al.*, 2001) (see Fig. 5.1b).

Brannerite is also formed in the titanate-based nuclear waste-form crystalline ceramics under reducing conditions. Finnie *et al.* (2003) and Colella *et al.* (2005) examined synthetic U(v) phases and natural brannerites with XPS and electron energy-loss spectroscopy. The average valence state in the natural brannerites was close to 5.0.

5.3.3 Uranium(VI) phases

Carbonate dominates the speciation of uranium in alkaline environments, while sulfate complexation is of importance in slightly acidic oxidizing media. The U(VI) phases represent an extremely diverse and complex series of minerals. In this section, the U(VI) minerals will be discussed by first introducing the various uranium mineral structures and then their occurrence on the basis of the major complexing anion, and finally a mention of uranium sorption on soil minerals.

Uranyl oxyhydroxides that form in U-rich aqueous solutions can be represented by the general formula $\{M_n[UO_2)_xO_y(OH)_z](H_2O)_m\}$, where M represents divalent cations, including Ca^{2+}, Pb^{2+}, Ba^{2+}, and Sr^{2+}. However, uranyl oxyhydroxides are only stable in groundwaters devoid of carbonate, sulfate, and/or vanadate ligands.

(a) Bonding in uranyl polyhedra

Burns *et al.* (1996) developed a hierarchical structural classification for U(VI) minerals and other inorganic phases, based on the polymerization of coordination polyhedra. The linear uranyl (Ur) ion is coordinated by four, five, or six anions (ϕ: O^{2-}, OH^-, H_2O), with the oxygen atoms of the uranyl ion forming the apices of square ($Ur\phi_4$), pentagonal ($Ur\phi_5$), and hexagonal ($Ur\phi_6$) bipyramids. The equatorial U–O bond lengths for $Ur\phi_4$, $Ur\phi_5$, and $Ur\phi_6$, are 2.26(8), 2.34(10), and 2.46(12) Å, respectively. The polyhedra possess very asymmetrical charge distributions, $O_{Ur} \sim -1.7$and $U\text{–}O_{eq} \sim -0.5$ as discussed in more detail in

Section 5.8. Uranyl minerals with uranium as the only high-valence cation invariably contain sheets [the exception being studtite (Burns and Hughes, 2003)], as do the naturally occurring uranyl vanadates, uranyl molybdates, and most uranyl sulfates. A majority of the uranyl silicates contain sheets except for soddyite $\{(UO_2)_2[SiO_4](H_2O)_2\}$ and weeksite $\{K_{1.26}Ba_{0.25}Ca_{0.12}[(UO_2)_2(Si_5O_{13})]H_2O\}$ (Jackson and Burns, 2001), which involve frameworks of U(VI) polyhedra. Uranyl carbonates are exceptional because they often contain isolated uranyl tricarbonate clusters, although rutherfordine, UO_2CO_3 (cf. Fig. 5.54), and roubaultite $\{Cu_2(UO_2)_3(CO_3)_2O_2(OH)_2](H_2O)_4\}$, contain uranyl carbonate sheets. The uranyl selenites demesmaekerite $\{Cu_5Pb_2(UO_2)_2(SeO_3)_6(OH)_6(H_2O)_2\}$, and derriksite, $\{Cu_4[(UO_2)(SeO_3)_2](OH)_6]\}$, contain chains of polyhedra, whereas guillemenite, $\{Ba[UO_2)_3(SeO_3)_2O_2](H_2O)_3\}$, and haynesite, $\{(UO_2)_3(OH)_2(SeO_3)_2 \cdot 5H_2O\}$, both contain uranyl selenite sheets. Uranyl arsenates either contain autunite-type sheets or chains, as in the structures of walpurgite, $\{(UO_2)Bi_4O_4(AsO_4)_2 \cdot 2H_2O\}$, and orthowalpurgite, $\{(UO_2)Bi_4O_4(AsO_4)_2 \cdot 2H_2O\}$.[19] Relatively few uranium minerals are based upon chains, although recent structural refinements indicate that these types of U^{6+} minerals are more common that previously thought. Examples include: the only know peroxide mineral, studtite (Burns and Hughes, 2003); the uranyl tellurides, moctezumite $\{PbUO_2(TeO_3)_2\}$, derriksite, and demesmaekerite; the uranyl sulfate uranopilite; the uranyl arsenates, walpurgite, orthowalpurgite, and their phosphate analog, phosphowalpurgite $\{(UO_2)Bi_4O_4(PO_4)_2 \cdot 2H_2O\}$ (Sejkora *et al.* 2004); and parsonsite $\{Pb_2[(UO_2)(PO_4)_2]\}$. Locock *et al.* (2005a) have also shown that the synthetic arsenic-bearing analog of parsonsite, hallimondite $\{Pb_2[(UO_2)(AsO_4)_2]\}$, is also a chain structure.

(b) Geometries of uranyl polyhedra

The crystal chemistry of U(VI) is rich in diversity, yet it is relatively rare for uranyl solids to form frameworks. The distribution of bond strengths within uranyl bipyramidal polyhedra generally permits polymerization only through the equatorial ligands, resulting in chains or sheets. Linkages in the third dimension may be facilitated by additional polyhedra such as silicate, molybdate, vanadate, or phosphate.

The U(VI) minerals that are based on infinite polyhedra sheets with edge- and corner-sharing polyhedra can be better described by the topological arrangement of anions that occur within the sheets (Miller *et al.*, 1996; Burns and Hill, 2000a). Similar to a method described by Aléonard *et al.* (1983) for U_3O_8 structures, the procedure is as follows: Each anion that is not bonded to at least two cations within the sheet, and not an equatorial anion of a bipyramid or

[19] The compositions of orthowalpurgite and walpurgite as written are identical; however, the structures are not (Mereiter, 1982b; Krause *et al.*, 1995).

pyramid within the sheet, is removed from further consideration. Cations are removed along with all cation–anion bonds, leaving an array of unconnected anions. Anions are joined by lines, with only those anions that may be considered as part of the same coordination polyhedra being connected. Anions are removed from further consideration, leaving a series of lines that represent the anion topology. The anion topology does not contain any information about the cation population of the sheet from which the topology was derived (see Fig. 5.2). The P chain is composed of edge-sharing pentagons, the R chain contains rhombs, and the H chain contains edge-sharing hexagons. The arrowhead chains (U and D), which have a directional aspect, contain both pentagons and triangles, arranged such that each triangle shares an edge with a pentagon and the opposite corner with another pentagon in the chain. Generation of anion topologies using chain-stacking sequences is an elegant method for describing the relationships among the complex U(VI) sheet recently found in several minerals. The following describes a number of the possible anion topologies in the U(VI) minerals (see Burns, 1999a for a more complete list).

(*i*) *Protasite* (α-U_3O_8) *anion topology*

The protasite anion topology is the basis of sheets that occur in protasite $\{Ba[(UO_2)_3O_3(OH)_2](H_2O)_3\}$, becquerelite (Burns and Li, 2002), billietite (Pagoaga *et al.*, 1987), richetite $\{M_xPb_{8.57}[(UO_2)_{18}(OH)_{12}]_2(H_2O)_{41}\}$ (Burns, 1998b), compreignacite (Burns, 1998c), agrinierite $\{K_2(Ca_{0.65}Sr_{0.35})[(UO_2)_3O_3(OH)_2]_2 \cdot 5H_2O\}$ (Cahill and Burns, 2000), and masuyite $\{Pb[(UO_2)_3O_3(OH)_2](H_2O)_3\}$ (Burns and Hanchar, 1999), as well as a synthetic cesium uranyl oxide hydrate (Hill and Burns, 1999). As such, it is apparent that sheets based on this topology are compatible with a range of interlayer configurations involving Ba, Ca, Pb, K, and Cs. This simple anion topology contains only triangles and pentagons (see Fig. 5.2a).

Only P and D chains are required to develop the protasite anion topology, with the repeat sequence PDPD... The protasite anion topology does not distinguish between O^{2-} and OH^- anions and the distribution of anions is not identical between different minerals possessing the protasite structure type. Becquerelite, billietite, and compreignacite have identical anion distributions, $[(UO_2)O_3(OH_3)]^-$ but masuyite and protasite do not.

(*ii*) *Fourmarierite anion topology*

Sheets based upon the fourmarierite anion topology (see Fig. 5.2b) occur in fourmarierite (Piret, 1985) and schoepite (Finch *et al.*, 1996a). In schoepite, the sheets are neutral, with H_2O groups being the only constituents of the interlayer. In fourmarierite, the sheets have a different distribution of O and OH^-, resulting in a charged sheet that is balanced by Pb^{2+} in the interlayer. The anion topology

can be obtained with a chain-stacking sequence involving P, D, and U chains, with the sequence PDUPUD.... Li and Burns (2000a) have refined the structures of several fourmarierite specimens from various localities. All the crystals are orthorhombic.

(*iii*) *Vandendriesscheite anion topology*

Vandendriesscheite is the most common Pb-bearing uranyl oxyhydroxide, occurring at numerous weathered uraninite deposits, often in association with schoepite. The anion topology of vandendriesscheite (see Fig. 5.2c) is exceptionally complex, with a primitive repeat of 41.4 Å (Burns, 1997). Only vandendriesscheite contains a sheet based upon this topology, which can be constructed using P, U and D chains in the sequence PDUPUPUPU DPDPDPDUPUPUP.... It contains sections that are identical to the PDPD... (or PUPU...) repeats of the protasite anion topology, with the junction between such sections involving the DU sequence of the fourmarierite anion topology. Thus, the vandendriesscheite anion topology is a structural intermediate between these two simpler anion topologies.

(*iv*) *Sayrite anion topology*

Sayrite $\{Pb_2[(UO_2)_5O_6(OH)_2](H_2O)_4\}$ (Piret *et al.*, 1983), is the only mineral that contains sheets based upon the sayrite anion topology, which involves U, D, P and R chains. The chains are arranged in such a way that each P chain is flanked by two arrowhead chains with the same sense (direction), giving UPU or DPD sequences. These two sequences alternate in the anion topology, and are separated by R chains, giving the sequence RUPURDPDRUPU...

(*v*) *Curite anion topology*

The structure of curite (Taylor *et al.*, 1981; Li and Burns, 2000b) contains sheets based upon the curite anion topology, which cannot be described as a simple chain-stacking sequence using only the U, D, P and R chains. A chain with pentagons, triangles, and squares is required. It has a directional sense owing to the presence of an arrowhead (a pentagon and a triangle sharing an edge), and is designated U_m and D_m, for up and down (modified) pointing chains, respectively. The curite anion topology can be characterized by the chain-stacking sequence U_mDU_mD...

(*vi*) *β-U_3O_8 anion topology*

The β-U_3O_8 sheet anion topology (see Fig. 5.2d) is the basis of the sheets in ianthinite (Burns *et al.*, 1997b), as well as the sheets in β-U_3O_8. This topology can conveniently be described using a chain-stacking sequence involving U, D, and R chains with the repeat sequence DRUDRU...

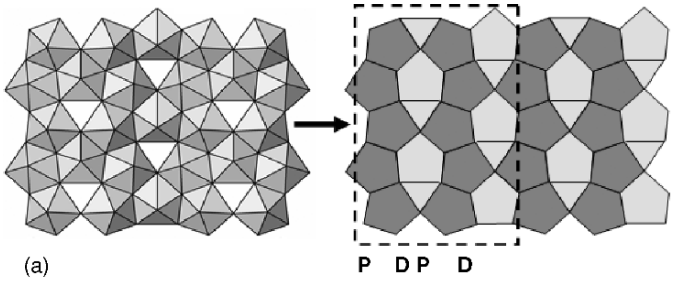

(a)

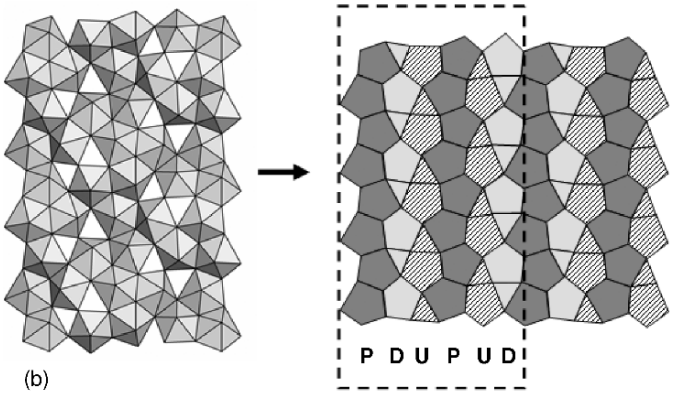

(b)

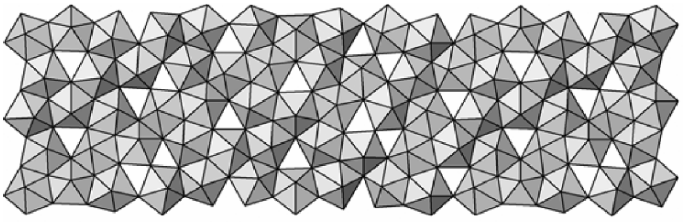

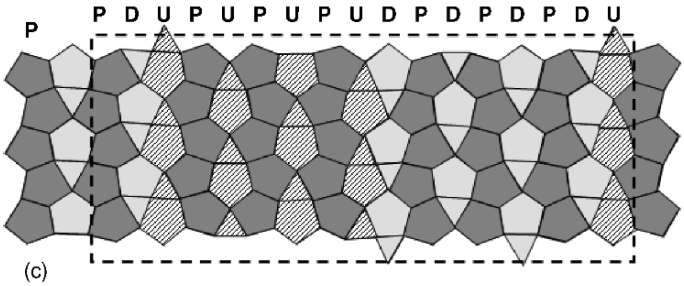

(c)

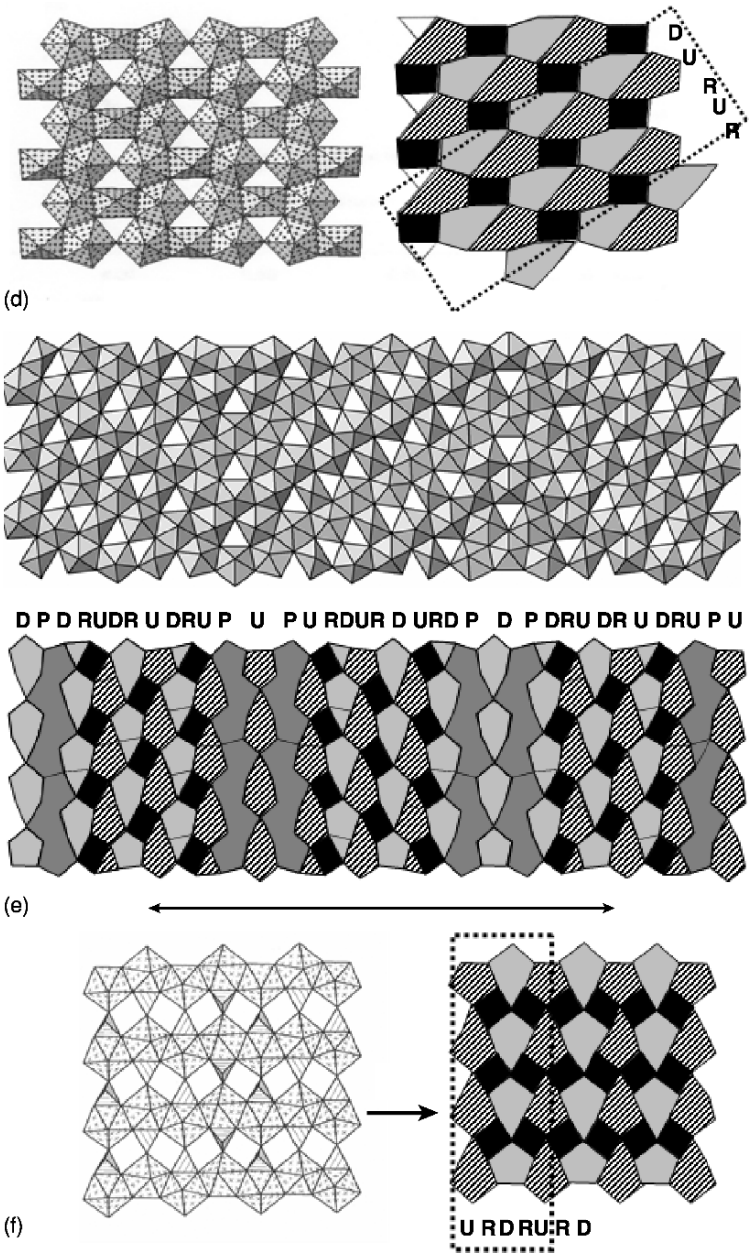

Fig. 5.2 (*a*) *Protasite* (α-U_3O_8) *structure and anion topology with anion repeat* (*adapted from Burns,* 1999). (*b*) *Fourmarierite structure and anion topology, showing the structural repeat.* (*c*) *Vandendriesscheite structure and anion topology.* (*d*) β-U_3O_8 *structure and anion topology* (*adapted from Brugger* et al., 2004). (*e*) *Wölsendorfite anion topology and the complex anion topology.* (*f*) *Uranophane anion topology showing anion repeat* (*adapted from Burns*, 1999).

(*vii*) *Wölsendorfite anion topology*

The versatility of this method for visualizing complex structures is beautifully demonstrated in the description of the structure of wölsendorfite (Burns, 1999b). The structure contains unique $Ur\phi_4$ square bipyramids and six unique $Ur\phi_5$ pentagonal bipyramids that link by sharing equatorial corners and edges to form infinite sheets that are parallel to (100). The interlayer between the uranyl sheets contains Pb^{2+} and Ba^{2+} cations, as well as H_2O groups that are either bonded to the interlayer cations or are held in the structure by H-bonding only. This complex anion topology possesses a primitive repeat of 56 Å (see Fig. 5.2e). It may be constructed using R, D, P, and U chains, with the repeat sequence DRUDRUDRUPDPDRUDRUDRUPDP... The repeat sequence involves the strings DRUDRUDRU and PDP, which are slabs of the β-U_3O_8 and protasite anion topologies, respectively. Thus, the wölsendorfite anion topology is structurally intermediate between the β-U_3O_8 and protasite anion topologies.

(*viii*) *Uranophane anion topology*

All minerals based on the uranophane topology contain pentagons of the anion topology (see Fig. 5.2f).

The uranophane sheet consists of chains of $Ur\phi_5$ bipyramids linked by bridging, isolated SiO_4 tetrahedra, and is common to uranophane, boltwoodite $\{K_{0.56}Na_{0.42}[(UO_2)(SiO_3OH)](H_2O)_{1.5}\}$, cuprosklodowskite, kasolite $\{Pb[(UO_2)(SiO_4)](H_2O)\}$, and sklodowskite. The difference between α-uranophane and β-uranophane depends on the orientation of the silicate tetrahedron. In kasolite, the apical O atoms of the SiO_4 tetrahedra bond to two Pb^{2+} cations in the interlayer (Catalano and Brown, 2004).

(c) Prediction of crystal morphology of U(VI) sheet minerals

The bond valence approach is commonly used to evaluate the analysis of a crystal structure. It provides a means to check bond lengths, the valence state of ions with the structure, as well as providing a method to describe hydrogen bonding (Burns, 1999a). The bond valence approach can be used to identify the valence state of the U cation in well-refined crystal structures. Schindler *et al.* (2004) and Schindler and Hawthorne (2004) have developed a method for predicting the stability of sheet uranyl minerals using the bond-valence deficiency of the sheet edges. Schindler *et al.* (2004) have shown that the surface structure of an edge is characterized by the bond-valence deficiency of anion terminations along chains of polyhedra parallel to the edge, and by the shift and orientation of adjacent layers. The stability of the edges also depends on the arrangement of the interstitial cations between the layers. The edges of the sheet-like uranyl minerals are more reactive than the basal surfaces because the equatorial O-atoms on the edges bond to fewer U^{6+} atoms than oxygen in the sheet, and hence must satisfy their individual bond-valence requirements through a higher degree of protonation (Schindler *et al.*, 2004). The interaction

of the uranyl mineral edge surface with aqueous species controls crystal growth, dissolution, and sorption of other species, including other actinides. These interactions depend on the surface structure of an edge, the pH, and saturation index with respect to the mineral.

(d) Uranyl oxyhydroxides

The uranyl oxyhydrates are not only of importance in the geochemistry of uranium, but they are also one of the primary phases generated during the oxidative dissolution of SNF. Uranyl oxyhydroxides form in U-rich aqueous solutions and develop early during the oxidative dissolution of uraninite ores deposits; hence, they are expected to be the older U(VI) minerals in an oxidized deposit. The complexity of these structures combined with their propensity to dehydrate made their structure characterization difficult; Finch *et al.* (1996a) reported the full structure determination of schoepite and Weller *et al.* (2000) refined the structure of meta-schoepite $\{(UO_2)_4O(OH)_6 \cdot 5H_2O\}$. The uranyl oxyhydroxides are based on electrostatically neutral polyhedral sheets of the form $[(UO_2)_xO_y(OH)_z]$ and no interlayer cations. Water molecules occupy the interlayer sites, linking adjacent sheets through H-bonds. Meta-schoepite possesses one less water molecule than schoepite, leading to 2.8% reduction in the *c*-axis and 0.6 and 0.9% in the *a*- and *b*-directions, respectively. Hughes-Kubatko *et al.* (2005) have shown that meta-schoepite is thermodynamically unstable relative to dehydrated schoepite and have suggested that sodium may be an essential element in natural meta-schoepite. The $U–O_{ax}$ and $U–O_{eq}$ bond lengths in schoepite vary with pH. Allen *et al.* (1996a) determined that $U–O_{ax}$ distances are 1.80, 1.84, and 1.86 Å and $U–O_{eq}$ distances are 2.38, 2.36 and 2.32 Å, at pH 7, 9, and 11, respectively. At pH 11, the uranyl group becomes elongated and the $U–O_{eq}$ bond contracts, such that the structure resembles a clarkeite-like alkali metal uranate. Clarkeite-like sodium uranates have been observed during dissolution of soddyite (Giammar and Hering, 2002) and in the highly caustic environment of the Hanford tank wastes in Washington, USA (Deutsch *et al.*, 2004). Pseudomorphic replacement of pegamatic uraninite by clarkeite $\{(NaCa_{0.5}Pb_{0.5})[(UO_2)O(OH)](H_2O)_{0–1}\}$ may occur during metasomatic alteration by oxidizing hydrothermal fluids (Finch and Ewing, 1997).

The alkali uranyl oxyhydroxides may play an important role in attenuating radionuclides in the environment, including neptunium (Li and Burns, 2001a; Burns *et al.*, 2004a), strontium (Burns and Li, 2002), and cesium (Hoskins and Burns, 2003).

(e) Pb–uranyl oxyhydroxides

As uranium decays to lead, the lead enters cation vacancies in the interlayer, leaving a uranium vacancy in the structural sheet. Although Pb–uranyl oxyhydroxides will form directly from uraninite alteration, many Pb–uranyl minerals are formed though the accumulation of radiogenic lead in nominally Pb-free uranium phases. Accumulation of lead will also destabilize the structure

of some U(VI) minerals. For example, Finch and Ewing (1997) have demonstrated that clarkeite will eventually transform to wölsendorfite or curite. Lead is not incorporated into rutherfordine, soddyite, or uranophane, minerals that may replace early-formed lead uranyl oxyhydroxides. However, several uranyl phosphates and arsenates will incorporate lead. Indeed, Finch and Ewing (1992) suggested that curite, one of the last minerals remaining after complete oxidative dissolution of uraninite, may act as substrate for nucleation of certain phosphates. Burns and Hill (2000b) have synthesized a strontium analog of curite that may be relevant to HLW disposal.

Spriggite, $\{Pb_3[(UO_2)_6O_8(OH)_2](H_2O)_3\}$, has been identified by Brugger *et al.* (2004). The structure is based on $[(UO_2)_6O_8(OH)_2]^{6+}$ sheets of uranyl polyhedra of the β-U_3O_8 anion topology with Pb^{2+} and H_2O in the interlayer. Spriggite has the highest Pb:U ratio (1:2.00) of all known lead uranyl oxide hydrates. Finch and Murakami (1999) have suggested a reaction pathway for increasing alteration of hydrated lead uranyl oxyhydroxides where the molar proportion of PbO can be correlated with the molar proportion of H_2O. With increasing PbO content, charge compensation in the sheet structure results in OH^- substitution for O^{2-}. The U–O_{eq} bonds in the Urϕ_5 pentagonal bipyramids are considerably longer and of lower bond valence than the U^{6+}–O bonds in the Urϕ_4 square bipyramids. The change in uranyl ion coordination from pentagonal to square helps satisfy bond-valence requirements of OH^- in the anion site. Hence, the spriggite adopts Urϕ_4 square bipyramids, whereas the structure of vandendriesscheite (Pb:U = 1:6.36) consists entirely of Urϕ_5 pentagonal bipyramids. Vandendriesscheite, one of the most common Pb-bearing uranyl oxyhydroxides, contains two symmetrically distinct Pb^{2+} cations in the interlayer; both bonded to H_2O groups. The two Pb^{2+} cations (Pb(1) and Pb(2)) are bonded to five and six O_{ur} atoms of adjacent sheets of uranyl polyhedra, respectively. Richetite possesses an extraordinarily complex structure (Burns, 1998b). The phase has been reported at the Shinkolobwe and Jáchymov U-deposits.

(f) Uranyl peroxides

The U-bearing phases, studtite and meta-studtite $\{(UO_2)O_2(H_2O)_2\}$, are the only known peroxide minerals that form during the buildup of α-generated H_2O_2 on the surface of natural uraninite (Walenta, 1974; Deliens and Piret, 1983a; Finch and Ewing, 1992). Burns and Hughes (2003) determined that the structure of studtite is monoclinic, contains one symmetrically distinct U^{6+} cation and four O atoms, two of which occur as H_2O groups. The U^{6+} cation occurs as part of a linear uranyl ion, and each U^{6+} cation is bonded to six additional O atoms, two of which are H_2O groups, and four that are O atoms of the peroxide groups. Unlike all other uranyl oxide hydrate minerals, studtite is not based upon sheet of uranyl polyhedra, but contains polymerized uranyl polyhedra in only one dimension. The occurrence of chains rather sheets in U(VI) minerals is usually due to distortions in the polyhedra, normally the result of lone pairs (e.g. in Se- and Bi-bearing uranium minerals); however, in studtite,

the presence of peroxide at the equatorial positions of the uranyl polyhedra results in distorted hexagonal bipyramids, with the peroxide O–O edge length of 1.46 Å. Typical O–O edge length in uranyl hexagonal bipyramid is 2.4 Å with nitrate or carbonate ligands. This distortion may prevent the formation of two-dimensional layer structures (see Fig. 5.56a).

Radiolysis of water at spent nuclear fuel may create an additional complexity for predicting UO_2 paragenesis in a geological repository (Satonnay *et al*., 2001; Amme, 2002). Studtite and meta-studtite have been identified by McNamara *et al*. (2003) on the surface of corroding commercial spent fuel replacing the meta-schoepite that precipitated earlier. As the H_2O_2 concentration increased with time, studtite and meta-studtite became the dominant alteration phases. H_2O_2 is consumed in the presence of carbonate (Sunder *et al*., 2004), forming peroxo complexes with H_2O_2 and U(VI) (Amme, 2002).

(g) Uranyl carbonates and calcite

Uranyl carbonates tend to form in evaporative environments or under high p_{CO_2} conditions. They are structurally diverse and only relatively few of the uranyl carbonates (rutherfordine (Finch *et al*., 1999b), roubaultite, bijvoetite $\{[M_8^{3+}(H_2O)_{25}(UO_2)_{16}O_8(OH)_8(CO_3)_{16}](H_2O)_{14}\}$, where M is Y or Ln (Li *et al*., 2000), and wyartite (Burns and Finch, 1999) consist of sheets of polyhedra that contain a cation of high valence. Other uranium carbonates contain isolated clusters similar to those observed in solution (Allen *et al*., 1995). The optical signature of the UO_2^{2+} bands in liebigite $\{Ca_2UO_2(CO_3)_3 \cdot 11H_2O\}$, andersonite $\{Na_2Ca[(UO_2)(CO_3)_3](H_2O)_5\}$, and schröckingerite $\{NaCa_3(UO_2)(CO_3)_3(SO_4)F \cdot 10H_2O\}$, that all contain uranyl tricarbonate clusters, are almost identical (Čejka, 1999).

The uranyl monocarbonates (rutherfordine, joliotite $[UO_2CO_3 \cdot nH_2O]$, blatonite $[UO_2CO_3 \cdot H_2O]$, and urancalcarite $\{Ca(UO_2)_3CO_3(OH)_6 \cdot 3H_2O)\}$) are thermodynamically stable, having solubilities comparable to some uranyl oxide hydrates. The uranyl carbonate mineral grimselite, $\{K_3Na[(UO_2)(CO_3)_3](H_2O)\}$ (Li and Burns, 2001b), contains uranyl tricarbonate complexes of composition $[(UO_2)(CO_3)_3]^{4-}$, which occur as an isolated polyhedra in each of the structures, cf. Fig. 5.53. Schröckingerite contains $Na\phi_6$ octahedron, an SO_4 tetrahedron, and three symmetrically distinct $Ca\phi_8$ polyhedra (Hayden and Burns, 2002). The structure contains isolated units of uranyl tricarbonate and sulfate tetrahedra that are coordinated to low-valence cations. Bayleyite, $\{Mg_2[(UO_2)(CO_3)_3](H_2O)_{18}\}$, contains three symmetrically distinct $Mg(H_2O)_6$ octahedra, as well as a $(UO_2)(CO_3)_3$ cluster, and six symmetrically distinct H_2O groups. Swartzite, $\{CaMgUO_2(CO_3)_3 \cdot 12H_2O\}$, contains $Ca\phi_8$ polyhedra and a $Mg(H_2O)_6$ octahedron.

At a partial pressure of $CO_2 > 10^{-2.2}$ atm, rutherfordine becomes the stable uranium phase with respect to dehydrated schoepite; however, the schoepite–rutherfordine equilibrium indicates that p_{CO_2} must be $>10^{-1.9}$ atm before schoepite becomes unstable with respect to rutherfordine. Schoepite is thus expected

to be the U-solubility-controlling phase in waters exposed to atmospheric conditions. Rutherfordine would be expected to replace schoepite in environments where the p_{CO_2} pressure is higher, possibly in a repository environment or in saturated soils. Replacement of schoepite by rutherfordine has been observed at the Shinkolobwe U-deposit (Finch and Ewing, 1992). The structure of rutherfordine was elucidated by Finch *et al.* (1999b) and can be represented by an anion topology that consists of edge-sharing hexagons that share corners, creating pairs of edge-sharing triangles. The rutherfordine sheet is obtained by populating all the hexagons in the anion topology with uranyl ions and one half of the triangles are populated with CO_3 groups. The sheets are held together via van der Waals forces. An identical sheet structure occurs in synthetic $(UO_2)(SeO_3)$.

Burns and Finch (1999) reported the structure of a mixed uranium valence mineral, wyartite that contains U(V) and U(VI). The structure of wyartite contains three symmetrically distinct U positions. The U1 and U2 cations are each strongly bonded to two O atoms with U–O bond lengths of ~1.8 Å, consistent with a linear uranyl ion, whereas the U3 site has seven anions at the corners of a pentagonal bipyramid, with U–O bond lengths of 2.07 and 2.09 Å. A bond valence analysis showed that the U3 site is coordinated by six O atoms and one H_2O group. Two of the O atoms of the bipyramid are shared with a CO_3 group and the sum of bond valences incident at the U3 site is 5.07, in agreement with the assignment of U(V) in this site. Urancalcarite is structurally similar to wyartite and commonly associated with wyartite in nature. Finch and Murakami (1999) suggest that wyartite may oxidize to uranocalcarite. Schindler and coworkers (Schindler and Hawthorne, 2004; Schindler *et al.*, 2004) proposed the formation of the mixed U(V)–U(VI) mineral, wyartite II, on surface of calcite during interaction of acidic and basic uranyl-bearing solutions with calcite.

The structure of fontanite, $\{Ca[(UO_2)_3(CO_3)_2O_2](H_2O)_6$, has been refined by Hughes and Burns (2003) as a monoclinic phase that consists of two symmetrically distinct $Ur\phi_5$ units, one $Ur\phi_6$ unit, and two CO_3 triangles. It is observed in the weathered zone of the Rabejac uranium deposit in Lodève, Hérault, France, where it is associated with billietite and uranophane. Both fontanite and roubaultite possess anion topologies similar to phosphuranylite $\{KCa(H_3O)_3(UO_2)[(UO_2)_3(PO_4)_2O_2]_2(H_2O)_8\}$.

Several uranyl carbonates that contain lanthanides have been described. Bijvoetite is found in association with uraninite, sklodowskite, and uranophane in the oxidized zone at the Shinkolobwe mine (Li *et al.*, 2000). The structure of bijvoetite is extremely complex and contains 16 unique carbonate groups, 39 symmetrically distinct H_2O groups, and 8 unique M^{3+} sites that are occupied by variable amounts of yttrium, dysprosium, and other lanthanides. Astrocyanite $\{Cu_2(Ce,Nd,La)_2UO_2(CO_3)_5(OH)_2 \cdot 1.5H_2O\}$, is another rare earth-bearing uranyl carbonate that is observed as an oxidation product of uraninite. These complex rare earth uranyl carbonates may play an important role in the long-term behavior of released transuranic elements following corrosion of nuclear materials in a geologic repository.

The occurrence of trace amounts of uranyl ions in natural calcite has posed a long-standing problem in crystal chemistry because of speculation that the size and shape of the uranyl ion may preclude its incorporation in a stable lattice position in calcite. The incorporation of uranium in calcite and aragonite provides the basis for U-series age-dating which are commonly adopted for marine and terrestrial carbonates. Uranium is enriched in aragonite relative to calcite owing to the nature of the coordination environment in U-bearing aragonite. Reeder *et al.* (2000) have demonstrated using EXAFS that the dominant aqueous species $UO_2(CO_3)_3^{4-}$ is retained by the uranyl in aragonite, essentially intact. In contrast, a different equatorial coordination occurs in calcite, characterized by fewer nearest oxygens at a closer distance, reflecting that the CO_3 groups are monodentate. The uranyl ion has a more stable and well-defined local environment when co-precipitated with aragonite; however, Reeder *et al.* (2000) argue that as aragonite is metastable with respect to calcite, retention of U(VI) by calcite is likely to be temporary. In contrast, Kelly *et al.* (2003) examined a 13 700-year-old U-rich calcite from a speleothem in northernmost Italy. X-ray absorption spectroscopy data indicated substitution of U(VI) for a Ca^{2+} and two adjacent CO_3^{2-} ions in calcite. This data implied that uranyl has a stable lattice position in natural calcite and suggested that uranium may become incorporated in calcite over long time scales.

Sturchio *et al.* (1998) reported the occurrence of U^{4+} in calcite based on XANES core spectroscopic analysis and concluded that this explained the anomalously high concentrations of uranium observed in calcite in reducing environments. Substitution of Ca^{2+} by Na^{+} was suggested as a possible mechanism to charge balance the structure. The calculated U–O distances reported by Sturchio *et al.* (1998) were (2.21 ± 0.02) Å and (2.78 ± 0.03) Å for U^{4+} in calcite, whereas Reeder *et al.* (2001) estimated $U–O_{eq}$ to be 2.33 Å and $U–O_{ax}$ as 1.80 Å. Interestingly, Sturchio *et al.* (1998) showed a good match of their measured U–O bond lengths with a natural brannerite, where U–O bond lengths were reported as 2.28 and 2.82 Å. However, natural brannerite minerals have recently been shown to be U(V) phases (Finnie *et al.*, 2003; Colella *et al.*, 2005).

(h) Uranyl sulfates

Uranyl sulfates are important in systems where sulfides (e.g. pyrite) are being oxidized. Initial oxidation causes an increase in acidity of the system; however, the acidity may be buffered by the dissolution of carbonate in the surrounding rock, leading to the formation of gypsum. Uranyl sulfates usually occur where uranyl carbonates are absent (and vice versa), owing to the different pH conditions where these minerals will dominate. Uranyl sulfate minerals typically occur as microcrystalline crusts, finely intergrown with other uranyl sulfates and/or monocarbonates. They are common at uranium mines where they form during evaporation of acid sulfate-rich mine drainage waters.

Burns (2001a) and Burns *et al.* (2003) have performed structural refinements on a number of monoclinic zippeite-group U(VI) phases, including zippeite

$\{K_3(H_2O)_3[(UO_2)_4(SO_4)_2O_3(OH)]\}$, sodium-zippeite $\{Na_5(H_2O)_{12}[(UO_2)_8(SO_4)_4O_5(OH)_3]\}$, Mg-zippeite $\{Mg(H_2O)_{3.5}[(UO_2)_2(SO_4)O_2]\}$, Zn-zippeite $\{Zn(H_2O)_{3.5}[(UO_2)_2(SO_4)O_2]\}$, and Co-zippeite $\{Co(H_2O)_{3.5}[(UO_2)_2(SO_4)O_2]$. Each structure contains the zippeite-type layers that consist of chains of edge-sharing $Ur\phi_5$ units that are cross-linked by vertex sharing with sulfate tetrahedra. Marecottite, $\{Mg_3(H_2O)_{18}[(UO_2)_4O_3(OH)(SO_4)_2]_2(H_2O)_{10}\}$, is based on uranyl layers composed of chains of edge-sharing $Ur\phi_5$ biyramids that are linked by vertex-sharing sulfate tetrahedra, identical to zippeite (Brugger *et al.*, 2003). Marecottite and zippeite can co-exist as has been observed in samples from the Jáchymov mine in the Czech Republic. Uranopilite is the only known uranyl sulfate mineral to form chains. The structure consists of clusters of six distinct $Ur\phi_5$ bipyramids that are linked together into a chain by sulfate tetrahedra bonded to two oxygens from each cluster. Adjacent chains are only hydrogen-bonded (Burns, 2001a).

(i) Uranyl silicates

Because of the ubiquity of dissolved silica in most groundwaters, uranyl silicates are the most abundant U(VI) minerals. The uranyl silicates are divided into three groups based on their U:Si ratios (Stohl and Smith, 1981). Accordingly, the structural trends in the uranyl silicates are also dependent on the U:Si ratio (Stohl and Smith, 1981; Finch and Murakami, 1999; Burns, 2001b). In phases with the U:Si ratio of 2:1 and 1:1, no polymerization of the SiO_4 tetrahedra occurs, whereas phases with 1:3 ratios contain chains of vertex-sharing silica tetrahedra. As the U:Si ratio approaches 1:4, the structures contain sheets of SiO_4 tetrahedra. In soddyite, with a ratio of 2:1, each silica tetrahedron shares two of its edges with other uranyl polyhedra, but in structures with the ratio 1:1, only one edge of each silica tetrahedron is shared with a second uranyl polyhedron and each silica tetrahedron is linked to other uranyl polyhedra by vertex sharing.

Uranophane is one of the most common uranyl minerals, and its ubiquity suggests that the uranyl silicates are important phases controlling uranium concentrations in groundwater (Finch and Ewing, 1992). α-Uranophane and β-uranophane have distinctly different crystallographic data and stabilities. Differences in stability were amply illustrated in the study by Cesbron *et al.* (1993) where they failed to synthesize β-uranophane whereas α-uranophane was produced. Both calcium uranyl silicates are common in most oxidized uranium deposits.

The 1:3 silicates (weeksite and haiweeite) are only known from Si-rich environments such as tuffaceous rocks but are commonly observed during the laboratory weathering of borosilicate waste glasses (Ebert *et al.*, 1991; Feng *et al.*, 1994). The structure of weeksite, originally described by Outebridge *et al.* (1960), has been refined by Jackson and Burns (2001). Haiweeite, named for the Haiwee reservoir, California, USA, has been identified at the Nopal I deposit in Peña Blanca, Mexico, where it is associated with uranophane. The structure of weeksite consists of chains of edge-sharing $Ur\phi_5$ pentagonal bipyramids that share edges with SiO_4 tetrahedra. The chains are linked through

disordered SiO_4 tetrahedra to form complex sheets, which in turn form a framework through linkage with SiO_4 tetrahedra (Burns, 1999b).

The only known thorium uranyl silicate mineral, coutinhoite, has been described by Atencio *et al.* (2004) as being isostructural with weeksite. The open channels created by the silicate framework structure are thought to permit the incorporation of Th^{4+}. Oursinite, $\{(Co_{0.86}Mg_{0.10}Ni_{0.04}) \cdot O_2 \cdot UO_2 \cdot 2SiO_2 \cdot 6H_2O\}$, was first reported by Deliens and Piret (1983b) from Shinklolobwe. The phase formed from the oxidation of Co- and Ni-bearing sulfides and demonstrates the ability for U(VI) phases to incorporate a range of elements. Lepersonnite, $\{CaO(Gd,Dy)_2O_3 \cdot 24UO_3 \cdot 8CO_2 \cdot 4SiO_2 \cdot 60H_2O\}$, is a pale yellow uranyl silicate from the Shinkolobwe mine that was first described by Deliens and Piret (1982). The reported compositions of oursinite, lepersonnite, and coutinhoite have immediate implications for radioactive waste disposal for the possible retention of radionuclides, including plutonium, in the environment.

Soddyite is the only known mineral with a U:Si ratio of 2:1; it is also the most common of the uranyl minerals that have structures based on frameworks of polyhedra of higher valence. The structure of soddyite consists of $Ur\phi_5$ units that share equatorial edges to form chains. The chains are cross-linked by sharing edges with SiO_4 tetrahedra in such a way that each tetrahedron shares two of its edges with adjacent chains (Burns, 1999b). Based on observations at the Nopal I site, Pearcy *et al.* (1994) suggested that the precipitation of soddyite may be kinetically more favorable than the formation of other U^{6+} silicates. Soddyite may form from uranophane exposed to dilute metoric waters that are low in carbonate and with a pH below 7. Uranosilite, $\{(Mg,Ca)_4(UO_2)_4(Si_2O_5)_{5.5}(OH)_5 \cdot 13H_2O\}$, has only been reported in nature at a site in Menzenschwand, Germany (Walenta, 1983). Burns *et al.* (2000) reported the occurrence of a new U(VI) silicate from the corrosion of a borosilicate glass with formula $\{KNa_3(UO_2)_2(Si_4O_{10})_2(H_2O)_4\}$, with a U:Si ratio of 1:4. This phase was demonstrated to be structurally distinct from the phase synthesized by Plesko *et al.* (1992). Burns and co-authors suggested that this novel U(VI) silicate may incorporate Np(V).

(j) Uranyl phosphates and arsenates

Uranyl phosphates and arsenates constitute about one-third of the ~200 described uranium minerals (see Table 5.3); yet only a fraction of these have well-defined structures. In groundwaters where $\log\{[PO_4^{3-}]_T/[CO_3^{2-}]_T\} > -3.5$, uranyl phosphate complexes dominate over uranyl carbonate complexes (Sandino and Bruno, 1992). Finch and Ewing (1992) suggested that the occurrence of uranyl phosphates in the most weathered zones of the Koongarra U-deposit indicated that higher oxidation potentials may be necessary for uranyl phosphate precipitation, as uranyl silicates were observed at depth. However, saléeite $(Mg(UO_2)_2(PO_4)_2 \cdot 10H_2O)$ was observed on the surface of apatite where the groundwater was undersaturated with respect to saléeite, indicating that the mineralization occurred by local saturation (Murakami *et al.*, 1997).

Laboratory studies have demonstrated that surface mineralization of saléeite on fluoro-apatite where localized release of Ca and P facilitates autunite formation and U^{6+} uptake (Ohnuki *et al.*, 2004).

Uranyl arsenates are often structurally analogous to the corresponding uranyl phosphates; e.g. the isostructural mineral species abernathyite, $\{K[(UO_2)(AsO_4)](H_2O)_3\}$, and meta-ankoleite, $\{K[(UO_2)(PO_4)](H_2O)_3\}$. Many of the natural uranyl phosphates and arsenates may exhibit complete solid solution formation between end-members. However, in hügelite, $\{Pb_2[(UO_2)_3O_2(AsO_4)_2](H_2O)_5\}$, the presence of arsenic makes the unit cell four times larger than that reported for dumontite, $\{Pb_2[(UO_2)_3(PO_4)_2(OH)_4](H_2O)_5\}$ (Locock and Burns, 2003b). Both structures possess the phospuranylite anion topology. In hügelite, the interlayer contains four symmetrically distinct Pb^{2+} cations. Unlike the lead uranyl oxyhydroxides, hügelite contains only $Ur\phi_5$ and $Ur\phi_6$ polyhedra; yet, it possesses a high U:Pb ratio.

Uranyl arsenates and phosphates may be divided into groups depending on the U:P or U:As ratio. However, a structural classification is more encompassing. The uranium phosphates and arsenates can be separated into four groups: (i) autunite structure; (ii) 3:2 phosphuranylite structure; (iii) uranophane structure; and (iv) chain structures.

(*i*) *Autunite structures*

The most important uranyl phosphates in terms of natural abundance are the autunites and meta-autunite groups. The autunite group of minerals is tetragonal uranyl arsenates and phosphates. The group possesses the general formula $M(UO_2)_2(XO_4)_2 \cdot 8\text{–}12H_2O$ where M may be Ba, Ca, Cu, Fe^{2+}, Mg, Mn^{2+} or $\frac{1}{2}$(HAl) and X is As or P. Takano (1961) obtained unit cell parameters for an autunite specimen from Ningyo Pass, Japan ($a = 6.989$ Å and $c = 20.63$ Å). These were virtually identical to those obtained by Locock and Burns (2003a) on a synthetic autunite. The Pb uranyl oxide hydrate, curite is commonly associated with uranium phosphates such as autunite, torbernite, and parsonsite (Vochten and Deliens, 1980). Finch and Ewing (1992) suggested that the (010) face of curite consists of $\equiv (UO_2) - OH_2^+$ surface species that may provide a reactive pathway for attachment of $(HPO_4)^{2-}$ groups, forming $\equiv (UO_2)$-OPO_3-H_3O^0. This species, once deprotonated, would have the equivalent stoichiometry of chernikovite. Heinrichite $\{Ba[(UO_2)(AsO_4)]_2(H_2O)_{10}\}$ was originally assumed by Gross *et al.* (1958) to be tetragonal, despite the observation of biaxial optical properties. Locock *et al.* (2005b) have refined the structures of several of the barium-bearing phases that possess the autunite sheet structure, including heinrichite and meta-uranocircite $\{Ba[(UO_2)(PO_4)]_2(H_2O)_7\}$ type I and II. There is only the loss of one H_2O group and a slight decrease in the interlayer spacing, from $d_{020} = 8.82$ Å to $d_{020} = 8.43$ Å from going from meat-uranocircite I to II; however, there is a significant re-arrangement in the Ba atomic positions. Table 5.3 lists new refinements from Locock *et al.* (2005b) for these autunite structures; however, because of the difficulties in obtaining

suitable natural specimens, some are based synthetic phases and predictions. These have been listed owing to the apparent inconsistencies in earlier published data. Locock *et al.* (2005c) have published a refinement of uranospathite $\{Al_{1-x}\square_x[(UO_2)(PO_4)]_2(H_2O)_{20+3x}\ F_{1-3x}\}$ with $0 < x < 0.33$ and confirmed the presence of fluorine, the absence of H_3O^+, and a higher Al content in the structure; the empty square in the formula indicates a vacancy. Locock *et al.* (2005c) have described uranospathite as the "Dogwood sandwich" of the autunite group with an interlayer spacing, d_{200} of 15.01Å, possessing 21 H_2O groups per formula unit (*pfu*). The discovery that uranospathite and other aluminum uranyl phosphates possess a number of different hydration states has called into question the traditional division of these minerals into autunite and meta-autunite sub-groups based on the 10-12 H_2O *pfu* and 6-8 H_2O *pfu*, respectively.

(*ii*) *Phosphuranylite structures*

The phosphuranylite group consists of mainly orthorhombic phases with structure sheets of the composition $[(UO_2)_3(O,OH)_2(PO_4)_2]$. Phosphuranylite is remarkable because it contains all three types of Ur polyhedra. The $Ur\phi_5$ and $Ur\phi_6$ occur in the uranyl sheet and the $Ur\phi_4$ occur in the interlayer (Burns, 1999a). It is one of the few minerals with uranium in an interlayer position. Torbernite and meta-torbernite are hydrous copper uranium phosphates, the only difference between the two being the number of water molecules present; the length of the *c*-axis depends on the water content. The structure of monoclinic bergenite, the barium phosphuranylite phase $\{Ca_2Ba_4[(UO_2)_3O_2(PO_4)_2]_3(H_2O)_{16}\}$, has been refined by Locock and Burns (2003c).

(*iii*) *Uranophane structures*

The uranophane structure type occurs in only a few uranium phosphates and arsenates. Ulrichtite, $Cu[Ca(H_2O)_2(UO_2)(PO_4)_2](H_2O)_2$, and the mixed valence arsenite–arsenate uranyl mineral, Séelite, $\{Mg(UO_2)(AsO_3)_{0.7}(AsO_4)_{0.3} \cdot 7H_2O\}$. The name ulrichite was once used as a term for pitchblende; however, the structure of this $Ca–Cu^{2+}$ mineral has now been refined by Kolitsch and Giester (2001).[20] The structure consists of elongated CuO_6 octahedra that are corner linked by two PO_4 octahedra, edge- and corner-sharing $Ur\phi_5$, CaO_8, and PO_4 polyhedra. These form heteropolyhedral sheets parallel to (001) that are linked by the elongated CuO_6 octahedra.

(*iv*) *Chain structures*

Chain structures occur in walpurgite, orthowalpurgite, phosphowalpurgite, hallimondite, and parsonsite. Burns (2000) solved the structure of parsonsite

[20] Problems with the ulrichite structure as described by Birch *et al.* (1988) were recognized by Burns (1999a).

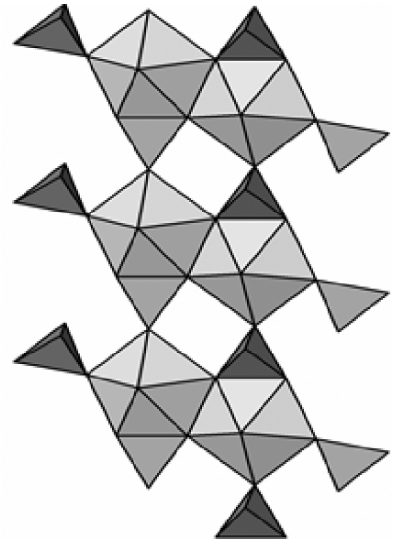

Fig. 5.3 *Parsonsite, the chain uranyl phosphate phase* (*adapted from Locock and Burns*, 2003).

and found that it was composed of uranyl phosphate chains rather than sheets as observed in the autunite and phosphuranylite minerals. The structure consists of $Ur\phi_5$ polyhedra edge-sharing dimers that are cross-linked with two distinct phosphate tetrahedra by edge- and vertex- sharing. Two symmetrically distinct Pb^{2+} cations link the uranyl phosphate chains (see Fig. 5.3).

One of the Pb positions, Pb(1) is coordinated by 9 oxygen atoms, with Pb–O bond lengths ranging from 2.35 to 3.16 Å. Pb(2) is coordinated by 6 oxygens with a distinctly one-sided polyhedral geometry owing to the presence of a lone pair of electrons on the Pb cation. The Pb(2)–O bond lengths range from 2.28 to 3.15 Å. Common to other uranium phases, the lone pair distortion may be responsible for the formation of chains rather than sheets.

Based on structural refinements and infrared spectroscopy, Locock *et al.* (2005a) have shown that parsonsite does not contain any structural water. In most uranyl phosphates and arsenates, water occurs as a hydrate H_2O, either coordinating interlayer cations, or occurring as interstitial H_2O groups. Although Locock *et al.* (2005a) detected water in hallimondite, this was determined not to be critical to structural integrity.

(*v*) *Synthetic uranyl phosphates and arsenates*

Synthetic varieties have also revealed structural differences between phosphate and arsenate uranyl phases that contain the large alkali cations cesium and rubidium. These phosphate and arsenate phases are not isostructural. For

example, cesium uranyl arsenates are not isostructural with cesium uranyl phosphates, but show a homeotypic framework with identical coordination geometries and polyhedral connectivity. The presence of arsenic expands the framework relative to phosphorus and so the cesium uranyl arsenate has a unit-cell volume ~7% greater than the corresponding phosphate.

(*vi*) *Uranium*(*VI*) *phosphates in the environment*

Because of their low solubilities, phosphate and arsenate minerals are of considerable environmental importance for understanding the mobility of uranium in natural systems and they may control the concentration of uranium in many groundwaters. In alkaline environments, dewindite $\{Pb(UO_2)_3(PO_4)_2(OH)_2 \cdot 3H_2O\}$ is stable at low lead concentrations; whereas dumontite is the stable phase in Pb-rich environments. In acid environments, parsonsite is prevalent at high lead levels and przhevalskite $\{Pb_2(UO_2)_3(PO_4)_2(OH)_4 \cdot 3H_2O\}$ occurs under low lead concentrations (Nriagu, 1984). Jerden and Sinha (2003) examined the long-term sequestration of uranium by U(VI) phosphate mineral precipitation at the Coles Hill uranium deposit in Virginia, USA where uranium is released by the oxidation and chemical weathering of an apatite-rich, coffinite–uraninite orebody. Meta-autunite was observed by Buck *et al.* (1996) and Morris *et al.* (1996) in contaminated soils from a former uranium processing plant at Fernald, Ohio, USA.

Significant uraniferous phosphorite deposits occur in Tertiary sediments in Florida, Georgia, and North and South Carolina and in the Hahotoé-Kpogamé U-deposits in Togo, West Africa (Gnandi and Tobschall, 2003). The Florida Phosphorite Uranium Province has yielded large quantities of uranium as a by-product of the production of phosphoric acid fertilizer (Finch, 1996). The discovery that bacteria can reduce U(VI), which appears to precipitate as uraninite, has led to the concept of *in situ* bioremediation of U-contaminated groundwater; however, another possible microbial process for uranium immobilization is the precipitation of U-phosphates. Macaskie *et al.* (2000) have demonstrated that *Citrobacter* sp. will bioprecipitate uranyl phosphate with exocellularly produced phosphatase enzyme. In a similar study by Basnakova *et al.* (1998) a nickel uranyl phosphate was observed in experiments with *Citrobacter* sp.

(k) Uranyl vanadates

Uranyl vanadates comprise some of the most insoluble uranyl minerals, forming whenever dissolved uranium comes in contact with dissolved vanadate anions. The K-bearing uranyl vanadate, carnotite, is possibly the most important source of secondary (U^{6+}) uranium ore minerals, providing ~90% of the uranium production from secondary deposits. It is a lemon-yellow mineral with an earthy luster, a yellow streak, and a specific gravity of about 4. It occurs most commonly in soft, powdery aggregates of finely crystalline material or in thin films or stains on rocks or other minerals. The most noted occurrences of

carnotite are in the Colorado Plateau (Zhao and Ewing, 2000), on the western edge of the Black Hills, South Dakota, USA, and in the Ferghana basin in Kyrgyzstan. It occurs in sandstones in flat-lying, irregular, partially bedded ore bodies. If present in sufficient quantity, carnotite will color the rock bright yellow; but in poorer deposits, particularly below 0.20 percent U_3O_8, it may be difficult to distinguish the uranium mineral from the sandstone itself.

Using solid state reactions, Dion *et al.* (2000) synthesized two new alkali uranyl vanadates, $M_6(UO_2)_5(VO_4)_2O_5$ with M = Na, K, by and determined their structures from single-crystal XRD. Both structures consisted of $[(UO_2)_5(VO_4)_2O_5]^{6-}$ corrugated layers parallel to the (100) plane. The layers contained VO_4 tetrahedra, Urϕ_5 pentagonal bipyramids, and distorted Urϕ_4 octahedra. The Urϕ_5 units were linked by sharing opposite equatorial edges to form zigzag infinite chains parallel to the *c*-axis. These chains were linked together on one side by VO_4 tetrahedra and on other side by Urϕ_4 and Urϕ_5 corner-sharing units.

(l) Uranyl selenites and tellurites

In nature, uranyl selenite minerals form where Se-bearing sulfides are undergoing oxidative dissolution. Selenium occurs as Se(IV), in the selenite anion, SeO_3^{2-}, however, Finch and Murakami (1999) suggested that Se(VI) minerals may be expected under sufficiently oxidizing conditions. Natural uranyl selenites and tellurites include the minerals derriksite, demesmaekerite, guilleminite, larisaite $\{Na(H_3O)(UO_2)_3(SeO_3)_2O_2 \cdot 4H_2O\}$ (Chukanov *et al.*, 2004), and marthozite, $\{Cu[(UO_2)_3(SeO_3)_2O_2](H_2O)_8\}$. The three known uranyl tellurites are cliffordite $\{UO_2(Te_3O_7)\}$, moctezumite $\{PbUO_2(TeO_3)_2\}$, and schmitterite $\{UO_2(TeO_3)\}$. The selenites and tellurites are based upon infinite chains of polymerized polyhedra of higher valence. The chain structures observed with moctezumite and derriksite contains Urϕ_5 and Urϕ_4 bipyramids as well as $Te^{4+}O_3$ and $Se^{4+}O_3$ triangles. They are strongly distorted owing to the presence of a lone pair of electrons on the cation. The crystal structure of marthozite has been refined by Cooper and Hawthorne (2001). There are two unique selenium sites, each occupied by Se^{4+} and coordinated by three O atoms, forming a triangular pyramid with Se at the apex, indicative of the presence of a stereoactive lone pair. The Se–O bond length is ~1.70 Å. The structure possesses one Cu site coordinated by 4 H_2O groups and two O atoms. The structural unit is a sheet of composition $[(UO_2)_3(SeO_3)_2O_2]$, which is topologically identical to the structural unit in guilleminite $\{Ba[(UO_2)_3(SeO_3)_2O_2](H_2O)_3\}$. Adjacent sheets are linked through interstitial Cu^{2+} cations *via* Cu^{2+}-O bonds and *via* H-bonds that involve both (H_2O) groups bonded to Cu^{2+} and interstitial (H_2O) groups.

A number of uranyl selenites containing alkaline metals (Almond *et al.*, 2002), as well as Ag and Pb (Almond and Albrecht-Schmitt, 2002) have been prepared. The structures consist of $[(UO_2)(SeO_3)_2]^{2-}$ sheets constructed from Urϕ_5 units that are linked by SeO_3^{2-} anions, similar to the natural minerals. Synthetic $Sr[(UO_2)_3(SeO_3)_2O_2] \cdot 4H_2O$ prepared in supercritical water was

found to possess the same anion topology as is found in guilleminite and marthozite; however, this phase could not be prepared under ambient or hydrothermal conditions (Almond and Albrecht-Schmitt, 2004).

(m) Uranyl molybdates

Uranyl molybdates are common minerals formed by weathering of uraninite and Mo-bearing minerals (Finch and Murakami, 1999). Umohoite $\{[(UO_2)(MoO_2)](H_2O)_4\}$, is commonly partially replaced by iriginite $\{[(UO_2)(MoO_3OH)_2(H_2O)](H_2O)\}$, which also consists of polyhedra sheets. Iriginite, however, has a distinctive anion-topology arrangement of chains of pentagons and squares that share edges, and zigzag chains of edge sharing squares and triangles (Krivovichev and Burns, 2000a). In the structure of iriginite, each pentagon of the anion topology is populated by an $Ur\phi_5$ polyhedron, two-thirds of the squares are populated with $Mo^{6+}O_6$ octahedra that occur as edge-sharing dimers; the triangles, as well as one-third of the squares, are empty. There have been reports of substantial variability of the *c* dimension of umohoite possibly due to variation of the H_2O content or polytypism that may account for the observed variation in unit-cell parameters (Krivovichev and Burns, 2000b).

The sheets of uranyl and molybdate polyhedra in iriginite and umohoite have features in common. The umohoite to iriginite transformation during alteration of U–Mo deposits, corresponding to a change of the U:Mo ratio from 1:1 to 1:2, involves a change of anion topology to one with a smaller number of edges shared between coordination polyhedra. The uranophane anion-topology is the basis of the umohoite sheet. Construction of the anion topology requires the U and D arrowhead chains as well as the R chain, with the chain-stacking sequence URDRURDR... The iriginite anion-topology contains the same chains as the umohoite (uranophane) anion-topology, but the chain-stacking sequence is DRRRURRRDRRRURRR... The ratio of arrowhead (U and D) chains to R chains in the umohoite and iriginite anion topologies is 1:1 and 1:3, respectively. In the umohoite sheet, all rhombs of the R chains are populated with Mo^{6+} cations, whereas in the iriginite sheet, only two-thirds of the rhombs contain Mo^{6+}, with the remaining third empty. The result is U:Mo ratios of 1:1 and 1:2 in the umohoite and iriginite sheets, respectively. The iriginite anion-topology may be derived from that of umohoite by expansion of the umohoite anion-topology along a vector within the sheet that is perpendicular to the arrowhead chain, together with the insertion of two additional **R** chains between adjacent arrowhead chains. This transformation mechanism requires addition of Mo^{6+} to populate the rhombs of the **R** chains. Another mechanism for obtaining the iriginite anion-topology from that of umohoite is the replacement of every second URD sequence in the umohoite anion-topology with an **R** chain. This mechanism requires the removal of the U^{6+} that populated the **D** and **U** arrowhead chains. Krivovichev and Burns (2000a,b) have suggested that this may appear to be the most likely mechanism of the umohoite-to-iriginite transformation (see Fig. 5.4).

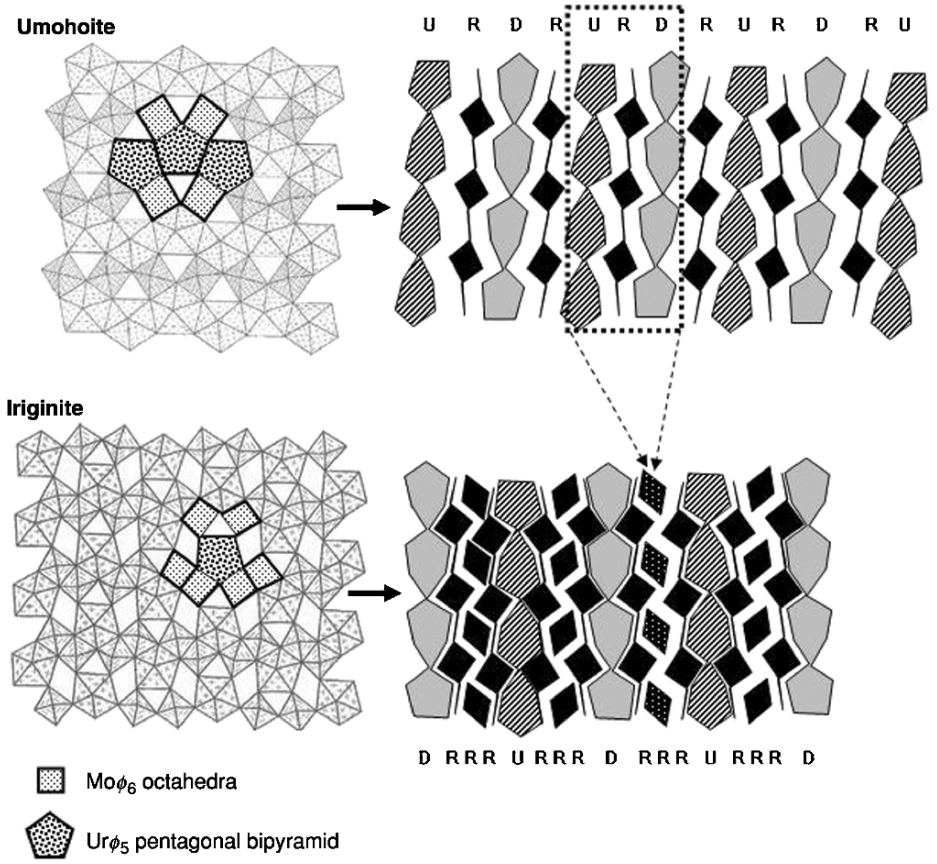

Fig. 5.4 *Diagram showing a possible mechanism for the umohoite to iriginite transformation (adapted from Krivovichev and Burns, 2000a,b). The iriginite structure can be obtained from umohoite through the replacement of every second URD sequence in the unmohoite anion topology with an R chain. This mechanism requires removal of the U^{6+} that occupied the D and U arrowhead chains.*

Mourite $\{U^{4+}Mo^{6+}{}_5O_{12}(OH)_{10}\}$, is a rare U^{4+} mineral containing molybdenum that is observed in oxidized zones in association with umohoite occurring as dark violet crusts and scaly aggregates in the Kyzylsai uranium deposit in Kazakhstan associated with umohoite. Krivovichev and Burns (2002a–c, 2003a) have described several synthetic uranyl molybdates, including Rb, Cs, Ag, and Tl species, respectively.

(n) Uranyl tungstates

Only one natural uranium tungstate is known, uranotungstite $\{(Fe^{2+},Ba,Pb)(UO_2)_2WO_4(OH)_4(H_2O)_{12}\}$; however, there are a wealth of synthetic U(IV) and U(VI) tungstates that have been reported in the literature. The phase UO_2WO_4 is isostructural with UO_2MoO_4, suggesting that the W^{6+} cations are tetrahedrally coordinated by O atoms. Given the structural similarities of Mo(VI) and W(VI), it might be expected that a variety of U(VI)–W(VI) phases should form. The phases $UO_2W_3O_{10}$ and $Na_2UO_2W_2O_8$, has been described but their structures are unknown. U(IV) tungsten bronzes have received considerable attention. The structures consist of ReO_3-type slabs of corner-sharing $W^{6+}O_6$ octahedra. A number of lithium uranyl tungstates ion conductors, such as $Li_2(UO_2)(WO_4)_2$ and $Li_2(UO_2)_4(WO_4)_4O$, have been prepared by high-temperature solid state reactions (Obbade *et al.*, 2004).

(o) Uranium association with clay minerals and zeolites

Chisholm-Brause *et al.* (2001) have identified four distinct uranyl complexes on montmorillonite that co-exist under certain conditions. Inner sphere and exchange-site complexes persist over a range of solution conditions. The uranyl ion sorbs onto montmorillonite at low pH *via* ion exchange, leaving the inner-sphere uranyl aquo-ion structure intact (Dent *et al.*, 1992; Sylwester *et al.*, 2000). At near neutral pH and in the presence of a competing cation, inner-sphere complexation with the surface predominates. Adsorption of the uranyl onto silica and γ-alumina surfaces appears to occur *via* an inner-sphere, bidentate complexation with the surface, with the formation of polynuclear surface complexes occurring at near-neutral pH (Sylwester *et al.*, 2000). Pabalan *et al.* (1993) have performed laboratory tests on the sorptive properties of zeolitic materials for uranium; the sorption is strongly dependent on pH. At near neutral pH U(VI) was strongly sorbed but under conditions where carbonate- and ternary hydroxyl-carbonate-complexes are present the sorption decreased substantially. Della Ventura *et al.* (2002) have discovered a new lanthanide borosilicate minerals of the hellandite group where uranium appears to be incorporated into a borosilicate cage structure. The phase, called ciprianiite $\{Ca_4[(Th,U)(REE)]Al_2(Si_4B_4O_{22})(OH,F)_2]\}$, formed with a syenitic ejectum[21] collected close at

[21] Literally, the violent volcanic explosion of mainly alkali feldspar (syenite) intrusive rock.

Tre Croci within a pyroclastic formation belonging to the Vico volcanic complex (Latium, Italy). Uvarova *et al*. (2004) reported another U^{4+} bearing silicate, arapovite $\{U(Ca,Na)_2(K_{1-x}\square_x)Si_8O_{20}\}$ from the Dara-i-Pioz moraine, Tien-Shan Mountains, Tajikistan.

The thorium and uranium uptake from their aqueous solutions by pristine and NaCl-pretreated zeolite-bearing volcanoclastic rock samples from Metaxades (Thrace, Greece) has been studied using a batch-type method (Misaelides *et al*., 1995). The concentration of the solutions varied between 50 mg L^{-1} and 20 g L^{-1}. The NaCl pretreatment of the materials improved the thorium, but not the uranium, uptake. The absolute thorium uptake by the pretreated material, determined using neutron activation and X-ray fluorescence techniques, reached 12.41 mg g^{-1}, whereas the uranium uptake by the raw material was 8.70 mg g^{-1}. The distribution coefficients (K_d) indicated that the relative thorium and uranium uptake is higher for initial concentrations below 250 mg L^{-1}. The zeolitic materials were very stable despite the initial low pH of the solutions used; however, the pH increased significantly with time due to the simultaneous hydrogen-ion uptake. The thorium and uranium uptake is a complex function of the aqueous chemistry of the elements, the nature of the constituent minerals, and the properties of the zeolitic rock specimens. The various metal species are bound through different sorption processes such as ion-exchange, adsorption, and surface precipitation. Microporous minerals (zeolites, phyllosilicates) are mainly responsible for the large sorption capacity of the rock samples studied.

5.4 ORE PROCESSING AND SEPARATION

Because of the complexity of many uranium ores and the usual low concentrations of uranium present, the economic recovery of uranium often poses a difficult problem for the chemist. Physical concentration methods (flotation, gravitational, electromagnetic, etc.) have met with only limited success for uranium. The chemical methods used for the recovery of uranium from ores thus have to be designed to treat large ore volumes economically. Because of this and because uranium is a very electropositive metal, most direct pyrochemical methods are not applicable and processes usually involve modern aqueous extractive metallurgy. In this section the more important aspects of the extractive metallurgy of uranium will be described with emphasis on the chemical principles involved.

Uranium ores vary in chemical complexity from the relatively simple pitchblendes, which are accompanied by perhaps 10 other minerals, to exceedingly complex and refractory uranium-bearing titanites, niobates, and tantalates containing rare earths and many other metals. Included are uranium minerals accompanied by major admixtures of ill-defined organic compounds. Some pitchblende ores may have as many as 40 elements present from which

uranium must be separated. Many uranium deposits are variable in composition, resulting in an almost daily variation in the composition of the starting materials. Such variations are minimized by stockpiling methods. Nevertheless there have been many *ad hoc* procedures elaborated to meet special chemical situations. Most such highly specialized methods will have little interest for this discussion. The general features common to most procedures will, however, be pertinent. All methods that have been commonly used comprise the following steps: (1) pre-concentration of the ore; (2) a leaching operation to extract the uranium into an aqueous phase – this step frequently being preceded by roasting or calcination to improve the extraction; and (3) recovery of the uranium from the pregnant leach liquors by ion exchange, solvent extraction, or direct precipitation, and in the case of ion-exchange or solvent extraction products by a final precipitation. Special methods may be used for recovery of by-product uranium. The product of these operations is a high-grade concentrate, which is usually further purified at a site other than the uranium mill.

The extractive metallurgy of uranium has been discussed in detail in various books (Vance and Warner, 1951; Clegg and Foley, 1958; Harrington and Ruehle, 1959; Chervet, 1960; Bellamy and Hill, 1963; Gittus, 1963; Galkin and Sudarikov, 1966; Merritt, 1971) and in collections of papers (United Nations, 1955, 1958, 1964; IAEA, 1966, 1970). There is also a bibliography on feed materials (Young, 1955). The most comprehensive collection of data is the multi-volume supplement to the *Gmelin Handbook of Inorganic Chemistry* (Gmelin, 1975–1996), more particularly its volume (A3) on Technology and Uses (Gmelin, 1981a). Many other references can be found in these sources.

5.4.1 Pre-concentration

Most uranium ores contain only small amounts of uranium, and because leaching is a relatively expensive operation, much effort has been expended to reduce the magnitude of the leaching operation by pre-concentration of the ore. Physical concentration methods (gravitational, electrostatic, flotation) and various sorting methods have been either used or proposed for upgrading of uranium ores. Unfortunately such beneficiation methods have not achieved great success, only a few of the uranium ores processed being amenable to physical beneficiation processes. Only in a few cases can appreciable concentration of uranium be achieved without excessive loss to tailings.

Uranium minerals as well as other minerals, with which they are closely associated, are denser than many gangue materials and successful gravity separation methods are sometimes possible. Such gravity separations are complicated by the fact that uranium minerals tend to concentrate in the fines upon crushing or grinding of some ores. This property has been used to some advantage in that a certain degree of mechanical concentration can be achieved by a gentle grinding followed by screening. Electrostatic methods generally give low recoveries or low concentration factors. Magnetic separation methods have

generally been used to remove gangue materials such as magnetite, ilmenite, garnet, etc. Flotation methods have received considerable laboratory attention although they do not appear to have been widely applied. Flotation of undesirable gangue materials such as sulfides has met with some success, but no flotation agents have been developed for uranium minerals that give concentration factors approaching those obtained in the processing of sulfide minerals. Flotation has met with some success in splitting carbonate-containing ores into a carbonate and a non-carbonate fraction so that the former fraction can be leached by the carbonate method and the other with sulfuric acid. Both manual and mechanical sorting methods have been applied to the upgrading of uranium ores. In this procedure individual lumps of ore are sorted either by hand or by mechanical devices usually on the basis of radiation readings for the individual lumps. Merritt (1971) reviewed various mechanical upgrading techniques in some detail.

5.4.2 Roasting or calcination

It is frequently desirable to subject ores to high-temperature calcination prior to leaching. Several functions can be performed by such roasting operations. An oxidizing roast can remove carbonaceous material and put the uranium in soluble form. It can oxidize sulfur compounds to avoid subsequent polythionate and sulfur poisoning of ion-exchange resins. It removes other reductants, which might consume oxidant during the leaching step. Reducing roasts can convert uranium to the reduced state and prevent dissolution of uranium during by-product recovery.

Roasting also improves the characteristics of many ores. Many of them contain clays (particularly of the montmorillonite class), which cause thixotropic slurries and create problems in leaching, settling, and filtering. Dehydration of these clays alters their physical properties and decreases these problems.

Roasting with sodium chloride is commonly used with vanadium-containing ores to convert the vanadium to a soluble form. Sodium vanadate is formed, which is believed to form soluble uranyl vanadates (Merritt, 1971). Salt roasting has also been used to convert silver to silver chloride for easier separation from soluble components.

5.4.3 Leaching or extraction from ores

The object of this procedure is to extract the uranium present in the ore into solution, usually aqueous, from which the recovery and purification of the uranium from accompanying metals can be carried out. The leaching operation is usually the first of the chemical manipulations to which the ore is subjected, and all present chemical processing methods for any type of ore involve digestion of the ore with either acid or alkaline reagents. The acid reagent may be

generated *in situ* by bacterial or high-pressure oxidation of sulfur, sulfides and Fe(II) in the ore to sulfuric acid and ferric [Fe(III)] species. The choice of a reagent for a particular case will be determined primarily by the chemical nature of the uranium compounds present in the ore and the gangue materials that accompany them.

The extraction of uranium from the majority of the ores is generally more complete by acid leaching than with alternative leaching procedures and is therefore used in most mills. While other acids can be used, sulfuric acid is employed because of its lower price, except when hydrochloric acid is available as a by-product of salt roasting. As a general principle only uranium (VI) minerals are readily dissolved in sulfuric acid. For uranium minerals, such as uraninite, pitchblende, and others, containing uranium in lower oxidation states, oxidizing conditions must be provided to ensure complete extraction. Oxidizing conditions are provided by agents such as manganese dioxide, chlorate ion, ferric ion, chlorine, or molecular oxygen. Manganese dioxide and chlorate ion are most commonly used and iron must be present in solution as a catalyst in order for either of them to be effective.

Manganese dioxide to the extent of perhaps 5 kg per ton (but typically about one-half of this in U.S. practice) or up to 1.5 kg $NaClO_3$ per ton of ore are usually adequate for all but the very refractory ores. Free ferric-ion concentrations larger than 0.5 g L^{-1} generally give adequate dissolution rates. Sufficient iron is normally provided by the ores themselves and by the ore-grinding process. Typical dissolution reactions are

$$UO_2 + 2Fe^{3+} \rightarrow UO_2^{2+} + 2Fe^{2+}$$

$$2Fe^{2+} + MnO_2 + 4H^+ \rightarrow 2Fe^{3+} + Mn^{2+} + 2H_2O$$

$$6Fe^{2+} + ClO_3^- + 6H^+ \rightarrow 6Fe^{3+} + Cl^- + 3H_2O$$

To avoid excessive consumption of oxidant this is in general not added to the acidified ore until the reaction with free iron and sulfides is practically complete. Manganese can be recovered at later stages as manganese(II) hydroxide followed by ignition in air at 300°C to the dioxide. When only a small fraction of the uranium is in reduced form, agitation with air is often sufficient to maintain oxidation by ferric ion. Various other oxidants are effective, including chlorine, permanganate, bromine, etc., but cost or difficulty of handling (corrosiveness, etc.), have relegated their use to very special situations. Proper addition of oxidizing agent can be controlled by an empiric potentiometric measurement of the redox potential. If the potential between a platinum and a calomel electrode inserted into the digesting ore mixture is adequately controlled, the iron will be present principally as Fe^{3+} and suitable oxidizing conditions will have been imposed (Woody and George, 1955).

The most common form in which acid leaching is applied is in the form of aqueous leaching with agitation. The sulfuric acid concentration is adjusted so that it close to pH 1.5 at the end of the leaching period; the period of extraction

is generally 4–48 h, in U.S. practice typically 4–24 h. Elevated temperatures and higher acid concentrations increase the rate of extraction but are often uneconomic and result in higher reagent consumption, increased corrosion, and increased dissolution of non-uranium minerals. Counter-current leaching in several stages is sometimes used but is less common than single stage processes. Recycle circuits have also been devised to use the acid leachant more efficiently. A less common procedure is acid pugging, in which a small amount of dry, ground ore is mixed with a more concentrated acid to form a plastic mass, which is allowed to cure and then leached with water. Percolation leaching, in which solution percolates slowly through an ore bed, is well-suited to ores in which the uranium minerals occur as coatings on sand grains, particularly when the ore is of low grade. A variation of percolation leaching that has important application to low-grade ores is heap leaching, in which 5–10 m deep piles of ore of about 100 m length are leached by slow percolation of an acid solution that is collected in the pile drainage. *In situ* leaching is another method that has been applied to certain ore bodies with low permeability of the rock underlying the deposit and adequate porosity of the ore body itself. In this procedure, wells are drilled into the ore body and leachant is pumped into some of these while the enriched solutions are pumped from other wells.

Two acid leaching methods require no reagent addition in some ores containing sulfides or sulfur. These methods are pressure leaching, in which air is the oxidant at elevated temperatures ($\sim$150°C) and pressures, and bacterial leaching, where air is also the oxidant but at temperatures near ambient. In both cases uranium dissolution is brought about by the oxidation of iron and sulfur compounds to Fe^{3+} and sulfuric acid. Typical reactions in pressure leaching are

$$4FeS_2 + 15O_2 + 2H_2O \rightarrow 2Fe_2(SO_4)_3 + 2H_2SO_4$$
$$UO_2 + Fe_2(SO_4)_3 \rightarrow UO_2SO_4 + 2FeSO_4$$
$$4FeSO_4 + 2H_2SO_4 + O_2 \rightarrow 2Fe_2(SO_4)_3 + 2H_2O$$

Similar overall reactions occur in bacterial leaching through the action of bacteria, such as *Thiobacillus ferrooxidans* and others, on ferrous ion, sulfur, and sulfides. Although there are several reported advantages of high-pressure leaching, such as improved extraction and shorter extraction times, particularly with refractory ores, there is also larger corrosion and higher maintenance costs and the method has received little actual use. Bacterial leaching appears to be particularly attractive as a low-cost recovery method for very low-grade ores when used with heap or *in situ* leaching.

While acid leaching is excellent for many ores, and is essential for primary refractory ores such as euxenite, davidite, and brannerite, it is subject to certain limitations. Most uranium minerals are soluble in dilute sulfuric acid with an oxidant present, but many ores contain other minerals such as calcite, dolomite, and magnesite, which consume sufficient amounts of acid to make

acid leaching uneconomic. In such cases, carbonate solutions are used to extract uranium.

Carbonate leaching is usually carried out with sodium carbonate. The utility of carbonate solutions arises from the high stability of the uranyl(VI) tricarbonate ion, $UO_2(CO_3)_3^{4-}$, in aqueous solution at low hydroxide-ion concentration. Uranium(VI) is thus soluble in carbonate solution, unlike the vast majority of other metal ions, which form insoluble carbonates or hydroxides in these solutions. The sodium carbonate leaching is thus inherently more selective than the sulfuric acid procedure. In general, compounds of uranium(VI) are readily soluble in carbonate leach solutions although silicates dissolve, albeit with some difficulty. Minerals containing uranium in its lower oxidation states are insoluble in carbonate solutions, and oxidants are required. Under oxidizing conditions, simple uranium oxides and some other uranium(IV) minerals such as coffinite can be leached, particularly at elevated temperature.

In addition to the advantage of low reagent consumption in carbonate-containing ores, carbonate leaching is relatively (but not completely) specific for uranium and carbonate solutions, which are moderately non-corrosive. Disadvantages include lower uranium extraction than by acid leaching and that the method is not suitable for ores having high gypsum or sulfide content. Important refractory minerals such as euxenite, brannerite, and davidite are not attacked significantly without a prior fusion step. Since few ore components other than uranium minerals are attacked to any appreciable extent by carbonate solutions, any uranium imbedded in gangue will escape leaching. A carbonate leach thus requires sufficiently fine grinding to liberate the uranium. Economics dictate that the reagents must be recovered and recycled in the carbonate leach process.

Oxygen (often under pressure) is the commonly used oxidant in carbonate leaching and the dissolution of simple uranium oxide follows the reactions (Merritt, 1971).

$$2UO_2 + O_2 \rightarrow 2UO_3$$
$$UO_3 + H_2O + 3CO_3^{2-} \rightarrow UO_2(CO_3)_3^{4-} + 2OH^-$$
$$OH^- + HCO_3^- \rightarrow CO_3^{2-} + H_2O$$

As shown in the equations above, bicarbonate is used to prevent increase in the hydroxide concentration, which would result in precipitation of uranates or polyuranates by the reaction

$$2UO_2(CO_3)_3^{4-} + 6OH^- + 2Na^+ \rightarrow Na_2U_2O_7 + 6CO_3^{2-} + 3H_2O$$

The detailed dissolution mechanisms are more complex than represented here and several possible alternatives have been proposed (Clegg and Foley, 1958; Wilkinson, 1962; Merritt, 1971). Although air is the most commonly used oxidant in carbonate leaching, other oxidants have been used. Potassium permanganate was commonly used in the past but was expensive and replaced

by pressurized leaching at 95–120°C in air. This was followed by the use of cupric–ammonia complexes, a catalyst for air oxidation, but current practice is toward simply using air at atmospheric pressure and longer dissolution times at about 75–80°C in Pachuca-type (air-agitated) tanks (Merritt, 1971). Pure oxygen has been used (Woody and George, 1955) in place of air with some advantages. Other oxidants that have been considered are NaOCl, H_2O_2, and $K_2S_2O_8$. Various catalysts such as $MgCl_2$, Ag_2SO_4, $K_3Fe(CN)_6$, copper–cyanide complexes, and copper–, nickel–, and cobalt–ammonia complexes have also been studied.

Although sodium carbonate is the only reagent used commercially in alkaline leaching, ammonium carbonate has been extensively tested in the laboratory and pilot plant (Merritt, 1971). Since the concentrations of sodium carbonate and bicarbonate used are typically 0.5–1.0 M, the recovery of reagents is necessary. The specificity of carbonate leaching for uranium is such that the uranium can usually be recovered from the leach solution by precipitation as sodium polyuranates ('diuranate') with sodium hydroxide. The filtrate is then treated with carbon dioxide to regenerate the desired carbonate/bicarbonate ratio.

While the amounts of carbonate, bicarbonate, and oxygen consumed during leaching are usually very small, side reactions may occur with other constituents of the ores, which consume substantial amounts of carbonate. Particularly important parasitic reactions are due to sulfide minerals and gypsum and, at higher temperatures and pressures, silica and alumina:

$$2FeS_2 + 15/2O_2 + 8CO_3^{2-} + 7H_2O \rightarrow 2Fe(OH)_3 + 4SO_4^{2-} + 8HCO_3^-$$

$$CaSO_4 + CO_3^{2-} \rightarrow CaCO_3 + SO_4^{2-}$$

$$SiO_2 + H_2O + 2CO_3^{2-} \rightarrow SiO_3^{2-} + 2HCO_3^-$$

$$Al_2O_3 \cdot 3H_2O + 2CO_3^{2-} \rightarrow 2AlO_2^- + 2HCO_3^- + 2H_2O$$

Flotation may be used to reduce the initial sulfide content to tolerable limits.

Organic materials in some ores cause difficulties in the carbonate leach process and various schemes for handling this problem are reviewed by Merritt (1971). A simplified flow sheet for carbonate leaching is shown in Fig. 5.5.

Clarification is the separation of ore slimes from the aqueous uranium extract and constitutes the final step in ore extraction of uranium. It is a necessary step except when the resin-in-pulp ion-exchange process is used, in which case only partial clarification is necessary, and when *in situ*, heap, or percolation leaching has been used, since the ore itself acts as an effective filter medium in these leaching techniques and clear solutions are obtained. Solution clarification has in the past been one of the most difficult problems in uranium recovery, but flocculants have been developed (Clegg and Foley, 1958) to improve settling of clays and other slimy ore constituents. These have greatly improved liquid–solid separation technology and most ores can now be handled satisfactorily in liquid–solid separation equipment with the proper choice and use of flocculants.

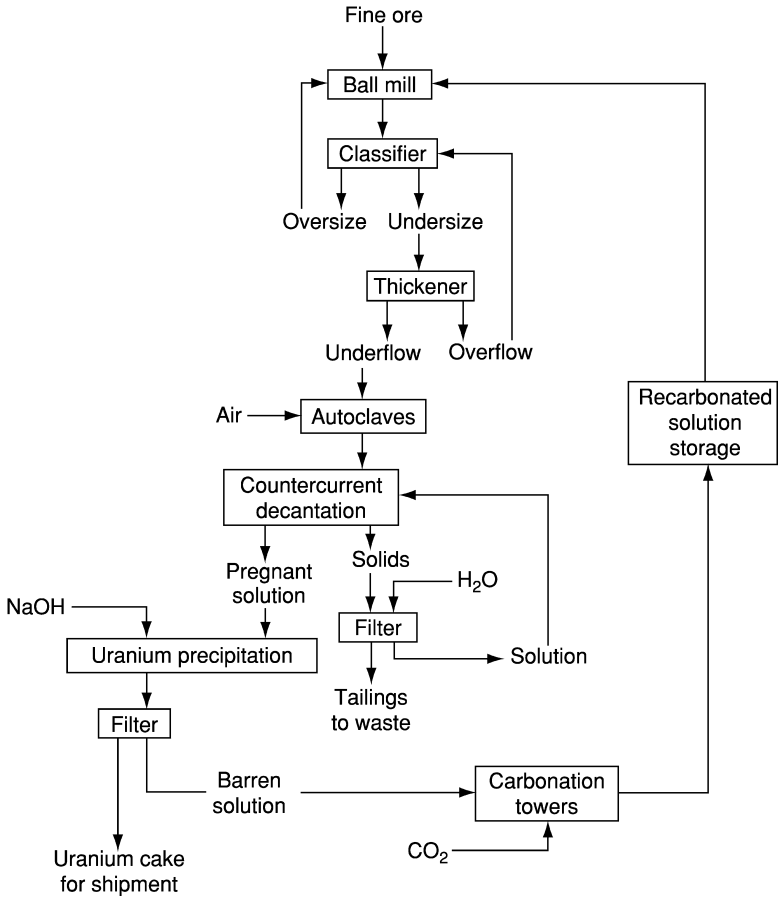

Fig. 5.5 *Flow sheet of raw ore leach for unoxidized or primary uranium of Eldorado Mining and Refining Ltd, Beaverlodge, Saskatchewan* (*Stephens and McDonald*, 1956).

Flocculants used include polyacrylamides, guar gums, and animal glues. For the resin-in-pulp process, only the coarser ore particles (325 mesh) are removed and slime contents of 5% to as high as 20% solids can be handled depending on exact process design. Clegg and Foley (1958) and Merritt (1971) review clarification in detail.

5.4.4 Recovery of uranium from leach solutions

The recovery of uranium from leach solutions can be achieved by a variety of methods including ion exchange, solvent extraction, and chemical precipitation. Each of the various procedures listed above can be applied to acid or alkaline

leach liquors, although in general they will not be equally applicable. Although various precipitation methods were extensively used in the past, they were generally cumbersome and complex if significant uranium purification was to be achieved. Currently operating uranium mills, with the exception of some that employ carbonate leaching, all use ion exchange or solvent extraction, or both, to purify and concentrate the uranium before a final product precipitation. Because of the selectivity of carbonate leaching, precipitation from carbonate leach solutions produces a fairly pure uranium concentrate, but for acid leach solutions, ion exchange or solvent extraction is always employed.

(a) Ion exchange

The recovery of uranium by ion exchange is of great importance. Uranium(VI) is selectively absorbed from both sulfate and carbonate leach solutions as anionic complexes using anion-exchange resins. The loaded resin is rinsed, and the uranium eluted with a sodium chloride or an acid solution. The uranium is then precipitated from the eluate and recovered as a very pure uranium concentrate. This process can be carried out with either stationary columns of ion-exchange resin through which clarified leach liquors are passed; alternatively the resin may be moved through the leach liquor in agitated baskets. This resin-in-pulp process does not require complete clarification of the leach liquor.

The degree of purification of the uranium by these ion-exchange processes is related to the selectivity of the anion-exchange resins for the anionic uranyl sulfate or carbonate complexes relative to that of impurity species. Cationic impurities are not absorbed and many anionic species are absorbed less strongly than are the uranyl complexes and are displaced by them. The impurities can be left in the ion exchangers during uranium elution, but often they are so strongly absorbed as to act as exchanger poisons that require elaborate removal steps.

The uranyl species absorbed by the exchangers from carbonate solution appears to be exclusively the $UO_2(CO_3)_3^{4-}$ complex, but from sulfate solutions more than one species is absorbed (Ryan, 1962). Although it has been reported (OECD-NEA, 1982) that below pH 2 the only uranyl sulfate complex in the resin is $UO_2(SO_4)_3^{4-}$, spectral studies of the resin phase (Ryan, 1962) indicate that, although $UO_2(SO_4)_3^{4-}$ is present over at least the pH range 0.5–4.5, it is not the only uranyl species. The ratio of uranyl species in the resin phase changes with pH but is almost unaffected by change in total aqueous phase sulfate concentration at any given pH. Even if the affinity of anion-exchange resins for complex anions may be very high, high distribution coefficients do not necessarily mean that an appreciable fraction of the uranium is present as anionic species in the aqueous phase. Both weak-base or strong-base resins can be used with the sulfate system, but only the strong-base resins in the basic carbonate solutions. In practice, the resin choice is governed by several factors, including absorption and elution kinetics, resin particle size, the physical and

chemical stability of the resin, the selectivity and ease of removal of resin poisons, hydraulic characteristics, and exchange capacity. Typically, resins of moderately low cross-linking and moderately large particle size are used and several resins have been marketed specifically for uranium processing.

Elution of the uranium from anion-exchange resins in either the sulfate or the carbonate processes is normally made with approximately 1 M sodium or ammonium chloride or nitrate solutions. In the sulfate process the eluent is acidified, and in the carbonate process some carbonate or bicarbonate is added to prevent hydrolysis. Special elution techniques are used for vanadium recovery when it is co-absorbed in the carbonate process (Merritt, 1971).

Although uranyl sulfate and carbonate complexes have a higher affinity for the resin than most impurity ions, they are not extremely strongly sorbed and some impurity ions are more strongly absorbed. In the acid system such ions include pentavalent vanadates, molybdenum sulfate complexes, polythionates, and in South African ores treated for gold recovery, cobalt cyanide complexes and thiocyanate. Vanadates are more strongly absorbed than uranium in the carbonate process except at high pH values. In addition, some other weakly sorbed ions may be present in sufficiently high concentration to compete for resin sites, resulting in decreased uranium loading; some of these may also alter absorption kinetics. Some of the strongly held ions and others such as silicate, titanium, thorium, hafnium, niobium, antimony, and arsenate and phosphate complexes, which polymerize or hydrolyze in the resin phase, are not readily removed during the normal elution process. They gradually build up in the resins where they act as poisons and require special removal procedures (Merritt, 1971).

Merritt (1971) and Clegg and Foley (1958) have reviewed the uranium ion-exchange processes in detail along with the various specialized problems encountered and their treatment. They have discussed specific flow sheets, processing rates, back-cycle methods for reagent conservation, and processing equipment for fixed-bed, moving-bed, basket resin-in-pulp, and continuous resin-in-pulp ion-exchange processes.

(b) Solvent extraction

Solvent extraction has a distinct advantage over ion exchange for uranium purification from leach liquors because of the ease with which it can be operated in a continuous counter-current flow process. It has a disadvantage, however, in the incomplete phase separation, due to emulsion formation, third-phase formation, etc. In addition solvent losses constitute both a monetary loss and a potential pollution problem in the disposal of spent leach liquor. Because solvent losses are related to overall solution volume, solvent extraction usually has an advantage for leach solutions with concentrations above about 1 g U per liter, and ion exchange has an advantage for low-grade solutions with concentrations appreciably less than 1 g U per liter (Merritt, 1971). Solvent extraction

processes are not economically advantageous for carbonate leach solutions. Two types of alkyl phosphoric acids and secondary and tertiary alkylamines, have been used industrially for uranium extraction from sulfate leach liquors. These extraction reagents are normally used as relatively dilute solutions in an inert diluent such as kerosene. Modifiers such as long-chain alcohols and neutral phosphate esters are typically added to prevent third-phase formation to increase amine salt solubility in the diluent, and to improve phase separation.

Amine extraction from sulfate leaching is analogous to anion exchange in that anionic uranyl sulfate complexes are extracted by the alkylammonium cations. The species extracted, at least by tertiary amines, is predominantly the $UO_2(SO_4)_3^{4-}$ complex in the pH range ($1 < pH < 2$) normally used in commercial processing. The concentration of other uranyl species increases with decreasing pH (Ryan, 1962). There is considerable variation in affinity and selectivity for uranium with the structure of the amine. Typical commercially used tertiary amines give extraction coefficients of 100–140, whereas *N*-benzylheptadecylamine gives extraction coefficients as high as 8000 (Merritt, 1971). Such specialized amines, if made available at a reasonable cost, will be capable of recovering uranium from very dilute leach solutions but might require more complex stripping procedures. Amines extract other anions to varying degree and thereby decrease uranium extraction efficiency. Nitrate interference is severe and chloride interference is more severe for secondary than for tertiary amines. These factors are important for the choice of stripping agent and the recycling of solutions. Molybdenum is extracted more strongly than uranium. It builds up as a poison in the amine, finally causing serious problems by precipitating at the organic–aqueous interface, and special molybdenum stripping procedures are used to counteract this problem (Merritt, 1971). Vanadium is also extracted to some extent. Various ions are effective in stripping uranium from the solvent. Nitrate has such high affinity for the amine that it must be removed in the carbonate or hydroxide regeneration step before the next extraction cycle; however this is not necessary in solutions containing chloride, except with secondary amines having high chloride affinity. Another procedure uses ammonium sulfate with pH carefully controlled in the range 4.0–4.3, since poor stripping or poor phase separation occurs outside this range. Direct precipitation of uranium from the organic phase has been proposed (Brown *et al*., 1958).

The alkylphosphoric acid extractants have the advantage over amines of fewer phase separation problems due to suspended solids and of having good extraction efficiency in the presence of dilute nitrate, chloride, and sulfate. On the other hand, they suffer from lower selectivity for uranium since the alkyl phosphates extract cations and many of the impurities including iron in the leach solutions. Special methods for removing or rendering these impurities non-extractable have been devised. Alkylphosphoric acid extraction has been referred to as 'liquid cation exchange'. The dialkyl phosphates appear to be

dimers and four dialkyl phosphates are required to extract one uranyl ion (Baes *et al.*, 1958; Blake *et al.*, 1958). Addition of neutral phosphate esters increases the uranium extraction coefficient of alkylphosphoric acids (synergistic effect). Stripping of bis(2-ethylhexyl)phosphoric acid is normally carried out with carbonate solution, but monodecylphosphoric acid requires 10 M HCl for stripping.

In addition to the solvent extraction procedures discussed above, mixed amine–alkylphosphoric acids have also been used. Other processes include both ion-exchange and solvent-extraction steps as well as special methods for removing and in some cases recovering interfering ions such as molybdenum. Solvent extraction methods have also been studied in cases where the leach solution is not clarified, solvent-in-pulp, but solvent losses are then very high. Merritt (1971) has reviewed the commercial practice in detail and gives many further references.

(c) Chemical precipitation

Before the use of ion-exchange and solvent extraction methods for the removal and purification of uranium from leach liquors, precipitation techniques were used on clarified leach liquors. Much effort was spent during the late 1940s to develop selective precipitation processes; most of these techniques are obsolete and will not be discussed here but they are reviewed by Wilkinson (1962) and by Merritt (1971).

The product from typical acid process anion-exchange or solvent extraction processes is an acid solution of mixed nitrate or chloride and sulfate. The two principal methods of precipitation of uranium from these are neutralization with sodium hydroxide, magnesia, or ammonia, or the precipitation of the peroxide $UO_4 \cdot xH_2O$ in the pH range 2.5–4.0 with hydrogen peroxide. In the neutralization procedure a preliminary pH adjustment to 3.5–4.2 is made to precipitate and remove iron if it exceeds specifications. Phosphate, if present, is also removed in this step as iron phosphate. Uranium precipitation is then accomplished at a pH of 6.5–8.0. Since the cations used (Na^+, M^{2+}, or NH_4^+) contaminate the product by formation of insoluble polyuranates, the choice of precipitant will depend on cost, physical nature of the precipitate formed, product specifications, etc. Most U.S. plants now use ammonia, which can be removed by heating of the product, but there is also some use of magnesia. The peroxide precipitation process is more specific although the cost is somewhat higher, a higher-purity product is obtained. Ferric ions must be removed to a concentration less than 0.5 g L^{-1} in order to prevent catalytic decomposition of hydrogen peroxide in a preliminary precipitation step; alternatively the decomposition is prevented by precipitation from very cold solutions or by complexing the iron. The precipitates ('yellow cake') are dried, and in the case of the ammonia, precipitated material of composition approximately $(NH_4)_2U_2O_7$ (ammonium diuranate) may be heated to form U_3O_8 or UO_3, depending on

temperature. The magnesium and sodium polyuranates are stable to low-temperature calcination.

Precipitation from alkaline solution is carried out with either clarified carbonate leach solution or with alkaline eluting or stripping solutions from ion exchange or solvent extraction. The three methods include addition of strong base, acidification followed by CO_2 removal and neutralization, and reduction to U(IV). The latter method is the only one capable of direct recovery of any vanadium present; the other ones do not result in complete recovery or complete separation. Sodium hydroxide does not completely precipitate uranium from carbonate solution; despite this, the filtrate is recarbonated and recycled. The product consists of sodium polyuranates. Acidification, carbon dioxide removal by boiling, and neutralization (usually with ammonia or magnesia) is preferred for the high-uranium-concentration carbonate strip solutions from solvent extraction since the volume is low and recycling of reagents is not so important. Reduction of uranyl(VI) carbonate solutions results in precipitation of hydrated U(IV) oxide. Reduction methods include hydrogen reduction under pressure in the range 100–200°C with appropriate catalyst, electrolytic reduction, and sodium amalgam reduction. Vanadium is reduced and co-precipitated with uranium. Merritt (1971) has reviewed precipitation conditions, flow sheets, and plant practice in detail.

(d) By-product uranium

In South Africa, uranium is recovered as a by-product of gold recovery by conventional methods after the recovery of gold by cyanide leaching. Uranium has also been recovered as a by-product from crude phosphoric acid by both ion exchange and solvent extraction methods. In anion exchange, U(VI) is absorbed and concentrated by absorption of uranyl phosphate complexes, but resin capacities are uneconomically low. Solvent extraction has normally involved use of alkyl pyrophosphate extraction of U(IV) (Greek *et al.*, 1957), but other schemes utilize extraction of U(VI) and synergistic combinations of phosphates. References to previous work in this field are given in a paper on this subject (Deleon and Lazarević, 1971).

(e) Refining to a high-purity product

The normal product of uranium milling operations, 'yellow cake' or calcined 'yellow cake', is not sufficiently pure to be of nuclear grade and is normally further refined to produce nuclear-grade material (IAEA, 1980). There has been some emphasis on further upgrading in the mill to produce a high-grade product by using multiple stages of solvent extraction and/or ion exchange, special stripping methods, more selective precipitation methods, or combinations of these (see Merritt, 1971 for further detail). The usual refining operation has

normally been carried out either by tri(*n*-butyl)phosphate (TBP) extraction from nitric acid solutions or by distillation of uranium hexafluoride, since this is the feed for isotope enrichment plants.

Solvent extraction and fluoride volatility processes are currently used for uranium refining. A schematic flow diagram of a typical TBP/kerosene extraction process is shown in Fig. 5.6; a fluoride volatility process flow sheet is shown in Fig. 5.7. The TBP extraction from nitric acid solution makes use of the very selective tendency of actinides to form nitrate- or mixed nitrate–solvent complexes, as discussed further in Chapters 23 and 24. This process replaces the earlier and more hazardous diethyl ether extraction from nitrate solution. The extraction reaction is

$$UO_2(NO_3)_x^{2-x} + (2-x)NO_3^- + 2TBP \rightarrow UO_2(NO_3)_2(TBP)_2$$

where $x = 0$–2. Thorium is the only normally encountered impurity element having an appreciable distribution coefficient into a kerosene-TBP phase from nitric acid solution, but its distribution is sufficiently low that it can be transferred to the aqueous phase by high uranium loading of the organic phase.

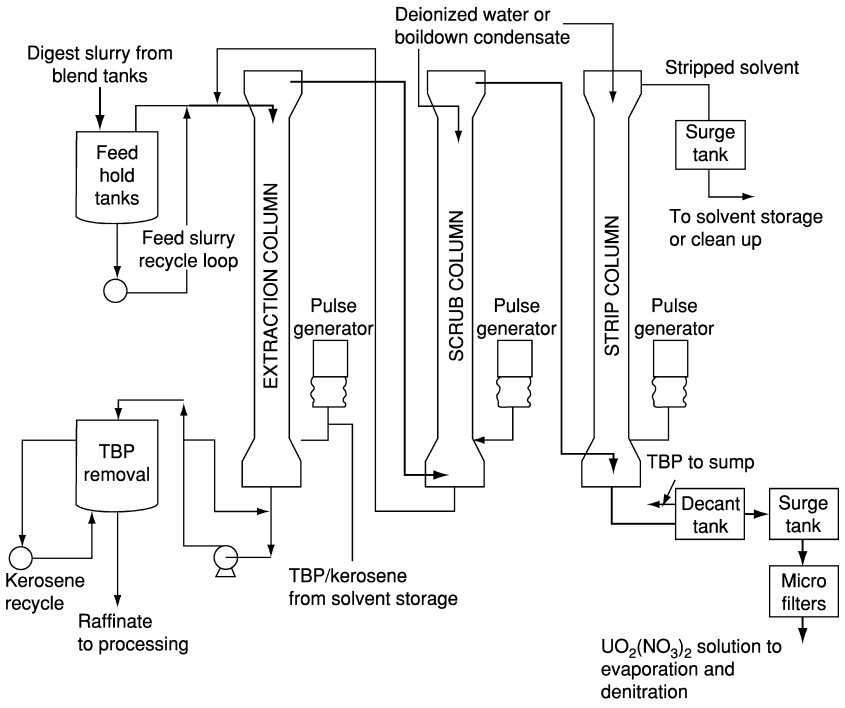

Fig. 5.6 *Schematic flow diagram: TBP/kerosene extraction system at the Fernald refinery* (*Harrington and Ruehle*, 1959).

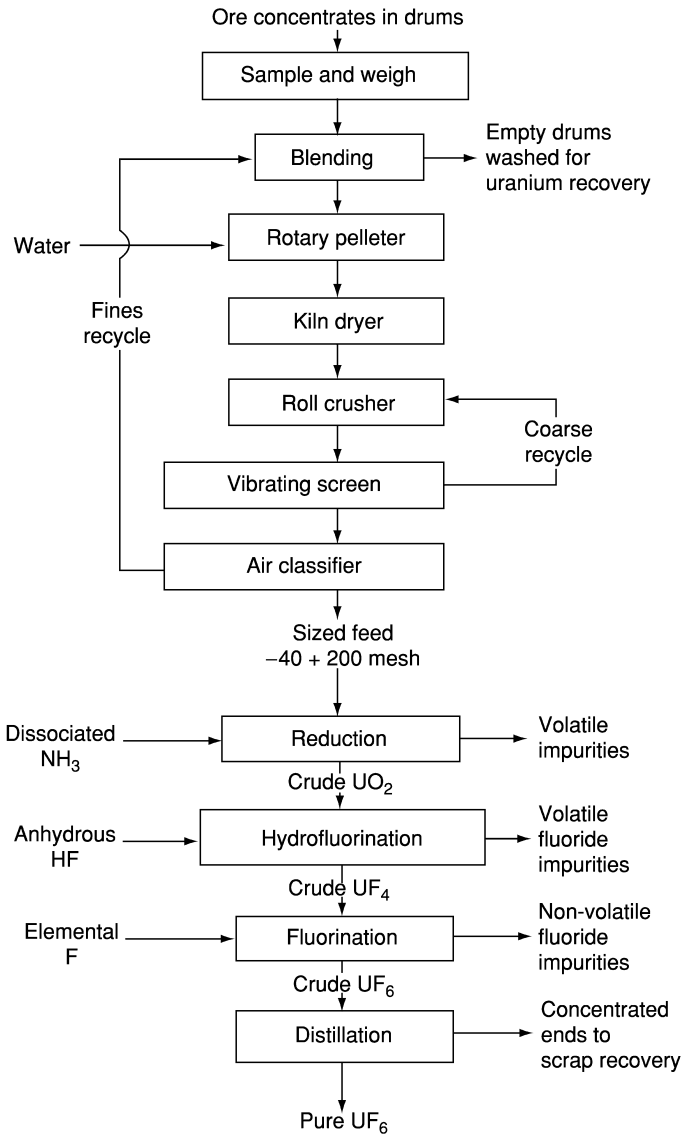

Fig. 5.7 *Overall process flow diagram for fluoride volatility process for the refining of ore concentrates* (*Ruch* et al., 1959).

The purified uranium is stripped from the organic phase with water, converted to UO_3, reduced with hydrogen to UO_2, and converted to UF_4 with hydrogen fluoride at elevated temperatures. The UF_4 can either be reduced to uranium metal for natural uranium reactors or be fluorinated to UF_6 for isotopic

enrichment for production of other types of reactor fuel. The fluoride volatility process makes use of reduction to UO_2 followed by direct fluorination, using the cheaper hydrogen fluoride to make UF_4 followed by F_2 to prepare UF_6. The UF_6 is fractionally distilled to produce a high-purity UF_6 for isotopic enrichment. The chemistry and operating conditions of the TBP refining process, the conversion to UO_3, UO_2, and finally to UF_4 are reviewed in detail in the book edited by Harrington and Ruehle (1959). Ruch *et al.* (1959) have described the refining of ore concentrates by uranium hexafluoride distillation.

Hyman *et al.* (1955) have converted uranium ore concentrates to UF_6 by means of liquid-phase fluorination using bromine trifluoride, BrF_3 (b.p. 126°C). While not applicable to raw ore, the procedure may be readily applied to concentrates. Results of experiments along these lines are summarized in Table 5.4. Since fluorine in the form of BrF_3 is rather expensive, it is worthwhile to introduce as much fluorine as possible via the inexpensive reagent hydrogen fluoride (which cannot, of course, be used to convert lower uranium fluorides to uranium hexafluoride), and then to complete the fluorination process with bromine trifluoride. This reduction of fluorine consumption may be readily accomplished by a preliminary hydrofluorination at 600°C. This treatment fluorinates silica and other gangue materials present in the ore concentrate and converts uranium(IV) to UF_4. Thus, two-thirds of the fluorine in the final UF_6 product is introduced by the relatively inexpensive hydrogen fluoride rather than by bromine trifluoride. Since uranium hexafluoride is used for the isotope separation of uranium, chlorination procedures have not received nearly as extensive investigation, because of the serious corrosion problems created by the use of chlorine at elevated temperatures.

Table 5.4 *Fluorination of various ore concentrates with BrF_3* (*Hyman* et al., 1955).

Ore concentrate			
Source	*U content* (%)	*Uranium retained by residue*[a,b] (%)	*F_2 consumption*[a,c] (cm^3 *F_2(STP) per* g U)
rand concentrate	68.1	0.16, 0.07	383, 419
rand concentrate	68.1	0.73, 0.10[d]	133, 138[d]
intermediate plant concentrate	23.3	1.45, 0.81	805, 767
intermediate plant concentrate	32.6	0.55, 1.00	552, 735

[a] Duplicate runs are given for each sample and treatment.
[b] (Grams U in residue/grams U in initial concentrate) × 100.
[c] To form UF_6 from 1 g U as metal requires 282.5 cm^3 F_2; to form UF_6 from 1 g U as UF_4 requires 94.2 cm^3 F_2.
[d] After hydrofluorination.

5.5 PROPERTIES OF FREE ATOMS AND IONS

Uranium, being one of the elements with the largest atomic number, has a very complex electronic structure. This is manifested in its spectral properties as they appear in the X-ray, UV/visible and fluorescence spectra. Details of the electronic energy levels deduced experimentally and from quantum chemical calculations are discussed in detail in Chapter 16 and in the following sections where the properties of compounds and complexes are described. The focus in Section 5.9 is on the interpretation of solid state spectra using the crystal field model and in Section 5.10 on solution spectra, including fluorescence spectroscopy of uranyl(VI) species.

5.6 URANIUM METAL

Uranium metal was used in earlier reactor systems but is now largely replaced in commercial reactors by ceramic uranium dioxide. Large-scale production of uranium metal requires elevated temperature where the high reactivity of uranium with most common refractory materials and metals makes the selection of reaction vessels a difficult problem. Finely divided uranium reacts even at room temperature with all the components of the atmosphere except the noble gases. However, contrary to the situation with titanium and zirconium, the introduction of small amounts of oxygen or nitrogen does not have an adverse effect on the mechanical properties of the metal. There are three different phases of metallic uranium below the melting point, α-, β-, and γ-uranium, each with its specific structure and physical properties. A detailed discussion of the physical properties is given in Chapter 21 on actinide metals and a short description on uranium metal and alloys in the following section.

5.6.1 Preparation of uranium metal

The element uranium is strongly electropositive, resembling aluminum and magnesium in this respect; consequently uranium metal cannot be prepared by reduction with hydrogen. Uranium metal has been prepared in a number of ways: reduction of uranium oxide with strongly electropositive elements, such as calcium, electro-deposition from molten-salt baths, thermal decomposition, decomposition of uranium halides (van Arkel de Boer 'hot wire' method), and reduction of uranium halides (UCl_3, UCl_4, UF_4) with electropositive metals (Li, Na, Mg, Ca, Ba). Only the last method is of current importance. For details, the reader is referred to two comprehensive surveys (Katz and Rabinowitch, 1951; Warner, 1953) and of older work to a review by Wilkinson (1962) and to the *Gmelin Handbook of Inorganic Chemistry* (1981a).

Both uranium tetrafluoride and tetrachloride are reducible with calcium and magnesium, while uranium dioxide can be reduced with calcium and probably magnesium. Finely divided uranium is pyrophoric and a massive metal product is therefore desired; this can be achieved by ensuring that the entire reaction mixture is fluid for a sufficiently long time for uranium metal to collect; this requires a slag with a moderately low melting point. Calcium oxide and magnesium oxide slags have melting points well above 2500°C, and are therefore less useful than calcium fluoride and magnesium fluoride, with melting points 1423°C and 1261°C, respectively. Uranium tetrachloride is very hygroscopic, and subject to oxidation in air and therefore the much more stable uranium tetrafluoride is preferred. Magnesium is the reagent of choice for reduction, since it is available in large quantities with a high degree of purity and can also be handled in air without special precautions. Details of a process based on these considerations are described by Wilhelm (1956) and in the books by Warner (1953) and by Harrington and Ruehle (1959).

For small-scale production of ^{233}U or ^{235}U in metallic state the batch size is limited by their critical mass of these isotopes and calcium is the preferred reductant. Bertino and Kirchner (1945), have described the special procedures for ^{233}U, and Patton *et al.* (1963) and Baker *et al.* (1946) those for ^{235}U.

Uranium ore concentrates are first purified by solvent extraction with TBP in kerosene as the immiscible solvent in the manner described in Section 5.4.4e. The purified uranyl nitrate is then decomposed thermally to UO_3. The trioxide is reduced with hydrogen to the dioxide, which in turn is converted to uranium tetrafluoride, 'green salt', by high-temperature hydrofluorination. The tetrafluoride is then reduced to metallic uranium with magnesium. A flow sheet of the production of uranium from ore concentrates is given in Fig. 5.8.

The temperature reached during the reduction reaction exceeds 1300°C where magnesium metal has a very high vapor pressure; hence, the reaction must be carried out in a sealed container (bomb). Such bombs are made in various sizes from standard seamless pipes. Their lengths range from 91.4 to 114.3 cm (36 to 45 in.), their diameters up to 33 cm (13 in.).

Uranium prepared by the metallothermic processes described above is of sufficient purity for most purposes. However, it may be further purified by molten-salt electrolysis (Slain, 1950; Noland and Marzano, 1953; Niedrach and Glamm, 1954; Blumenthal and Noland, 1956) using alkali or alkaline-earth chloride as electrolytes. UF_4, UCl_4, or UCl_3 are dissolved in these electrolytes. The material to be purified is used as the anode, molybdenum, or tantalum as the cathode; a diaphragm, usually of a sintered, porous ceramic material, separates the anode and the cathode.

Other methods that have been employed in uranium purification include zone melting (Whitman *et al.*, 1955; Antill, *et al.*, 1961) and hot-wire deposition (Fine *et al.*, 1945; Prescott *et al.*, 1946). Because of the low melting point of uranium, the latter method is only of limited value.

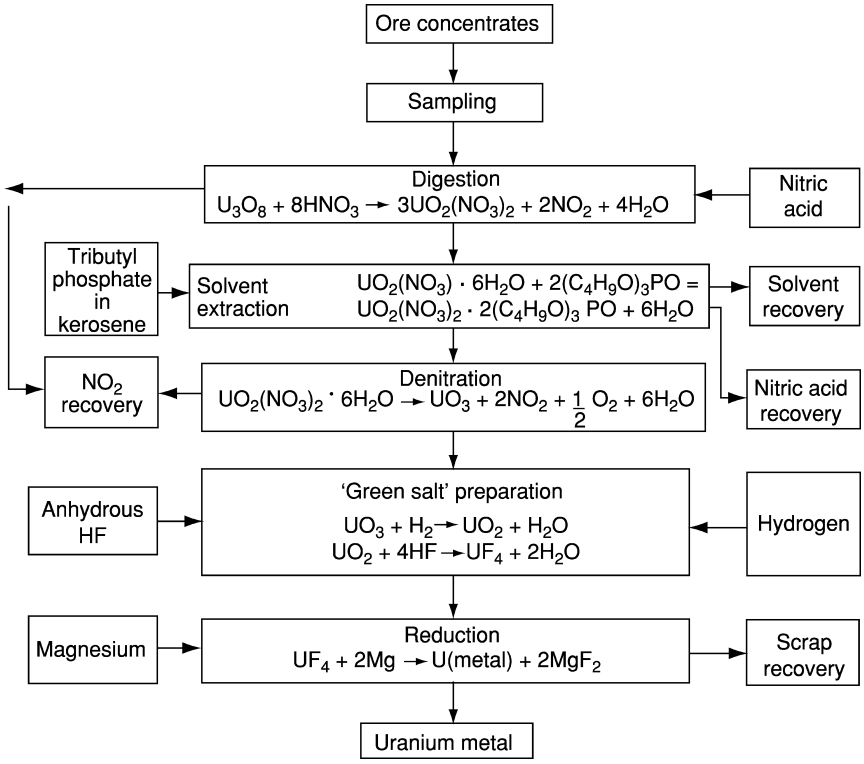

Fig. 5.8 *Flow sheet for the production of uranium metal by reduction of* UF_4 *with magnesium* (*Kelley,* 1955).

(a) Physical properties of uranium metal

(*i*) *Crystal structure*

Uranium metal has three crystalline phases below the melting point at (1134.8 ± 2.0)°C. The α-phase is the room-temperature modification of uranium; it is orthorhombic with space group No. 63, *Cmcm* and unit cell parameters $a = 2.854$ Å, $b = 5.87$ Å, and $c = 4.955$ Å (Barrett *et al.*, 1963; Lander and Müller, 1970) and one uranium at the site 4c in the space group.

The structure consists of corrugated sheets of atoms, parallel to the *ac*-plane and perpendicular to the *b*-axis. Within the sheets the atoms are tightly bonded, whereas the forces between atoms in adjacent sheets are relatively much weaker (Fig. 5.9). This arrangement is highly anisotropic and resembles the layer structures of arsenic, antimony, and bismuth. In the α-uranium structure, the U–U distances in the layer are (2.80 ± 0.05) Å and between adjacent layers

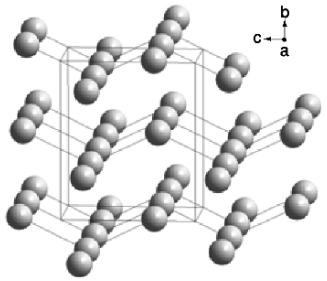

Fig. 5.9 *The structure of α-uranium from Lander and Müller* (1970). *It is a layer structure with puckered ac-layers perpendicular to the b-axis; the uranium–uranium distances in the layer are* (2.80 ± 0.05) Å *and between the layers* 3.26 Å.

3.26 Å. The physical properties of the α-phase are a reflection of its structure, e.g. the strongly anisotropic coefficient of thermal expansion. The average value of the thermal expansion coefficient over the temperature range 25–325°C is 26.5, –2.4, and 23.9 × 10^{-6} $°C^{-1}$, respectively, along *a*, *b*, and *c*. A chemical consequence of the unique orthorhombic structure of α-uranium is that the formation of solid solutions with metals of the common structure types is severely restricted.

The β-phase of uranium exists between 668 and 775°C; it has a complex structure with six crystallographically independent atoms in the tetragonal unit cell (Donohue and Einspahr, 1971). The space group is $P4_2/mnm$, $P4_2nm$, or $P4n2$, with unit cell parameters $a = 5.656$ Å and $b = c = 10.759$ Å. The lattice parameters were determined in an alloy with 1.4% chromium at 720°C, and in uranium powder in the temperature range where the phase is stable. The tetragonal lattice is a stacked layer structure with layers parallel to the *ab* plane of the unit cell at *c*/4, *c*/2, and 3*c*/4. Additional high-precision measurements are required to solve the structure completely (Donohue and Einspahr, 1971).

The γ-phase of uranium is formed at temperatures above 775°C; it has a body-centered cubic (bcc) structure with the cell parameter $a = 3.524$ Å; the phase stabilized at room temperature by the addition of molybdenum that forms an extensive series of solid solutions with γ-uranium.

(b) General properties

Foote (1956), Holden (1958), and Wilkinson and Murphy (1958) have described the physical metallurgy of uranium and Oetting *et al.* (1976) and Rand and Kubaschewski (1963) the thermodynamic properties of uranium metal.

A number of physical and thermal properties of elemental uranium are collected in Table 5.5. Uranium is not a refractory metal like chromium, molybdenum, or tungsten; it is among the densest of all metals, being exceeded in this respect only by some of the platinum metals and by α-Np and α-Pu.

Table 5.5 *Physical and thermal properties of uranium* (*Oetting* et al., 1976).

melting point	(1408 ± 2) K
vapor pressure	
1720–2340 K	$\log p(\text{atm}) = -(26210 \pm 270)\ T^{-1}$
(Pattoret *et al.*, 1964)	$+ (5.920 \pm 0.135)$
1480–2420 K	$\log p(\text{atm}) = -(25230 \pm 370)\ T^{1}$
(Ackerman and Rauh, 1969)	$+ (5.71 \pm 0.17)$
X-ray density (α-uranium)	19.04 g cm^{-3}
(Lander and Müller, 1970)	
enthalpy of sublimation	
$\Delta_f H°$(U, g, 298.15 K)	(533 ± 8) kJ mol^{-1}[a]
enthalpy	
$H°(298.15\ K) - H°(0\ K)$	6364 J mol^{-1}
entropy	
$S°(298.15\ K)$	(50.20 ± 0.20) J K^{-1} mol^{-1}[a]
heat capacity	
$C_p°(298.15\ K)$	(27.669 ± 0.050) J K^{-1} mol^{-1}
transformation points	
α to β	(942 ± 2) K
β to γ	(1049 ± 2) K
enthalpies of transformation	
$\Delta_{trs}H$ (α to β)	2791 J mol^{-1}
$\Delta_{trs}H$ (β to γ)	4757 J mol^{-1}
$\Delta_{fus}H$ (γ to liq)	9142 J mol^{-1}
enthalpy and specific heat functions	
α-uranium (298–942 K)	$H_T - H_{298} = 26.920T - 1.251 \times 10^{-3}T^2 + 8.852 \times 10^{-6}T^3 + 0.7699 \times 10^{5}T^{-1} 8407.828$ (J mol^{-1})
	$C_p = 26.920 - 2.502 \times 10^{-3}T + 26.556 \times 10^{-6}T^2 - 0.7699 \times 10^{5}T^{-2}$ (J K^{-1} mol^{-1})
β-uranium (942–1049 K)	$H_T - H_{298} = 42.920T - 14326.020$ (J mol^{-1})
	$C_p = 42.92$(J K^{-1} mol^{-1})
γ-uranium (1049–1408 K)	$H_T - H_{298} = 38.280T - 4698.690$ (J mol^{-1})
	$C_p = 38.28$ (J K^{-1} mol^{-1})
uranium (liquid)	$H_T - H_{298} = 48.650T - 10137.120$ (J mol^{-1})
	$C_p = 48.65$ (J K^{-1} mol^{-1})
thermal conductivity at 298.15 K (Ho *et al.*, 1972)	27.5 J m^{-1} s^{-1} K^{-1}
electrical resistivity (300 K) (Arajs and Colvin, 1964)	28×10^{-8} Ω m

[a] CODATA key value (Cox *et al.*, 1989).

The electrical resistivity of uranium is about 16 times higher than that of copper, 1.3 times that of lead and approximates that of hafnium (Gale and Totemeier, 2003).

An important mechanical property (Table 5.6) of uranium is its plastic character, allowing easy extrusion. The mechanical properties are very sensitive

Table 5.6 *Average mechanical properties of uranium* (*Grossman and Priceman,* 1954; *Wilkinson and Murphy,* 1958).

modulus of elasticity	1758×10^6 kPa
Poisson ratio at zero stress	0.20
shear modulus	73.1×10^6 kPa
bulk modulus	97.9×10^6 kPa
proportional limit	2.068×10^4 kPa
yield strength	
0.1% offset	1.8617×10^5 kPa
0.2% offset	2.2754×10^5 kPa
compressibility	
β_{100}	$0.758 \pm 7\%$
β_{010}	$0.296 \pm 16\%$
β_{001}	$0.141 \pm 16\%$
β_v	$1.195 \pm 6\%$

to the pre-history of the sample, and are strongly dependent on crystal orientation, fabrication, and heat treatment. Despite its plastic nature, uranium has a definite yield point with a well-defined, but very low, proportional limit. The ultimate tensile strength of uranium varies between 3.44×10^5 and 13.79×10^5 kPa, depending on the cold working and previous thermal history of the sample. Uranium rapidly loses strength at elevated temperatures, the tensile strength falling from 1.862×10^5 kPa at 150°C to 0.827×10^5 kPa at 600°C.

The Brinell hardness of rolled polycrystalline α-uranium varies between 2350 and 2750 MN m^{-2} at 23°C (Samsonov, 1968). The hardness is strongly affected by impurities. Cold working increases the hardness with up to 50%. Above 200°C, the hardness falls off rapidly. γ-Uranium is so soft as to make fabrication difficult, while the β-phase is harder and considerably more brittle than the α-phase.

(c) Magnetic susceptibility and related properties

The solid-state properties of uranium have been the subject of a relatively recent exhaustive review (Lander *et al.*, 1994). Some pertinent physical properties taken from this review are given here. Although many measurements have been performed on uranium metal, the description and full understanding of its properties is still not complete. Uranium metal is weakly paramagnetic and exhibits almost temperature-independent paramagnetism with a room temperature value of 390×10^{-9} emu mol^{-1}. (Fournier and Troć, 1985). α-Uranium exhibits an anomaly at 43 K apparent in the magnetic susceptibility data and in other measurements. This anomaly and further phase transformations observed at 37 and 23 K have been attributed to charge density waves. α-Uranium exhibits a superconducting transition at low temperatures that can be described by the Bardeen–Cooper–Schreiffer (BCS) theory. The maximal T_c value for

Table 5.7 *Components of uranium resistivity tensor at* 273 K.

References	ρ[100] (μΩ cm)	ρ[110] (μΩ cm)	ρ[110] (μΩ cm)
Brodsky *et al.* (1969)	36.1 ± 0.2	20.6 ± 0.2	26.0 ± 0.2
Berlincourt (1959)	39.4	25.5	26.2
Pascal *et al.* (1964)	39.1	23.6	30.2
Raetsky (1967)	34.7	23.6	20.3

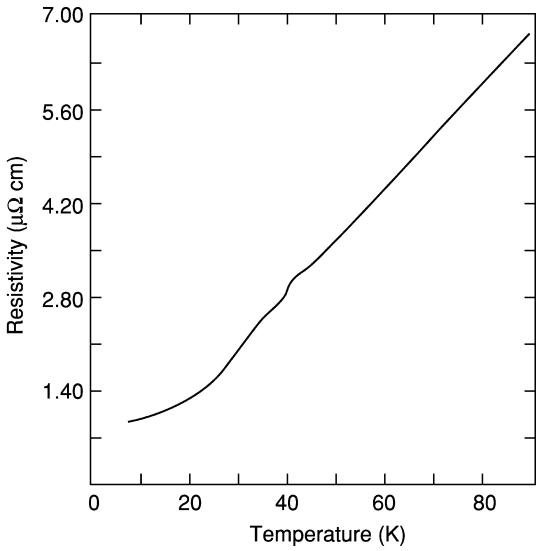

Fig. 5.10 *Resistivity–temperature curve for* α*-uranium along the* [010] *axis* (*Brodsky* et al., 1969).

α-uranium is ∼2–2.3 K at a pressure of ∼1.0–1.1 GPa. The 0.1013 MPa (1 atm) value of T_c is taken as ≤0.1 K.

(d) Electrical and related properties

The temperature dependence of the resistivity of uranium single crystals has been measured by a number of authors and the components of the resistivity tensor are given in Table 5.7. The resistivity–temperature curve for α-uranium along the [010] direction is shown in Fig. 5.10. Many other physical properties of elemental uranium have been determined, such as elastic moduli, heat capacity, de Haas-van Alphen measurements, transport properties and others. The reader is referred to Lander *et al.* (1994) and to Chapter 21 for further discussion.

Table 5.8 *Reactions of uranium with various metals* (*Saller and Rough,* 1955*; Rough and Bauer,* 1958*; Chiotti* et al., 1981). *IS and SS denote intensely studied and slightly studied, respectively*.

Class	*Behavior*		*Metals*
I	form intermetallic compounds	IS	Al, As, Au, B, Be, Bi, Cd, Co, Cu, Fe, Ga, Ge, Hg, Ir, Mn, Ni, Os, Pb, Pd, Pt, Rh, Ru, Sb, Sn
II	form solid solutions but no intermetallic compounds	SS	In, Re, Tc, Tl, Mo, Nb, Pu, Ti, Zr
III	form neither solid solutions nor intermetallic compounds	IS	Ag, Cr, Mg, Ta, Th, V, W
		SS	lanthanides, Li, Na, K, Ca, Sr, Ba

5.6.3 Uranium intermetallic compounds and alloys

The most noticeable features of the behavior of uranium with other metals are the formation of intermetallic compounds with a wide variety of alloying metals and the extensive ranges of solid solutions in α- and β-uranium. Table 5.8 summarizes the alloying behavior with the metallic elements. Saller and Rough (1955), Pfeil (1956), Rough and Bauer (1958), Hansen and Anderko (1958), Elliott (1965), Shunk (1969), and Wilkinson (1962) have given comprehensive and informative descriptions of the general behavior of the alloying elements, including numerous phase diagrams. The thermodynamics of uranium alloy systems was reviewed by Chiotti *et al*. (1981).

A large number of intermetallic compounds have been characterized by X-ray crystallographic methods and by conventional metallographic techniques. The *Gmelin Handbook of Inorganic Chemistry* gives a comprehensive review of the properties of the uranium alloys with alkali metals, alkaline earths, and elements of main groups III and IV (Gmelin, 1989, vol. B2), with transition metals of groups IB to IVB (Gmelin, 1994, vol. B3), and with transition metals of groups VB to VIIB (Gmelin, 1995a, vol. B4), including the effects of irradiation, which are also discussed in the volume on technology and uses of uranium (Gmelin, 1981a, vol. A3).

Among uranium intermetallic phases of interest may be mentioned the transition-metal compounds U_6Mn, U_6Fe, U_6Co, and U_6Ni, which are distinguished by their hard and brittle nature. Uranium forms intermetallic phases with noble metals and the phase diagrams for U–Ru, U–Rh, U–Pd, U–Os, U–Ir, and U–Pt systems have been assessed by Chiotti *et al*. (1981), a compilation that also provides information on a number other intermetallic phases. The compounds of uranium with the light platinum metals, Ru, Rh, and Pd, are of interest in the pyrometallurgical reprocessing of metallic fuels, because the

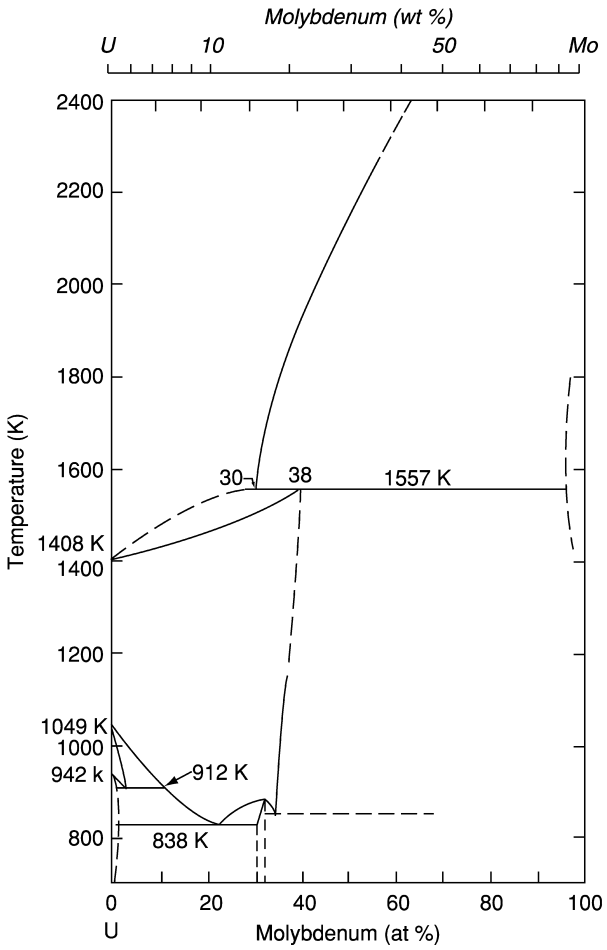

Fig. 5.11 *Phase diagram of the uranium–molybdenum system* (*Chiotti* et al., 1981).

noble metals form alloys that remain with the uranium when the fuel is processed for fission-product removal by oxidative slagging.

Elements of class III in many cases form simple eutectic systems. Molybdenum, titanium, zirconium, niobium, and plutonium form extensive solid solutions with uranium at elevated temperatures. No intermediate phases are detected for the U–Nb system, whereas the U–Mo, U–Pu, U–Ti, and U–Zr systems all show metastable phases. The uranium–molybdenum system is shown in Fig. 5.11 and illustrates the general features of the small but important class of true alloying elements. The uranium alloys have unusual physical properties that are discussed in Chapter 21.

Table 5.9 *Chemical reactions of uranium metal.*

Reactant	*Reaction temperature*[a] (°C)	*Products*
H_2	250	α- and β-UH_3
C	1800–2400	UC; U_2C_3; UC_2
N_2	700	UN, UN_2
P	1000[b]	U_3P_4
O_2	150–350	UO_2, U_3O_8
S	500	US_2
F_2	250	UF_6
Cl_2	500	UCl_4, UCl_5, UCl_6
Br_2	650	UBr_4
I_2	350	UI_3, UI_4
H_2O	100	UO_2
HF(g)	350[b]	UF_4
HCl(g)	300[b]	UCl_3
NH_3	700	$UN_{1.75}$
H_2S	500[b]	US, U_2S_3, US_2
NO	400	U_3O_8
N_2H_4	25	$UO_2(NO_3)_2 \cdot 2NO_2$
CH_4	635–900[b]	UC
CO	750	UO_2 + UC
CO_2	750	UO_2 + UC

[a] Reaction temperature with massive metal.
[b] Reaction temperature with powdered uranium (from decomposition of UH_3).

5.6.4 Chemical properties of uranium and its alloys

Uranium metal is a highly reactive substance that can react with practically all of the elements in the periodic table with the exception of the noble gases. Some of the more important chemical reactions of uranium are listed in Table 5.9.

Wilkinson (1962) has discussed in detail the corrosion of massive uranium by various gaseous agents, such as dry oxygen, dry air, water vapor, carbon monoxide, carbon dioxide, and others, as well as the pyrophoricity of this element. Totemeier (1995) has written a more recent review of the corrosion and pyrophoricity behavior of uranium (and plutonium) with oxygen, water vapor, and aqueous solutions in terms of reaction rates, products, and reaction mechanisms.

From a practical point of view, the reactions of uranium with oxygen, nitrogen, and water are probably the most significant. Uranium metal exposed to oxygen, water, or air undergoes reaction even at room temperature. The kinetics of corrosion of uranium by various reagents such as dry and moist oxygen, dry and moist air, water vapor and hydrogen, and the pyrophoricity of uranium, as well as that of plutonium, are discussed in detail in Chapter 29

devoted to handling, storage, and disposal of these elements and their relevant compounds.

Uranium dissolves very rapidly in aqueous hydrochloric acid. The reaction frequently yields considerable amounts of a black solid, presumably a hydrated uranium oxide but very likely containing some hydrogen. The addition of a small amount of fluorosilicate ion prevents the appearance of the black solid during dissolution in hydrochloric acid. Non-oxidizing acids, such as sulfuric, phosphoric, and hydrofluoric, react only very slowly with uranium, whereas nitric acid dissolves massive uranium at a moderate rate. With finely divided uranium, the dissolution in nitric acid may approach explosive violence. Uranium metal is inert to alkalis. Addition of oxidizing agents such as peroxide to sodium hydroxide solution leads to the dissolution of uranium and to the formation of ill-defined water-soluble peroxyuranates.

5.7 COMPOUNDS OF URANIUM

Ever since the discovery of uranium in 1789, its compounds have been synthesized and studied, so that a wealth of information has accumulated over the years. Much of this information may be found in the books by Katz and Rabinowitch (1951, 1958) and in the various volumes of the Supplement Series of the *Gmelin Handbook of Inorganic Chemistry* (1975–1996), which constitute probably the most comprehensive collection of information on uranium compounds.

For obvious reasons, such as lack of space, it is impossible to give a complete account of every uranium compound known to date. Rather, representative examples will be discussed with emphasis on preparation, structure, and chemical properties; information and discussion of thermodynamic properties of uranium and other actinide compounds are found in Chapter 19. In its compounds, uranium exhibits the oxidation states 3+, 4+, 5+, and 6+, with 4+ and 6+ as the predominant ones. Also, mixed valence and non-stoichiometric compounds are known.

While general features of the structures of uranium compounds, both from coordination and chemical points of view, will be discussed in Section 5.9, structures pertaining to each family of compounds will be described in the following subsections.

5.7.1 The uranium–hydrogen system

The uranium–hydrogen system has been reviewed by Katz and Rabinowitch (1951), Mallett *et al.* (1955), Libowitz (1968), Flotow *et al.* (1984), and Ward (1985). An extensive review has been given in the *Gmelin Handbook* (Gmelin, 1977, vol. C1). The kinetics of the reaction of hydrogen on uranium is discussed

in detail in Chapter 29, describing the handling, storage, and disposition of plutonium and uranium. This topic will therefore not be developed here.

(a) Preparative methods

β-UH_3 forms rapidly as fine black or dark gray powder when uranium turnings or powder, as well as large massive lumps, are heated to 250°C in a vacuum followed by the introduction of H_2 gas into the reaction system (Spedding *et al.*, 1949; Libowitz and Gibb. Jr, 1957). Crystalline β-UH_3 may be prepared as gray, fibrous crystals at 30 atm H_2 and 600–700°C in an autoclave using a uranium nitride crucible as the primary container inside the pressure vessel.

α-UH_3 can only be prepared by slow reaction at temperatures below about −80°C. The α-phase is unstable, and the products are usually a mixture with more than 50% β-UH_3 (Mulford *et al.*, 1954; Abraham and Flotow, 1955). Purer α-UH_3 has been obtained by the diffusion method: Fine reactive uranium metal powder, formed by thermal decomposition of β-UH_3, was kept below −78°C in an Ar (or He) filled cryostat at a pressure of 0.25–0.40 atm, to which H_2 was introduced with an adequately low rate (reaction period: 20 days). More than 80% of the product was α-UH_3 (Wicke and Otto, 1962).

(b) Crystal structures

α-UH_3 is cubic with space group *Pm*3*n*. Two uranium atoms occupy (0,0,0) and (1/2,1/2,1/2), and six hydrogen atoms ±(1/4,0,1/2), ±(1/2,1/4,0), and ±(0,1/2,1/4) positions. The crystallographic data are listed in Table 5.10.

β-UH_3 also has a cubic structure with space group *Pm*3*n*, the same as in α-UH_3, but with different atom positions, $2U_I$ in (0,0,0) and (1/2,1/2,1/2), and

Table 5.10 *Crystallographic data of uranium hydrides.*

Compound	*Symmetry*	*Space group*	*a* (Å)	*z*	*X-ray density* (g cm^{-3})	*References*
α-UH_3	cubic	*Pm*3*n*	4.160(1)	2	11.12	Mulford *et al.* (1954); Wicke and Otto (1962);
			4.153(2)			Caillat *et al.* (1953)
α-UD_3	cubic	*Pm*3*n*	4.150	2	11.34	Wicke and Otto (1962); Grunzweig-Genossar *et al.* (1970);
			4.147(3)		11.36	Johnson *et al.* (1976)
α-UT_3	cubic	*Pm*3*n*	4.142(2)	2	11.55	Johnson *et al.* (1976)
β-UH_3	cubic	*Pm*3*n*	6.6444(8)	8	10.92	Rundle (1947, 1951)
β-UD_3	cubic	*Pm*3*n*	6.633(3)	8	11.11	Rundle (1947, 1951)
β-UT_3	cubic	*Pm*3*n*	6.625(3)	8	11.29	Johnson *et al.* (1976)

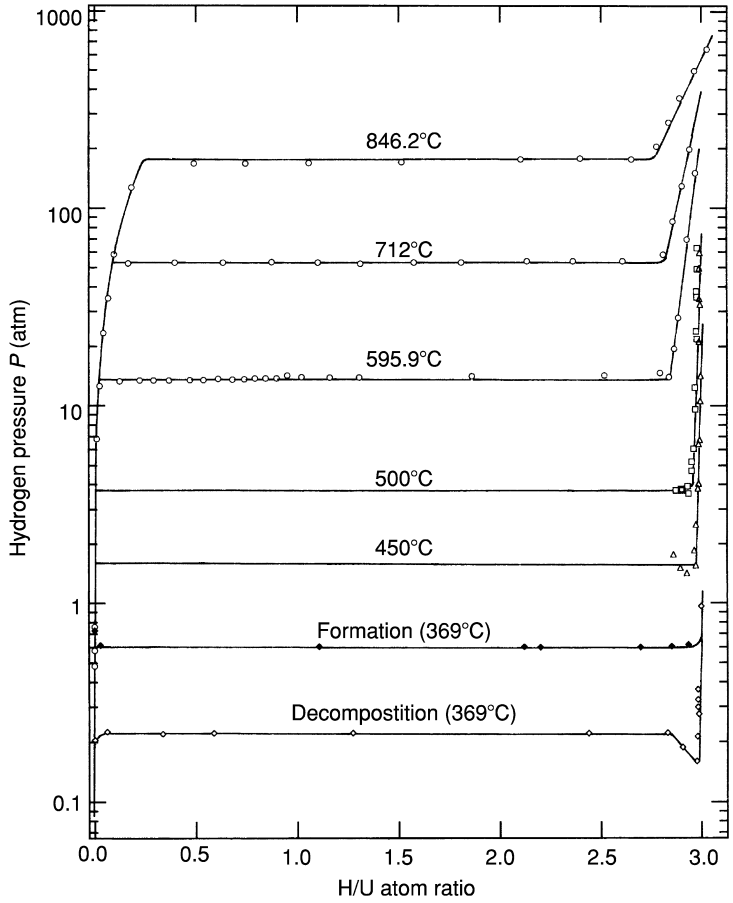

Fig. 5.12 *Hydrogen pressure versus composition isotherms for the system U–UH_3–H_2. Formation and decomposition curves at* 369°C: *Wicke and Otto* (1962); 450 *and* 500°C *curves: Libowitz and Gibb, Jr.* (1957); 595.9, 712, *and* 846.2°C *curves: Northrup, Jr.* (1975).

$6U_{II}$ in $\pm(1/4,0,1/2)$ and their equivalent positions. The hydrogen position was determined by neutron diffraction of β-UD_3 (Rundle, 1951). The hydrogen atoms are located in the 24(*k*) position, where each hydrogen atom is equidistant from four uranium neighbors within the experimental error, i.e., $12H_I$ in $\pm(5/16,0,\pm5/32)$ and $12H_{II}$ in $\pm(11/32,\pm1/2,3/16)$.

(c) Phase relations and dissociation pressures

A pressure–composition (isotherm) diagram of the U–UH_3–H_2 system is shown in Fig. 5.12; the region of the existence of α-hydride phase is not given because this phase is unstable and transforms irreversibly to β-UH_3 at higher

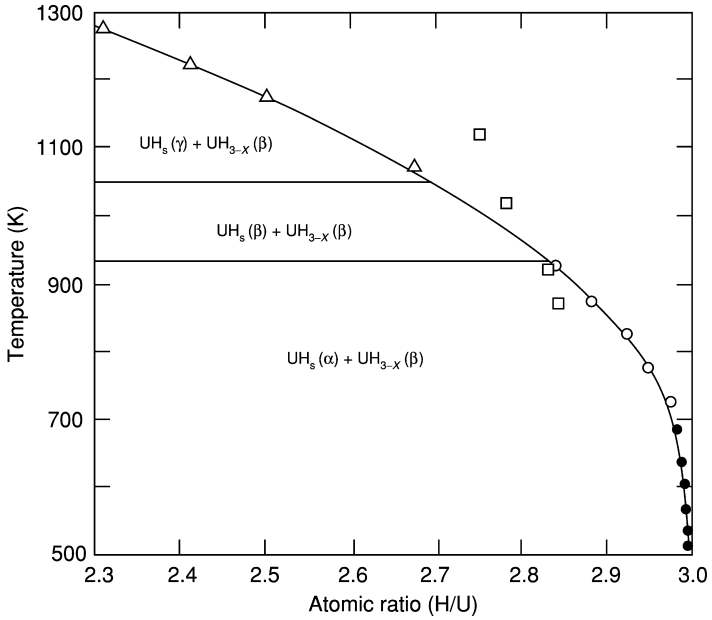

Fig. 5.13 *Phase diagram of the uranium–hydrogen system in the range H/U* = 2.3–3.0 (*from Flotow* et al., 1984). *UH_s (α, β, and γ) represent uranium metal phases (α, β, and γ), respectively, with dissolved hydrogen.* •: *Besson and Chevallier* (1964); ○: *Libowitz and Gibb, Jr.* (1957); □: *Northrup, Jr.* (1975); △: *Lakner* (1978). *Reproduced by the permission of the Atomic Energy Agency, Vienna.*

temperatures. The equilibrium H_2 pressure over α-UH_3 is much higher than that over β-UH_3, but no quantitative data are available. The rate of the α → β transformation is relatively low; α-UH_3 changes to β-UH_3 in a few hours at 250°C (Wicke and Otto, 1962).

The β-hydride phase, β-UH_{3-x}, has a relatively wide range of hydrogen hypostoichiometry at higher temperatures. The slight hyperstoichiometry at 846.2°C shown in Fig. 5.12 is an experimental artefact caused by hydrogen permeation from the sample vessel (Northrup, Jr., 1975).

Fig. 5.13 shows the hypostoichiometric range for uranium trihydride up to 1300 K (Flotow *et al.*, 1984). At 1280 K, the lower limit of the β-hydride phase attains to $UH_{2.3}$.

The solubility of hydrogen in uranium metal increases with increasing temperature (Fig. 5.12). The data determined by Mallett and Trzeciak (1958) obey Sieverts law.

$$\alpha\text{-U: } \log S(\mathrm{H/U}) = 1/2 \log p_{\mathrm{H_2}}(\mathrm{atm}) - 2.874 - 388\, T^{-1} \quad (T < 942\,\mathrm{K}),$$
$$\beta\text{-U: } \log S(\mathrm{H/U}) = 1/2 \log p_{\mathrm{H_2}}(\mathrm{atm}) - 1.778 - 892\, T^{-1} \quad (942 < T < 1049\,\mathrm{K}),$$
$$\gamma\text{-U: } \log S(\mathrm{H/U}) = 1/2 \log p_{\mathrm{H_2}}(\mathrm{atm}) - 2.238 - 227\, T^{-1} \quad (1049 < T < 1408\,\mathrm{K}),$$
$$\text{Liquid U: } \log S(\mathrm{H/U}) = 1/2 \log p_{\mathrm{H_2}}(\mathrm{atm}) - 1.760 - 587\, T^{-1} \quad (T > 1408\,\mathrm{K}),$$

where S is the solubility measured as the atom ratio. It may be noteworthy that finely divided uranium chemisorbs much larger amounts of hydrogen than those given by the previous equations (e.g. about 100 times larger at 295°C and 0.15 mmHg H_2).

Below 400°C the hydrogen pressure for formation of hydrides is not the same as that for the decomposition in the region of two solid phases (plateau region). Spedding *et al.* (1949) reported that the decomposition and formation pressures at 357°C were 0.176 and 0.188 atm, respectively. Wicke and Otto (1962) indicated that this difference is 170% at 369°C as shown in Fig. 5.12. Various explanations of the hysteresis and the dip in the decomposition process have been proposed (Libowitz, 1968; Condon and Larson, 1973); there is a possibility that traces of oxygen play a role. Using very pure uranium samples, no evidence of hysteresis was found and the time to attain equilibrium was quite short (Meusemann and von Erichsen, 1973; Condon, 1980).

The plateau hydrogen pressures are given by the equation

$$\ln p(\text{atm}) = A - BT^{-1}$$

where $A = 14.55$ and $B = 10233$ for UH_3 in the temperature range 298–942 K (Chiotti, 1980). For uranium trideuteride, UD_3, Flotow *et al.* (1984) assessed the measured data by Spedding *et al.* (1949), Wicke and Otto (1962), Destriau and Sériot (1962), and Carlson (1975), and recommended the values $A = 15.046$ and $B = 10362$ (500–800 K), which were obtained by averaging the results of Spedding *et al.* (1949) and Wicke and Otto (1962). The data for uranium tritritide, UT_3, are meager. The recommended A and B values (Flotow *et al.*, 1984) are those obtained by averaging the results of Flotow and Abraham (1951) and of Carlson (1975); they are $A = 14.57$ and $B = 9797$ in the temperature range 600–800 K. The above equilibrium pressures are considerably lower than the pressures derived from calorimetric data for UH_3, UD_3, and UT_3 (Flotow *et al.*, 1984).

(d) Thermodynamic properties

The heat capacity, entropy, and enthalpy of formation of UH_3, UD_3, and UT_3 (β forms) at 298 K are listed in Table 5.11.

Table 5.11 *Heat capacity, entropy, and enthalpy of formation of β-UH_3, β-UD_3, and β-UT_3 at* 298.15 K (*Flotow* et al., 1984).

Compound	C_p°(298.15 K) ($JK^{-1}mol^{-1}$)	S°(298.15 K) ($JK^{-1}mol^{-1}$)	$\Delta_f H^\circ$ (298.15K) ($kJ\ mol^{-1}$)
β-UH_3	49.29 ± 0.08	63.68 ± 0.13	– 126.98 ± 0.13
β-UD_3	64.98 ± 0.08	71.76 ± 0.13	– 129.79 ± 0.13
β-UT_3	74.43 ± 0.75	79.08 ± 0.79	–130.29 ± 0.21

Flotow and Osborne (1967) and Flotow *et al.* (1959) have measured the low-temperature heat capacity of $UH_3(\beta)$ from 1.4 to 23 K and from 5 to 350 K, respectively. Abraham *et al.* (1960) have reported the low-temperature heat capacity of UD_3 from 5 to 350 K and Ward *et al.* (1979) that from 4 to 17 K.

Although no experimental heat capacity data have been published for $UT_3(\beta)$, Flotow *et al.* (1984) obtained the estimated C_p values using semiempirical equations to estimate the optical mode contributions of the hydrogen lattice vibrations. Abraham *et al.* (1960) found that the sum of the lattice heat capacity associated with the acoustic modes, the electronic heat capacity, and the magnetic heat capacity, agreed within 0.08 $JK^{-1}mol^{-1}$ for $UH_3(\beta)$ and $UD_3(\beta)$, which means that this part of heat capacity is virtually the same for UH_3, UD_3, and UT_3. Moreover, they showed that this could be represented by a linear function of temperature. On this basis, Flotow *et al.* (1984) calculated the optical mode contributions of UT_3 by using the Einstein heat capacity function to estimate the heat capacity of UT_3.

The heat capacity of UH_3 and UD_3 up to 800 K was also obtained by this method as shown in Fig. 5.14. The sharp anomaly in the vicinity of 170 K is due to the ferromagnetic–paramagnetic transition of the β-hydride phases.

(e) Electrical resistivity

The electrical resistivity, ρ, of β-hydride increases with increasing temperature as in metals. Ward *et al.* (1979) measured the electrical resistivity of β-UD_3 from 2.4 to 300 K. The ρ vs T curve has an anomaly due to a magnetic transition at 166 K. These resistivities are in good agreement with the unpublished data of Flotow for β-UH_3 communicated to Grunzweig-Genossar *et al.* (1970). The resistivity of β-hydride is about ten times higher than that of uranium metal.

(f) Magnetic properties and the nature of bonding

The history of magnetic studies of uranium hydrides is described in the review of Troć and Suski (1995). In the earlier work, α-UH_3 was considered to be ferromagnetic at low temperatures with T_C the same as, or close to that of β-UH_3. However, the neutron diffraction study on α-UD_3 (Lawson *et al.*, 1991) revealed the α-hydride phase to be non-magnetic at least above 15 K, i.e. the apparent ferromagnetism was due to β-hydride impurities in the α-hydride samples.

β-Hydride is ferromagnetic at low temperatures. The magnetic data for β-UH_3 and β-UD_3 are shown in Table 5.12. At the Curie temperature, the λ-type heat capacity anomaly has also been observed at 170.5 and 167.6 K for β-UH_3 and β-UD_3, respectively (Fig. 5.14). The lower Curie temperature in the deuteride is associated with the somewhat shorter U–U distance, resulting in a change of the exchange integrals for the Weiss field (Ward, 1985). The electrical

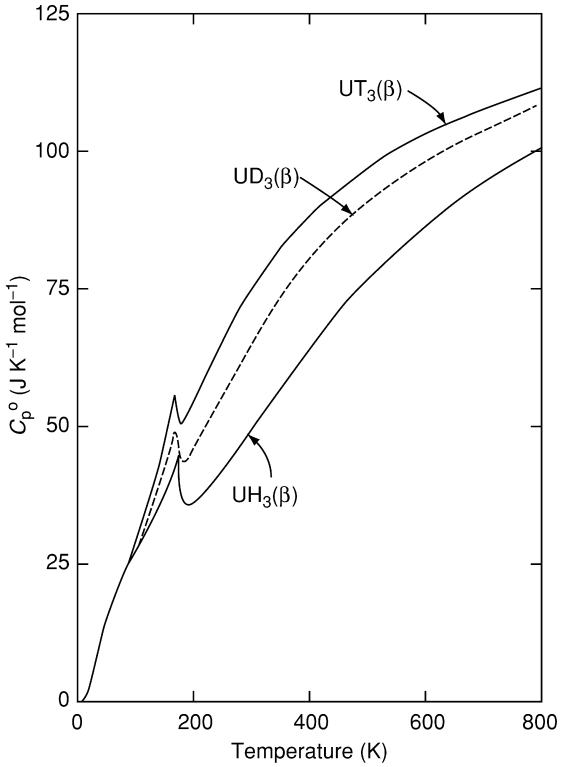

Fig. 5.14 *Heat capacities of $UH_3(\beta)$, $UD_3(\beta)$, and $UT_3(\beta)$* (*Flotow* et al., 1984).

resistivity for β-UD_3 changed at the Curie temperature (166 K) (Ward *et al.*, 1979). Andreev *et al.* (1998) report that the Curie temperature of β-UH_3 decreases with increasing external pressure from 175 K (0 kbar) to 169 K (8 kbar). In Table 5.12, the saturation uranium magnetic moments obtained by neutron diffraction are far larger than those obtained by magnetization measurements, possibly a result of a large magnetic anisotropy in β-UH_3 (Bartscher *et al.*, 1985). The neutron diffraction studies of β-UH_3 carried out at the ferromagnetic temperatures revealed that the two U_I and six U_{II} atoms, which occupy different crystallographic positions in space group *Pm*3*n*, are magnetically equivalent giving the same magnetic moment; no (110) reflection peak was observed in the diffraction patterns (Wilkinson *et al.*, 1955; Bartscher *et al.*, 1985; Lawson *et al.*, 1990). Increased external pressure lowers the saturation magnetic moment of uranium from $1\mu_B$(0 kbar) to $0.985\mu_B$(10 kbar) at 4.2 K (Andreev *et al.*, 1998). The effective uranium moments in Table 5.12 are those obtained from the slope of the Curie–Weiss curves in the paramagnetic range of temperatures.

Table 5.12 *Magnetic data for β-UH_3 and β-UD_3.*

Hydride	*Ferromagnetic Curie temperature* T_C(K)	*Paramagnetic Curie temperature* θ_p(K)	*Saturation uranium moment* $\mu_S(\mu_B)$	*Effective paramagnetic uranium moment* $\mu_{eff}(\mu_B)$	*References*
β-UH_3	174	174	0.65 (80 K)	2.44	Trzebiatowski *et al.* (1954)
	173		0.9 (78 K)	2.79	Gruen (1955)
	181	173	0.9 (2.1 T, 4.2 K)		Lin and Kaufmann (1956)
	168	180	1.18 (6 T, 1.3 K)		Henry (1958)
	181	176	0.7	2.24	Karchevskii and Buryak (1962)
	175		1.0 (40 T, 4.2 K)		Andreev *et al.* (1998)
	175		1.39 (ND)		Shull and Wilkinson (1955)
			1.45 (NMR)		Barash *et al.* (1984)
			1.54 (ND)		Lawson *et al.* (1990)
β-UD_3	172	172		2.44	Trzebiatowski *et al.* (1954)
			0.98 (6 T, 1.3 K)		Henry (1958)
	177.5	175.2		2.24	Karchevskii and Buryak (1962)
		166	0.87 (5.34 T)	2.26	Ward *et al.* (1979)
			1.39 (ND)		Wilkinson *et al.* (1955)
	178		1.45 (ND, 10 K)		Bartscher *et al.* (1985)

ND: neutron diffraction.

Grunzweig-Genossar *et al.* (1970) assume that uranium is composed of uranium ions and protons (deuterons) in a high-density interacting electron gas. The magnetic moments arise from 5f electrons. The uranium ions are magnetically coupled through the polarized conduction electrons by the RKKY interaction, which can explain the ferromagnetic ordering below ~180 K and the large Knight shift obtained by their nuclear magnetic resonance (NMR) measurement, i.e. $K = 0.40\chi_M$, where χ_M is the molar magnetic susceptibility. The second moment and line-shape data suggest that the 5f electrons ($Z \sim 2.5$ conduction electrons per uranium atom) are localized and do not form a band as in metallic uranium.

Cinader *et al.* (1973) measured the NMR spin-lattice relaxation time in the paramagnetic state at 189–700 K. In addition to the time-dependent dipolar interaction through hydrogen diffusion, the relaxation time was dependent on (1) the direct interaction between the conduction electrons and the protons (deuterons) causing Korringa relaxation, and (2) the indirect RKKY (Ruderman-Kittel-Kasuya-Yosida) interaction. The density of states of the s-type conduction electrons at the Fermi level was 1.65 states per eV. A model with a spherical Fermi surface and free electron behavior in the RKKY interaction, results in U^{3+} and H^- as the ionic species.

(g) Chemical properties

Uranium hydride is very reactive and, in most respects its reactions resemble those of the finely divided uranium metal; in fact, reactions that occur at temperatures where the hydrogen decomposition pressures are high may be those of the metal. Uranium hydride ignites spontaneously in air, but gradual oxidation at low oxygen pressures at room temperature results in the formation of a protective film of oxide on the surface of hydride particles, which prevents the hydride from ignition. Adsorption of a variety of electron-pair-donor compounds can reduce the pyrophoric properties.

Uranium hydride is used as a starting material in many reactions, including the preparation of finely divided uranium metal. Hydrogen, deuterium, and tritium may be stored as UH_3, UD_3, and UT_3, respectively. These gases are released when the compounds are heated to the decomposition temperatures. Gram quantities of UH_3 reacts slowly with water, but larger samples react violently and produce high temperatures (Newton *et al.*, 1949). UH_3 reacts slowly with solution of non-oxidizing acids such as HCl and weak acids such as CH_3COOH, but vigorously with HNO_3. UH_3 reacts with H_2SO_4 to form S, SO_2, and H_2S, and with H_3PO_4 to form UPO_4. UH_3 is unstable in strong bases and reduces aqueous solutions of $AgNO_3$ and $HgCl_2$. At elevated temperatures, UH_3 reacts with O_2, hydrogen halides, H_2S, HCN, NH_3, N_2, CO_2, CH_4, and C_2H_2 (acetylene), but not with liquid hydrocarbons and chlorinated solvents, although an explosive reaction occurs with CCl_4. The reactions of UH_3 with most compounds are thermodynamically favored, and many cases where the

Table 5.13 *Reactions of uranium hydride.*

Reagent	*Reaction temperature* (°C)	*Product*
O_2	ignites at room temperature	U_3O_8
H_2O	350	UO_2
H_2S	400–500	US_2
N_2	250	U_2N_3
NH_3	250	U_2N_3
PH_3	400	UP
Cl_2	250	UCl_4
CCl_4	250 possibility of explosion at 25°C	UCl_4
HCl	250–300	UCl_3
HF	200–400	UF_4
Br_2	300–350	UBr_4
HBr	300	UBr_3
CO_2	300	UO_2

reactions do not proceed are a result of kinetic inhibition (Haschke, 1991). Typical reactions of uranium hydride are given in Table 5.13.

(h) Other uranium hydride compounds

(*i*) *Uranium*(IV) *borohydride,* $U(BH_4)_4$

The volatile $U(BH_4)_4$ is obtained as dark green crystals by the reaction

$$UF_4 + 2Al(BH_4)_3 \rightarrow U(BH_4)_4 + 2Al(BH_4)F_2.$$

Purification is made by vacuum sublimation (Schlesinger and Brown, 1953).

$U(BH_4)_4$ is tetragonal with space group $P4_32_12$ having four formula units in the unit cell. The lattice parameters are $a = (7.49 \pm 0.01)$ Å and $c = (13.24 \pm 0.01)$ Å. The positions of U, B, and H have been determined by X-ray and neutron diffraction analyses (Bernstein *et al.*, 1972a,b).

In vacuo and in an inert-gas atmosphere, $U(BH_4)_4$ is fairly stable, but it is immediately decomposed by oxygen or moisture. Bernstein and Keiderling (1973) determined the molecular structure from optical and nuclear magnetic resonance spectra.

The vapor pressure of $U(BH_4)_4$ is given by the equation

$$\log p(\text{mmHg}) = 13.354 - 4265T^{-1}.$$

$U(BH_4)_3$ is a red solid, which has been observed as a by-product in the synthesis of $U(BH_4)_4$. Because of its pyrophoric properties, it has not been well characterized (Schlesinger and Brown, 1953).

(*ii*) *$UNiAlH_y$ and related compounds*

The intermetallic compounds UXAl (X = Ni, Co, Mn) absorb hydrogen on heating in the temperature range 20–250°C at high H_2 pressures. The maximum hydrogen content attained at 20°C corresponds to $UNiAlH_{2.74}$ ($p_{H_2} = 55$ atm), $UCoAlH_{1.2}$ (40 atm), and $UMnAlH_{0.15}$ (40 atm) (Drulis *et al.*, 1982). UNiAl absorbs the largest amount of hydrogen in these compounds, though lower maximum hydrogen absorption values have been reported, at room temperature and 70 atm viz. $UNiAlH_{2.5}$ (Jacob *et al.*, 1984), and $UNiAlD_{2.2}$ at 30°C and 50 atm D_2 (Yamamoto *et al.*, 1998). The lower limit of the hydride phase is $y = 0.7$–0.8 (Yamamoto *et al.*, 1994, 1998; Yamanaka *et al.*, 1999). The hydrogen solubility in the UNiAl metal appears to obey Sieverts law in the hydrogen concentration region below 0.02 H per formula unit UNiAl (Yamanaka *et al.*, 1999).

The symmetry and space group of $UNiAlH_y$ are the same as those for UNiAl. The structure consists of alternate planes containing three Al (in 3f) and two Ni (2c) atoms at $z = 0$ and three U (3g) and one Ni (1b) atoms at $z = 1/2$. The hydrogen atoms are located in the center of one of the adjacent U_3Ni tetrahedra, in the bipyramid U_3Al_2, and in the bipyramid Al_3Ni_2 (Kolomiets *et al.*, 2000). The lattice parameter a increases whereas b decreases slightly with increasing value of y (Drulis *et al.*, 1982; Jacob *et al.*, 1984; Yamamoto *et al.*, 1994; Yamanaka *et al.*, 1999; Kolomiets *et al.*, 2000). This variation, expressed in Å, is approximately represented by the equations $a = 6.736 + 0.187y$ and $c = 4.037 - 0.028y$ in the range $0.8 \leq y \leq 2.7$. The hydrogenation of UNiAl is accompanied by a volume change. The quotient $\Delta V/V$ attains a value of 0.124 for both hydride ($y = 2.3$) and deuteride ($y = 2.1$). In addition, the X-ray diffraction peak intensities indicate a positional shift of the U atoms from (0.572, 0, 1/2) in UNiAl to (2/3, 0, 1/2) in $UNiAlH_{2.3}$. These changes are supposed to favor the accommodation of a larger amount of hydrogen (Kolomiets *et al.*, 2000).

The desorption isotherms of $UNiAlH_y$ have two sloping plateaus, which suggests the existence of two hydride phases (Jacob *et al.*, 1984). The partial molar enthalpy and entropy of hydrogen for the non-stoichiometric $UNiAlH_y$ varies with the y value. $\Delta\bar{H}(H_2)$ and $\Delta\bar{S}(H_2)$ were –53 kJ (mol H_2)$^{-1}$ and –88 J K^{-1} (mol H_2)$^{-1}$, respectively, for $UNiAlH_{1.35}$, and –41 kJ (mol H_2)$^{-1}$ and –95 J K^{-1} (mol H_2)$^{-1}$ for $UNiAlH_{2.30}$ (Drulis *et al.*, 1982). The values measured by Jacob *et al.* (1984) are comparable with the above values: $\Delta\bar{H}(H_2)$ and $\Delta\bar{S}(H_2)$ were −64 kJ (mol H_2)$^{-1}$ and –90 J K^{-1} (mol H_2)$^{-1}$, respectively, for $UNiAlH^{1.2}$, and −47 kJ (mol H_2)$^{-1}$ and –94 J K^{-1} (mol H_2)$^{-1}$, respectively, for $UNiAlH_{2.0}$.

The incorporation of hydrogen into UNiAl leads to a large increase in the antiferromagnetic ordering temperature from 19 K to 90–100 K. The transition temperatures for $UNiAlH_{2.3}$ and $UNiAlD_{2.1}$ are 99 and 94 K, respectively (Kolomiets *et al.*, 2000). According to Zogal *et al.* (1984), $UNiAlH_{1.9}$ has

magnetic transitions at 122 and 34 K, where the second transition possibly refers to the hydride at the lower phase limit. The magnetic susceptibility in the paramagnetic region is represented by the modified Curie–Weiss equation. The effective moment, μ_{eff}, the paramagnetic Curie temperature, θ_{p}, and the temperature-independent susceptibility, χ_{o}, are 2.42 μ_{B}/f.u., –42 K and 7×10^{-9} m^3 mol^{-1}, respectively, for $UNiAlH_{2.3}$. The values are 2.43 μ_{B}/f.u., –50 K and 8×10^{-9} m^3 mol^{-1}, respectively, for $UNiAlD_{2.1}$ (Kolomiets *et al.*, 2000).

$U(Fe_{1-x}Ni_x)Al$ with $x \geq 0.7$ absorbs hydrogen forming $U(Fe_{1-x}Ni_x)AlH_y$ hydrides. Raj *et al.* (2000) studied the magnetic properties of $U(Fe_{0.3}Ni_{0.7})AlH_y$, and found that no other hydride phase was formed above or below $y = 0.8$. $U(Fe_{0.3}Ni_{0.7})AlH_y$ is ferromagnetic with $T_{\text{C}} = 15$ K ($y = 0$) and 90 K ($y = 0.8$). Magnetization of $U(Fe_{0.3}Ni_{0.7})Al$ at 5.5 T gave a saturation moment of $\cong 0.3\mu_{\text{B}}$/f.u. The value for the hydride ($y = 0.8$) was much higher, $\cong 0.9\mu_{\text{B}}$/f.u., indicating considerable increase in the ferromagnetic correlations. Other intermetallic hydrides, e.g. $U_5Ni_4PdH_{1.0}$ (Drulis *et al.*, 1982), $UCoH_{2.7}$ (Andreev *et al.*, 1986; Yamamoto *et al.*, 1991), and UTi_2D_y (Yamamoto *et al.*, 1995) have also been studied.

5.7.2 The uranium–oxygen system

(a) Binary uranium oxides

(*i*) *Preparative methods*

Comprehensive information on the preparation of actinide oxides including uranium oxides is given in a monograph by Morss (1991).

UO(*s*)

Although UO gas is one of the main species over U(l)+UO_{2-x} at high temperatures, solid UO ($Fm\bar{3}m$, $a = 4.92$ Å) with NaCl-type structure is very unstable and its formation has not been definitely established. When UO_2 was heated with uranium metal at high temperatures, a fcc phase was produced only in cases of considerable carbon contamination (Rundle *et al.*, 1948). Carbon is thought to promote the reaction. It is possible that UC or UN must be present for the formation of the UO phase (Rundle *et al.*, 1948; Cordfunke, 1969).

UO_2(*s*)

UO_2 is prepared by hydrogen reduction of UO_3 or U_3O_8 between 800 and 1100°C (Katz and Rabinowitch, 1951; Belle, 1961; Wedermeyer, 1984). The H_2 gas used for this purpose should not contain impurity of O_2 in order to avoid oxidation to hyperstoichiometric UO_{2+x}, which occurs on cooling at temperatures below 300°C. The UO_2 pellets for reactor fuel are reduced at much higher temperatures around 1700°C in order to approach the theoretical density. For laboratory use, other reductants such as CO, C, CH_4, and C_2H_5OH may be

used, but they offer no advantages over H_2 (Katz and Rabinowitch, 1951; Wedermeyer, 1984; Roberts and Walter, 1966). NH_3 is not suitable (Belle, 1961). Commercial methods of UO_2 synthesis start from the peroxide $UO_4 \cdot 2H_2O$, ammonium diuranate with the approximate composition $(NH_4)_2U_2O_7$ or ammonium uranyl carbonate $(NH_4)_4UO_2(CO_3)_3$ followed by air calcination at 400–500°C. Subsequent H_2 reduction at 650–800°C yields UO_2 with high surface area. The nuclear fuel pellets are produced by cold pressing of these powders, followed by sintering.

$U_4O_9(s)$

U_4O_9 can be prepared from the stoichiometric amounts of UO_2 and U_3O_8 according to the reaction $5UO_2 + U_3O_8 = 2U_4O_9$. The reactants are ground in an agate mortar and the mixture is sealed in an evacuated quartz ampoule, and then heated at 1000°C for about 2 weeks until the sample is completely homogenized. The sample is slowly cooled to room temperature over a period of 2 weeks (Gotoo and Naito, 1965; Westrum, Jr. *et al.*, 1965). U_4O_9 has three phases: α-U_4O_9 that transforms into β-U_4O_9 on heating to ~350 K, and β-U_4O_9 that transforms into γ-U_4O_9 at ~850 K (Labroche *et al.*, 2003b). These transformations are reversible.

$U_3O_7(s)$

Three polymorphs of α, β, and γ are known for U_3O_7; all of them are tetragonal. α-U_3O_7 with *c/a* ratios 0.986–0.991 is prepared by oxidizing UO_2 at temperatures below 160°C (Hoekstra *et al.*, 1961; Westrum, Jr. and Grønvold, 1962). To prepare a single phase with O/U $\approx$ 2.33, the use of reactive UO_2, which is obtained by low-temperature reduction of UO_3 by H_2, is recommended (Hoekstra *et al.*, 1961). Oxidation of UO_2 in air at 200°C yields β-U_3O_7 with *c/a* ratios between 1.027 and 1.032 (Garrido *et al.*, 2003). The oxidation of standard uranium dioxide ceases at $UO_{2.33}$ at temperatures below 200°C and no formation of U_3O_8 takes place (Hoekstra *et al.*, 1961). Allen and Tyler (1986) report that well-crystallized single-phase β-U_3O_7 was obtained by oxidation at 230°C for 16 h. The γ-U_3O_7 ($U_{16}O_{37}$) phase, which has *c/a* ratios of 1.015–1.017 and smaller O/U ratios of 2.30–2.31 (Hoekstra *et al.*, 1961; Westrum, Jr. and Grønvold, 1962; Hoekstra *et al.*, 1970; Nowicki *et al.*, 2000), is formed when U_4O_9 is oxidized at 160°C (Hoekstra *et al.*, 1961). This compound has also been prepared as a mixture with monoclinic U_8O_{19} on heating a pellet of mixed UO_2 and UO_3 at $\geq$400°C under high pressures (15–60 kbar) (Hoekstra *et al.*, 1970).

$U_2O_5(s)$

High-pressure syntheses by Hoekstra *et al.* (1970) identified three U_2O_5 phases (α-U_2O_5, β-U_2O_5 and γ-U_2O_5). α-U_2O_5 was prepared by heating a mixture of UO_2 and U_3O_8 at 400°C and 30 kbar for 8 h. At 500°C, a pressure of 15 kbar was enough to prepare α-U_2O_5. Hexagonal β-U_2O_5 is formed at 40–50 kbar pressure at temperatures higher than 800°C. Monoclinic γ-U_2O_5 was sometimes

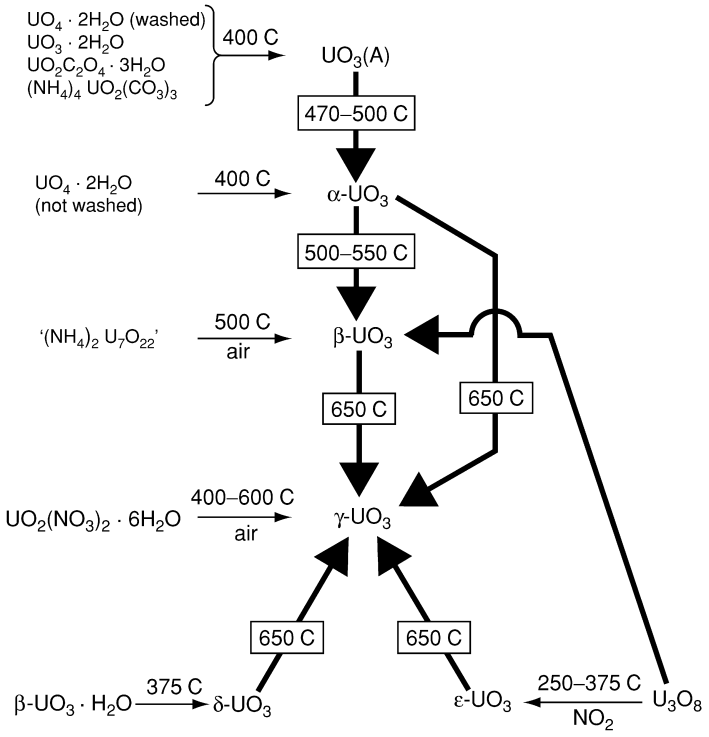

Fig. 5.15 *Flow sheet for the preparation of various UO_3 modifications: Bold lines refer to high O_2 pressure* (*Hoekstra and Siegel,* 1961; *Cordfunke*, 1969).

obtained when the UO_2 and U_3O_8 mixture was heated above 800°C at a pressure of 60 kbar.

$U_3O_8(s)$

α-U_3O_8 is prepared by oxidation of UO_2 in air at 800°C followed by slow cooling (Loopstra, 1970a). β-U_3O_8 is prepared by heating α-U_3O_8 to 1350°C in air or oxygen, followed by slow cooling (cooling rate: 100 K per day) to room temperature (Loopstra, 1970b).

$UO_3(s)$

Seven modifications are known for UO_3: A, α, β, γ, δ, ε, and ζ-UO_3. The methods of their syntheses are outlined in the flow sheet of Fig. 5.15 (Hoekstra and Siegel, 1961; Cordfunke, 1969).

Amorphous UO_3 (A-UO_3) forms when any of the compounds $UO_4 \cdot 2H_2O$ (washed with H_2O), $UO_3 \cdot 2H_2O$, $UO_2C_2O_4 \cdot 3H_2O$ and $(NH_4)_4UO_2(CO_3)_3$ is heated in air at 400°C. Because of the difficulty to remove residual traces of nitrogen and carbon, it is preferable to use either of the first two of the above

compounds (Hoekstra and Siegel, 1961). α-UO_3 is prepared by crystallization of A-UO_3 at 485°C for 4 days. The heating time can be shortened at 500°C but a pressure of 40 atm oxygen is then needed (Hoekstra and Siegel, 1961). β-UO_3 is prepared by heating 'ammonium diuranate' or uranyl nitrate rapidly in air at 450–500°C. The crystallinity of β-UO_3 is improved by keeping the sample at 500°C (not higher) for 4–6 weeks (Debets, 1966). This compound is also obtained by heating at 500–550°C under 30–40 atm O_2. γ-UO_3 is formed slowly at 500–550°C in 6–10 atm O_2. At 650°C and 40 atm O_2, all α, β, δ, and ε-UO_3 compounds convert to the γ-phase. γ-UO_3 can be prepared directly in air by heating uranyl nitrate hexahydrate to 400–600°C (Hoekstra and Siegel, 1958; Engmann and de Wolff, 1963). Stoichiometric δ-UO_3 is obtained by heating β-$UO_2(OH)_2$ (= β-$UO_3 \cdot H_2O$) at 375–400°C for more than 24 h (Hoekstra and Siegel, 1961). At 415°C, the oxygen-deficient δ-phase forms (Wait, 1955). ε-UO_3 is prepared by oxidizing U_3O_8 at 350°C in NO_2(g). The reaction goes to completion in a few seconds (Gruen *et al.*, 1951). At a temperature of 400°C, the reaction rate levels off as the stability limit of ε-UO_3 is approached (Hoekstra and Siegel, 1961). The high-pressure modification ζ-UO_3 forms at 30 kbar and 1100°C (Hoekstra *et al.*, 1970).

UO_3 hydrates

The existence of six compounds, i.e. $UO_3 \cdot 2H_2O$, α-$UO_3 \cdot 0.8H_2O$, α-$UO_2(OH)_2$, β-$UO_2(OH)_2$, γ-$UO_2(OH)_2$, and $U_3O_8(OH)_2$, has been confirmed in the UO_3–water system. $UO_3 \cdot 2H_2O$ is prepared by exposure of anhydrous UO_3 to water at 25–75°C. An alternative method is to add 0.65 g $La(OH)_3$ to 50 mL 0.2 M $UO_2(NO_3)_2$ solution. The hydroxide dissolves slowly, accompanied by an increase in solution pH from 2.2 to 4.0. Digestion of the clear solution at 55°C causes a gradual precipitation of a portion of the uranium as bright yellow crystals of $UO_3 \cdot 2H_2O$ (Hoekstra and Siegel, 1973). Water-deficient α-phase monohydrate, α-$UO_3 \cdot 0.8H_2O$, was prepared by heating $UO_3 \cdot 2H_2O$ in air at 100°C or by heating either $UO_3 \cdot 2H_2O$ or UO_3 in water at 80–200°C (Dell and Wheeler, 1963). Stoichiometric α-$UO_2(OH)_2$ (= α-$UO_3 \cdot H_2O$) was prepared in hydrothermal experiments at temperatures approaching 300°C (Harris and Taylor, 1962; Taylor, 1971).

Stoichiometric β-$UO_2(OH)_2$ (or β-$UO_3 \cdot H_2O$) is prepared by the action of water on $UO_3 \cdot 2H_2O$ or UO_3 at 200–290°C in a sealed reactor (Dawson *et al.*, 1956). It is also formed by the hydrolysis of uranyl salt solutions (cf. γ-$UO_2(OH)_2$). γ-$UO_2(OH)_2$ (or γ-$UO_3 \cdot H_2O$) is obtained when 0.65 g $La(OH)_3$ is added to 50 mL of 0.2 M $UO_2(NO_3)_2$ and subsequent heating of the solution to 80–90°C; digestion of the solution leads to slow precipitation of γ-$UO_2(OH)_2$ (Hoekstra and Siegel, 1973). There may be no region of true thermodynamic stability for the γ-phase. Continued digestion for several weeks eventually gives β-$UO_2(OH)_2$ as the sole product. $U_3O_8(OH)_2$ (= $UO_3 \cdot 1/3H_2O$ or $H_2U_3O_{10}$, i.e. hydrogen triuranate) is prepared by hydrothermal reaction of $UO_3 \cdot 2H_2O$ or UO_3 at temperatures between 300 and 400°C. Although no solid solution range

has been observed for this compound, appreciable variations in water content from 0.33 to 0.50 have been reported (Siegel *et al.*, 1972).

Uranium peroxide tetrahydrate, $UO_4 \cdot 4H_2O$, is obtained when the precipitate, grown from the uranyl nitrate solution of pH = 2 on addition of hydrogen peroxide solution, is dried at room temperature (Silverman and Sallach, 1961); the dihydrate, $UO_4 \cdot 2H_2O$, is prepared by heating $UO_4 \cdot 4H_2O$ at 90°C.

(*ii*) *Preparation of single crystals*

The basic method to prepare single crystals of UO_2 is to melt UO_2 powders. Arc melting (Brit and Anderson, 1962) and solar furnace heating (Sakurai *et al.*, 1968) techniques have been adopted for this purpose. The vapor deposition method has also been used, where an electric current was passed through a hollow cylinder of UO_2. UO_2 sublimed from the hot central part of the inner surface of the cylinder and deposited at the cooler end, forms large hemispherical single crystals of 4–12 mm (van Lierde *et al.*, 1962). Recrystallization also yields single crystals in the central part of UO_2 rod when the current is directly passed through the specimen (Nasu, 1964).

Single crystals of the length 5 cm have been prepared by means of the floating zone technique. In this case, the preheated UO_2 rods were heated by induction eddy-currents (Chapman and Clark, 1965). Robins (1961) obtained single crystals of 3 mm length by electrolysis of uranyl chloride in fused alkali chloride melts.

Formation of single crystals by chemical transport reactions has been studied by a number of researchers. Naito *et al.* (1971) examined the transport of UO_2, U_4O_9, and U_3O_8 from 1000 to 850°C in sealed quartz tubes using the transporting agents HCl, Cl_2, I_2, Br_2, and Br_2+S_2. Although the transport rate was very low in I_2 (0.002 mg h^{-1}), it was high enough in Cl_2 of 4 mmHg pressure (23 mg h^{-1}) and in Br_2+S_2 with partial pressures (2.5 ± 0.2) mmHg (12.5 mg h^{-1}) to obtain single crystals. Single crystals of UO_2 were deposited on UO_2 substrates with (100) and (111) orientations by the chemical transport method using Cl_2 as the transporting agent (Singh and Coble, 1974). At Cl_2 pressures below 10 mmHg and high substrate temperatures (>950°C), good single crystals free from cracking caused by epitaxial growth were obtained.

Faile (1978) reported the formation of large single crystals of UO_2 by the use of $TeCl_4$ as transport agent. UO_2 was transported in a sealed fused quartz tube from the source end at 1050°C over a temperature gradient to the deposition end at 950°C. The maximum weight of the obtained single crystals was 1 g. $TeCl_4$ has also been used successfully for the preparation of single crystals of other actinide dioxides (Spirlet *et al.*, 1979).

(*iii*) *Crystal structures*

The crystal structures of uranium oxides in the composition range $2.00 \leq O/U \leq 2.375$, which includes UO_2 and polymorphs of U_4O_9 and U_3O_7, are closely related to the fluorite structure. On the other hand, the crystal structures of

U_3O_8 and many of the UO_3 polymorphs are based on the layer structures, which are characterized by the existence of UO_2^{2+} uranyl groups arranged normal to the plane of the layers. The lattice parameters of the uranium oxides are shown in Table 5.14.

UO_2, UO_{2+x}

Stoichiometric uranium dioxide crystallizes in a fcc structure (space group $Fm\bar{3}m$), where the uranium atoms occupy the positions 0,0,0; 1/2,1/2,0; 1/2, 0, 1/2 and 0, 1/2, 1/2 and the oxygen atoms occupy the 1/4, 1/4, 1/4 and its equivalent positions. As the temperature is raised, the anisotropic thermal vibration causes the oxygen atoms to move to the $1/4 + \delta$, $1/4 + \delta$, $1/4 + \delta$ positions, where $\delta = (0.016 \pm 0.001)$ at 1000°C (Willis, 1964a).

In the hyperstoichiometric uranium dioxide, UO_{2+x}, the interstitial oxygen atoms occupy two different sites of the UO_2 lattice, which are displaced by about 1 Å along the <110> and <111> directions from the cubic coordinated interstitial position. These oxygen atoms are denoted as O′ and O″, respectively. Together with these interstitial atoms, it was observed that vacancies were formed at the normal oxygen sites, although the uranium sublattice remained undisturbed (Willis, 1964b). Willis (1978) later analyzed the neutron diffraction data for $UO_{2.12}$ at 800°C by taking into account the anharmonic contribution to the Debye–Waller factor. The occupancy numbers of O′ and O″ and the vacant lattice oxygens were calculated to be equal within one standard deviation, indicating that the defect complex has a 2:2:2 configuration of oxygen defects. The two O″ oxygen atoms displace two normal oxygen atoms forming two O′ atoms and two oxygen vacancies.

A model that assumes a chain-like coordination of the 2:2:2 clusters along <110> directions has been proposed (Allen *et al.*, 1982). However, it failed to give a satisfactory agreement between the observed and calculated neutron intensities (Willis, 1987). There may be a similarity between the clusters present in UO_{2+x} and $Fe_{1-x}O$. In the non-stoichiometric $Fe_{1-x}O$, the Roth clusters (Roth, 1960) or Koch–Cohen clusters (Koch and Cohen, 1969) are thought to be statistically distributed. These clusters have different structures but their compositions are close to that of Fe_3O_4 (Anderson, 1970), which is formed as an ordered phase when the concentration of clusters exceeds a certain value. In the case of UO_{2+x}, the possibility of disordered arrangement of cuboctahedral clusters exists, as U_4O_9 might be composed of ordered cuboctahedral clusters.

U_4O_9

The low-temperature phase α-U_4O_9 transforms to β-U_4O_9 at 340–350 K, which is accompanied by an anomaly in the specific heat at 348 K (Westrum, Jr. *et al.*, 1965) or 330 K (Gotoo and Naito, 1965) and of a dilatation at 293–359 K (Grønvold, 1955). The lattice parameter decreases with increasing temperature in this range (Ferguson and Street, 1963), but no anomaly was observed in the

Table 5.14 *Physical properties of the stoichiometric uranium oxides.*

					Lattice parameters					*Density* ($g\ cm^{-3}$)		
Formula	*Color*	*m.p.*(K)	*Space group*	*Symmetry*	*a* (Å)	*b* (Å)	*c* (Å)	*Angle* (deg)	*Z*	*Exp.*	*X-ray or ND*	*References*
UO_2	brown to black	3138	$Fm\bar{3}m$	fcc	5.4704				4	10.95	10.964	IAEA (1965); Winslow (1971)
U_4O_9	black		$I\bar{4}3d$	bcc	5.441 × 4				64		10.299	IAEA (1965); Ishii *et al.* (1970a); Bevan *et al.* (1986)
$U_{16}O_{37}$(*)	black			tetragonal	5.407		5.497				11.366	Hoekstra *et al.* (1970)
U_8O_{19}(*)	black			monoclinic	5.378	5.559	5.378	β = 90.27		11.34	11.402	Hoekstra *et al.* (1968)
α-U_3O_7	black			tetragonal	5.447		5.400			10.62		Hoekstra *et al.* (1961); Westrum, Jr. and Grønvold (1962)
β-U_3O_7	black			tetragonal	5.383		5.547			10.60		Hoekstra *et al.* (1961); Garrido *et al.* (2003)
γ-U_3O_7 ($U_{16}O_{37}$)	black			tetragonal	5.407		5.497					Hoekstra *et al.* (1970)
α-U_2O_5	black			monoclinic	12.40	5.074	5.675	β = 99.2	4	10.5	10.47	Hoekstra *et al.* (1970); Spitsyn *et al.* (1972)
β-U_2O_5	black			hexagonal	3.813		13.18		2	10.76 to 11.38	11.15	Hoekstra *et al.* (1970)
γ-U_2O_5	black			monoclinic	5.410	5.481	5.410	β = 90.49	2	10.36	11.51	Hoekstra *et al.* (1970)
$U_{13}O_{34}$	black		*Cmcm* (or *Cmc* or *Ama*)	orthorhombic	6.740	3.964×13	4.143×2		4		8.40	Spitsyn *et al.* (1972)

U_8O_{21}			*Pmma*	orthorhombic	6.796	3.958×8	4.145×2		4		8.341	Spitsyn *et al.* (1972)
$U_{11}O_{29}$			*Pnma* (or *Pna*$_2$)	orthorhombic	6.765	3.956×11	4.140×2		4		8.40	Spitsyn *et al.* (1972)
α-U_3O_8	green black		*C*2*mm*	orthorhombic	6.716	11.960	4.147		2		8.395	Loopstra (1970b)
β-U_3O_8	green black		*Cmcm*	orthorhombic	7.069	11.445	8.303		4		8.326	Loopstra (1970b)
$U_{12}O_{35}$(*)	olive green			orthorhombic	6.91	3.92	4.16		2	7.72	8.39	Hoekstra *et al.* (1970)
A-UO_3	orange	723(d)		amorphous						6.80		Hoekstra and Siegel (1961)
α-UO_3	beige	723(d)	(*C*222 derived)	orthorhombic	6.84	43.45	4.157		19	7.30	7.44	Siegel and Hoekstra (1971a); Greaves and Fender (1972)
β-UO_3	orange	803(d)	*P*2$_1$	monoclinic	10.34	14.33	3.910	β = 99.03	10	8.25	8.30	Hoekstra and Siegel (1961); Debets (1966)
γ-UO_3	yellow	923(d)	*Fddd*	orthorhombic	9.813	19.93	9.711		32	7.80	8.00	Hoekstra and Siegel (1961); Siegel and Hoekstra (1971b)
δ-UO_3	deep red	673(d)	*Pm*3*m*	cubic	4.16				1	6.69	6.60	Wait (1955); Hoekstra and Siegel (1961)
ε-UO_3	brick red	673(d)		triclinic	4.002	3.841	4.165	α = 98.10 β = 90.20 γ = 120.17	1	8.54	8.67	Hoekstra and Siegel (1961); Kovba *et al.* (1963)
ζ-UO_3	brown		*P*2$_1$2$_1$2$_1$	orthorhombic	7.511	5.466	5.224		4	8.62	8.86	Siegel *et al.* (1966); Hoekstra *et al.* (1970)

(d): decomposes.
(*): Parameters for these phases refer to a pseudo-cell.

magnetic susceptibility (Gotoo and Naito, 1965). The transition was claimed to be due to disordering of oxygen with U^{4+}–U^{5+} rearrangement (Naito *et al.*, 1967; Fournier and Troć, 1985). Belbeoch *et al.* (1967) reported that α-U_4O_9 has a rhombohedral structure, slightly distorted from a cubic structure with the lattice parameters $a = 5.4438n$ (*n*: an integer) and $\alpha = 90.078°$ at 20°C. The transition is possibly of order–disorder type coupled with a small change in crystal structure.

Another transition from β-U_4O_9 to γ-U_4O_9 occurs at higher temperatures around 850 K. An X-ray diffraction analysis showed the transition temperature to be 823–973 K (Blank and Ronchi, 1968), while the heat capacity measurement gave 900–950 K (Grønvold *et al.*, 1970). A transition between 813–893 K was observed for the specimens of $2.228 \leq O/U \leq 2.25$ (Naito *et al.*, 1973) using X-ray diffraction and electrical conductivity measurements. This β/γ transition is assumed to be based on the order–disorder mechanism (Blank and Ronchi, 1968; Naito *et al.*, 1973). According to Seta *et al.* (1982), there was no clear anomaly or variation in the heat capacity curves in the above temperature range. Instead they observed two small peaks for hypostoichiometric U_4O_{9-y} ($UO_{2.22}$ and $UO_{2.235}$) at 1000 and 1100 K.

The crystal structure of α-U_4O_9 has not yet been solved, but it is supposed to be closely related to that of strictly cubic β-U_4O_9, with the space group $I\bar{4}3d$. Electron diffraction measurements on α-U_4O_9 showed that the superlattice reflections all obeyed the special extinction rules for the $\bar{4}$ sites of the space group $I\bar{4}3d$ (Blank and Ronchi, 1968). Bevan *et al.* (1986) suggest that α-U_4O_9 consists of cuboctahedral clusters centered on 12(a) or 12(b) sites similar to the crystal structure of β-U_4O_9, although the anion sublattice may be perturbed.

Bevan *et al.* (1986) collected single-crystal neutron diffraction data for β-U_4O_9 at 230 and 500°C. A partial Patterson synthesis obtained using only the superlattice reflections supported the cuboctahedral cluster model. Fig. 5.16 shows a sketch of the cuboctahedral oxygen cluster formed by 12 anions located at the vertices of a cuboctahedron and with a 13th oxygen atom situated in its center. The cube surrounding the cluster has an edge length close to the lattice parameter of the fcc cell of the uranium sublattice (the individual cations are not shown in the figure). In β-U_4O_9, the discrete U_6O_{37} cuboctahedral clusters are arranged on $\bar{4}$ axes with positions 12(b) of $I\bar{4}3d$.The displacement of oxygen in the cluster gives rise to the O′ interstitial atoms of Willis. The cuboctahedral cluster contains the Willis 2:2:2 clusters as a component. The structure contains twelve U_6O_{37} clusters per unit cell. There are 60 extra anions per unit cell, and the composition is then $U_{256}O_{572}$, i.e. the β-U_4O_9 phase has the composition U_4O_{9-y} with $y = 0.062$.

U_3O_7

The U_3O_7 polymorphs all crystallize in the tetragonal system but none of their space groups have been specified. The axial ratio *c/a* is here an important parameter to classify the different polymorphs. α-U_3O_7, which is prepared by

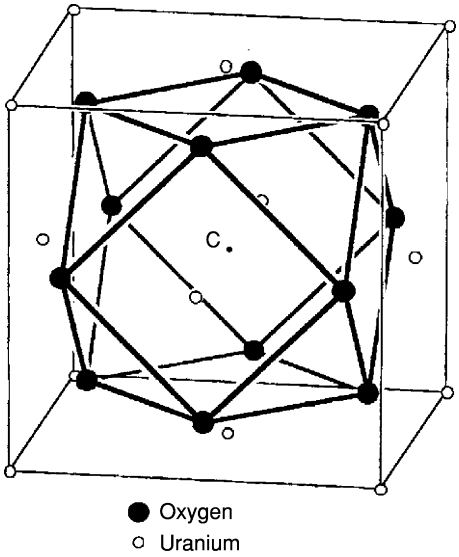

Fig. 5.16 *A schematic diagram of the cuboctahedral cluster. Eight oxygen anions inside the cationic cube are replaced by* 12 *anions located along the* <110> *directions from the center C.* (*from Garrido* et al. (2003), *reproduced by the permission of Elsevier*).

oxidation of UO_2 in air at temperatures of 120–175°C, has *c/a* ratios less than 1 (0.986–0.991) (Pério, 1953b; Westrum, Jr. and Grønvold, 1962). The *c/a* ratios for β-U_3O_7, prepared by oxidizing UO_2 in air at temperatures 160–250°C, are 1.027–1.032 (Hoekstra *et al.*, 1961; Simpson and Wood, 1983; McEachern and Taylor, 1998). In the range of O/U ratios between 2.26 and 2.33, the *c/a* ratio of α-U_3O_7 did not vary in a systematic way between 0.986 and 0.989, while that of β-U_3O_7 seemed to increase very slightly with increasing O/U ratio (Hoekstra *et al.*, 1961). The γ-U_3O_7 ($U_{16}O_{37}$) phase with *c/a* ratios of 1.015–1.016 appears in a range where the O/U ratios are 2.30–2.31 (Westrum, Jr. and Grønvold, 1962; Hoekstra *et al.*, 1970; Tempest *et al.*, 1988), which are significantly smaller than those of α-U_3O_7 and β-U_3O_7.

In the recent studies on β-U_3O_7, it was found that all the uranium atoms and 70% of the oxygen atoms were hardly affected by the oxidation of UO_2 to U_3O_7; however, the remaining 30% of the oxygen atoms changed their location to new sites which are shifted 0.31 Å along $\langle 110 \rangle$ vectors from the holes in the fluorite framework of UO_2. This result, based on a neutron diffraction analysis, is consistent with the assumption that the excess oxygen atoms in β-U_3O_7 are accommodated in the cuboctahedral oxygen clusters (Garrido *et al.*, 2003) as in the case of β-U_4O_9.

According to a theoretical study by Nowicki *et al.* (2000), the crystal structures of U_3O_7 differ from that of UO_2 by the presence of the cuboctahedral

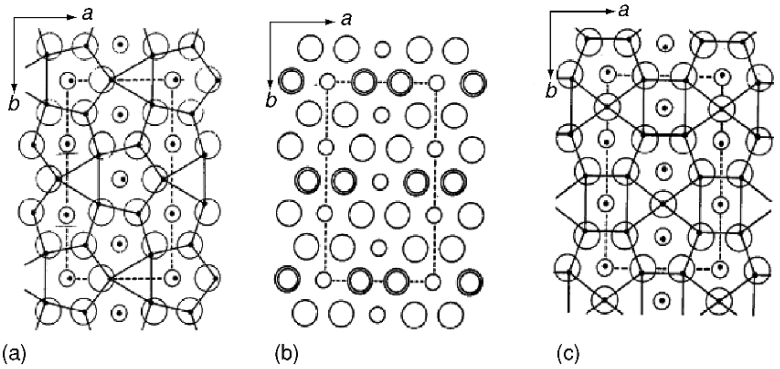

Fig. 5.17 *Atom arrangements on the sections perpendicular to the c-axis* (*Loopstra,* 1970*b*). (*a*) *α-U_3U_8*; (*b*) *hypothetical 'ideal' UO_3*; (*c*) *β-U_3O_8. The dots in the figure represent the actual positions. Isolated dots: uranium atoms; dots connected by full-drawn lines denote oxygen atoms. In* (*a*), *the section is at* $z = 0$, *and in* (*c*), *the origin is shifted b/3 at* $z = 1/4$. *Reproduced by permission of the International Union of Crystallography*.

clusters centered at specified ordered positions, and the arrangement of the clusters can be expressed as a stacking of identical polyatomic modules. A single module contains clusters arranged in a square pattern. The square sides have a length approximately equal to $R_1 = \sqrt{2.5}a_{UO_2} \approx 0.86$ Å. The thickness of the modules is close to $1.5a_{UO_2} \approx 0.82$ Å. The various polytypes found in U_3O_7 can be rationalized with different stacking order of these modules; the small change in the energy of formation of the crystal reflects the interaction between the clusters.

U_3O_8

α-U_3O_8 is orthorhombic (*C*2*mm*; $a = 6.716$ Å, $b = 11.96$ Å, $c = 4.1469$ Å; $z = 2$) (Loopstra, 1962). β-U_3O_8 is also orthorhombic (*Cmcm*; $a = 7.069$ Å, $b = 11.445$ Å, $c = 8.303$ Å; $z = 4$) (Loopstra, 1970b), and the crystal structures of these two modifications are very similar. Fig. 5.17 depicts the relation of α- and β-U_3O_8 with the hypothetical 'ideal' UO_3 structure. The idealized α-U_3O_8 structure (Fig. 5.17a) is derived from a layer of the hypothetical 'ideal' UO_3 (Fig. 5.17b) by removing one oxygen atom from every third row. The idealized β-U_3O_8 structure is obtained by replacing two oxygen atoms by a single one, located halfway between them (Fig. 5.17c). Fig. 5.17a and c show that the actual structures are only slightly distorted from the hypothetical ideal positions, which are represented in Fig. 5.17 by small circles (uranium atoms) and large circles (oxygen atoms). In α-U_3O_8, all uranium atoms are coordinated with oxygen atoms forming pentagonal bipyramids. In β-U_3O_8 the layers are stacked along the *c*-axis so that a set of chains of uranium atoms is formed at $x = 0$, $y = 0$ and $x = 1/2$, $y = 1/2$. The other uranium atoms form chains in the *c* direction, in which the oxygen coordination is alternately pentagonal bipyramidal and distorted octahedral.

α-U_3O_8 shows a λ-type anomaly in the specific heat at 208.5°C (Girdhar and Westrum, Jr., 1968). At this first-order phase transformation temperature, the orthorhombic pseudo-hexagonal α-U_3O_8 changes to a hexagonal structure ($P\bar{6}2m$; $a = 6.812$ Å, $c = 4.142$ Å; $z = 1$) (Loopstra, 1970a). Although the high- and low-temperature phases are closely related, there is an essential difference in the atom arrangement. In the high-temperature phase the uranium atoms occupy a single three-fold position, whereas at room temperature (in the low-temperature phase) they are located at two-fold and four-fold positions making it possible for the uranium atoms to have different localized charges.

Allen and Holmes (1995) pointed out the resemblance in the crystal structures of UO_2 and α-U_3O_8. The UO_2 fluorite structure can be transformed to the layer structure of α-U_3O_8 by displacing the (111) planes in UO_2. A displacement of 2.23 Å along the $\langle 112 \rangle$ direction in the (111) plane brings the outermost uranium layer directly above the second layer of the structure of α-U_3O_8.

UO_3

The crystal structure of α-UO_3 was first reported as trigonal ($P\bar{3}m1$; $a = 3.971$ Å, $c = 4.170$ Å) (Zachariasen, 1948a). However, the later neutron powder diffraction data could not be adequately described in this way. Loopstra and Cordfunke (1966) published a structure assignment using an orthorhombic unit cell ($C2mm$; $a = 3.961$ Å, $b = 6.860$ Å, $c = 4.166$ Å). This structure is close to the former one, since in both cases there are linear chains of O–U–O–U–O with the uranium surrounded by six additional oxygen atoms lying approximately in a plane normal to the chains. The reassignment to the orthorhombic cell reduced the *R*-value from 0.35 to 0.19, but this is still high. Neither of the structures proposed could explain the abnormally low experimental density and the infrared absorption spectrum; the experimental densities were 7.25 g cm^{-3} (Loopstra and Cordfunke, 1966) or 7.30 g cm^{-3} (Siegel and Hoekstra, 1971a), which are much lower than the X-ray density of 8.39 g cm^{-3}. Strong infrared absorption was observed around 930 cm^{-1} (Hoekstra and Siegel, 1961; Carnall *et al.*, 1966). This is typical of the antisymmetric stretching vibration of the linear uranyl group with the U–O bond distance of about 1.7 Å (Jones, 1959), but isolated uranyl groups do not exist in either of the above crystal structures.

A characteristic feature of a large number of solid uranium(VI) oxides is that they contain uranyl groups (UO_2^{2+}) with collinear atom arrangement (O–U–O) (Zachariasen, 1954b). The U–O bond (primary bond) of the uranyl group is a strong covalent bond (cf. Section 5.8.3c), giving short bond distances of 1.7–1.9 Å. The antisymmetric vibration of O_I–U–O_I, where O_I denotes the oxygen atoms in the uranyl group, gives rise to a strong infrared absorption in the frequency range of 600–950 cm^{-1}. The oxygen atoms (O_{II}), bound to uranium in a plane perpendicular to the linear uranyl group, form secondary bonds which are weaker than the U–O_I bonds. The U–O_{II} bond distances are longer, usually between 2.1 and 2.5 Å. The uranyl groups are often seen in the uranium oxides having layer structures. The collinear axis of the uranyl group is along the *c*-axis of such crystals with the four to six U–O_{II} bonds formed in the *a*–*b* plane.

Greaves and Fender (1972) carried out a structure refinement based on the assumption that α-UO_3 is formed by introducing statistically distributed vacancies into the uranium sublattice of α-U_3O_8 so as to re-establish an O/U ratio of three. For each missing uranium atom there were two displaced oxygen atoms in the *z*-direction. Refinement of diffraction data using this model for the α-U_3O_8 structure (space group *C*222) of Andresen (1958) decreased the *R*-value to 0.031 and the theoretical density to 7.44 g cm^{-3}; the U–O distance in the uranyl groups was 1.64 Å. The same refinement based on the *C*2*mm* space group of Loopstra (1962) yielded fairly reasonable values of the uranium occupation number, 0.82, and the U–O distance, 1.58 Å, but the *R*-value (0.13) and the uranium and oxygen temperature factors were somewhat higher. The superlattice reflections observed in both the neutron and electron diffraction patterns could be indexed on an orthorhombic unit cell with dimensions $a = 6.84$ Å, $b = 43.45$ Å, and $c = 4.157$ Å.

The crystal structure of high-pressure phase, ζ-UO_3, is orthorhombic ($P2_12_12_1$; $a = 7.511$ Å, $b = 5.466$ Å, $c = 5.224$ Å) (Siegel *et al.*, 1966). There are no uranium vacancies in this UO_3 modification as shown by the agreement of the measured density (8.62 g cm^{-3}) with the X-ray density (8.85 g cm^{-3}). In this structure each uranium atom is bonded to seven oxygen atoms, leading to shared [UO_7] configurations with bridging oxygen atoms in the plane perpendicular to the UO_2-axis, identified by two short collinear bonds of 1.80 and 1.85 Å. The other five coordinated oxygen atoms form a puckered pentagonal coordination geometry around the uranyl groups.

(*iv*) *Phase relations*

There have been numerous reports on the phase relations and thermodynamic properties of the uranium–oxygen system. Rand *et al.* (1978) made an assessment of thermodynamic data and presented a phase diagram of this system. Recently, Chevalier *et al.* (2002) and Guéneau *et al.* (2002) published critical reviews. In two recent papers Labroche *et al.* (2003a,b) critically assessed the composition range and oxygen potential of uranium oxides in the UO_2–U_3O_8 region taking into account the uncertainties of the published data.

Uranium–uranium dioxide region

Hypostoichiometric UO_{2-x} exists as a single phase or as a mixture with liquid. Since the formation energy of an oxygen vacancy in UO_2 is much higher than that of interstitial oxygen, the lower phase boundary of single phase UO_{2-x} is very close to O/U = 2.0 up to ~1500 K. In the phase diagram of Rand *et al.* (1978), this phase boundary has been obtained up to 2500 K by using the relation $\ln x = (3.877 \pm 0.094) - (13130 \pm 210)T^{-1}$ proposed by Winslow (1973) based on examination of the relevant experimental data. In the recent critical review on the thermodynamic properties in the uranium–oxygen system, Chevalier *et al.* (2002) presented the phase diagram of the U–UO_2 region by careful selection of the experimental data from Blum *et al.* (1963),

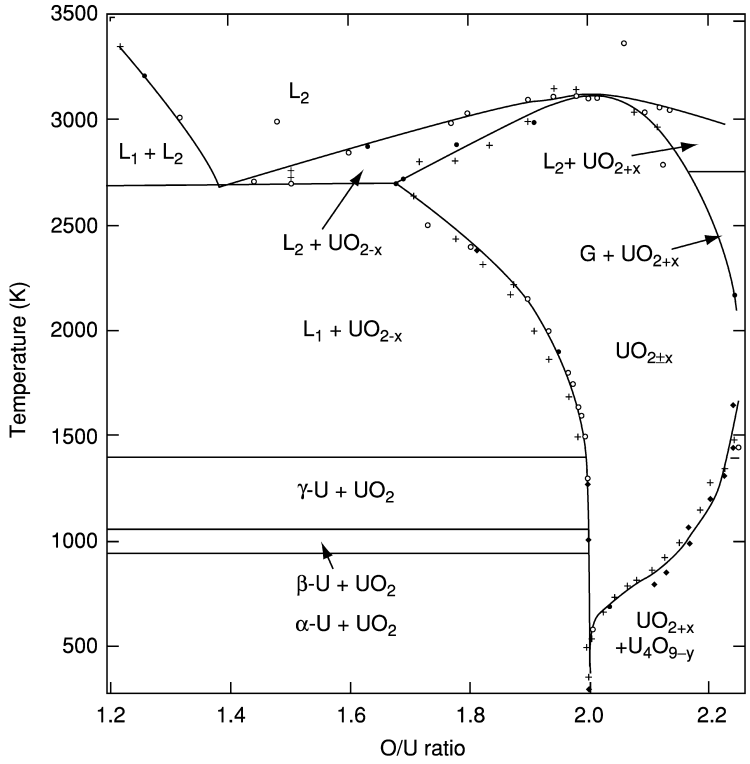

Fig. 5.18 *Partial phase diagram of the U–UO_2 system assembled from values in Rand* et al. (1978), *Chevalier* et al. (2002), *and Guéneau* et al. (2002).

Bates (1964, 1966), Martin and Edwards (1965), Edwards and Martin (1966), Guinet *et al.* (1966), Bannister (1967), Tetenbaum and Hund (1968, 1970), Ackermann *et al.* (1969), Latta and Fryxell (1970), Ackermann and Rauh (1972), Garg and Ackermann (1977, 1980), and Guéneau *et al.* (1998). Guéneau *et al.* (2002) presented the phase diagram of this region using the data from Cleaves *et al.* (1945), Martin and Edwards (1965), Edwards and Martin (1966), Bannister (1967), Hein *et al.* (1968), Ackermann *et al.* (1969), Kjaerheim and Rolstad (1969), Latta and Fryxell (1970), Tachibana *et al.* (1985), and Guéneau *et al.* (1998). Fig. 5.18 shows a phase diagram of the U–UO_2 region ($1.2 \leq O/U \leq 2.0$) and the UO_{2+x} region with $x \leq 0.25$ drawn by using the selected values from Rand *et al.* (1978), Chevalier *et al.* (2002), and Guéneau *et al.* (2002).

The monotectic temperatures for the reaction $L_2 = UO_{2-x} + L_1$ are (2773 ± 30) K (Edwards and Martin, 1966), (2743 ± 30) K (Guinet *et al.*, 1966) and (2693 ± 70) K (Bannister, 1967). The reported compositions of the liquid L_2 phase at the monotectic temperature are $O/U = (1.3 \pm 0.1)$ (Edwards and Martin, 1966), 1.18 (Guinet *et al.*, 1966), (1.53 ± 0.05) (Bannister, 1967) and

1.46 (Latta and Fryxell, 1970). The measured composition of the liquid L_1 phase at this temperature was O/U = 0.05 (Edwards and Martin, 1966; Latta and Fryxell, 1970). The O/U ratios of solid UO_{2-x} are in reasonable agreement: 1.67 (Latta and Fryxell, 1970; Rand *et al.*, 1978), 1.64 (Edwards and Martin, 1966), 1.60 (Guinet *et al.*, 1966), and (1.62 ± 0.06) (Bannister, 1967). The ratio O/U is decreased to ≈1.67 at the lower phase boundary of single phase UO_{2-x} at the monotectic temperature. Above the monotectic temperature the O/U ratio at the lower phase boundary increases to $UO_{2.00}$, until the maximum melting temperature is reached. At the monotectic temperature, three condensed phases, i.e. oxygen-saturated liquid uranium metal L_1 ($UO_{0.05}$), liquid L_2 of a composition $UO_{1.39}$, and solid UO_{2-x} ($UO_{1.67}$) coexist in equilibrium.

$UO_{2.00}$–$UO_{2.25}$ region

Stoichiometric uranium dioxide, UO_2, shows a first-order transition at 30.8 K. This is a magnetic transition, and below that temperature UO_2 is antiferromagnetic, with a structure of type I (Fournier and Troć, 1985), accompanied by an internal distortion in the oxygen sublattice (Faber, Jr. and Lander, 1976). At the transition temperature, a discontinuity in the lattice parameter vs temperature curve (Marples, 1976) and a sharp anomaly in the heat capacity with an entropy increment of 3.6 $J\,K^{-1}\,mol^{-1}$ (Westrum, Jr. and Grønvold, 1962; Huntzicker and Westrum, Jr., 1971) were observed.

Uranium dioxide is stoichiometric at low temperatures, but exhibits a hyperstoichiometric (UO_{2+x}) homogeneity range above 500 K; this range increases with increasing temperature. The upper phase boundary of single phase UO_{2+x} has been extensively studied at temperatures between 500 and 1950 K. The boundary increases with increasing temperature up to (1398 ± 8) K (Blackburn, 1958; Roberts and Walter, 1961; Anthony *et al.*, 1963; Belbeoch *et al.*, 1967; Blank and Ronchi, 1968; van Lierde *et al.*, 1970; Dodé and Touzelin, 1972; MacLeod, 1972; Matsui and Naito, 1975; Labroche *et al.*, 2003b), at which the U_4O_9 phase decomposes to UO_{2+x} and U_3O_{8-z} ($UO_{2.61}$) peritectoidally. The upper phase boundary of UO_{2+x} above that temperature increases only slightly with increasing temperature up to 1950 K.

The phase diagram in the region $2.0 \leq O/U \leq 3.0$ is shown in Fig. 5.19, where the upper phase boundary of UO_{2+x} was obtained by referring to the literature (Blackburn, 1958; Schaner, 1960; Aronson *et al.*, 1961; Roberts and Walter, 1961; Kiukkola, 1962; Markin and Bones, 1962a; Hagemark and Broli, 1966; Kotlar *et al.*, 1967a; Bannister and Buykx, 1974; Saito, 1974; Picard and Gerdanian, 1981; Labroche *et al.*, 2003b). The U_4O_9 phase has a narrow homogeneity range; the reported lower phase boundary is located between the O/U ratios of 2.228 and 2.235 (Blackburn, 1958; Schaner, 1960; Roberts and Walter, 1961; Kotlar *et al.*, 1968; van Lierde *et al.*, 1970; Inaba and Naito, 1973; Picard and Gerdanian, 1981; Labroche *et al.*, 2003b). This boundary is almost unchanged with temperature from room temperature to the peritectic temperature. The reported upper phase boundaries have the O/U values mostly between

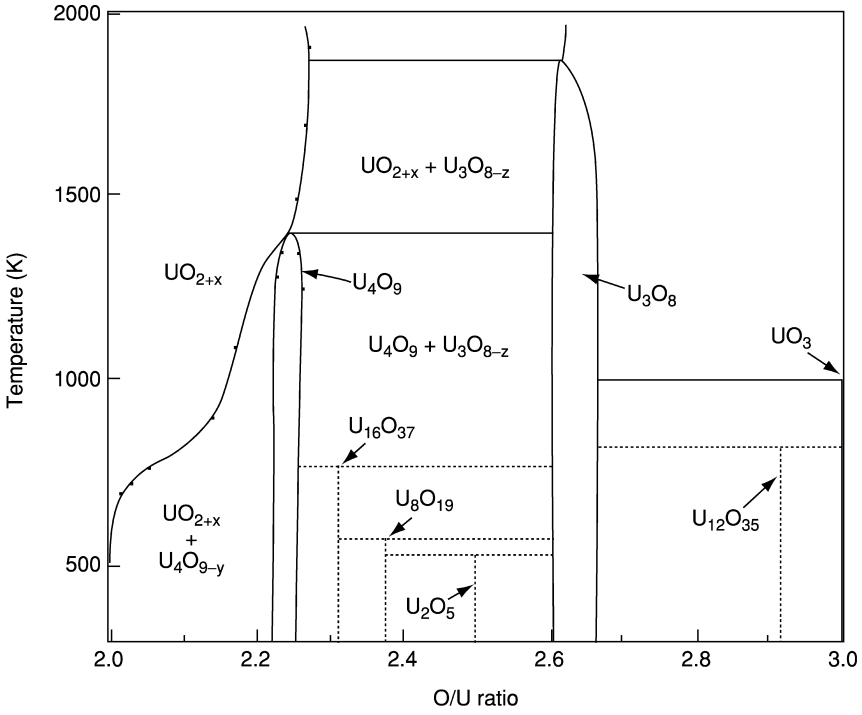

Fig. 5.19 *Phase diagram of the U–O system in the region* $2.0 \leq O/U \leq 3.0$.

2.24 and 2.25 (Blackburn, 1958; Schaner, 1960; Roberts and Walter, 1961; Kotlar *et al.*, 1968; van Lierde *et al.*, 1970; Inaba and Naito, 1973; Picard and Gerdanian, 1981; Labroche *et al.*, 2003b), and many of the papers indicate the uppermost composition to have O/U = 2.242. It is generally assumed that also the upper phase boundary does not change substantially with temperature.

U_4O_9 shows no low-temperature anomaly in the heat capacity due to a magnetic transition observed for UO_2. This is interesting if one considers the close resemblance in the crystal structures between U_4O_9 and UO_2. Instead, the low-temperature modification α-U_4O_9 undergoes a non-magnetic second-order transition to β-U_4O_9 at 340–350 K giving rise to a λ-type specific heat anomaly. The enthalpy and entropy increments of this transition for U_4O_{9-y} with O/U = 2.246–2.254 are 630–710 J mol^{-1} and 1.9–2.2 J K^{-1} mol^{-1}, respectively (Gotoo and Naito, 1965; Westrum, Jr., *et al.*, 1965; Grønvold *et al.*, 1970; Inaba and Naito, 1973). β-U_4O_9 transforms into γ-U_4O_9 at around 850 K. According to Bevan *et al.* (1986), the maximum O/U atom ratio of the β-U_4O_9 phase should be 2.2345 (cf. section on U_4O_9), which supports the hypostoichiometries at the upper phase boundary observed for U_4O_9. The phase transitions α/β and β/γ are reversible, as described in the crystal structure section.

$UO_{2.25}$–$UO_{2.667}$ region

Most compounds in the composition range of $2.25 \leq O/U \leq 2.5$, i.e. α- and β-U_3O_7, γ-U_3O_7 ($U_{16}O_{37}$), U_8O_{19}, and β- and γ-U_2O_5 have fluorite-type structures. α-, β-, and γ-U_3O_7 have been prepared under ambient atmosphere, but U_8O_{19} and α-, β-, and γ-U_2O_5 were formed only at high pressures (15–60 kbar). On this basis, U_8O_{19} and U_2O_5 are regarded as metastable phases, which are thermodynamically unstable at atmospheric pressure (Hoekstra *et al.*, 1970). The phases for which the stability has not been established are indicated in Fig. 5.19 by broken lines. U_3O_7 decomposes at 700°C in air to U_4O_9 and U_3O_8 (Pério, 1953a; Grønvold, 1955). Although β-U_3O_7 shows no low-temperature transitions, α-U_3O_7 exhibits a small λ-type anomaly at 30.5 K with enthalpy and entropy increments of 11 J mol^{-1} and 0.4 J K^{-1} mol^{-1}, respectively. This transition is assumed to be of magnetic origin (Westrum, Jr. and Grønvold, 1962). The other oxides $U_{13}O_{34}$ ($UO_{2.615}$) and $U_{11}O_{29}$ ($UO_{2.636}$) have been described (Kovba *et al.*, 1972; Spitsyn *et al.*, 1972), but no information is given for their stability at low temperatures and pressures.

Two modifications of U_3O_8, i.e. α- and β-U_3O_8, crystallize both in orthorhombic system and their crystal structures are very similar. These compounds are not based on the fluorite structure but are composed of the layer structures related to the hypostoichiometric 'ideal' UO_3 structure (Section 5.7.2a(iii)), which has uranyl bonds perpendicular to the layer planes. The difficulty to rearrange the oxygen atoms in these infinite layer structures is probably the reason for the slow equilibration between U_3O_8 and the gas phase at different temperatures and the oxygen partial pressures. The O/U ratio of the U_3O_8 phase varies with the experimental methods (Gerdanian and Dodé, 1965; Fujino *et al.*, 1981; Srirama Murti *et al.*, 1989). Labroche *et al.* (2003a) suggested that the reason for the scattered data is dissolution of atmospheric nitrogen in the oxides. Although the measured data at the lower phase boundary of U_3O_8 phase are not in good agreement above 1000 K (Labroche *et al.*, 2003b), the ratios O/U are in general between 2.595 and 2.62 (Blackburn, 1958; Hagemark and Broli, 1966; Kotlar *et al.*, 1967b; Ackermann and Chang, 1973; Caneiro and Abriata, 1984). This phase boundary does not change with temperature up to ~1600 K. Above 1000 K, the upper phase boundary was observed to have $O/U = 2.667$ (stoichiometric U_3O_8) up to ~1400 K (Ackermann and Chang, 1973; Caneiro and Abriata, 1984). At an ambient pressure of 0.21 atm O_2, however, the compound becomes hypostoichiometric above 873 K (Cordfunke and Aling, 1965; Rodriguez de Sastre *et al.*, 1967; Ackermann and Chang, 1973). On the other hand, at lower temperatures of 773–873 K, freshly prepared U_3O_8 samples often show hyperstoichiometry with $O/U = 2.670$. Moreover, a hysteresis is seen in the O/U ratio in heating and cooling cycles. Repetition of the heating and cooling cycle results in formation of compounds of lower O/U ratios (Dharwadkar *et al.*, 1975; Fujino *et al.*, 1981). Similar hysteresis phenomena for U_3O_{8-z} have also been observed in oxygen partial pressure vs O/U ratio isotherms (Caneiro and Abriata, 1984) and the electrical conductivity (Ishii *et al.*, 1970b;

Dharwadkar *et al.*, 1978). Slow formation of another phase in α-U_3O_8 may take place at temperatures of 1273–1573 K; according to Hoekstra *et al.* (1955); this is possibly the U_8O_{21} phase with a homogeneity range extending between the compositions $UO_{2.60}$ and $UO_{2.65}$. A slightly different composition range, $UO_{2.617}$–$UO_{2.655}$, has also been reported (Caneiro and Abriata, 1984). It is possible that the proper stoichiometry of β-U_3O_8 is U_8O_{21}, since β-U_3O_8 has been prepared by heating α-U_3O_8 to 1623 K followed by slow cooling to room temperature (Loopstra, 1970b). However in the majority of reports, the phase in this region of compositions is considered to be hypostoichiometric U_3O_8 (i.e. U_3O_{8-z}) (Kotlar *et al.*, 1967a; Ackermann and Chang, 1973; Labroche *et al.*, 2003a,b).

α-U_3O_8 shows a λ-type transition in the heat capacity at 25.3 K with associated enthalpy and entropy increments of 50 J mol^{-1} and 2.3 J K^{-1} mol^{-1}, respectively (Westrum, Jr. and Grønvold, 1959, 1962). This is due to a para-antiferromagnetic transition (Leask *et al.*, 1963). α-U_3O_8 shows three other transitions at higher temperatures: 490, 570, and 850 K. The reported temperature for the 490 K transition varies between 480 and 490 K (Girdhar and Westrum, Jr., 1968; Maglic and Herak, 1970; Inaba *et al.*, 1977; Naito *et al.*, 1982). For the 570 K transition, the reported temperatures are between 562 and 576 K (Inaba *et al.*, 1977; Naito *et al.*, 1982, 1983). The 850 K transition has been observed in one study using adiabatic calorimetry (Inaba *et al.*, 1977). Naito *et al.* (1983) proposed an electronic ordering on uranium atoms with displacement of oxygen atoms as the origin of the above transitions.

$UO_{2.667}$–UO_3 region

Hoekstra and Siegel (1961) regard the $UO_{2.9}$ phase ($U_{12}O_{35}$), which is formed by partial decomposition of amorphous UO_3, as a distinct compound because on heating amorphous UO_3 the O/U ratio remains virtually constant over a 100 K temperature interval from 450 to 550°C. The pycnometric density measured for $UO_{2.9}$ is considerably lower than the theoretical density. This is similar to the case of α-UO_3 assigned to a *C*2*mm* orthorhombic cell with $a = 3.961$ Å, $b = 6.860$ Å, and $c = 4.166$ Å (Loopstra and Cordfunke, 1966). Thus the crystal structure of $UO_{2.9}$ may also have vacant uranium sites as in the α-UO_3 structure.

For UO_3, one amorphous and six crystalline modifications are known. When α-UO_3 is heated in air with a constant heating rate, it decomposes to U_3O_8 passing through a non-stoichiometric range with the O/U ratios between 3.0 and ca. 2.95 (Hoekstra and Siegel, 1961). The δ- and ε-UO_3 compounds convert to U_3O_8 at about 450°C in air with no evidence of a non-stoichiometric oxide range. However, if the heating rate is low, they do not decompose directly, instead re-oxidation of the partially reduced oxides to γ-UO_3 takes place. Also in the γ-UO_3 there is no measurable oxygen non-stoichiometry. The γ-phase is more stable and decomposes to U_3O_8 at higher temperatures of 620–700°C. ζ-UO_3 is formed by heating U_3O_8 at 500°C under high pressures of 15–60 kbar interval produced by a pyrophyllite tetrahedral assembly. This compound is unstable at the ambient pressure (Hoekstra *et al.*, 1970). No magnetic transition has been observed for UO_3 (Jones *et al.*, 1952).

In the uranium trioxide–water system, six compounds have been well established (Dawson *et al.*, 1956; Harris and Taylor, 1962; Debets and Loopstra, 1963; Dell and Wheeler, 1963; Cordfunke and Debets, 1964; Bannister and Taylor, 1970; Taylor, 1971; Siegel *et al.*, 1972; Hoekstra and Siegel, 1973; Vita *et al.*, 1973; Tasker *et al.*, 1988). The physical properties for these compounds are listed in Table 5.15 together with those for uranium peroxide hydrates.

(*v*) *The heat capacity of UO_2*

The low-temperature heat capacity of UO_2 shows a very sharp λ-type anomaly of magnetic origin (Fournier and Troć, 1985) at 30.44 K (Huntzicker and Westrum, Jr., 1971) or 28.7 K (Jones *et al.*, 1952). The entropy increment is 3.6 J K^{-1} mol^{-1} (Westrum, Jr, and Grønvold, 1962). Faber, Jr. and Lander (1976) carried out a neutron diffraction and scattering study on this transition. They showed that the anomaly took place at 30.8 K and that it could be explained as a first-order transition from the low-temperature antiferromagnetic state of type I, associated with an internal distortion of the oxygen sublattice, to the paramagnetic state. The low-temperature (5–346 K) heat capacity data of Huntzicker and Westrum, Jr. (1971) are in good agreement with those of Grønvold *et al.* (1970) (304–1006 K) in the range of overlapping temperatures.

The high-temperature heat capacity of UO_2 has been studied extensively because of the importance of this compound as nuclear fuel; several critical reviews have also been published (Browning, 1981; Browning *et al.*, 1983; Naito, 1989; Ronchi and Hyland, 1994; Fink, 2001; Carbajo *et al.*, 2001). The selected data of heat capacities are shown in Fig. 5.20 together with the correlations calculated by the MATPRO equation (Hagrman, 1995) and by the Fink equations with functional and polynomial forms. In the figure two sets of data of Ronchi *et al.* (1999) are shown for high temperatures, and the data of Huntzicker and Westrum, Jr. (1971) and Grønvold *et al.* (1970) are shown for low and intermediate temperatures. Since the heat capacities of the functional and polynomial equations differ by at most 1%, the latter equation is recommended because of its simplicity (Fink, 2001). This equation, which is based on a combined analysis of the reported data (Moore and Kelley, 1947; Hein and Flagella, 1968; Hein *et al.*, 1968; Ogard and Leary, 1968; Leibowitz *et al.*, 1969; Fredrickson and Chasanov, 1970; Grønvold *et al.*, 1970; Huntzicker and Westrum, Jr., 1971; Ronchi *et al.*, 1999), for $298.15 \leq T \leq 3120$ K is:

$$C_p(T)(\text{J K}^{-1}\,\text{mol}^{-1}) = 52.1743 + 87.951\,\tau - 84.2411\,\tau^2 + 31.542\,\tau^3 - 2.6334\,\tau^4 - 0.71391\,\tau^{-2},$$

where, $\tau = T(\text{K})/1000$. The MATPRO equation (Hagrman, 1995) gives somewhat lower C_p values at higher temperatures.

The λ-type transition found by Bredig (1972) at 2670 K has been confirmed by other researchers (Hutchings *et al.*, 1984; Ralph and Hyland, 1985; Hiernaut *et al.*, 1993). Hiernaut *et al.* (1993) modeled the transition in $UO_{2.00}$ as

Table 5.15 *Physical properties of the uranium trioxide hydrates and of the uranium peroxide hydrates.*

Formula	*Color*	*Space group*	*Symmetry*	*Lattice parameters*				*Z*	*Density* ($g\ cm^{-3}$)		*References*
				a (Å)	*b* (Å)	*c* (Å)	*Angle* (deg)		*Exp.*	*X-ray or ND*	
α-$UO_3 \cdot 0.8H_2O$			orthorhombic	4.27–4.30	10.19–10.24	6.86–6.96		4	6.63		Dawson *et al.* (1956)
α-$UO_2(OH)_2$ (=α-$UO_3 \cdot H_2O$)	greenish yellow	*Cmca*	orthorhombic	4.242	10.302	6.868		4	6.73		Taylor (1971); Hoekstra and Siegel (1973)
β-$UO_2(OH)_2$ (=β-$UO_3 \cdot H_2O$)	yellow-green	*Pbca*	orthorhombic	5.6438	6.2867	9.9372		4	5.73		Bannister and Taylor (1970); Hoekstra and Siegel (1973)
γ-$UO_2(OH)_2$ (=γ-$UO_3 \cdot H_2O$)	gray-chamois	$P2_1/c$	monoclinic	6.419	5.518	5.561	$\beta = 112.77$	2	5.56		Cordfunke and Debets (1964); Hoekstra and Siegel (1973)
$UO_2(OH)_2 \cdot H_2O$ (=$UO_3 \cdot 2H_2O$) (schoepite)	bright yellow	*Pbna*	orthorhombic	13.977	16.696	14.672		32	5.00		Debets and Loopstra (1963); Tasker *et al.* (1988); Hoekstra and Siegel (1973)
$U_3O_8(OH)_2$	violet		triclinic	6.802	7.417	5.556	$\alpha = 108.5$ $\beta = 125.5$ $\gamma = 88.2$	1		6.85	Siegel *et al.* (1972)
$UO_4 \cdot 4H_2O$	pale yellow	*C*2, *Cm* or *C*2/*m*	monoclinic	11.85	6.78	4.245	$\beta = 93.47$	2	5.15		Debets (1966)
$UO_4 \cdot 2H_2O$	pale yellow	*Immm*	orthorhombic	6.502	4.216	8.778		2			Debets (1966)

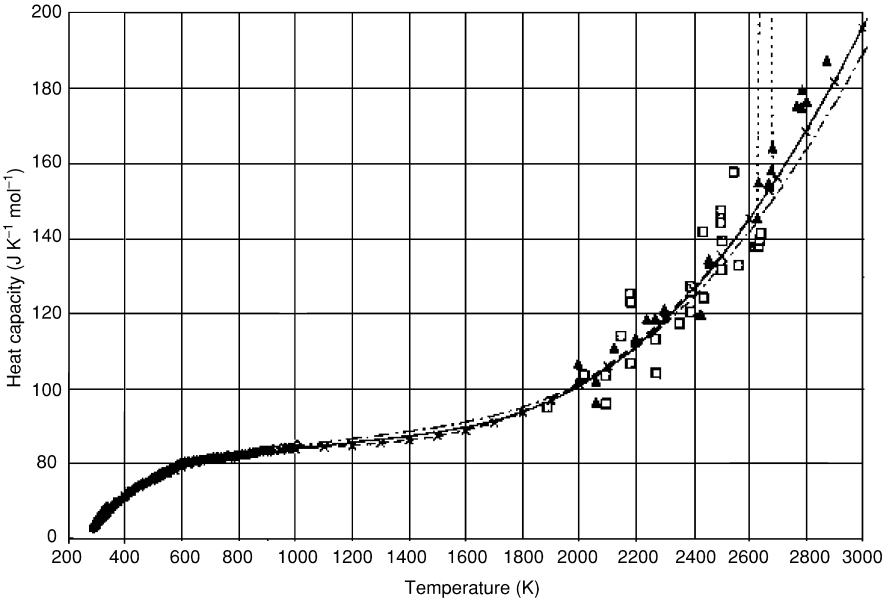

Fig. 5.20 *Recommended equations and data for the heat capacity of UO_2* (*Fink,* 2001). ▲: *Table data of Ronchi* et al. (1999); □: *Graph data of Ronchi* et al. (1999); ◇ *Grønvold* et al. (1970); ○: *Huntzicker and Westrum, Jr.* (1971); ——: *Functional form equation* (*Fink*, 2001); –×–×–: *Polynomial form equation* (*Fink*, 2001); ------: *Phase transition*; —·—·—: *MATPRO equation* (*Hagrman*, 1995).

a second-order transition involving oxygen Frenkel disorder. The transition temperature of hypostoichiometric uranium dioxide (UO_{2-x}) increases with increasing x. Their model explains the shift as due to the change from a λ-transition to a first-order phase transition in UO_{2-x}.

The discussion on the heat capacity of UO_2 can be divided into the following four regions (Ronchi and Hyland, 1994):

(1) *Room temperature – 1000* K *region*. The increase in the heat capacity is caused by the harmonic lattice vibrations with a smaller contribution from thermal excitation of localized electrons of U^{4+} in the crystal field.
(2) *1000–1500* K *region*. The heat capacity increases with increasing anharmonicity of the lattice vibrations as shown by thermal expansion.
(3) *1500–2670* K *region*. The heat capacity increase in this region is mainly ascribed to the formation of lattice and electronic defects. The C_p peak at 2670 K is due to the oxygen Frenkel defects as determined by neutron scattering measurements.
(4) *Region above 2670* K. The peak of the heat capacity drops sharply by rapid saturation of the defects. At temperatures from 2700 K to the melting point, the concentration of Schottky defects increases.

(*vi*) *Oxygen potential and other thermodynamic properties*

A large number of reports have been published on the partial molar thermodynamic quantities $\Delta\bar{G}(O_2)$, $\Delta\bar{H}(O_2)$, and $\Delta\bar{S}(O_2)$ for non-stoichiometric uranium oxides. These studies have been carried out mainly by means of thermogravimetric method (Gerdanian, 1964; Gerdanian and Dodé, 1965; Hagemark and Broli, 1966; Kotlar *et al.*, 1967b; Ugajin, 1983; Matsui and Naito, 1985a) and emf method (Aronson and Belle, 1958; Kiukkola, 1962; Markin and Bones, 1962a,b; Marchidan and Matei, 1972; Saito, 1974; Nakamura and Fujino, 1987); however, tensimetric (Roberts and Walter, 1961), quenching (Anthony *et al.*, 1963), and Knudsen effusion (Blackburn, 1958) techniques have also been used.

In the two-phase regions of solid oxides, the equilibrium oxygen pressure over uranium oxides, p_{O_2}(atm), which is related with the oxygen potential of the oxides $\Delta\bar{G}(O_2)$ by the equation $\Delta\bar{G}(O_2) = RT \ln p_{O_2}$, is a function of only temperature. For the UO_{2+x}–U_4O_{9-y} two-phase region, Saito (1974) showed that $\log p_{O_2}$ is:

$$\log p_{O_2}(\text{atm}) = -105.7 - 5136\, T^{-1} + 33.46 \log T \tag{5.1}$$

The previous equation describes the measured data from the literature (Aronson and Belle, 1958; Blackburn, 1958; Roberts and Walter, 1961; Kiukkola, 1962; Markin and Bones, 1962b; Kotlar *et al.*, 1967b; Marchidan and Matei, 1972; Saito, 1974; Nakamura and Fujino, 1987), although it gives gradually too low values at temperatures above 1323 K (Roberts and Walter, 1961; Nakamura and Fujino, 1987).

For the U_4O_9–U_3O_{8-z} two-phase region, $\log p_{O_2}$ is represented by (Saito, 1974)

$$\log p_{O_2}(\text{atm}) = 7.996 - 16\,330\, T^{-1} \tag{5.2}$$

or (Roberts and Walter, 1961)

$$\log p_{O_2}(\text{atm}) = 8.27 - 16\,760\, T^{-1}. \tag{5.3}$$

The difference in $\log p_{O_2}$ of equations (5.2) and (5.3) is 0.20 at $T = 900$ K, which decreases to 0.033 at $T = 1400$ K.

The oxygen potential of UO_{2+x} in the single-phase region is a function of the composition x and temperature. A number of experimental $\Delta\bar{G}(O_2)$ isotherms plotted against O/U ratio of UO_{2+x} for various temperatures in the range 1173–1773 K have been reported (Aukrust *et al.*, 1962; Markin and Bones, 1962a,b; Hagemark and Broli, 1966; Ugajin, 1983; Matsui and Naito, 1985a). The scatter in the experimental $\Delta\bar{G}(O_2)$ data seems to increase as the O/U ratio decreases in the composition range below 2.01, where $\Delta\bar{G}(O_2)$ rapidly decreases with decreasing O/U ratio.

Fig. 5.21 shows $\Delta\bar{G}(O_2)$ for UO_{2+x} as a function of the O/U ratio expressed by an equation which consists of component equations giving experimental values in polynomial forms (Nakamura and Fujino, 1987) with small modifications for

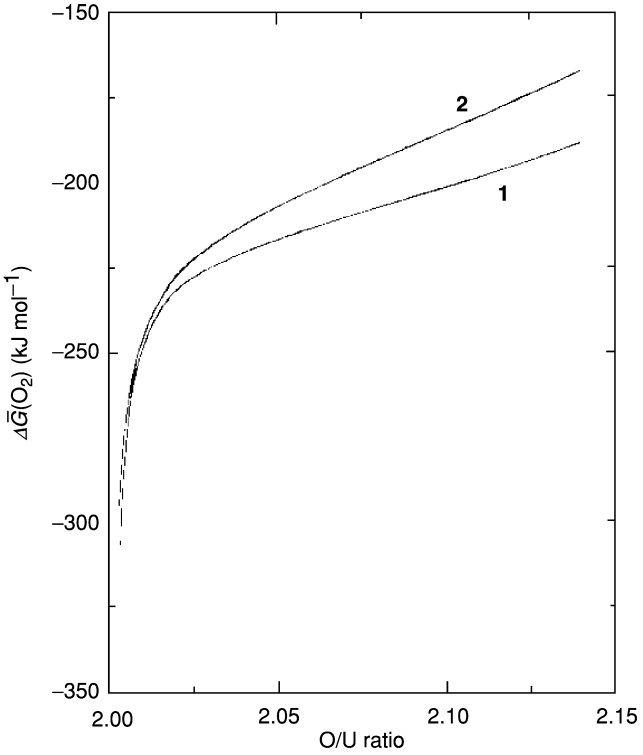

Fig. 5.21 *Oxygen potential as a function of O/U ratio. Curve* 1, 1173 K; *curve* 2, 1373 K.

$\Delta\bar{G}(O_2)$ below O/U = 2.02. The lowest O/U ratio shown in the figure is 2.003, below which the $\Delta\bar{G}(O_2)$ values approach those at $x = 0$, i.e. –633.3 and –588.4 kJ mol^{-1} for 1173 and 1373 K, respectively. These values are obtained from the equation $\Delta\bar{G}(O_2) = -897\,000 + 224.8\,T$ J mol^{-1} at $x = 0$ assessed by Lindemer and Besmann (1985) for temperatures between 873 and 1673 K.

The partial molar entropy of oxygen, $\Delta\bar{S}(O_2) = -d\Delta\bar{G}(O_2)/dT$, was in most papers regarded as temperature independent and on this basis differentiation of $\Delta\bar{G}(O_2)$ was made without specifying temperature. There have been rather wide scattering in the reported values of the partial molar enthalpy of oxygen, $\Delta\bar{H}(O_2)$, and the entropy, $\Delta\bar{S}(O_2)$. This is significantly reduced when $\Delta\bar{S}(O_2)$ is treated as a temperature-dependent quantity: $d\Delta\bar{S}(O_2) = \bar{C}_p(O_2)dT/T$ where $\bar{C}_p(O_2)$ is the partial molar heat capacity of oxygen expressed as a polynomial of $\log x$ (Nakamura and Fujino, 1987). In this case, $\Delta\bar{H}(O_2)$ also becomes temperature-dependent because of the relation $\Delta\bar{H}(O_2) = \Delta\bar{G}(O_2) + T\Delta\bar{S}(O_2)$.

Fig. 5.22a compares the calculated $\Delta\bar{H}(O_2)$ vs x curves obtained by using the above $\bar{C}_p(O_2)$ values with the literature data. Fig. 5.22b compares the $\Delta\bar{S}(O_2)$ vs x curves. The derived $\Delta\bar{H}(O_2)$ curve at 1323 K is in good agreement

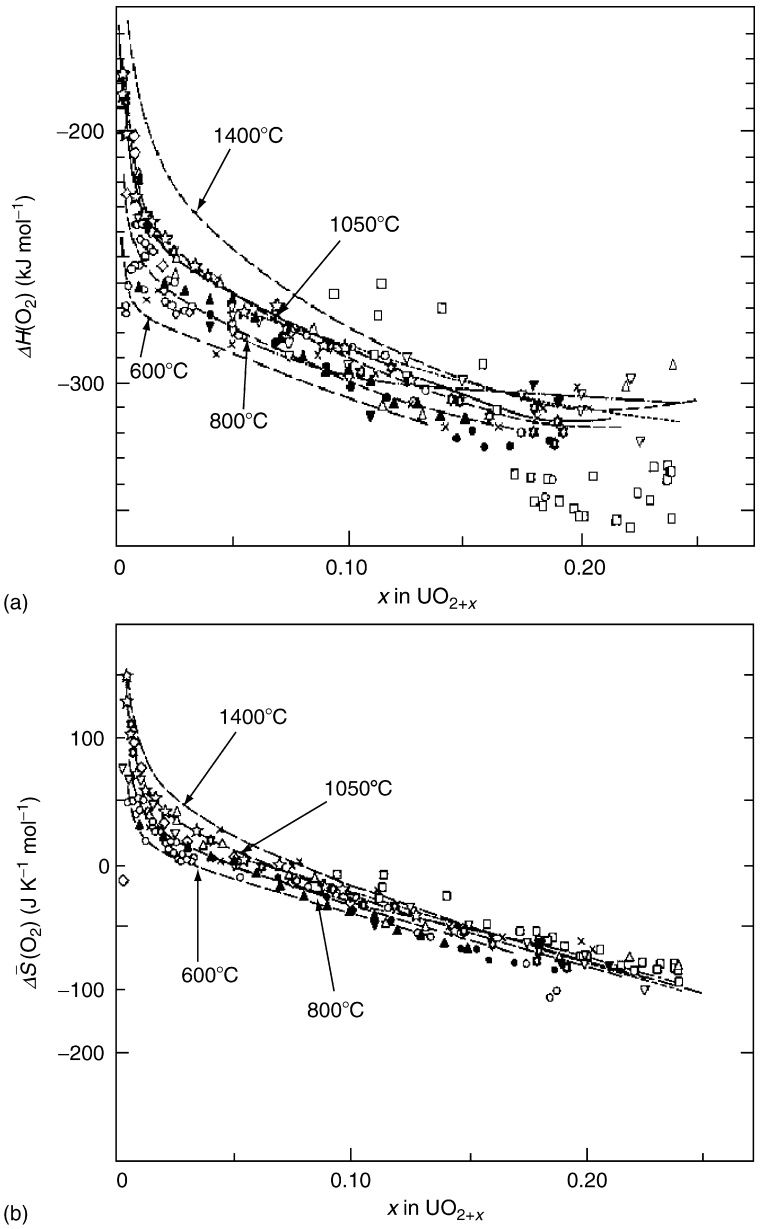

Fig. 5.22 (*a*) and (*b*): *Variation of* $\Delta\bar{H}(O_2)$ *and* $\Delta\bar{S}(O_2)$, *respectively*, *with composition x at* 873, 1073, 1323, *and* 1673 K *in the region* $0 \leq x \leq 0.25$ (*Nakamura and Fujino,* 1987). ★: *sample a* (*Nakamura and Fujino,* 1987); ☆: *sample b* (*Nakamura and Fujino,* 1987); — — —: *least squared* $\Delta\bar{H}(O_2)$ *and* $\Delta\bar{S}(O_2)$ *curves* (*Nakamura and Fujino* 1987); ——: *Picard and Gerdanian* (1981) *at* 1323 K; ○: *Markin and Bones* (1962*a,b*); △: *Kiukkola* (1962); ●: *Saito* (1974); ▲: *Gerdanian and Dodé* (1965); ▽: *Hagemark* et al. (1962, 1966); ▼: *Marchidan and Matei* (*1972*); ×: *Aronson and Belle* (1958); ◇: *Ugajin* (1983); □: *Roberts and Walter* (1961); -----: *Rand and Kubaschewski* (1963) *at* 1273 K; —·—·—: *Rand* et al. (1978). *Reproduced by the permission of Elsevier*.

with the measured curve of Picard and Gerdanian (1981). Most reported values of the temperature-independent $\Delta\bar{H}(O_2)$ and $\Delta\bar{S}(O_2)$ are within the curves derived using temperature-dependent $\Delta\bar{H}(O_2)$ and $\Delta\bar{S}(O_2)$ in the range 1073–1323 K.

Labroche *et al.* (2003a) made a critical assessment of the thermodynamic data for UO_{2+x} taking into account the uncertainties in the measurements. The result showed that $\log p_{O_2}$ could be represented by equations of the form $\log p_{O_2} = A - B\,T^{-1}$ with A and B varying with the O/U ratio in the range 2.01–2.23. On the other hand, this treatment revealed that the x dependence of $\log p_{O_2}$ could not be given with adequate accuracy by the above simple formulas if the temperature range is larger.

Gerdanian and Dodé (1968) determined $\Delta\bar{H}(O_2)$ by measuring the evolved heat when a small amount of oxygen was passed over UO_{2+x} in a Calvet-type microcalorimeter. This technique made it possible to measure $\Delta\bar{H}(O_2)$ close to the stoichiometric composition as shown in Fig. 5.23.

In this figure, $\Delta\bar{H}(O_2)$ increased very sharply with increasing O/U ratio from $<$–800 kJ mol^{-1} at $UO_{2.0003}$, and then attained a maximum of about

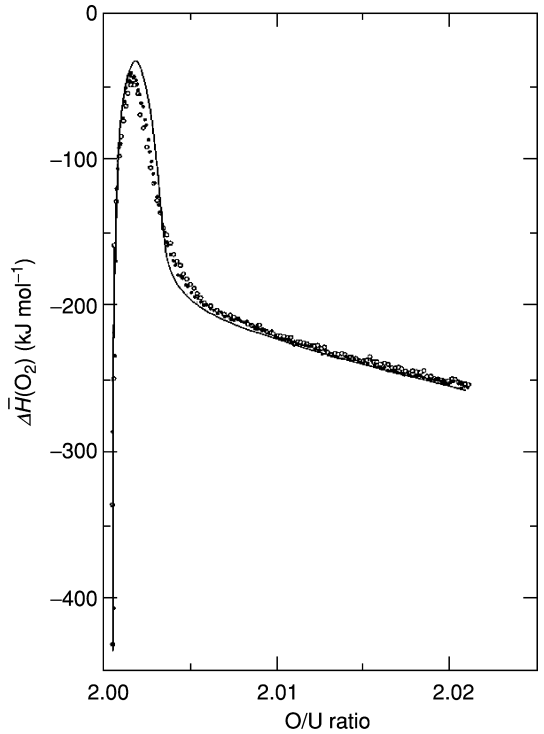

Fig. 5.23 *Change of* $\Delta\bar{H}(O_2)$ *close to stoichiometric* UO_2 (*Gerdanian and Dodé*, 1968). •: run 1; ○: *run* 2;———: $\Delta\bar{H}(O_2)$ *corrected for systematic experimental errors.*

–29 kJ mol^{-1} at $UO_{2.0018}$. The curve afterwards decreased and became progressively linear above O/U = 2.01.

No significant anomaly has been observed for $\Delta\bar{G}(O_2)$ in the above composition range (Markin and Bones, 1962a), though precise determination could not be made at small O/U ratios near stoichiometric UO_2 due to rapid change of $\Delta\bar{G}(O_2)$. When there is no anomaly in $\Delta\bar{G}(O_2)$, $\Delta\bar{S}(O_2)$ should have the sharp peak at the same composition as $\Delta\bar{H}(O_2)$. Gerdanian (1974) showed that the $\Delta\bar{H}(O_2)$ anomaly could be well described by assuming that the formation of the Willis (2:2:2) cluster is the predominant reaction. At the same time he commented that the choice of cluster structures and ionic charges was not crucial and it could be changed if another appropriate and consistent set of $\Delta\bar{H}(O_2)$ and $\Delta\bar{S}(O_2)$ was selected. Actually, the $\Delta\bar{H}(O_2)$ anomaly can also be interpreted by the oxygen Frenkel disorder and Willis (2:1:2) cluster formation reactions coupled with the intrinsic hole–electron formation reaction (Nakamura and Fujino, 1986).

(*vii*) *Vaporization of UO_2*

The vaporization of uranium oxides has been studied mainly on stoichiometric and hypostoichiometric uranium dioxides. The vaporization data concerning U_3O_8 and U_4O_9 phases (Ackermann *et al.*, 1960; Ackermann and Chang, 1973) have attracted only little attention (Naito and Kamegashira, 1976). The vaporization behavior of uranium dioxide may be discussed for the temperature regions below and above the melting point. In the region below the melting point, vaporization has been studied using a variety of techniques such as Knudsen mass effusion, Langmuir surface evaporation, mass spectrometry, and transpiration. The important gaseous species are U(g), UO(g), UO_2(g), UO_3(g), O(g), and O_2(g). The transpiration method can only give total pressures. The partial pressures of each of the uranium-bearing species are measured by means of the Knudsen cell - mass spectrometer technique. In the temperature range 1890–2420 K, the partial pressure of UO_2(g) measured by the latter method (Pattoret *et al.*, 1968) was $\log p_{UO_2}(\text{atm}) = 8.60 - 30850\,T^{-1}$.

In order to obtain the total pressure, it is necessary to measure the pressures of the other gaseous species. However, since the partial pressure p_{UO_2} over uranium dioxide near the stoichiometric composition is (94 ± 3)% of the total pressure at 2150 K (Pattoret *et al.*, 1968; Ackermann *et al.*, 1979), the total pressure is very close to p_{UO_2}. Ackermann *et al.* (1979) compared, at 2150 K, the reported values of the total pressure (10^{-6} atm), the apparent heat of sublimation (kJ mol^{-1}) obtained from a plot of $\log p_{total}$ versus $1/T$, and the apparent entropy of sublimation for UO_2(s) (J K^{-1} mol^{-1}). The values are 1.21, 596.2, and 164 (Ackermann *et al.*, 1956); 1.91, 627.6, and 182 (Ivanov *et al.*, 1962); 0.577, 587.9, and 154 (Voronov *et al.*, 1962); 1.32, 635.1, and 183 (Ohse, 1966); 0.914, 589.5, and 159 (Alexander *et al.*, 1967); 1.97, 617.1, and 178 (Gorban, *et al.*, 1967); 1.81, 590.8, and 165 (Pattoret *et al.*, 1968) and 1.16,

598.7, and 165 (Tetenbaum and Hunt, 1970), respectively. The ΔH_V values spread in a range from 585 to 635 kJ mol^{-1}. The Langmuir method (Voronov *et al.*, 1962) yields low total pressures. The pressure data obtained by the transpiration method (Alexander *et al.*, 1967; Tetenbaum and Hunt, 1970) also tend to be low, which is supposed to be caused by more rapid loss of material giving rise to composition gradient in uranium dioxide during transpiration evaporation. The transpiration total pressures in the form of $\log p_{\text{total}} = A - B\,T^{-1}$, measured at temperatures between 2500 and 2900 K for $UO_{1.88}$(s) (Szwarc and Latta, 1968), were in good agreement with those of Tetenbaum and Hunt (1970) measured over the temperature range 2080–2705 K, but the total pressures for $UO_{1.92}$ (s) and $UO_{1.94}$ (s) were low; approximately two-third to half of the values of Tetenbaum and Hunt (1970).

For hypostoichiometric uranium dioxide, the pressure of UO(g) becomes comparable to p_{UO_2}or, depending on the composition of the solid, higher than p_{UO_2}. Storms (1985) measured p_{UO} as a function of composition between U(l) + UO_{2-x}(s), and $UO_{2.0}$(s) in the temperature range 1667–2175 K using a mass spectrometer equipped with a tungsten Knudsen cell. The gas-phase reaction $2UO_2(g) = UO(g) + U(g)$ was assumed to be in equilibrium in the cell and its equilibrium constant should be independent of the solid composition. Thus, the uranium activity, a_U, and the partial enthalpy of vaporization of U(g), $\Delta\bar{H}_U$, were obtained by adopting the two-phase mixture U(l) + UO_{2-x}(s) as the reference in which a_U was measured to be unity below 2100 K. The partial pressures of U(g), UO(g), and UO_2(g) were expressed as a function of temperature and a_U. From the gas-phase equilibrium $UO_3(g) + UO(g) = 2UO_2(g)$, p_{UO_3} was also given as a (T, a_U) function using the $\Delta_f G^o(UO_3, g)$ data. The pressures p_U and p_{UO_2} were then obtained in terms of temperature, a_U, and $\Delta_f G^o(UO_2, s)$. The partial pressures and the total pressures over various compositions of UO_{2-x}(s) at 2000 K are shown in Fig. 5.24.

The sum of the partial pressures of U(g), UO(g), and UO_2(g) over U(l) + UO_2(s) at 2300 K was in good agreement with that of Ackermann *et al.* (1969), but it was about one-third that of Pattoret *et al.* (1968). The partial pressures of O_2 over U(l) + UO_{2-x} measured recently by Baïchi *et al.* (2002) using the twin-cell method are, for example, $\sim 1 \times 10^{-19}$, $\sim 1 \times 10^{-18}$, and $\sim 1 \times 10^{-17}$ atm for 2000, 2100, and 2200 K, respectively. The above O_2 pressure at 2000 K is in accord with that of Fig. 5.24.

The congruently vaporizing composition (CVC) changes with temperature as reported in the literature (Ackermann *et al.*, 1960, 1969; Pattoret *et al.*, 1968; Edwards *et al.*, 1969). The calculated relation between temperature and the O/U ratio for CVC by Storms (1985) is in reasonable accord with these data: Up to 2100–2200 K, CVC is O/U = 2.00. As the temperature rises above these temperatures, CVC decreases nearly linearly with increasing temperature to O/U = 1.95–1.96 at 2700 K.

The total vapor pressures over uranium dioxide above its melting point measured by the transpiration technique (Reedy and Chasanov, 1972), pulsed

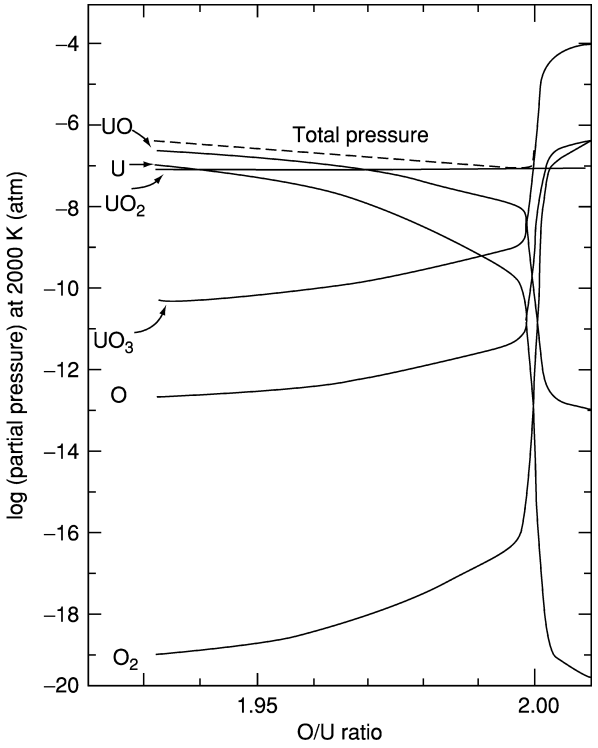

Fig. 5.24 *Partial pressures and total pressure over* UO_{2-x} *of various compositions at* 2000 K (*from Storms*, 1985, *reproduced by the permission of Elsevier*).

laser surface heating (Asami *et al.*, 1975; Bober *et al.*, 1975; Tsai *et al.*, 1975; Babelot *et al.*, 1977), and electron beam heating (Benson, 1977) have been compared by Ohse *et al.* (1979). In the latter monograph, a discussion was made of the methods to measure the equilibrium pressure from the evaporation rate of the gaseous species generated by dynamic, non-equilibrium pulse heating techniques. The upper temperature limit of the transpiration measurements was 3400 K for hypostoichiometric uranium dioxide of O/U = 1.94 (Reedy and Chasanov, 1972). The total pressure data above 4200 K showed a small curvature toward high pressures due to the composition change of liquid uranium dioxide to hypostoichiometry (Babelot *et al.*, 1977). In the case where the correction was made for this deviation by normalizing to O/U = 2.00 in forced congruency evaporation mode, a straight line was obtained in the $\log p_{\text{total}}$ vs. $1/T$ plot. The scattering of the corrected data (Asami *et al.*, 1975; Bober *et al.*, 1975; Tsai *et al.*, 1975; Babelot *et al.*, 1977; Benson, 1977) around the straight line is reasonable in the temperature range 3120–5000 K.

The suggested total pressure up to 5000 K by the IAEA Specialists' Meeting (1978) is

$$\log p_{\text{total}}(\text{MPa}) = 28.65 - 34\,930\,T^{-1} - 5.64 \log T.$$

The data of the equation of state for UO_2 were obtained using the principle of corresponding states (Browning *et al.*, 1978), the method of rectilinear diameters (Partington, 1949; Ohse *et al.*, 1979), and significant structure theory (Vilcu and Misdolea, 1967; Lu *et al.*, 1968). The values of critical temperature, T_c(K), critical pressure, p_c(atm), and critical density, ρ_c(g cm^{-3}) calculated by means of the principle of corresponding states are: 7300, 1915, and 3.16 (Meyer and Wolfe, 1964); 7300, 1900, and 3.16 (Menzies, 1966). The values obtained by the method of rectilinear diameters are 9110, 1230, and 1.59 (Miller, 1965). Gillan (1975) obtained the critical values on the basis of the significant structure theory. The values changed greatly when using the vapor pressures measured over UO_2(s) at lower temperatures from 6960, 1070, and 1.64 (Ohse, 1966) to 9330, 1450, and 1.63 (Tetenbaum and Hunt, 1970), respectively. Fischer *et al.* (1976), obtained the values 7560, 1210, and 1.66 using the experimental data of Ohse (1966).

(*viii*) *Diffusion*

Oxygen self-diffusion in hypostoichiometric uranium dioxide takes place by the vacancy mechanism. The self-diffusion coefficient, D^*, is expressed as

$$D^* \cong D_V^O = A_V \theta_V (1 - \theta_V) \exp(-\Delta H_V^O / RT),$$

where D_V^O, A_V, θ_V and ΔH_V^O are the oxygen self-diffusion coefficient of vacancy, pre-exponential factor, oxygen vacancy concentration (site fraction), and migration enthalpy of vacancy motion, respectively. Most of the observed values for ΔH_V^O are between 48 and 58 kJ mol^{-1} (Matzke, 1981, 1987; Bayovlu and Lorenzelli, 1984). Kim and Olander (1981) report 48.9 kJ mol^{-1}. The theoretically calculated enthalpy is 52 kJ mol^{-1} (Jackson *et al.*, 1986).

For stoichiometric UO_2, the oxygen diffusion mechanism changes with temperature: At low temperatures, thermal oxygen vacancies are the primary species contributing to oxygen mobility, whereas thermal interstitial oxygens predominate at high temperatures. In the range of 800–1800°C, both defects have significant mobility. Calculation suggests $D_i \approx D_V$ at 1400°C (Kim and Olander, 1981). The activation enthalpy of oxygen migration for stoichiometric UO_2, Q, has been determined to be 247 kJ mol^{-1} (Marin and Contamin, 1969), which is related to the enthalpy of oxygen Frenkel defect formation, H_F, by $Q = \Delta H_V^O + H_F/2$. This equation gives $H_F = 396$ kJ mol^{-1} for $\Delta H_V^O = 50$ kJ mol^{-1} (Murch and Catlow, 1987).

For hyperstoichiometric uranium dioxide, UO_{2+x}, the oxygen self-diffusion is considered to occur via the structural interstitial oxygen ions. By plotting D^* against $1/T$, the migration enthalpy of interstitial oxygens, ΔH_i^O, has been measured to be ca. 96 kJ mol^{-1} (Belle, 1969; Contamin *et al.*, 1972; Murch

and Catlow, 1987) or 99.6 kJ mol^{-1} (Breitung, 1978) for x values between 0.01 and 0.1. The calculated ΔH_i^O value is 62 kJ mol^{-1} (Jackson *et al.*, 1986).

The chemical diffusion coefficient of oxygen, $\tilde{D}^O$, describes the movement of oxygen ions under the oxygen concentration gradient of hyperstoichiometric UO_{2+x}; it is expressed as (Lay, 1970; Breitung, 1978):

$$\tilde{D}^O = D^* \frac{(2+x)}{2RT} \frac{d[\Delta\overline{G}(O_2)]}{dx}$$

The $\tilde{D}^O$ values are higher than the oxygen self-diffusion coefficient, D^*, by several orders of magnitude. The $\tilde{D}^O$ values calculated by the above equation are comparable with the experimental values for the x values up to 2.14 (Marin, 1968; Bittel *et al.*, 1969; Carter and Lay, 1970; Lay, 1970).

Uranium self-diffusion in uranium dioxide also depends on oxygen non-stoichiometry. For $x \geq 0$, the uranium vacancies are mainly responsible for uranium diffusion, while in the range of significant hypostoichiometry the interstitial uranium atoms become predominant. The activation enthalpies of uranium migration, Q_U, were measured to be 540 and 250 kJ mol^{-1} for UO_2 and UO_{2+x}, respectively (Matzke, 1987).

The calculated Q_U values are 1200 and 750 kJ mol^{-1} for UO_2 and UO_{2+x}, respectively (Jackson *et al.*, 1986). The uranium self-diffusion coefficient, D_U^*, is smaller than oxygen diffusion coefficient, D^*, by a factor of 10^5 at 1400°C. Another feature is the pronounced dependence of D_U^* on non-stoichiometry. D_U^* increases approximately proportionally with increasing x^2 from UO_2 to $UO_{2.20}$ at 1400–1600°C by about five orders of magnitude (Marin and Contamin, 1969).

(*ix*) *Electrical conductivity*

UO_2, UO_{2+x}

The electrical conductivity of hyperstoichiometric uranium dioxide is caused by positive holes (Tagawa *et al.*, 1975). Although the measured values of mobility of the holes are scattered over a rather wide range, viz. from 0.0015 $cm^2\ V^{-1}\ s^{-1}$ at room temperature (Nagels *et al.*, 1964) to 0.021 $cm^2\ V^{-1}\ s^{-1}$ at 600°C or 0.055 $cm^2\ V^{-1}\ s^{-1}$ at 1100°C (Aronson *et al.*, 1961), these mobilities are much lower than those for usual band-type semiconductors for which the mobility is larger than 1 $cm^2\ V^{-1}\ s^{-1}$ (Tuller, 1981).

To explain the above conduction behavior of uranium dioxide, the small polaron model is used, where the holes are assumed to move in the oxide structure dragging the local distortion of the lattice caused by the electrical interaction. de Coninck and Devreese (1969) measured the electrical conductivity and thermoelectric power of UO_{2+x} having $x = 0.001$ and reported that the small polaron model could be applied with a nearly linear dependence of $\ln(\sigma T^{3/2})$ against $1/T$, where σ is the electrical conductivity. The holes and electrons are localized on individual atoms, giving the species of U^{5+} and U^{3+}, respectively; the electrical conduction occurs as a result of their hopping

in the crystal (Catlow and Pyper, 1979). For wider range of x values of UO_{2+x}, the electrical conductivity follows (Aronson *et al.*, 1961; Winter, 1989)

$$\sigma T = 3.8 \times 10^6 (n+p)(1-n-p)e^{-0.3/kT},$$

where n and p are the electron and hole concentrations, respectively. The activation energy of conduction was measured to be 0.3 eV.

Based on Seebeck data, Winter (1989) claims the same mobility for electrons and holes in UO_{2+x}. The ratio σ_p/σ_n is larger than 1 for $x > 0$, and smaller than 1 for $x < 0$. Since one of the electronic defects always has a concentration higher than that of the ionic defects and the electronic mobilities are much higher, the ionic conductivity is insignificant. The conductivities for nominally stoichiometric UO_2 with $x \sim 10^{-3}$ can be represented by the above equation (Bates *et al.*, 1967; Winter, 1989). At $x = 0$, the intrinsic conductivity by the U^{5+} and U^{3+} charge carriers produced by a disproportionation reaction $2U^{4+} = U^{5+} + U^{3+}$ becomes important. The above reaction parameters were given by a band gap of 2 eV and a vibrational entropy of $2k$ (Winter, 1989).

For UO_{2+x} at 500–1400°C, the electrical conductivities plotted against x decrease nearly linearly with decreasing x below $x = 0.1$ in the direction $\sigma \to 0$. The conductivity changes in the different measurements, but there is a fairly good consistency in the σ values of the samples having larger x values: For $x = 0.1$ at 1000°C, for example, $\sigma \approx 30\ \Omega^{-1}\ cm^{-1}$ (Aronson *et al.*, 1961), which is close to the conductivity obtained by Dudney *et al.* (1981). The other reported values are $\approx 10\ \Omega^{-1}\ cm^{-1}$ (Matsui and Naito, 1985b) and $\approx 1.5\ \Omega^{-1}\ cm^{-1}$ (Ishii *et al.*, 1970c), while the measured values of Lee (1974) are much lower.

U_3O_{8-z}

There are no large differences in the electrical conductivity between U_3O_{8-z} and UO_{2+x}. The conductivities for U_3O_{8-z} are $\sigma \approx 10^{-1}$ and $10^{-3}\ \Omega^{-1}cm^{-1}$ at 730 and 230°C, respectively, when the oxygen partial pressure is 150 mmHg. Contrary to the conduction behavior of UO_{2+x}, however, σ for U_3O_{8-z} increases with decreasing p_{O_2} (in the range 10^2 to 10^{-2} mmHg O_2), suggesting that the main carriers are electrons (George and Karkhanavala, 1963). A change of slope in the $\log\sigma$ vs $1/T$ plots, resulting from a phase transition, was observed at 723 K. The activation energies of conduction were 0.64 and 1.10 eV below and above the transition, respectively. The transition temperature varies with non-stoichiometry from 658 K ($UO_{2.667}$, i.e. stoichiometric U_3O_8) to 923 K ($UO_{2.558}$ to $UO_{2.650}$) (Ishii *et al.*, 1970b). At higher temperatures of 1111–1190 K, another σ anomaly has been measured, presumably due to the formation of U_8O_{21+x} (Dharwadkar *et al.*, 1978).

(*x*) *Chemical properties*

UO_2 is oxidized to U_3O_8 on heating in air at temperatures of 600–1300°C. When UO_3 is heated in air above 600°C, the compound is reduced to U_3O_8. U_3O_8 has been used as a standard material for chemical analysis of uranium oxides

Table 5.16 *Reactions of uranium oxides.*

Reagent	*Temperature* (°C)	*Products of the following oxides*		
		UO_2	*U_3O_8*	*UO_3*
H_2(g)	>750	—	UO_2	UO_2
CO(g)	>750	—	UO_2	UO_2
HF(g)	550	UF_4	$UO_2F_2 + UF_4$	UO_2F_2
F_2(g)	400	UF_6 (>500°C)	UF_6	UF_6
CCl_4(g)	400	UCl_4	$UCl_4 + UCl_5$	$UCl_4 + UCl_5$
$SOCl_2$(g)	450	UCl_4	UCl_4	UCl_4
H_2S(g)	1000	UOS	UOS	UOS
C(s)	1500–1700	UC (UC_2)	UC (UC_2)	UC (UC_2)
C(s) + Cl_2(g)	1000	UCl_4	UCl_4	UCl_4
C(s) + CS_2(g)	1000	US_2	US_2	US_2
C(s) + N_2(g)	1700–1900	UN	UN	UN

because of its high stability in air. However, U_3O_8 is now recognized as a compound that is rather difficult to obtain in strictly stoichiometric composition; the O/U ratio deviates significantly from 8/3 depending on the heating temperature, time, and thermal history.

Stoichiometric UO_2 can be obtained by heating uranium oxides in H_2 or CO gas streams at temperatures 750–1700°C (Table 5.16). However, if the H_2 gas contains an O_2 impurity, the formed UO_2 is oxidized to non-stoichiometric UO_{2+x} during the cooling process at temperatures below 300°C. The reaction of UO_2 with air at room temperature deserves special attention, as the reaction is dependent on particle size and reactivity. Very fine UO_2 powder formed by the hydrogen reduction at lower temperatures below 800°C may be pyrophoric. Even though large particles are usually not pyrophoric, the O/U ratio increases steadily with time of exposure to air. UO_2 can take up appreciable quantities of oxygen for particle diameters of about 0.05–0.08 μm. When the particle size is 0.2–0.3 μm or larger, UO_2 is fairly stable to oxidation (Belle, 1961). UO_2 pellets sintered at around 1700°C are not oxidized for years due to protection by slightly oxidized thin surface films.

Some reactions of uranium oxides with chemical reagents are shown in Table 5.16. For the reaction with C(graphite), the product is UC if the mixing mole ratio of carbon and UO_2 is $C/UO_2 = 3$, and UC_2 if $C/UO_2 = 4$.

An interesting reaction between uranium oxides and liquid N_2O_4 has been observed (Gibson and Katz, 1951). Anhydrous uranium oxides react with liquid N_2O_4 to yield $UO_2(NO_3)_2 \cdot N_2O_4$. A similar reaction with N_2O_5 (Gibson *et al.*, 1960) may be used to prepare anhydrous $UO_2(NO_3)_2$. It was found that the reaction between metal and liquid N_2O_4 also gives $UO_2(NO_3)_2 \cdot N_2O_4$ (Addison and Hodge, 1961).

Uranium oxides dissolve in mineral acids such as HNO_3, $HClO_4$, HCl, and H_2SO_4. In HCl, H_2SO_4, and strong phosphoric acid, the mean valence of

uranium does not change from that in the solid state before dissolution. Sintered UO_2 pellets dissolve in HNO_3 with a slow rate, but the dissolution can be accelerated if a small amount of NH_4F is added, due to the formation of fluoro-complexes of uranium. The addition of a small amount of H_2O_2 to HNO_3 is also effective to enhance the dissolution rate of UO_2 in laboratory experiments; in this way no contamination of the solution takes place.

The mechanism of dissolution of UO_2 in H_2O_2 aqueous solution has been studied by a number of researchers. It is regarded as a second-order reaction with a rate constant 8×10^{-7} m min^{-1} (based on the surface-to-solution volume ratio) (Ekeroth and Jonsson, 2003). The plausible mechanism is a slow electron transfer step producing $UO^{+}_{2(surface)} + OH^{\bullet}$ followed by a rapid reduction of the radical $OH^{\bullet}$ to OH^{-}. The $UO^{+}_{2(surface)}$ ions are oxidized to $UO^{2+}_{2(surface)}$ by $OH^{\bullet}$ or by disproportionation (Shoesmith and Sunder, 1994; Ekeroth and Jonsson, 2003). Carbonate ions increase the solubility of $UO^{2+}_{2(surface)}$ (Grenthe *et al.*, 1984). The above mechanism is consistent with the results by other oxidants, viz. $IrCl_6^{2-}$, MnO_4^{-}, $Fe(EDTA)^{-}$, $CO_3^{\bullet-}$, $HO_2^{\bullet}$, and O_2 (Bard and Parsons, 1985; Wardman, 1989; Huie *et al.*, 1991).

(b) Alkali metal uranates and alkaline-earth metal uranates

In Table 5.17, some physico-chemical properties and crystal structures are shown for ternary alkali metal uranates and alkaline-earth metal uranates.

(*i*) *Uranates*(VI)

The most frequently encountered uranates(VI) are a series of compounds of types $M_2^{+}U_nO_{3n+1}$ (M^{+}: alkali metals) and $M^{2+}U_nO_{3n+1}$ (M^{2+}: alkaline-earth metals), but other compounds such as $M_4^{+}UO_5$, $M_2^{2+}UO_5$, $M_3^{2+}UO_6$, and $M_2^{2+}U_3O_{11}$ are also well known.

Preparation

Carbonates, nitrates, or chlorides of alkali or alkaline-earth elements are mixed with the calculated amounts of U_3O_8 or UO_3. Uranates(VI) are obtained by heating the mixtures in air or oxygen at temperatures 500–1000°C. Because of higher volatility of rubidium and cesium oxides, the uranates of these elements are prepared by heating at lower temperatures of 600–700°C (Hoekstra, 1965). The alkaline-earth oxides are also used as starting materials. Reaction temperatures above 1000°C can be used for the preparation of alkaline-earth uranates on account of very low vapor pressures of alkaline-earth oxides.

A number of stoichiometric sodium uranates (α- and β-Na_2UO_4, $Na_2U_2O_7$, α-Na_4UO_5, etc.) have been prepared following a procedure described by Jayadevan *et al.* (1974) by calcining well-characterized thermally labile double sodium uranium salts such as carbonates, oxalates, and acetates. This technique avoids high-temperature treatment and decreases losses by vaporization. This is

Table 5.17 *Some physico-chemical properties and crystal structures for alkali and alkaline earth metal uranates.*

Formula	*Physico-chemical properties*	*Space group*	*Symmetry*	*Lattice parameters*				*Z*	*Density* ($g\ cm^{-3}$)		*References*
				a (Å)	*b* (Å)	*c* (Å)	*Angle* (deg)		*Exp*	*X-ray or ND*	
U(VI) compounds											
Li_2UO_4	not hygroscopic.	α-phase:	orthorhombic						6.13		Zachariasen (1946); Kovba *et al.*
	α→β transformation	(*Fmmm*)		(6.04	5.11	10.52)					(1958); Efremova *et al.* (1959, 1961c);
	1573 K. excitation	*Pnma*		10.547	6.065	5.134					Neuhaus and Recker (1959); Spitsyn
	and infrared	β-phase:	hexagonal	3.912		16.52					*et al.* (1961a); Bereznikova *et al.*
	spectra										(1961); Prigent and Lucas (1965);
											Hoekstra (1965); Ohwada (1970a);
											Kovba (1971a); O'Hare and Hoekstra
											(1974b); Hauck (1974); Krol (1981);
											Volkovich *et al.* (1998)
Na_2UO_4	yellow.	α-phase:	orthorhombic	9.76	5.73	3.50			5.71		Wisnyi and Pijunowski (1957); Spitsyn
	hygroscopic.	*Cmmm*									*et al.* (1961a,b); Kovba *et al.* (1961a);
	infrared spectra	β-phase:	orthorhombic						5.51		Scholder and Glser (1964); Hoekstra
		(*Fmmm*)		5.98	5.807	11.70					(1965); Ohwada (1970a); Kovba
		Pnma		11.708	5.804	5.970					(1971a); Cordfunke and Loopstra
											(1971); O'Hare and Hoekstra (1973);
											Osborne *et al.* (1974); Gebert *et al.*
											(1978); Volkovich *et al.* (1998)
K_2UO_4	yellow. hygro-	α-phase:	tetragonal	4.344		13.13			4.66		Hoekstra and Siegel (1956); Wisnyi
	scopic. infrared	*I4/mmm*		4.335		13.13					and Pijunowski (1957); Spitsyn *et al.*
	spectra		orthorhombic	7.98	6.91	19.78					(1961a,b); Hoekstra (1965); Ohwada
		β-phase:	pseudo-cubic	4.32							(1970b); Kovba (1971a); O'Hare and
											Hoekstra (1974b); Volkovich *et al.*
											(1998)
Rb_2UO_4	yellow.	*I4/mmm*	tetragonal	4.354		13.86			4.52	6.02	Spitsyn *et al.* (1961a,b); Hoekstra
	hygroscopic.			4.353		13.869					(1965); Ohwada (1970b); Kovba and
	infrared spectra										Trunova (1971); O'Hare and
											Hoekstra (1974b)
Cs_2UO_4	orange. very	*I4/mmm*	tetragonal	4.39		14.82					Spitsyn *et al.* (1961a,b); Hoekstra
	hygroscopic.			4.3917		14.803					(1965); Ohwada (1970b); O'Hare
	infrared spectra										and Hoekstra (1974a); van Egmond
											(1976b)
$MgUO_4$	yellow. not	*Imma*	orthorhombic	6.520	6.595	6.924				7.28	Zachariasen (1954a); Lambertson and
	hygroscopic,										Mueller (1954); Rüdorff and Pfitzer
	infrared spectra										(1954); Klíma *et al.* (1966); Jakeš and
				6.499	6.592	6.921					Schauer (1967); Ohwada (1972); Jakeš
											and Křivý (1974); O'Hare *et al.* (1977)

$CaUO_4$	yellow, not hygroscopic, infrared and far infrared spectra	$R\bar{3}m$	rhombohedral	6.266 6.2683 3.87 3.876		 17.54 17.558	$\alpha = 36.03$ $\alpha = 36.04$	1			Zachariasen (1948b); Wisnyi and Pijunowski (1957); Leonidov (1960); Kovba *et al.* (1961b); Anderson and Barraclough (1963); Carnall *et al.* (1965); Jakeš *et al.* (1966); Loopstra and Rietveld (1969); Voronov *et al.* (1972)
$SrUO_4$	α-phase: orange red. β-phase: yellow, infrared and Raman spectra	α-phase: $R\bar{3}m$ (isostructural with $CaUO_4$)	rhombohedral	6.54 6.551 3.991		 18.361	$\alpha = 35.53$ $\alpha = 34.82°$		7.84		Zachariasen (1948b); Rüdorff and Pfitzer (1954); Ippolitova *et al.* (1959, 1961b); Keller (1962a); Klíma *et al.* (1966); Reshetov and Kovba (1966); Cordfunke and Loopstra (1967); Loopstra and Rietveld (1969); Ohwada (1970a); Brisi (1971); Sawyer (1972); Voronov *et al.* (1972); Fujino *et al.* (1977); Tagawa and Fujino (1977); Tagawa *et al.* (1977)
		β-phase: *Pbcm* (isostructural with $BaUO_4$)	orthorhombic	5.4896	7.9770	8.1297				7.26	
$BaUO_4$	orange yellow. infrared spectra	*Pbcm*	orthorhombic	5.751 5.7553 5.744	8.135 8.1411 8.136	8.236 8.2335 8.237		4			Samson and Sillén (1947); Rüdorff and Pfitzer (1954); Wisnyi and Pijunowski (1957); Ippolitova *et al.* (1961c); Allpress (1964); Klíma *et al.* (1966); Reis, Jr. *et al.* (1976)
$LiU_{0.83}O_3$	α, β, and γ-phases ($Li_2O \cdot 1.60UO_3 = Li_{22}U_{18}O_{65}$)		orthorhombic	20.382	11.511	11.417		2	6.6	6.66	Kovba (1971b); Hauck (1974); Prins and Cordfunke (1983); Griffiths and Volkovich (1999)
$Li_2U_2O_7$	yellow. existence confirmed. electronic and infrared spectra		rhombohedral orthorhombic	 20.4	 11.6	 11.1					Efremova *et al.* (1961c); Kovba *et al.* (1961b); Spitsyn *et al.* (1961c); Hoekstra (1965); Kovba (1971b); Toussaint and Avogadro (1974); Hauck (1974); Prins and Cordfunke (1983); Volkovich *et al.* (1998); Griffiths and Volkovich (1999)
$Na_2U_2O_7$	orange colored. infrared and far-infrared spectra		hexagonal orthorhombic	3.94 3.725	 6.660	17.80 11.88					Sutton (1955); Neuhaus (1958); Kovba *et al.* (1961b); Spitsyn *et al.* (1961c); Hoekstra (1965); Carnall *et al.* (1965, 1966); Kovba (1970, 1972a); Cordfunke and Loopstra (1971); Battles *et al.* (1972); Volkovich *et al.* (1998)
		C2/m	monoclinic	12.796	7.822	6.896	$\beta = 111.42$				
$K_2U_2O_7$	infrared and far-infrared spectra. possibility of two phases	α-phase: $R\bar{3}m$	hexagonal	3.99 3.985 3.998		19.71 19.643 19.77					Kovba *et al.* (1958, 1961b); Ippolitova and Kovba (1961); Spitsyn *et al.* (1961c); Hoekstra (1965); Carnall *et al.* (1965); Allpress *et al.* (1968); Anderson (1969); Kovba (1972a); Volkovich *et al.* (1998)

Table 5.17 (*Contd.*)

Formula	*Physico-chemical properties*	*Space group*	*Symmetry*	*Lattice parameters*				*Z*	*Density* ($g\ cm^{-3}$)		*References*
				a (Å)	*b* (Å)	*c* (Å)	*Angle* (deg)		*Exp*	*X-ray or ND*	
$Rb_2U_2O_7$	decomposes at 1473 K. infrared spectra	$R\bar{3}m$	hexagonal	4.01 4.00 4.004		20.81 20.57 20.83			6.33	6.50	Kovba *et al.* (1961b); Spitsyn *et al.* (1961c); Hoekstra (1965); Allpress *et al.* (1968); Anderson (1969); Kovba and Trunova (1971)
$Cs_2U_2O_7$	orange yellow. infrared spectra	α-phase: $C2/m$ β-phase: $C2/m$ γ-phase: $P6/mmc$	monoclinic monoclinic hexagonal	14.528 14.516 4.106	4.2638 4.3199	7.605 7.46 14.58	$\beta = 112.93$ $\beta = 113.78$		6.62		Hoekstra (1965); Kovba and Trunova (1971); Kovba *et al.* (1974); Cordfunke *et al.* (1975); van Egmond (1976c)
CaU_2O_7	yellow or orange green. infrared spectra	two orthogonal axes with 14.06 and 4.00 Å exist									Hoekstra and Katz (1952); Bereznikova *et al.* (1961); Jakeš *et al.* (1966); Cordfunke and Loopstra (1967); Brochu and Lucas (1967)
SrU_2O_7	magnetic susceptibility. infrared spectra										Hoekstra and Katz (1952); Klíma *et al.* (1966); Cordfunke and Loopstra (1967); Brochu and Lucas (1967)
BaU_2O_7	yellow. infrared spectra	$I4_1/amd$	tetragonal	7.127		11.95					Hoekstra and Katz (1952); Allpress (1964, 1965)
$Li_2U_3O_{10}$	infrared spectra	 α-phase: $P2_1/c$ β-phase: $P2$	tetragonal monoclinic monoclinic	5.63 6.821 6.805	 18.91 19.067	12.28 7.300 7.250	 $\beta = 121.56$ $\beta = 121.12$	2	 6.85	7.62 7.35 7.32	Efremova *et al.* (1961c); Spitsyn *et al.* (1961c); Hoekstra (1965); Kovba (1970, 1972c); Prins and Cordfunke (1983); Volkovich *et al.* (1998)
$K_2U_3O_{10}$	infrared spectra										Prigent and Lucas (1965); Anderson (1969)
$Cs_2U_3O_{10}$	no existence claimed										Efremova *et al.* (1961b); Cordfunke *et al.* (1975)
MgU_3O_{10}	yellow or orange yellow. infrared spectra		hexagonal	3.79 7.57		4.080 16.32					Rüdorff and Pfitzer (1954); Polunina *et al.* (1961); Klíma *et al.* (1966)
$K_2U_4O_{13}$	existence not confirmed	$P6_3$	hexagonal	14.29		14.014			6.7	6.6	Efremova *et al.* (1959); Allpress *et al.* (1968); Anderson (1969); Kovba (1970)
$Rb_2U_4O_{13}$	yellow. decomposes at 1473 K	Pb_3/m (or Pb_3)	hexagonal	14.307		14.298		8	6.85	7.0	Ippolitova *et al.* (1961a); Spitsyn *et al.* (1961c); Kovba and Trunova (1971)
$Cs_2U_4O_{13}$	forms by $Cs_2CO_3 + 4UO_3$ at 873 K	$Cmcm$	orthorhombic	13.494	15.476	39.56			6.8	6.88	Efremova *et al.* (1959); Spitsyn *et al.* (1961c); Cordfunke (1975); Cordfunke *et al.* (1975); van Egmond (1976a)
CaU_4O_{13}	tan colored. decomposes to CaU_2O_7 at 1333 K in air		orthorhombic	6.656	4.161	4.030					Cordfunke and Loopstra (1967)

SrU_4O_{13}	dark purple. decomposes to $Sr_2U_3O_{11}$ at 1403 K		monoclinic (pseudo-orthorhombic)	6.734	4.193	4.065	$\beta = 90.16$				Cordfunke and Loopstra (1967)
$Cs_2U_5O_{16}$	solid solution with $Cs_2U_4O_{13}$		monoclinic	13.465	15.561	15.928	$\beta = 92.78$			6.82	Cordfunke *et al.* (1975); van Egmond (1976a)
$Li_2U_6O_{19}$	decomposes to $Li_2U_{2.7}O_9$ at 1263 K		othorhombic	6.701	4.01	4.148					Kovba (1970); Hauck (1974); Fujino *et al.* (1983)
$K_2U_6O_{19}$	existence doubtful		orthorhombic	6.95	3.90	7.19					Efremova *et al.* (1959); Kovba (1961); Spitsyn *et al.* (1961c); Allpress *et al.* (1968); Anderson (1969)
$K_2U_7O_{22}$	forms by the reaction of K_2CO_3 and $UO_4 \cdot nH_2O$	*Pbam*	orthorhombic	6.945	19.533	7.215		2	7.1	7.11	Kovba (1961, 1970)
$Rb_2U_7O_{22}$	decomposes at 1273 K	*Pbam*	orthorhombic	6.958	19.590	7.279				7.32	Efremova *et al.* (1959); Spitsyn *et al.* (1961c); Kovba and Trunova (1971)
$Cs_2U_7O_{22}$	decomposes at 1273 K	*Pbam*	orthorhombic	6.949	19.711	7.3955				7.485	Efremova *et al.* (1959); Spitsyn *et al.* (1961c); Cordfunke *et al.* (1975); van Egmond (1976b)
Li_4UO_5	gold colored. hygroscopic. excitation and infrared spectra	*I4/m*	tetragonal	6.736 6.720		4.45 4.451			5.28	5.41	Scholder (1958); Efremova *et al.* (1959, 1961c); Kovba (1962); Hoekstra and Siegel (1964); Reshetov and Kovba (1966); Ohwada (1971); Hauck (1974); Krol (1981)
Na_4UO_5	red to salmon pink. very hygroscopic. infrared spectra	*I4/m*	tetragonal	7.576 7.536		4.641 4.630			4.95	5.11	Findley *et al.* (1955); Efremova *et al.* (1959); Kovba (1962); Hoekstra and Siegel (1964); Cordfunke and Loopstra (1971); Ohwada (1971); Battles *et al.* (1972)
K_4UO_5	possibility of no existence remains		othorhombic	3.50	8.58	12.95				4.19	Efremova *et al.* (1959, 1961a); Hoekstra and Siegel (1964)
Rb_4UO_5	preparation $Rb_2CO_3 + UO_3$ at 1273 K		tetragonal	8.18		13.73				6.00	Efremova *et al.* (1959); Ippolitova *et al.* (1961a)
Ca_2UO_5	yellow. infrared spectra	$P2_1/c$	monoclinic	7.9137	5.4409	11.4482	$\beta = 108.803$		5.55	5.67	Bereznikova *et al.* (1961); Sawyer (1963); Jakeš *et al.* (1966); Cordfunke and Loopstra (1967); Loopstra and Rietveld (1969)
Sr_2UO_5	yellow. infrared and Raman spectra	$P2_1/c$	monoclinic	8.1043	5.6614	11.9185	$\beta = 108.985$		6.08	6.34	Sawyer (1963); Keller (1964); Cordfunke and Loopstra (1967); Loopstra and Rietveld (1969); Allen and Griffiths (1977)
Li_6UO_6	yellow. infrared spectra	α-phase:	hexagonal	8.338		7.352					Scholder and Glser (1964); Hauck (1973); Prins and Cordfunke (1983)
Ca_3UO_6	pale yellow. decomposes at 1773 K. infrared spectra	$P2_1$ (cryolite structure)	monoclinic	5.7275	5.9564	8.2982	$\beta = 90.568$		5.1	5.34	Rüdorff and Pfitzer (1954); Ippolitova *et al.* (1959); Bereznikova *et al.* (1961); Jakeš *et al.* (1966); Rietveld (1966); Brisi (1969); Loopstra and Rietveld (1969); Voronov *et al.* (1972); Kemmler-Sack and Seemann (1975)

Table 5.17 (*Contd.*)

Formula	*Physico-chemical properties*	*Space group*	*Symmetry*	*Lattice parameters*				*Z*	*Density* ($g\ cm^{-3}$)		*References*
				a (Å)	*b* (Å)	*c* (Å)	*Angle* (deg)		*Exp*	*X-ray or ND*	
Sr_3UO_6	pale yellow. infrared and Raman spectra	$P2_1$	monoclinic	5.9588	6.1795	8.5535	$\beta = 90.192$	2		6.17	Rüdorff and Pfitzer (1954); Scholder and Brixner (1955); Ippolitova *et al.* (1959); Sleight and Ward (1962); Rietveld (1966); Cordfunke and Loopstra (1967); Loopstra and Rietveld (1969); Kemmler-Sack and Seemann (1975); Allen and Griffiths (1977)
Ba_3UO_6	pale yellow. stable up to high temperatures. infrared and charge transfer spectra	$Fm\bar{3}m$ $(NH_4)_3FeF_6$ type structure	cubic tetragonal orthorhombic	8.922 8.90 6.825 44.63	 44.31	 8.943 8.973			6.75	6.98	Rüdorff and Pfitzer (1954); Scholder and Brixner (1955); Ippolitova *et al.* (1959, 1961c); Rietveld (1966); Kemmler-Sack and Seemann (1975)
$Ca_2U_3O_{11}$	ocher. decomposes to CaU_2O_7 and $CaUO_4$ at 1173 K		triclinic	6.186	6.212	6.186	$\alpha = \gamma = 37.12$ $\beta = 37.56$				Cordfunke and Loopstra (1967)
$Sr_2U_3O_{11}$	cognac colored. stable to 1573 K. infrared and Raman spectra		triclinic	6.484	6.523	6.484	$\alpha = \gamma = 35.44$ $\beta = 36.10$				Cordfunke and Loopstra (1967); Allen and Griffiths (1977)
$Ba_2U_3O_{11}$	orange. stable to 1773 K. infrared spectra										Allpress (1964)
U(v) and U(iv) compounds											
$LiUO_3$	black purple. magnetic properties. electronic spectra	$R3c$ $LiNbO_3$ type	rhombohedral	5.901			$\alpha = 54.60$	1	7.46	7.67	Rüdorff and Leutner (1957); Rüdorff and Menzer (1957); Kovba (1960); Rüdorff *et al.* (1962); Kemmler (1965); Kemmler-Sack *et al.* (1967); Kemmler-Sack (1968b); Keller (1972); Selbin *et al.* (1972a)
$NaUO_3$	red brown. magnetic susceptibility. electronic spectra. no existence of uranyl group	*Pbnm* $GdFeO_3$ type	orthorhombic	5.775 5.776	5.905 5.910	8.25 8.283				7.33	Rüdorff and Leutner (1957); Rüdorff and Menzer (1957); Ippolitova *et al.* (1961d); Rüdorff *et al.* (1962); Prigent and Lucas (1965); Kemmler-Sack *et al.* (1967); Kemmler-Sack and Rüdorff (1967); Kemmler-Sack (1968b); Bartram and Fryxell (1970); Cordfunke and Loopstra (1971); King (1971); Battles *et al.* (1972); Keller (1972); Selbin *et al.* (1972a); Lyon *et al.* (1977)

Na_xUO_3	green. $0 < x \leq 0.14$		orthorhombic ($Na_{0.025}UO_{3-x}$)	6.718	11.90	4.142		8.0	8.29	Greaves *et al.* (1973)
			hexagonal ($Na_{0.10}UO_3$)	3.955		4.163		7.2	7.69	
KUO_3	brown. magnetic susceptibility. electronic spectra	*Pm*3*m* $CaTiO_3$ type	cubic	4.290 4.299				6.85	6.84	Ippolitova *et al.* (1961d); Rüdorff *et al.* (1962); Kemmler-Sack *et al.* (1967); Kemmler-Sack and Rüdorff (1967); Kemmler-Sack (1968b); Selbin *et al.* (1972a)
$RbUO_3$	pale brown. Rb_xUO_3 ($0.8 \leq x \leq 1$). magnetic susceptibility. electronic spectra	*Pm*3*m*	cubic	4.323				7.5	7.63	Ippolitova and Kovba (1961); Rüdorff *et al.* (1962); Kemmler-Sack *et al.* (1967); Kemmler-Sack and Rüdorff (1967); Kemmler-Sack (1968b); Selbin *et al.* (1972a)
$CaUO_3$	black. no existence claimed	*Iam* Mn_2O_3 type	cubic (high pressure form: *fcc*, $a = 5.38$ Å)	10.727						Alberman *et al.* (1951); Young and Schwartz (1963); Brochu and Lucas (1967)
$SrUO_3$	dark brown	(deformed $CaTiO_3$ type)	orthorhombic	6.101 6.03	8.60 6.18	6.17 8.62				Scholder and Brixner (1955); Lang *et al.* (1956); Furman (1957); Brisi (1960); Keller (1964)
$BaUO_3$	brown. magnetic susceptibility	*Pm*3*m* $CaTiO_3$ type	cubic	4.40 4.387 (pseudo-cubic) 4.411				7.98		Rüdorff and Pfitzer (1954); Scholder and Brixner (1955); Lang *et al.* (1956); Furman (1957); Trzebiatowski and Jabloński (1960); Fujino and Naito (1969); Braun *et al.* (1975)
$Ca_{2.5}U_{1.33}O_{5.83}$	electronic spectra	deformed $CaTiO_3$ type	monoclinic	5.767	5.974	8.349	$\beta = 89.8$		6.10	Kemmler-Sack and Seemann (1974)
$Sr_{2.5}U_{1.33}O_{5.83}$	same crystal structure as $Ca_{2.5}U_{1.33}O_{5.83}$.		monoclinic	6.178	6.023	8.629	$\beta = 89.8$	6.33	6.51	Kemmler-Sack and Seemann (1974)
$Ba_{2.67}U_{1.33}O_6$	brown. magnetic susceptibility. electronic spectra		cubic	8.901				7.10	7.34	Kemmler-Sack and Wall (1971)
Ca_2UO_4	forms by the reaction of $CaO+UO_2$ below 2023 K									Alberman *et al.* (1951)
Sr_2UO_4	forms by heating Sr_2UO_5 in H_2.									Scholder and Brixner (1955)
Ba_2UO_4	forms by the same method as Sr_2UO_4. possibility of no existence									Scholder and Brixner (1955); Trzebiatowski and Jabloński (1960)
Ba_3UO_5	no existence reported	α-phase: β-phase: $Fm\bar{3}m$	tetragonal cubic	6.291 8.915		8.982				Trzebiatowski and Jabloński (1960); Keller (1964); Charvillat *et al.* (1970); Braun *et al.* (1975)
Li_3UO_4	ocher colored. magnetic susceptibility. electronic spectra		tetragonal	4.49		8.5				Scholder (1960); Scholder and Glser (1964); Blasse (1964); Kemmler-Sack *et al.* (1967); Kemmler-Sack (1968b)

Table 5.17 (*Contd.*)

Formula	*Physico-chemical properties*	*Space group*	*Symmetry*	*Lattice parameters*				*Z*	*Density* ($g\ cm^{-3}$)		*References*
				a (Å)	*b* (Å)	*c* (Å)	*Angle* (deg)		*Exp*	*X-ray or ND*	
Na_3UO_4	pale brown.	$Fm\bar{3}m$	cubic	4.77					6.5		Scholder (1960); Pepper (1964);
	low temperature C_p.	NaCl type		4.79–4.80							Scholder and Glser (1964); Addison
	high temperature			4.74							(1969); Bartram and Fryxell (1970);
	C_p (298–1200 K).	$P4_232$	cubic	9.543 (to explain superstructure lines)							Marcon (1972); O'Hare *et al.* (1972);
	formula claimed to be $Na_{11}U_5O_{16}$	$Fd3m$	cubic	9.574							Osborne and Flotow (1972); Fredrickson and Chasanov (1972)
Li_7UO_6	pale green. magnetic		rhombohedral	6.61			$\alpha = 53.27$				Scholder and Glser (1964); Keller
	susceptibility.		(hexagonal indexing)	5.52		15.80					*et al.* (1965); Kemmler-Sack *et al.*
	electronic spectra			5.55		15.76					(1967); Kemmler-Sack (1968b); Hauck (1969); Selbin *et al.* (1965)
$Cs_2U_4O_{12}$	$\alpha \rightarrow \beta$ at 898 K, and	α-phase: $R\bar{3}m$	rhombohedral	10.9623			$\alpha = 89.402$				Cordfunke *et al.* (1975); Cordfunke
	$\beta \rightarrow \gamma$ at 968 K. stable	β-phase: $P2_1$	monoclinic	7.886	8.002	10.793	$\beta = 92.62$				(1975); van Egmond (1975); Cordfunke
	in air up to 1523 K	γ-phase: $Fd3m$	cubic	11.2295							and Westrum, Jr. (1979)
MgU_2O_6	black. magnetic	$Fm\bar{3}m$	cubic	5.284							Hoekstra and Katz (1952); Keller
	susceptibility.	CaF_2 type		5.275							(1964); Kemmler-Sack *et al.* (1967);
	electronic spectra.			5.281							Kemmler-Sack and Rüdorff (1967);
	Mg and U atoms statistically distributed.										Kemmler-Sack (1968b); Fujino and Naito (1970); Selbin *et al.* (1972a); Fujino (1972)
CaU_2O_6	black. magnetic susceptibility	$Fm\bar{3}m$ CaF_2 type	cubic	5.379						8.71	Hoekstra and Katz (1952); Hoekstra and Siegel (1956); Brochu and Lucas (1967)
SrU_2O_6	black. magnetic susceptibility	$Fm\bar{3}m$ CaF_2 type	cubic	5.452						9.07	Hoekstra and Katz (1952); Hoekstra and Siegel (1956); Brochu and Lucas (1967); Tagawa *et al.* (1977)
BaU_2O_6	black. magnetic susceptibility (85–300 K)	$Fm\bar{3}m$ CaF_2 type	cubic	5.63							Hoekstra and Katz (1952); Scholder and Brixner (1955); Hoekstra and Siegel (1956); Keller (1964); Brochu and Lucas (1967)
CaU_3O_9	non-stoichiometric region in CaU_3O_{9-x}		cubic	super-structure line							Young and Schwartz (1962, 1963)
$Ba_2U_2O_7$	magnetic susceptibility. electronic spectra		monoclinic (pseudo tetragonal)	11.56	11.31	11.56	$\beta \approx 90$		7.46	7.58	Kemmler-Sack and Rüdorff (1967); Kemmler-Sack (1968a,b)

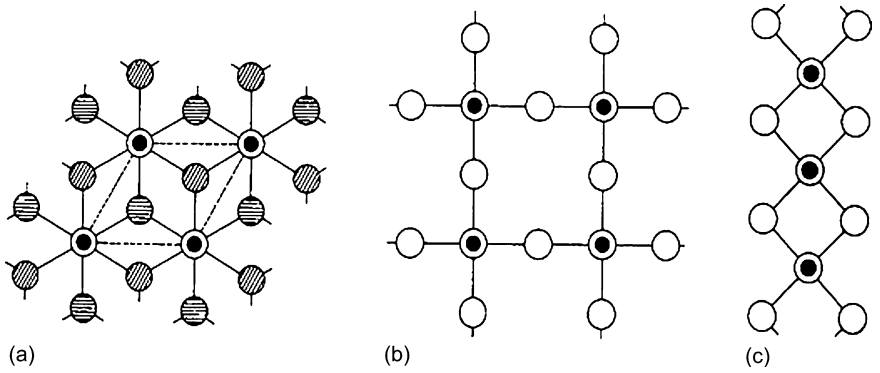

Fig. 5.25 *Schematic atom arrangement around a uranyl group* (*Zachariasen,* 1954*b*); *the notation is as follows:* ◉: *the inner filled circles show U in the plane of the page; the outer empty circles denote* O_I, *one above and the other below the plane of the page*; ○: *denotes* O_{II} *in the plane of the page*; ◍: *denotes* O_{II} *slightly above the plane of the page and* ◍: *denotes* O_{II} *slightly below the plane.* (*a*) *Hexagonal coordination by six* O_{II} *atoms* (β-Li_2UO_4, $CaUO_4$, α-$SrUO_4$). *Each uranium atom is coordinated with six oxygen atoms in an approximately planar arrangement. The axis of the collinear* U_I–U–O_I *group is normal to the plane of the page.* (*b*) *Tetragonal coordination by four* O_{II} *atoms forming an infinite plane* ($BaUO_4$). *Uranium is octahedrally coordinated by four* O_{II} *atoms and two* O_I *atoms. Each octahedron shares four corners with adjacent octahedra forming a layer structure extended in the bc plane. The Ba atoms are located between the layers and link them by electrostatic force.* (*c*) *Tetragonal coordination by four* O_{II} *atoms forming an infinite chain* ($MgUO_4$). *The octahedra share two opposite edges, resulting in formation of chains along the a-axis. Reproduced by the permission of the International Union of Crystallography.*

discussed in Tso *et al.* (1985). Note that the technique is also discussed by Keller (1972) for BaU_2O_7 and $Ba_2U_3O_{11}$.

Crystal structures

An important feature of $M_2^+U_nO_{3n+1}$ and $M^{2+}U_nO_{3n+1}$ type uranates(VI) is their layer structure and the existence of the uranyl groups, UO_2^{2+}, in the crystals.

The structure of monouranates ($n = 1$) is characterized by the layer planes; the oxygen atoms on this plane are coordinated to uranium atoms forming secondary bonds. The primary bonds between the uranium and oxygen atoms of the uranyl group, O_I–U–O_I, are collinear and perpendicular to the layer plane. The atom arrangements around the uranyl groups are schematically drawn in Fig. 5.25 (Zachariasen, 1954b).

For β-Li_2UO_4 (Zachariasen, 1945), $CaUO_4$ and α-$SrUO_4$ (Zachariasen, 1948b), each uranium atom is coordinated to six oxygen atoms (cf. Fig. 5.25a, viewed from the *c*-axis). The axis of the UO_2^{2+} group in the figure is normal to the page, while three of six O_{II} atoms are located about 0.5 Å above and remaining three O_{II} atoms about 0.5 Å below the plane through uranium and perpendicular to the UO_2^{2+} axis. The oxygen atoms coordinated to uranium in

$BaUO_4$ and $MgUO_4$ form a deformed octahedron, where each O_{II} oxygen atom acts as a bridge between two adjacent uranium atoms. In $BaUO_4$ the octahedra share corners (Fig. 5.25b), but in $MgUO_4$ they share edges (Fig. 5.25c). As a consequence, infinite layers are formed in $BaUO_4$ and infinite chains in $MgUO_4$. The alkali or alkaline-earth metals occupy the positions between the layers and bind them together by electrostatic force (Zachariasen, 1954b).

There are no uranyl groups in Li_4UO_5 and Na_4UO_5, and the structure instead contains four orthogonal planar $U–O_I$ bonds (with the distance 1.99 Å in both Li_4UO_5 and Na_4UO_5), yielding UO_4^{2-}; in addition, there are also two collinear $U–O_{II}$ bonds (Li_4UO_5: 2.23 Å; Na_4UO_5: 2.32 Å) (Hoekstra and Siegel, 1964). The octahedra produced in this way are linked to bridges through the diagonally located O_{II} atoms, resulting in formation of a structure containing octahedral chains running along the *c*-axis. $M_3^{2+}UO_6$-type compounds (M = Ca, Sr, Ba) crystallize into distorted perovskite structures ($2[M_{1/4}U_{1/4}][M_{5/4}U_{1/4}]O_3$), where the alkaline-earth atoms and uranium atoms corresponding to $[M_{1/4}U_{1/4}]$ occupy the octahedral sites in an ordered manner (Keller, 1964; Morss, 1982; Williams *et al.*, 1984).

Physicochemical properties

Alkali metal monouranates(VI) are hygroscopic except for Li_2UO_4, and mostly yellow colored; some diuranates are orange or red-orange. The uranates(VI) of the heavy alkali metals are volatile on heating in air. The antisymmetric stretching vibration of UO_2^{2+} in uranates(VI) gives a strong absorption in the IR range of 600–900 cm^{-1}. The frequency changes depending on the bonding strength of the coordinated oxygen atoms. Since the $U–O_I$ bonds of the uranyl group are much stronger, this vibration can be treated approximately as an isolated linear three-atom system of CO_2-type (Jones, 1958). The $U–O_I$ distances calculated from the infrared frequencies using the empirical Badger equation are mostly in good agreement with those obtained by diffraction experiments (Hoekstra and Siegel, 1964; Allpress, 1965; Hoekstra, 1965; Carnall *et al.*, 1966).

A phase transformation coupled with oxygen non-stoichiometry has been observed for $SrUO_4$ and $CdUO_4$ (Tagawa and Fujino, 1978, 1980). α-$SrUO_4$ can be reduced to non-stoichiometric $SrUO_{4-x}$ with the maximum x value of 0.2–0.3. On heating α-$SrUO_4$ at different oxygen partial pressures from 10 to 600 mmHg and heating rates of 1–5 K min^{-1}, the compound is rapidly reduced to $SrUO_{3.8–3.9}$ at about 800°C. The solid is then immediately re-oxidized to stoichiometric composition by absorbing oxygen from the gaseous phase. At the same time, it transforms into β-$SrUO_4$. The atom rearrangement in the phase transformation may be accelerated by the formation of vacancies in the oxygen sublattice of α-$SrUO_4$.

Magnetic susceptibilities have been measured for $MgUO_4$, $SrUO_4$, $BaUO_4$, CaU_2O_7, SrU_2O_7, and BaU_2O_7 (Brochu and Lucas, 1967). In these compounds U(VI) is expected to be diamagnetic, but a weak paramagnetism was observed; this is ascribed to covalency in the uranyl group (Bell, 1969).

(*ii*) *Uranates* (*V*) *and* (*IV*)

Uranates(V) of $M^{+}UO_3$ (M = Li, Na, K, Rb), $M_3^{+}UO_4$ (M = Li, Na), and $M^{2+}U_2O_6$ (M = Mg, Ca, Sr, Ba) types are the most well known, as are the uranates(IV) of $M^{2+}UO_3$ (M = Ca, Sr, Ba) type.

Preparation

To prepare uranates(V), a symproportionation reaction is widely used, where the uranates(IV) and (VI) are first mixed in 1:1 uranium atom ratio, after which the mixture is heated in an evacuated sealed quartz ampoule. An example is the reaction $Li_2UO_4 + UO_2 = 2LiUO_3$, which takes place at 650–750°C. Another method is to reduce uranates(VI) by H_2 at elevated temperatures; the reaction condition should be carefully defined in order to form uranates(V). Since the uranates of alkaline-earth metals are not volatile, the high-temperature reduction method by H_2 can be used to prepare the corresponding uranates(IV).

For some uranates(VI) having high equilibrium oxygen pressures, uranates(V) can be prepared by heating the uranate(VI) in a vacuum at high temperature. The $M^{2+}U_2O_6$ compounds are prepared by the reaction

$$M^{2+}U_2O_7 = M^{2+}U_2O_6 + 1/2O_2$$

at 1100°C (M = Mg, Ca, Sr, Ba). It is, however, rather difficult to obtain stoichiometric uranates(V) by this method.

Crystal structures

Uranates(V) and (IV) do not contain uranyl groups and as a result, their crystal structures are in general not of the layer type and in many cases simpler. The compounds of $M^{+}UO_3$ and $M^{2+}UO_3$, with the exception of $CaUO_3$ (cubic Mn_2O_3-type structure), have perovskite or deformed perovskite-type structures. $LiUO_3$ crystallizes into a rhombohedrally distorted $LiNbO_3$ structure, as a result of the small ionic radius of Li^{+}. $NaUO_3$ has an orthorhombic $GdFeO_3$ structure with small distortions from cubic perovskite structure. KUO_3 and $RbUO_3$ have cubic perovskite structures, and $BaUO_3$ a cubic or pseudo-cubic perovskite structure.

In the uranates(V) of $M_3^{+}UO_4$-type, Li_3UO_4 crystallizes in a tetragonally distorted NaCl-type structure, in which the lithium and uranium atoms are located in the cation sites in an ordered manner with an atom ratio of 3:1. All $M^{2+}U_2O_6$ compounds have cubic fluorite-type structures, where the alkaline-earth metal atoms and uranium atoms are statistically distributed with an atom ratio of 1:2 over the cation sites.

Physico-chemical properties

Most uranates(V) and (IV) are brown to black. An exception is the pale green Li_7UO_6. Uranates(V) and (IV) dissolve in dilute mineral acids. The dissolution rate in HNO_3 is higher than those in HCl and H_2SO_4 (Trzebiatowski and

Jabloński, 1960; Scholder and Gläser, 1964; Brochu and Lucas, 1967). Li_3UO_4 is oxidized to Li_2UO_4 in air even at room temperature. Na_3UO_4 absorbs significant amounts of oxygen, water, and CO_2 at room temperature. On heating the uranates(V) or uranates(IV) in air, they are readily oxidized to uranates(VI).

Electronic spectra have been measured for $LiUO_3$, $NaUO_3$, KUO_3, $RbUO_3$, MgU_2O_6, CdU_2O_6, Li_3UO_4, Li_7UO_6, $Ba_2U_2O_7$, etc. in the range 4000–40000 cm^{-1} (Kemmler-Sack *et al.*, 1967). The crystal field parameters were determined for $LiUO_3$ and Li_3UO_4 from the optical absorption electronic spectra (Lewis *et al.*, 1973; Kanellakopulos *et al.*, 1980; Hinatsu *et al.*, 1992a,b). For KUO_3 and $RbUO_3$, the octahedral crystal field around a U^{5+} atom was consistently calculated with a spin–orbit coupling constant of 1770 cm^{-1} (Kemmler-Sack *et al.*, 1967; Selbin *et al.*, 1972a).

Magnetic susceptibilities have been measured for $LiUO_3$, $NaUO_3$, KUO_3, $RbUO_3$, Li_3UO_4, Li_7UO_6, MgU_2O_6, CdU_2O_6, and $Ba_2U_2O_7$ at temperatures 85–473 K (Rüdorff and Menzer, 1957; Kemmler-Sack, 1968a). In the paramagnetic temperature range, the Curie constant changed with the coordination number. The magnetic susceptibilities for M^+UO_3 (M = Li, Na, K, Rb) were measured in a wider temperature range from 4.2 K to room temperature (Keller, 1972; Miyake *et al.*, 1979, 1982; Kanellakopulos *et al.*, 1980). The electron paramagnetic resonance (EPR) spectra for U^{5+} ions doped in $LiNbO_3$, which has the same crystal structure as $LiUO_3$, gave a signal at $g = 0.727$ (Lewis *et al.*, 1973). The EPR signals were also observed for pure M^+UO_3 but they were very broad (Miyake *et al.*, 1979, 1982). $LiUO_3$ showed a ferromagnetic transition at 16–17 K (Miyake *et al.*, 1979, 1982; Hinatsu *et al.*, 1992b).

Li_3UO_4 has a distorted NaCl-type structure and its magnetic properties have been studied by measuring the EPR spectra and magnetic susceptibility in an extended temperature range down to 4.2 K (Keller, 1972; Lewis *et al.*, 1973; Kanellakopulos *et al.*, 1980; Miyake *et al.*, 1982; Hinatsu *et al.*, 1992a). The experimental magnetic susceptibility can be well described by assuming the $5f^1$ electron of U^{5+} in an octahedral crystal field with a small tetragonal distortion with the crystal field parameters obtained from the electronic spectra (Hinatsu *et al.*, 1992a). $NaUO_3$ gives a magnetic transition at 32 K (Miyake *et al.*, 1977) or 35 K (Keller, 1972), for which a λ-type anomaly has also been observed in the heat capacity (Lyon *et al.*, 1977). The EPR and magnetic susceptibility studies for $M^{2+}U_2O_6$ (M = Mg, Ca, Cd, Sr) have been carried out (Brochu and Lucas, 1967; Miyake *et al.*, 1993; Miyake and Fujino, 1998). The anomalies of magnetic origin have been observed at 4–7 K.

(*iii*) *Non-stoichiometry*

The non-stoichiometry in uranates can be classified into three types. The first type occurs when part of the alkali metal in the uranate is lost as an oxide by vaporization on heating, viz. $Na_{2-2x}U_2O_{7-x}$ is formed from $Na_2U_2O_7$ by the loss of xNa_2O ($0 \leq x \leq 0.07$) (Carnall *et al.*, 1966; Anderson, 1969). The second type

is caused by non-stoichiometric dissolution of alkali metal in a uranium oxide. An example is Na_xUO_3 ($0 \leq x \leq 0.14$) (Greaves *et al.*, 1973). The third type is the most common non-stoichiometry, i.e. the oxygen non-stoichiometry. Examples of such uranates are $Na_2U_2O_{7-x}$ ($0 \leq x \leq 0.5$) (Anderson, 1969), $K_2U_2O_{7-x}$ (Spitsyn *et al.*, 1961b), $Cs_2U_4O_{13-x}$ (Cordfunke *et al.*, 1975), $CaUO_{4-x}$ ($0 \leq x \leq 0.5$) (Anderson and Barraclough, 1963), α-$SrUO_{4-x}$ ($0 \leq x \leq 0.5$) (Tagawa and Fujino, 1977), CaU_2O_{7-x} ($0 \leq x \leq 0.13$) and SrU_2O_{7-x} ($0 \leq x \leq 0.4$) (Hoekstra and Katz, 1952), SrU_4O_{13-x} (Cordfunke and Loopstra, 1967; Tagawa *et al.*, 1977). Rhombohedral $CaUO_4$ and α-$SrUO_4$, which crystallographically are very similar to ionic UO_2, show a wide range of non-stoichiometries, while β-$SrUO_4$ and $BaUO_4$ with increased covalency have virtually no non-stoichiometry. Examples of the third type of non-stoichiometric compounds derived from uranate(v) are MgU_2O_{6+x} ($-0.16 \leq x \leq 0.03$), CaU_2O_{6+x} ($-0.05 \leq x \leq 0.05$), SrU_2O_{6+x} ($-0.05 \leq x \leq 0.4 \sim 0.6$), and BaU_2O_{6+x} ($x \leq 0.86$) (Hoekstra and Katz, 1952).

The non-stoichiometric uranates are produced by heating in reducing atmospheres, but generally the U(VI) state is more stable in ternary uranates than in binary uranium oxides. This trend is more pronounced for the uranates with higher M/U ratios (M = alkali metals or alkaline-earth metals). The experimental fact that alkali and alkaline-earth metal uranates(VI) strictly without U(V) and U(IV) are formed under certain conditions when heated in air was utilized for the determination of oxygen in uranium oxides (Fujino *et al.*, 1978b).

(c) Transition metal uranates

Table 5.18 shows the crystallographic properties of ternary transition metal uranates. In this section the uranates of some non-transition metals such as Sb, Tl, Pb, and Bi are included because of the resemblance of their properties. Here we present an overview of preparation methods and crystal structures. For more detailed information, the reader is referred to the following review articles (Hoekstra and Marshall, 1967; Keller, 1972, 1975).

(*i*) *Preparative methods*

The most general 'dry' method for preparation is to heat thoroughly ground mixtures of transition metal oxides and UO_3 (or U_3O_8) in air. $CrUO_4$, $MnUO_4$, and $CoUO_4$ can be synthesized by heating the mixed oxides for 1 day at 1000–1100°C (Hoekstra and Marshall, 1967). $CuUO_4$ is obtained by heating below 875°C. Triuranates, MU_3O_{10} (M = Mn, Co, Ni, Cu, Zn), are prepared by heating the mixtures of M/U = 1/3 at 875°C. Although Ni, Cu, and Zn triuranates are readily obtained as stoichiometric compounds, Mn and Co triuranates tend to remain oxygen-deficient.

Nitrates, viz. $M(NO_3)_2 + UO_2(NO_3)_2$ (Weigel and Neufeldt, 1961), can also be used as starting materials for preparing MUO_4 (M = Cu, Zn, Cd, Hg),

Table 5.18 *Crystallographic properties of transition metal uranates.*

Formula	*Color*	*Space group*	*Symmetry*	*Lattice parameters*					*Density* ($g\ cm^{-3}$)		*References*
				a (Å)	*b* (Å)	*c* (Å)	*Angle* (deg)	*Z*	*Exp.*	*X-ray or ND*	
$EuUO_3$			orthorhombic	6.020	6.165	8.606					Berndt *et al.* (1976)
$U_{0.25}NbO_3$	brown		tetragonal	7.727		7.792			5.72		Keller (1975)
$U_{0.25}TaO_3$	brown		tetragonal	7.739		7.773			8.23		Keller (1975)
U_xWO_3 (x<0.16–0.2)			cubic	3.78–3.81							Keller (1975)
$CrUO_4$	dark brown	*Pbcn*	orthorhombic	4.871	11.787	5.053			7.72	8.12	Rüdorff *et al.* (1967); Hoekstra and Marshall (1967); Keller (1975)
$MnUO_4$		*Imma*	orthorhombic	6.645	6.983	6.749					Hoekstra and Marshall (1967); Keller (1972)
$FeUO_4$	black	*Pbcn*	orthorhombic	4.888	11.937	5.110					Rüdorff *et al.* (1967); Hoekstra and Marshall (1967); Keller (1972, 1975)
$CoUO_4$	dark brown	*Imma*	orthorhombic	6.497	6.952	6.497				8.17	Hoekstra and Marshall (1967); Keller (1972, 1975)
α-$NiUO_4$		*Pbcn*	orthorhombic	4.820	11.627	5.188					Hoekstra and Marshall (1967); Keller (1972, 1975)
β-$NiUO_4$		*Imma*	orthorhombic	6.472	6.870	6.472					Hoekstra and Marshall (1967); Keller (1972, 1975)
$CuUO_4$	coffee brown	$P2_1/n$	monoclinic	5.475	4.957	6.569	$\beta = 118.87$	2			Hoekstra and Marshall (1967); Siegel and Hoekstra (1968); Keller (1972)
$ZnUO_4$	bright red	*Imma*	orthorhombic	6.492	6.994	6.574					Hoekstra and Marshall (1967); Keller (1972)
α-$CdUO_4$	brownish yellow		orthorhombic	7.01	6.836	3.519					Ippolitova *et al.* (1961e); Keller (1972)

β-$CdUO_4$	brownish yellow	$R\bar{3}m$	rhombohedral	3.587		17.41		2			Ippolitova *et al.* (1961e); Keller (1972)
$HgUO_4$	orange		orthorhombic	11.12	6.87	6.48					Keller (1972)
$PbUO_4$	red	*Pbcm*	orthorhombic	5.528	7.952	8.180					Keller (1972)
$BiUO_4$	gray black	$Fm\bar{3}m$	cubic	5.481				4	10.3	10.31	Rüdorff *et al.* (1967)
α-Ag_2UO_4	deep brown		tetragonal	11.70		5.87			7.57	7.41	Keller (1972)
β-Ag_2UO_4	deep brown		tetragonal	4.66		6.38			6.46	6.20	Keller (1972)
Tl_2UO_4	yellow orange		tetragonal	4.468		13.10					Keller (1972)
Cd_2UO_5	orange yellow	$P2_1/c$	monoclinic	8.074	5.312	11.52	$\beta = 100.52$	4		7.74	Keller (1972)
$UTiO_5$			orthorhombic	6.31	7.35	15.56					Dickens *et al.* (1993)
UVO_5	black	*Pbma*	orthorhombic	12.31	7.19	4.115					Keller (1975)
$UNbO_{5(+x)}$			orthorhombic	6.459	3.785	4.036					Keller (1975)
$UTaO_{5.17}$	dark gray		orthorhombic	6.463	3.780	3.980					Keller (1975)
$UMoO_5$		*Pbcm*	orthorhombic	4.115	12.761	7.338					Keller (1975)
$UTeO_5$		$Pca2_1$	orthorhombic	10.161	5.363	7.862					Meunier and Galy (1973)
CoU_2O_6	dark brown		hexagonal	9.095		4.990			8.55	8.79	Kemmler-Sack and Rüdorff (1967); Keller (1975)
NiU_2O_6	red brown	*P*321	hexagonal	9.015		5.103			8.64	8.75	Kemmler-Sack and Rüdorff (1967); Keller (1975)
CdU_2O_6			cubic	5.357					9.66	9.858	Kemmler-Sack and Rüdorff (1967)
Cr_2UO_6	black	$P\bar{3}1m$	hexagonal	4.988		4.620			7.01	7.31	Keller (1975)
Cd_3UO_6	light orange		monoclinic	8.262	5.733	5.623	$\beta = 89.53$				Keller (1972)
Pb_3UO_6	dark red	*Pnam*	orthorhombic	13.71	12.36	8.21					Keller (1972)
UV_2O_6		$P\bar{3}1m$	hexagonal	4.988		4.768			7.09	7.06	Keller (1975)

Table 5.18 (*Contd.*)

Formula	*Color*	*Space group*	*Symmetry*	*Lattice parameters*				Z	*Density* ($g\ cm^{-3}$)		*References*
				a (Å)	*b* (Å)	*c* (Å)	*Angle* (deg)		*Exp.*	*X-ray or ND*	
CdU_2O_7	yellow										Keller (1972)
$Cd_2U_2O_7$			rhombohedral	10.72			$\alpha = 91.30$				Kemmler-Sack and Rüdorff (1967)
$Tl_2U_2O_7$			orthorhombic	6.902	7.971	19.643					Keller (1972)
$U_{2/3}Nb_2O_7$		*Fd*3	cubic	10.38					5.2	5.4	Keller (1975)
$Co_3U_2O_8$		*Pnnm*	orthorhombic	5.11	10.30	6.15		2			Bacmann (1973); Keller (1975)
UV_2O_8	yellow green	*Pnma*	orthorhombic	5.70	11.78	10.42			4.50	4.45	Keller (1975)
UTa_2O_8	yellow	$P\bar{3}1m$	hexagonal	6.41		3.95			8.3		Keller (1975)
UMo_2O_8		*Pban*	orthorhombic	20.08	7.32	4.11			6.13		Keller (1975)
U_2MoO_8		$P2_12_12$	orthorhombic	6.734	23.24	4.115					Keller (1975)
U_2WO_8		$P2_12_12$	orthorhombic	6.711	23.28	4.091					Keller (1975)
MnU_3O_{10}	light brown		hexagonal	3.80		4.14					Hoekstra and Marshall (1967); Keller (1972)
FeU_3O_{10}			orthorhombic	6.51	7.53	16.14					Keller (1972, 1975)
CoU_3O_{10}	deep brown		hexagonal	3.79		4.08					Hoekstra and Marshall (1967); Keller (1972, 1975)
NiU_3O_{10}	yellow brown		monoclinic	7.525	6.545	16.126	$\beta = 91$				Hoekstra and Marshall (1967); Keller (1972, 1975)
CuU_3O_{10}	deep red		monoclinic	7.575	6.473	16.679	$\beta = 91$				Hoekstra and Marshall (1967); Keller (1972)

ZnU_3O_{10}	red brown		hexagonal	7.56			16.418			Hoekstra and Marshall (1967); Keller (1972)
UV_3O_{10}	black	*Fddd*	orthorhombic	12.00	6.926	16.17				Keller (1975)
$UNb_3O_{10(+x)}$		*Fddd*	orthorhombic	7.38	12.78	15.96		5.95	5.98	Keller (1975)
$UTa_3O_{10(+x)}$			hexagonal	7.416		15.770		8.41		Keller (1975)
$U(WO_4)_2$			orthorhombic	9.545	10.245	14.26				Keller (1975)
$U_2V_2O_{11}$	green	$P2_1/m$	monoclinic	9.29	13.24	7.27	$\beta \approx 100$			Keller (1975)
Y_6UO_{12}	pale yellow-green	$R\bar{3}$	hexagonal	9.934	9.364			5.91	6.00	Aitken *et al.* (1964); Bartram (1966)
La_6UO_{12}	reddish-orange	$R\bar{3}$	hexagonal	10.473		9.984			9.63	Aitken *et al.* (1964); Hinatsu *et al.* (1988)
Pr_6UO_{12}		$R\bar{3}$	hexagonal	10.301		9.800				Aitken *et al.* (1964)
Nd_6UO_{12}		$R\bar{3}$	hexagonal	10.254		9.748				Aitken *et al.* (1964)
Sm_6UO_{12}		$R\bar{3}$	hexagonal	10.148		9.630				Aitken *et al.* (1964)
Gd_6UO_{12}		$R\bar{3}$	hexagonal	10.076		9.529				Aitken *et al.* (1964)
Tb_6UO_{12}		$R\bar{3}$	hexagonal	10.013		9.465				Aitken *et al.* (1964)
Ho_6UO_{12}		$R\bar{3}$	hexagonal	9.935		9.368				Aitken *et al.* (1964)
Tm_6UO_{12}		$R\bar{3}$	hexagonal	9.826		9.248				Aitken *et al.* (1964)
Yb_6UO_{12}		$R\bar{3}$	hexagonal	9.826		9.248				Aitken *et al.* (1964)
Lu_6UO_{12}		$R\bar{3}$	hexagonal	9.797		9.204				Aitken *et al.* (1964); Bartram (1966)
$Y_5U_2O_{12}$		$R\bar{3}$	hexagonal	10.01		9.36		6.88	6.83	Bartram (1966)
$U_2V_6O_{21}$	brown	*Fddd*	orthorhombic	11.995	6.94	16.17				Keller (1975)
$UMo_{10}O_{32}$		*Cccm*	orthorhombic	16.18	14.48	19.18				Keller (1975)
$UMo_{11}O_{35}$			orthorhombic	19.66	14.41	16.11		5.01		Keller (1975)
α-$U_3Mo_{20}O_{64}$		*Cccm*	orthorhombic	8.246	28.76	19.78				Keller (1975)
γ-$U_3Mo_{20}O_{64}$		*Pbmn*	orthorhombic	4.134	14.33	9.873		5.08	5.18	Keller (1975)
$U_5W_{19}O_{67}$		*Pcmm*	orthorhombic	7.814	7.271	38.67				Keller (1975)

because of their high reactivity. In this case, reaction temperatures not higher than 600°C are recommended for M = Cu, Zn, and Cd to avoid the formation of U_3O_8. $HgUO_4$ forms at 400°C. Ag_2UO_4 has been synthesized by heating a mixture of $AgNO_3$ and UO_2 to 500°C and maintaining this temperature for a period of 15 min. Above 500°C, Ag_2UO_4 begins to decompose with precipitation of metallic silver.

For preparing $FeUO_4$ and FeU_3O_{10}, the symproportionation reaction method in a sealed tube gives a good result. $FeUO_4$ is synthesized by heating either a mixture of $FeO + UO_3$ or $2Fe_2O_3 + U_3O_8 + UO_2$ at 1050°C in evacuated sealed quartz tubes. When a mixture of $Fe_2O_3 + U_3O_8 + 3UO_3$ is heated at 880°C, FeU_3O_{10} forms (Hoekstra and Marshall, 1967). $BiUO_4$ is prepared by heating a mixture of $2Bi_2O_3 + U_3O_8 + UO_2$ at 900–1000°C (Rüdorff *et al.*, 1967). The compounds MU_2O_6 (M = Co, Ni, Cd) have been prepared by heating the mixtures of $MUO_4 + UO_2$ at 800°C (Kemmler-Sack and Rüdorff, 1967). Single crystals of CuU_3O_8 and NiU_3O_{10} were grown by the reaction of UO_3 with the molten anhydrous transition metal chlorides in evacuated sealed silica tubes at 600–650°C for several weeks (Hoekstra and Marshall, 1967).

MU_3O_{10} with M = Mn, Co, and Zn were prepared by hydrothermal reactions using a platinum-lined Morey bomb in which the transition metal oxides and γ-UO_3 were heated in 0.06 M H_2SO_4 solution for 5 days at 350°C (Hoekstra and Marshall, 1967).

MUO_4 (M = Ni, Zn, Co, Mn) was successfully synthesized in experiments where a mixture of oxides was heated for 30 min at 1000°C under high pressures of 30–40 kbar using a tetrahedral anvil. However, the triuranates of these transition metals and $FeUO_4$ did not form by this method (Hoekstra and Marshall, 1967).

(*ii*) *Crystal structures*

$MnUO_4$ and $CoUO_4$ have the infinite chains of edge-sharing oxygen octahedra in the direction normal to the *c*-axis, characteristic of the $MgUO_4$ structure; these compounds crystallize in the same space group. The space group of $CrUO_4$, $FeUO_4$, and α-$NiUO_4$ is different from that of the above two compounds, and the lengths of the uranium–oxygen bonds that are expected to belong to uranyl groups are longer (2.05–2.06 Å) than those in $MnUO_4$ and $CoUO_4$. In these three compounds, the distorted UO_6 octahedra form infinite chains along the *c*-axis and less deformed MO_6 (M = Cr, Fe, Ni) octahedra are running parallel in the direction of the *c*-axis. Similar chain structures are also observed in the crystals of $USbO_5$, $UTiO_5$, and $UMoO_5$ (Dickens *et al.*, 1993). These structures are built from parallel layers of edge-sharing UO_m and MO_n polygons, linked together by metal–oxygen–metal chains or pillars running perpendicularly to the layers. In Pb_3UO_6, the infinite chains are formed by sharing the corners of distorted UO_6 octahedra in the direction of the *c*-axis.

The crystal structure of Pb_3UO_6 is wholly different from those of Ca_3UO_6 and Sr_3UO_6 (Sterns, 1967).

In the system PbO–U_2O_5, cubic $Pb_{1.5}U_2O_{6.5}$ ($a = 11.16$ Å) accommodates PbO until the $Pb_{2.5}U_2O_{7.5}$ composition is attained, resulting in a slight distortion to a rhombohedral structure ($a = 11.23$ Å, $\alpha = 90.25°$). This homogeneity range is regarded as derived from pyrochlore-type $Pb_2U_2O_7$ by addition or subtraction of PbO (Kemmler-Sack and Rüdorff, 1966).

$CuUO_4$ comprises a third group of crystal structures among the transition metal monouranates (Siegel and Hoekstra, 1968). The compound is monoclinic with space group $P2_1/n$. The coordination geometry is distorted octahedral with short collinear uranyl bonds, each of length 1.90 Å. The uranyl groups are in the direction nearly normal to a planar and almost square array of secondary uranium–oxygen bonds of lengths 2.15 and 2.24 Å.

Rare-earth oxides form solid solutions with UO_2 in an extended composition range. At the high atom ratio of RE/U = 6 (RE = rare-earth metals), however, the compounds of the composition RE_6UO_{12} crystallize in rhombohedral systems. In RE_6UO_{12} the uranium atom is surrounded by six oxygen atoms that form a distorted octahedron. All the U–O bond distances in the octahedron are 2.34 Å (La_6UO_{12}), and no uranyl groups exist in the crystal (Hinatsu *et al.*, 1988). $Y_5U_2O_{12}$ is produced along with Y_6UO_{12} giving a very similar crystal structure with similar lattice parameters. In $Y_5U_2O_{12}$, half the uranium atoms occupy the Y position (18f) in a disordered manner (Bartram, 1966).

(d) Solid solutions with UO_2

Uranium dioxide forms solid solutions with the oxides of alkaline-earth elements, rare-earth elements, some transition elements (Mn, Zr, Nb, Cd), and actinide elements (Th, Np, Pu, Am, Cm, etc.). The solid solution with PuO_2 (MOX) is important as nuclear fuel. Description on mixed oxide fuel, MOX, is given in Chapter 7.

The solid solutions are prepared by heating intimate mixtures of metal (M) oxides and uranium oxides usually in reducing atmosphere at temperatures between 1000 and 2000°C. The oxide powders are in most cases mechanically mixed, but other techniques such as coprecipitation (Keller *et al.*, 1972; Miyake *et al.*, 1986) and evaporation from aqueous solutions (Markin *et al.*, 1970; Lindemer and Sutton, Jr., 1988) have also been adopted. In the solid solutions, the dissolved foreign metal atoms and host uranium atoms are statistically distributed on the metal sites of the fluorite-type cubic crystals of UO_2 (Rüdorff *et al.*, 1967; Keller *et al.*, 1969; Hutchings *et al.*, 1985; Martin *et al.*, 2003). The solid solution can be written as $M_yU_{1-y}O_{2+x}$, where x is defined (in this section) to take on both positive and negative values. A considerable number of publications on the magnetic properties are available since the magnetic properties of uranium and metals, M, of varying oxidation state can be studied in the same fluorite-type fcc crystal field in these solid solutions; detailed description is given

in Chapter 20. Recent progress on this subject is written in a review (Fujino and Miyake, 1991).

(*i*) *Lattice parameter change with composition*

The lattice parameter of cubic solid solution changes nearly linearly with the increase of y and x in $M_yU_{1-y}O_{2+x}$. The differential coefficient, $\partial a/\partial y$, where a is the lattice parameter in Å, can have both negative and positive values depending on the metal ion M^{n+}. Table 5.19 shows the observed $\partial a/\partial y$ and $\partial a/\partial x$ for various solid solutions (Fujino and Miyake, 1991). The underlined values in the table are those obtained from the lattice parameters of the stoichiometric solid solutions at the upper limit of the y-values, i.e. $M^{3+}_{0.5}U_{0.5}O_{2.00}$ and $M^{2+}_{0.33}U_{0.67}O_{2.00}$.

As seen in the table, the coefficient $\partial a/\partial y$ is large for the metals with large ionic radii, although correction for valence state of the metals is required for a more detailed discussion. Investigations to determine the functional relation between these quantities have been performed (Ohmichi *et al*., 1981; Fujino and Miyake, 1991). The differential coefficient of the oxygen non-stoichiometry, $\partial a/\partial x$, in Table 5.19 have in general the values $-0.3 \leq \partial a/\partial x \leq -0.24$ for $x < 0$ and $-0.13 \leq \partial a/\partial x \leq -0.11$ for $x > 0$ regardless of the M metal.

(*ii*) *The solid solution regions*

$M^{4+}_yU_{1-y}O_{2+x}$

Zr SOLID SOLUTIONS The solubility data on this system are diverse. The Zr solid solution with $y = 0.15$ was obtained by heating at 1500°C (Une and Oguma, 1983a); at 1750°C, solid solutions with y values up to 0.3 were obtained (Aronson and Clayton, 1961). The solid solution with the highest y value, 0.35, has been obtained by heating the mixture of $UO_2(NO_3)_2 \cdot 6H_2O$ and $ZrOCl_2 \cdot 8H_2O$ in H_2 at 1650°C (Hinatsu and Fujino, 1985). The Zr solid solution is regarded as metastable at lower temperatures.

Th SOLID SOLUTIONS Th solid solutions are formed continuously from $y = 0$ to 1 for $x = 0$. However, for $x > 0$, there is an upper limit in the solubility. According to Paul and Keller (1971), the single-phase solid solutions under 1 atm O_2 exist below $y = 0.45$, 0.40, and 0.36 at 1100, 1400, and 1550°C, respectively. The lower limits at $p_{O_2} = 0.2$ atm are $y = 0.383$, 0.359, 0.253, and 0.068 for 700, 1200, 1400, and 1500°C, respectively (Gilpatrick *et al*., 1964), which is in agreement with the value of $y = 0.22$ below 1400°C reported by Anderson *et al*. (1954). The maximum x value is 0.25 at temperatures between 1250 and 1550°C for $y \leq 0.5$. At lower temperatures of 600–1100°C, the upper limit of x decreases to 0.12–0.14 for y values below 0.4 (Cohen and Berman, 1966; Paul and Keller, 1971).

Table 5.19 *Lattice parameter change with composition of solid solutions* $M_yU_{1-y}O_{2+x}$ (*Fujino and Miyake,* 1991).

Element	$\partial a/\partial y$	$\partial a/\partial x$	*References*
Zr	–0.302		Cohen and Schaner (1963);
	–0.301		Hinatsu and Fujino (1985)
Th	0.163 ($y \leq 0.05$)	–0.14 ($x > 0$)	Cohen and Berman (1966)
	0.127		
	($0.1 \leq y \leq 0.5$)		
Np	–0.146		Tabuteau *et al.* (1984)
Pu	–0.0747 ($x = 0$)	–0.345 ($x < 0$)	Schmitz *et al.* (1971);
	–0.0727 ($x < 0$)		
		–0.313 ($x < 0$)	Martin and Shinn (1971);
		–0.274 ($x < 0$)	Mignanelli and Potter (1986)
Sc	–0.438		Hinatsu and Fujino (1986);
	–0.521		Keller *et al.* (1972)
Y	–0.233		Fukushima *et al.* (1981);
	–0.254		Weitzel and Keller (1975);
	–0.266		Ohmichi *et al.* (1981)
La	0.094 ($x > 0$)	–0.131 ($x > 0$)	Hinatsu and Fujino (1987);
	0.06 ($x < 0$)	–0.2 ($x < 0$)	
	0.073 ($x = 0$)		Weitzel and Keller (1975);
		–0.285 ($x < 0$)	Hill *et al.* (1963)
Ce	–0.067		Mignanelli and Potter (1983);
	–0.06		Lorenzelli and Touzelin (1980);
	–0.057 ($x = 0$)		Hinatsu and Fujino (1988a);
		–0.321 ($x < 0$)	Markin *et al.* (1970);
		–0.288	Norris and Kay (1983)
		($y = 0.282$,	
		$-0.015 \leq x < 0$)	
Pr	–0.007	–0.127 ($x > 0$)	Yamashita *et al.* (1985);
		–0.397 ($x < 0$)	
	–0.015		Hinatsu and Fujino (1988c)
Nd	–0.047	–0.112 ($x > 0$)	Hinatsu and Fujino (1988b);
	–0.057		Fukushima *et al.* (1983);
	–0.058		Weitzel and Keller (1975);
	–0.075		Ohmichi *et al.* (1981);
		–0.30 ($x < 0$)	Wadier (1973)
Sm	–0.118		Fukushima *et al.* (1983);
	–0.121		Rüdorff *et al.* (1967)
Eu	–0.138		Fukushima *et al.* (1983);
	–0.144		Ohmichi *et al.* (1981);
	–0.151	–0.30 ($x < 0$)	Fujino *et al.* (1990)
Gd	–0.164		Fukushima *et al.* (1982);
	–0.171		Rüdorff *et al.* (1967);
	–0.173	–0.24 ($x < 0$)	Ohmichi *et al.* (1981)
Ho	–0.267		Weitzel and Keller (1975)
Yb	–0.315		Rüdorff *et al.* (1967)
Lu	–0.356		Weitzel and Keller (1975)
Mg	–0.568	–0.117 ($x > 0$)	Fujino and Naito (1970);
	–0.546		Kemmler-Sack and Rüdorff (1967);
	–0.559		Keller (1964)

Table 5.19 (*Contd.*)

Element	$\partial a/\partial y$	$\partial a/\partial x$	*References*
Ca	–0.310	–0.102 ($x > 0$) –0.190 ($x < 0$)	Yamashita and Fujino (1985);
	–0.213	–0.10 ($x > 0$)	Hinatsu and Fujino (1988d);
	–0.289		Loopstra and Rietveld (1969)
Sr	–0.098	–0.109 ($x > 0$) –0.244 ($x < 0$)	Fujino *et al.* (1988);
	–0.055		Hoekstra and Katz (1952)
Mn	–0.499		Kemmler-Sack and Rüdorff (1967)
Cd	–0.340		Keller (1962b); Kemmler-Sack and Rüdorff (1967)
Bi	0.149		Rüdorff *et al.* (1967)

$M_y^{4+\sim3+}U_{1-y}O_{2+x}$

Ce SOLID SOLUTIONS Ce solid solutions are formed continuously from $y = 0$ to 1 for $x = 0$. For $x < 0$, the region of the single-phase solid solution is restricted to $y \leq 0.35$ (Markin *et al.*, 1970) or $y \leq 0.2$ (Lorenzelli and Touzelin, 1980). Above this value up to $y = 0.7$, the products are two phases $(Ce,U)O_{2.00}$ and $(Ce,U)O_{2-x}$ at room temperature. Further reduction results in formation of single-phase solid solutions. The x values for the single-phase solid solutions are $x < -0.04$, –0.12, –0.19, and –0.24 for $y = 0.1$, 0.3, 0.5, and 0.7, respectively (Lorenzelli and Touzelin, 1980).

In the hyperstoichiometric range of $0 \leq x \leq 0.18$, the solid solutions with $y < 0.5$ are a single phase at room temperature. Air-oxidized hyperstoichiometric solid solutions crystallize in a fluorite-type single phase in the region of high Ce concentrations (Hoch and Furman, 1966). Single-phase regions exist in $y = 0.56$–1.0 (1100°C), 0.43–1.0 (1250 °C), and 0.26–1.0 (1550°C) (Paul, 1970). Single phases with $y = 0.6$–1.0 at 1100°C have also been reported (Tagawa *et al.*, 1981a).

$M_y^{n+}U_{1-y}O_{2+x}$ ($n = 3$ and 2)

SOLID SOLUTIONS IN REDUCING ATMOSPHERE The solid solutions obtained by heating in reducing atmospheres are generally hypostoichiometric. The x values are highly negative when strong reductants such as H_2 or CO are used. The single-phase regions of fcc solid solutions with M metals (M = rare-earth elements, alkaline-earth metals, and Cd) are shown in Table 5.20. In reducing atmosphere, the single-phase solid solution forms essentially in a range starting from $y = 0$. For M^{2+} metals, the maximum y values are around 1/3. If the monoxides of Mg and Ba are heated with UO_2 in a vacuum, the solubility is very low even at high temperatures due to shortage of oxygen (cf. Table 5.20).

Table 5.20 *Single phase regions of fcc solid solutions* $M_yU_{1-y}O_{2+x}$ *with M elements (rare-earth elements, alkaline-earth elements and Cd) prepared in reducing atmospheres. Concentrations of the M elements are shown in* mol%.

	Temperature (°C)					
Element	1100	1250	1400	1550	1700	*References*
Sc	0–1.6	0–1.8	0–2.1	0–2.9 (H_2)		Keller *et al.* (1972)
Y					0–50 (H_2)	Bartram *et al.* (1964);
					0–65 (2000°C, vacuum)	Ferguson and Fogg (1957)
La		0–82				Diehl and Keller (1971);
				0–54 (1750°C, vacuum)		Wilson *et al.* (1961);
				0–75 (1750°C, H_2 or vac.)		Hill *et al.* (1963)
Pr		0–70 (1350°C, vacuum)				Yamashita *et al.* (1985)
Eu		0–42 (Ar)				Berndt *et al.* (1976);
				0–53 (1600°C, vacuum)		Grossman *et al.* (1967);
				0–50∼60 (vacuum)		Fujino *et al.* (1990)
Gd					0–80 (H_2)	Beals and Handwerk (1965)
					0–50 (Ar)	
Mg	0–33 ($MgUO_4$+MgU_3O_{10}+UO_2, 1100–1300°C, He)					Fujino and Naito (1970);
				0–5 (MgO+UO_2, 2350°C, vac.)		Anderson and Johnson (1953)
Ca	0–33 ($CaUO_4$+U_3O_8+UO_2, 1100–1300°C, vacuum)				0–40 (2000°C)	Brisi *et al.* (1972);
						Voronov and Sofronova (1972);
		3–33 (1200–1400°C, He)		0–20(CaO+UO_2, 1650°C, vac.)		Yamashita and Fujino (1985);
						Alberman *et al.* (1951)
Sr	0–30 ($SrUO_4$+U_3O_8+UO_2, 1200–1400°C, ∼1 Pa O_2)					Fujino *et al.* (1988);
	33 (SrU_2O_7, vacuum)					Hoekstra and Siegel (1956);
						Ippolitova *et al.* (1961b);
		0–20 (1300°C)				Brisi *et al.* (1972)
Ba	33 (BaU_2O_7, 1200°C, vacuum)					Hoekstra and Siegel (1956);
	33 (BaU_2O_7, 600°C, NH_3)					Brochu and Lucas (1967);
				0–3 (BaO+UO_2, vac.)		Kleykamp (1985)
Cd	0–33 ($CdUO_4$+UO_2, vacuum sealed tube)					Kemmler-Sack and Rüdorff (1967)

SOLID SOLUTIONS IN OXIDIZING ATMOSPHERE The single-phase regions of fcc solid solutions prepared in oxidizing atmospheres are shown in Table 5.21. UO_2 is oxidized to U_3O_8 when heated in oxidizing atmospheres unless mixed with the M elements. Hence, the lower limit of the fcc single phase is not $y = 0$ but at higher values. The x value changes with y value in a rather simple way for rare-earth solid solutions: For Nd solid solutions heated under $p_{O_2} = 1$ atm at 1100°C for example, the mean uranium valence remains constant (+5) when the y value is in a region between ~0.3 and 0.5, i.e. x changes as $x=1/2-y$. The uranium valence then increases linearly from +5 to +6 when y increases from 0.5 to 0.67, during which $x = 0$. For the solid solutions in a higher y range, 0.67–0.75, the uranium valence is U(VI). Here, the x value decreases linearly from 0 to –0.125 ($x=1-3y/2$) with increasing y value in order to satisfy the charge neutrality condition (Keller and Boroujerdi, 1972).

(*iii*) *Oxygen potentials*

$M_y^{4+}U_{1-y}O_{2+x}$

Zr SOLID SOLUTIONS The oxygen potential of $Zr_yU_{1-y}O_{2+x}$ solid solution is lower than that of UO_{2+x}. At 1250 K, the $\Delta\bar{G}(O_2)$ value for Zr solid solution with $y = 0.3$ is –270 kJ mol^{-1} at $x = 0.05$ (Aronson and Clayton, 1961), while that for UO_{2+x} at $x = 0.05$ is ca. –210 kJ mol^{-1}. The low $\Delta\bar{H}(O_2)$ of $Zr_yU_{1-y}O_{2+x}$ has been suggested to explain the low $\Delta\bar{G}(O_2)$ of this solid solution. The $\Delta\bar{H}(O_2)$ values vary between –480 and –355 kJ mol^{-1} for $Zr_yU_{1-y}O_{2+x}$, which are significantly lower than those between –355 and –270 kJ mol^{-1} for $Th_yU_{1-y}O_{2+x}$ (Aronson and Clayton, 1960, 1961; Une and Oguma, 1983a).

Th SOLID SOLUTIONS Dissolution of Th causes an increase in $\Delta\bar{G}(O_2)$ with increasing value of y. The difference in $\Delta\bar{G}(O_2)$ between Th solid solution and UO_{2+x} is small if the concentration of Th is low (viz., $y = 0.1$). However, at high Th concentration with $y = 0.71$ ($x = 0.05$), $\Delta\bar{G}(O_2)$ of the solid solution at 1250 K is as high as –150 kJ mol^{-1} (Aronson and Clayton, 1960). This value is 60 kJ mol^{-1} higher than $\Delta\bar{G}(O_2)$ of $UO_{2.05}$ at the same temperature. There have been other thermodynamic studies on this solid solution (Tanaka *et al.*, 1972; Ugajin, 1982; Ugajin *et al.*, 1983; Matsui and Naito, 1985a).

$M_y^{4+\sim3+}U_{1-y}O_{2+x}$

Ce SOLID SOLUTIONS Because two oxidation states, Ce^{3+} and Ce^{4+}, are possible for Ce in oxides, the oxygen potential of Ce solid solution changes over a wide range of x-values from negative to positive values, giving rise to a rapid ('vertical') change of $\Delta\bar{G}(O_2)$ at $x = 0$. The shape of the $\Delta\bar{G}(O_2)$ curve is very similar to that of $Pu_yU_{1-y}O_{2+x}$, but the $\Delta\bar{G}(O_2)$ values of $Ce_yU_{1-y}O_{2+x}$ are markedly higher. Namely, $\Delta\bar{G}(O_2)$ for $Ce_{0.25}U_{0.75}O_{1.95}$ is as high as –460 kJ mol^{-1} at 1200°C, compared to the value of –570 kJ mol^{-1} for $Pu_{0.25}U_{0.75}O_{1.95}$.

Table 5.21 *Single-phase regions of fcc solid solutions* $M_yU_{1-y}O_{2+x}$ *with M elements (rare-earth elements and Mg) prepared in oxidizing atmospheres. Atmosphere is* O_2 (1 atm) *unless otherwise described. Concentrations of the M elements are shown in* mol%.

	Temperature (°C)					
Element	1100	1200	1300	1400	1500	*References*
Sc	49.5–63.8	48.5–64.0 (1250°C)		45.5–64.9	42.1–65.5 (1510°C) ~0–65.7 (1550°C)	Keller *et al.* (1972)
Y	33–60 (1000°C, air)	30–65 (air)				Bartram *et al.* (1964); Hund *et al.* (1965)
La	31.5–51.5 68.5 79.5–82 30–45, 70–90 (1000°C, air)	28.5–55 63.5–69.5 79–82	26.5–75 77–82	25–82	24–82 (1550°C) 30–80 (1650°C)	Diehl and Keller (1971); Hill *et al.* (1963); Tagawa *et al.* (1983)
Pr	38.6–71.9	39.9–71.2 30–60 (1250°C)	41.4–70.2 32–71 (1350°C, air)	43.2–69.0	45.3–67.1	de Alleluia *et al.* (1981); Jocher (1978); Yamashita *et al.* (1985)
Nd	35.0–74.5	33–81 (1250°C)		25–81	13–81 (1550°C)	Boroujerdi (1971); Keller and Boroujerdi (1972)
Sm	50–60 (1000°C, air)					Tagawa *et al.* (1981b)
Eu	39–72 38–64 (air)	36–72 (1250°C)		30–72	25–72	Tanamas (1974); Haug and Weigel (1963)
Gd					30–60 (1700°C, air)	Beals and Handwerk (1965)
Dy	48.4–74.9	44.1–72.8 (1250°C)		35.0–72.8	14.2–72.2 (1550°C)	de Alleluia *et al.* (1981)
Ho	47.0–64.0	43.0–64.0 (1250°C)		33.0–64.0	19.0–64.0 (1550°C)	Keller *et al.* (1969)
Er	49.0–62.5	45.0–62.5 (1250°C)		41.0–62.5	21.5–62.5 (1550°C)	Keller *et al.* (1969)
Tm	48.5–64.0	45.0–64.0 (1250°C)		34.0–64.0	15.0–64.0 (1550°C)	Keller *et al.* (1969)
Yb	48.5–64.5	45.0–64.5 (1250°C)		38.5–64.5	16.5–64.5 (1550°C)	Keller *et al.* (1969)
Lu	48.0–65.5	45.0–65.5 (1250°C)		43.0–65.5	41.0–65.5 (1550°C)	Keller *et al.* (1969)
Mg			36–39 (1300°C, air)	12–39 (1500°C, air)	~0–39 (1600°C, air) max. 37 (1600–1700°C, air)	Sugisaki *et al.* (1973); Budnikov *et al.* (1958)

This difference has been attributed to the higher $\Delta\bar{G}(O_2)$ value of CeO_{2-x} (Panlener *et al.*, 1975) compared with that of PuO_{2-x} (Woodley, 1981). The $\Delta\bar{G}(O_2)$ measurements of the Ce solid solutions have been carried out by a number of researchers (Hoch and Furman, 1966; Markin and Crough, 1970; Ducroux and Baptiste, 1981; Norris and Kay, 1983; Nagarajan *et al.*, 1985).

Pr AND Am SOLID SOLUTIONS The Pr solid solutions have lower values of $\Delta\bar{G}(O_2)$ than the solid solutions with solely M^{3+} rare-earth ions, because of the two possible oxidation states, Pr^{3+} and Pr^{4+} (Jocher, 1978; Fujino and Miyake, 1991). The situation is the same for Am solid solutions, although their $\Delta\bar{G}(O_2)$ values are markedly higher than those of Pu and Ce solid solutions (Bartscher and Sari, 1983).

$M_y^{3+}U_{1-y}O_{2+x}$

A large number of oxygen potential measurements for the M^{3+} solid solutions have been carried out. These comprise solid solutions of Y (Aitken and Joseph, 1966; Hagemark and Broli, 1967; Nakajima *et al.*, 2002), La (Hagemark and Broli, 1967; Stadlbauer *et al.*, 1974; Matsui and Naito, 1986), Pr (Jocher, 1978; Fujino and Miyake, 1991), Nd (Wadier, 1973; Une and Oguma, 1983c), Eu (Tanamas, 1974; Lindemer and Brynestad, 1986; Fujino *et al.*, 1990, 1999), and Gd (Une and Oguma, 1982, 1983b; Lindemer and Sutton, Jr. 1988).

$\Delta\bar{G}(O_2)$ for $M_y^{3+}U_{1-y}O_{2+x}$ can be defined from $x = -y/2$ to positive x values; the measured oxygen potential increases with increasing x value, passing through an inflection point at $x = 0$, where $\Delta\bar{G}(O_2)$ increases very rapidly. The dissolution of M^{3+} metals enhances $\Delta\bar{G}(O_2)$ more than do the M^{4+} metals. The $\Delta\bar{G}(O_2)$ value increases with increasing y, but the $\Delta\bar{G}(O_2)$ curve gradually levels off at high M^{3+} concentrations. In a series of rare-earth solid solutions, the La solid solution shows the highest $\Delta\bar{G}(O_2)$ values, which is assumed to be associated with the fact that La^{3+} has the largest ionic radius of these M^{3+} ions. With increasing atomic number of the lanthanides, $\Delta\bar{G}(O_2)$ is lowered, although the $\Delta\bar{G}(O_2)$ difference between the Nd and Gd solid solutions is small. Fig. 5.26 shows the oxygen potential of $Gd_yU_{1-y}O_{2+x}$ as a function of O/(Gd+U) ratio ($=2 + x$).

The Eu solid solutions show a much higher value of $\Delta\bar{G}(O_2)$ than the other M^{3+} solid solutions (Lindemer and Brynestad, 1986). This is possibly due to the coexistence of Eu^{2+} and Eu^{3+} in the solid solutions (Fujino *et al.*, 1990). It is noteworthy that the inflection point of $\Delta\bar{G}(O_2)$ for Eu solid solutions is shifted to a range of $x < 0$ values. This is also observed for $M_y^{2+}U_{1-y}O_{2+x}$, supporting the presence of Eu^{2+} in the Eu solid solutions.

$M_y^{2+}U_{1-y}O_{2+x}$

The oxygen potential of $Mg_yU_{1-y}O_{2+x}$ (Fujino and Naito, 1970; Fujino *et al.*, 1978a; Tateno *et al.*, 1979) is significantly higher than those of $M_y^{3+}U_{1-y}O_{2+x}$. Moreover, the x values at which the 'vertical' change of $\Delta\bar{G}(O_2)$ takes place,

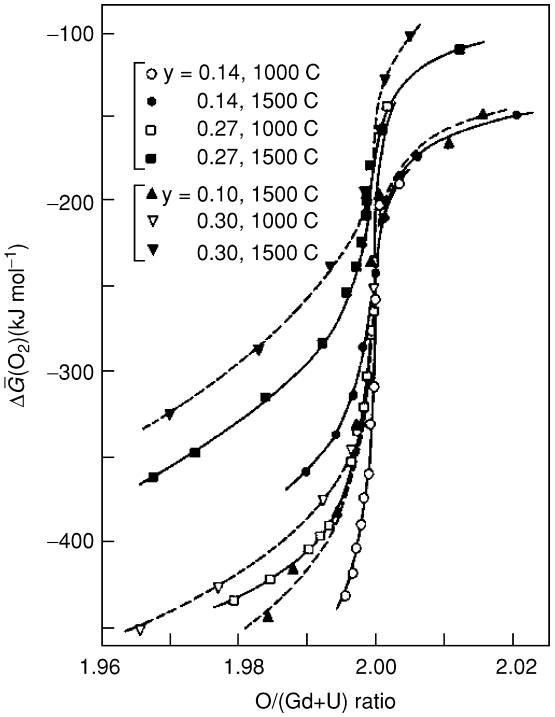

Fig. 5.26 *Oxygen potential of* $Gd_yU_{1-y}O_{2+x}$ *as a function of O/(Gd+U) ratio* (*Fujino and Miyake,* 1991). *Solid lines: Une and Oguma* (1983*b*)*; Broken lines: Lindemer and Sutton, Jr.* (1988). *Reproduced by the permission of Elsevier*.

which are also the inflection points, are negative in contrast to the M^{4+} and M^{3+} solid solutions, where the value of x at the inflection is zero. This negative shift for $Mg_yU_{1-y}O_{2+x}$ becomes more pronounced at higher values of y, viz., $x = -0.07$ at $y = 0.3$ (1200–1500°C) (Sugisaki and Sueyoshi, 1978).

The high $\Delta\bar{G}(O_2)$ values are supposed to be rationalized by a configurational entropy change. Dissolution of M^{2+} metals in UO_2 results in formation of a larger number of U^{5+} ions in the solid solution crystals, which increases the number of ways, W, of arranging the cations on the cation sites. The entropy, $\Delta\bar{S}(O_2)$, described by the relation $\Delta\bar{S}(O_2) = 2R\,\partial \ln W/\partial(xN)$, where N is the Avogadro's number (Aronson and Clayton, 1960; Hagemark and Broli, 1967; Fujino and Miyake, 1991), shows therefore a significant decrease. For the Mg solid solutions Fujino *et al.* (1992, 1995, 1997b) claim that the $\Delta\bar{G}(O_2)$ shift is explained if the charge complexes of the form, ($M^{2+}2U^{5+}$), in which the corresponding cations have their normal sites, are formed together with ($M^{2+}U^{5+}$) complexes. In the oxygen potential curves for $(Mg,Gd,U)O_{2+x}$ (Fujino *et al.*, 2001a) and $(Mg,Ce,U)O_{2+x}$ (Fujino *et al.*, 2001b), the shift to negative x values is even larger than in the Mg solid solution.

When the oxygen partial pressure is very low, high concentrations of Mg cannot dissolve in UO_2. The solubility of Mg is in a range $0.1 < y < 0.15$ for $p_{O_2} = 10^{-15}$–10^{-19} atm at 1200°C (Fujino *et al.*, 1997a).

5.7.3 Uranium borides, carbides, silicides, and related compounds

Non-oxide p-block compounds of uranium represent a large family that share certain similarities with oxides in that non-stoichiometric compounds exist; these are especially well noted for the heavy p-block elements of a semi-metallic nature (e.g. Sb and Te). Oxidation state assignment for uranium in some of these compounds can be very tedious, owing to the presence of homoatomic bonding between main group elements where the E ··· E (E = main group element) contacts between main group elements is intermediate in length between a full single bond and a van der Waals contact. This phenomenon is particularly common in antimonides and tellurides. Full descriptions of all known binaries and especially of ternary and quaternary phases are not possible in the present context. Further historical details can be found in Waber *et al.* (1964), Eding and Carr (1961), Freeman and Darby (1974), and in a series of IAEA bibliographies (Maximov, 1963, 1965, 1967).

(a) Uranium–boron system

The only known binary uranium borides are UB_2, UB_4, and UB_{12}. The crystal structure data for these compounds are given in Table 5.22. The former compounds have been prepared by direct reaction of the elements at high temperatures (Wedekind and Jochem, 1913). Mixtures of UB_{12} and UB_4 have also been deposited by fused-salt electrolysis (Andrieux, 1948; Andrieux and Blum, 1949). It has recently been demonstrated that UB_4 can be prepared by the solid-state metathesis reaction of UCl_4 with MgB_2 at 850°C (Lupinetti *et al.*, 2002).

$$UCl_4 + 2MgB_2 \rightarrow UB_4 + 2MgCl_2$$

A view of the structure of UB_4 is shown in Fig. 5.27.

The phase diagram of the U–B system is shown in Fig. 5.28 (Howlett, 1959, 1960; Elliott, 1965; Chiotti *et al.*, 1981).

In addition, there is mass spectroscopic evidence that supports the existence of UB and UB_2 in the gas phase (Gingerich, 1970). The dissociation energies D_0^o were reported as (318 ± 33) kJ mol^{-1} for UB and (949 ± 42) kJ mol^{-1} for UB_2.

Uranium borides are remarkably inert, and borides have been proposed as a potential form for storing transuranium waste generated from the nuclear fuel cycle (Lupinetti *et al.*, 2002). There are some differences in reactivity of the uranium borides with respect to one another. UB_4 is generally more reactive

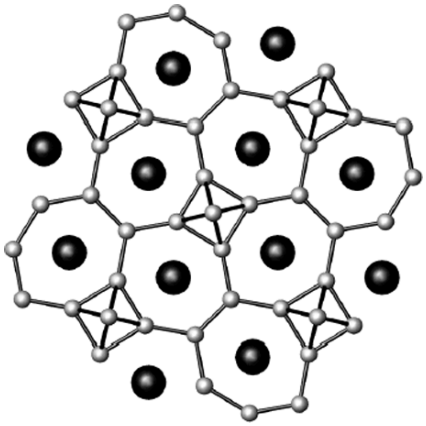

Fig. 5.27 *A view down the c-axis of the structure of UB_4. U–B bonds have been omitted for clarity.*

than UB_{12}. For example, boiling HF, HCl, and H_2SO_4 attack UB_{12} very slowly, but react more rapidly with UB_4, allowing for the separation of the two compounds. Both UB_4 and UB_{12} can be dissolved in HNO_3–H_2O_2 mixtures.

Ternary uranium borides have been extensively investigated for their rich variation in bonding and their complex physical properties. Compounds in this class include $U_5Mo_{10}B_{24}$, which contains three different kinds of B polyanions: two-dimensional puckered sheets formed from six- and eight-membered rings, planar ribbons composed of six-membered B rings, and chains of condensed eight-membered rings (Konrad and Jeitschko, 1996). UNi_4B has been extensively investigated and is a geometrically frustrated antiferromagnetic compound that partially orders below $T_N = 20$ K (Mentink *et al.*, 1998).

(b) Uranium–carbon system

The uranium–carbon system has been studied by a number of teams including Rundle *et al.* (1948), Esch and Schneider (1948), Litz *et al.* (1948), Wilhelm *et al.* (1949), and Mallett *et al.* (1952). The uranium–carbon system bear some similarities with that of uranium with other first-row p-block elements in that in addition to discrete, stoichiometric compounds, there are three known phases, UC, UC_2, and U_2C_3 that can be of variable composition. The complex phase diagram of the uranium–carbon system is shown in Fig. 5.29.

Among other things this diagram demonstrates that UC and UC_2 are completely miscible with one another at elevated temperatures and under these conditions the entire range UC–UC_2 is homogeneous. At lower temperatures, miscibility is much more limited and the exact extent of variability in composition for each of the carbides is still to be determined.

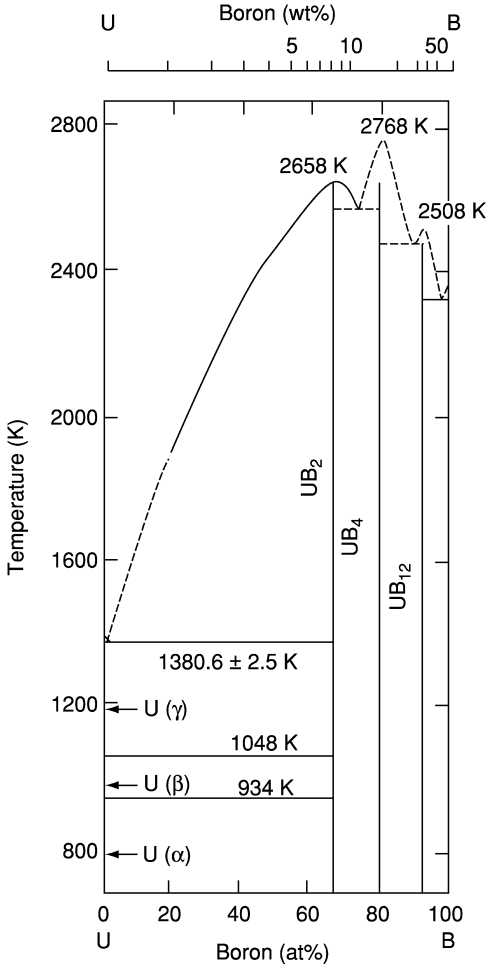

Fig. 5.28 *Phase diagram of the uranium–boron system* (*Chiotti* et al., 1981).

Litz *et al.* (1948) were the first to study the preparation of UC and UC_2. U_2C_3 is an unusual compound in that it has not been prepared by the direct reaction of the elements at high temperatures; this reaction invariably yields UC and UC_2 (Mallet *et al.*, 1952). However, U_2C_3 is obtained when a mixture of UC and UC_2 is heated in the range 1250–1800°C *in vacuo*. It is essential that the fused mixture be given a certain amount of stressing and cold working to initiate the nucleation necessary for the formation of the U_2C_3 phase; once formed it is stable at room temperature. Table 5.22 lists some of the crystallographic data for the uranium carbides. An illustration of the structure of UC_2 is shown in Fig. 5.30.

Table 5.22 *Crystallographic data for the stoichiometric binary uranium compounds with boron and group* IV *elements* (*Chiotti* et al., 1981).[a]

				Lattice parameters				*Density* (g cm^{-3})	
Formula	*Color*	*Space group*	*Symmetry*	*a* (Å)	*b* (Å)	*c* (Å)	*Z*	*Meas.*	*X-ray*
UB_2	metallic	*P*6/*mmm*	hexagonal	3.1293[b]		3.9893[b]	1	12.8	12.82
				3.1314[c]		3.9857[c]			
UB_4	metallic	*P*4/*mbm*	tetragonal	7.075		3.979	4	9.32	9.38
UB_{12}	metallic	*Fm*3*m*	fcc	4.4773			4	5.65	5.825
$UC(\delta_1)$	gray-black	*Fm*3*m*	fcc	4.961			4		13.63
U_2C_3	black	$I\bar{4}3d$	cubic	8.088			8		12.88
$UC_2(\zeta)$	light gray	*I*4/*mmm*	tetragonal	3.5266		6.0023	2		11.68
$UC_2(\delta_2)$	light gray		cubic	5.488			4		
$USi_3(1)$		*Pm*3*m*	cubic	4.060			1		8.15
$USi_{1.88}(\eta)$[d]	silvery	$I4_1/amd$	tetr. bc	3.948		13.67	4	7.27	8.98
				3.930		14.06			
$U_3Si_5(\tau)$[e]	silvery	*P*6/*mmm*	hexagonal	3.843		4.069	1	7.27	9.25
$USi(\zeta)$[f]	black	*Pbnm*	orthorhombic	5.66	7.67	3.91	4	9.30	10.40
$U_3Si_2(\varepsilon)$		*P*4/*mbm*	tetragonal	7.3299		3.9004	2	11.31	12.20
$U_3Si(\delta)$		*I*4/*mcm*	tetr. bc	6.029		9.696	4		15.58
UGe_3	metallic	*Pm*3*m*	cubic	4.2062			1		10.37
UGe_2[g]	metallic	*Cmmm*	orthorhombic	4.036	14.928	4.116	4		10.26
UGe[f]	metallic	*Pbcm*	orthorhombic	9.827	8.932	5.841	12		12.07
U_5Ge_4[k]	metallic	$P6_3/mcm$	hexagonal	8.744		5.863	2		12.67
U_3Ge_3	metallic								
U_5Ge_3[l,m]		$P6_3/mcm$	hexagonal	8.58		5.79	2		12.66
U_7Ge[h,m]									

Table 5.22 (*Contd.*)

Formula	*Color*	*Space group*	*Symmetry*	*Lattice parameters*			*Z*	*Density* (g cm^{-3})	
				a (Å)	*b* (Å)	*c* (Å)		*Meas.*	*X-ray*
USn_3	metallic	*Pm*3*m*	cubic	4.626			1		10.0
U_3Sn_5	metallic								
U_5Sn_4									
UPb_3[g]	metallic	*Fm*3*m*	cubic	4.7915					12.93
UPb[g,i]	metallic		tetr. bc	11.04		10.60			
			tetr. fc	4.579		5.259			13.27

[a] Unless otherwise mentioned, the data are taken from Chiotti *et al.* (1981).
[b] Boron-rich phase.
[c] Boron-poor phase.
[d] $USi_{1.88}$ is also referred to as α-USi_2.
[e] U_3Si_5 is also referred to as β-USi_2.
[f] According to Laugier *et al.* (1971), USi is tetragonal. The orthorhombic structure is due to oxygen.
[g] Boulet *et al.*, (1997a).
[h] Existence of these compounds deduced from vapor pressure data taken by Alcock and Grieveson (1962, 1963).
[i] The different lattice constants are due to different interpretations of powder patterns.
[j] Boulet *et al.* (1997b).
[k] Boulet *et al.* (1997c).
[l] Marakov and Bykov (1959). May be the same phase as U_5Ge_4.
[m] The existence of U_5Ge_3 and U_7Ge has been called into question (Boulet *et al.*, 1997c), and they are likely mixture of U_5Ge_4 and U metal dissolving 3% of germanium.

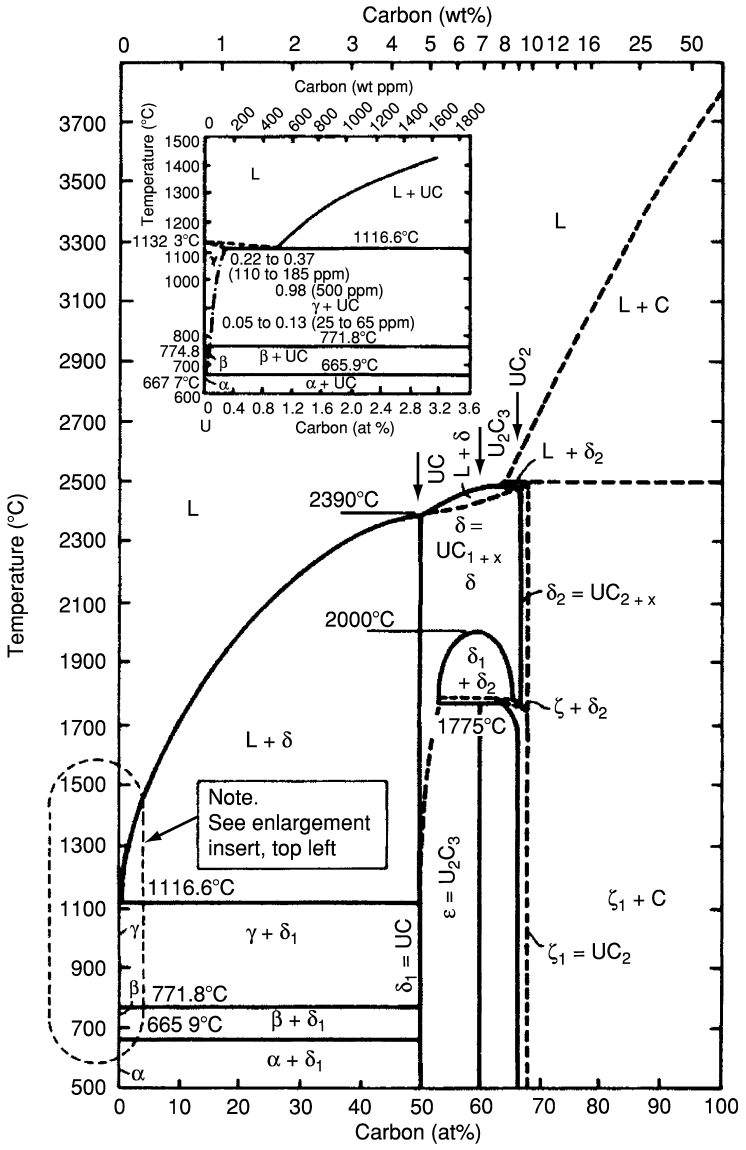

Fig. 5.29 *Phase diagram of the uranium–carbon system* (*Wilkinson,* 1962).

The uranium carbides can undergo a number of hydrolysis reactions; finely divided UC_2 is pyrophoric. The carbides react with water to yield a variety of products. Lebeau and Damien (1913) found that upon hydrolysis of UC_2, in addition to hydrogen, methane, and ethane, significant amounts of liquid and

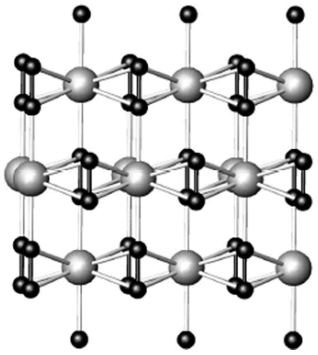

Fig. 5.30 *A view down the a-axis of the structure of UC_2.*

solid hydrocarbons are produced. Litz (1948) made an exhaustive study of the hydrolysis of UC and UC_2, the value of which is limited by the fact that he worked only at temperatures above 83°C and did not measure the quantity of gas evolved or analyze the solid residue for carbon compounds. Bradley and Ferris (1962, 1964) made a very careful study of the hydrolysis of arc-melted UC (1962) and of UC_2, U–UC mixtures, and UC–UC_2 mixtures (1964) at temperatures between 25 and 99°C. In the case of UC, the hydrolysis yielded a gelatinous, hydrous uranium(IV) oxide and a gaseous mixture (93 mL (STP) per gram UC), which consisted of 86 vol% methane, 11 vol% hydrogen, 1.8 vol% ethane, and small quantities of saturated C_3–C_6 hydrocarbons. The gaseous products contained all the carbon originally present in the carbide.

The total amount of carbon originally present in the carbide was also recovered in the hydrocarbon hydrolysis products of UC_2, U–UC, and UC–UC_2 mixtures. In the case of arc-melted $UC_{(1.85 \pm 0.03)}$, 36 different hydrocarbons were identified. The reaction product contained 15 vol% methane, 28 vol% ethane, 7 vol% C_3–C_6 alkanes, 8 vol% alkenes, 0.6 vol% alkynes, 1 vol% unidentified un-saturates, and 40 vol% hydrogen. Approximately 25% of the total carbon was found as a water-insoluble wax. In the hydrolysis of UC–UC_2 mixtures, a linear decrease of the volume percentage of CH_4 and linear increases of the percentages of hydrogen and the C_2–C_8 hydrocarbons were observed as the combined C/U atom ratio increased from 1.0 to 1.85. For UC–UC_2 mixtures, less methane than expected was evolved. This indicates that some polymerization of C units had occurred.

Bunnell *et al.* (1975) studied the hydrolysis of bare and defect-coated UC_2 fuel bead cores by water vapor at $p_{H_2O} = 24$–76 mmHg. They studied the reaction products by optical and scanning electron microscopies, identified hydrogen, methane, and ethane as the major reaction products, and measured the activation energy to be (25.4 ± 2.9) kJ mol^{-1}.

In air, UC_2 decomposes completely in a week, presumably as a result of hydrolysis. According to Mallet *et al.* (1952), U_2C_3 does not react appreciably with water even at 75°C. UC_2 appears to be stable in air at 300°C, but is completely converted to oxide in air within 4 h at 400–500°C. UC_2 reacts at 1100°C with nitrogen to form uranium nitride. Since the reactions of the carbides are greatly affected by the particle size of the solid and the previous thermal history of the sample, no far-reaching conclusions should be drawn regarding the relative reactivity of the uranium carbides.

The uranium carbides have found an important application as nuclear fuels in fast reactors. This type of application and related properties has been discussed in a number of uranium carbide conferences (see Proceedings, 1960a,b, 1961, 1963). One of the problems with reprocessing the spent fuels from these reactors is that oxalic acid is also produced in the dissolution of mixed uranium and plutonium carbides in HNO_3. Complexation of UO_2^{2+} by oxalate can account for the problems of incomplete uranium and plutonium extraction in the PUREX process for fuel reprocessing (Choppin *et al.*, 1983).

Ternary carbides, such as $U_2Al_3C_4$, can be prepared by melting the elements in a carbon crucible in a high-frequency radiofrequency (RF) furnace (Gesing and Jeitschko, 1995). The structure of $U_2Al_3C_4$ is closely related to that of Al_4C_3. Much like binary uranium carbides, $U_2Al_3C_4$ undergoes hydrolysis reactions in dilute HCl resulting in the formation of 74 (wt.)% methane, 8% ethane and ethylene, and 18% saturated and unsaturated higher hydrocarbons.

Laser-ablated U atoms react with CO in a noble gas matrix to form CUO (Li *et al.*, 2002). This molecule exhibits different stretching frequencies in a solid Ar matrix from those in a solid Ne matrix. Further experiments suggest that Ar atoms interact directly with CUO molecules to form an actinide–noble gas compound. The combination of experimental and theoretical methods suggests that multiple Ar atoms interact with a single CUO molecule.

(c) Uranium–silicon system

The uranium–silicon system is remarkably rich and a large number of uranium silicides including U_3Si, U_3Si_2, USi, U_3Si_5, $USi_{1.88}$, and USi_3 have been prepared and crystallographically characterized (Zachariasen, 1949a; Kaufman *et al.*, 1957). The phase diagram, shown in Fig. 5.31, is based on earlier work reported in the compilations by Hansen and Anderko (1958), Elliott (1965), and Shunk (1969), and in the paper by Vaugoyeau *et al.* (1971), which has been assessed and discussed by Chiotti *et al.* (1981).

Further details on the composition ranges of the two phases U_3Si_5 and $USi_{1.88}$ are given by Vaugoyeau *et al.* (1971). U_3Si_5 melts congruently at 2043 K (1770°C) and has a composition range $USi_{1.71}$ to $USi_{1.78}$ (63–64 at % Si) in the temperature range 1000–1300°C. The phase $USi_{1.88}$, in the same temperature range, has a composition span $USi_{1.79}$ to $USi_{1.84}$ (64–64.8 at % Si).

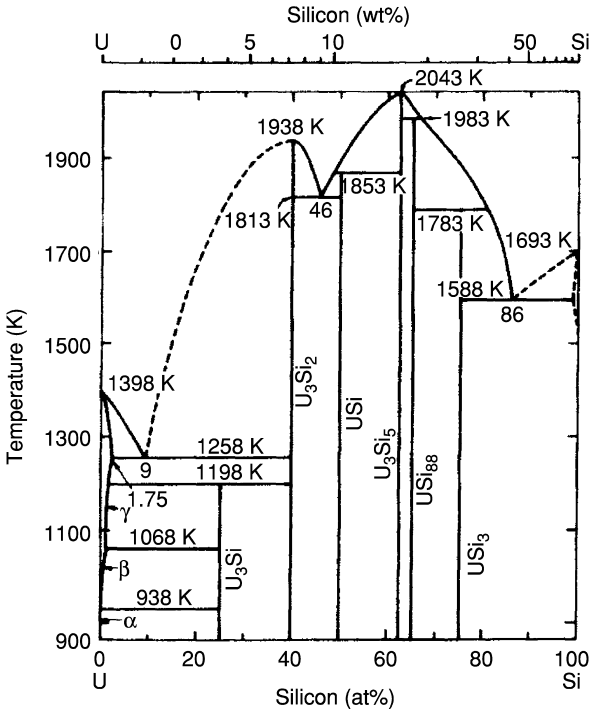

Fig. 5.31 *Phase diagram of the U–Si system* (*Chiotti* et al., 1981).

The two-phase region between the two compounds is very narrow. The compound USi was shown to decompose peritectically at 1580°C and has a narrow homogeneity range. The eutectic between U_3Si_2 and USi occurs at 1540°C and 46 at % Si.

As can be inferred from this information and from the data in Table 5.22, the U–Si phase diagram is very complicated. However, the uranium silicides are of technical importance. For instance, compounds such as $U(Al,Si)_3$ are formed in the layer between the uranium metal and the aluminum can in natural uranium fuel elements (Cunningham and Adams, 1957). Because of the chemical inertness of some of the uranium silicides, these compounds promise more applications. Crystal structures of the U–Si compounds are also summarized in Table 5.22.

Ternary uranium silicides are well established from compounds such as UCu_2Si_2 (Fisk *et al.*, 2003), $U_2Nb_3Si_4$ (Le Bihan *et al.*, 2000), and URu_2Si_2 (Sugiyama and Onuki, 2003). Single crystals of UCu_2Si_2 prepared from a Cu flux undergo a 50 K antiferromagnetic transition below the 100 K ferromagnetic transition (Fisk *et al.*, 2003).

$U_2Nb_3Si_4$ is weakly ferromagnetic below 35 K (Le Bihan *et al.*, 2000). Finally, URu_2Si_2 is one of the most studied heavy fermion materials (Sugiyama and Onuki, 2003).

(d) Uranium–germanium, uranium–tin, and uranium–lead systems

The uranium–germanium system is as complex as that of uranium silicides. U_7Ge (*vide infra*), U_5Ge_3 (*vide infra*), U_5Ge_4, UGe_2, and UGe have all been characterized and subjected to extensive physical property measurements (Onuki *et al*., 1992). The compound originally formulated as U_3Ge_4 has been shown to be a mixture of UGe and U_3Ge_5. Detailed studies including magnetic structure determination via neutron diffraction have been performed on UGe_2, which is an unusual example of a ferromagnetic superconductor (Saxena, 2000; Sheikin *et al*., 2000; Nishioka *et al*., 2002).

This compound was originally reported to crystallize in the $ZrSi_2$ (*Cmcm*) structure type, but in fact crystallizes in the $ZrGa_2$ (*Cmmm*) type (Oikawa *et al*., 1996; Boulet *et al*., 1997a). U_5Ge_3 and U_7Ge both undergo a transition to a superconducting phase below 2 K (Onuki *et al*., 1990). However, the existence of both of these compounds has been called into question (Boulet *et al*., 1997c), and they are likely mixture of U_5Ge_4 and U metal dissolving 3% of germanium.

The uranium–tin phase diagram has been described by Palenzona and Manfrinetti (1995). U_5Sn_4 (Ti_5Ga_4-type), USn (ThIn-type), USn_2 ($ZrGa_2$-type), U_3Sn_7 (Ce_3Sn_7-type), and USn_3 ($AuCu_3$-type) were identified from this work. Dhar *et al*. (1998) have assessed the magnetic properties of these compounds. U_5Sn_4 and USn are ferromagnetically ordered below 62 and 49 K, respectively; USn_2 and U_3Sn_7 attain an antiferromagnetic state near 80 K. Shunk (1969) and Chiotti *et al*. (1981) have reported the phase diagram for the uranium–lead system.

5.7.4 Uranium pnictides

The systems U–N, U–P, U–As, U–Sb, and U–Bi have been studied in great detail. In particular, the monopnictides UN, UP, and UAs have found major interest because of their solid-state properties, which are relatively easy to study because of their cubic (NaCl) structure. Physical and crystallographic data of the pnictides are summarized in Table 5.23.

The thermodynamic properties of uranium and other actinide nitrides are briefly summarized in Chapter 19. Additional information on uranium nitrides and heavier pnictides is available in Gmelin (1981b, vol. C7; 1981d, vol. C14).

(a) Uranium–nitrogen system

Rundle *et al*. (1948) established the existence of the following uranium nitride phases: UN, U_2N_3, and $UN_{1.75}$, while the phase UN_2 could not be confirmed. Berthold *et al*. (1957) and Berthold and Delliehausen (1966) succeeded, however, in preparing a phase $UN_{1.90}$ by reacting uranium hydride with ammonia at

Table 5.23 *Crystallographic data of uranium pnictides* (*Rough and Bauer,* 1958*; Hansen and Anderko,* 1958*; Waber* et al., *1964; Elliot,* 1965*; Shunk,* 1969).[a]

					Lattice parameters			*Density*	
Formula	*Color*	*m.p.* (°C)	*Space group*	*Symmetry*	*a* (Å)	*c* (Å)	Z	*X-ray*	*Exp.*
UN	metallic	2850	$Fm3m$	fcc	4.889		4	14.32	
UN[b]			$R\bar{3}m$	rhombohedral	3.170	8.635	3	16.7	
α-U_2N_3			$Ia3$	cubic	10.678		16	11.24	
β-U_2N_3[c]			$P\bar{3}m1$	hexagonal	3.700	5.825		12.45	
$UN_{1.45}$	black				10.700				
UN_x[d]									
$UN_{1.76}$	black			bcc	10.628				
$UN_{1.90}$	black								
UP	metallic	2610	$Fm3m$	fcc	5.5889		4	10.23	
UP[b]			$R\bar{3}m$	rhombohedral	7.583	9.433	12	11.41	
U_3P_4	metallic		$I\bar{4}3d$	bcc	8.207		4		
UP_2	grey		$P4/nmm$	tetragonal	3.808	7.780	2		
UAs	metallic	2705[e]	$Fm3m$	fcc	5.7788		4	10.77	
U_3As_4	metallic		$I\bar{4}3d$	bcc	8.507		4		

UAs_2	metallic		$P4/nmm$	tetragonal	3.954	8.116	2	9.8	
U_5Sb_4[g]	metallic		$P6_3/mcm$	hexagonal	9.237	6.211	2	12.14	
USb	metallic	1850	$Fm\bar{3}m$	fcc	6.203		4		
U_3Sb_4	metallic	1695[f]	$I\bar{4}3d$	bcc	9.113		4	10.84	10.7
USb_2	metallic	1335[f]	$P4/mmm$	tetragonal	4.272	8.759	2	10.04	10.5
α-UBi(δ_1)	metallic		$Fm\bar{3}m$	cubic	6.364		4	11.52	
β-UBi(δ_2)	metallic	1400–1450[e]	$P4/nmm$	tetr.bc	11.12	10.55	24	13.6	
U_3Bi_4 (ε)	metallic	1150[f]	$I\bar{4}3d$	bcc	9.350		4	12.57	12.8
UBi_2	metallic	1010[f]	$P4/nmm$	tetragonal	4.445	8.908	2	12.38	12.36

[a] Unless otherwise mentioned, the data are taken from Rough and Bauer (1958), Hansen and Anderko (1958), Waber *et al.* (1964), Elliot (1965), Shunk (1969).
[b] High-pressure phase (Olsen *et al.*, 1985, 1988).
[c] Masaki and Tagawa (1975).
[d] Solid solutions ranging from $UN_{1.45}$ through $UN_{1.76}$, lattice constant decreasing from 10.700 to 10.628 Å.
[e] With decomposition.
[f] With peritectic decomposition.
[g] Paixão *et al.* (1994). This phase was originally formulated as U_4Sb_3.

elevated temperatures. Bugl and Bauer (1964) have studied the U–N system in detail.

The nitrides can be prepared by reaction of very pure uranium metal (or uranium hydride prepared from such metal) with nitriding agents. The surface of the uranium metal has to be pickled with nearly concentrated HNO_3, and then washed with organic solvents to remove even traces of oxide and oil films, which might lead to the formation of oxide or carbide contaminants. The nitriding agents also have to be of high purity. Uranium mononitride can be prepared (i) by reaction of uranium metal (or uranium hydride) with nitrogen or ammonia, (ii) by the thermal decomposition of higher nitrides at or above 1300°C, or (iii) by the reduction of higher nitrides with uranium metal. U_2N_3 can be prepared by reacting UC with NH_3 or a N_2/H_2 gas mixture (Nakagawa *et al.*, 1997). The reaction with ammonia is advantageous because NH_3 acts as both a nitriding agent and as a carbon-clearing agent. Fitzmaurice and Parkin (1994) report that various uranium nitrides could be prepared from the self-propagating reaction of UCl_4 with Li_3N.

Mallett and Gerds (1955) made a kinetic study of the reaction of uranium metal with nitrogen in the temperature range 550–900°C and at atmospheric pressure. Surface reaction products were identified by X-ray diffraction methods. At 775–900°C it was found that all three nitride phases were present. The intermediate nitride U_2N_3 is prepared by similar methods or by reduction of $UN_{1.75}$ with hydrogen. Since U_2N_3 loses nitrogen above 700°C *in vacuo*, the preparative procedure must take this into account. The nitride $UN_{1.75}$ cannot be prepared at all by reaction of the metal with nitrogen, unless a high pressure of nitrogen is used. There appears to be a two-phase region between UN and U_2N_3, but the region between U_2N_3 and $UN_{1.75}$ appears to be homogeneous. A tentative phase diagram of the system is shown in Fig. 5.32.

All of the higher uranium nitrides are thermally unstable relative to UN. UN is easily oxidized by air and is decomposed by water vapor; it is not attacked by either hot or cold hydrochloric or sulfuric acids, but is attacked by molten alkali. U_2N_3 can be used for the catalytic cracking of ammonia (Rizzo da Rocha *et al.*, 1995). Schmitz-Dumont *et al.* (1954) described the interesting uranium compound uranyl amide, $UO_2(NH_2)_2$. This compound can be prepared by the reaction of potassium uranyl nitrate, $KUO_2(NO_3)_3$, with potassium amide in liquid ammonia. Uranyl amide is a brown, amorphous substance that is unaffected by dry oxygen at room temperature. Moisture, however, converts the amide to ammonium diuranate. The uranium amido chlorides, UNH_2Cl_2 and $U(NH_2)_2Cl$, can be obtained by reacting UCl_3 with ammonia at 450 to 500°C. Increased heating of these compounds results in their conversion to U(NH)Cl and then $UN_{1.73–1.75}$ (Berthold and Knecht, 1965a).

The reaction of Li_3N with UH_3 at 900°C results in the formation of $LiUN_2$ (Jacobs *et al.*, 2003). The structure is related to the anatase type with the octahedral sites occupied by Li. Ca_3UN_4 can be prepared by reacting Ca $(NH_2)_2$ and UH_3 between 600 and 1000°C (Heckers *et al.*, 2003). X-ray and

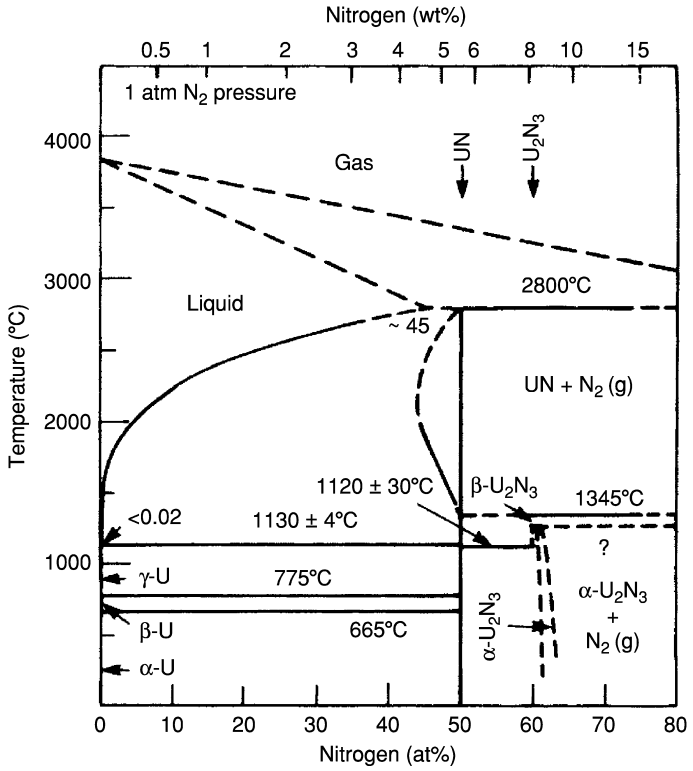

Fig. 5.32 *Phase diagram of the U–N system* (*Shunk*, 1969).

neutron diffraction studies on this phase show that it crystallizes in the NaCl structure type with statistical occupation of the cation site by three Ca atoms and one U atom.

(b) Uranium–phosphorus, uranium–arsenic, and uranium–antimony, and uranium–bismuth systems

In the systems U–P, U–As, U–Sb, and U–Bi, the compounds UX, U_3X_4, and UX_2 (where X = P, As, Sb, or Bi) have been reported. Compounds UX have the cubic NaCl structure for all X, with the exception of β-UBi, which is tetragonal body-centered. U_3X_4 is body-centered cubic and UX_2 tetragonal for all X.

At least four methods have been applied for preparation of the pnictides: direct synthesis from the elements in an autoclave (Albutt *et al.*, 1964) or in a sealed tube, for instance (Iandelli, 1952).

$$2U + P_4 \rightarrow 2UP_2$$

the reaction of uranium hydride with phosphine or arsine, for instance

$$UH_3 + PH_3 \rightarrow UP + 3H_2$$

and finally by circulating gaseous phosphine or arsine over slightly heated hydride (Baskin and Shalek, 1964; Baskin, 1969). For the preparation of the phosphides, a PH_3-loaded stream of argon is passed over the hydride, which is heated at 400–500°C. For the preparation of the arsenides, AsH_3 is reacted with UH_3 at 300°C. The reaction products are annealed at 1200–1400°C. Single crystals of UAs_2 have been grown by reacting uranium metal with a Cs_3As_7 flux (Albrecht-Schmitt *et al.*, 2000). Finally, uranium phosphides, arsenides, and antimonides can be prepared from the reaction of UCl_4 with sodium pnictides (Fitzmaurice and Parkin, 1994).

Buhrer (1969), Spirlet (1979), and Vogt (1982) succeeded in growing single crystals of most uranium pnictides by gas-phase transport, using $TeCl_4$, I_2, and other transporting agents. The crystals grown in this manner allow the determination of physical properties such as magnetic susceptibilities, magnetic phase diagrams (Busch *et al.*, 1979a), or the measurement of the de Haas–van Alphen effect (Henkie *et al.*, 1981); the uranium pnictides are particularly well suited for such measurements. Normally, they should exhibit isotropic behavior because of their structure, but the presence of anisotropy in the cubic crystals suggests the formation of magnetic domains. U_3P_4 and U_3As_4 are both metallic ferromagnets with itinerant 5f electrons (Inada *et al.*, 2001).

The binary compounds of the systems U–Sb and U–Bi may be prepared directly from the elements, or by reacting uranium with alkali metal antimonide and bismuthide fluxes. The binary phase diagram of U–Sb was originally investigated by Beaudry and Daane (1959). Among the binary compounds discovered in this system was a uranium-rich phase (δ) that forms a eutectic with USb at 1770°C. This compound was originally formulated as U_4Sb_3. Magnetic susceptibility measurements on a compound with this nominal composition show ferromagnetic behavior below 86 K (Troć, 1992). However, later microprobe analysis, neutron scattering, and single crystal X-ray diffraction data were utilized to establish that the actual composition of this phase is U_5Sb_4 (Paixão *et al.*, 1994); this compound crystallizes in the Ti_5Ga_4 structure type. Paixão *et al.* (1994) have demonstrated that U_5Sb_4 shows highly anisotropic ferromagnetic behavior below 86 K.

5.7.5 Uranium chalcogenides

The binary, ternary, and quaternary uranium sulfides, selenides, and tellurides have been the subject of intense investigation for more than 160 years. U–Po compounds are currently unknown owing to the high radioactivity and rarity of polonium. A significant number of the chalcogenide phases deduced before 1980 were reinvestigated over the past two decades, primarily by single-crystal X-ray diffraction, as a number of previously known compounds were assigned incorrect space groups, unit cells, and compositions.

(a) Uranium–sulfur system

Uranium sulfide in the form of US_2 was first prepared in the mid-1800s (Péligot, 1842; Herrmann, 1861). This compound was followed by the preparation of US and U_2S_3, which were identified by Alibegoff (1886); these studies pre-date the discovery of X-rays. Systematic X-ray powder diffraction investigations did not take place until 1943 (Strotzer *et al.* 1943), when seven distinct phases were identified from their powder patterns, but these were not indexed. The phase diagram of the uranium–sulfur system is shown in Fig. 5.33.

Based on later systematic studies of the uranium–sulfur system by Eastman *et al.* (1950), Zachariasen (1949b) was able to elucidate the crystal structures of many of the previously synthesized phases. Mills (1974) has compiled thermodynamic data for these phases. Crystal structure data for the uranium chalcogenides and oxychalcogenides are given in Table 5.24.

The uranium sulfides can be prepared by heating uranium or uranium hydride with H_2S, or by heating the elements together in a sealed tube. Lower sulfides may be obtained by thermal decomposition of the higher sulfides *in vacuo* at high temperatures. γ-US_2 can be prepared from what is thought to be a topotactic reaction of U_3S_5 with sulfur (Kohlmann and Beck, 1997).

α-UX_2 compounds (X = S, Se) were previously reported to crystallize in *I*4/*mcm*, but based on single crystal X-ray data they are now known to crystallize in *P*4/*ncc* (Noël and Le Marouille, 1984). U_3S_5 has been the subject of a large number of studies that have concluded that the compound is mixed-valent, containing both U^{3+} and U^{4+}; it can be formulated as $(U^{3+})_2(U^{4+})(S^{2-})_5$ (Noël and Prigent, 1980; Kohlmann and Beck, 2000). A view of the structure of U_3S_5 is shown in Fig. 5.34.

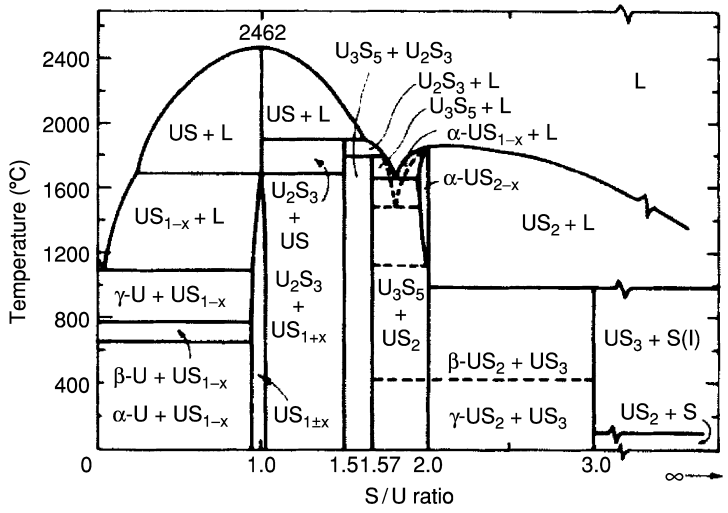

Fig. 5.33 *Tentative phase diagram of the U–S system* (*Cordfunke,* 1969).

Table 5.24 *Crystallographic data for uranium chalcogenides and oxychalcogenides.*[a]

Formula	*Color*	*m.p.* (°C)	*Space group*	*Symmetry*	*Lattice parameters*				*Z*	Density (g/cm^3)		*References*
					a	*b*	*c*	β		*Obs.*	*Calc.*	
UOS	Black		*P4/nmm*	tetrag.	3.483		6.697		2		9.64	Picon and Flahaut (1968)
US	silvery black	2462	*Fm*$\bar{3}$*m*	cubic	5.484				4		10.87	Zachariasen (1949b)
U_2S_3	Blue-black	1850	*Pbnm*	orthor.	10.34	10.58	3.885		4	8.94	8.96	Picon and Flahaut (1968)
U_3S_5	Blue-black			orthor.	7.42	8.11	11.74		4	8.16	8.26	Potol *et al.* (1972)
α-US_2[b]	Steel gray	1850	*P4/ncc*	tetrag.	10.293		6.374		10		8.01	Noël and Le Marouille (1984)
β-US_2	Steel gray		*Pbab*	orthor.	4.4803	7.439	4.1209		4	8.07	8.09	Suski *et al.* (1972)
γ-US_2	Steel gray		*P*$\bar{6}$*2m*	hexag.	7.236		4.062		3	8.12	8.17	Picon and Flahaut (1968); Daoudi *et al.* (1996); Kohlmann and Beck (1997)
US_3	Black, shiny		$P2_1/m$	monoc.	5.40	3.90	18.26	80.5	4	5.9	5.86	Picon and Flahaut (1968); Marcon (1969)
UOSe	black[c]		*P4/nmm*	tetrag.	3.9035		6.9823		2	10.40	10.38	Murasik *et al.* (1968)
USe	Black		*Fm*$\bar{3}$*m*	fcc	5.7399				4		11.13	Kruger and Moser (1967)
U_3Se_4	Black, shiny	1680[d]	*I*$\bar{4}$3*d*	cubic	8.820				4	10.07	9.97	Khodadad (1960); Khodadad (1961); Noël (1985a)

U_2Se_3	Black	1610	*Pnma*	orthor.	10.94	11.33	4.06	4	9.42	9.40	Khodadad (1959, 1961)
U_3Se_5	Black	1560[d]	*Pnma*	orthor.	12.292	8.459	7.799	4	9.04	9.14	Breeze and Brett (1972)
U_7Se_{12}	Black		$P6_3/m$	hexag.	11.385		4.099	1			Breeze and Brett (1972)
α-USe_2[e]	Black	1460	*I4/mcm*	tetrag.	10.765		6.660	10		9.03	Noël and Le Marouille (1984)
β-USe_2	black[f]		*Pnma*	orthor.	7.455	4.2320	8.964	4	9.08	9.3	Breeze and Brett (1972); Noël *et al.* (1996)
γ-USe_2	Black		$P\bar{6}2m$	hexag.	7.6376		4.1924	3	9.07	9.31	Breeze and Brett (1972); Kohlmann and Beck (1997)
USe_3	Black, shiny	1160[d]	$P2_1/m$	monoc.	5.652	4.056	10.469	2	7.25	7.25	Breeze and Brett (1972); Ben Salem *et al.* (1984)
UOTe	Gray-black		*P4/nmm*	tetrag.	4.004		7.491	2	10.55		Klein-Haneveld and Jellinek (1964); Breeze *et al.* (1971)
U_2O_2Te	Gray-black		*I4/m*	tetrag.	3.9640		12.564	2			Breeze *et al.* (1971)
UTe	Gray-black	1740	$Fm\bar{3}m$	fcc	6.150			4	10.37	10.55	Kruger and Moser (1967); Klein-Haneveld and Jellinek (1964)
U_3Te_4	Black	1540[d]	$I\bar{4}3d$	cubic	9.3980			4	9.80	9.81	Matson *et al.* (1963)
α-U_2Te_3	Black, shiny		$I\bar{4}3d$	cubic	9.3960			4	9.02	9.81	Matson *et al.* (1963)

Table 5.24 (*Contd.*)

Formula	*Color*	*m.p.* (°C)	*Space group*	*Symmetry*	*Lattice parameters*				*Z*	Density (g/cm^3)		*References*
					a	*b*	*c*	β		*Obs.*	*Calc.*	
β-U_2Te_3	Black	1500[d]	*Pnma*	orthor.	12.175	4.370	11.828		4		9.06	Suski *et al.* (1976); Tougait *et al.* (1998b)
α-U_3Te_5	Black			hexag.	12.25		4.23					Ellert *et al.* (1975)
β-U_3Te_5	Black	1300[d]		orthor.	7.99	8.73	12.88					Slovyanskikh *et al.* (1977)
γ-U_3Te_5	Black		*Pnma*	orthor.	16.098	4.210	14.060		4		9.42	Tougait *et al.* (1998a)
U_7Te_{12}	Black		$P\bar{6}$	hexag.	12.312		4.260		1		9.49	Breeze *et al.* (1971); Breeze and Brett (1971); Tougait *et al.* (1998c)
$UTe_{1.77}$	Black		*P4/nmm*	tetrag.	4.243		8.946		2		9.8	Klein-Haneveld and Jellinek (1969); Klein-Haneveld and Jellinek (1970)
$UTe_{1.78}$	Black			orthor.	4.162	6.134	13.973		4			Breeze *et al.* (1971)

α-UTe_2	Dark gray	1180[d]	*Immm*	orthor.	4.1619	6.1277	13.961		4	9.20	Klein-Haneveld and Jellinek (1970); Boehme *et al.* (1992)
β-UTe_2	Black		*Pnnn*	orthor.	4.24	6.16	14.52		4	8.68	Ellert *et al.* (1971)
U_3Te_7	Black	950[d]									Montignie (1947)
α-UTe_3	Black	935[d]	$P2_1/m$	monoc.	6.0987	4.2229	10.325	98.2	2	7.83	Breeze *et al.* (1971); Boehme *et al.* (1992); Stoewe (1996a)
β-UTe_3	Black		*Cmcm*	orthor.	4.338	24.743	4.338		4	8.85	Noël and Levet (1989)
U_2Te_5	Black		*C2/m*	monoc.	34.42	4.181	6.074	95.4	4	8.5	Stoewe (1996b); Tougait *et al.* (1997)
$U_{0.9}Te_3$[g]	Black		*Cmcm*	monoc.	4.3537	24.792	4.3541		4	8.4	Stoewe (1997a)
UTe_5		490[d]	*Pnma*	orthor.	17.915	10.407	4.220		4		Slovyanskikh *et al.* (1967); Noël (1985b)

[a] Compiled from Gmelin (1981, vol. C11, 1984, vol. C10) and from original literature.
[b] Old sources listing α-US_2 refer to $US_{1.80}$-$US_{1.93}$. The single crystal structure of α-US_2 is known.
[c] Most of the selenides and tellurides, if prepared in sealed tubes, are obtained as free-running black powders. In some cases, single crystals have been prepared by gas-phase transport.
[d] Peritectic decomposition temperature of the solid-state phase.
[e] α-USe_2 can refer to the phase $USe_{1.88}$ and has variable lattice parameters.
[f] Obtained as black crystals with metallic luster.
[g] This compound has been previously reported in the literature as $UTe_{3.38}$. Powder diffraction data suggests that the uranium content may equal $U_{0.724}Te_3$ (Boehme *et al.*, 1992).

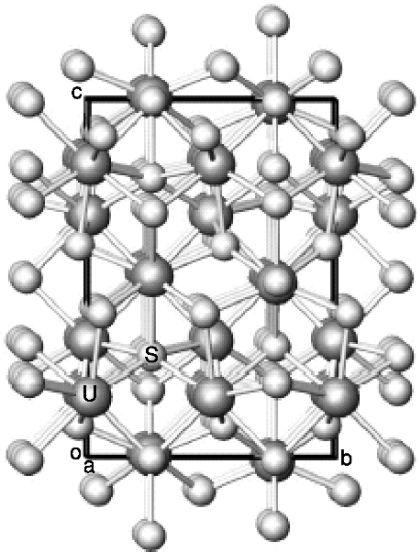

Fig. 5.34 *A view down the a-axis of the structure of* U_3S_5. *This is a mixed valence compound and should be formulated as* $(U^{3+})_2(U^{4+})(S^{2-})_5$.

(b) Uranium–selenium and uranium-tellurium systems

The selenides and tellurides of uranium have also been studied extensively. A large number of individual phases have been identified and characterized by their X-ray patterns. The crystallographic data of the individual phases have also been summarized in Table 5.24. The phase diagrams of the systems U–Se and U–Te are shown in Figs. 5.35 and 5.36, respectively.

The β modification of UTe_3, which was originally thought to adopt the $NdTe_3$ structure type, has been shown to be non-stoichiometric with uranium defects, giving rise to a formulation of $U_{0.9}Te_3$ (Stoewe, 1997a). This compound is identical to the previously known binary uranium telluride, formulated as $UTe_{3.38}$, and shows variable composition with U content ranging from 0.87 to 0.93. X-ray powder diffraction data suggest even a larger defect concentration consistent with a formula of $U_{0.724}Te_3$ (Boehme *et al.*, 1992). Te–Te bonding exists in a number of uranium telluride phases, making oxidation state assignment difficult. For example, one-dimensional tellurium chains exist in UTe_2. Therefore the compound is not $(U^{4+})(Te^{2-})_2$ but rather $(U^{3+})(Te^{2-})(Te^{1-})$ (Stoewe, 1997b). A view of the structure of UTe_2 is shown in Fig. 5.37.

The selenides and tellurides can be prepared by similar methods as the sulfides, i.e. reaction of uranium powder prepared from the hydride with H_2Se or H_2Te, synthesis from the elements at controlled temperatures in sealed tubes, or thermal decomposition of the higher selenides or tellurides. For a more detailed description of the solid-state properties of USe and UTe,

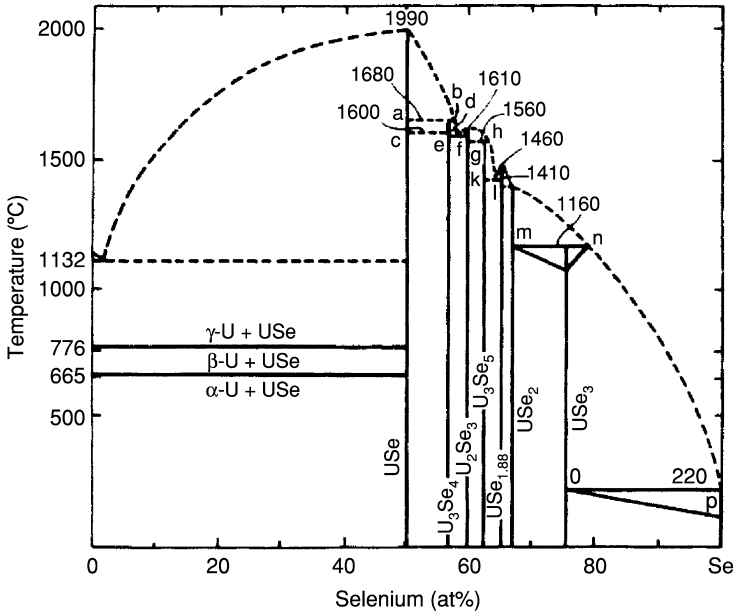

Fig. 5.35 *Phase diagram of the U–Se system* (*Klein-Haneveld and Jellinek*, 1964).

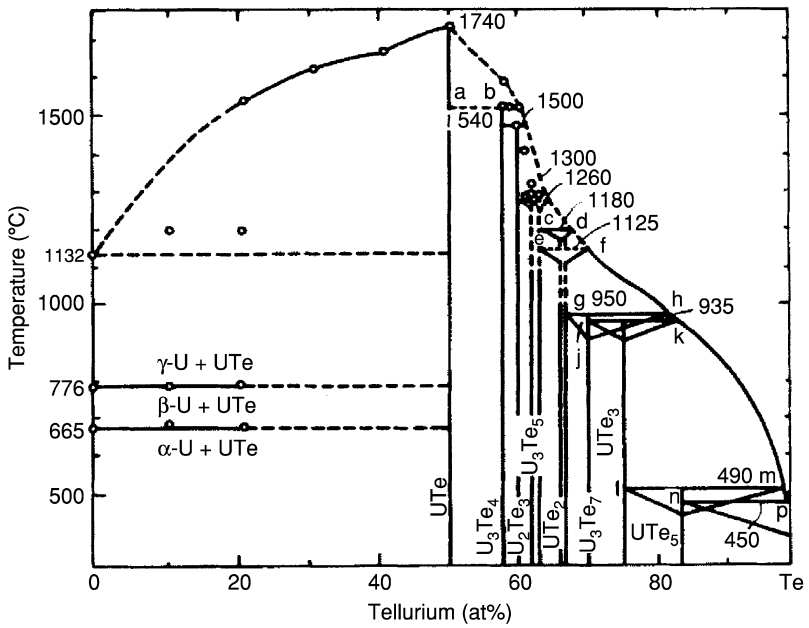

Fig. 5.36 *Phase diagram of the U–Te system* (*Slovyanskikh* et al., 1977).

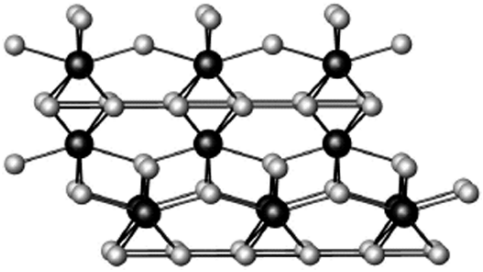

Fig. 5.37 *A view down the a-axis of the structure UTe_2. There are one-dimensional chains formed from Te–Te bonding, leading to the composition $(U^{3+})(Te^{-})(Te^{2-})$.*

see *Gmelin* (1981c, vol. C11) and the Proceedings of the International Conference on the Physics of Actinides and Related 4f Materials (Wachter, 1980). U_2Te_5 has been prepared from the direct reaction of the elements, and single crystals grown by using $TeBr_4$ as a chemical transport reagent (Stoewe, 1996b). Uranium chalcogenides can also be prepared by reacting UCl_4 with Li_2X (X = S, Se, Te) (Fitzmaurice and Parkin, 1994). Narducci and Ibers (1998) have reviewed the ternary and quaternary uranium chalcogenides. These compounds range from simple perovskite-type compounds with ABX_3 (X = S, Se, Te) formula to complex, tellurium-deficient compounds such as one-dimensional $Cs_8Hf_5UTe_{30.6}$ (Cody *et al*., 1995; Cody and Ibers, 1995). The oxidation state of uranium in these compounds is often called into question due to the presence of Te ··· Te contacts on the order of 3 Å, which are considerably shorter than the van der Waals distance (4.10 Å), but longer than a full Te–Te single bond (2.76 Å). This results in a formal oxidation state for the tellurium with a non-integral value; hence, the oxidation state of uranium is ambiguous.

5.7.6 Uranium halides and related compounds

The halides and complex halides are one of the most thoroughly studied classes of uranium compounds. They have found use in many industrial applications, uranium hexafluoride, tetrachloride, and trichloride in large-scale isotope separation of ^{235}U and uranium tetrafluoride as a component of molten-salt reactor fuels as well as for the preparation of uranium metal. The most stable halides are formed with uranium in the 6+ and 4+ oxidation states. Experimental investigations gave evidence for increasing U 5f participation in the chemical bonds in the more covalent compounds. Ionicity is largest for halides with uranium in higher oxidation states and with the more electronegative halogens. An exception to this rule is UF_3, which is reported to be more covalent than UCl_3 (Thibaut *et al*., 1982). Uranium in oxidation states 5+ and 6+ forms linear uranyl groups UO_2^+ and UO_2^{2+}. These possess covalent, substitution inert bonds and act like single species with respect to the halogen atoms. Lau and Hildenbrand (1982, 1984) have presented thermochemical data for gaseous

U–F_n and U–Cl_n species (where $n = 1, 2, 3, 4$, or 5), obtained from mass spectrometric investigations of high-temperature reaction equilibria.

The chemistry of uranium halides has been reviewed in numerous papers and books, e.g. Katz and Sheft (1960), Hodge (1960), Pascal (1962–1970), Bagnall (1967, 1987), Caillat (1961), Chatalet (1967), Brown (1968, 1972, 1973, 1979), Johnson *et al*. (1974), Manes (1985), and Eick (1994). Several reviews were devoted to particular aspects of the halides: the crystallographic data of actinide halides have been reported by Taylor (1976a) and of their binary compounds with non-metallic elements by Benedict (1987); the results of spectroscopic investigations were presented by Carnall (1982), Carnall and Crosswhite (1985), Baer (1984), and Wilmarth and Peterson (1981); the magnetism of actinide compounds by Santini *et al*. (1999); EPR by Kanellakopulos (1983); the thermodynamic data by Kubaschewski and Alcock (1979), Fuger *et al*. (1983), Grenthe *et al*. (1992), and Guillaumont *et al*., (2003); the industrial production of uranium hexafluoride by Hellberg and Schneider (1981), and the properties of uranium in molten salts and metals by Martinot (1984, 1991). A number of review papers have been also devoted to a particular oxidation state or group of uranium halides, e.g. *Structural systematics in actinide fluoride complexes* (Penneman *et al*., 1973), *Verbindungen mit Fluor* (Bacher and Jacob, 1980), *Actinide fluorides* (Freestone and Holloway, 1991), *Uranium hexafluoride. Its chemistry related to its major application* (Bacher and Jacob, 1986), *Compounds of uranium with chlorine, bromine, iodine* (Brown, 1979), *Heptavalent actinides* (Keller, 1985), *Complex compounds of uranium* (Bagnall, 1979), *Comprehensive coordination chemistry II – The Actinides* (Burns *et al*., 2004), *Magnetochemistry of uranium*(v) *complexes and compounds* (Miyake, 1991), *Chemistry of tervalent uranium* (Drożdżyński, 1991). In order to keep the reference number at a reasonable limit these review articles will be frequently cited as the source of chemical and physical properties of the compounds. In each of the following subsections the uranium halides and related compounds are discussed in order of increasing valence state and some of their physical properties summarized in subsequent tables. Although references to original literature data have been kept in these tables, the citation of thermodynamic data have been limited to the most important binary compounds as Chapter 19 of this work is devoted to thermodynamic properties of the actinides.

(a) Tervalent halides and complex halides

The first tervalent uranium compound, UCl_3, was prepared by Péligot (1842), and until the end of the 1960s the binary trihalides have been almost the only ones investigated. The crucial reason was the large sensitivity to oxidation and very poor solubility in aprotic organic solvents of all at that time known uranium(III) compounds. During the last 30 years the development of new experimental methods made it possible to prepare almost 150 uranium(III)

compounds (Drożdżyński, 1991). However, the uranium trihalides and complex halides still remain the only relatively well-investigated group.

The stability of the trihalides decreases with increase in the atomic number of the halide. Apart from UF_3, all the halides are more or less hygroscopic and easily oxidized in air. In aqueous solutions they are rapidly oxidized but in pure, thoroughly deoxygenated solvents the U^{3+} ions are fairly stable. Concentrated hydrochloric acid gives intensely deep-red solutions, characteristic of the $[UCl_n]^{3-n}$ complex anions. With the exception of UF_3, UCl_3 and uranium(III) fluoro complexes, the halides are also readily soluble in some more polar solvents. The compounds exhibit a variety of colors (see Table 5.25). The preparation of somewhat more stable hydrated uranium(III) complexes have also been reported. Since all of them are readily soluble in water they are efflorescent in a humid atmosphere. For binary halides the following anion polyhedra have been identified: five capped trigonal prism (UF_3), tricapped trigonal prism (UCl_3, UBr_3), and bicapped trigonal prism (UI_3).

The synthesis of uranium(III) halides and complex halides requires a rather complex equipment and strictly oxygen-free conditions. At temperatures higher than 600°C the syntheses ought to be carried out in tantalum or molybdenum tubes in order to avoid side reactions with silica; Drożdżyński (1991) has reported a survey of the preparation methods.

Trivalent uranium has a [Rn] $5f^3$ electronic configuration with the $^4I_{9/2}$ ground state. A number of crystal-field analyses of high-resolution low-temperature absorption spectra have been reported for U^{3+}-doped single crystals of $LiYF_4$ (S_4) (Simoni *et al.*, 1995), $LaCl_3$ (C_{3h}) (Crosswhite *et al.*, 1980; Carnall, 1989; Karbowiak *et al.*, 2002a), $LaBr_3$ (C_{3h}) (Sobczyk *et al.*, 2005), RbY_2Cl_7 (C_{2v}) (Karbowiak *et al.*, 1997), K_2UX_5 (C_s) (X = Cl, Br or I) (Karbowiak *et al.* 1998a), Cs_2NaYCl_6 (O_h) and Cs_2LiYCl_6 (O_h) (Karbowiak *et al.*, 1998b), Ba_2YCl_7 (C_1) Karbowiak *et al.*, 2002b, Cs_2NaYBr_6 (Karbowiak *et al.*, 2003a), $CsCdBr_3$ (Karbowiak *et al.*, 2003b), $Cs_3Lu_2Cl_9$(C_{3v}) and $Cs_3Y_2I_9$ (C_{3v}) (Karbowiak *et al.* 2005a). Such analyses have been also performed for polycrystalline samples of UCl_3 and UBr_3 (C_{3h}) (Sobczyk *et al.*, 2003), $UCl_3 \cdot 7H_2O$ (C_i) (Karbowiak *et al.*, 2001), $CsUCl_4 \cdot 3H_2O$ (C_s), $NH_4UCl_4 \cdot 4H_2O$ (C_2) (Karbowiak *et al.*, 2000), and $ZnCl_2$-based glass (Dereń *et al.*, 1998). However, only the U^{3+}-doped single crystals of $LaCl_3$ and $LiYF_4$ exhibit suitable site symmetry for precise energy-level investigations, using selection rules for electric and magnetic dipole transitions. The energy levels of the U^{3+} ion in the different site symmetries were assigned and fitted to a semiempirical Hamiltonian representing the combined atomic and crystal-field interactions. *Ab initio* calculations made it possible to use a simplified parametrization and the determination of the starting values in the angular overlap model in cases where the U^{3+} ion had the lowest site symmetry (Karbowiak *et al.*, 2000). The free ion and crystal-field parameters obtained from an analysis of low-temperature absorption spectra of thin films of UF_3, UCl_3, and UBr_3 are presented in Table 5.25. In addition, an analysis of low-temperature absorption, luminescence, and excitation

Table 5.25 *Properties of selected uranium(III) halides and complex halides.*[a]

Formula	*Selected properties and physical data*[b]	*Lattice symmetry, lattice constants* (Å)*, conformation and density* (g cm^{-3})[c]	*Remarks regarding information available and references*
UF_3	grey to black powder or purplish black crystals. density: 8.9 g cm^{-3}; disproportionates above 1000°C UF_3(cr): $\Delta_f G_m^o = -1432.5$ (4.7)†, $\Delta_f H_m^o = -1501.4$(4.7)†, $S_m^o = 123.4$ (0.4)†; $C_{p,m}^o = 95.1$(0.4)†. UF_3(g): $\Delta_f G_m^o = -1062.9$ (20.2)†, $\Delta_f H_m^o = -1065.0$ (20)†, $S_m^o = 347.5$(10)†; $C_{p,m}^o = 76.2$(5.0)†. $\log p$(mm Hg) = $4187T^{-1} + 3.945$ $\mu_{eff.} = 3.67$ B.M. (125–300 K)[d]; $\theta = -110$ K. $\mu_{eff.} = 3.66$ B.M. (293–723K)[d]; $\theta = -98$ K, Atomic and crystal-field parameters: $E_{avg} = 20\,006$ (30), $F^2 = 38\,068$ (108), $F^4 = 32256$ (177), $F^6 = 16372$ (198), $\zeta_{5f} = 1613$ (11); $\alpha = 26.1$ (6), $\beta = -793$ (40), $\gamma = 2085$ (104); $T^2 = [298.0]$, $T^3 = [48.0]$, $T^4 = [255.0]$, $T^6 = [-285.0]$, $T^7 = [332.0]$, $T^8 = [305.0]$; $M^0 = [0.67]$, $M^2 = [0.37]$, $M^4 = [0.26]$; $P^2 = [1276]$, $P^4 = [608]$, $P^6 = [122]$;$B_0^2 = 216(60)$, $B_2^2 = -319(49)$, $B_0^4 = 1479$ (78), $B_2^4 = 679(62)$, $B_4^4 = 1615(62)$, $B_0^6 = 2373$ (79), $B_2^6 = -2201$ (62), $B_4^6 = -1631(630)$, $B_6^6 = -1106$ (63); $n = 75$; *rms* = 33.6.	hexagonal; C_{6v}^3, $P6_3cm$, No. 185; $Z = 6$; or trigonal: $P\bar{3}c1$, D_{3d}^4, No. 165; Z = 6, CN = 11, $a = 7.173$, $c = 7.341$; d(calc.) = 8.95 to 8.99; d(exp.) = 9.18. LaF_3 structure type; The bond lengths to the corresponding prism atoms in $P\bar{3}cl$ are 3.01 (2×), 2.48 (2×) and 2.63 (2×) and in $P6_3cm$ these are 2.53 (2×), 2.81 (2×), 2.45 and 3.09, respectively. The cap atoms in both structures have fit firmly (bond lengths 2.42–2.48.)	*X-ray single-crystal and neutron diffraction data* (Zalkin *et al.*, 1967; Taylor 1976a; Zachariasen, 1975); *Synthesis* (Runnals, 1953; Warf, 1958; Friedman *et al.*, 1970; Berndt, 1973); *absorption spectra* (Schmieder *et al.*, 1970); *photoelectron spectra* (Thibaut *et al.*, 1982); *crystal-field analysis* (Drożdżyński *et al.*, 2002); *mechanical and thermal properties* (Bacher and Jacobs, 1980); *EPR, NMR and magnetic susceptibility data* (Berger and Sienko, 1967; Dao, Nguyen Nghi *et al.*, 1964; Kanellakopulos, 1983); *fused-salt systems* (Martinot, 1984); *thermodynamic properties* (Brown, 1973, 1979; Grenthe *et al.*, 1992; Guillaumont *et al.*, 2003)

Table 5.25 (*Contd.*)

Formula	*Selected properties and physical data*[b]	*Lattice symmetry, lattice constants* (Å)*, conformation and density* (g cm^{-3})[c]	*Remarks regarding information available and references*
$NaUF_4$	peritectic decomposition point of α-$NaUF_4$: 775°C; α–β transformation temp. 595°C	hexagonal, C_{3h}^1, $P\bar{6}$, No. 174; a = 6.167, c = 3.770; d(calc.) = 5.92; tricapped trigonal prism sharing ends to form chain	*X-ray powder diffraction data; fused salt systems* (Brunton *et al*., 1965; Bacher and Jacob, 1980)
Na_2UF_5		cubic, space centered, Z = 4; a = 7.541(6); d(calc.) = 5.87	*X-ray powder diffraction data; fused salt systems* (D'Eye and Martin, 1957; Bacher and Jacob, 1980)
KUF_4	dark-blue		(Bacher and Jacob, 1980)
K_2UF_5	peritectic point: 848°C	cubic; CaF_2 structure type ; a = 6.62 (1); Z = 1.6; d(calc.) = 3.74	*X-ray powder diffraction data; fused salt systems* (Volkov *et al*., 1979)
K_3UF_6	purple-brown, extremely moisture sensitive	cubic, face centered; a = 9.20	*X-ray powder diffraction data; fused salt systems* (Thoma and Penneman, 1965; Thoma *et al*., 1966)
$K_3U_2F_9$	peritectic point: 750°C	cubic; CaF_2structure type ; a = 6.00 (1); Z = 0.8; d(calc.) = 4.67	*X-ray powder diffraction data; fused salt systems* (Volkov *et al*., 1979)
$RbUF_4$		hexagonal; KYF_4 structure type ; a = 8.54(1), c = 10.72(2); Z = 6, d(calc.) = 5.84	*X-ray powder diffraction data; fused salt systems* (Boraopkova *et al*., 1971)
Rb_3UF_6	purple-brown, extremely moisture sensitive	cubic, face centered; a = 9.5074	*X-ray powder diffraction data; fused salt systems* (Thoma and Penneman, 1965; Thoma *et al*., 1966; Chirkst, 1981)
Cs_3UF_6	purple-brown, extremely moisture sensitive	cubic, face centered; a = 10.6	*X-ray powder diffraction data; fused salt systems* (Thoma and Penneman, 1965; Thoma *et al*., 1966; Chirkst, 1981)

$UZrF_7$	reddish-brown, slowly oxidizes in air at room temperature; $\mu_{eff.} = 3.80$ B.M. (100–300 K)[d]; $\theta = -85$ K	monoclinic, isotypic with $SmZrF_7$, $a = 6.1000(6)$, $b = 5.833(8)$ $c = 8.436(10)$; $\beta = 102.69(7)$; $Z = 2$; $V = 292.81$; d(calc) = 5.25; d(exp.) = 5.40.	*X-ray powder diffraction data; magnetic susceptibility data* (Fonteneau and Lucas, 1974)
UZr_2F_{11}	slowly oxidizes in air at room temperature. $\mu_{eff.} = 3.90$ B.M. (100–300 K)[d]; $\theta = -101$ K	monoclinic; $a = 5.308(6)$, $b = 6.319(8)$, $c = 8.250(8)$, $\beta = 105.41(5)^\circ$, $Z = 2$; $V = 266.81$; d(calc.) = 5.22	*X-ray powder diffraction data; magnetic susceptibility data* (Fonteneau and Lucas, 1974). *general properties* (Bacher and Jacob, 1980)
UCl_3	dark red needles or fine crystalline olive-green powder; hygroscopic; soluble in acetic acid.m.p. = 835°C; b.p. = 1657 °C; density: 5.51 g cm^{-3}; Oxidizes in air at room temperatures; UCl_3(cr): $\Delta_f G^o_m = -796.1$ (2.0)†, $\Delta_f H^o_m = -863.7$ (2.0)†, $S^o_m = 158.1$ (0.5)†; $C^o_{p,m} = 95.10$ (0.5)†. UCl_3(g): $\Delta_f G^o_m = -521.7$ (20.2)†, $\Delta_f H^o_m = -523.0(20)$†, $S^o_m = 380.3$ (10.0)†; $C^o_{p,m} = 82.4$ (5.0)†. $\log p$(mmHg) = $-11149\ T^{-1} + 8.90$ (590–790 K) $\log p$(mmHg) = $-11552 T^{-1} + 8.97$ (>790 K); Atomic and crystal-field parameters: $\mu_{eff.} = 3.76$ B.M. (70–300 K)[d]; $\theta = -75$ K; $T_N = 20$ K; $\mu_{eff.} = 3.03$ B.M. (350–509 K)[d]; $\theta = -29$ K; $E_{avg} = 19331(42)$, $F^2 = 37719(154)$, $F^4 = 30370(202)$, $F^6 = 19477(218)$, $\zeta_{5f} = 1606(13)$; $\alpha = 31(5)$, $\beta = -939(40)$, $\gamma = 2087(115)$; $T^2 = 460(81)$; $T^3 = 59(25)$, $T^4 = 159(39)$, $T^6 = -144(46)$, $T^7 = 356(42)$, $T^8 = [300]$; $M^0 = [0.663]$; $P^2 = 1639(65)$; $B^2_0 = 370(42)$, $B^4_0 = -359(76)$, $B^6_0 = -1704(74)$; $B^6_6 = 935(60)$; $n = 58$; $rms = 35.8$	hexagonal; C^2_{6h}, $P6_3/m$, No. 176; the coordination polyhedron is a symmetrically tricapped trigonal prism arranged in columns in the c-direction; $a = 7.452(6)$, $c = 4.328(4)$; d(U–Cl) = 2.928(3), (6×); d(U–Cl) = 2.934(5), (3×); d(U–Cl) = 4.816(4) (to neighbor chain); d(Cl–Cl) = 3.342(5); d(Cl–Cl) = 3.410(3); (face atom-cape atom); d(calc.) = 5.51	*X-ray single crystal data* (Schleid *et al.*, 1987; Murasik *et al.*, 1985; Taylor and Wilson, 1974f); *synthesis* (Brown, 1968, 1979; Drożdżyński, 1991, 1988a); *thermodynamic properties* (Rand and Kubaschewski, 1963; Brown, 1973, 1979; Grenthe *et al.*, 1992; Guillaumont *et al.*, 2003). *magnetic susceptibility data*, (Handler and Hutchison, 1956; Jones *et al.*, 1974; Dawson, 1951); *NIR, visible and UV low temperature absorption spectra and crystal-field analysis of UCl_3 and U^{3+}:$LaCl_3$*, (Carnall, 1989; Karbowiak *et al.*, 2002; Sobczyk *et al.*, 2003); *photoelectron spectra* (Thibaut *et al.*, 1982)

Table 5.25 (*Contd.*)

Formula	*Selected properties and physical data*[b]	*Lattice symmetry, lattice constants* (Å)*, conformation and density* (g cm^{-3})[c]	*Remarks regarding information available and references*
$UCl_3 \cdot 7H_2O$	grayish-ink-blue needles, readily soluble in numerous organic solvents; relatively resistant to oxidation by air at temperatures lower than 15°C; loses some of its crystallization water at higher temperatures or at high vacuum; may be completely dehydrated at 260°C. $\mu_{eff.} = 2.95$ B.M. (10–300 K)[d]; $\theta = -32.7$ K; Atomic and crystal-field parameters: $E_{avg} = 19827(17)$, $F^2 = 40488(58)$, $F^4 = 32544(81)$, $F^6 = 22866(75)$, $\zeta_{5f} = 1622(10)$; $\alpha = 28(5)$, $\beta = -622(35)$, $\gamma = 1148$; $T^2 = 306$, $T^3 = 42$, $T^4 = 188$, $T^6 = -242$, $T^7 = 447$, $T^8 = 300$; $M^0 = 0.672$, $M^2 = 0.372$, $M^4 = 0.258$; $P^2 = 1216$, $P^4 = 608$, $P^6 = 122$; $B_0^2 = -126(76)$, $B_1^2 = [-109]$, $\mathrm{Im}B_1^2 = -423(47)$, $B_2^2 = -209(53)$, $\mathrm{Im}B_2^2 = -350(55)$, $B_0^4 = 188(106)$, $B_1^4 = [-99]$, $\mathrm{Im}B_1^4[-81]$, $B_2^4 = [-66]$, $\mathrm{Im}B_2^4 = [-238]$, $B_3^4 = [136]$, $\mathrm{Im}B_3^4 = -529(83)$, $B_4^4 = [374]$, $\mathrm{Im}B_4^4 = [-491]$, $B_0^6 = [-130]$, $B_1^6 = 428(90)$, $\mathrm{Im}B_1^6 = [-77]$, $B_2^6 = [171]$, $\mathrm{Im}B_2^6 = 133$ [100], $B_3^6 = [-251]$, $\mathrm{Im}B_3^6 = [-14]$, $B_4^6 = -489(110)$, $\mathrm{Im}B_4^6 = -1832(81)$, $B_5^6 = [160]$, $\mathrm{Im}B_5^6 = 1197(96)$, $B_6^6 = -498(98)$, $\mathrm{Im}B_6^6 = -241(91)$; *rms* = 36; $n = 94$	triclinic; $P\bar{1}$, C_i^1, No.2; $a = 7.902(1)$; $b = 8.210(2)$, $c = 9.188(2)$; $\alpha = 70.53(3)$; $\beta = 73.14(3)$; $\gamma = 81.66(3)$; $V = 537.0(2)$; $Z = 2$; d(calc.) = 2.910. The crystals are built up from separate $[U_2Cl_2(H_2O)_{14}]^{4+}$ units and Cl^- ions. The characteristic features of this structure are dimers, formed by two uranium ions connected through the (Cl1) bridging chlorine atoms. d(U–Cl) = 2.915(1) and 2.894(1); d(U–O) = from 2.515(3) to 2.573(3)	*X-ray single crystal data* (Mech *et al.*, 2005); *magnetic susceptibility data; NIR and visible absorption spectrum, decomposition* (Drożdżyński, 1985); *crystal-field analysis, low temperature absorption spectrum* (Karbowiak *et al.*, 2001)

$UCl_3{\cdot}6H_2O$	purple plates	monoclinic; *P*12/*n*l; $a = 9.732(2)$, $b = 6.593(1)$, $c = 8.066(2)$, $\alpha = 90$, $\beta = 93.56(3)$; $\gamma = 90$; $V = 516.51$; $Z = 2$; d(calc.) = 2.909; The basic units of the crystal structure are Cl^- anions and $[UCl_2(H_2O)_6]^+$ cations. The U as well as O(1), O(2) and O(3) atoms are each eight-coordinated, whereas the Cl(2) and Cl(1) chloride atoms are seven and six coordinated, respectively. The characteristic feature of this structure is the existence of hydrogen bonds, which link the uranium eight–coordinated polyhedra, forming a three–dimensional network	*X-ray single crystal data* (Mech *et al.*, 2005)
$UCl_3{\cdot}CH_3CN{\cdot}5H_2O$	deep-red; soluble in polar organic solvents; IR (cm^{-1}): 2260m, 2270sh (ν_2, symm. C ≡ N stretching); 1367 (ν_3, symm. CH_3 deform.); 926m (ν_4, symm. C–C stretching); 2298 ($\nu_3 + \nu_4$, combination band); 1035 (ν_7, degenerate CH_3 rocking); $\mu_{eff.} = 3.39$ B.M .(65–300 K)[d], $C = 1.430$ emu·K·mol^{-1}, $\theta = -65.7$ K, $T_N = 12$ K	monoclinic; $a = 12.96(2)$, $b = 12.98(3)$, $c = 6.62(1)$; $\beta = 101.7(2)$; $Z = 4$, $V = 1007.2$; d(calc.) = 3.14	*X-ray powder diffraction data; magnetic susceptibility data; IR, NIR and visible absorption spectra; decomposition*, (Zych and Drożdżyński, 1986)
$UCl_3{\cdot}2H_2O{\cdot}2CH_3CN$	deep dark reddish needles	$P\bar{1}$, C_i^1, No.2; $a = 7.153(1)$, $b = 8.639(2)$, $c = 10.541(2)$; $\alpha = 108.85(3)$, $\beta = 105.05(3)$, $\gamma = 93.57(3)$; $V = 587.6(3)$; $Z = 2$; d(calc.) = 2.61; d(U–Cl) = 2.775; d(U–Cl) to the bridging anions = 2.860–2.901; d(U–O) = 2.468–2.485; d(U–U) = 4.605.	*X-ray single crystal data* (Mech *et al.*, 2005)

Table 5.25 (*Contd.*)

Formula	*Selected properties and physical data*[b]	*Lattice symmetry, lattice constants* (Å), *conformation and density* (g cm^{-3})[c]	*Remarks regarding information available and references*
		The U^{3+} ion is eight coordinated by five chloride ions, two water molecules and one methyl cyanide, which are forming a distorted bicapped trigonal prism The characteristic feature of this structure is the link of the uranium atoms through the two common edges of the Cl1 and Cl3 chlorine atoms into an infinitive zigzag chain in the [010] direction	
$CsUCl_4$	deep ink-blue; soluble in polar organic solvents; $\mu_{eff.} = 3.16$ B.M. (60–300 K)[d]; $\theta = -36$ K; $C = 1.2146$ emu·K·mol^{-1}	could not be unambiguously indexed	*X-ray powder diffraction data; magnetic susceptibility data; NIR, Vis, and UV absorption spectra* (Karbowiak and Drożdżyński, 1998a)
K_2UCl_5	purple; soluble in polar organic solvents, m.p. = 608°C – congruently; $\mu_{eff.} = 3.77$ B.M. (130–300 K)[d)]; $\theta = -33.5$ K; $T_N = 13.2$ K; IR(cm^{-1}): ν(U–Cl, stretching) = 140–220	orthorhombic; D_{2h}^{16}, *Pnm*, No. 62; Z = 4; Monocapped trigonal prisms $[UCl_7]$ are connected via two opposite common edges to chains; $a = 12.7224(7)$, $b = 8.8064(6)$, $c = 7.9951(5)$; $V = 1348.8(1)$; d(calc.) = 3.68	*single crystal and X-ray powder diffraction data; IR, NIR, and Vis absorption spectra; magnetic susceptibilities* (Drożdżyński and Miernik, 1978; Krämer *et al*., 1994); *luminescence and low temperature spectra of* U^{3+}*:*K_2LaCl_5 (Andres *et al*., 1996); *magnetic phase transitions* (Keller *et al*., 1995); *crystal-field analysis* (Karbowiak *et al*., 2000); *fused salt systems* (Suglobova and Chirkst, 1981)

Rb_2UCl_5	violet-red; soluble in polar organic solvents; m.p. = 575°C– incongruently; $\mu_{eff.} = 3.44$ B.M. (150–300 K)[d]; $\theta = -32.0$ K; $T_N = 8.6$ K; IR (cm^{-1}): ν(U–Cl, stretching) = 100–260	orthorhombic; D_{2h}^{16}, *Pnma,* No. 62; $Z = 4$; Monocapped trigonal prisms [UCl_7] are connected via two opposite common edges to chains; $a = 13.1175(8)$, $b = 8.9782(6)$, $c = 8.1871(7)$; $V = 1451.19(2)$; d(calc.) = 4.04; d(U–Cl) = 2.774 to 2.846; d(U–U) = 4.651 (interchain); d(U–U) = 7.88 (intrachain)	*X-ray powder diffraction data; IR, NIR and visible absorption spectrum; magnetic susceptibilities* (Drożdżyński and Miernik, (1978); Krämer *et al.*, 1994); *fused salt systems* (Suglobova and Chirkst, 1981)
Cs_2UCl_5	m.p. = 370°C – decomposition in solid state	rhombic; $a = 12.03$, $b = 9.76$, $c = 9.37$; $Z = 4$, d(calc.) = 4.08	*X-ray powder diffraction data; fused salt systems* (Suglobova and Chirkst, 1981)
$(NH_4)_2UCl_5$	violet; $\mu_{eff.} = 3.54$ B.M. (17–220 K)[d]; $\theta = -26.0$ K; $\mu_{eff.} = 3.47$ B.M. (220–300 K)[c]; $\theta = -37.5$ K; $T_N = 7.8$ K; IR(cm^{-1}): ν(U–Cl, stretching) = 140–260		*IR, NIR,and Vis absorption spectra; magnetic susceptibilities* (Drożdżyński and Miernik, 1978)
$SrUCl_5$	deep olive-green; $\mu_{eff.} = 3.65$ B.M. (90–300 K)[d] $C = 1.653$ emu·K·$mole^{-1}$, $\theta = -127$ K	could not be indexed	*X-ray powder diffraction data; magnetic susceptibility data; NIR and Vis absorption spectra*, (Karbowiak and Drożdżyński, 1998b)
$[(CH_3)_3N]_3 \cdot UCl_6$	dark violet-blue; IR (cm^{-1}): 110m [$\delta(UCl_6)$ A_u]; 123m,b [$\delta(UCl_6)$ E_u] 203s [lattice or cation vib.]; 236s [$\nu_s(UCl_6)$ A_u]; 259s [$\nu_{as}(UCl_6)$ E_u]. Raman (cm^{-1}): 79sh [lattice]; 89w [$\delta(UCl_6)$ E_g]; 104w [$\delta(UCl_6)$ B_g]; 131m [lattice or cation vib.]; 226vs [$\nu_{as}(UCl_6)$ A_g]; 237sh [$\nu'(UCl_6)$ A_g]; 268w [$\nu_s(UCl_6)$ B_g]; $\mu_{eff.} = 3.36$ B.M. (200–300K)[d]; $\theta = 17$; $T_N = 4.8$ K; $C = 1.5058$ emu·K·$mole^{-1}$	tetragonal; $a = 13.020$, $c = 7.825$; $Z = 2$; $V = 1326.48$; d(calc.) = 1.68	*X-ray powder diffraction data; IR, Raman, NIR and Vis absorption spectra; magnetic susceptibility data* (Karbowiak *et al.*, 1996a)

Table 5.25 (*Contd.*)

Formula	*Selected properties and physical data*[b]	*Lattice symmetry, lattice constants* (Å), *conformation and density* (g cm^{-3})[c]	*Remarks regarding information available and references*
RbU_2Cl_7	pale-brown; soluble in polar organic solvents; IR (cm^{-1}):281s, 271s, 210s, 202vs, 195sh, 190vs, 181vs, 169vs, 150sh [ν(U–Cl)]; 130m, 125m, 114m, 90m [δ(Cl–U–Cl)]; 83sh, 70m, 55w [T'(Rb/U)]; RS (in cm^{-1}): 262w, 227 s,b, 189s,165s [ν(U–Cl)]; 142m, 120m, 95w [δ(Cl–U–Cl)]; 85m, 62m T'(Rb/U); $\mu_{eff.} = 3.76$ B.M., $C = 1.750$ emu·K·$mole^{-1}$, $\theta = -80$ K	rhombic; $a = 12.86(5)$, $b = 6.89(1)$, $c = 12.55(2)$; $Z = 4$, d(calc) = 4.80(3), $RbDy_2Cl_7$ structure type	*X-ray powder diffraction data* (Suglobova and Chirkst, 1981); Volkov *et al*., 1987); *NIR and Vis low temperature absorption spectrum; magnetic susceptibility data; IR transmission and Raman spectra* (Karbowiak *et al*., 1996b); *luminescence and excitation spectra* (Karbowiak *et al*., 1996d); *low temperature absorption spectrum and crystal-field analysis of* U^{3+}*:*RbY_2Cl_7 (Karbowiak *et al*., 1997)
Ba_2UCl_7	deep black-brown; soluble in polar organic solvents; $\mu_{eff.} = 3.25$ B.M., (105–300 K)[d], $C = 1.310$ emu·K·$mole^{-1}$, $\theta = -95$ K	monoclinic; C_{2h}^5, $P2_1/c$, No. 14; $a = 7.20$, $b = 15.61$, $c = 10.66$; $\beta = 91.1°$, $V = 1197$; d(calc.) = 4.22	*X-ray powder diffraction data* (Volkov *et al*., 1987); Suglobova and Chirkst, 1981); *magnetic susceptibility data; IR, NIR and Vis absorption spectra* (Karbowiak and Drożdżyński, (1998b)
Cs_2LiUCl_6	deep ink-blue; $\mu_{eff.} = 3.56$ B.M. (85–300)[d]; $C = 1.571$ emu·K·$mole^{-1}$, $\theta = -103$ K	regular; O_h^5, $Fm3m$, No. 225; $a = 10.671$; $Z = 4$; $V = 1218.03$; d(calc.) = 3.9444	*X-ray powder diffraction data, NIR, Vis and UV absorption spectra, magnetic susceptibilities* (Karbowiak and Drożdżyński, 1998a); *absorption, vibronic and emission spectra; crystal-field analysis* (Karbowiak *et al*., 1996e; Karbowiak *et al*., 1998b)

K_2NaUCI_6		hexagonal; C_{3v}^1, $P3m1$, No.156; isostructural with α-K_2LiAlF_6; a = 7.28(1), c = 17.79(2); Z = 3; V = 816.53; d(calc.) = 3.35(1)	*X-ray powder diffraction data* (Volkov *et al*., 1987; Aurov *et al*., 1983); *thermodynamic data* (Aurov and Chirkst, 1983)
Rb_2NaUCI_6		trigonal; a = 7.27(2), c = 35.51(10); Z = 6; d(calc.) = 3.93(3), d(exp.) = 3.98(2); Rb_2LiAlF_6 and Cs_2NaCrF_6 structure type	*X-ray powder diffraction data* (Volkov *et al*., 1987; Aurov *et al*., 1983); *thermodynamic data* (Aurov and Chirkst, 1983)
Cs_2NaUCl_6	ink-blue; soluble in polar organic solvents; $\mu_{eff.}$ = 2.49 B.M. (4–20)[d]; θ = 0.53 K. $\mu_{eff.}$ = 2.92 B.M. (25–50)[d]; θ = 9.6 K	cubic; O_h^5, $Fm3m$, No.225; a = 10.937 (1); V = 1308.3(5); Z = 4, d(U–Cl) = 2.723(9), d(U–U) = 7.734; d(calc.) = 3.754	*single crystal data* (Spirlet *et al*., 1988); *magnetic properties* (Hendricks *et al*., 1974); *thermodynamic properties* (Aurov and Chirkst, 1983; Schoebrechts *et al*., 1989); *NIR, Vis and UV low temperature absorption and luminescence spectra; crystal-field analysis* (Karbowiak *et al*., 1998b); *IR spectra* (Mazurak *et al*., 1988).
NaU_2Cl_6 or $(Na^+)(U^{3+})_2(e^-)(Cl^-)_6$		hexagonal; C_{6h}^2, $P6_3/m$., No 176; a = 7.5609(3), c = 4.3143(3); Z = 1; d(U–Cl) = 2.945(6×) and 2.977(3×), d(Na–Cl) = 2.878(6×)].	*single crystal data* (Schleid and Meyer, 1989)
$KUCl_4{\cdot}4H_2O$	violet-red; soluble in polar organic solvents; IR (cm^{-1}): 650, 610 (U–OH_2 rocking); 470s (U–OH_2 wagging); 300w ν(U–OH_2 stretching); 222sh, 214s, 198s ν(U–Cl, stretching); 166s ν(U–Cl–U, stretching or lattice); 130s δ(Cl–U–Cl, stretching or lattice); 107s, 88sh (lattice modes); $\mu_{eff.}$ = 3.72 B.M. (100–300 K)[d]; C = 1.716 emu·K·$mole^{-1}$; θ = −69.3 K	orthorhombic; a = 6.971, b = 6.638, c = 11.317; Z = 2; V = 523.6; d(calc.) = 3.11	*X-ray powder diffraction data; magnetic susceptibility data; IR, NIR and Vis spectra* (Drożdżyński, 1988b)

Table 5.25 (*Contd.*)

Formula	*Selected properties and physical data*[b]	*Lattice symmetry, lattice constants* (Å), *conformation and density* ($g\ cm^{-3}$)[c]	*Remarks regarding information available and references*
$RbUCl_4 \cdot 4H_2O$	violet-red; soluble in polar organic solvents; IR (cm^{-1}): 660 (U–OH_2, rocking); 486s (U–OH_2, wagging); 300sh, 290ms [ν(U–OH_2), stretching]; 228s, 216sh, 197s [ν(U–Cl) stretching]; 165ms [ν(U–Cl–U), stretching or lattice]; 130s [δ(Cl–U–Cl), bending]; 99 ms (lattice modes); $\mu_{eff.} = 3.74$ B.M. (100–300 K)[d]; $C = 1.734$ emu·K·$mole^{-1}$, $\theta = -66.2$ K	orthorhombic; $a = 6.999$, $b = 6.673$, $c = 11.375$; $Z = 2$; $V = 531.3$; d(calc.) = 3.36	*X-ray powder diffraction data; magnetic susceptibility data; IR, NIR and Vis absorption spectra* (Drożdżyński, 1988b)
$NH_4UCl_4 \cdot 4H_2O$	dark red-violet; soluble in polar organic solvents; IR (cm^{-1}): 650, 610 (U–OH_2, rocking); 494s (U–OH_2, wagging); 299ms [ν(U–OH_2) stretching]; 222s, 202s ν(U–Cl, stretching); 175ms [ν(U–Cl–U), stretching or lattice]; 130s [δ(Cl–U–Cl), bending]; 114ms, 84sh (lattice modes); $\mu_{eff.} = 3.53$ B.M. (100–240 K)[d]; $C = 1.560$ emu·K·$mole^{-1}$, $\theta = -72.5$ K. Atomic and crystal-field parameters: $F^2 = 39911(85)$, $F^4 = 33087(149)$, $F^6 = 22048(160)$, $\zeta_{5f} = 1627.3(8.8)$; $\alpha = 33.0(3.7)$, $\beta = -973.1(29.3)$, $\gamma = 1316.9(85.4)$; $T^2 = 306$, $T^3 = 42$, $T^4 = 188$, $T^6 = -242$, $T^7 = 447$, $T^8 = 300$;	orthorhombic; D_2^3, $P2_12_12$, No. 18; $a = 7.002(2)$, $b = 11.354(3)$, $c = 6.603(2)$; $Z = 2$; $V = 524.94(14)$. The U^{3+} cation is coordinated by four Cl^-, ions and four H_2O molecules. The crystal is build up from eight-coordinated U^{3+} polyhedrons, which are connected together by O-H··Cl hydrogen bonds. d(U–Cl) (2×) = 2.845(4); d(U–Cl)) (2×) = 2.847(4); d(U–O) (2×) = 2.510(11); d(U–O) (2×) = 2.568(10); d(calc.) = 2.973, d(exp.) = 2.97	*single crystal diffraction data; magnetic susceptibility data; IR, NIR and Vis low temperature absorption spectra* (Drożdżyński, 1988b); *low temperature absorption spectra and crystal-field analysis* (Karbowiak *et al*., 2000)

	$M^0 = 0.672$, $M^2 = 0.372$, $M^4 = 0.258$; $P^2 = 1216$, $P^4 = 608$, $P^6 = 122$; $B_0^2 =$ 721(47) / [698], $B_2^2 = 428$ (39) / [403], $\mathrm{Im}B_2^2 = -460$ (39) / [–515], $B_0^4 =$ [–814], $B_2^4 =$ [–858], $\mathrm{Im}B_2^4 =$ [118], $B_4^4 =$ [–670], $\mathrm{Im}B_4^4 =$ [–22], $B_0^6 =$ [–403], $B_2^6 =$ [–612], $\mathrm{Im}B_2^6 =$ [838], $B_4^6 =$ [–549], $\mathrm{Im}B_4^6 =$ [–197], $B_6^6 =$ [–1063], $\mathrm{Im}B_6^6 =$ [–96], *rms* = 30, $n = 83$		
$KUCl_4 \cdot 3H_2O$	green; hygroscopic and air sensitive; IR(cm^{-1}): ν(U–OH_2, rocking) = 635s, 575s; ν(U–OH_2, wagging) = 480; *ν*(U–OH), stretching = 425, 280sh; *ν*(U–Cl), stretching = 260s, 238, 202; *ν*(U–Cl–U), stretching or lattice = 169, 125; *δ*(Cl–U–Cl), bending = 144, 125; *ν*(stretching and bending modes of coordinated water) = 1600; (3170, 3215, 3360, 3420); $\mu_{\mathrm{eff.}} = 3.70$ B.M. (150–300 K)[d]; $C =$ 1.7033 emu·K·$mole^{-1}$, $\theta = -80$ K	monoclinic; $a = 6.9373$, $b = 7.2658$, $c = 9.5209$; $\beta = 96.71$; $Z = 2$; $V = 476.62$; *d*(calc.) = 3.30	*X-ray powder diffraction data; IR, NIR and Vis absorption spectra; magnetic susceptibility data* (Karbowiak and Drożdżyński, 1993)
$RbUCl_4 \cdot 3H_2O$	greenish-brown to brown; hygroscopic and air sensitive; IR (cm^{-1}): *ν*(U–OH_2, rocking) = 650, 615, 600; *ν*(U–OH_2, wagging) = 485; *ν*(U–OH), stretching = 380, 285sh; *ν*(U–Cl), stretching = 255s, 220, 190; *ν*(U–Cl–U), stretching or lattice = 151, 157; *δ*(Cl–U–Cl), bending = 132, 127, 121, 118; *ν*(stretching and bending modes of coordinated water) = 1565, 1580, 1605, 3470; (93180, 3210, 3350, 3420, 3470); $\mu_{\mathrm{eff.}} = 3.57$ B.M. (100–300 K)[d], $C =$ 1.5766 emu·K·$mole^{-1}$, $\theta = -64$ K	monoclinic; $a = 8.8986$, $b = 6.9738$; $c = 8{,}0517$; $\beta = 100$; $Z = 2$; $V = 490.75$; *d*(calc.) = 3.51	*X-ray powder diffraction data; IR, NIR and Vis absorption spectra; magnetic susceptibility data* (Karbowiak and Drożdżyński, 1993)

Table 5.25 (*Contd.*)

Formula	*Selected properties and physical data*[b]	*Lattice symmetry, lattice constants* (Å)*, conformation and density* (g cm^{-3})[c]	*Remarks regarding information available and references*
$CsUCl_4 \cdot 3H_2O$	brown-green; soluble in polar organic solvents; $CsUCl_4 \cdot 3H_2O$; $\mu_{eff.} = 3.39$ B.M., $C = 1.430$ emu·K·$mole^{-1}$, $\theta = -67.7$ K. Free ion and crystal-field parameters: $F^2 = 39876(58)$, $F^4 = 33279(77)$, $F^6 = 23598(68)$, $\zeta_{5f} = 1648.3(10.3)$; $\alpha = 26.2(4.3)$, $\beta = -889(38)$, $\gamma = 1131(94)$; $T^2 = 306$, $T^3 = 42$, $T^4 = 188$, $T^6 = -242$, $T^7 = 447$, $T^8 = 300$; $M^0 = 0.672$, $M^2 = 0.372$, $M^4 = 0.258$; $P^2 = 1216$, $P^4 = 608$, $P^6 = 122$; $B_0^2 = -411(46)$ / [–390], $B_2^2 = 614(45)$ / [573], $\mathrm{Im}B_2^2 = 610(46)$ / [614], $B_0^4 =$ [–699], $B_2^4 =$ [–398], $\mathrm{Im}B_2^4 =$ [–525], $B_4^4 =$ [–1039], $\mathrm{Im}B_4^4 =$ [–49], $B_0^6 =$ [–1046], $B_2^6 =$ [–58], $\mathrm{Im}B_2^6 =$ [794], $B_4^6 =$ [–119], $\mathrm{Im}B_4^6 =$ [–173], $B_6^6 =$ [–27], $\mathrm{Im}B_6^6 =$ [–691], *rms* = 34; $n = 77$	monoclinic; C_{2h}^2, $P2_1/m.$, No. 11; $a = 7.116(1)$, $b = 8.672(2)$, $c = 8.071(2)$; $\beta = 99.28(3)$; $Z = 4$; $V = 956.96$; d(U–Cl) = 2.957(3×), d(U–O) = 2.552 (3×) (mean values); tricapped trigonal prism consisting of six Cl and three O atoms (representing the water molecules)	*single crystal diffraction data* (Krämer *et al.*, 1991*)*; *synthesis, magnetic susceptibility data; IR, NIR and Vis low temperature absorption spectra; crystal-field analysis* (Karbowiak *et al.*, 1993, 2000)
$NH_4UCl_4 \cdot 3H_2O$	greenish-brown to brown; hygroscopic and air sensitive; IR (cm^{-1}): ν(U–OH_2, rocking) = 615sh, 590s; ν(U–OH_2, wagging) = 470s; ν(U–OH), stretching = 385, 290sh; ν(U–Cl), stretching = 266s, 232; ν(U–Cl–U), stretching or lattice = 172; δ(Cl–U–Cl), bending = 147, 128; ν(stretching and bending modes	monoclinic; $a = 13.7693$, $b = 8.8990$, $c = 7.8643$; $\beta = 95.65$; $Z = 4$; $V = 956.95$; d(calc.) = 3.12	*X-ray powder diffraction data; IR, NIR and Vis absorption spectra; magnetic susceptibility data* (Karbowiak and Drożdżyński, 1993)

	of coordinated water) = 1585, 1600; $\nu_4(NH_4)$ = 1404 vs; $\nu_2(NH_4)$ = 1670, $\nu_4 + \nu_6(NH_4)$ = 1770, $2\nu_4 - \nu_5(NH_4)$ = 2710, $\nu_1(NH_4)$ = 3040, $\nu_3(NH_4)$ = 3110vs. $\mu_{eff.}$ = 3.71 B.M. (75–300 K)[d]; C = 1.7073 emu·K·mole^{-1}, $\theta = -54$ K		
UOCl	red; UOCl (cr): $\Delta_f G^o_m = -785.7$ (4.9)[†], $\Delta_f H^o_m = -833.9(4.2)^{\dagger}$, S^o_m = 102.5 (8.4)[†]; $C^o_{p,m} = 71.0$ (5.0)[†]. $\mu_{eff.}$ = 3.40 B.M. (240–300 K)[d]; $\theta = -145$ K	tetragonal; D^7_{4h}, $P4/nmm$, No. 129; (PbFCl type of unit cell); a = 4.043, c = 6.882; Z = 2; CN = 9; d(U–Cl) = 2.373(2×), d(U–Cl) = 3.074(1×), d(U–Cl) = 3.150(4×)	*single crystal diffraction data* (Schleid and Meyer; 1988; Brown and Edwards, 1972); *IR and magnetic susceptibility data* (Levet and Noël, 1981); *photo-electron spectra* (Thibaut *et al.*, 1982); *themodynamic data* (Grenthe *et al.*, 1992; Guillaumont *et al.*, 2003)
U(NH)Cl		tetragonal; D^7_{4h}, $P4/nmm$, No.129; a = 3.972(5), b = 3.972(5), c = 6.81 (1); Z = 2; V = 107.44; d(calc.) = 8.91	*crystallographic data* (Berthold, and Knecht, 1966)
$Cs_2U[Cl_9O_3(TaCl)_6]$		trigonal/rhombohedral; D^2_{3d}, $P\bar{3}1c$, No.163; a = 9.1824(5), c = 17.146(2); Z = 2; V = 1252.01; d(calc.) = 5.75	*structural and theoretical studies of bondings in the cluster* (Ogliaro *et al.*, 1998)
UBr_3	reddish-brown; air sensitive; soluble in acetic acid, dimethylacetamid; density: 6.53 g cm^{-3}; m.p. = 835°C, b.p. = 1537°C UBr_3(cr): $\Delta_f G^o_m = -673.2$ (4.2)[†], $\Delta_f H^o_m = -698.7$ (4.2)[†], S^o_m = 192.98 (0.50)[†]; $C^o_{p,m} = 105.83$ (0.50)[†]. UBr_3(g): $\Delta_f G^o_m = -408.1$ (20.5)[†], $\Delta_f H^o_m = -371$ (20)[†], S^o_m = 403.0 (15.0)[†]; $C^o_{p,m} = 85.2$ (5.0)[†]. $\log p(\text{mmHg}) = -16420T^{-1} + 22.95 - 3.02 \log T$ (298–1000 K). $\log p(\text{mmHg}) = -15000T^{-1} + 27.54 - 5.03 \log T$ (1000–1810 K)	hexagonal, (UCl_3 type of structure), C^2_{6h}, $P6_3m$, No.176; a = 7.942(2), c = 4.441(2), (a = 7.9519, c = 4.448; Z = 2, CN = 9; d(calc.) = 6.54; d(U–Br) = 3.145 (3.150) to the three capping Br atoms, d(U–Br) = 3.062(3.069∼) to the six Br atoms at the prism vertices, d(Br–Br) = 3.652(3.663) at the trigonal prism face edge and d(U–U) = 4.441Å (4.448) along the c-direction. The face Br–U–Br angle is 73.21(73.3). Values in parentheses were taken from Krämer and Meyer (1989)	*X-ray single crystal data* (Levy *et al.*, 1975; Krämer and Meyer, 1989); *magnetic susceptibility data*: (Jones *et al.*, 1974); *thermodynamic properties* (Rand and Kubaschewski, 1963; Grenthe *et al.*, 1992; Guillaumont *et al.*, 2003); *NIR, Vis and UV absorption spectra; fused salt systems* (Sobczyk *et al.*, 2003; Karbowiak *et al.*, 2003a; Brown, 1979); *photoelectron spectra* (Thibaut *et al.*, 1982)

Table 5.25 (*Contd.*)

Formula	*Selected properties and physical data*[b]	*Lattice symmetry, lattice constants* (Å)*, conformation and density* ($g\ cm^{-3}$)[c]	*Remarks regarding information available and references*
	$\mu_{eff.} = 3.57$ B.M. (25–76K)[d]; $\theta = -54$ K, $T_N = 15$ K; $\mu_{eff.} = 3.29$ B.M. (350–483K)[d]; $\theta =$ 25K, $T_N = 15$ K; Atomic and crystal-field parameters: $E_{avg} = 19213(74)$, $F^2 = 37796(265)$, $F^4 = 30940(313)$, $F^6 = 20985(315)$, $\zeta_{5f} = 1604(19)$; $\alpha = 27(8)$, $\beta = -823$ (54), $\gamma = 1647(168)$; $T^2 = 374(125)$, $T^3 = 29(34)$, $T^4 = 262(58)$, $T^6 = -258(77)$, $T^7 = 264(60)$, $T^8 = [300]$; $M^0 = [0.6630]$; $P^2 = 1707(89)$; $B_0^2 = 410(50)$, $B_0^4 = -452(86)$, $B_0^6 = -1637$ (77), $B_6^6 = 722(63)$; $n = 47$; *rms* = 36.5		
$UBr_3 \cdot 6H_2O$	red	monoclinic; *P*2/*n*; $a = 10.061$, $b =$ 6.833, $c = 8.288$; $\beta = 92.99$; $V =$ 285.00	*X-ray powder diffraction and thermal decomposition data* (Brown *et al.*, 1968)
K_2UBr_5	dark violet; Polar organic solvents; m.p. = 625°C – congruently; ν(U–Br) stretching vibrations (cm^{-1}): 110m, 124m, and 145s,br	orthorhombic; D_{2h}^{16}, *Pnma,* No. 62; $a = 13.328(1)$, $b = 9.2140(7)$, $c =$ 8.4337(5), $Z = 4$, $V = 1559.5(2)$; CN = 6; *d*(calc.) = 4.53	*X-ray powder diffraction data; magnetic data; NIR, Vis an UV absorption spectra* (Krämer *et al.*, 1993, 1994); *magnetic phase transitions* (Keller *et al.*, 1995); *IR and thermodynamic data* (Suglobova and Chirkst, 1978a; Fuger *et al.*, 1983); melting point diagrams (Vdovenko *et al.*, 1974a)
Rb_2UBr_5	violet; polar organic solvents; m.p. = 600°C – congruently; ν(U–Br) stretching vibrations (cm^{-1}): 111m, 124m, and 144s,br	orthorhombic; D_{2h}^{16}, *Pnma,* No. 62; $a = 13.670(1)$, $b = 9.3900(8)$, $c =$ 8.6046(4); $Z = 4$; $V = 1663.1(2)$. CN = 6	*X-ray powder diffraction data; magnetic data; NIR, Vis an UV absorption spectra* (Krämer *et al.*, 1994); *IR and thermodynamic data*:

			(Suglobova and Chirkst, 1978a; Fuger *et al.*, 1983); melting point diagrams (Vdovenko *et al.*, 1974a)
Cs_2UBr_5	violet; m.p. = 420°C, congruently; ν (U–Br) stretching vibrations(cm^{-1}): 110m, 124m, and 149s,br	rhombic; isostructural with Cs_2DyCl_5; $a = 15.79(4)$, $b = 9.85(5)$, $c = 7.90(1)$; $Z = 4$, CN = 6, d(calc.) = 4.85(4)	*X-ray powder diffraction data* (Volkov *et al.*, (1987); *IR and thermodynamic data* (Suglobova and Chirkst, 1978a,b; Fuger *et al.*, 1983); melting point diagrams (Vdovenko *et al.*, 1974a)
Rb_3UBr_6	dark-violet; m.p. = 695°C, congruently	cubic; face centered; $a = 11.03(2)$, d(calc.) = 4.79	*X-ray powder diffraction data* (Vodovenko *et al.*, 1974a).
Cs_3UBr_6	dark-violet; m.p. = 758°C, congruently;	cubic; face centered; $a = 11.51(2)$; d(calc) = 4.83	*X-ray powder diffraction data; thermodynamic properties* (Aurov and Chirkst, 1983)
K_2NaUBr_6	–	tetragonal; D_{4h}^3, *P4/nbm*, No. 125; $a = 10.81(1)$, $c = 11.30(1)$; $Z = 4$, d(calc.) = 4.09, d(exp.) = 4.04	*X-ray powder diffraction and thermodynamic data* (Aurov *et al.*, 1983); *thermodynamic properties* (Aurov and Chirkst, 1983)
Cs_2NaUBr_6	–	P-cubic; T_h^6, *Pa*3, No. 205; $Z = 4$, $a = 11.439(2)$, d(calc.) = 4.44	*X-ray powder diffraction and thermodynamic data* (Aurov *et al.*, 1983); *thermodynamic properties* (Aurov and Chirkst, 1983)
UOBr	$\mu_{eff.} = 3.67$ B.M. (250–300K)[d]; $\theta = -140$ K	tetragonal; (PbFCl type of unit cell), D_{4h}^7, *P4/nmm*, No.129; $a = 4.063(1)$, $c = 7.447(2)$; CN = 9	*X-ray powder diffraction data; IR and magnetic susceptibility data* (Levet and Noël, 1981; *photoelectron spectra* (Thibaut *et al.*, 1982)
$K_2UBr_5 \cdot 2CH_3CN \cdot 6H_2O$	brown-red		*magnetic susceptibility data; decomposition; IR, NIR and Vis and UV absorption spectra* (Zych and Drożdżyński, 1991)
$Rb_2UBr_5 \cdot CH_3CN \cdot 6H_2O$	blue-violet		*magnetic susceptibility data; decomposition; IR, NIR and Vis absorption spectra* (Zych and Drożdżyński, 1991)

Table 5.25 (*Contd.*)

Formula	*Selected properties and physical data*[b]	*Lattice symmetry, lattice constants* (Å), *conformation and density* ($g\ cm^{-3}$)[c]	*Remarks regarding information available and references*
$(NH_4)[UBr_2 \cdot (CH_3CN)_2 \cdot (H_2O)_5]Br_2$	grayish-green to brown crystalline solid; air sensitive; soluble in organic solvents like methanol, ethanol, formic acid, dimethyl-formamide, tributhylphosphate etc. IR (cm^{-1}): $\nu(H_2O)$ with hydrogen bond character = 3325s,b; (3114s,b; 2952w); $\nu(CH_3)$ = 2921w; (2851w); combination band = 2307w; $\nu_s(C{\equiv}N)$ = 2273w; $\delta(HOH)$ = 1606m; $\delta_{as}(CH_3)$ = 1399s; (1378s); $\delta_s(CH_3)$ = 1189w, 1144w; $\delta(U{-}OH_2)$ = 1078w; $\rho(CH_3)$ = 1044w; $\nu(C{-}C)$ = 971w, 938w, 922w; $\rho(U{-}OH_2)$ = 887w, 770w,721w; $\omega(U{-}OH_2)$ = 663vs,b, 670vs,b, 400–590s,vb; $\nu(U{-}OH_2)$ = 387m, 306m; $\nu(UN_2)$ = 202m; $\nu(UBr_2)$ = 157m,b, 115sh; $\delta(UBr_2)$ = 82w; (62w, 59w,47w, 37w) Raman; $\nu_s(C{\equiv}N)$ = 2280m; $\delta(HOH)$ = 1631m;$\delta_{as}(CH_3)$ = 1415w; (1356m); $\delta_s(CH_3)$ = 1261w, 1186w; $\delta(U{-}OH_2)$ = 1123m; $\rho(CH_3)$ = 1063m; $\nu(C{-}C)$ = 952w, 826w;	orthorhombic; D_{2h}^{16}, *Pnma* No. 62; $a = 8.98(2)$, $b = 9.99(2)$, $c = 20.24(4)$; $Z = 4$; $V = 1816(7)$ Å^3; d(U–Br1) = 3.074(4) (2×), d(U–O1) = 2.538(12) (2×), d(U–O2) = 2.549(14) (2×), d(U–N1) = 2.517(30) (1×), d(U–N2) = 2.688(26) (1×), d(U–O3) = 2.652(20) (1×), d(calc.) = 2.74	*single crystal diffraction data; magnetic susceptibility data; IR, Raman, NIR, Vis and UV spectra; factor group analysis* (Zych *et al.*, 1993; Zych and Drożdżyński, 1990b)

	$\rho(U–OH_2) = 729w$; $\omega(U–OH_2) =$ 651w, 611w, 536w; $\nu(U–OH_2) =$ 536w, 455m,b, 326w; $\nu(UN_2) =$ 282w; $\nu(UBr_2) = 195sh$, 149		
UI_3	black; extremely moisture sensitive, soluble: methanol, ethanol, ethyl acetate, dimethyl-acetamide, acetic acid; m.p. = 766°C; UI_3(cr): $\Delta_f G^o_m = -466.1$ (4.9)†, $\Delta_f H^o_m = -466.9$ (4.2)†, $S^o_m = 221.8$ (8.4)†; $C^o_{p,m} = 112.1$ (6.0)†; UI_3(g): $\Delta_f G^o_m = -198.7$ (25.2)†, $\Delta_f H^o_m = -137$ (25)†, $S^o_m = 431.2$ (10.0)†; $C^o_{p,m} = 86.0$ (5.0)†. $\mu_{eff.} = 3.65$ B.M. (25–200 K)[d]; $\theta = -34$ K, $T_N = 3.4$ K; $\mu_{eff.} = 3.31$ B.M. (350–394 K)[d]; $\theta = 5$ K	orthorhombic; ($TbCl_3$ and $PuBr_3$ structure type); D^{17}_{2h}, *Cmcm*, No. 63; $a = 4.334(6)$, $b = 14.024(18)$, $c = 10.013(13)$; $Z = 4$. The coordination polyhedron is a bicapped trigonal prism the third capping Br^- anion being withdrawn by bonding with another U atom; d(U–I1) = 3.165(12) (2×) and d(U–I2) = 3.244(8) (4×) (to the prism iodine atoms), d(U–I2) (2×) = 3.456(11) (to the cap iodine atoms), d(I2–I2) = 3.679(18) Å and d(U–U) = 4.328(5) Å. d(calc.) = 6.78	*X-ray single crystal and neutron diffraction data* (Zachariasen, 1948a; Levy *et al*., 1975; Murasik *et al*., 1981); *thermodynamic data* (Brown, 1979; Guillaumont *et al*., 2003); *e diffuse reflectance spectra* (Barnard *et al*., 1973); *magnetic data* (Dawson, 1951; Jones *et al*., 1974; Murasik *et al*., 1981; 1985)
$UI_3{\cdot}4CH_3CN$	dark-brown	monoclinic; $a = 9.6168$, $b = 8.7423$, $c = 7.1858$; $\beta = 92.99$; $Z = 2$; $V = 603.31$; d(calc.) = 4.08; d(U–Il) = 3.165(12) (2×) and d(U–I2) (4×) = 3.244(8) (to prism iodines), d(U–I2) (2×) = 3.456(11) (to cap iodine atoms), d(I2–I2) = 3.679(18) and d(U–U) = 4.328(5) Å	*X-ray powder diffraction data; magnetic susceptibility data; IR, NIR, Vis and UV absorption spectra* (Drożdżyński and du Preez, 1994)
$UI_3(THF)_4$	dark-purple	monoclinic; C^5_{2h}, $P2_1/c$; No. 14; $a = 8.750(3)$, $b = 16.706(16)$, $c = 17.697(16)$; $\beta = 93.64(3)$; $Z = 4$; $V = 2582$	*synthesis and reactivity; single crystal X-ray diffraction data; thermal gravimetric analysis; vibrational spectrum;* ^1H *NMR spectrum; electronic absorption spectrum* (Avens *et al*., 1994)

Table 5.25 (*Contd.*)

Formula	*Selected properties and physical data*[b]	*Lattice symmetry, lattice constants* (Å)*, conformation and density* (g cm^{-3})[c]	*Remarks regarding information available and references*
K_2UI_5	deep-blue	orthorhombic; D_{2h}^{16}, *Pnma*, No. 62; monocapped trigonal prisms [UCl_7] are connected via two opposite common edges to chains; CN = 6; $a = 14.293(1)$, $b = 9.8430(5)$, $c = 9.1067(5)$; $Z = 4$; $V = 1929.1(2)$; d(U–I) = 3.182 to 3.275; d(U–U) = 5.143 (interchain); d(U–U) = 7.778 (intrachain)	*X-ray powder diffraction data, magnetic data, NIR, Vis an UV absorption spectra, magnetic phase transitions* (Krämer *et al.*, 1994; Keller *et al.*, 1995); *low temperature absorption spectrum of* U^{3}*:*K_2LaI_5 (Andres *et al.*, 1996); *crystal-field analysis* (Karbowiak *et al.*, 1998a); *IR and thermodynamic data* (Suglobova and Chirkst, 1978)
Rb_2UI_5	blue-violet	orthorhombic; D_{2h}^{16}, *Pnma*, No.62; $a = 14.546(2)$, $b = 9.249(1)$, $c = 10.026(2)$; $Z = 4$; $V = 2031.1(5)$Å, CN = 6	*X-ray powder diffraction data; magnetic data; NIR, Vis and UV absorption spectra* (Krämer *et al.*, 1994); *IR and thermodynamic data* (Suglobova and Chirkst, 1978)
UOI	deep blue; $\mu_{eff.} = 3.56$ B.M. (220–300K)[d]; $\theta = -150$ K	tetragonal; (PbFCl type of unit cell), D_{4h}^{7}, *P4/nmm*; No. = 129; $a = 4.062(1)$, $c = 9.208(2)$; CN = 9	*X-ray powder diffraction data;IR and magnetic susceptibility data* (Levet and Noel, 1981)
$UBrCl_2$	black with a greenish tinge; m.p. = 800°C; $UBrCl_2$(cr): $\Delta_f G_m^o = -760.3(9.8)^{\dagger}$, $\Delta_f H_m^o = -812.1(8.4)^{\dagger}$, $S_m^o = 175.7(16.7)$		*thermodynamic data* (MacWood, 1958; Brown, 1979; Grenthe *et al.*, 1992; Guillaumont *et al.*, 2003)

UBr_2Cl	black with a greenish tinge; m.p. = 775°C; UBr_2Cl(cr) $\Delta_f G^o_m = -714.4$ (9.8)†, $\Delta_f H^o_m = -750.6$ (8.4)†, $S^o_m =$ 192.5 (16.7)†	*thermodynamic data* (MacWood, 1958; Brown,1979; Grenthe *et al.*, 1992; Guillaumont *et al.*, 2003)
other mixed halides: (i) UCl_2I; (ii) $UClI_2$; (iii) UBr_2I; (iv) $UBrI_2$.	extremely moisture sensitive; (i) black, m.p. ~750; (ii) black, m.p. ~725; (iii) black, m.p. ~700; (iv) black, m.p. ~690	

* Estimated values.

† Values recommended by the Nuclear Energy Agency (Guillaumont *et al.*, 2003).

[a] Values have been selected in part from review articles (Brown, 1979; Bacher and Jacob, 1980; Freestone and Holloway, 1991; Grenthe *et al.*,1992; Guillaumont *et al.*, 2003).

[b] m.p. = melting point (°C); b.p.. = boiling point (°C); (cr) = crystalline; (g) = gaseous; thermodynamic values in kJ mol^{-1}, or J K^{-1} mol^{-1} at 298.15 K, unless otherwise mentioned; $\Delta_f G^o_m$, standard molar Gibbs energy of formation; $\Delta_f H^o_m$, standard molar enthalpy of formation; S^o_m, standard molar entropy; $C^o_{p,m}$(J K^{-1} mol^{-1}), standard molar heat capacity; log p (mmHg) = $-AT^{-1} + B - C \log T$: vapor pressure equation for indicated temperature range; IR = infrared active; lat. = lattice vibrations; val. = valence vibrations; def. = deformation vibrations; all values in cm^{-1}; vs: very strong; s: strong; m: medium; ms: medium strong; w: weak; sh: shoulder; b: broad; C, Θ, paramagnetic constants from the Curie Weiss law $C = \chi_M(T-\Theta)$; $\mu_{eff} = 2.84\sqrt{C}$ - effective magnetic moment; T_N, ordering temperature; atomic and crystal-field parameters; F^k and ζ_{5f} = electrostatic and spin–orbit interaction; α, β, γ; = two-body correction terms; $T^i t_i$ (i = 2,3,4,6,7,8) = three-particle configuration interaction; M^j (j = 0, 2 and 4) = spin–spin and spin–other–orbit relativistic corrections; P^k (k = 2, 4 and 6) = electrostatically correlated spin-orbit perturbation; B^k_q, crystal-field parameters; values in brackets indicate parameter errors; parameters in square brackets were kept constant during the final fitting procedure; standard deviation: $rms = \sum \left[(\Delta_i)^2/(n-p)\right]^{1/2}$ [cm^{-1}], where Δ_i is the difference between the observed and calculated energies, n is the number of levels fitted and p is the number of parameters freely varied.

[c] All values are in Å and angles are in degrees; d, density [g cm^{-3}]; CN, coordination number, V = molar volume [cm^3 mol^{-1}].

[d] Temperature range with linear relationship of χ_M^{-1} against T.

spectra of co-doped (U^{4+},U^{3+}):Ba_2YCl_7 single crystals has been also reported (Karbowiak *et al.*, 2003c) Efficient luminescence was observed at 7 K from both the $^4G_{7/2}$ and $^4F_{9/2}$ levels of the U^{3+} ions and from the $^1D_2$ and $^1I_6$ levels of U^{4+}. For the U^{4+}ions a very strong anti-Stokes emission was noticed due to energy transfer processes. Contrary to U^{4+} for which emission was observed even at room temperature the emission of U^{3+} ions is strongly quenched by temperature. Owing to the presence of U^{3+} and U^{4+} ions in the host crystal, an energy transfer between these ions has been proved. Analyses of the nephelauxetic effect and crystal field splittings of the K_2UX_5 (X = Cl, Br or I) series of compounds have also been reported (Karbowiak *et al.*, 1998a).

The absorption spectra of $NH_4UCl_4 \cdot 4H_2O$ and $CsUCl_4 \cdot 3H_2O$ recorded at 298 and 4.2 K, presented in Fig. 5.38 (Karbowiak *et al.*, 2000) are typical for most uranium(III) compounds. In the 4000–15800 cm^{-1} region the spectra consist of relatively intense, sharp, and well-separated absorption lines.

A comparison of the spectra shows significant differences in the visible range connected with the appearance of strong and broad f–d bands, allowed by the Laporte rule. For $CsUCl_4 \cdot 3H_2O$ the first f–d bands are located at about 23000 cm^{-1}, while in $NH_4UCl_4 \cdot 4H_2O$ they are shifted about 5000 cm^{-1} toward the infrared region. For the isostructural series of complex halides of the composition U^{3+}:K_2LaX_5 (X = Cl, Br, I), the substitution of the Cl^- by I^- results in a significantly smaller shift of about 1000 cm^{-1} (Karbowiak *et al.*, 1998a). Drożdżyński (1985, 1991) and Karbowiak *et al.* (1996c) report a close relationship between the increase of covalence/decrease of the uranium–halogenide distances, and the red shift of the first intense f–d bands. The crystal-field symmetry is another factor, which can influence the position of the f–d bands. However, this seems to be a minor factor, since there is no simple dependence of the energy of the first f–d transition on the site symmetry of the U^{3+} ion. For example in K_2UCl_5 (C_s) and Cs_2NaUCl_6 (O_h) (Karbowiak *et al.*, 1998a,b) the first f–d transitions occur at similar energies of 14300 and 15000 cm^{-1}, respectively, while for UCl_3 (D_{3h}) they appear at 23000 cm^{-1} (Karbowiak *et al.*, 2002a). An extensive analysis of the $5f^3 \rightarrow 5f^26d^1$ transitions in low temperature absorption spectra of U^{3+} ions incorporated in various single crystals were reported by Seijo and Barandiran (2001), Karbowiak and Drożdżyński (2004) and Karbowiak (2005a,b). Temperature-induced line broadening and line shift measurements have been chosen as method for the determination of the electron–phonon coupling parameters for U^{3+} doped in K_2LaCl_5 (Ellens *et al.*, 1998), $LaCl_3$ and $LaBr_3$ single crystals (Karbowiak *et al.*, 2003d). The value of the electron–phonon coupling parameter, $\bar{\alpha}$, was found to be considerably lower in $LaCl_3$ than in K_2LaCl_5 but larger than that of Nd^{3+} in $LaCl_3$. The electron–phonon coupling is also stronger for U^{3+} in the tribromide as compared with the trichloride host; this has been attributed to a larger covalency of the first compound.

Intensity calculations of $5f^3 \rightarrow 5f^3$ transitions in tervalent uranium, based on the Judd–Ofelt theory were performed both for solution (Drożdżyński, 1978, 1984) and solid-state spectra (Drożdżyński and Conway, 1972, Karbowiak and

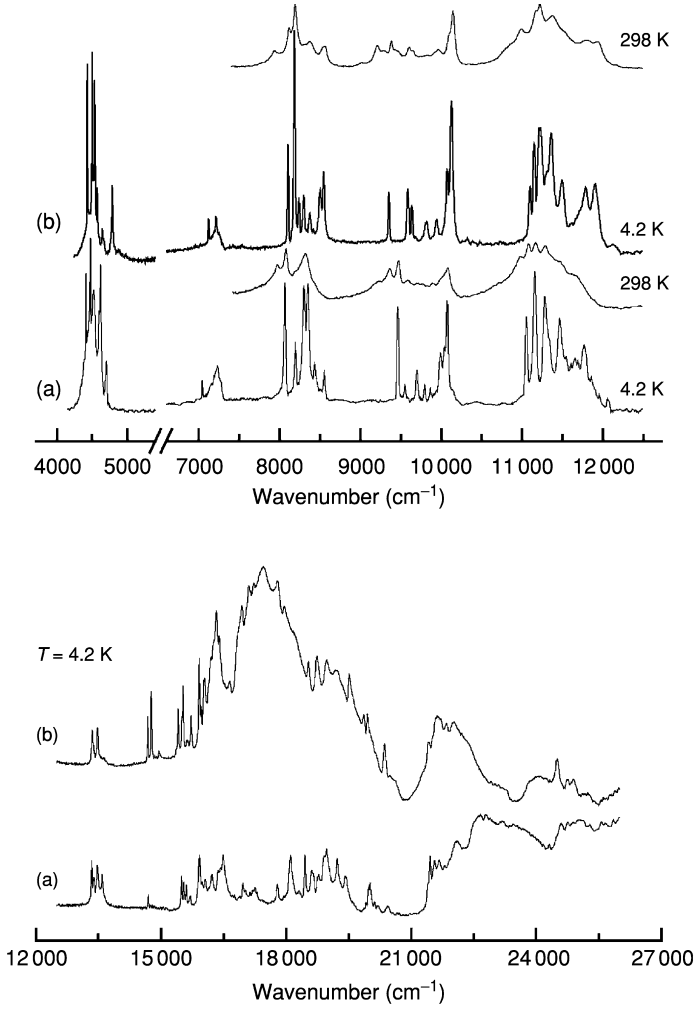

Fig. 5.38 *Absorption spectra of thin films of* $CsUCl_4 \cdot 3H_2O$ (*a*) *and* $NH_4UCl_4 \cdot 4H_2O$ *recorded at* 4.2 *and* 298 K (*from Karbowiak* et al., 2000 *reproduced by the permission of Elsevier*).

Drożdżyński, 2003). The analyses have shown a rather poor agreement between the observed and calculated oscillator strengths. So far, a relatively small r.m.s. deviation, of the order 10^{-6} to 10^{-7}, has been obtained only for the absorption spectra of UCl_3 in hexamethylphosphortriamide (Drożdżyński and Kamenskaya, 1978) and of UCl_3-doped $ZnCl_2$-based glass (Dereń *et al.*, 1998).

For almost all the halides and complex halides, magnetic susceptibility measurements were carried out over wide temperature ranges. The paramagnetic

constants from the Curie–Weiss law $\chi'_{m.} = C/(T - \theta)$ and the effective magnetic moments $\mu_{eff} = 2.84\mu_B$ were determined for a large number of compounds (see Table 5.25). The trihalides show remarkable cooperative effects, which were studied both experimentally (Murasik *et al*., 1980, 1985, 1986) and theoretically (Łyżwa and Erdös, 1987; Plumer and Caillé, 1989). UCl_3 and UBr_3 undergo an unusual magnetic phase transition for actinide compounds. A one-dimensional, short-range magnetic order along the *z*-axis of the hexagonal lattice develops at about 15 K for UBr_3 and 22 K for UCl_3, which results from strong antiferromagnetic interactions between the nearest neighbors. A three-dimensional ordering appears in UBr_3 and UCl_3 when the uranium magnetic moments order to a '0+–' configuration in each plane perpendicular to the *z*-axis at $T_N = 6.5$ and 5.3 K, respectively. At temperatures below $T_t = 2.7$ K for UBr_3 and $T_t = 2.5$ K for UCl_3 the magnetic moments exhibit smaller values and become oriented parallel to the equivalent *x*- or *y*-axis. The observed reorientation of the moments is reported to be rare in the actinide ions due to a usually strong anisotropy, which determines the direction of the moment (Santini *et al*., 1999).

An extensive physical analysis of the magnetic interactions and magnetic ordering phenomena, as well as the crystal-field splitting in the K_2UX_5 (X = Cl, Br or I) series of compounds, were performed on the basis of the Ising model (Keller *et al*., 1995). The application of elastic and inelastic neutron scattering experiments along with specific heat measurements made it possible to obtain a consistent picture of the magnetic phases. An analysis of the IR and Raman spectra of this series of compounds and of RbU_2Cl_7 is also available (Karbowiak *et al*., 1996a; Hanuza *et al*., 1999). Drożdżynski (1991) has summarized paramagnetic resonance measurements for U^{3+} ions substituted in CaF_2, SrF_2, and $LaCl_3$ single crystals. Some physical properties of tervalent uranium halides and related compounds are collected in Table 5.25.

(*i*) *Uranium trifluoride and uranium(III) fluoro complexes*

Uranium trifluoride

Uranium trifluoride is most conveniently prepared by reduction of UF_4 with metallic aluminum or finely powdered uranium. In the former case the reagents are placed in a graphite crucible and heated up to 900°C where the reaction proceeds smoothly and the excess of aluminum and by-products sublime from the reaction zone (Runnals, 1953). In the latter one, stoichiometric quantities of cleaned uranium turnings and UF_4 are placed in a nickel tube and heated to about 250°C in a stream of pure hydrogen (Warf, 1958). The finely divided UH_3 was decomposed at 400°C, after which the tube should be shaken in order to obtain an intimate mixture that was then heated to 700–900°C to give the pure trifluoride (Friedman *et al*., 1970). The reduction with other metals such as Be, Mg, Ti, or Zr, as well as UN or U_2N_3, at 900–950°C has also been found suitable for the synthesis. The use of the nitrates has some technical advantages since they prevent the formation of corrosive by-products. Reduction with Li,

Na, Cs, Mg, Ca, Sr, and Ba yields metallic uranium. The preparation of ultrapure UF_3 by reduction of UF_4 with hydrogen at 1020 to 1050 ($\pm$ 20)°C has been reported by Berndt and Erdman (1973).

Uranium trifluoride is a gray to black solid. Separate crystals show a deep-violet color under the microscope. As compared to other uranium(III) compounds the trifluoride is remarkably stable on air at room temperature. At higher temperatures UF_3 oxidizes and at 900°C it is quantitatively converted into U_3O_8. The compound is thermally unstable even in an inert atmosphere and disproportionates to UF_4 and U at about 1000°C and to a smaller extent (0.1% per hour) also at 800°C. UF_3 is insoluble in water and cold aqueous acids but slowly undergoes oxidation. This proceeds with the formation of uranium(IV) and uranyl compounds at 100°C. UF_3 dissolves rapidly in nitric acid–boric acid mixtures. Chlorine, bromine, and iodine react to give UF_3X (X = Cl, Br or I).

UF_3 has the LaF_3-type structure but the symmetry is reported to be either trigonal (space group $P\bar{3}c1$, D^4_{3d}, No. 185) or hexagonal (space group $P6_3cm$, C^3_{6v}, No. 165). Two coordination numbers 9 and 11 are also taken into consideration (Taylor, 1976a). Both structures may be considered as distorted ideal polyhedra with a bimolecular hexagonal cell (space group $P6_3/mmc$) (Schlyter, 1953). The polyhedra are fully capped trigonal prisms in which fluorine atoms (CN = 11) are located on all corners and outside the two triangular and the three square boundary planes. The main difference between the different structures is a slight displacement of the atoms forming the prism and the atoms outside the triangular surfaces normal to *c*-axis (Taylor, 1976a). Other crystallographic data are listed in Table 5.25.

A good quality absorption spectrum of UF_3 was obtained by means of the teflon disk technique (Schmieder *et al.*, 1970) and in chlorinated naphthalene at 4.2 K (Drożdżyński and Karbowiak, 2005). For the latter data a crystal-field analysis has also been performed. There is a large shift of the L′S′J′ multiplets towards higher wave numbers, as compared with other U^{III} low-temperature spectra. Some absorption spectra were also recorded in fused-salt systems: LiF–Be_2, LiF–BeF_2–ZrF_4, and LiF–NaF–KF (Martinot, 1984).

The magnetic susceptibility of UF_3 has been measured between 2 and 300 K (Berger and Sienko, 1967) and between 293 and 723 K (Nguyen-Nghi *et al.*, 1964). For both temperature ranges a linear relationship of $1/\chi'_M$ vs T was reported. The effective magnetic moment of 3.67 BM is close to the free ion value.

Uranium trifluoride monohydrate and uranium(III) fluoro complexes

$UF_3 \cdot H_2O$ was prepared from an uranium(III) solution in 1 M HCl or in anhydrous methanol by precipitation with ammonium fluoride (Barnard *et al.*, 1973). The green gelatinous precipitate appears in the latter case to be brown after drying due to some U(IV) impurities. The hydrate is reported to be far more reactive than the anhydrous fluoride and is immediately oxidized in air, giving a pale green uranium(IV) substance. The compound was characterized by magnetic susceptibility measurements, but the results may not be reliable.

The formation of a number alkali fluorouranates(III) and complexes of UF_3 with ZrF_4 has been known for a long time (Bacher and Jacob, 1980). KUF_4, K_2UF_5, K_3UF_6, Rb_3UF_6, and Cs_3UF_6 were prepared by heating UF_4 and metallic uranium with the appropriate alkali fluoride at 1000°C (Thoma *et al.*, 1966). $NaUF_4$ and Na_2UF_5 were identified during investigations of the binary fused-salt system $NaF–UF_3$. Some of the complex fluorides were characterized by X-ray powder diffraction (Table 5.25) but more detailed information is still not available.

$UZrF_7$ was prepared by reduction of a mixture of UF_4 and ZrF_4, either with metallic zirconium or with metallic uranium at about 800°C; UZr_2F_{11} was identified in a systematic study of the $UZrF_7–ZrF_4$ binary system (Fonteneau and Lucas, 1974). The fluorides are not stable and slowly oxidize even at room temperature. The compounds were characterized by magnetic susceptibility measurements in the 100–300 K range and by X-ray powder diffraction analyses (Table 5.25).

(*ii*) *Uranium trichloride and uranium(III) complex chlorides*

Uranium trichloride

Uranium trichloride may be prepared by a number of methods (Brown, 1979; Drożdżyński, 1991). One of the most convenient is the action of gaseous hydrogen chloride on uranium hydride. Attractive alternative methods involve the reduction of uranium tetrachloride with zinc, metallic uranium, or uranium hydride.

$$UH_3 + 3HCl \overset{350^\circ C}{\rightarrow} UCl_3 + 3H_2$$

$$3UCl_4 + Al \overset{400^\circ C}{\rightarrow} 3UCl_3 + AlCl_3$$

Small amounts of pure UCl_3 may also be prepared by thermal vacuum decomposition of $NH_4UCl_4 \cdot 4H_2O$ (Drożdżyński, 1988a, 1991). The compound obtained by the latter method is reactive and tractable for synthetic purposes, in contrast to that obtained by reduction with metals.

Uranium trichloride is obtained either in the form of a fine olive-green powder or as dark-red crystals. It is not soluble in anhydrous organic solvents but it dissolves somewhat in glacial acetic acid, showing a characteristic transient red color. UCl_3 dissolves in polar organic solvents, provided the compound or the solvents have absorbed some gaseous hydrogen chloride before. In aqueous solutions it is more or less rapidly oxidized. UCl_3 reacts with chlorine to form a mixture of higher valence chlorides, and with bromine and iodine to yield $UBrCl_3$ and UCl_3I, respectively. The reaction with ammonia, acetonitrile, tetrahydrofuran (THF), and phenazine yields a number of unstable adducts.

UCl_3 is hygroscopic, but in contrast to other uranium halides no absorption of water is reported at p_{H_2O} less than 320 Pa (2.4 mmHg). It is a strong reducing agent both in solution and in solid state. Several metals such as calcium or

lithium reduce UCl_3 to metallic uranium but the reaction has not been widely applied. UCl_3 melts at 837°C and disproportionates to U and UCl_4 at 840°C. A number of fused-salt systems containing UCl_3 have been investigated and the formation of some chloro complexes has also been reported (Bacher and Jacob, 1980).

Uranium trichloride has hexagonal symmetry (Zachariasen, 1948a,c; Murasik *et al.*, 1985; Schleid *et al.*, 1987) with the space group $P6_3/m - C_{6h}^2$. The coordination polyhedron is a symmetric tricapped trigonal prism arranged in columns in the *c*-direction. Each column is surrounded trigonally by three others at 1/2*c* in such a manner that the prism atoms of one chain become the cap atoms of the neighboring one. The packing view of UCl_3 along the [001] direction is shown on Fig. 5.39. The trichlorides Ac–Am and La–Nd have the same type of structure; some of the crystal data are listed in Table 5.25.

High-resolution polarized absorption spectra of $LaCl_3:U^{3+}$ single crystals (Karbowiak *et al.*, 2002) and unpolarized spectra of a polycrystalline UCl_3 sample in chlorinated naphathalene have been recorded at 4.2 K in the 4000–30000 cm^{-1} range (Sobczyk *et al.*, 2003). The experimental energy levels of the U^{3+} ion in the compounds were fitted to a semi-empirical Hamiltonian employing free-ion operators, one-electron crystal-field operators, and two-particle correlation crystal-field (CCF) operators, resulting in the determination of crystal-field parameters and the assignment/reassignment of the recorded $5f^3 \rightarrow 5f^3$ transitions. The effects of selected CCF operators on the splitting of

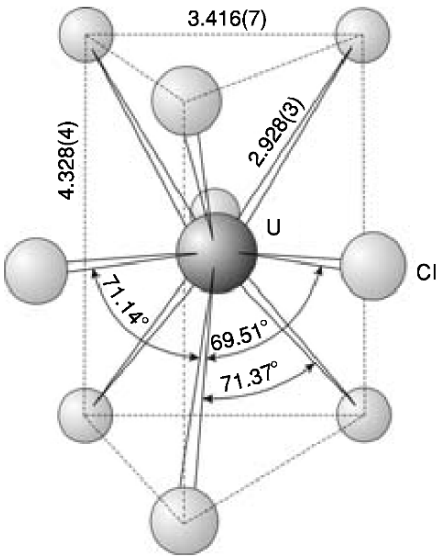

Fig. 5.39 *The tricapped trigonal prism configuration of halogen atoms in UCl_3 and UBr_3 (distances in* Å *are for UCl_3; after Murasik* et al., 1985).

some specific U^{3+} multiplets have also been investigated. The so far most accurate analysis of the band intensity, based on the Judd–Ofelt theory (Karbowiak and Drożdżyński, 2003), has been based on the obtained electronic wave functions and a room temperature absorption spectrum of UCl_3. A good agreement between the observed and calculated oscillator strengths has been obtained by combining the recorded band areas of some multiplets. In order to check the correctness of the calculations, the obtained intensity parameters, Ω_λ, have been used for the determination of transition probabilities and these in turn for the calculations of radiative lifetimes. A good-quality UCl_3 absorption spectrum has been obtained also by means of teflon disk technique (Schmieder *et al.*, 1970).

The magnetic properties of uranium trichloride have been the subject of extensive investigations (Santini *et al.*, 1999; Drożdżyński, 1991). The inverse magnetic susceptibility as a function of the temperature follows the Curie-Weiss law in two different temperature ranges and exhibits an antiferromagnetic transition at 22 K. Neutron diffraction studies revealed the existence of three-dimensional long-range anti-ferromagnetic ordering below the Néel temperature $T_N = 6.5$K (Murasik *et al.*, 1981, 1985).

Uranium trichloride hydrates and hydrated uranium(III) chloro complexes

Two hydrates of UCl_3 are known, the heptahydrate, $UCl_3 \cdot 7H_2O$ and the hexahydrate, $UCl_3 \cdot 6H_2O$. The heptahydrate was obtained by reduction of an UCl_4 solution consisting of acetonitrile, propionic acid, and water (Drożdżyński, 1985) with liquid zinc amalgam in an inert atmosphere whereas the reduction is most conveniently accomplished in an all glass apparatus with provisions for precipitation, filtration, and drying in an inert gas atmosphere (Drożdżyński, 1979). It is interesting to note that a few years earlier Habenschuss and Spedding (1980) predicted the possible formation of this compound on the basis of ionic size considerations. $UCl_3 \cdot 7H_2O$ is a crystalline ink-blue solid, readily soluble in numerous organic solvents. The compound is relatively resistant to oxidation by air at temperatures lower than 15°C. At higher temperatures it loses some of its crystallization water and in high vacuum it may be completely dehydrated at 200°C (Drożdżyński, 1985).

X-ray single crystal analyses of the heptahydrate and of the less hydrated $UCl_3 \cdot 6H_2O$ compound have been reported (Mech *et al.*, 2005) (see Table 5.25). In the heptahydrate the crystals are built from separate $[U_2Cl_2(H_2O)_{14}]^{4+}$ units and Cl^- ions. The characteristic features of this structure are dimers, formed by two uranium ions connected through the (Cl1) bridging chlorine atoms. Whereas the basic units of the crystal structure of $UCl_3 \cdot 6H_2O$ are Cl^- anions and $[UCl_2(H_2O)_6]^+$ cations. The basic units of the crystal structure of $UCl_3 \cdot 6H_2O$ are Cl^- anions and $[UCl_2(H_2O)_6]^+$ cations. The U atom is eight-coordinated through six water molecules and two chlorine atoms. In this structure the characteristic feature is the existence of hydrogen bonds, which link the uranium eight-coordinated polyhedra, forming a three-dimensional network.

The presence of water molecules in the inner coordination sphere was also confirmed by the solid-state absorption spectrum of $UCl_3 \cdot 7H_2O$, which is very similar with that of the U^{3+} aquo ion (Drożdżyński, 1978) and exhibits significant differences in comparison to those of the less hydrated uranium(III) complex chlorides (Zych and Drożdżyński, 1986; Drożdżyński, 1988b). A detailed crystal-field level analysis, based on a very good quality low-temperature spectrum, is also available (Karbowiak *et al.*, 2001). The heptahydrate exhibits Curie–Weiss dependence in the temperature range 10 to 300 K. The derived magnetic moment $\mu_{\text{eff.}} = 2.95$ B.M. is much lower than the 'free ion' value of ca. 3.7 B.M., presumably due to the crystal field of the water molecules.

The synthesis and characterization of a number of hydrated complex chlorides of the formulas $MUCl_4 \cdot 5H_2O$ (Barnard *et al.*, 1972b), $MUCl_4 \cdot 4H_2O$ (M = K, Rb or NH_4) (Drożdżyński, 1988b; Karbowiak and Drożdżyński, 1993), $MUCl_4 \cdot 3H_2O$ (M = Cs, K, Rb, or NH_4) (Karbowiak and Drożdżyński, 1993, 1999), and $UCl_3 \cdot CH_3CN \cdot 5H_2O$ (Zych and Drożdżyński, 1986) have been reported.

The pentahydrates were prepared by shaking a U(III) solution in 11 M HCl with the appropriate halide MCl (M = K, Rb, or NH_4) at 0°C. The U^{III} solution was prepared either by dissolving $U_2(SO_4)_3 \cdot 8H_2O$ or by dissolving a uranium (III) double sulphate in 11 M HCl (Barnard *et al.*, 1972a). The preparation of the tetrahydrates can be achieved using a general route reported by Drożdżyński (1979). In this method the reduction of a solution of UCl_4, methyl cyanide, propionic acid, and water with zinc amalgam in anaerobic conditions generates an immediate precipitation of the tetrachlorouranate(III) tetrahydrate (Drożdżyński, 1988b). The formation of the pentahydrates has not been confirmed by X-ray investigations. Apart from some expected similarities between the compounds of the series, one can also note differences, e.g. that the tetrahydrates are reported to be readily soluble in dry methanol or ethanol, in contrast to the pentahydrates. The tetrahydrates are also much more resistant to oxidation and hydrolysis in dry air and temperatures below 15°C, and can be easily transformed into the anhydrous salts by thermal dehydration at high vacuum. One may note also a red shift of the $5f^3 \rightarrow 5f^3$ transitions and relatively large differences in the plots of the reciprocal susceptibilities as well as in the derived effective magnetic moments.

Structure investigations revealed that $(NH_4)UCl_4 \cdot 4H_2O$ belongs to the orthorhombic system, space group $P2_12_12$. The crystal is built up from separate $[U(H_2O)_4Cl_4]^-$ and NH_4^+ ions. The eight-coordinated U^{3+} polyhedra are connected by O–H $\cdots$ Cl hydrogen bonds forming a three-dimensional network (Karbowiak *et al.*, 1996c). X-ray powder diffraction patterns show that the other members of the series could also be indexed on the basis of the orthorhombic cell (Karbowiak *et al.*, 1996c). $(NH_4)UCl_4 \cdot 4H_2O$ is an excellent starting material for the preparation of numerous other uranium(III) compounds.

The $MUCl_4 \cdot 3H_2O$ series of compounds was also obtained by reduction of appropriate acetonitrile solutions of UCl_4 and MCl (where M = K, Rb, Cs, or NH_4) with liquid zinc amalgam, but using somewhat different conditions than those used to prepare the tetrahydrates (Karbowiak and Drożdżyński, 1993). In contrast to the deep purple-red colors of the penta- and tetrahydrates the latter ones show green to brown colors. In this series the first broad and strong $5f^3 \rightarrow 5f^26d^1$ bands were observed in the absorption spectra at wavenumbers higher than 21000 cm^{-1}.

Single-crystal X-ray analysis is available for $CsUCl_4 \cdot 4H_2O$ (Krämer *et al.*, 1991). The compound crystallizes in the monoclinic system, space group: $P2_1/m$ (Table 5.25). Uranium has a coordination number of nine (tricapped trigonal prism) consisting of six chlorine atoms and three oxygen atoms (representing water) with mean distances of 2.957 and 2.552 Å, respectively. Cesium is surrounded by eight chlorine atoms in the shape of a distorted cube, which is capped by two non-bonded water ligands at a mean distance of 3.602 Å. One can view the structure as a linking of the polyhedra $[U(Cl1)_4(Cl2)_2(H_2O)_3]$ through two common edges of chloride (Cl1) ligands at two triangular faces of the trigonal prism of chloride ions to an infinite zigzag chain in the [010] direction. X-ray powder diffraction analyses show that the remaining three members of the series could be indexed on the basis of the same monoclinic cell, and that they presumably are isostructural.

For the tri- and tetrahydrates the first broad and strong $5f^3 \rightarrow 5f^26d^1$ bands are observed in the absorption spectra at about 21500 and 16000 cm^{-1}, respectively. The red shift of these bands has been attributed to the formation of inner sphere complexes with some of the uranium–ligand bond lengths of a markedly more covalent character than that of the U^{3+} aqua-ion, e.g. in $UCl_3 \cdot 7H_2O$ (Drożdżyński, 1991; Karbowiak *et al.*, 1996c). The magnetic susceptibility constants from the Curie–Weiss law are listed in Table 5.25.

Anhydrous uranium(III) chloro complexes

The largest group of well-characterized uranium(III) compounds is formed by chloro complexes such as $CsUCl_4$ (Karbowiak and Drożdżyński, 1998c), M_2UCl_5 (M = K, Rb, Cs. or NH_4) (Drożdżyński and Miernik, 1978; Meyer *et al.*, 1983), $SrUCl_5$ (Karbowiak and Drożdżyński, 1998b), $[(CH_3)_3N]_3UCl_6$ (Karbowiak *et al.*, 1996a); MU_2Cl_7 (M = K, Rb, Ph_4As or Ph_4P) (Drożdżyński, 1991; Karbowiak *et al.*, 1996b); Ba_2UCl_7 (Karbowiak *et al.* 1998d); M_2NaUCl_6 (M = K, Rb or Cs) (Aurov *et al.*, 1983; Volkov *et al.*, 1987), and Cs_2LiUCl_6 (Karbowiak and Drożdżyński, 1998a).

Most of the complex chlorides can be conveniently prepared by heating stoichiometric amounts of the component halides in graphite-coated quartz tubes. The $(NH_4)_2UCl_5$, $Ph_4AsU_2Cl_7$, and $Ph_4PU_2Cl_7$ compounds were obtained by reduction of appropriate uranium tetrachloride solutions in

acetonitrile with liquid zinc amalgam (Drożdżyński, 1991; Drożdżyński and Miernik, 1978). Also the complexes with the general formulas M_2UCl_5 and MU_2Cl_7 can be prepared in this way (Drożdżyński, 1979). All the syntheses were carried out in an inert atmosphere or high vacuum of ca. 10^{-4} Pa. Spectroscopic studies and crystal-field analysis of U^{3+}:RbY_2Cl_7 and U^{3+}:Li_2NaYCl_6 single crystals were reported by Karbowiak *et al.* (1996b, 1977) and Karbowiak *et al.* (1996e, 1998b), respectively.

The formation of number of uranium(III) chloro complexes has also been observed during investigations of binary and ternary phase systems (Brown, 1979). The complexes display a variety of colors (Table 5.25). All of them are hygroscopic but are somewhat resistant to oxidation in dry air. Unlike UCl_3 the complex chlorides are readily soluble in numerous polar organic solvents.

K_2UCl_5 and Rb_2UCl_5 crystallize in the orthorhombic system and are isotypical with the K_2PrCl_5/Y_2HfS_5 structures, their space group is *Pnma*, $Z = 4$ (Krämer *et al.*, 1994). The coordination polyhedron is a monocapped trigonal prism [UCl_7], connected via two opposite common edges to chains, $[UCl1_{1/1}Cl2_{1/1}Cl3_{1/1}Cl4_{4/2}]^{-2}$, that run in the [010] direction of the unit cell. The relatively short U^{3+}–U^{3+} distance through the common edge, equal to 4.556 Å, is assumed to be responsible for antiferromagnetic transitions at 8.6 to 13.2 K. The temperature dependence of the inverse molar susceptibilities in the 20–300 K range follows the Curie–Weiss law in two temperature ranges, separated by a slight but apparent break at 130, 150, and 220 K, respectively, for K_2UCI_5, Rb_2UCl_5, and $(NH_4)_2UCl_5$. The effective magnetic moments range from 3.47 B.M. for $(NH_4)_2UCl_5$ to 3.99 B.M. for K_2UCI_5 (Drożdżyński and Miernik, 1978). Some other magnetic susceptibility constants determined from the Curie–Weiss law are listed in Table 5.25.

Solid-state electronic spectra of thin mulls of the compounds show all characteristic features of the uranium(III) complex anions with strong $5f^3 \rightarrow 5f^26d^1$ bands starting at ca. 18000 cm^{-1}. The complexes exhibit very similar far-IR spectra with one broad and not well-resolved band in the region 100–240 cm^{-1} assigned to U-Cl stretching modes. An analysis of magnetic phase transitions and crystal-field splittings in the K_2UX_5 (X = Cl, Br, or I) series of complex halides is reported by Keller *et al.*(1995).

Single-crystal X-ray data show that Cs_2NaUCl_6 (Spirlet *et al.*, 1988) crystallizes with the ideal cryolite arrangement. Each of the uranium or sodium ions is octahedrally surrounded by six chloride ions at the distance of 2.723(9) and 2.746(9) Å, respectively. The cesium ions (site symmetry T_d) are surrounded by 12 equidistant chloride ions with d(Cs–Cl) = 3.867(8) Å (for other data see Table 5.25). The enthalpies of formation of the hexachloro complexes are also available (Aurov and Chirkst, 1983; Schoebrechts *et al.*, 1989).

It is interesting to note the preparation of a reduced metallic uranium chloride which has been formulated as NaU_2Cl_6 or $(Na^+)(U^{3+})_2(e^-)(Cl^-)_6$ (Schleid and

Meyer, 1989). The extra electrons provided by the incorporation of the sodium atom are reported to occupy the 6d band of uranium. The compound is isostructural with $NaPr_2Cl_6$ and may be described as a stuffed derivative of UCl_3 (hexagonal symmetry, space group $P6_3/m$). Other available information about the compounds is compiled in Table 5.25.

Complexes of UCl_3 with neutral donor ligands

Ammonia adducts of the composition $UCl_3 \cdot 7NH_3$ and $UBr_3 \cdot 6NH_3$ were obtained by treatment of the halides with gaseous ammonia at room temperature and a pressure of 1013 hPa (Eastman and Fontana, 1958; Berthold and Knecht, 1965b, 1968). Since heating in a stream of nitrogen up to 45°C formed a relatively stable $UCl_3 \cdot 3NH_3$ complex, indicating that the compounds contain some loosely bound ammonia. At higher temperatures this adduct decomposes into $UCl_3 \cdot NH_3$, which is stable up to 300°C.

According to MacCordick and Brun (1970) the heating of UCl_3 with an excess of acetonitrile in sealed tube at 80°C results in the separation of a brown, hygroscopic solid of the formula $UCl_3 \cdot CH_3CN$. However, an attempt to repeat the preparation was unsuccessful (Barnard *et al.*, 1973).

A purple adduct of the composition $UCl_3(THF)_x$ has been prepared by reduction of a UCl_4 solution in THF with stoichiometric amounts of NaH or an excess of Na_2C_2. The obtained purple solution of $UCl_3(THF)_x$ is reported to be a useful starting material for numerous syntheses (Moody and Odom, 1979; Andersen, 1979; Moody *et al.*, 1982).

Hart and Tajik (1983) have reported the preparation of numerous air sensitive uranium(III) complexes with cyclic polyethers and aromatic diamines by reduction with liquid zinc amalgam in acetonitrile or acetonitrile/propionic acid solutions of UCl_4 and the appropriate ligand, e.g. $(UCl_3)_3$(benzo-15-crown-5)$_2 \cdot 1.5CH_3CN$ (yellow-orange), $(UCl_3)_3$(benzo-15-crown-5)$_2$ (deep red), UCl_3 (cyclohexyl-15-crown-5) (red-purple), $(UCl_3)_3$(18-crown-6)$_2$ (red-brown), $(UCl_3)_5$(dibenzo-18-crown-6)$_3$ (deep-red), $(UCl_3)_5$(*cis-syn-cis*-dicyclohexyl-18-crown-6)$_3$ (red), UCl_3(1,10 phenantroline)$_2$ (violet-purple) and UCl_3(2,2′-bipyridile)$_2$. The complexes are insoluble or react with common organic solvents. The preparation of several trivalent uranium complexes with crown ethers, oxygen donor or amine ligands has also been reported by other authors e.g. UCl_3(15-crown-5)(red), UCl_3(18-crown-6), UCl_3(benzo-15-crown-5) (red) by Moody *et al.* (1979, 1982), as well as $(UCl_3)_3$(18-crown-6)$_2$ (red-brown), $(UCl_3)_2$(2,2′-bipyridine)$_3$ (bright-green) and $(UCl_3)_2$(dimethoxyethane)$_3$ (brown) by Rossetto *et al.* (1982). All complexes are hygroscopic and more or less rapidly oxidized by atmospheric air. They exhibit some characteristic features of U(III) absorption spectra with very intense f–d transitions in the visible and/or ultraviolet region. Infrared data are indicative to decide if the coordination takes place through the ligand nitrogen or oxygen atoms. Some of the complexes have also been characterized by magnetic susceptibility measurements at 298 K (Hart and Tajik, 1983).

(*iii*) *Uranium tribromide and uranium(III) bromo complexes*

Uranium tribromide

Uranium tribromide can most conveniently be prepared by the reaction of uranium hydride with gaseous hydrogen bromide at 300°C. The method is also suitable for a large-scale preparation (Brown, 1979). Alternative methods include the reduction of UBr_4 by metallic zinc or finely divided uranium at about 600°C. Since UBr_3 reacts with quartz at that temperature, the reaction ought to be performed in a sealed tantalum or molybdenum vessel. In small quantities it may be readily prepared by thermal vacuum decomposition of $NH_4UBr_4 \cdot 5CH_3CN \cdot 6H_2O$ (Zych and Drożdżynski, 1990a). Other preparation procedures such as a direct combination of the elements or the reaction between uranium oxalate and gaseous hydrogen bromide seem to be less convenient (Brown, 1979).

UBr_3 is a dark-brown substance, much more hygroscopic and sensitive to oxidation in air than UCl_3. Rapid oxidation occurs on dissolution in water and in numerous organic solvents. It gives, however, somewhat more stable solutions in formamide, methyl acetate, dimethylacetamide, and acetic acid. Reactions with chlorine and bromine yield UCl_4 and UBr_4, respectively. UBr_3 is reduced by calcium to metallic uranium at high temperatures.

Uranium tribromide is isostructural with UCl_3. The unit cell data are given in Table 5.25. The interatomic distances of the tricapped trigonal prismatic coordination polyhedron obtained from neutron diffraction studies (Levy *et al.*, 1975) and by Krämer and Meyer (1989) (values in parentheses) are: d(U–Br) = 3.145 Å (3.150 Å) to the three capping Br atoms, d(U–Br) = 3.062 Å (~3.069 Å) to the six Br atoms at the prism vertices, d(Br–Br) = 3.652 Å (3.663 Å) at the trigonal prism face edge and d(U–U) = 4.441 Å (4.448 Å) along the c-direction.

Using low-temperature, high-resolution absorption and fluorescence spectra of UBr_3 doped into single crystals of $LaBr_3$ (Paszek, 1978) and K_2LaBr_5 (Karbowiak *et al.*, 1998a) a complete crystal-field analysis in the 4000–22000 cm^{-1} absorption range has been performed. Magnetic susceptibility measurements in the 4.5–483 K range show an antiferromagnetic transition at $T_N = (15 \pm 0.5)$ K. The effective magnetic moments equal to 3.92 and 3.57 B.M. have been determined from the temperature ranges where a plot of $1/\chi_M$ against T is linear.

Uranium tribromide hexahydrate

Uranium tribromide may be converted to the hexahydrate by controlled exposure to oxygen-free water vapor (Brown *et al.*, 1968). On prolonged pumping the obtained red-colored hexahydrate slowly loses most of the coordinated water until the composition approximates $UBr_3 \cdot H_2O$. Complete dehydration occurs with a slow and gradual increase of temperature to about 100°C. X-ray powder diffraction pattern shows that $UBr_3 \cdot 6H_2O$ is isostructural with the

monoclinic lanthanide trihalide hexahydrates (Table 5.25). Further information is not available.

Uranium(III) bromo complexes

Bromouranates(III) of the composition M_2UBr_5 and M_3UBr_6 (M = K, Rb or Cs) have been identified during investigations of the binary fused-salt systems (Vdovenko *et al.*, 1974a; Volkov *et al.*, 1987). The pentabromouranates(III) may also be prepared by fusion of the appropriate components. Complexes of the M_3UBr_6 type are high-temperature phases and decompose on cooling into the alkali bromide and the corresponding pentabromouranate(III). The melting points and regions of existence of the hexabromouranates(III) increase with an increase in the atomic number of the alkali metal. An opposite tendency is observed in the series of pentabromouranates(III) (Vdovenko *et al.*, 1974a). Suglobova and Chirkst (1978a) have reported the thermodynamic properties of some of the bromo complexes.

X-ray powder diffraction analyses reveal that the hexabromouranates(III) have a face-centered cubic symmetry whereas the pentabromouranates(III) are isostructural with the rhombic Tl_2AlF_6. On this basis, it has been assumed (Suglobova and Chirkst, 1978b) that the structure of the pentabromouranates (III) contains distorted UBr_6 octahedra, which combine into parallel chains through common vertices. Aurov *et al.* (1983) and Aurov and Chirkst (1983) have reported X-ray powder diffraction and thermodynamic data for K_2NaUBr_6 and Cs_2NaUBr_6 by (Table 5.25).

A royal-blue $UBr_3(THF)_4$ adduct has been obtained by a gentle dissolution of uranium metal turnings in THF at a reaction temperature near 0°C (Avens *et al.*, 1994). The compounds $K_2UBr_5 \cdot 2CH_3CN \cdot 6H_2O$, $Rb_2UBr_5 \cdot CH_3CN \cdot 6H_2O$ and $(NH_4)[UBr_2(CH_3CN)_2(H_2O)_5]Br_2$ were obtained from acetonitrile solutions of UBr_4 and the appropriate ammonium or alkali metal bromide, by reduction with liquid zinc amalgam (Zych and Drożdżyński, 1990b, 1991; Zych *et al.*, 1993). All compounds are well characterized by various physical methods (Table 5.25). Single crystal X-ray data are available for $(NH_4)[UBr_2(CH_3CN)_2(H_2O)_5]Br_2$, (Zych *et al.*, 1993).

(*iv*) *Uranium(III) iodide and uranium(III) iodo complexes*

Uranium triiodide

A convenient and widely used method for the preparation of uranium triiodide involves the action of iodine vapors on finely divided uranium metal, either in sealed or flow systems at 570 and 525°C, respectively. Large quantities of high purity UI_3, in the form of black crystals, are collected in the 375–450°C condensing zone of a flow system apparatus first reported by Gregory (1958). Alternative procedures employ the reduction of uranium tetraiodide with zinc metal or finely divided uranium metal, reaction between uranium hydride and

methyl iodide, and vacuum thermal decomposition of UI_4 at 225–235°C (Brown, 1979).

UI_3 is a jet-black, highly hygroscopic crystalline solid, sensitive to oxidation in air. Even at elevated temperatures the triiodide is corrosive and attacks glass, which at 800°C is reduced to silicon. The compound reacts with iodine, methylchloride, and uranium tetrachloride to yield UI_4, UCl_4, and $UClI_3$, respectively. UI_3 dissolves in aqueous solutions, methanol, ethanol, ethyl acetate, dimethylacetamide, and acetic acid forming unstable U(III) solutions. Spontaneous oxidation within 1 min was observed in organic solvents like dioxan, pyridine, acetonitrile, dimethylformamide, or acetone (Barnard *et al.*, 1973).

UI_3 possesses the orthorhombic $PuBr_3$-type structure (Zachariasen, 1948a). The structure (space group *Ccmm* - D_{2h}^{17}) was studied in detail also by neutron diffraction profile analysis (Levy *et al.*, 1975; Murasik *et al.*, 1981). The coordination polyhedron is a distorted bicapped trigonal prism layered in planes perpendicular to the *a*-axis.

Diffuse reflectance spectra have been reported in the 4000–30000 cm^{-1} range at room temperature and 90 K (Barnard *et al.*, 1973). In the series of uranium (III) halides one may observe a pronounced red shift of the first $5f^3 \rightarrow 5f^2 6d^1$ bands from about 23000 cm^{-1} in the spectrum UF_3 to about 13400 cm^{-1} forUI_3.

Magnetic susceptibility measurements have shown an antiferromagnetic transition at $T_N = (3.4 \pm 0.2)$ K as well as a second susceptibility maximum at 1.5 K. UI_3 exhibits a first-order magnetic phase transition. The compound orders antiferromagnetically at $T_N = 2.6$ K, resulting in the appearance of a magnetic sublattice (Parks and Moulton, 1968). Neutron scattering investigations reveal hysteresis of the integretated neutron intensity of the magnetic reflections versus temperature, which confirms that the phase transition is of the first order (Murasik *et al.*, 1986).

Complexes with neutral donor ligands

The reaction of elemental iodine with an excess of oxide-free uranium metal turnings in appropriate coordinating solvents at 0°C yields dark purple $UI_3(THF)_4$, purple $UI_3(dme)_4$, black $UI_3(py)_4$ (Avens *et al.*, 1994), and a dark brown $UI_3(CH_3CN)_4$ (Drożdżyński and du Preez, 1994) (THF, tetrahydrofuran; dme, 1,2-dimethoxyethane; py, pyridine). These organic-solvent soluble Lewis base adducts are reported to be key starting materials for the preparation of variety of inorganic and organometallic uranium complexes. Single-crystal X-ray diffraction data show that $UI_3(THF)_4$ is mononuclear with a pentagonal bipyramidal coordination geometry about the uranium ion. Two iodide atoms, with an average U–I lengths of 3.111(2) Å are axially coordinated. The third iodide atom and the four THF ligands lie in the equatorial plane with the U–I distance of 3.167(2) Å and average U–O distances of 2.52(1) Å (Avens *et al.*, 1994). Other available information is listed in Table 5.25.

(*v*) *Uranium*(III) *oxide halides and mixed halides*

The uranium(III) oxide halides UOCI, UOBr, and UOI were prepared by heating stoichiometric mixtures of UO_2X_2, UO_2, and U or UX_4, U_3O_8 and U (X = Cl, Br or I), for 24 h at 700°C (Levet and Noël, 1981). The chemical properties of UOCI, UOBr, and UOI have not been reported.

The X-ray powder diffraction patterns are consistent with the tetragonal PbFCl-type of structure (*P*4/*nmm*). In a recent investigation, the structure was refined by single-crystal X-ray analysis and the atomic positions were determined (Schleid and Meyer, 1988). A plot of the inverse paramagnetic susceptibility against temperature follows the Curie–Weiss law from about 220 to 300 K with μ_{eff} of 3.40, 3.67, and 3.56 B.M. for UOCl, UOBr, and UOI, respectively. All of the oxide halides are weak ferromagnets with nearly the same transition temperatures ranging from 190 to 183 K. Some IR data are also available (Levet and Noël, 1981).

The preparation of a number of uranium(III) mixed halides with the general formulas UXY_2 and UX_2Y, where X = Cl or Br and Y = Cl or I were reported (Gregory, 1958), but very little information about their properties is available. $UClBr_2$ was obtained by reduction of UCl_3Br with hydrogen at 400°C. The UBr_3 by-product is removed from the substance by treatment with iodine. One of the most convenient methods for the preparation of UCl_2Br is reported to be the fusion of a 2:1 molar ratio of UCl_3 and UBr_3 at 850°C. The solid-state reaction between UCl_3 and UI_3 has been also applied successfully for the preparation of $UClI_2$. The remaining mixed halides, i.e. UCl_2I, UBr_2I, and $UBrI_2$ have usually been obtained by thermal decomposition of UCl_2I_2 and UBr_2I_2 at 400°C, and of $UBrI_3$ at 375°C (see also Table 5.25).

(b) Tetravalent halides and complex halides

Uranium tetrahalides and complex halides have so far been the most extensively investigated group of uranium compounds besides those in the 6+ oxidation state. The tetrahalides are not stable on exposure to air however with some exceptions, e.g. that of UF_4. They are more or less hygroscopic and after a time the compounds get oxidized in air. The large chemical stability of UF_4 is mainly due to its high lattice energy. Apart from the fluorides most of the compounds are readily soluble in polar solvents. Aqueous solutions are slowly oxidized to U(VI) species, but in pure and thoroughly deoxygenated solvents U^{4+} is fairly stable. The typical colors vary from pale olive green to deep bluish-green. In few cases black, brown, and blue colors have also been noticed (Table 5.26). The synthesis of binary uranium(IV) halides usually requires strictly oxygen-free conditions. The coordination polyhedra in the binary tetrahalides are more or less distorted forms of a square antiprism (UF_4), a dodecahedron (UCl_4), or a pentagonal bipyramid (UBr_4). The tetrahalides form stable solid complexes with a large variety of ligands, e.g. of the UX_4L_2-type (X = Cl. Br, or I)

Table 5.26 *Properties of selected uranium(IV) halides and complex halides.*[a]

Formula	*Selected properties and physical constants*[b]	*Lattice symmetry, lattice constants* (Å), *conformation and density* (g cm^{-3})[c]	*Remarks regarding information available and references*
UF_4	emerald green; non-volatile; almost insoluble in water and organic solvents; soluble in oxidizing solutions; m.p. = 1036°C; density: 6.70 g cm^{-3}; $\mu_{eff.} = 3.28$ B.M.; $\theta = -116$ K (77–500 K)[d]; $\mu_{eff.} = 2.83$ B.M.; $\theta = -146$ K (75–295K)[d]; $\mu_{eff.} = 2.79$ B.M; (1–300 K)[d] UF_4(cr): $\Delta_f G^o_m = -1823.5$ (4.2)†, $\Delta_f H^o_m = -1914.2$ (4.2)†, $S^o_m = 151.7$ (0.2)†; $C^o_{p,m} = 116.0$ (0.1)†. UF_4(g): $\Delta_f G^o_m = -1576.9$ (6.7)†, $\Delta_f H^o_m = -1605.2$ (6.5)†, $S^o_m = 360.7$ (5.0)†; $C^o_{p,m} = 95.1$ (3.0)†. log$p$(mmHg) = 22.60–16400T^{-1} – 3.02 log$T$ (298–1309 K). log p(mmHg) = 28.05–15300·T^{-1} –5.03 log$T$ (1309–1755 K); IR (cm^{-1}): 404(s)[ν(U–F)]; 194 (s) [ν(F–U–F), bending]; Energy levels parameters (cm^{-1}): $F^2 = 44\,784$, $F^4 = 43107$, and $F^6 = 25654$; $\zeta_{5f} = 1761.0(3.4)$, $\alpha = 34.74$, $\beta = -767.3$, and $\gamma = 913.9$; $P^2 = 2715$ (94); $B^2_0 = 1183(28)$, $B^2_2 = 29(27)$, $B^4_0 = -2714(99)$, $B^4_2 = 3024(71)$, $B^4_4 = -3791(53)$, $B^6_0 = -1433$ (148),$B^6_2 = 1267(101)$, $B^6_4 = -1391$ (93) and $B^6_6 = 1755(82)$; $rms = 31$; $n = 69$	monoclinic; C^6_{2h}, $C2/2$, No. 15; $a =$ 12.73 [12.7941], $b = 10.753$ [10.7901]; $c = 8.404$ [8.3687 90]; $\beta = 126.33$ [126.25]; [$V = 931.68$]; $Z = 12$; d(calc.) = 6.71], d(exp.) = 6.71; d(U–F) distances: 2.23–2.354. Antiprism linked in 3-dimensions by sharing all corners. Each uranium atom has eight fluorine neighbours arranged in a slightly distorted square antiprism. In square brackets are given the data of Kern *et al*., (1994)	*synthesis* (Halstead *et al*., 1982; Bacher and Jacob, 1980, Freestone and Holloway, 1990); *crystallographic data and temperature variation of structural parameters*, (Larson *et al*., 1964; Keenan and Asprey, 1969; Kern *et al*., 1994); *thermodynamic data* (Grenthe *et al*., 1992; Guillaumont *et al*., 2003); *magnetic data, IR, NIR; Raman spectra; Photo-acoustic spectra, ESCA spectra; redox reactions; applications for nuclear fuel* (Conway, 1959; Bacher and Jacob, 1980; *crystal-field spectra* (Carnall *et al*., 1991); *Vis and UV spectra* (Conway, 1959; Bacher and Jacob, 1980); *photo-electron spectra* (Thibaut *et al*., 1982)

Table 5.26 (*Contd.*)

Formula	*Selected properties and physical constants*[b]	*Lattice symmetry, lattice constants* (Å), *conformation and density* (g cm^{-3})[c]	*Remarks regarding information available and references*
$UF_4 \cdot 4/3H_2O$	grass-green	monoclinic; $d = 5.79$. The water molecules are bonded through O–H–F bridges	*crystallographic data* (Gagarinskii *et al.*, 1965; Khanaev *et al.*, 1967)
$UF_4 \cdot 2H_2O$	IR (cm^{-1}): 2950, 3365, and 3840	cubic; O_h^5, $Fm\bar{3}m$, No.225; a = 5.701(0.012); d(calc.) = 6.32; $Z = 2$; d(U–U) = 2.465, d(F–F) = 2.846	*crystallographic data* (Dawson *et al.*, 1954; Bakakin, 1965), *NMR data* (Gabuda *et al.*, 1969)
$UF_4 \cdot 2.5H_2O$	slightly soluble in water (0.1g L^{-1}), soluble in dimethylammonium acetate; stable up to 100°C; $UF_4 \cdot 2.5H_2O$ (cr): $\Delta_f G_m^o$ = –2440.3 (6.2)†, $\Delta_f H_m^o$ = –2671.5(4.3)†, S_m^o = 263.5(15.0)†; $C_{p,m}^o$ = 263.7 (15.0)†	orthorhombic; D_{2h}^{16}, *Pnam,* No.62; a = 12,75, b = 11.12, c = 7.05; d(calc.) = 4.74; $Z = 8$; d(U1–F) (5×) = 2.29; d(U1–O) (4×) = 2.63–2.84; d(U2—F) (9×) = 2.39	*crystallographic data* (Dawson *et al.*, 1954; Borisov and Zaniedporovski, 1971; Zadneporovskii and Borisov, 1971); *^{1}H-NMR, ^{19}F-NMR, IR data*, *thermodynamic data* (Bacher and Jacob, 1980; Grenthe *et al.*, 1992; Guillaumont *et al.*, 2003).
$UF_4 \cdot 7H_2O$		cubic; O_h^5, $Fm\bar{3}m$, No.225; a = 5.65 (1); V = 180.36; $Z = 2$; d(calc.) = 6.01	*crystallographic data* (Dawson *et al.*, 1954)
$LiUF_5$	dark-green; m.p. 605°C*	tetragonal; C_{4h}^6, $I4_1/a$; No.88; a = 14.8592(96), c = 6.5433(9); $Z = 16$; V = 90.3; d(calc.) = 6.23; the U atom is surrounded by nine F ions in a tricapped trigonal prismatic array. Adjacent prisms share edges and corners to form network	*crystallographic data* (Brunton, 1966; Keenan, 1966; Penneman *et al.*, 1973)

Li_3UF_7		tetragonal; D_{4h}^7, *P*4*nmn*, No.129; $a = 6.132$, $c = 6.391$	*crystallographic data* (Thoma and Penneman, 1965)
Li_4UF_8	m.p. = 496°C (incongr.)	orthorhombic; D_{2h}^{16}, *Pnma*; No.62; $a = 9.960$, $b = 9.883$, $c = 5.986$; $Z = 4$; d(calc.) = 4.71; $V = 589.23$; the coordination polyhedron is a triangular prism with pyramids on two of the prism faces; each U atom has 8 F^- neighbours at 2.29 (0.02) and a ninth at 3.30(0.03); CN. = 8	*crystallographic data; IR spectra* (Barton *et al.*, 1958; Brunton, 1967)
LiU_4F_{17}	yellowish-green or green square prism; 775°C*	$a = 8.990$, $c = 11.387$	*crystallographic data* (Jove and Cousson, 1977; Cousson *et al.*, 1977)
Li_2CaUF_8		tetragonal; D_{2d}^9, $I\bar{4}m2$, No. 119; $a = 5.2290(12)$, $c = 11.0130(18)$; $Z = 2$; $V = 301.12$; d(exp.) = 4.85, d(calc.) = 4.9.	*crystallographic data* (Védrine *et al.*, 1973; 1979)
Li_2CdUF_8		tetragonal; D_{2d}^9, $I\bar{4}$ (or $I\bar{4}m2$), No.119; $a = 5.222(0.002)$, $c = 10.952(0.005)$; $Z = 2$; d(exp.) = 4.85, d(calc.) = 4.86.	*crystallographic data* (Védrine *et al.*, 1973)
α-Na_2UF_6	blue; m.p. = 673°C; IR(cm^{-1}): ν(U–F) = 375(s); ν(F–U–F), bending = 192(s); 258(m), ν(Na–F) = 258(m); other: 146w	cubic; O_h^5, $Fm\bar{3}m$, No 225; $a = 5.565(4)$; $Z = 4$; $V = 172.34$; d(calc.) = 5.11	*crystallographic data* (Zachariasen, 1948d; Mighell and Ondik, 1977)
β_2-Na_2UF_6		trigonal/rhombohedral; D_3^2, *P*321, No 150; $a = 5.95(1)$, $c = 3.7(1)$; $Z = 1$; $V = 114.97$; d(calc.) = 5.75; tricapped trigonal prism sharing ends to form chain	*crystallographic data* (Zachariasen, 1948d)

Table 5.26 (*Contd.*)

Formula	*Selected properties and physical constants*[b]	*Lattice symmetry, lattice constants* (Å), *conformation and density* (g cm^{-3})[c]	*Remarks regarding information available and references*
γ-Na_2UF_6	$\mu_{eff.} = 3.13$ to 3.23 B.M.; $\theta = -84$ to –89 K (14–300 K)[d]	orthorhombic; D_{2h}^{25}, *Immm*, No 71; $a = 5.56$, $b = 4.01$, $c = 11.64$; the coordination geometry in UF_9 chains is a tricapped trigonal prism (structure type of β_1-K_2UF_6)	*crystallographic data* (Zachariasen, 1948d; Mighell and Ondik, 1977); *magnetic data* (Bacher and Jacob, 1980)
δ-Na_2UF_6	m.p. = 648°C	hexagonal; C_3^1, *P*3, No.143; $a = 6.112(2)$, $c = 7.240(2)$; $Z = 2$; $V = 234.23$; d(calc.) = 5.64; in the asymmetric unit cell are two U ions; each has nine nearest F^- ions at the corners of capped trigonal prisms; d(U–F) ranges from 2.23 to 2.42(1)	*crystallographic data* (Brunton *et al.*, 1965; Cousson *et al.*, 1979)
Na_3UF_7	geenish-blue; m.p. = 629°C; $\mu_{eff.} = 3.40$ B.M.; $\theta = 290$ K (74–300 K)[d] or $\mu_{eff.} = 3.30$ B.M.; θ = 81 K $\mu_{eff.} = 3.38$ B.M.; $\theta = 290$ K; (for 195–473 K range). IR (cm^{-1}): ν(U–F) = 380(s); ν(F–U–F), bending = 217(s); ν(Na–F) = 240 (m); other, 146w	tetragonal; D_{4h}^{17}, *I*4/*mmm,* No.139; $a = 5.488$, $c = 10.896$	*crystallographic data* (Zachariasen, 1948a; Mighell and Ondik, 1977); *magnetic data* (Bacher and Jacob, 1980)
NaU_2F_9	yellowish-green; m.p. = 660°C (dec.); IR (cm^{-1}): ν(U–F) = 360(s); ν(F–U–F), bending = 194(s); ν(Na-F) = 260(m); other, 145w		*IR data* (Ohwada *et al.*, 1972)

$Na_7U_2F_{15}$	green	orthorhombic; D_{2h}^{23}, *Fmmm*, No.69; $a = 17{,}7$, $b = 29.8$, $c = 12.7$	*crystallographic data* (Thoma *et al.*, 1963; Mighell and Ondik, 1977)
$Na_5U_3F_{17}$		cubic; $a = 5.589$	*crystallographic data* (Thoma *et al.*, 1963).
$Na_7U_6F_{31}$	green; m.p. = 718°C; IR(cm^{-1}): ν(U–F) = 383(s); ν(F–U–F), bending = 193(s); ν(Na–F) = 241(m)	rhombohedral; C_{3i}^2, $R\bar{3}$, No.148; $a = 14.72$, $c = 9.84$; $Z = 3$; $V =$ 615.5 $Å^3$; CN = 8; isostructural with $Na_7Zr_6F_{31}$ in which the basic coordination geometry about central ion is approx. square antiprismatic, and six antiprisms share corners to form an octahedral cavity which encloses the additional F atom.	*crystallographic data* (Thoma *et al.*, 1963; Mighell and Ondik, 1977)
$NaKUF_6$		hexagonal; C_3^1, *P*3, No.143; $a = 6.24$, $c = 7.80$; $Z = 2$; d(calc.) = 5.23	*crystallographic data* (Brunton *et al.*, 1965)
$NaRbUF_6$	pale green, purple interference	hexagonal; C_3^1, *P*3, No. 143; $a = 6.29$, $c = 8.13$; $Z = 2$; d(calc.) = 5.49	*crystallographic data* (Brunton *et al.*, 1965); *optical data* (Bacher and Jacob, 1980)
α-K_2UF_6	green; $\mu_{eff.} = 3.45$ B.M.; $\theta =$ –108K (74–300 K)[d]; IR(cm^{-1}): ν(U–F)val. = 360s, 292s; ν(F–U–F)def. = 217sv; 161m, ν(F–U–F)def. or ν(K–F)lat. = 147m; ν(K–F)lat. = 84w	cubic with disordered cations; O_h^5, $Fm\bar{3}m$, No 225; $a = 5.946(1)$; $Z = 4$; $V = 210.22$; d(calc.) = 4.53	*crystallographic data* (Zachariasen, 1948d); *magnetic data* (Bacher and Jacob, 1980)
β_1-K_2UF_6	drab olive; m.p. = 755°C[*]; stable between 608 –and 755°C; below 608°C decomposes to K_3UF_7 + $K_7U_6F_{31}$	hexagonal; D_{3h}^3, $P\bar{6}2m$, No.189; $a = 6.5528(2)$, $c = 3.749(1)$; $Z = 1$; $V = 139.41$; d(calc.) = 5.1235; tricapped trigonal prisms share the triangular faces perpendicular to the three fold axis of the ideal polyhedron to form infinite chains	*crystallographic data* (Zachariasen, 1948a; Brunton, 1969a, Penneman *et al.*, 1973; Bacher and Jacob, 1980; *IR spectra* (Soga *et al.*, 1972)

Table 5.26 (*Contd.*)

Formula	*Selected properties and physical constants*[b]	*Lattice symmetry, lattice constants* (Å), *conformation and density* (g cm^{-3})[c]	*Remarks regarding information available and references*
β_2-K_2UF_6	green	hexagonal; D_3^2, *P*321, No.150; a = 6.54(2); c = 4.04; Z = 1; V = 150.02; d(calc.) = 4.76. tricapped trigonal prism sharing ends to form chain	*crystallographic data* (Zachariasen, 1948d); *IR spectra* (Soga *et al.*, 1972)
α-K_3UF_7	deep-green; m.p. = 957°C; IR (cm^{-1}): ν(U–F)val. = 362s; ν(F–U–F)def. = 206s; ν(F–U–F)def. or ν(K–F)lat. = 120m; ν(K–F)lat. = 80w	cubic; O_h^5, $Fm\bar{3}m$, No.225; a = 9.22 (2); Z = 4; V = 783.78, d(calc.) = 4.14; the seven F atoms are statistically distributed over fluorite lattice sites	*crystallographic data, IR spectra* (Zachariasen, 1954c; Burns and Duchamp, 1962; Bacher and Jacob, 1980); *IR spectra* (Soga *et al.*, 1972)
β-K_3UF_7		orthorhombic; D_{2h}^{13}, *Pmmn*, No.59 or $Pmn2_1$, C_{2v}^7, No. 31; a = 6.58, b = 8.31, c = 7.22	*crystallographic data* (Burns and Duchamp, 1962)
$K_7U_6F_{31}$	green; m.p. = 789°C (congr.); IR: ν(U–F)val. = 380s, 319m; 244sh, 200m; ν(F–U–F) def. = 244sh, 200m; ν(F–U–F) def. or ν(K–F) lat. = 153m, 114m; ν(K–F) lat. = 80w	rhombohedral; C_{3i}^2, $R\bar{3}$, No. 148; a = 9.376, α = 107.20; Z = 1; CN = 8; d(calc.) = 5.58; isostructural with $Na_7Zr_6F_{31}$; square antiprisms sharing corners, with one fluorine atom in a cavity	*crystallographic data, IR spectra* (Brunton *et al.*, 1965); *IR spectra* (Soga *et al.*, 1972)
KU_2F_9	green; m.p. = 765°C (incongr.) with formation of UF_6; IR (cm^{-1}): ν(U–F)val. = 360s, 331s, 290sh; ν(F–U–F) def. = 235m, 204m; ν(F–U–F)def. or ν(K–F)lat. = 160m, 148m, 118w; ν(K–F)lat. = 85w	orthorhombic; D_{2h}^{16}, *Pnma,* No 62; a = 8.7021, b = 11.4769, c = 7.0350; Z = 4; V = 702.61; CN = 9; d(calc.) = 6.4851; tricapped trigonal prism, sharing ends and edges; d(U–F) = 2.29–2.39	*X-ray powder diffraction and single crystal data, IR spectra* (Brunton *et al.*, 1965; Brunton, 1969b); *IR spectra* (Soga *et al.*, 1972)

KU_6F_{25}	metastable	hexagonal; D_{6h}^4, $P6_3/mmc$, No.194; $a = 8.18$, $c = 16.42$; d(calc.) = 6.73; $Z = 2$; tricapped trigonal prism, sharing edges and corners to form double rings of six polyhedra each	*crystallographic data* (Burton *et al.*, 1965; Zachariasen, 1948d); *IR spectra* (Soga *et al.*, 1972)
RbU_6F_{25}	deep-green; m.p. = 832°C (incongr. with formation of UF_4)	hexagonal; D_{6h}^4, $P6_3/mmc$, No.194; $a = 8.195$, $c = 16.37$; $Z = 2$; d(calc.) = 6.908; tricapped trigonal prism, sharing edges and corners to form double rings of six polyhedra each	*crystallographic data* (Mighell and Ondik, 1977; Brunton *et al.*, 1965); *IR spectra* (Soga *et al.*, 1973)
Rb_2UF_6	green; m.p. = 818°C (incongr)	orthorhombic; D_{2h}^{17}, *Cmcm*, No.63; $a = 6.958(2)$, $b = 12.042(5)$, $c = 7.605(5)$; $Z = 4$; $V = 637.21$; d(calc.) = 5.45; the structure is of the K_2ZrF_6 type and consists of infinitive chains of UF_8 polyhedra in the form of dodecahedra with triangular faces (ideal symmetry D_{2d})	*X-ray powder and single crystal diffraction data* (Kruse, 1971; Kruse and Asprey, 1962); *IR spectra* (Soga *et al.*, 1973)
Rb_3UF_7	pale green; m.p. = 995°C (congr.)	cubic; O_h^5, $Fm\bar{3}m$, No.225; $a = 9.5667$; the seven F atoms are statistically distributed over fluorite lattice sites	*crystallographic data* (Bacher and Jacob, 1980); *IR spectra* (Soga *et al.*, 1973)
$Rb_7U_6F_{31}$	green; m.p. = 675°C (incongr.)	rhombohedral; C_{3i}^2, $R\bar{3}$, No. 148; $a = 9.595$; $\alpha = 107.67$, $Z = 1$; CN = 8; d(calc.) = 6.02; structure type of $Na_7Zr_6F_{31;}$ square antiprisms sharing corners, with one fluorine atom in a cavity	*crystallographic data* (Burton *et al.*, 1965; Thoma *et al.*, 1958); *IR spectra* (Soga *et al.*, 1973)

Table 5.26 (*Contd.*)

Formula	*Selected properties and physical constants*[b]	*Lattice symmetry, lattice constants* (Å), *conformation and density* (g cm^{-3})[c]	*Remarks regarding information available and references*
other complex fluorides with rubidium: $RbUF_5$ (green blue, m.p. = 735°C; IR(cm^{-1}):ν_{UF} = 370, 330, 302 cm^{-1}, RbU_3F_{13}, $Rb_2U_3F_{14}$ (m.p. = 722°C*)			*general properties* (Bacher and Jacob, 1980)
$CsUF_5$	greenish-blue (or sky blue); m.p. = 735°C.		
CsU_2F_9	deep-green crystals	monoclinic; C_{2h}^6, *C*2/*c*, No.15; *a* = 15.649(3), *b* = 7.087(1), *c* = 8.689 (2); β = 118·11(2); *Z* = 4, *V* = 849.98; CN = 8 1/2 (effective); *d*(exp.) = 6.4; *d*(calc.) = 6.09; tricapped trigonal prism, one prism corner statistically only half-occupied. Contains 8-coordinate U in edge-sharing polyhedra forming U_4F_{16} sheets	*crystallographic data* (Rosenzweig *et al.*, 1973)
CsU_6F_{25}	deep-green; m.p. = 867°C (incongr.) with formation of UF_4	hexagonal; D_{6h}^4, $P6_3/mmc$, No.194; *a* = 8.2424(4), *c* = 16.4120(20); *Z* = 2; *V* = 965.61; *d*(calc.) = 7; tricapped trigonal prism, sharing edges and corners to form double rings of six polyhedra each	*crystallographic data* (Brunton *et al.*, 1965, 1971)

Cs_2UF_6	greenish- blue to light blue; m.p. = 800°C*		*general properties* (Bacher and Jacob, 1980)
$Cs_2U_3F_{14}$	bluish-green; m.p. = 737°C (incongr.) with formation of $Cs_2U_3F_{14}$	monoclinic; C_{2h}^2, $P2_1/m$, No.11 or $P2_1$, C_2^2, No.4; $a = 8.39$, $b = 8.46$, $c = 20.88$; $\beta = 119.89°$	*crystallographic data* (Brunton *et al.*, 1965); *magnetic susceptibilities* (Bacher and Jacob, 1980)
Cs_3UF_7	pale blue; m.p. = 970°C	cubic; O_h^5, $Fm\bar{3}m$, No.225; $a =$ 9.90; CN = 7; structure type of K_3UF_7; d(calc.) = 7.92.	*crystallographic data* (Penneman *et al.*, 1973; Brunton *et al.*, 1965)
α-NH_4UF_5	over 190°C decomposes partly to β-NH_4UF_5	rhombohedral; C_{3i}^2, $R\bar{3}$, No.148; $a = 9.55$; $\alpha = 107.4$	*crystallographic data* (Benz *et al.*, 1963; Penneman *et al.*, 1974); *magnetic susceptibilities* (Bacher and Jacob, 1980)
β-NH_4UF_5	polymeric	monoclinic; C_{2h}^5, $P2_1/c$, No.14; $a =$ 7.799(5), $b = 7.158(5)$, $c = 8.762$ (7); $\beta = 116.45$; $Z = 4$; $V = 437.94$; d(calc.) = 5.32; CN = 9	*crystallographic data* (Penneman and Ryan, 1974) *magnetic susceptibilities* (Bacher and Jacob, 1980)
γ-$(NH_4)_2UF_6$	decomposes under He over 220°C to NH_4F+$(NH_4)_7U_6F_{31}$	orthorhombic; C_{2v}^2, $Pmc2_1$, No.26 or D_{2h}^5, $Pmcm$, No.51; $a = 4.05$, $b = 7.03$, $c = 11.76$; $Z = 2$; d(calc.) = 3.9	*crystallographic data* (Penneman *et al.*, 1964a); *magnetic and optical data* (Bacher and Jacob, 1980)
$(NH_4)_4UF_8$	deep green; over 130°C decomposes in air to NH_4F + $(NH_4)_2UF_6$	monoclinic; C_{2h}^6, $C2/c$, No.15; $a =$ 13.126, $b = 6.692$, $c = 13.717$; $\beta =$ 121.32; $Z = 4$; CN = 8; d(exp.) = 2.96; d(calc.) = 2.982; d(U–F) = 2.25–2.33; discrete distorted tetragonal antiprismatic array	*X-ray powder and single crystal data*; (Rosenzweig and Cromer, 1970); *thermodynamic data, magnetic and optical data* (Bacher and Jacob, 1980)
$NH_4U_3F_{13}$	decomposes in vacuum at 300–400°C to UF_4	orthorhombic; C_{2v}^2, $Pmc2_1$, No. = 26; $a = 8.045(2)$, $b = 8.468(2)$, $c =$ 7.375(2); $V = 502.42$; $Z = 2$; d(calc.) = 6.47	*crystallographic data* (Abazli *et al.*, 1980)

Table 5.26 (*Contd.*)

Formula	*Selected properties and physical constants*[b]	*Lattice symmetry, lattice constants* (Å), *conformation and density* (g cm^{-3})[c]	*Remarks regarding information available and references*
$(NH_4)_7U_6F_{31}$	m.p. > 150°C (dec.); under He gas to UF_4; exists in α, β, γ and δ forms	rhombohedral; C_{3i}^2, $R\bar{3}$, No.148; $a = 9.55$; $\alpha = 107.4$; CN = 8; square antiprisms sharing corners, with one fluorine atom in a cavity; structure type of $Na_7Zr_6F_{31}$.	*crystallographic data* (Benz *et al.*, 1963; Penneman *et al.*, 1964a); *thermodynamic data, magnetic and optical properties* (Bacher and Jacob, 1980)
$(NH_3OH)UF_5$		orthorhombic; D_2^1, $P222$, No.16; C_{2v}^1, $Pmm2$, No.25 or D_{2h}^1, $Pmmm$, No.47; $a = 10.963$, $b = 14.9024$, $c = 10.4391$	*crystallographic data* (Ratho *et al.*, 1969)
$N_2H_5UF_5$		orthorhombic; D_2^1, $P222$, or C_{2v}^1, $Pmm2$; $a = 7.941$, $b = 6.372$, $c = 7.478$; $Z = 4$	*crystallographic data* (Ratho and Patel, 1968); *thermodynamic data; magnetic susceptibilities; IR spectra, decomposition data.* (Bacher and Jacob, 1980)
$[N(C_2H_5)_4]_2UF_6$	white cryst.; air and moisture sensitive; IR (cm^{-1}):ν(U–F) = 405; $F^2 = 49699$, $\varsigma_{5f} = 1970$; $B_0^4 = 10\,067(113)$, $B_0^6 = 22(72)$; *rms* = 67		*general properties* (Ryan *et al.*, 1974); *electronic spectra, crystal-field parameters* (Wagner *et al.*, 1977)
other complex fluorides with hydrazinium: $(N_2H_5)_2UF_6$, $(N_2H_5)_3UF_7$			*general properties* (Bacher and Jacob, 1980)
$UN_{0.95}F_{1.2}$	uranium oxidation number = +4.05	tetragonal; D_{2h}^5, $P4/n$, No.85; $a = 3.951$ $c = 5.724$; $Z = 2$; $V = 89.35$; d(calc.) = 10.19	*crystallographic data* (Jung and Juza, 1973)

$Ca_{0.925}\ U_{0.075}\ F_{2.15}$		cubic; O_h^5; $Fm\bar{3}m$; No.225; a = 5.507(3), $Z = 4$; $V = 167.01$; d(calc.) = 3.81	*neutron diffraction data* (Laval *et al.*, 1987)
$CaUF_6$	green; $\mu_{eff.} = 3.25$ B.M.; $\theta = -101$ (74–300 K)[d]	hexagonal (LaF_3 type); D_{3d}^4, $P\bar{3}c1$, No.165; $a = 6.928$, $c = 7.127$; d(calc.) = 6.59	*crystallographic data* (Keller and Salzer, 1967) *magnetic data* (Bacher and Jacob, 1980)
$SrUF_6$		hexagonal (LaF_3 type); D_{3d}^4, $P\bar{3}c1$, No.165; $a = 7.122$, $c = 7.293$; d(calc.) = 6.83	*crystallographic data* (Keller and Salzer, 1967)
$BaUF_6$		hexagonal (LaF_3 type); D_{3d}^4, $P\bar{3}c1$, No.165; $a = 7.403$, $c = 7.482$; d(calc.) = 6.86	*crystallographic data* (Keller and Salzer, 1967)
$PbUF_6$	green	hexagonal (LaF_3 type); D_{3d}^4, $P\bar{3}c1$, No.165; $a = 7.245$, $c = 7.355$; d(calc.) = 8.33	*crystallographic data* (Keller and Salzer, 1967)
other complex fluorides with lead: $Pb_3U_2F_{14}$, Pb_6UF_{16}.			*general properties* Bacher and Jacob (1980)
$TlUF_5$	m.p. = 640°C	monoclinic; C_{2h}^5, $P2_1/c$; No.14; $a = 8.222(2)$, $b = 13.821(4)$, $c = 8.317(5)$; $\beta = 102.53(3)$; $Z = 8$; $V = 922.6$; d(calc.) = 7.74; tricapped trigonal prismatic at U	*infrared spectra* (Soga *et al.*, 1973); *crystallographic data* (Avignant *et al.*, 1980, 1982)
Tl_2UF_6	m.p. = 598°C (eutec.)	orthorhombic; $a = 4.07$, $b = 6.97$, $c = 11.56$; $Z = 2$; d(calc.) = 7.54	*crystallographic data* (Avignant and Cousseins, 1971)
Tl_3UF_7	m.p. = 542°C (incongr.)	cubic; $a = 9437$; $Z = 2$; $d = 7.92$	*crystallographic data* (Avignant and Cousseins, 1971)
Tl_4UF_8	m.p. = 317°C*		
$Tl_7U_6F_{31}$		hexagonal; $a = 15.39$, $c = 10.80$; $Z = 3$; d(calc.) = 7.74	*crystallographic data* (Avignant and Cousseins, 1977; Avignant *et al.*, 1977)
TlU_3F_{13}	m.p. = 674°C (incongr)	orthorhombic; $a = 8.49$, $b = 8.04$, $c = 7.38$.; Z = 2; d(calc.) = 7.68	*crystallographic data* (Avignant *et al.*, 1977)

Table 5.26 (*Contd.*)

Formula	*Selected properties and physical constants*[b]	*Lattice symmetry, lattice constants* (Å), *conformation and density* (g cm^{-3})[c]	*Remarks regarding information available and references*
TlU_6F_{25}		hexagonal; $a = 8.18$, $c = 16.46$; $d = 7.19$	*crystallographic data* (Avignant *et al.*, 1977)
$TlUO_3F_{11}$		monoclinic; C_s^3, *Cm*, No. 8; $a = 14.051(3)$, $b = 8.106(3)$, $c = 8.389(2)$, $\beta = 90.00(3)$; $Z = 4$; $V = 955.49$; d(calc.) = 7.95	*crystallographic data* (Hsini *et al.*, 1986)
YUF_7		monoclinic; $a = 8.19$, $b = 8.27$, $c = 11.17$; $\beta = 92.66$	*crystallographic data; magnetic properties* (Denes *et al.*, 1973)
$TmUF_7$		monoclinic; $a = 8.19$, $b = 8.27$, $c = 11.19$; $\beta = 92.73$	*crystallographic data; magnetic properties* (Denes *et al.*, 1973)
$YbUF_7$		monoclinic; $a = 8.18$, $b = 8.25$, $c = 11.20$; $\beta = 92.70$; d(calc.) = 6.93	*crystallographic data; magnetic properties* (Denes *et al.*, 1973)
$LuUF_7$		monoclinic; $a = 8.17$, $b = 8.24$, $c = 11.18$; $\beta = 92.48$	*crystallographic data; magnetic properties* (Denes *et al.*, 1973)
$CuU_2F_{10}{\cdot}8H_2O$		orthorhombic; $a = 8.73$, $b = 7.16$, $c = 20.78$, $Z = 4$, d(calc.) = 4.48.	*crystallographic data* (Charpin *et al.*, 1968)
$ZnUF_6{\cdot}5H_2O$		orthorhombic; $a = 14.34$, $b = 15.72$, $c = 8.05$; $Z = 8$; d(calc.) = 3.71	*crystallographic data* (Charpin *et al.*, 1969)
$MnUF_6{\cdot}8H_2O$		monoclinic; $a = 12.37$, $b = 6.98$, $c = 8.06$; $\beta = 93.33$; $Z = 4$; d(calc.) = 4.41	*crystallographic data* (Charpin *et al.*, 1969)
$CoU_2F_{10}{\cdot}5H_2O$		monoclinic; $a = 11.07$, $b = 7.10$, $c = 8.81$; $\beta = 94.17$; $Z = 2$; d(calc.) = 4.16	*crystallographic data* (Charpin *et al.*, 1968)
InU_2F_{11}		monoclinic; $a = 5.430$, $b = 6.407$, c = 8.402, $\beta = 104.62(4)$	*crystallographic data* (Champarnaud-Mesjard and Gaudreau, 1976)

$NiU_2F_{10}{\cdot}8H_2O$		monoclinic; $a = 11.05$, $b = 7.08$, $c = 8.86$; $\beta = 93.33$; $Z = 2$; d(calc.) = 4.17	*crystallographic data* (Charpin *et al.*, 1968)
UOF_2	UOF_2(cr): $\Delta_f G^o_m = -1434.1$ (6.4)†, $\Delta_f H^o_m = -1504.6$ (6.3)†, $S^o_m = 119.2$ (4.2)$^{\dagger.}$		*thermodynamic data* (Grenthe *et al.*, 1992; Guillaumont *et al.*, 2003)
$UO_2F_{0\cdot25}$	dark grey to black; mixed valence compound (U^{IV} and U^{V}); oxidation state 4.25	octahedral; fluorite type of structure; $a = 5.49$; $Z = 4$; d(exp.) = 11.0. One anion per unit cell is occupying inter-net places	(Kemmler-Sack, 1967, 1969)
$UOF_2{\cdot}H_2O$	$UOF_2{\cdot}H_2O$(cr): $\Delta_f G^o_m = -1674.5$ (4.1)†, $\Delta_f H^o_m = -1802.0$(3.3)†, $S^o_m = 161.1$(8.4)†		*IR spectra* (Jacob and Bacher, 1980); *thermodynamic properties*, (Grenthe *et al.*, 1992; Guillaumont *et al.*, 2003)
UCl_4	light green needles or dark-green octahedra; m.p. = 590°C; b.p. = 789°C; density: 4.725 g cm^{-3}; $\mu_{eff.} = 3.29$ B.M.; $\theta = -65$ K (90 – 551 K)[d] hygroscopic; soluble in polar organic solvents; insoluble in ethyl acetate, chloroform and benzene. UCl_4(cr): $\Delta_f G^o_m = -929.6$ (2.5)†, $\Delta_f H^o_m = -1018.8$ (2.5)†, $S^o_m = 197.200$(0.8)†; $C^o_{p,m} = 121.8$ (0.4)†. UCl_4(g): $\Delta_f G^o_m = -789.4$ (4.9)†, $\Delta_f H^o_m = -815.4$ (4.7)†, $S^o_m = 409.3$ (5.0)†; $C^o_{p,m} = 103.5$ (3. 0)† $\log p$ (mmHg) = $-11350T^{-1} + 23.21 - 3.02 \log T$ (298–863 K) $\log p$(mmHg) = $-9950\ T^{-1} + 28.96 - 5.53 \log T$ (863–1062 K); IR and Raman vibrations(cm^{-1}): 311 (R), 270 (R, IR), 240 (R, IR),	tetragonal; D^{19}_{4h}, $I4_1/amd$, No.141; $a = 8.3018(4)$, $c = 7.4813(6)$, $Z = 4$; d(calc.) = 4.87; each uranium atom is bonded to eight chlorine atoms; the coordination polyhedron is a dodecahedron ($\bar{4}2m$); d(U–Cl) = 2.889(1) and 2.644(2) (4 times each); Cl–U–Cl angles: 3.141(8) and 3.540(1). The Cl–Cl approaches are 3.141(8), 3.097(8) and 3.540(1); structure refined data: $a = 8.3018(4)$, $b = 8.3018(4)$, $c = 7.4813(6)$; $V = 515.61$; d(calc.) = 4.89	*crystallograhic data* (Brown, 1979; Taylor and Wilson, 1973a); *structural transitions anticipating melting* (Bros *et al.*, 1987); *structure refinement* (Schleid *et al.*, 1987) *temperature absorption spectra, crystal-field energy level structure* (Malek *et al.*, 1986a,b); Brown, 1979; Hecht and Gruber, 1974; Clifton *et al.*, 1969; McLaughlin, 1962; Żołnierek *et al.*, 1984; *thermodynamic data* (Rand and Kubaschewski, 1963 ; Grenthe *et al.*, 1992; Brown, 1979; Guillaumont *et al.*, 2003); *magnetic properties* (Hendricks *et al.*, 1971; Dawson, 1951; Gamp *et al.*, 1983); *electrical and optical properties* (Brown, 1979); *IR and*

Table 5.26 (*Contd.*)

Formula	*Selected properties and physical constants*[b]	*Lattice symmetry, lattice constants* (Å), *conformation and density* (g cm^{-3})[c]	*Remarks regarding information available and references*
	172 (R), 153 (R, IR), and 102(R, IR); $\mu_{eff.} = 3.29$; $\theta = -62$ K Energy level parameters: $F^2 = 42561(235)$, $F^4 = 39440(634)$, and $F^6 = 24174(185)$; $\zeta_{5f} = 1805$ (8), $\alpha = 30.9(1)$, $\beta = -576(168)$; $B_0^2 = -903(151)$, $B_0^4 = 766(220)$, $B_4^4 = -3091(185)$, $B_0^6 = -1619(482)$ and $B_4^6 = -308(280)$. $F_2 = 172.6$, $F_4 = 38.79$, $F_6 = 2.565$; $M^0 = [0.99]$, $M^2 = [0.55]$ and $M^4 = [0.38]$; $P^2 = P^4 = P^6 = [500]$		*Raman spectra* (Bohres *et al.*, 1974); *photoelectron spectra* (Thibaut *et al.*, 1982)
$UCl_4(CH_3CN)_4$	grey-green cryst; soluble in CH_3CN; loses CH_3CN *in vacuo* >40°C; IR (cm^{-1}): ν(CN) = 2278; $\mu_{eff.} = 2.89$ B.M.; $\theta = -158$ K	monoclinic; C_{2h}^6, *C*2/*c*, No.15; $a = 14.677(4)$; $b = 8.452(2)$; $c = 13.9559(3)$; $\beta = 91.77(2)$; $Z = 4$; d(calc.) = 2.087; d(U–Cl) = 2.624 (2) and 2.614(2); d(U–N) = 2.599 (6) and 2.567(6). The U atom is eight-coordinated with a dodecahedral arrangement. The C atoms occupy the dodecahedral B sites and the N atoms the A site	*crystallographic data* (Cotton *et al.*, 1984; Van den Bossche *et al.*, 1986); *infrared data* (Kumar and Tuck, 1984)
Li_2UCl_6	m.p. = 448.8 °C ; IR (cm^{-1}): ν(U–Cl) = 232w, 258, 287w	hexagonal; D_{6h}^4, $P6_3/mmc$, No. 194; $a = 11.191(5)$, $b = 11.191(5)$, $c = 6.0365(1)$; $Z = 3$; $V = 654.72$; d(calc.) = 3.53	*crystal structure from multiphase powder neutron profile refinement* (Bendall *et al.*, 1983); *magnetic properties* (Trzebiatowski and Mulak, 1970); *thermodynamic data* Vdovenko *et al.*, 1974b; Fuger *et al.*, 1983)

Na_2UCl_6	m.p. = 445.6 °C; IR (cm^{-1}): ν(U–Cl) = 240w, 260, 286w	trigonal/rhombohedral; D^3_{3d}, $P\bar{3}m1$, No.164; a = 11.8062(9), b = 11.8062(9), c = 6.3243(2); Z = 3; V = 763.42; d(calc.) = 3.24	*crystal structure from multiphase powder neutron profile refinement* (Bendall *et al.*, 1983); *magnetic properties* (Trzebiatowski and Mulak, 1970); *thermodynamic data* Vdovenko *et al.*, 1974b; Fuger *et al.*, 1983)
Rb_2UCl_6	IR (cm^{-1}):ν(U–Cl) = 267; 285w	trigonal; D^5_{3d}, $R\bar{3}m$, No.166; a = 7.34, c = 5.89; d(calc.) = 3.68; each U atom is surrounded by six Cl atoms at the vertices of an octahedron	*crystallographic data* (Vdovenko *et al.*, 1972a); *magnetic properties* (Trzebiatowski and Mulak, 1970); *thermodynamic data* (Vdovenko *et al.*, 1974b; Fuger *et al.*, 1983)
α-Cs_2UCl_6	green crystals; m.p. = 670°C; IR and Raman data (cm^{-1}): ν_1 = 307, ν_3 = 262, ν_4 = 115, ν_5 = 125, ν_6 = 88; Energy level parameters (T_d): F_2 = 189.358, F_4 = 33.469, F_6 = 3.927, F^2 = 42605, F^4 = 36447, F^6 = 28909; ς_{5f} = 1800.104; $A^o_4\langle r^4\rangle$ = 901.381 $A^o_6\langle r^6\rangle$ = 85.426; B^4_0 = 7211.0, B^4_4 = (4309) B^6_0 = 1366.8 B^6_4 = (–2554); *rms* = 163; n = 21	trigonal; D^5_{3d}, $R\bar{3}m$, No 166; a = 7.478, c = 6.026; each U atom is surrounded by six Cl atoms at the vertices of an octahedron	*crystallographic data* (Siegel, 1956); *IR and Raman data* (Brown *et al.*, 1975; Brown, 1979); *crystal-field spectra* (Johnston *et al.*, 1966); *magnetic properties* (Trzebiatowski and Mulak, 1970); *thermodynamic data* Vdovenko *et al.*, 1974b; Fuger *et al.*, 1983)
β-Cs_2UCl_6	appears in a polymorphic transition at 510°C; IR and Raman data: ν_1 = 308, ν_2 = 230, ν_3 = 267, ν_4 = 116, ν_5 = 126, ν_6 = 89	trigonal; a = 7.50, c = 12.00; d(calc.) = 4.04; (for a rapidly quenched sample); for the refined structure: trigonal/rhombohedral; D^3_{3d},$P\bar{3}m1$; No.164; a = 7.5037(3), b = 7.5037(3), c = 6.0540(4); Z = 1; V = 295.21; 95.21	*crystallographic data* (Vdovenko *et al.*, 1972b); *structure refinement* (Schleid *et al.*, 1987) *IR and Raman data* (Shamir and Silberstein, 1975; Shamir *et al.*, 1975)
$Cs_2U[O_3Cl_9(Nb\ Cl)_6]$		trigonal/rhombohedral; D^2_{3d}, $P\bar{3}1c$, No.163; a = 9.2080(7), c = 17.0950(30); Z = 2; V = 1255.25; d(calc.) = 4.34	*crystal structure* (Cordier *et al.*, 1997)

Table 5.26 (*Contd.*)

Formula	*Selected properties and physical constants*[b]	*Lattice symmetry, lattice constants* (Å), *conformation and density* (g cm^{-3})[c]	*Remarks regarding information available and references*
$[N(CH_3)_4]_2UCl_6$	green cryst.; soluble in CH_3CN, H_2O; IR and Raman data (cm^{-1}): $\nu_1 = 284$, $\nu_2 = 230$, $\nu_5 = 123$, $\nu_6 = 87$	cubic face centered; $a = 13.06$; d(calc.) = 1.788, d(exp.) = 1.791	*crystallographic data* (Staritzky and Singer, 1952); *IR and Raman data* (Silberstein, 1972; Brown, 1979)
$[N(C_2H_5)_4]_2UCl_6$	green cryst.; soluble in CH_3CN, H_2O; crystals undergo reversible phase change at 94°C; IR and Raman data (cm^{-1}): $\nu_1 = 293$, $\nu_3 = 254$, $\nu_4 = 110$, $\nu_5 = 110$, $\nu_6 = 78$; $F^2 = 43170(2181)$, $\varsigma_{5f} = 1774(35)$; $B_0^4 = 7463(432)$, $B_0^6 = 992(258)$; *rms* = 168	orthorhombic; D_{2h}^{23}, *Fmmm*, No.69; $a = 14.23$, $b = 14.73$, $c = 13.33$; d(calc.) = 1.693	*crystallographic data* (Staritzky and Singer, 1952); *IR and Raman data* (Brown *et al.*, 1975; Brown, 1979); *electronic spectra, crystal-field parameters* (Wagner *et al.*, 1977)
$[P(C_6H_5)_3C_2H_5]_2UCl_6$		triclinic; C_1^1, $P\bar{1}$, No.2; $a = 10.53$ (1), $b = 10.95(1)$, $c = 10.31(1)$; $\alpha = 113.22(5)^o$, $\beta = 105.20(5)$, $\gamma = 80.40(5)$; $Z = 1$; d(calc.) = 1.631, d(exp.) = 1.64; d(U-Cl): = 2.621 (2), 2.627(1) and 2.623(1)	*crystallographic data* (Caira *et al.*, 1978)
$UCl(H_2PO_2)_3(H_2O)_2$		orthorhombic; D_{2h}^{11}, *Pbcm*, No.57; $a = 7.559(2)$, $b = 10.111(2)$, $c = 14.680(2)$; $Z = 4$; $V = 1121.98$, d(calc.) = 2.99	*synthesis, structure, vibrational spectra* (Tanner *et al.*, 1992)
$UCl(PO_4)2H_2O$		tetragonal; C_{4h}^5, *I4/m*, No.87; $a = 14.631(2)$, $b = 14.631(2)$, $c = 6.662$ (1); $Z = 8$; $V = 1426.11$; d(calc.) = 3.77	*crystallographic data* (Benard-Rocherulle *et al.*, 1997)

other uranium(IV) chloro complexes: (i) $KUCl_5$; (ii) $RbUCl_5$; (iii) $CsUCl_5$, (iv) K_2UCl_6; (v) Cs_2UCl_6 (vi) Ag_2UCl_6; (vii) $KNaUCl_6$; (viii) $SrUCl_6$; (ix) $BaUCl_6$; (x) Rb_4UCl_8; (xi) KU_3Cl_{13}; (xii) $KNaUCl_6$; (xiii) CsU_2Cl_9; (xiv) $Cs_3U_2Cl_{11}$	(i) m.p. = 345°C* (ii) m.p. = 360°C* (iii) (iv) IR (cm^{-1}):ν(U–Cl) = 250w, 263, 286w (v) green cryst.; m.p. 670°C (vi) m.p. = 407°C; ΔH^o_{fus} = 35.4 (2.1) (vii) (viii) m.p. = 560°C (ix) m.p. = 382°C* (x) m.p. = 406.3°C (xi) (xii) (xiii)		*thermodynamic and IR data* (Brown, 1979; Suglobova and Chirkst, 1978a, Vdovenko *et al.*, 1974b; Fuger *et al.*, 1983); *magnetic properties* (Brown, 1979)
$UOCl_2$	green; moisture sensitive; insoluble in organic solvents; soluble in H_2O; b.p.>400°C; $UOCl_2$(cr): $\Delta_f G^o_m$ = –998.5 (2.7)†, $\Delta_f H^o_m$ = –1069.3 (2.7)†, S^o_m = 138.32 (0.21)†; $C^o_{p,m}$ = 95.06 (0.42)†; paramagnetic $\mu_{eff.}$ = 3.13 B.M. (above 40 K); exhibits magnetic ordering below 31 K	orthorhombic; D^9_{2h}, *Pbam*, No.55; a = 15.255, b = 17.828, c = 3.992; d(U(1)–O) = 2.20–2.40; d(U(1)–Cl) = 2.66–3.15; d(U(2)–O) = 2.17–2.33; d(U(2)–Cl) = 2.88–3.01; d(U(3)–O) = 2.22–2.35; d(U(3)–Cl) = 2.70–3.51; the arrangement around U(1) is dodecahedral (CN = 8; 3O, 5Cl); that around U(2) is trigonal (CN = 7; 3O, 4Cl) and that around U (3) is approx. dodecahedral-1 (C.N. = 7; 3O, 4Cl)	*crystallographic data, neutron diffraction data* (Bagnall *et al.*, 1968; Taylor and Wilson, 1974a); *infrared spectra* (Bagnall *et al.*, 1968) *thermodynamic data* (Brown, 1979; Grenthe *et al.*, 1992;Guillaumont *et al.*, 2003); *magnetic properties, ir spectra* (Levet.and Noël, 1979); *photoelectron spectra* (Thibaut *et al.*, 1982)
UNCl		tetragonal; D^7_{4h}, *P4/nmm*, No.129; a = 3.979, c = 6.811; Z = 2; V = 107.83; d(calc.) = 8.85; d(exp) = 8.78. The compound is isostructural with PbFCl;	*crystallographic data* (Juza and Sievers, 1965; Juza and Meyer, 1969; Yoshihara *et al.*, 1971)

Table 5.26 (*Contd.*)

Formula	*Selected properties and physical constants*[b]	*Lattice symmetry, lattice constants* (Å), *conformation and density* (g cm^{-3})[c]	*Remarks regarding information available and references*
		d(U–Cl_1) = 3.17 (4×); d(U–N) = 2.30; d(Cl_1–Cl_1) = 3.98; d(Cl_1–Cl_2) = 3.23; d(N–Cl) = 3.29; d(N–N) = 2.81	
$UClF_3$	emerald green cryst.; m.p. = 444°C*; b.p. = 550–650°C (in vacuo subl.) $UClF_3$(cr): $\Delta_f G^o_m$ = –1606 (5.)†, $\Delta_f H^o_m$ = –1690 (5)†, S^o_m = 185.4 (4.2)†; $C^o_{p,m}$ = 120.9 (4.2)†	orthorhombic; *Abam* or C^{17}_{2v}, *Aba*2, No.41; a = 8.673(2), b = 8.69(1), c = 8.663(5); Z = 8; d(calc.) = 6.72	*crystallographic data* (Savage, 1956; Staritzky and Douglass, 1956); *thermodynamic data; fused salt system* (Brown, 1979; Grenthe *et al.*, 1992; Guillaumont *et al.*, 2003)
other chloride fluorides: (i) UCl_2F_2, (ii) UCl_3F.	(i) green; m.p. = 460°C*. UCl_2F_2(cr): $\Delta_f G^o_m$ = –1376(6)†, $\Delta_f H^o_m$ = –1466 (5)†, S^o_m = 174.1 (8.4)†; $C^o_{p,m}$ = 119.7 (4.2)†. (ii) m.p. = 530°C*; UCl_3F(cr): $\Delta_f G^o_m$ = –1147(5)†, $\Delta_f H^o_m$ = –1243 (5)†, S^o_m = 162.8 (4.2)†; $C^o_{p,m}$ = 118.8(4.2)†		*thermodynamic data; fused salt system* (Brown, 1979; Grenthe *et al.*, 1992; Guillaumont *et al.*, 2003)
UBr_4	brown to black-brown cryst; moisture sensitive; soluble in Me_2CO, EtOH; m.p. = 519°C; b.p. = 777°C; sublimes in a Br_2-N_2 stream. $\mu_{eff.}$ = 3.12 B.M; θ = –35 K; (77–569 K)[d] . UBr_4(cr): $\Delta_f G^o_m$ = –767.4 (3.5)†, $\Delta_f H^o_m$ = –802.1 (2.5)†, S^o_m = 238.5 (8.4)†; $C^o_{p,m}$ = 128.0 (4.2)†. UBr_4(g): $\Delta_f G^o_m$ = –634.6 (5.0)†, $\Delta_f H^o_m$ =	monoclinic; C^3_{2h}, *C*2/*m*, No.12; a = 10.92(2), b = 8.69(3), c = 7.05(1); β = 93.9(1); Z = 4; d(calc.) = 5.55, d(exp.) = 5.35. The Br anions form a pentagonal bipyramid around the U atom. The bipyramids are linked into two-dimensional sheets by double bromide bridging of the U cations. d(U–Br) = 2.85(2) to 2.95(2)	*synthesis* (Brauer, 1981) *crystallographic data* (Douglass and Staritzky, 1957; Taylor and Wilson, 1974d,e; Levy *et al.*, 1975; Korba, 1983); *thermodynamic data;* (Grenthe *et al.*, 1992; Guillaumont *et al.*, 2003); *magnetic data* (Dawson, 1951; Hendricks, 1971); *photoelectron spectra* (Thibaut *et al.*, 1982)

	–605.6 (4.7)†, S^o_m = 451.9 (5.0)†; $C^o_{p,m}$ = 106.9 (3.0)†. log*p* (mmHg) = –10800 T^{-1} +23.15–3.02 log*T* (298–792 K) log *p* (mmHg) = –8770 T^{-1} + 27.93 – 5.53 log*T* (792–1050 K); Energy level parameters: F_2 = 191, F_4 = 34, F_6 = 4, ζ_{5f} = 1976, $A(r^4)$ = –490 and $A(r^6)$ = –15 (in cm^{-1}); ν_{U-Br} = 233 cm^{-1} (vapor)	(in the pentagonal ring) and 2.78 (3) and 2.61(4) (to the apical bromides); the axial Br–U–Br angle = 177(1)°	
$[UBr(H_2O)_8]Br_3(H_2O)$		triclinic; C_i^1, $P\bar{1}$, No.2; *a* = 8.234 (4), *b* = 12.781(7), *c* = 7.168(2), α = 97.76(3), β = 98.36(2)° γ = 85.38(4); *Z* = 2; *V* = 738.07; *d*(calc.) = 3.24	*crystallographic data* (Rabinovich *et al*., 1998)
Li_2UBr_6		trigonal/rhombohedral; D^2_{3d}, $P\bar{3}1c$; No = 163; *a* = 6.8896(4), *c* = 12.6465(9); γ = 120; *Z* = 2; *V* = 519.86	*crystallographic data; phase transitions by neutron diffraction* (Maletka *et al*., 1998)
Na_2UBr_6	m.p. = 533°C; ν(U–Br)as. = 164w, 180, 202w	trigonal/rhombohedral; D^3_{3d}, $P\bar{3}m1$; No. = 164; *a* = 12.4368(1), *c* = 6.6653(2); *V* = 892.83; *Z* = 3	*crystallographic data* (Vdovenko *et al*., 1973b; Bogacz *et al*., 1980); *thermodynamic data* (Vdovenko *et al*., 1973a, 1974c; Fuger *et al*., 1983); *Visible and, IR data* (Brown, 1979; Suglobova and Chirkst, 1978)
K_2UBr_6	m.p. = 672°C; ν(U–Br)as. = 185, 208w	trigonal; *a* = 10.94, *c* = 10.67; *d*(calc.) = 4.11, *d*(exp.) = 4.12	*crystallographic data* (Vdovenko *et al*., 1973b); *thermodynamic data* (Vdovenko *et al*., 1973a, 1974c; Fuger *et al*., 1983); *Visible and IR data* (Suglobova and Chirkst, 1978a; Brown, 1979)

Table 5.26 (*Contd.*)

Formula	*Selected properties and physical constants*[b]	*Lattice symmetry, lattice constants* (Å), *conformation and density* (g cm^{-3})[c]	*Remarks regarding information available and references*
Rb_2UBr_6	m.p. = 722°C[*]; ν(U–Br)as. = 192	cubic face centered; O_h^5, $Fm\bar{3}m$, No.225; $a = 10.94$; $V = 1309.34$. The U atoms are surrounded by an octahedral array of Br atoms at distances of 2.74; d(calc.) = 4.48, d(exp.) = 4.048	*crystallographic data* (Vdovenko *et al.*, 1973a; Maletka *et al.*, 1996b); *thermodynamic data* (Vdovenko *et al.*, 1973a, 1974c; Fuger *et al.*, 1983); *visible-near IR data* (Suglobova and Chirkst, 1978a; Brown, 1979)
Cs_2UBr_6	m.p. = 756°C; vibrational modes (cm^{-1}): ν_1(R) = 197, ν_2(R) = (155), ν_3(IR) = 195, ν_4 = (IR) = 84, ν_5(R) = 87, $L = 5$; $F_2 = 84.112$, $F_4 = 35.542$, $F_6 = 3.818$, $\zeta_{5f} = 1792.306$, $B_0^4 = 6593$, $B_0^6 = 1195$	cubic face centered; O_h^5, $Fm\bar{3}m$, No.225; $a = 11.07$; $V = 1356.57$. The U atoms are surrounded by an octahedral array of Br atoms at distances of 2.767; d(Br–Br) = 3.914; d(calc.) = 4.78, d(exp.) = 4.74	*crystallographic data*, (Vdovenko *et al.*, 1973a); *thermodynamic data* (Vdovenko *et al.*, 1973a, 1974c; Fuger *et al.*, 1983); *visible and IR spectral data* (Johnston *et al.*, 1966; Chodos, 1972; Suglobova and Chirkst, 1978a; Brown, 1979); *crystal-field analysis* (Johnston *et al.*, 1966)
UNBr		tetragonal; D_{4h}^7, $P4/nmm$, No.129; $a = 3.944$, $c = 7.950$; $Z = 2$; d(calc.) = 8.913; d(exp.) = 8.64; The compound is isostructural with BiOCl; d(U–Br) = 3.234; d(U–N) = 2.280	*crystallographic data*; (Juza and Meyer, 1969)
$[N(CH_3)_4]_2UBr_6$	vibrational modes (cm^{-1}): ν_3(IR) = 181; ν(U–Br) = 190–195	cubic face centered; O_h^5, $Fm\bar{3}m$, No.225; $a = 13.37$; d(calc.) = 2.405	*crystallographic data* (Brown, 1966)
$[N(C_2H_5)_4]_2UBr_6$	IR (cm^{-1}): ν(U–Br) = 178; energy level parameters: $F_2 = 181.63(12)$ (or $F^2 = 40867$), $\zeta_{5f} = 1756(41)$, $B_0^4 = 6946(609)$, $B_0^6 = 999(252)$; *rms* = 176		*IR and energy level analyses* (Brown, 1966; Wagner *et al.*, 1977)

$[P(C_6H_5)_3C_2H_5]_2UBr_6$		monoclinic; C_{2h}^2, $P2_1/m$, No.11; $a = 10.45(1)$, $b = 13.51(1)$, $c = 15.46(1)$; $\beta = 96.67(5)$; $Z = 2$; d(calc.) = 1.990, d(exp). = 1.96; d(U–Br): = 2.757(2), 2.776 (2) and 2.777(2)	*crystallographic data* (Caira *et al.*, 1978)
$[P(C_6H_5)_4]_2[UBr_6]\cdot 4CH_3CN$	green crystals; extremely sensitive towards oxygen and moisture	monoclinic; C_{2h}^5, $P2_1/c$, No.14; $a = 9.818(3)$, $b = 20.101(4)$, $c = 15.493(3)$, $\beta = 98.79(2)$; $Z = 2$; $V = 3022$; d(calc.) = 1.72; d(U–Br1) = 2.754 (1); d(U–Br2) = 2.778(1); d(U–Br3) or O = 2.768(1); Br(1)–U–Br(2) = 89.2(1); Br(1)–U–Br(3) (or O) = 90.4(1); Br(2)–U–Br(3) (or O) = 89.6(1).	*synthesis and crystallographic data* (Bohrer *et al.*, 1988)
$UBr(PO_2H_2)_3\cdot 2H_2O$		orthorhombic; D_{2h}^{11}, *Pbcm*, No. 57; $a = 7.488(5)$, $b = 10.192(2)$, $c = 15.203(5)$; $Z = 2$; $V = 1160.26$.	*X-ray crystallographic and spectroscopic structural studies* (Tanner *et al.*, 1993)
$UBr(PO_4)(H_2O)_2$		tetragonal; C_{4h}^5, $I4/m$, No.87; $a = 14.7480(7)$, $c = 6.6810(4)$; $V = 1453.14$; $Z = 8$; d(calc.) = 4.1.	*crystallographic data* (Benard-Rocherulle *et al.*, 1997)
$UBrCl_3$	greenish brown; hygroscopic; m.p. = 521°C; b.p. = 784°C; $UBrCl_3$(cr): $\Delta_f G_m^o = -893.5\ (9.2)^\dagger$, $\Delta_f H_m^o = -967.3\ (8.4)^\dagger$, $S_m^o = 213.4\ (12.6)^\dagger$	tetragonal; $a = 8.434$, $c = 7.690$	*thermodynamic data* (MacWood, 1958; Brown, 1979; Grenthe *et al.*, 1992; Guillaumont *et al.*, 2003)
UBr_2Cl_2	dark green; hygroscopic; m.p. = 510°C; b.p. = 1053 °C; UBr_2Cl_2 (cr): $\Delta_f G_m^o = -850.9\ (9.8)^\dagger$, $\Delta_f H_m^o = -907.9\ (8.4)^\dagger$, $S_m^o = 234.3\ (16.7)^\dagger$		*thermodynamic data* (MacWood, 1958; Brown, 1979; Grenthe *et al.*, 1992; Guillaumont *et al.*, 2003)
UBr_3Cl	greenish brown; hygroscopic; m.p. = 502°C; b.p. = 774°C UBr_3Cl(cr): $\Delta_f G_m^o = -807.1\ (9.8)^\dagger$, $\Delta_f H_m^o = -852.3\ (8.4)^\dagger$, $S_m^o = 238.5\ (16.7)^\dagger$		*thermodynamic data* (MacWood, 1958; Brown, 1979; Grenthe *et al.*, 1992; Guillaumont *et al.*, 2003)

Table 5.26 (*Contd.*)

Formula	*Selected properties and physical constants*[b]	*Lattice symmetry, lattice constants* (Å), *conformation and density* (g cm^{-3})[c]	*Remarks regarding information available and references*
$UOBr_2$	greenish yellow: $UOBr_2$(cr): $\Delta_f G^o_m$ = –929.6 (8.4)†, $\Delta_f H^o_m$ = –973.6 (8.4)†, S^o_m = 157.57 (0.29)†; $C^o_{p,m}$ = 98.0 (0.4)†		*thermodynamic data* (Greenberg and Westrum, 1956; Rand and Kubaschewski, 1963; Brown, 1979; Grenthe *et al.*, 1992; Guillaumont *et al.*, 2003); *photoelectron spectra* (Thibaut *et al.*, 1982)
UI_4	black lustrous crystals; moisture sensitive; m.p. = 506°C; density: 5.6 g cm^{-3}; m.p. = 506°C; b.p. = 757°C; $\mu_{eff.}$ = 2.98 B.M; (1–300 K)[d] . UI_4(cr): $\Delta_f G^o_m$ = –512.7 (3.8)†, $\Delta_f H^o_m$ = –518.3 (2.8)†, S^o_m = 263.6 (8.4)†; $C^o_{p,m}$ = 126.4 (4.2)†. UI_4(g): $\Delta_f G^o_m$ = –369.6 (6.2)†, $\Delta_f H^o_m$ = –305.0 (5.7)†, S^o_m = 499.1 (8.0)†; $C^o_{p,m}$ = 108.8 (4.0)†. log p (mmHg) = –12330 T^{-1} + 26.62 – 3.52 log$T$ (298–779 K), log p (mmHg) = –9310 T^{-1} + 28.57 – 5.53 log$T$ (779–1030 K): IR data (cm^{-1}): 178m, 165s, 132,s, 122m, 104vw, 92m, 55m	monoclinic; C^6_{2h}, $C2/c$, No. 15; a = 13.967(6), b = 8.472(4), c = 7.510 (3); β = 90.54(5); Z = 4; V = 888.7; d(calc.) = 5.57. Close-packed hexagonal iodine atoms form zigzag chains of edge-sharing octahedra ($UI_2I_{4/2}$). d(U–I(1) bridging) = 3.08(2) and 3.11(2); d(U-I(2) terminal) = 2.92(2)(2×); d(U—U) = 4.55	*crystallographic and neutron diffraction data* (Levy *et al.*, 1980, Taylor, 1987); *thermodynamic data*; (Fuger and Brown, 1973; Brown, 1979; Guillaumont *et al.*, 2003)
Li_2UI_6		trigonal/rhombohedral; D^2_{3d}, $P\bar{3}1c$, No. = 163; a = 7.3927(8), c = 13.826(2); V = 654.39; Z = 2; d(U–I) = 3.013	*neutron diffraction and electrical conductivity data* (Maletka *et al.*, 1996a)

Na_2UI_6		trigonal/rhombohedral; C_{3i}^2, $R\bar{3}$, No.148; $a = 7.7001(6)$, $c = 20.526$; $Z = 3$; $V = 1053.97$; d(U–I) = 2.992	*crystallographic data* (Maletka *et al*., 1992, 1995)
$EuUI_6$		monoclinic; C_s^4, Cc, No.9; $a = 8.006(4)$, $b = 12.998(5)$, $c = 15.194(5)$; $\beta = 106.2(1)$; $V = 1518.34$; $Z = 4$; d(U–I) = 3.035 to 3.218	*X-ray powder diffraction data* (Beck and Kuehn, 1995)
$BaUI_6$		monoclinic; C_s^4, Cc, No.9; $a = 8.845(5)$, $b = 13.834(7)$, $c = 15.753(8)$; $\beta = 107.5(1)$; $V = 1838.35$; $Z = 4$; d(U–I) = 3.164 to 3.241	*X-ray powder diffraction data* (Beck and Kuehn, 1995)
M_2UI_6 (M = N$(C_2H_5)_4$, N$(C_4H_9)_4$, N$(C_6H_5)(CH_3)_3$, As$(C_6H_5)_4$).	red; extremely moisture sensitive; soluble in anhydrous methyl cyanide and acetone; vibrational mode in (cm^{-1}) UI_6^{2-}: $\nu_1 = 143$ to 156; $\nu_2 = 119$, $\nu_3 = 135$ to 143; $\nu_4 = 60$ to 65, $\nu_5 = 62$ to 66; $\nu_6 = 44$ to 47; energy level parameters for $[N(C_2H_5)_4]_2UI_6$: $F^2 = 38188$ (2422), $\zeta_{5f} = 1724(39)$, $B_0^4 = 6338(676)$, and $B_0^6 = 941$ (289)		*electronic and IR spectra; crystal-field analysis; magnetic susceptibility data* (Wagner *et al*., 1977; Brown, 1979)
UOI_2	rose-brown cryst; decomposes slowly at room temp; hygroscopic; soluble in H_2O; U–O vibrations (cm^{-1}): 520(w), 475(m), 420 (m), 280(w), and 250(sh); paramagnetic; $\mu_{eff.} = 3.34$ B.M	orthorhombic; D_{2h}^9, *Pbam*, No.55; isostructural with $UOCl_2$ ($PaOCl_2$ struct. type); $a = 17.853(5)$, $b = 20.05(2)$, $c = 4.480(5)$	*crystallographic data; magnetic susceptibility data, infrared spectra* (Levet and Noël, 1979)
UNI		tetragonal; D_{4h}^7, *P4/nmm*, No.129; $a = 3.990$, $c = 9.206$; $Z = 2$;	*crystallographic data*; (Juza and Meyer, 1969)

Table 5.26 (*Contd.*)

Formula	*Selected properties and physical constants*[b]	*Lattice symmetry, lattice constants* (Å), *conformation and density* (g cm^{-3})[c]	*Remarks regarding information available and references*
		$V = 146.56$; d(calc.) = 8.58; d(exp) = 8.50; isostructural with BiOCl	
(i) UF_3I; (ii) $UClI_3$; (iii) UCl_2I_2; (iv) UCl_3I; (v) $UBrI_3$; (vi) UBr_2I_2; (vii) UBr_3I; (viii) UCl_2BrI; (ix) $UClBr_2I$.	(i) brownish black; (ii) black, m.p.<500°C; $UClI_3$ (cr): $\Delta_f G^o_m = -615.8\ (11.4)^\dagger$, $\Delta_f H^o_m = -643.8\ (10.0)^\dagger$, $S^o_m = 242\ (18)^\dagger$; (iii) black, m.p.<500°C; UCl_2I_2 (cr): $\Delta_f G^o_m = -723.4\ (11.3)^\dagger$, $\Delta_f H^o_m = -768.8\ (10.0)^\dagger$, $S^o_m = 237\ (18)^\dagger$; (iv) black, m.p.<490°C, UCl_3I(cr): $\Delta_f G^o_m = -829.9\ (8.8)^\dagger$, $\Delta_f H^o_m = -898.3\ (8.4)^\dagger$, $S^o_m = 213.4\ (8.4)^\dagger$; (v) black, m.p.<500°C $UBrI_3$(cr): $\Delta_f H^o_m = -589.6\ (10.0)^\dagger$;		*thermodynamic data*, (MacWood, 1958; Brown, 1979; Grenthe *et al*., 1992; Guillaumont *et al*., 2003)

(vi) dark, brown; m.p.<500°C
UBr_2I_2 (cr): $\Delta_f H_m^o = -660.4$ (10.0)†;
(vii) dark brown, m.p. 478°C,
UBr_3I $\Delta_f H_m^o = -727.6$ (8.4)†,
sublimes without decomposition;
(viii) black, m.p. < 500°C;
(ix) black, m.p. < 500°C.

---

* Peritectic decomposition point.

† Values recommended by the Nuclear Energy Agency (Guillaumont *et al.*, 2003) .

[a] Values have been selected in part from review articles (Brown, 1979, Bacher and Jacob, 1980; Freeman,1991; Grenthe *et al.*,1992; Guillaumont *et al.*, 2003);

[b] m.p. = melting point (°C); b.p(°C). = boiling point; (cr) = crystalline; (g) = gaseous; thermodynamic values in kJ mol^{-1}, or J $K^{-1}mol^{-1}$ at 298.15 K, unless otherwise mentioned; $\Delta_f G_m^o$, standard molar Gibbs energy of formation; $\Delta_f H_m^o$– standard molar enthalpy of formation; S_m^ostandard molar entropy; $C_{p,m}^o$, standard molar heat capacity; log p (mm Hg) $= -AT^{-1} + B - C \log T$: vapour pressure equation for indicated temperature range; IR = infrared active; L = lattice vibrations; val. = valence vibrations; def. = deformation vibrations; all values in cm^{-1}; s:strong; m: medium; w: weak; sh: shoulder; Energy levels parameters: F_k, F^k, ζ_{5f} = electrostatic and spin–orbit interaction parameters; α, β, γ; = two-body correction; M^j ($j = 0$, 2 and 4) = spin-spin and spin-other-orbit relativistic corrections; P^k = the electrostatically correlated spin-orbit perturbation parameters; B_q^k = crystal-field parameters; values in brackets indicate parameter errors; standard deviation: $rms = \sum \left[(\Delta_i)^2/(n-p)\right]^{1/2}$[$cm^{-1}$], where Δ_i is the difference between the observed and calculated energies, n is the number of levels fitted and p is the number of parameters freely varied.

[c] All values are in Å and angles are in degrees; CN, coordination number; d represents density in g cm^{-3}, V = molar volume [cm^3 mol^{-1}].

[d] Temperature range with linear relationship of χ_M^{-1} against T.

with arsine oxides or phosphine oxides (du Preez *et al*., 1977b; du Preez and Zeelie, 1987).

Tetravalent uranium has a [Rn]$5f^2$ electronic configuration. The ground state is nominally $^3H_4$. The earlier studies of absorption spectra of tetravalent halides in the solid state, aqueous solutions, organic solvents, and in doped host crystals have been compiled in a review article by Carnall (1982). Krupa (1987) analyzed the spectroscopic properties of the ions in solids with their characteristic $5f^2 \rightarrow 5f^2$ transitions. In contrast to the uranium(III) spectra, the spin–orbit interactions in different compounds are of the same order of magnitude and the f–d transitions have been observed at higher energies beginning near 40000–45000 cm^{-1}. For a number of halides and complex halides, low-temperature absorption spectra have been recorded and the energy levels of the U^{4+} ion in different site symmetries were assigned and fitted to a semiempirical Hamiltonian representing the combined atomic and crystal-field interactions. An analysis of octahedral UX_6^{2-} spectra for a series of $(NEt_4)_2UX_6$ salts (X = F, Cl, Br or I) was reported by Wagner *et al*. (1977). The authors have noticed that the Slater parameter F^2 diminishes by ~20% for the series and the crystal-field parameters are different from those of the comparable octahedral PaX_6^{2-} and UX_6^{2-} halides. Analyses of the energy-level structure of U^{4+} ion doped in an isomorphic series of tetragonal ($I4_1/amd$) host crystals such as $ThSiO_4$, $ThCl_4$, and $ThBr_4$ (Delamoye *et al*., 1983; Simoni *et al*., 1988; Malek *et al*., 1986a,b; Malek and Krupa, 1994) led to consistent sets of free ion and crystal-field parameters with a least square deviation (r.m.s.) between 36 and 71 cm^{-1}. In these host crystals, U^{4+} experiences a rather weak crystal field, which justifies the same theoretical approach as for the Ln^{3+} ions; this is in contrast to that in higher symmetry sites as found in $U(BD_4)_4/Hf(BD_4)_4$ (site symmetry T_d; Rajnak *et al*., 1998), Cs_2UX_6 (X = Cl or Br) (site symmetry O_h; Johnston *et al*., 1966; Satten *et al*., 1983) or U^{4+}: $CsCdBr_3$ (disturbed O_h site symetry; Karbowiak *et al*., 2005b) where the crystal field splitting is approximately twice as large with the r.m.s. deviation of 100 to 150 cm^{-1}. As a result, mixing of crystal field components of different multiplets in close proximity may occur. In an analysis of the absorption spectrum of Cs_2UBr_6 single crystals, Faucher *et al*. (1996) have shown that the inclusion of configuration interactions with the higher lying $5f^17p^1$ electronic configuration in the fitting procedure may considerably improve the r.m.s. deviation.

An analysis of (U^{4+}, U^{3+}):BaY_2Cl_7 single crystals (Karbowiak *et al*., 2003b) enabled the assignment of 60 observed $5f^2 \rightarrow 5f^2$ transitions from absorption, excitation, and luminescence spectra, which encompasses all but the $^1S_0$ multiplet. A comparison of the scalar crystal field parameters,

$$N_v = \left[\sum_{k,2} (B_2^k)^2 \frac{4\pi}{(2k+1)}\right]^{1/2}$$

(Auzel and Malta, 1983), indicates that the main factor determining the crystal-field strength is not the nature of the ligand but the site symmetry of the central ion; this is in contrast to that for Ln^{3+} and U^{3+} ions. Energy transfer has been demonstrated between uranium ions in the 3+ and 4+ oxidations states. A very strong anti-Stokes emission was observed for the U^{4+} ions.

In all cases in which the uranium ions are occupying sites of inversion symmetry, as in UCl_6^{2-}, the observed band structure consists almost exclusively of vibronic side bands and their progressions could be used to deduce the electronic transitions. The analysis of absorption spectra of UF_4 in a KBr pellet at 4 K as well as of U^{4+}(aq.) at 298 K have been reported by Cohen and Carnall (1960) and Carnall *et al.* (1991). The authors have also compared the crystal-field interactions of UF_4, NpF_4, and PuF_4. The absorption spectrum of thin films of a mixture of UF_4 with chlorinated naphthalene (refraction index 1.635) at 7 K is shown in Fig. 5.40 (Drożdżyński and Karbowiak, 2005) and is typical for most uranium(IV) compounds. In this region the spectra consist of relatively intense and sharp absorption lines. The intra-configurational $5f^3 \rightarrow 5f^3$ transitions result in 91 non-degenerated crystal field levels.

Magnetic susceptibility measurements have been carried out over wide temperature ranges for almost all halides and complex halides. The paramagnetic constants from the Curie–Weiss law $\chi'_m = C/(T - \theta)$ and the effective magnetic moments ($\mu_{eff} = 2.84\sqrt{c}\mu_{B+}$) for some of the compounds are collected in Table 5.26. Hexachloro uranates(IV) show temperature-independent paramagnetism between 4 and 300 K with $\chi_M = 2000 \times 10^{-6}$ emu.

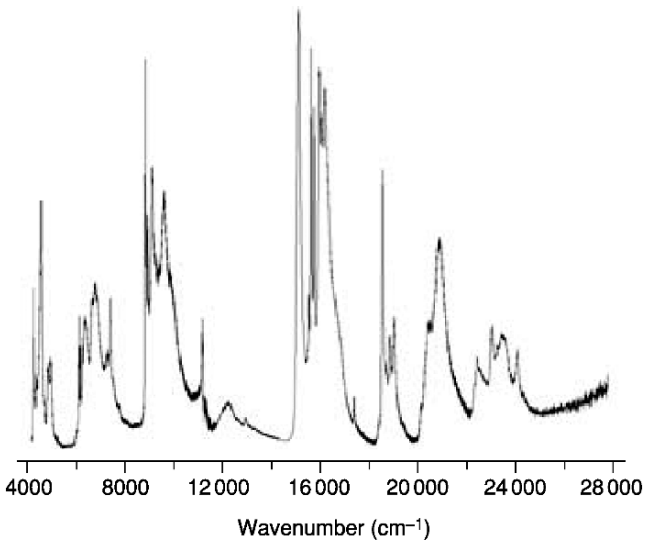

Fig. 5.40 *Absorption spectrum of thin films of a mixture of UF_4 with chlorinated naphthalene at* 7 K (*Drożdżyński and Karbowiak*, 2005).

(*i*) *Uranium tetrafluoride and complex uranium(IV) fluoro compounds*

Uranium tetrafluoride

Uranium tetrafluoride has important industrial applications in the conversion of uranium ore to UF_6 and in the production of UO_2. The former is a key compound in the uranium enrichment process and UO_2 is a nuclear fuel. The usefulness of UF_4 in these two processes depends on its large chemical stability and an almost complete insolubility in aqueous solutions. Fluoride melts containing UF_4 have also proved to be suitable in 'homogeneous reactors'. The preparation of UF_4 has been extensively investigated (Brown, 1968, 1979; Bacher and Jacob, 1980; Freestone and Holloway, 1991). Most of the procedures are based either on precipitation from aqueous solutions or on high-temperature reactions in anhydrous conditions. In the first method, aqueous uranyl solutions are reduced to U(IV) by $SnCl_2$, $Na_2S_2O_4$, $FeSO_4$, CuCl, $CrCl_3$, $TiCl_3$, and SO_2 (combined with Cu^{2+}ions), or electrochemically; after reduction, two hydrates, $UF_4 \cdot 2.5H_2O$ and $UF_4 \cdot nH_2O$, with $0.5 < n < 2$, are obtained by precipitation with F^- (Allen *et al.*, 1950; Anderson *et al.*, 1950; Dawson *et al.*, 1954). The preparation from aqueous solutions based on electrolytic reductions of uranyl solutions has found industrial application in the Excer Process (ion exchange conversion, electrolytic reduction (Higgins and Roberts, 1956; Marinsky, 1956; Bacher and Jacob, 1980).

Since it is difficult to remove water without hydrolytic reactions, UF_4 produced by aqueous processes is not suitable for reduction to metal or for conversion to UF_6. Consequently, it has been customary to prepare UF_4 by high-temperature reactions. One of the most convenient methods to produce UF_4 on a large scale employs heating of UO_2 in an excess of anhydrous HF at 400–600°C.

$$UO_2 + 4HF \overset{550°C}{\rightarrow} UF_4 + 2H_2O$$

This and similar methods result in the formation of a highly reactive form of the dioxide. If the starting material is a non-stoichiometric oxide, it is essential to insert H_2 in order to avoid reactions such as:

$$U_3O_8 + 8HF \rightarrow 2UO_2F_2 + UF_4 + 4H_2O$$

Ruehle (1959) describe the synthesis of UF_4 using a stirred fluidized-bed hydrofluorination reactor. The chemistry of the reaction has been discussed by Dawson *et al*. (1954).

On a large scale the compound may be prepared by thermal decomposition of $UO_4 \cdot 2H_2O$ to UO_3 at 250°C followed by reduction with hydrogen to UO_2 at 600°C and fluorination to UF_4 with NH_4HF_2 at 150°C (Van Impe, 1954). Alternatively, UF_4 may be obtained in a similar route using uranium(IV) acetate or by reaction of UO_2 with SF_4 at 500°C.

Other satisfactory methods involve the direct reduction of UO_3 to UF_4 by ammonia–hydrogen fluoride mixtures at 500–750°C and by NH_4F, NH_4HF_2, or

a mixture of NH_4HF_2 and hydrazine fluoride. Also various freons, in particular, CF_2Cl_2, are useful fluorinating agents for UO_2, UO_3, and $(NH_4)_3U_4O_{16}F_3$ (Evers and Reynolds, 1954; Van Impe, 1954).

Attractive alternatives for the preparation of smaller amounts include the heating of metallic uranium with anhydrous hydrogen fluoride in a sealed tube at 225–250°C and treating UH_3 or uranium with hydrogen fluoride vapours at 250–350°C or with a mixture of $H_2 + HF$ at 250°C (Brown, 1979).

Since UF_6 is the starting material for ^{235}U enrichment, it is also a convenient preparatory material for enriched metallic uranium via uranium tetrafluoride. The preparation of UF_4 from UF_6 may be performed by:

(i) reduction with H_2 in the gaseous phase (Smiley and Brater, 1958, 1960; Bacher and Jacob, 1980)

$$UF_6 + H_2 \overset{630°C}{\rightarrow} UF_4 + 2HF$$

(ii) reduction with chlorinated hydrocarbons C_2HCl_3, C_2Cl_4, and CCl_4 (Bacher and Jacob, 1980, 1986)

$$UF_6 + 2CCl_4 \xrightarrow{200°C,\ p=29\ bar} UF_4 + 2CCl_3F + Cl_2$$

(iii) the reaction with Me_3SiX (Brown *et al.*, 1983)

$$UF_6 + 2Me_3SiX \rightarrow 2Me_3SiF + X_2 + UF_4 (X = Cl \text{ or } Br)$$

On technical scale the reaction (i) may be performed either in a 'hot-wall reactor', by heating the outside wall of the reactor up to 650°C, or in a 'cold-wall reactor' in which the energy is supplied by the reaction

$$F_2 + H_2 \rightarrow 2HF$$

The temperature of the reactor wall is kept between 150 and 200°C. In order to achieve a complete conversion in the reactions (ii) and (iii), a substantial excess of CCl_4 and a molar ratio 1:2 of UF_6 to Me_3SiX is essential (Bacher and Jacob, 1980; Hellberg and Schneider, 1981).

Uranium tetrafluoride is an emerald-green high melting polymeric solid, entirely insoluble in water. However it may be dissolved in the presence of reagents that can form fluoride complexes, such as Fe^{3+}, Al^{3+}, or boric acid, for example. It is a good starting material for the synthesis of UF_6 and production of uranium metal by reduction with calcium or magnesium. The reduction may also be performed with Li, La, or Al whereas Zr, Be, Ti, or hydrogen leads to uranium trifluoride. The compound is stable in air at room temperature, which makes it useful as an intermediate product in the conversion of uranium ore to UF_6. For sublimation *in vacuo*, a stainless steel tube with a molybdenum liner has been used (Dawson *et al.*, 1954). Uranium tetrafluoride reacts with strong oxidizing reagents such as Ce^{4+}, concentrated perchloric acid, nitric acid and, nitric acid–boric acid or sulphuric acid–ammonium persulphate mixtures with the formation of the appropriate uranyl salt solutions.

UF_4 is monoclinic, with the same structures as those of zirconium and hafnium tetrafluorides. The structure at different temperatures has been examined in detail by Kern *et al.* (1994), using neutron diffraction on polycrystalline samples. The unit cell of UF_4 contains 12 formula units with four (U1) and eight (U2) sites having C_2 symmetry. Each uranium atom has eight fluorine neighbors arranged in a slightly distorted square antiprism. A basic repeating unit of five uranium atoms is arranged in a slightly distorted pyramid. Four of them are forming a rhomb-shaped base, and the fifth comprises the apex of the pyramid. For other details see Table 5.26.

The thermodynamic properties of UF_4 have been analyzed in detail by Rand and Kubaschewski (1963), Kubaschewski and Alcock (1979), and Fuger *et al.* (1983). The heat capacity from 1.3 to 20 K has been measured by Burns *et al.* (1960) and between 5 and 300 K by Osborne *et al.* (1955).

Carnall *et al.* (1991) have reported an analysis of the low-temperature crystal-field absorption spectrum of UF_4. The authors found a good agreement between the experimentally observed and calculated band structure using an effective Hamiltonian with orthogonalized free-ion operators. The initial crystal-field parameter values were calculated on the basis of a superposition model for An^{4+} sites with C_2 symmetry. The values obtained are listed in Table 5.26. The parameters have been obtained in a fit of 69 observed crystal-field levels of UF_4; the r.m.s. error is 31 cm^{-1}. The spin–spin and spin–orbit parameters, $M^0 = 0.775$, $M^2 = 0.434$, and $M^4 = 0.294$, were assigned on the basis of *ab initio* calculations and were not varied in the fitting. The electrostatically correlated spin–orbit perturbation parameters P^4 and P^6 were constrained by keeping the ratios P^4/P^2 and P^6/P^2 constant, equal to 0.5 and 0.1, respectively. The magnitude of the total crystal-field strength expressed by the scalar parameter N_v (Auzel and Malta, 1983), is equal to 2700 (assuming the C_{2v} approximation).

Uranium tetrafluoride hydrates

The reaction of U(IV) solutions with 4–20% aqueous fluoride solutions results in the precipitation of $UF_4 \cdot 2.5H_2O$. A number of hydrates with smaller water content, $UF_4 \cdot nH_2O$ (where $0.5 < n < 2$), was obtained by controlled thermal decomposition. $UF_4 \cdot 2.5H_2O$ is the most stable one: in vacuum up to 25°C and in air up to 100°C. The compound may be converted to $UF_4 \cdot 0.5H_2O$ at 100–120°C with the maintenance of its structure. A complete dehydration occurs at 500–550°C in a stream of N_2 or HF. However, it still retains some of the structure of $UF_4 \cdot 2.5H_2O$ and, contrary to UF_4, it may be readily rehydrated to $UF_4 \cdot 2.5H_2O$. All UF_4 hydrates with lower water content may also be gradually converted back to this stable form. The solubility of $UF_4 \cdot 2.5H_2O$ in water is 0.1 $g \cdot L^{-1}$ (Bacher and Jacob, 1980).

$UF_4 \cdot 2.5H_2O$, $UF_4 \cdot 2H_2O$, and $UF_4 \cdot 4/3H_2O$ have orthorhombic *Pnma*, cubic $Fm\bar{3}m$, and a monoclinic structure, respectively, as revealed by X-ray diffraction and NMR data. Crystallographic data are given in Table 5.26.

The three-dimensional network contains channels in which coordinated and free water molecules are located (Zadneporovskii and Borisov, 1971).

Complex uranium(IV) fluorides

Metal fluoride–uranium tetrafluoride fused salt systems have been extensively studied because of their usefulness as fertile fuel materials, coolants, and heat transfer media in the Molten-Salt Reactor Experiment (MSRE), Molten-Salt Breeder Reactor, and the Aircraft Nuclear Propulsion (ANP) projects. Numerous ternary and polynary uranium(IV) fluorides have been characterized by determination of their crystallographic parameters (see Table 5.26) but there are fewer studies of their chemical and thermodynamic properties. The application of the compounds in molten-salt reactor technology has been reviewed in a number of articles (Thoma and Grimes, 1957; Thoma, 1959, 1971, 1972; Grimes and Cuneo, 1960; Rosenthal *et al.*, 1972; Grimes, 1978). Caillat (1961), Brown (1968), Bacher and Jacob (1980), Martinot (1984), Bagnall (1987), Freestone and Holloway (1991) and others have reviewed their general properties. Various complex compounds are listed in Table 5.27 with an indication of their melting behavior when available.

A number of ternary and quaternary fused salt systems such as $LiF–BeF_2–UF_4$ (Thoma, 1959; Jones *et al.*, 1959) and $NaF–BeF_2–UF_4$ (Thoma, 1959) were important for the MSRE and ANP projects. The $MgUF_6$ and $CaUF_6$ fluorides are of importance for the production of uranium by high-temperature reduction of UF_4 with calcium or magnesium. Systems with ammonium or hydrazinium cations have found application in the preparation of high-purity UF_4 by decomposition of the corresponding complex fluorides. A typical phase diagram of some importance for the molten-salt reactor projects is presented in Fig. 5.41.

The general methods for the preparation of the compounds (Bacher and Jacob, 1980; Freestone and Holloway, 1991) include: (i) solid state reaction between the component fluorides in an inert atmosphere; (ii) reactions between UF_4 or UO_2 and the alkali metal fluoride or carbonate in HF or $HF–O_2$ mixtures; (iii) reductions of UF_6 with appropriate alkali metal fluorides; (iv) controlled thermal decomposition of tetravalent uranium fluoro complexes of higher stoichiometry (e.g. $(NH_4)_4U^{IV}F_8$) or the treatment of other fluoro complexes with fluorine, (v) precipitation from aqueous solutions, followed by heating in air, *in vacuo* or fluorine, and (vi) hydrogen reduction of higher valence state fluoro complexes and precipitation from aqueous solutions.

The structures for the majority of the fluoro complexes are well established; typical examples are those with the UF_7^{3-}, UF_8^{4-} anions, but octahedral UF_6^{2-} complexes are also known. The cubic K_3UF_7 structure contains UF_7^{3-} pentagonal bipyramids, while the uranium coordination in Li_4UF_8 is described as a bicapped triangular prism (Brunton, 1967; Freestone and Holloway, 1991). Compounds of the $M^{II}UF_6$ (M^{II} = Ca, Sr, Ba, or Pb) adopt the LaF_3 structure (Keller and Salzer, 1967). U(IV) in $LiUF_5$, KU_2F_9, and $M^IU_3F_{13}$ (M^I = Rb or

Table 5.27 *Melting behavior of uranium(IV) complex fluorides and chlorides.*

System	*Complex fluorides*[a]
$LiF\text{-}UF_4$	LiU_3F_{13}, Li_2UF_6, Li_4UF_8 (P), Li_3UF_7, $LiUF_5$ (P), LiU_4F_{17} (P)
$NaF\text{-}UF_4$	$NaUF_5$, $Na_7U_2F_{15}$, Na_3UF_7 (C), Na_2UF_6 (P), $Na_5U_3F_{17}$ (P), $Na_7U_6F_{31}$ (C), NaU_2F_9 (D)
$KF\text{-}U_4$	KUF_5, K_3UF_7 (C), K_2UF_6 (P), KU_3F_{14}, $K_7U_6F_{31}$ (P), KU_2F_9 (P), KU_6F_{25}
$RbF\text{-}UF_4$	RbU_2F_9, Rb_3UF_7 (C), Rb_2UF_6 (P), $Rb_7U_6F_{31}$ (P), $RbUF_5$ (C), $Rb_2U_3F_{14}$ (P), RbU_3F_{13} (P), RbU_6F_{25} (P)
$CsF\text{-}UF_4$	Cs_3UF_7 (C), Cs_2UF_6 (P), $CsUF_5$ (C), $Cs_2U_3F_{14}$, CsU_2F_9, CsU_6F_{25}
$NH_4F\text{-}UF_4$	$(NH_4)_4UF_8$, $(NH_4)_2UF_6$, $(NH_4)_7U_6F_{31}$, NH_4UF_5, $NH_4U_3F_{13}$
$N_2H_5F\text{-}UF_4$	$(N_2H_5)_3UF_7$, $(N_2H_5)_2UF_6$, $N_2H_5UF_5$
$NH_3OHF\text{-}UF_4$	$(NH_3OH)UF_5$
$LiF\text{-}CaF_2\text{-}UF_4$	Li_2CaUF_8
$LiF\text{-}CdF_2\text{-}UF_4$	Li_2CdUF_8
$MgF_2\text{-}UF_4$	$MgUF_6$
$CaF_2\text{-}UF_4$	$CaUF_6$ (P)
$BaF_2\text{-}UF_4$	$BaUF_6$
$SrF_2\text{-}UF_4$	$SrUF_6$
$TlF\text{-}UF_4$	Tl_4UF_8, Tl_2UF_6, $Tl_7U_6F_{31}$, $TlUF_5$, TlU_3F_{13}, TlU_6F_{25}
$SnF_2\text{-}UF_4$	Sn_2UF_8 (P), $SnUF_6$ (P)
$PbF_2\text{-}UF_4$	$PbUF_6$, Pb_6UF_{16} (C), $Pb_3U_2F_{14}$ (C)
	complex chlorides[a]
$LiCl\text{-}UCl_4$	Li_2UCl_6 (C)
$NaCl\text{-}UCl_4$	Na_2UCl_6 (C)
$KCl\text{-}Ucl_4$	K_2UCl_6 (C), $KUCl_5$ (P), KU_3Cl_{13} (P), K_2UCl_6 (C)
$RbCl\text{-}UCl_4$	Rb_2UCl_6 (C), $Rb_3U_2Cl_{11}$ (P), $RbUCl_5$ (C), RbU_3Cl_{13} (P)
$CsCl\text{-}UCl_4$	Cs_2UCl_6 (C), CsU_2Cl_9 (P), $Cs_3U_2Cl_{11}$ (P), $CsUCl_5$ (P)

[a] C: congruent melting, E: eutectic, P: incongruent melting, D: decomposition.

NH_4) has tricapped trigonal prism coordination geometry. A structure with linear chains of polyhedra with a distorted cubic arrangement has been proposed for $\gamma\text{-}Na_2UF_6$ (Zachariasen, 1948a). Infinite chains are also present in the $\beta_1\text{-}K_2UF_6$ structure, where they are formed by tricapped trigonal prisms that share the triangular faces perpendicular to the three-fold axis of the ideal polyhedron (Zachariasen, 1948a). The structure of Rb_2UF_6 (Kruse, 1971) consists of infinite chains of $[UF_8]$ units with triangular faced dodecahedral geometry (of the K_2ZrF_6-type) whereas in $(NH_4)_2UF_6$ the chains of antiprism are linked by s edges on opposite square faces (Penneman *et al.*, 1974). Compounds of the $M^I_7U_6F_{31}$ type (M^I = Na, K, Rb, or NH_4) are isostructural with $Na_7Zr_6F_{31}$ (Burns *et al.*, 1968) and have a coordination geometry that is approximately square antiprismatic. The six antiprisms share corners to form an octahedral cavity, which encloses one F atom. Additional information on the structures and crystallographic data of uranium(IV) fluoro complexes are given in Table 5.26.

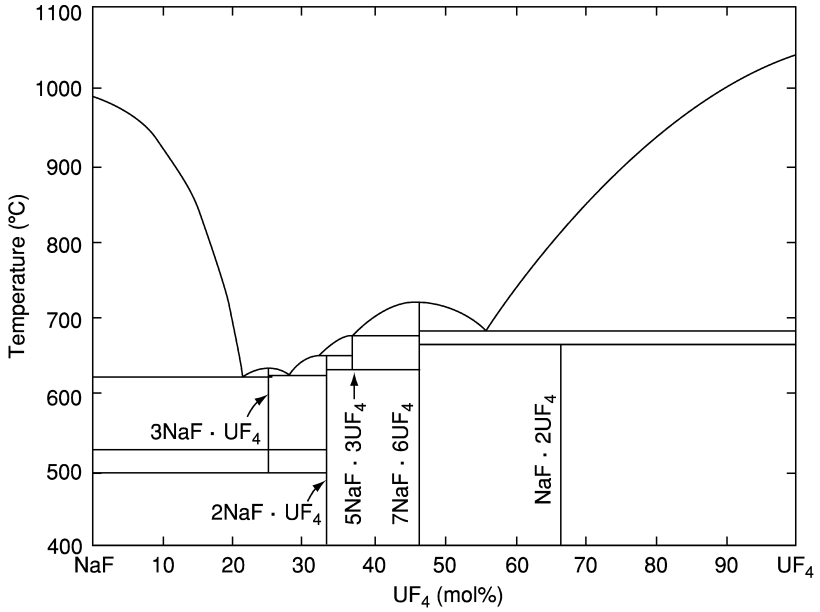

Fig. 5.41 *Phase diagram of the NaF–UF_4 system* (*Thoma,* 1959).

Numerous UF_4 complexes with quaternary ammonium compounds such as amines, pyridine, quinoline, and guanidine have been chemically and structurally characterized (Bacher and Jacob, 1980).

(*ii*) *Uranium*(IV) *oxide fluorides and nitride fluorides*

The melting of stoichiometric amounts of UO_2 and UF_4 yields UOF_2. From aqueous U(IV) solutions, the green hydrates $UOF_2 \cdot 2H_2O$ and $UOF_2 \cdot H_2O$ precipitates. Numerous non-stoichiometric uranium oxide fluorides, rich in oxygen, have been obtained by interactions of UF_4 with uranium oxides in the absence of oxygen at 400–550°C (Bacher and Jacob, 1980). The uranium atoms have an oxidation number that is either 5+, or a mixture of 5+ and 6+. In $UO_2F_{0.25}$, the oxidation number is 4+ and 5+. The compounds are non-volatile or difficult to volatilize; they have structures related to that of uranium oxide. The crystallographic data of $UO_2F_{0.25}$ are given in Table 5.26.

Heating of uranium nitride ($UN_{1.33}$) and uranium tetrafluoride leads to the formation of nitride fluorides of composition between UNF and $UN_{0.98}F_{1.20}$. The formal oxidation number of uranium in these compounds varies between 4 and 4.14. A tetragonal high-temperature and an orthorhombic low-temperature phase have been claimed to exist in this composition range. X-ray investigations of the tetragonal phase revealed a close structural relationship with lanthanum oxide fluoride (Jung and Juza, 1973). The interaction of uranium nitride with an

excess of UF_4 at 950°C leads to UF_3 and with an excess of UN to UNF (Tagawa, 1975).

(*iii*) *Uranium tetrachloride and uranium*(*IV*) *complex chlorides*

Uranium tetrachloride

Uranium tetrachloride is a suitable starting material for the synthesis of a large range of uranium compounds due to its ease of preparation and solubility in numerous polar organic solvents. It has also found application as charge material for calutron ion sources in the electromagnetic separation of uranium isotopes (Akin *et al.*, 1950). Since it has been the subject of an extensive research, numerous methods for the synthesis have been developed (Brown, 1979). Most of them are based on chlorination of uranium oxides with an extensive range of powerful chlorinating agents such as CCl_4, $COCl_2$, $SOCl_2$, S_2Cl_2, Cl_2, $Cl_2C{=}CClCCl_3$ as well as of S_2Cl_2/Cl_2 and Cl_2/He mixtures that can be used both in gaseous and liquid phases. The direct combination of uranium and chlorine leads to a complex mixture of uranium chlorides and does not yield pure UCl_4. This may most conveniently be obtained either by liquid-phase chlorination of UO_3, $UO_4 \cdot 2H_2O$, U_3O_8, UO_2Cl_2 (but not UO_2) with hexachloro propene, $Cl_2C{=}CCl{-}CCl_3$ (Hermann and Suttle, 1957) or by converting UO_2 to the tetrachloride by carbon tetrachloride at 450°C (Brown, 1979):

$$UO_2 + CCl_4 \overset{450^\circ C}{\rightarrow} UCl_4 + CO_2$$

Since the particle size of uranium dioxide is important for the synthesis, a reactive form of UO_2 should be used, formed by decomposition of uranyl oxalate in presence of hydrogen at 300°C. On laboratory scale, the simplest method involves the refluxing of UO_3 with a five-fold excess of hexachloro propene (b.p. 210°C) at atmospheric pressure. Uranium tetrachloride is insoluble in the reaction mixture and precipitates quantitatively as the reaction progresses. Due to extensive hydrolysis, the anhydrous chloride cannot be recovered from aqueous solutions.

In syntheses involving chlorine or the higher uranium oxides, usually small amounts of UCl_5 are formed. This is, however, thermally unstable and loses chlorine by heating in a stream of carbon dioxide or nitrogen. Uranium tetrachloride may be easily purified by sublimation *in vacuo*, or in a stream of a dry inert gas. A recommended route is also vapor-phase transport by the $UCl_4 \cdot AlCl_3$ complex, which proceeds rapidly already at 350°C (Gruen and McBeth, 1968). The chorination of UO_3 using liquid CCl_4 was used on a large scale to obtain UCl_4, which was used as charge material for the calutron ion sources used in the electromagnetic separation of uranium isotopes. Under a pressure of 20 atm, the chlorination yielded UCl_5, which was thermally decomposed to UCl_4 in an inert gas. Details of these processes can be found in Akin *et al.* (1950).

Uranium tetrachloride forms dark-green hygroscopic crystals, which must be handled in a dry atmosphere. At 600°C, in air it converts into U_3O_8. The compound is insoluble in non-polar organic solvents such as chloroform or

carbon tetrachloride but dissolves readily in numerous polar solvents, usually with complex formation, which enables the recovery of the anhydrous compound by evaporation. In water, it undergoes hydrolysis, which is complete at 100°C. The reaction of UCl_4 with hydrogen, zinc, or UN results in the formation of uranium trichloride. Reaction with HBr or HI yields UBr_3 and UI_3, respectively. Reduction to uranium metal takes place when the tetrachloride is heated with Li, Na, K, Mg, Ca, and Al.

Metallic uranium is also obtained by electrolytic reduction of molten UCl_4 or its solutions in fused salts media such as NaCl–KCl. Reduction with magnesium also leads to metallic uranium, whereas insoluble U(III) species are formed on reduction with Zn, Pb, and Bi. Uranium trichloride is formed in a LiCl–KCl melt by reduction with uranium or aluminum. The interaction of UCl_4 with chlorine at 115–125°C yields mixtures of UCl_5 and UCl_6, whereas in fused salt media at 400–700°C it leads to the formation of UCl_6. The reaction with fluorine gas, HBr, or HI converts UCl_4 to UF_6, UBr_4, and mixed chloride iodides, respectively.

Uranium tetrachloride crystallizes in the space group $I4_1/amd$, with tetragonal symmetry; it is isostructural with other actinide tetrachlorides. Each uranium atom is bonded to eight chlorine atoms in a dodecahedral arrangement. The crystallographic data are listed in Table 5.26. High-quality absorption spectra of UCl_4 were obtained (Brown, 1979) both for powdered samples, single crystals, in the vapor phase, and in a nitrogen matrix at 4 K (Clifton *et al.*, 1969). Numerous spectra were also recorded in different non-aqueous solvents. Successful investigations of U^{4+} spectra in the solid state started with a parametric analysis of U^{4+}-doped $ThBr_4$ single crystals by Delamoye *et al.* (1983). On this basis, consistent sets of atomic and crystal field parameters have been obtained also for isomorphic $ThCl_4$:U^{4+} and UCl_4 of D_{2d} symmetry (Malek *et al.*, 1986a,b). The data for UCl_4 are listed in Table 5.26. The parameters have been obtained by fitting 60 observed crystal-field levels of UCl_4 with a r.m.s. error of 60 cm^{-1}. The configuration interaction parameter $\gamma = 1200$, the spin–spin and spin–other orbit parameters, $M^0 = 0.99$, $M^2 = 0.55$ and $M^4 = 0.38$, and the electrostatically correlated spin–orbit perturbation parameters $P^2 = P^4 = P^6 = 500$ (all in cm^{-1}) have been used as constants in the fitting (Malek *et al.*, 1986b). The magnitude of the total crystal-field strength expressed by the scalar parameter (Auzel and Malta, 1983) N_v is equal to 1224.

The magnetic susceptibility of UCl_4 has been measured in wide temperature ranges: 100–350 K, $\mu_{eff} = 3.18$ B.M.; 350–500 K, $\mu_{eff} = 3.18$ B.M., $\theta = -31$ K (Bommer, 1941); 77–500 K, $\mu_{eff} = 3.29$ B.M., $\theta = -62$ K (Dawson, 1951); 77–450–775; 825–1200 K, $\mu_{eff} = 3.33$, 3.50, and 3.60 B.M., respectively (Trzebiatowski and Mulak, 1970). A deviation from the Curie–Weiss law was found at very low temperatures. The best fit between the experimental and the calculated curves was achieved using the values obtained by Hecht and Gruber (1974) with $A_6^4\langle r^6\rangle$ increased to 1561.8 cm^{-1}. The crystal-field parameters deduced by Mulak and Żołnierek (1977) are different from those obtained from spectroscopic data.

It has been shown (Gamp *et al.*, 1983) that the previous susceptibility measurements made on powdered UCl_4 samples are not reproducible because of a re-orientation effect caused by the high anisotropy of the susceptibility of this material. For single crystals, the anisotropic magnetic susceptibility $\chi_{\parallel}$ (along the tetragonal axis), measured between 1.6 and 350 K, is found to be almost temperature-independent and about 30 times smaller than $\chi_{\perp}$ at low temperatures (Gamp *et al.*, 1983). Chlorine-35 nuclear quadrupole resonance has been observed in solid UCl_4 at 77 K and a frequency of (6.24 $\pm$0.03) MHz (Carlson, 1969). Some other physical data are summarized in Table 5.26.

Complex uranium(IV) chlorides

A large number of hexachloro uranium(IV) compounds of the formulas $M^{I}_2UCl_6$ and $M^{II}UCl_6$ have been prepared by reactions in non-aqueous and aqueous media and by solid state reactions of the component halides (where M^{I} = Li, Na, K, Rb, Cs, Ag, $N(CH_3)_4$, $N(C_2H_5)_4$, $As(C_6H_5)_4$, C_5H_5NH, $N(CH_3)_2(C_6H_5CH_2)_2$, $P(C_2H_5)_3H$, $P(C_4H_9)_3H$, $P(C_6H_5)_2H_2$, $P(C_2H_5)_4$ etc. and M^{II} = Be, Ca, Ba, Sr, etc.). The chlorination of a mixture of U_3O_8 and NaCl at high temperatures yields Na_2UCl_6. The formation of numerous complex tetravalent chloro compounds (see Table 5.27) has also been observed during investigations of binary and ternary fused salt systems containing UCl_4.

The results of investigations on phase equilibria, spectroscopic and electrochemical properties of uranium tetrachloride in molten salt systems have been reviewed by Brown (1979) and Martinot (1984). Investigations of Gruen and McBeth (1968, 1969) and Schäfer (1975) and Binnewies and Schäfer (1974) have given evidence for the existence of uranium(IV) vapor phase complexes such as $UCl_4 \cdot AlCl_3$, $TlUCl_5$, $CuUCl_5$, Tl_2UCl_6, TlU_2Cl_9, $BeUCl_8$, In_2UCl_{10}, $ThUCl_8$, and Cu_2UCl_5. In the UCl_4–HCl–H_2O system, five hydrates have been identified among which $UCl_4 \cdot 9H_2O$ and $UCl_4 \cdot 5H_2O$ are stable at 0 and 40°C, respectively (Brown, 1979).

The action of oxygen and nitrogen donor ligands on UCl_4 solutions in non-aqueous solvents results in the formation of stable adducts of different UCl_4 to ligand stoichiometries (Brown, 1979; du Preez and Zeelie, 1989):

- (1:1): methylene bis-diphenylphosphine, ethylene bis-diphenylphosphine, α-α-dimethylmalonamide;
- (1:2): pyridine, triphenylphosphine oxide, 1,2–dimethoxyethane, 1,2-bis-methylthioethane, 1,10-phenanthroline, 1,8-diaminonaphthalene, 1,2-diaminobenzene, dimethyl sulfoxide, di-*tert*-butylsulfoxide;
- (1:2, 1:6): trimethylphosphine oxide;
- (1:2, 1:4): ammonia;
- (1:3): dioxan, tetrahydrofuran, trimethylphosphine, pyrrolidine;
- (1:4): phosphorous oxide trichloride, ROH (R = CH_3, C_2H_5, C_3H_9, i-C_3H_9), ethylenediamine, piperidine, methyl cyanide;
- (1:6): acetamide, hydrazine;

- (1:7, 1:5, 1:3): dimethylsulphoxide;
- (2:3): malonamide, glutaramide, dimethylglutaramide;
- (2:5):dimethylformamide, pyrazine, 1,2-diaminobenzene, pyrazine-2-carboxamide; dimethylacetamide.

In alternative syntheses, the reaction between uranium tetraacetate and acetates of M^I cations (M^I = K, Rb, Cs, NH_4, or $N(CH_3)_4$) in an acetyl chloride–acetic acid mixture has been used. The use of $CsUCl_6$ as a convenient starting material for the preparation of the complexes has also been reported.

The chlorine atoms may by replaced by a variety of anions in metathetic reactions involving uranium tetrachloride in non-aqueous media such as formic acid, acetic acid, sodium diethyldithiocarbamate (Nadtc), tertaethylammonium diethyldiselenocarbamate ($N(C_2H_5)_4$dsc), sodium acetylacetonate (Na-acac), tropolone (Htrop), $LiNR_2$ (R = C_2H_5, C_3H_7, C_6H_5, KC_5H_5), $NaNH_2$ (in NH_3), $NaBH_4$, and many other compounds. Electrochemical oxidation of anodic uranium into acetonitrile solutions of Cl_2 results in the formation of $UCl_4 \cdot 4CH_3CN$ in good yield. The compound may be converted into other UCl_4 adducts, e.g. with dimethylsulfoxide (1:3), 2,2′-bipyridine (1:2), Ph_3PO (1:2) etc. (Kumar and Tuck, 1984).

The chloro complexes are to some extent soluble in organic solvents such as ethanol, methyl cyanide, thionyl chloride, nitromethane, etc. with the exception of the compounds containing alkali metal cations. In aqueous hydrochloric acid solutions, the solubility of the complexes decreases markedly with the increase of the acid concentration. Liquid zinc amalgam reduction of solutions of M_2UCl_6 (where M = NH_4, K, or Rb) with an excess of NH_4Cl, KCl, or RbCl in anhydrous methyl cyanide results in the formation of the trivalent complexes, M_2UCl_5 (Drożdżyński and Miernik, 1978).

The crystallographic data of the hexachloro uranium(IV) compounds are listed in Table 5.26. The compounds with Cs^+, Rb^+, $N(CH_3)_4^+$, $As(C_2H_5)_4^+$, $P(C_6H_5)H^+$, and other cations exhibit a non-magnetic ground state A_1 with no thermal population of the excited states of the ground multiplet $^3H_4$, resulting in a temperature-independent paramagnetism between 4 and 350 K with $\chi_{mole} \cong 2000 \times 10^6$ cm^3 mol^{-1}. The magnetic susceptibility of Rb_2UCl_6 and Cs_2UCl_6 has been measured at higher temperatures and show an approximate Curie–Weiss dependence above 400 K. The magnetic susceptibilities of other chloro compounds (with M = Li, Na, or K) have a somewhat more complex temperature dependence with limited ranges of temperature-independent paramagnetism, e.g. $KUCl_5$ exhibits Curie–Weiss dependence in the 77 to 600 K and 600–1200 K ranges with μ_{eff} = 3.52 and 3.64 B.M., respectively. Solid state reactions of stoichiometric mixtures of Cs_2UCl_6 and Sb_2O_3 at 300°C *in vacuo* yields a dark olive brown uranium(IV) oxochloro compound of the formula Cs_2UOCl_4, for which Watt *et al.* (1974) reported infrared and powder diffraction data.

(*iv*) *Uranium*(IV) *oxychloride and oxochloro complexes*

$UOCl_2$ can be prepared by heating uranium dioxide in an excess of molten uranium tetrachloride followed by vacuum sublimation of the excess of tetrachloride at about 450°C (Brown, 1979), or by the following reaction:

$$3UCl_4 + Sb_2O_3 \rightarrow 3UOCl_2 + 2\,SbCl_3$$

This latter synthesis ought to be carried out *in vacuo* around 400°C where by-products sublimate from the reaction zone (Bagnall *et al*., 1968).

Uranium(IV) oxide dichloride is a green, moisture-sensitive, and thermally unstable solid. It readily dissolves in water and aqueous nitric acid, but is insoluble in organic solvents. At 170°C, CCl_4 may convert the compound to the tetrachloride; anhydrous liquid hydrogen fluoride may convert it to the tetrafluoride.

$UOCl_2$ is isostructural with some $MOCl_2$ oxychlorides (where M = Pa, Th, or Np). The oxychlorides crystallize in the orthorhombic system (see Table 5.26) and the structure contains $U_3O_3Cl_3$ chains running parallel to the *c*-axis that are linked by chlorine bridges. There are three types of polyhedra around the non-equivalent uranium atoms in the chains: around U(1), dodecahedra (CN = 8; from 3O and 5 Cl); around U(2), tricapped trigonal prism (CN = 9; 4O, 5Cl) and around U(3) monocapped trigonal prisms (CN = 7; 3O, 4Cl) (Taylor and Wilson, 1974a); all coordination polyhedra are distorted from the ideal shape. A dark olive-brown to blue-brown oxochloro complex of the formula Cs_2UOCl_4 was prepared by heating together Cs_2UCl_6 with Sb_2O_3 at 300°C *in vacuo* (Watt *et al*., 1974).

(*v*) *Uranium*(IV) *perchlorates*

Uranium(IV) perchlorate, $U(ClO_4)_4$, is unknown, but a few uranium(IV) perchlorato compounds have been isolated. Bagnall *et al*. (1962) and Bagnall and Wakerley (1974) have described the preparation and reactions in non-aqueous media of oxygen donor complexes of the formula $U(ClO_4)_4 \cdot 4L$ (L = octamethyl phosphoramide) and $U(ClO_4)_4 \cdot 4L'$ (L′ = dimethylacetamide, trimethylphosphine oxide, or hexamethylphosphoramide). Interaction of solid $U(HPO_4)_2 \cdot xH_2O$ with 10 M $HClO_4$ results in the formation of hydrated phosphate perchlorates of the formula $U(H_2PO_4)_2(ClO_4)_2 \cdot xH_2O$ ($x = 4$ and 6).

(*vi*) *Uranium tetrabromide and uranium*(IV) *complex bromides*

Uranium tetrabromide

A wide variety of methods for the preparation of uranium tetrabromide have been reported (Brown, 1979); the product may then be purified by sublimation *in vacuo* or in a stream of an inert gas. Since the compound is extremely moisture-sensitive, the carrier gases must be carefully dried. The most convenient and widely used preparation methods involve (i) the conversion of UO_2 or

U_3O_8 to the tetrabromide by heating, with a mixture of carbon, in a stream of bromine at 700–900°C, (ii) reactions between UO_2, UO_3, or $UOBr_3$ with carbon tetrabromide at about 170°C, (iii) reactions between UO_2 and a sulfur–bromine mixture under reflux at about 170°C, and (iv) direct bromination of uranium metal, either in a flow system, for example, a helium–bromine mixture at about 650°C, or in sealed evacuated vessels at 500–700°C.

Uranium tetrabromide is a deep brown, very hygroscopic solid, insoluble in non-polar organic solvents but soluble or reacting with numerous polar solvents. HBr is evolved on dissolution in methanol, ethanol, phenol, acetic acid, aniline, or on exposure to moist air. In non-aqueous solvents, the tetrabromide forms complex compounds with numerous organic ligands such as nitriles, amides, sulfoxides, phosphine oxides, or arsine oxides, e.g. $UBr_4 \cdot 4CH_3CN$, $UBr_4 \cdot 4CH_3CON(CH_3)_2 \cdot CH_3COCH_3$, $UBr_4 \cdot nCH_3CON(CH_3)_2$ ($n = 2.5$ or 5), $UBr_4 \cdot 8CO(NH_2)_2$, $UBr_4 \cdot 6(CH_3)_2SO$, $UBr_4 \cdot 2L$ (L = $(C_6H_5)_3PO$, $[(CH_3)_2N]_3PO$, $(C_2H_5)_3PO$, $(CH_3)_3AsO$, $(C_6H_5)_3AsO$, $(C_2H_5)_3AsO$, $(CH_3)_3AsO$, $UBr_4 \cdot 6(CH_3)_3PO$, $UBr_4 \cdot 6L'$ (L′ = $(CH_3)_3AsO$ and $(C_2H_5)_3AsO$). Reduction with alkali or alkaline earth metals at high temperatures and hydrogen at 450–700°C yields uranium metal and uranium tribromide, respectively. Uranium tetrabromide may be converted to the tetrachloride by chlorine and to UO_2Br_2 by dry oxygen at 150–160°C. The preparation and crystal structure of octaaquabromo uranium(IV) tribromide monohydrate, $[UBr(H_2O)_8]Br_3(H_2O)$ (Table 5.26) have been reported by Rabinovich *et al.* (1998).

Uranium tetrabromide crystallizes in the monoclinic space group *C*2/*m* (see Table 5.26), with pentagonal bipyramid coordination at the uranium atom; the polyhedra are linked into infinite two-dimensional sheets by double bromine bridges between the uranium atoms (Taylor and Wilson, 1974d,e).

Good-quality low-temperature absorption spectra as well as solution, reflectance, and transmission spectra of UBr_4 are available. The energy level parameters obtained from least-squares fitting of the observed and calculated energy levels are listed in Table 5.26. Absorption bands observed in the range 41400–32160 cm^{-1} were assigned to $5f^2 \rightarrow 5f^16d^1$ transitions; a charge transfer band was identified at 30165 cm^{-1}. Magnetic susceptibility measurements reveal a Curie–Weiss behavior in the temperature range 77–569 K, with $\theta = -35$ K and $\mu_{eff} = 3.12$ B.M (Brown, 1979; Dawson, 1951).

Uranium(IV) ternary and polynary bromides and bromo compounds

Cooling curves obtained from melting point diagrams show that only complexes of the M_2UBr_6-type are formed in the UBr_4–MBr system (M = Na, K, Rb, or Cs). They may conveniently be prepared by heating the component bromides in evacuated silica ampoules (Vdovenko *et al.*, 1973a,b). In addition to synthetic methods, phase transitions and crystallographic data for Li_2UBr_6 have been reported (Maletka *et al.*, 1998). Hexabromo compounds containing large organic cations are formed in anhydrous methyl cyanide solutions as a result of reactions at 0°C between UBr_4 and a number of alkylammonium or

phosphonium bromides, e.g. $[N(CH_3)_4]_2UBr_6$, $[N(C_2H_5)_4]_2UBr_6$, (Brown, 1979). Hexabromouranates(IV) may also be prepared by reactions of UBr_4 with aniline, ethylenediamine, and 8-hydroxyquinoline (Sara, 1970).

$UBr_4 \cdot 2CH_3CN$ in good yield is formed by electrochemical oxidation of uranium in CH_3CN/Br_2 solution under an inert atmosphere. Using a two-fold excess of different neutral ligands in a solution of this compound in acetone gives rise to UBr_4 adducts, e.g. $UBr_4 \cdot 2Ph_3O$ and $UBr_4 \cdot 6$dmso (dmso = dimethylsulfoxide) (Kumar and Tuck, 1984). The preparation of UBr_4 adducts has also been reported by du Preez and Zeelie (1989), e.g. $UBr_4 \cdot (tbso)_2$ (tbso = di-*tert*-butyl phosphoxide), $UBr_4(dmso)_2$ (dimethylsulfoxide) and $UBr_4 \cdot 4CH_3CN$. Evaporation of UBr_5 solutions containing 1 or more than 3 mol equivalents of methyl cyanide in dichloromethane yields $UBr_4 \cdot CH_3CN$ and $UBr_4 \cdot 3CH_3CN$, respectively. The synthesis, crystal structure, and IR data of $P(C_6H_5)_4UBr_6$, $P(C_6H_5)_4[UBr_6] \cdot 2CCl_4$, $[P(C_6H_5)_4]_2[UBr_6] \cdot 4CH_3CN$, and $[P(C_6H_5)_4]_2[UO_2\ Br_4] \cdot 2CH_2Cl_2$ were reported by Bohrer *et al.* (1988) (see Table 5.26).

The hexabromo complexes containing large organic cations have green-blue color; they dissolve readily in water, aqueous hydrobromic acid, and a number of polar non-aqueous organic solvents. They may be purified by crystallization, e.g. from methylcyanide or nitromethane. The compounds react with aqueous ammonia and liquid ammonia forming hydrous oxides and the insoluble $[N(C_2H_5)_4]_2UBr_6$ complex, respectively.

Rb_2UBr_6, Cs_2UBr_6, and $[N(CH_3)_4]_2UBr_6$ crystallize with face-centered cubic symmetry. The crystallographic data of these and some other hexabromouranates(IV) are listed in Table 5.26. Spectroscopic and magnetic susceptibility investigations performed for a number of octahedral uranium(IV) chloro- and bromo-complex compounds by Day and Venanzi (1966) show a temperature-independent paramagnetism, which results from interactions between the A_1 ($^3H_4$) ground state and the first excited state T_1 ($^3H_4$). Using the relative field strengths obtained from magnetic data, the authors have obtained the following values of the energy parameters: $\Delta = 1177\ cm^{-1}$ and $\theta = 2096\ cm^{-1}$ [where $\Delta = 8/33\ (B_0^4 + 35/13B_0^6)$ and $\theta = 2/33\ (5B_0^4 - 210/13B_0^6)$; $B_0^4 = 6481.5\ cm^{-1}$, $B_0^6 = 804\ cm^{-1}$]. The observed interactions are in an octahedral field best described by the orbital energy differences $\Delta(a_{2u} \rightarrow t_{2u})$ and $\theta(t_{2u} \rightarrow t_{1u})$.

Spectroscopic investigations reveal a coordination geometry with octahedral geometry both in the solid and in non-aqueous solutions; vibronic side bands are prominent in the spectra of the complexes and permit the assignment of a number of electronic transitions and the determination of the electrostatic, spin–orbit, and crystal-field parameters, e.g. for Cs_2UBr_6: (Johnston *et al.*, 1966) and for $[N(C_2H_5)_4]_2UBr_6$: (Wagner *et al.*, 1977) (see Table 5.26). From the spectral data the following ligand field parameters have been obtained: $\theta = 2378$, $\Delta = 828\ cm^{-1}$, $\zeta_{5f} = 1792\ cm^{-1}$ (or $B_0^4 = 6592.5\ cm^{-1}$, $B_0^6 = 1194.8\ cm^{-1}$) and $\theta = 2336$, $\Delta = 1127\ cm^{-1}$, $\zeta_{5f} = 998.95\ cm^{-1}$ (or $B_0^4 = 6946.5\ cm^{-1}$, $B_0^6 = 998.95\ cm^{-1}$) for Cs_2UBr_6 and $[N(C_2H_5)_4]_2UBr_6$, respectively. As one would

expect the $5f^2 \rightarrow 5f^16d^1$ transitions, recorded for $[N(C_2H_5)_4]_2UBr_6$, lie between those observed for the hexachloro and hexaiodo uranates(IV), i.e. at 27400(sh), 29400, 30400, 31500(sh), 33100, 37000, and 39000 cm^{-1} (Ryan, 1972). Spectral investigations of the compound in non-aqueous solvents reveal hydrogen bonding to primary, secondary, and tertiary alkylammonium ions that partially distorts the octahedral field in the UBr_6^{2-}complex, making the $5f^2 \rightarrow 5f^2$ electronic transitions allowed. The analysis of the visible and near IR spectra demonstrates vibronic frequencies within the ranges: 180–184 cm^{-1} (ν_3), 72–74 cm^{-1} (ν_4), and at 58 cm^{-1} (ν_6).

(*vii*) *Uranium(IV) oxide dibromide and nitride bromides*

Useful preparative methods for $UOBr_2$ (Brown, 1979) involve heating of UO_2 in a stream of CS_2 at 900°C to form $U_3O_2S_4$ followed by bromination at 600°C:

$$U_3O_2S_4 + 6Br_2 \rightarrow 2UOBr_2 + UBr_4 + 2S_2Br_2$$

or by heating of stoichiometric amounts of Sb_2O_3 and UBr_4 at about 150°C *in vacuo* (Bagnall *et al.*, 1968):

$$Sb_2O_3 + 3UBr_4 \rightarrow 3\,UOBr_2 + 2SbBr_3$$

Uranium(IV) oxide dibromide is a non-volatile, pale yellow, air-sensitive solid, readily soluble in water with the formation of a green solution from which a black solid slowly deposits. It decomposes above 600°C *in vacuo* to form UO_2 and UBr_4. The reported thermodynamic data (Greenberg and Westrum, Jr., 1956; Rand and Kubaschewski, 1963; Grenthe *et al.*, 1992; Guillaumont *et al.*, 2003) are listed in Table 5.26.

As in the corresponding chloride systems, the ammonolysis of UBr_4 at elevated temperatures leads to the formation of uranium nitride via amido, imido, and nitride bromides (Burk, 1967; Burk and Naumann, 1969). Since the composition of the decomposition products varies with temperature, the pure phases cannot easily be obtained (Brown, 1959). Juza and Meyer (1966, 1969) have obtained a dark-brown $UN_{1.03}Br_{1.03}$ phase on heating UBr_4-ammoniates at 400°C in gaseous ammonia. The compound can also be prepared by solid-state reactions of UN with UBr_4 at 600–900°C. It is insoluble in water and has the BiOCl-type structure with the space group *P*4/*nmm*. The crystallographic data are listed in Table 5.26.

(*viii*) *Uranium tetraiodide and uranium(IV) complex iodides*

Uranium tetraiodide

The most convenient and widely used method for the preparation of UI_4 involves the direct combination of the elements at about 500°C, either in a gas-flow system or in sealed vessels (see Brown, 1979); it is a black, moisture-sensitive solid. It rapidly decomposes on exposure to air and is also thermally

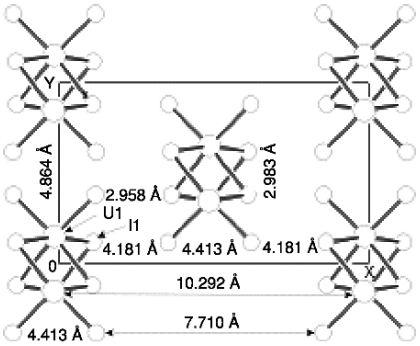

Fig. 5.42 *View along zigzag chains in UI_4 (distances are taken from Levy* et al., 1980).

unstable, liberating iodine with the formation of UI_3. The tetraiodide may also readily be reduced to UI_3 by hydrogen at moderate temperatures. The interaction of UI_4 with chlorine yields UCl_4, and with uranium tetrahalides it forms the mixed halides: UCl_2I_2, $UClI_3$, UBr_2I_2, and $UBrI_3$. Like other uranium halides the tetraiodide also forms complexes with organic ligands, e.g. $UI_4 \cdot 4$dma (dma = dimethylacedamide), $UI_4 \cdot 2$tbso (tbso = di-*tert*-butyl sulfoxide), $UI_4 \cdot 8$dmso (dmso = dimethyl sulfoxide), $UI_4 \cdot 6$dibso (dibso = di-isobutylsulfoxide), $UI_4 \cdot xNH_3$ (x = 4, 5, or 10) and $UI_4 \cdot 8$L (L = ε-caprolactam, α-$UI_4 \cdot tpao_2$, β-$UI_4 \cdot tpao_2$, $UI_4 \cdot tpao_4$, and $UI_4 \cdot tpao_6$ (tpao = triphenylarsine oxide) (Brown, 1979; du Preez and Zeelie, 1987, 1989).

The crystal structure of UI_4 has been solved using X-ray and powder neutron diffractions (Levy *et al.*, 1980; Taylor, 1987). The monoclinic structure (Table 5.26) contains uranium atoms with an approximately octahedral coordination, where the uranium atoms are linked by double iodide bridges, forming zigzag chains (Fig. 5.42). Two terminal iodide ions in the *cis* position are completing the coordination sphere of the uranium atom.

Uranium(IV) iodo complexes

Hexaiodo uranium(IV) compounds of the M_2UI_6-type (where M = $N(C_2H_5)_4$, $N(C_4H_9)_4$, $N(C_6H_5)(CH_3)_3$, and $As(C_6H_5)_4$) have been obtained from reactions of the component halides in anhydrous methyl cyanide followed by crystallization in an ice bath or by vacuum evaporation of the solvent. Alternatively, the treatment of uranium(IV) hexachloro or hexabromo complexes with anhydrous liquid hydrogen iodide may be used (Bagnall *et al.*, 1965; Brown *et al.*, 1976). The hexaiodo uranium(IV) compounds are stable, but extremely moisture-sensitive, red colored solids. Exposure to the atmosphere, addition of dilute aqueous acids, or ammonia results in immediate decomposition. The compounds are soluble in anhydrous methyl cyanide and acetone and liberate iodine on heating above 200°C.

From an analysis of the spectral data for $[N(C_2H_5)_4]_2UI_6$ the following electrostatic, spin–orbit, and crystal-field parameters were obtained (in cm^{-1}): $F^2 = 38188(2422)$, $\zeta_{5f} = 1724(39)$, $B_0^4 = 6338(676)$, and $B_0^6 = 992(252)$ (Wagner *et al.*, 1977). Magnetic susceptibility measurements of $[As(C_6H_5)_4]_2UI_6$ have shown that the compound exhibits a temperature-independent paramagnetism in the 84–300 K range with $\chi_{mole} = 2146(30) \times 10^{-6}$ cm^3 mol^{-1} (Bagnall *et al.*, 1965), analogous to that in the hexachloro and hexabromo uranium(IV) compounds.

(*ix*) *Uranium(IV) oxide di-iodide and nitride iodide*

UOI_2 can be prepared by heating U_3O_8, U, and I_2 at 450°C in a sealed Pyrex tube. The compound is iso-structural with $UOCl_2$ (orthorhombic symmetry in space group *Pbam*, see Table 5.26) and has $\mu_{eff} = 3.34$ B.M, as determined from magnetic susceptibility measurements (Levet and Noël, 1979).

The reaction of uranium tetraiodide with gaseous ammonia at temperatures above ~350°C yields uranium nitride iodide, UNI. It may be also obtained by heating uranium nitride with uranium tetraiodide. The compound has tetragonal symmetry (space group *P4/nmm*) and is iso-structural with the chloride and bromide analogues (see Table 5.26).

(*x*) *Uranium(IV) mixed halides and mixed halogeno compounds*

Phases of the composition of $UClF_3$, UCl_2F_2, and UCl_3F occur in the UCl_4–UF_4 system. All are melting incongruently and are thermally unstable, the order being $UClF_3 > UCl_2F_2 > UCl_3F$. The last compound may be prepared by (i) chlorination of UO_2F_2 in refluxing hexachloropropene, (ii) chlorination of UF_3 with chlorine at 350–380°C and by heating of UF_4 in a CCl_4 vapor at 420°C. UCl_3F, obtained in this way, is somewhat contaminated with unreacted starting materials and by-products (UCl_4 or $UOCl_2$). The X-ray powder data obtained for UCl_3F are listed in Table 5.26. A number of ternary chloride fluorides were identified in the $M^{I}Cl$–UF_4 and $M^{II}Cl_2$–UF_4 phase diagrams (where M^{I} = Li, Na, K, Rb, or Cs and M^{II} = Mg or Ca) (Brown, 1979).

The preparation and thermodynamic data of uranium(IV) mixed halides containing bromine have been reported by MacWood (1958). Solid-state reactions of stoichiometric quantities of UCl_4 and UBr_4 yield $UBrCl_3$ at 750°C and UBr_2Cl_2 and $UBrCl_3$ at 590°C. The former may also be prepared by bromination of UCl_3 at 500°C. Some thermodynamic data of these compounds are listed in Table 5.26.

The following mixed tetravalent halides containing iodide anions: (i) UCl_3I, (ii) UCl_2I_2, (iii) $UClI_3$, (iv) UBr_3I, (v) UBr_2I_2, and (vi) $UBrI_3$ (Brown, 1979) have be obtained in pure form. Satisfactory preparation methods involve: (i) iodination of UCl_3 at 500°C in a atmosphere of iodine, (ii) fusion of equimolar

amounts of UI_4 and UCl_4 in the presence of small amount of iodine, (iii) fusion of UCl_4 and either UI_3 (at 600°C) or UI_4, (iv) iodination of UBr_3 at 500°C, (v) iodination of UBr_2I at 500°C, or fusion of UBr_4 and UI_4 at 520°C followed by sublimation in a stream of iodine, and (vi) fusion of a 1:3 mole ratio of UBr_4 and UI_4, followed by sublimation at a low pressure of iodine. The compounds are dark-brown or black and undergo rapid hydrolysis in a humid atmosphere. Their melting points range from 478 and 490°C for UBr_3I and UCl_3I, respectively, to somewhat less than 500°C for the remaining mixed halides. All compounds readily lose iodine on heating *in vacuo*, except of $UBrI_3$, which can be sublimed without decomposition. A number of thermodynamic data are available for these compounds (see Table 5.26). The stability of the chloride iodides increases with increasing iodide content. A reverse stability trend is reported for the bromide iodides.

The preparation of uranium(IV) mixed halgeno-compounds by fusion methods and mixed halgeno compounds with donor ligand have been also reported, e.g. $M^{I}_2UX_2Y_2$ (where M^{I} = Na, K or Cs, X = Cl, and Y = Br), $K_2UCl_4I_2$, $K_2UBr_4I_2$, $UCl_3I \cdot 8CO(NH_2)_2$, $UI_2Cl_2 \cdot 5DMA$ (DMA = *N*,*N*-dimethylacetamide), and $UClI_3 \cdot 5DMA$ (Gregory, 1958; Brown, 1968).

(*xi*) *Nitrogen-containing uranium halides*

Uranium nitride chlorides, bromides, and iodides

High-temperature ammonolysis of UCl_4, UBr_4, or UI_4 leads to the corresponding uranium nitride chloride, bromide, and iodide. The formation of UNCl and UNBr proceeds via a number of intermediates such as $U(NH_2)Cl_3$, $U(NH)_2Cl_2$, or UNCl. Other routes to UNCl involve high-temperature interaction of UCl_4 and $UN_{1.33}$ as well as solid-state reactions between UCl_4 and aluminium or silicium at about 800°C in a nitrogen atmosphere. Crystallographic data for UNCl (Juza and Sievers, 1965; Juza and Meyer, 1969) are listed in Table 5.26.

A dark brown compound of the formula $UN_{1.03}Br_{1.03}$ was obtained on heating uranium tetrabromide ammoniates in gaseous ammonia for 48–60 h. The compound may also be prepared by heating uranium nitride and the tetrabromide at 600–900°C (Juza and Meyer, 1969). It is insoluble in water but dissolves slowly in 2 M H_2SO_4 with the formation of a green solution. UNBr is converted to uranium nitride in gaseous ammonia at temperatures over 750°C. The compound crystallizes in the BiOCl-type of structure, space group *P4/nmm*, D^7_{4h}, the same as the corresponding UNCl and UNI compounds (see Table 5.26).

The preparation of UNI can be achieved by ammonolysis of uranium tetraiodide at about 350°C or by heating uranium nitride with UI_4. The compound has the BiOCl-type structure and is isostructural with the chloride and bromide analogs (Juza and Meyer, 1969; see Table 5.26).

(c) Pentavalent halides and complex halides

Uranium halides in the pentavalent oxidation state exhibit a tendency to hydrolysis and disproportionation into U(IV) and U(VI) species. However, in the absence of substances that cause hydrolysis, diproportionation does not occur spontaneously (Bacher and Jacob, 1980). Stable solutions of uranium(V) have been obtained, for example, by heating a mixture of UO_3 with thionyl chloride under prolonged refluxing, or by dissolving UF_5 in methyl cyanide, dimethylformamide or Me_2SO as well as of UCl_5 and UBr_5 in some organic solvents (Selbin and Ortego, 1969; Brown, 1979; Halstead *et al.*, 1979). Uranium hexachloride decomposes easily in solvents like carbon tetrachloride, methylene dichloride, or 1,2-dichlorethane and is therefore a suitable starting material for the preparation of uranium(V) compounds on a laboratory scale. The synthesis and properties of various uranium(V) compounds and complexes have been reviewed by Selbin and Ortego (1969). The preparation of UX_6^- (X = F, Cl, Br or I) complexes and the oxohalide complexes $[UOF_5]^{2-}$, $[UOCl_5]^{2-}$, and $[UOBr_5]^{2-}$ has been reported by Ryan (1971). The chemical properties of the compounds, their stability against disproportionation in various non-aqueous halide solutions as well as some aspects of their absorption spectra are also discussed. The halides and complex halides have a variety of colors – from pale blue and red brown to yellow (Table 5.28). The coordination geometry of uranium(V) halides are: octahedral (α-UF_5), pentagonal bipyramidal (β-UF_5), and edge-sharing octahedral (U_2Cl_{10} units).

Uranium(V) has a $[Rn]5f^1$ electronic configuration with the $^4F_{5/2}$ (Γ_7) ground state. A number of spectra in solutions, solids, and gas phase are available (Ryan, 1971; Edelstein *et al.*, 1974; Leung and Poon, 1977; Bacher and Jacob, 1980; Eichberger and Lux, 1980; Carnall and Crosswhite, 1985). The analysis of the spectra has been based on a strong ligand-field model. The site symmetry of the U^{5+} ion is frequently found to be octahedral or distorted octahedral (Carnall and Crosswhite, 1985). The combined ligand field and spin–orbit interaction split the parent ^2F state into the Γ_7, Γ_8, Γ_7', Γ_8', and Γ_6 components. The spectra of U^{5+} in the approximate octahedral sites of the different compounds have very similar f–f band energy and relative intensities, e.g. the spectra of $[N(C_2H_5)_4]_2UOCl_5$ (Selbin *et al.*, 1972a), UCl_5 single crystals (Leung and Poon, 1977), UCl_5 in $SOCl_2$ (Karraker, 1964), and $(UCl_5)_2$ or $UCl_5 \cdot AlCl_3$ in the vapor phase (Gruen and McBeth, 1969). Spectroscopic studies and semi-empirical theoretical calculations of energy levels of UOX_5^{2-} species (X = F, Cl, or Br) in the corresponding tetraethylammonium oxopentahalide complexes reveal that each of the six electronic transitions is shifted to higher energy in the expected order: $Br^- < Cl^- < F^-$. The spin–orbit coupling constants obtained in the best fits also increase in this same order: 1750, 1770, and 1850 cm^{-1}. For a number of uranium(V) halides and complex halides, magnetic susceptibility measurements were carried out over wide temperature ranges. The paramagnetic constants from the Curie–Weiss law $\chi'_M = C/(T-\theta)$ and the effective

Table 5.28 *Properties of selected uranium(v) halides, mixed valence halides and complex halides.*[a]

Formula	*Selected properties and physical constants*[b]	*Lattice symmetry, lattice constants* (Å), *polyhedron type and density* (g cm^{-3})[c]	*Remarks regarding information available and references*
α-UF_5	grayish-white or bluish-white crystals; moisture sensitive; soluble in CH_3CN, C_2H_5CN, DMF and Me_2SO; disproportionate over 150°C to $U_2F_9 + UF_6$; m.p. = 348 (+13, –16)°C in a UF_6 atmosphere of 1.6–4.6 bar; density = 5.81g cm^{-3}; α-UF_5: $\Delta_f G^o_m = -1968.7\ (7.0)^\dagger$, $\Delta_f H^o_m = -2075.3\ (5.9)^\dagger$, $S^o_m = 199.6\ (12.6)^\dagger$, $C^o_{p,m} = 132.2\ (4.2)^\dagger$. UF_5(g): $\Delta_f G^o_m = -1862.1\ (15.3)^\dagger$, $\Delta_f H^o_m = -1913\ (15)^\dagger$, $S^o_m = 386.4\ (10.0)^\dagger$; $C^o_{p,m} = 110.6\ (5.0)$. IR: 580s,br, 398s; $\log p_{solid}(mmHg) = -(8001 \pm 664)/T^{-1} + (13.994 \pm 1.119)\log p_{liquid}(mmHg) = -(5388 \pm 803)\ T^{-1} + (9.819 \pm 1.236)$.Raman (cm^{-1}): 627.5s, 503m, 223m; $\lvert g\rvert = 0.892$;	tetragonal; C^5_{4h}, $I4/m$, No. 87; a = 6.5259(3), c = 4.4717(2), Z = 2; V = 190.44; CN = 6; d(calc.) = 5.81; UF_6 octahedra are bridged by *trans*-fluorides with d(U–F1) = 2.235(1) to give an infinite linear chain parallel to the c-axis. The remaining four F atoms in the octahedron are bound to one U atom with d(U–F2) = 1.995(7)	*crystallographic and neutron powder data; UV, Vis, IR and Raman spectra; heat capacity* (Zachariasen, 1949c; Osborne *et al*., 1955; Burns *et al*., 1960; Paine *et al*., 1976; Eller *et al*., 1979; Howard *et al*., 1982); *thermodynamic data* (Rand and Kubaschewski, 1963; Kubaschewski and Alcock, 1979; Fuger *et al*., 1983; Grenthe *et al*., 1992; Guillaumont *et al*., 2003); *magnetic susceptibility data, chemical properties* (Eller *et al*., 1979; Brown, 1968, 1973); *optical spectra and crystal-field analysis* (Hecht *et al*., 1986b); *photoelectron spectra* (Thibaut *et al*., 1982)
β-UF_5	pale yellow; moisture sensitive; soluble in CH_3CN, C_2H_5CN, DMF and Me_2SO; β-UF_5: $\Delta_f G^o_m = -1970.6(5.6)^\dagger$, $\Delta_f H^o_m = -2083.2\ (4.2)^\dagger$, $S^o_m = 179.5\ (12.6)^\dagger$; $C^o_{p,m} = 132.2\ (12.0)^\dagger$. IR (cm^{-1}): 623s,sh, 567s, 508s, 405s; Raman: 623s, 610s, 280m.	tetragonal; D^{12}_{2d}, $I\bar{4}2d$, No. 122; a = 11.469(5), c = 5.215(2); Z = 8; CN = 7; V = 685.97; d(calc.) = 6.45	*crystallographic and neutron diffraction data, IR and Raman spectra, thermodynamic data, chemical properties* (Brown, 1968; Paine *et al*., 1976; Ryan *et al*., 1976; Bacher and Jacob, 1980; Taylor and Waugh, 1980; Grenthe *et al*., 1992; Guillaumont *et al*.,

	$\mu_{\text{eff.}} = 2.24$ B.M.; $\theta = -75.4$ K (125–420 K)		2003); *magnetic susceptibility data* (Nguyen-Nghi *et al.*, 1964b) *optical spectra and crystal-field analysis* (Hecht *et al.*, 1986b); *solution spectra* (Halstead *et al.*, 1979)
U_2F_9 (mixed valence)	black; uranium oxidation number = +4.5; disproportionates into UF_4 and UF_6; U_2F_9(cr): $\Delta_f G^o_m = -3812$ (17)†, $\Delta_f H^o_m = -4016$ (18)†, $S^o_m = 329$ (20)†; $C^o_{p,m} = 251.0$ (16.7)†	cubic; body centered; T^3_d, $I\bar{4}3m$, No. 217; $a = 8.462(2)$; [$a = 8.4716$: (Howard *et al.* 1982)]; $Z = 4$; $V = 607.99$; CN = 9; d(calc.) = 7.091; the structure consists of a three-dimensionally bridged network composed of tricapped trigonal prismatic UF_9 units; $d(U–F_1) = 2.37(2)$, 2.21(2); $d(U–F_2) = 2.266$ (3); F1–U–F1 = 119.5(1), 71.2(3); F1–U–F2 = 67.0(5), 128.4(9)	*crystallographic and neutron diffraction data; reflectance spectrum* (Zachariasen,1949d; Eller *et al.*, 1979; Laveissière, 1967; Taylor, 1976a,b; Howard *et al.*, 1982); *thermodynamic data* (Bacher and Jacob, 1980; Grenthe *et al.*, 1992; Guillaumont *et al.*, 2003)
U_4F_{17} (mixed valence)	black; uranium oxidation number = +4.25; disproportionates into UF_4 and UF_6; U_4F_{17}(cr) $\Delta_f G^o_m = -7464$ (30)†, $\Delta_f H^o_m = -7850$ (32)†, $S^o_m = 631$ (40)†, $C^o_{p,m} = 485.3$ (33.0)†	monoclinic; deformed UF_4 lattice; C^6_{2h}, $C2/c$, No. 15; $a = 12.09(0.08)$, $b = 10.81(2)$, $c = 8.29(4)$; $\beta = 128.0(8)$; $Z = 12$; CN = 8 (UF_4); d(calc.) = 7.07	*crystallographic data* (Chatelet, 1967); *thermodynamic data* (Bacher and Jacob, 1980; Grenthe *et al.*, 1992; Guillaumont *et al.*, 2003)
$(H_3O)UF_6$	blue-green; above 68(1) °C decomposes to $UF_4 + UO_2F_2$; $(H_3O)UF_6$(cr): $\Delta_f H^o_m = -2641.4$ (3.2)†	cubic; $a = 5.2229(5)$	*X-ray powder diffraction data; VIS, NIR and IR spectra, EPR data* (Masson *et al.*, 1976); *thermodynamic data* (Grenthe *et al.*, 1992; Guillaumont *et al.*, 2003)
Other hydrated fluorides: $HUF_4 \cdot 2.5H_2O$; $HUF_4 \cdot 1.25H_2O$;	blue or light blue		*general properties* (Bacher and Jacob, 1980)

Table 5.28 (*Contd.*)

Formula	*Selected properties and physical constants*[b]	*Lattice symmetry, lattice constants* (Å), *polyhedron type and density* (g cm^{-3})[c]	*Remarks regarding information available and references*
$LiUF_6$	pale blue; EPR: $g_o = -0.768$; $\|\Delta g\| = 0.022$; $\Delta H = 109$ Oe; angle of distortion 0.13°; $\|g\| = 0.768$; $g_\parallel = -0{,}801$, $g\perp = -0.753$; $\varsigma = 1969$; IR and Raman(cm^{-1}): $\nu_1 = 622$, $\nu_2 = 439$, $\nu_3 = 515$, $\nu_4 = 152$, $\nu_5 = 222, 232$, $\nu_6 = 107$[e]	rhombohedral; C_{3i}^2, $R\bar{3}$, No. 148; structure type of $LiSbF_6$; $a = 5.262$, $c = 14.295$	*crystallographic data* (Brown, 1968, 1973; Penneman *et al.*, 1973); *absorption spectra, IR data, ESR data* (Hecht *et al.*, 1986a; Rigny and Plurien, 1967; Allen *et al.*, 1978; Halstead *et al.*, 1979; Bacher and Jacob, 1980)
α-$NaUF_6$	pale blue; air sensitive; EPR: $g_o = -0.745$; angle of distortion 0.65° $g_\parallel = -0.8175$, $g\perp = -0.708$; $\varsigma = 1965$; IR and Raman (cm^{-1}): $\nu_1 = 621$, $\nu_2 = 449$, $\nu_3 = 520$, $\nu_4 = 122$[e], 132[e], $\nu_5 = 206, 209$, $\nu_6 = 72$[e]	rhombohedral; C_{3i}^2, $R\bar{3}$, No.148; structure type of $LiSbF_6$; $a = 5.596$, $c = 15.526$	*crystallographic data* (Brown, 1968, 1973; Penneman *et al.*, 1973); *absorption spectra* (Bacher and Jacob, 1980; Hecht *et al.*, 1986a); *thermodynamic data* (Kudriashov *et al.*, 1978; Fuger *et al.*, 1983); *ESR data* (Rigny and Plurien, 1967; Halstead *et al.*, 1979)
β-$NaUF_6$	pale blue; air sensitive; EPR: $\|g\| = 0.748$; $\|\Delta g\| = 0.107$; $\Delta H = 57$ Oe; angle of distortion = 0.65°	cubic fcc; O_h^5, *Fm*3*m*, No. 225; $NaTaF_6$ structure type; $a = 8.608$	*crystallographic data* (Brown, 1968, 1973; Penneman *et al.*, 1973) *thermodynamic data* (Kudriashov *et al.*, 1978; Fuger *et al.*, 1983); *spectroscopic data* (Moskvin and Zaitseva, 1962)
KUF_6	yellow-green; air sensitive	orthorhombic; D_{2h}^{18}, *Cmca*, No. 64; CN = 6; $RbPaF_6$ structure type; $a = 5.61$, $b = 11.46$, $c = 7.96$; dodecahedron sharing edges to form chains	*crystallographic data* (Brown, 1968, 1973; Penneman *et al.*, 1973); *absorption sp*ectra (Bacher and Jacob, 1980) *thermodynamic data* (Kudriashov *et al.*, 1978; Fuger *et al.*, 1983)
$RbUF_6$	yellow-green;		*crystallographic data* (Penneman *et al.*, 1973 ; Brown, 1968, 1973);

		orthorhombic; D_{2h}^{18}, *Cmca*, No. 64; $RbPaF_6$ structure type; $a = 5.82$, $b = 11.89$, $c = 8.03$	*absorption spectra* (Bacher and Jacob, 1980); *thermodynamic data* (Kudriashov *et al*., 1978; Fuger *et al*., 1983); *crystal-field calculations* (Amberger *et al*., 1983)
$CsUF_6$	pale blue to green blue; (ν(U–F) = 503s; EPR: $\|g\| = 0.709$; $\|g\| = 0.709$; $\|\Delta g\| = 0.210$; angle of distortion = 1.25°; $g_{\|} = -0{,}928$, $g\perp = -0.681$; $\varsigma = 1985\ cm^{-1}$; IR and Raman ($cm^{-1}$): $\nu_1 = 608$, $\nu_2 = 452$, $\nu_3 = 505$, $\nu_4 = 126$–130^e, $\nu_5 = 190, 213$, $\nu_6 = 60^e$	rhombohedral; C_{3i}^2, $R\bar{3}$, No. 148; $KCsF_6$ structure type, $a = 8.04$, $c = 8.39$; dodecahedron sharing edges to form chains	*crystallographic data* (Brown, 1968, 1973; Penneman *et al*., 1973); *absorption spectra, NMR-spectra; IR and Raman spectra* (Bacher and Jacob, 1980, Carnall and Crosswhite, 1985; Hecht *et al*., 1986a; Geichman *et al*., 1962); *magnetic susceptibilities* (Mulak and Żołnierek, 1972); *ESR spectra* (Rigny and Plurien, 1967); *thermodynamic data* (Kudriashov *et al*., 1978; Fuger *et al*., 1983)
NH_4UF_6	yellow-green; $\mu_{eff} = 1.74$ B.M. (93–200 K); $\mu_{eff} = 2.25$ B.M. (200–390 K)[d]	orthorhombic; D_{2h}^{18}, *Cmca*, No.64; $RbPaF_6$ structure type; $a = 5.83$, $b = 11.89$, $c = 8.03$; dodecahedron sharing edges to form chains	*crystallographic data* (Brown, 1968, 1973; Penneman *et al*., 1973; *absorption spectra; magnetic susceptibility* (Nguyen-Nghi *et al*., 1965; Bacher and Jacob, 1980)
$AgUF_6$	decomposes at 230°C to F_2, UF_4 and AgF	tetragonal; $a = 5.42$, $c = 7.95$	*crystallographic data* (Brown, 1968, 1973; Penneman *et al*., 1973)
$TlUF_6$		orthorhombic; D_{2h}^{18}, *Cmca,* No.64; $a = 5.96$, $b = 11.55$, $c = 8.00$.	*crystallographic data* (Charpin, 1965)
$UF_5(SbF_5)_2$		monoclinic; C_{2h}^5, $P2_1/c$, No. = 14; $a = 8.110(4)$, $b = 14.129(6)$, $c = 10.032(6)$; $\beta = 96.97(5)°$; $Z = 4$; $V = 1141.03$; d(calc.) = 4.46	*crystallographic data* (Sawodny *et al*., 1980)

Table 5.28 (*Contd.*)

Formula	*Selected properties and physical constants*[b]	*Lattice symmetry, lattice constants* (Å), *polyhedron type and density* (g cm^{-3})[c]	*Remarks regarding information available and references*
$NOUF_6$	greenish-white; IR (cm^{-1}): ν(U–F) = 2333, 550s, 509sh; Raman: 616, 495, 441, 225, 206; $\|g\| = 0.748$	cubic; T_h^7, *Ia*3, No. 206; a = 10.464; d(exp.) = 4.30(5)	*crystallographic data* (Brown, 1973; Penneman *et al.*, 1973; *chemical reactivity, absorption spectra; IR and Raman spectra* (Geichman *et al.*, 1962; Bacher and Jacob, 1980); *ESR spectra* (Rigny *et al.*, 1971)
$C_{36}H_{30}P_2NUF_6$ bis (triphenylphosphine) iminium hexafluorouranate(V)	exhibits an unusual g-tensor with $\|g_1\| = 0.79$, $\|g_2\| = 0.69$, $\|g_3\| = 0.65$ which is attributed to low site symmetry and/or very small distortions of the UF_6^- octahedron	triclinic; C_i^1, $P\bar{1}$, No. 2; a = 14.553 (9), b = 12.110(7), c = 12.384(8); α = 73.08(4)°, β = 95.40(5)°, γ = 64.64(4)°; Z = 2; d(exp.) = 1.62, d(calc.) = 1.62; the U atom lies in a general position in the cell; d(U–F) = distances range between 2.00(1) and 2.061.	*crystal structure, EPR spectra* (Eastman *et al.*, 1981)
$Co(UF_6)_2{\cdot}4H_2O$		triclinic; a = 11.52, b = 10.11, c = 5.22; α = 91.30°, β = 91.30°, γ = 90.0°; d(exp.) = 4.52	*crystallographic data* (Montoloy and Plurien, 1968)
other hexa- and heptafluoro complexes: (i) K_2UF_7; Rb_2UF_7; (ii) Cs_2UF_7; (iii), (iv) $(NH_4)_2UF_7$; (v) $N_2H_6UF_7$; (vi) $N_2H_6(UF_6)_2$; (vii) NO_2UF_6; (viii) $(NH_3OH)UF_6$; (ix) $As(C_6H_5)_4UF_6$; (x) $Cu(UF_6)_2{\cdot}4H_2O$.			*general properties* (i–iv) Penneman *et al.*, 1964b; (v) Frlec *et al.* (1966), (vi) Frlec and Hyman (1967) (vii) Gleichman *et al.*,1961 (i–x) Bacher and Jacob, 1980

Na_3UF_8	pale blue; $\mu_{eff.} = 2.29$ B.M.	tetragonal; D_{4h}^{17}, *I*4/*mmm*, No.139; Na_3PaF_8 structure type; $a = 5.470$, $c = 10.940$	*crystallographic data* (Brown, 1973; Penneman *et al.*, 1973; Freestone and Holloway, 1991); *magnetic susceptibility, ^{19}F-NMR spectra* (Bacher and Jacob, 1980)
K_3UF_8	pale blue	fcc cubic; O_h^5, $Fm\bar{3}m$, No. 225, $a = 9.20$	*crystallographic data* (Brown, 1973; Penneman *et al.*, 1973; Freestone and Holloway, 1991); *IR spectra* (Bacher and Jacob, 1980)
Rb_3UF_8		fcc cubic; O_h^5, $Fm\bar{3}m$, No. 225, $a = 9.60$	*crystallographic data* (Brown, 1968; Bacher and Jacob, 1980; Freestone and Holloway, 1991); *absorption spectra and spectral data* (Bacher and Jacob, 1980; Penneman *et al.*, 1964b)
Cs_3UF_8		fcc *cubic;* O_h^5, $Fm\bar{3}m$, No.225	*X-ray powder diffraction data, absorption spectra, magnetic susceptibilities* (Bacher and Jacob, 1980)
Ag_3UF_8		cubic; $a = 4.36$; d(exp.) = 6.49	*crystallographic data* (Brown, 1973; Penneman *et al.*, 1973; Freestone and Holloway, 1991); *IR spectra* (Bacher and Jacob, 1980)
Tl_3UF_8		cubic; $a = 4.75$	*crystallographic data* (Bougon and Plurien, 1965; Freestone and Holloway, 1991). (Bacher and Jacob, 1980)

Table 5.28 (*Contd.*)

Formula	*Selected properties and physical constants*[b]	*Lattice symmetry, lattice constants* (Å), *polyhedron type and density* (g cm^{-3})[c]	*Remarks regarding information available and references*
other octafluoro complexes:			
$(NH_4)_3UF_8$.			
$N_2H_6(UF_6)_2$	bluish-green; $\mu_{eff} = 1.61$ B.M. (80–293 K)		*magnetic susceptibility, IR and Raman data* (Frlec *et al*., 1966; Frlec and Hyman, 1967)
$N_2H_6UF_7$	yellow; $\mu_{eff} = 1.66$ B.M. at 273 K (160–280 K); $\theta = 111$ K		*magnetic susceptibility, IR and Raman data* (Frlec *et al*., 1966; Frlec and Hyman, 1967)
$(NH_3OH)UF_6$	blue; $\mu_{eff} = 152$ B.M. at 300 K; (the Curie–Weiss law is not obeyed)		*magnetic susceptibility, IR and Raman data* (Frlec and Hyman, 1967)
$[N(C_2H_5)_4]_2UOF_5$	pink; air sensitive; IR data (cm^{-1}): ν(U–O) = 852, 760 cm^{-1}; $\lvert g \rvert$ = 0.58		*IR data* (Ryan, 1971); *EPR and crystal-field spectra* (Selbin and Sherrill, 1974)
$[N(C_2H_5)_4]_2$ $UOF_5{\cdot}2H_2O$	pink; air sensitive; IR data: ν(U–O) = 872, 780 cm^{-1}		*IR data* (Ryan, 1971)
UO_2F		monoclinic; $a = 8.22$, $b = 6.81$, $c = 32.08$; $\beta = 90.5$	*X-ray powder diffraction, optical and magnetic data* (Kemmler-Sack, 1967, 1969)
$UO_2F_{0.25}$	deep-gray to black	cubic; fluorite type of structure; $a = 5.49$; $Z = 4$; d(calc.) = 11.4; d(exp.) = 11.0	*X-ray powder diffraction, optical and magnetic data* (Kemmler-Sack, 1967, 1969)
(i) $NaSrU_2O_6F$		cubic; O_h^7, $Fd3m$, No. 227;	*crystallographic data* (Kemmler-Sack, 1968c)
(ii) $KSrU_2O_6F$		(i) $a = 11.16$	
(iii) $RbSrU_2O_6F$		(ii) $a = 11.27$	
(iv) $TlSrU_2O_6F$		(iii) $a = 11.34$	
(v) $NaBaU_2O_6F$		(iv) $a = 11.27$	

(vi) $KBaU_2O_6F$ (vii) $RbBaU_2O_6F$ (viii) $TlBaU_2O_6F$ (ix) $KPbU_2O_6F$ (x) $RbPbU_2O_6F$ (xi) $TlPbU_2O_6F$		(v) $a = 11.31$ (vi) $a = 11.39$ (vii) $a = 11.45$ (viii) $a = 11.40$ (ix) $a = 11.33$ (x) $a = 11.36$ (xi) $a = 11.36$	
$UZr_6O_{14}F$		orthorhombic; C_{2v}^9, $Pna2_1$, No.33; $a = 5.328(1)$, $b = 36.64(1)$, $c = 5.065(1)$; $Z = 4$; $V = 988.78$; d(calc.) = 6.91	*crystallographic data* (Papiernik *et al.*, 1980, 1983)
α-UCl_5	red-brown; very moisture sensitive; in water disproportionates to U(IV) and U(VI); soluble in CS_2, CCl_4 and $SOCl_2$. m.p. = dec; density = 3.81 g cm^{-3}. UCl_5(cr): $\Delta_f G_m^o = -930.1$ (3.9)†, $\Delta_f H_m^o = -1039.0$ (3.0)†, $S_m^o = 242.7$ (8.4)†; $C_{p,m}^o = 150.6$ (8.4)†. UCl_5(g): $\Delta_f G_m^o = -849.6$ (15.1)†, $\Delta_f H_m^o = -900$ (15)†, $S_m^o = 438.7$ (10.0)†; $C_{p,m}^o = 123.6$ (5.0)†. log p (mmHg) = $-3307\ T^{-1} + 3.361$ $\mu_{eff.} = 2.00$ B.M, $\theta = -99$ K, (14–300 K); ESR: $\lvert g \rvert = 1.188$; IR (cm^{-1}): 360, 340, 320, 308sh, 263, 227, 177, 169, 150, 127, 116, 102, 64; Raman (cm^{-1}): 367, 324, 130;crystal-field data (cm^{-1}): $B_0^4 = 134.79$ (1125), $B_0^6 = 158.6(745)$, $\varsigma_{5f} = 1559(115)$	monoclinic; C_{2h}^2, $P2_1/n$, No.11; structure based on cubic close packing of Cl atoms in which U atoms occupy one-fifth of the octahedral holes; two such octahedra share one edge forming a U_2Cl_{10} unit; d[U–Cl(1)] = 2.70, d[U–Cl(1')] = 2.67, d[U–Cl(2)] and d[U–Cl(4)] = 2.43, d[U–Cl(3)] and d[U–Cl(5)] = 2.44; $a = 7.99$, $b = 10.69$, $c = 8.48$; $\beta = 91.5$; $Z = 4$; d(calc.) = 3.81	*synthesis:* (Rediess and Sawodny, 1982); *crystallographic data* (Smith *et al.*, 1967; Brown, 1973); *thermodynamic data* (Grenthe *et al.*, 1992; Guillaumont *et al.*, 2003); *electrical properties, optical data and crystal-field analysis* (Leung and Poon, 1977; Brown, 1979; Carnall and Crosswhite, 1985); *photoelectron spectra* (Thibaut *et al.*, 1982); *IR and Raman spectra*; (Brown, 1979); *magnetic properties and electron spin resonance data* (Handler and Hutchison, 1956; Fuji *et al.*, 1979; Miyake, 1991)
β-UCl_5	red-brown	triclinic; C_i^1, $P\bar{1}$, No.2; $a = 7.07$, $b = 9.65$, $c = 6.35$; $\alpha = 89.1$,	*crystallographic data* (Müller and Kolitsch, 1974)

Table 5.28 (*Contd.*)

Formula	*Selected properties and physical constants*[b]	*Lattice symmetry, lattice constants* (Å), *polyhedron type and density* (g cm^{-3})[c]	*Remarks regarding information available and references*
		$\beta = 117.36$, $\gamma = 108.54$; structure based on hexagonal close packing of Cl atoms. In the U_2Cl_{10} units the U–Cl distances of the bridging atoms are 2.70 and those involving the terminal Cl atoms are ranging from 2.43 to 2.45	
$Cl_4UCl_2UCl_4$		triclinic; C_i^1, $P\bar{1}$, No.2; $a = 7.07$, $b = 9.65$, $c = 35.89$; $\alpha = 89.1$, $\beta = 117.36$, $\gamma = 108.54$; $Z = 1$; $V = 360.4$; d(calc.) = 3.83	*crystallographic data* (Müller and Kolitsch, 1974); *spectral data* (Gruen and McBeth, 1969)
$(SCl_3)(UCl_6)$		orthorhombic; D_2^4, $P2_12_12_1$, No. 19; $a = 10.668(10)$, $b = 10.712(4)$, $c = 11.333(6)$; $Z = 4$; $V = 1295.09$; d(calc.) = 3.02	*crystallographic data* (Sawodny *et al*., 1983)
UCl_5 adducts: $UCl_5{\cdot}Cl_2C = CClCOCl$; $UCl_5{\cdot}Ph_3PO$; $UCl_5{\cdot}SOCl_2$; $UCl_5{\cdot}AlCl_3$(g).			*general properties* (Sillén and Martell, 1964; Bagnall *et al*., 1964; Gruen and McBeth, 1969)
$LiUCl_6$	IR data (cm^{-1}): $\nu_1 = 343$; $\nu_2 = 293$; $\nu_5 = 160$		*infrared and Raman data* (Stumpp and Piltz, 1974)
α-$NaUCl_6$	yellow; IR data (cm^{-1}): $\nu_1 = 343$; $\nu_2 = 273$; $\nu_5 = 136$	cubic; O_h^5, $Fm\bar{3}m$, No. 225, $a = 9.86(2)$; $Z = 4$; d(U-Cl) = 4.93; d(calc.) = 3.26	*X-ray powder diffraction data*; *thermodynamic data* (Kudryashov *et al*., 1978; Fuger *et al*., 1983); *infrared and Raman data* (Stumpp and Piltz, 1974)
β-$NaUCl_6$	yellow	trigonal; C_{3i}^2, $R\bar{3}$, No.148; $a = 6.56(1)$, $c = 18.68(3)$; $Z = 3$; d(U-Cl) =	*X-ray powder diffraction data; thermodynamic data* (Kudryashov

		4.90; d(calc.) = 3.37, d(exp.) = 3.15	*et al.*, 1978; Fuger *et al.*, 1983); *infrared and Raman data* (Stumpp and Piltz, 1974)
$KUCl_6$	yellow; IR data (cm^{-1}): $\nu_1 = 343$; $\nu_2 = 286$; $\nu_5 = 141$	orthorhombic; D_{2h}^{18}, *Cmca*, No.64; $a = 6.97(1)$, $b = 14.14(3)$, $c = 9.66(2)$; $Z = 4$; d(U-Cl) = 6.23; d(calc.) = 3.40	*X-ray powder diffraction data; thermodynamic data* (Kudryashov *et al.*, 1978; Fuger *et al.*, 1983); *infrared and Raman data* (Stumpp and Piltz, 1974)
$RbUCl_6$	deep yellow; moisture and oxygen sensitive; m.p. >280 °C;; IR data (cm^{-1}): $\nu_1 = 341$; $\nu_2 = 273$; $\nu_5 = 136$	orthorhombic; D_{2h}^{18}, *Cmca,* No. 64; $a = 6.92(1)$, $b = 14.14(3)$, $c = 9.66(2)$; $Z = 4$; d(U-Cl) = 6.23; d(calc.) = 3.74	*X-ray powder diffraction data*; *thermodynamic data* (Kudryashov *et al.*, 1978; Fuger *et al.*, 1983); *infrared and Raman data* (Stumpp and Piltz, 1974)
$CsUCl_6$	yellow; moisture sensitive; soluble in $SOCl_2$; m.p. = 360°C; μ_{eff} = 1.71 B.M., θ = –161 K, (83–308 K); IR data (cm^{-1}): $\nu_1 = 342$; $\nu_2 = 280$; $\nu_5 = 139$	cubic; O_h^5, $Fm\bar{3}m$, No. 225; a = 10.22(1); $Z = 4$; d(calc.) = 3.61, d(U–Cl) = 5.11	*X-ray powder diffraction data; thermodynamic data* (Kudryashov *et al.*, 1978; Fuger *et al.*, 1983); *infrared and Raman data* (Stumpp and Piltz, 1974)
$TlUCl_6$	orange yellow; IR data (cm^{-1}): $\nu_1 = 348$; $\nu_2 = 283$; $\nu_5 = 147$		*infrared and Raman data* (Stumpp and Piltz, 1974)
$UCl_5 \cdot PCl_5$ (= $[PCl_4]^+[UCl_6^-]$)	orange-red; air sensitive; IR data (cm^{-1}): $\nu_1 = 343$; $\nu_2 = 271$; $\nu_5 = 130$	triclinic; C_i^1, $P\bar{1}$, No.2; a = 7.038(4), b = 7.373(4); c = 13.706(8); α = 89.38(3), β = 88.80(3)°, γ = 105.20(3)°; $Z = 2$; V = 686.09, d(calc.) = 3.02; d(U–Cl) = 2.474(13) to 2.517(14); Cl–U–Cl = 88.6(5) to 92.1(6); the compound is isomorphous with $PCl_5 \cdot NbCl_5$ and $PCl_5 \cdot TaCl_5$, consisting of an assemblage of octahedral $U(1)Cl_6^-$, $U(2)Cl_6^-$ and tetrahedral PCl_4^+ groups. The array of the chlorine atoms are hexagonal	*crystal and molecular structure* (Taylor and Waugh, 1983); *infrared and Raman data* (Stumpp and Piltz, 1974)

Table 5.28 (*Contd.*)

Formula	*Selected properties and physical constants*[b]	*Lattice symmetry, lattice constants* (Å), *polyhedron type and density* (g cm^{-3})[c]	*Remarks regarding information available and references*
		close packed, while the polyhedra are regular within experimental errors	
$[P(C_6H_5)_3CH_2(C_6H_5)]UCl_6$	orange crystals; discolors on exposure to air	monoclinic; C_{2h}^5, $P2_1/c$, No.14; $a = 11.72(1)$, $b = 18.78(1)$, $c = 13.61(1)$; $\beta = 105.71(2)$; $Z = 4$; d(calc.) = 1.851, d(exp.) = 1.85(1). Each uranium atom is surrounded by a slightly distorted octahedron of six crystallographically independent Cl atoms at U–Cl distances ranging from 2.469(7) to 2.513(7)	*crystallographic data* (de Wet *et al.*, 1978)
$[C(N_3)_3]UCl_6$	IR data (cm^{-1}): $\nu_1 = 347$; $\nu_3 = 314$; $\nu_4 = 127$; $\nu_5 = 129$	hexagonal; D_{3d}^1, $P\bar{3}1m$, No.162; $a = 8.19(2)$, $c = 6.43(5)$; d(U–Cl) = 2.56	*crystallographic data; infrared and Raman data* (Kolitsch and Müller, 1974)
$[N(CH_3)_4]UCl_6$	yellow; air sensitive; soluble in $MeNO_2$, MeCN, Me_2CO, Et_2O; $\mu_{eff.} = 1.62$ B.M.; $\theta = -161$K; IR data (cm^{-1}): $\nu_1 = 345$; $\nu_2 = 278$; $\nu_5 = 134$; $\nu_6 = 95$; ν(U–Cl)as = 310		*Infrared and Raman data* (Shamir and Silberstein, 1975, Shamir *et al.*, 1975)
$[N(C_2H_5)_4]UCl_6$	deep yellow cryst.; soluble in $MeNO_2$, MeCN, Me_2CO, Et_2O; IR data (cm^{-1}): $\nu_3 = 310$; $\nu_4 = 122$; ν(U–Cl)as. = 303–310; $\|g\| = 1.12$		*absorption spectra and crystal-field analysis* (Ryan, 1971; Edelstein *et al.*, 1974); *infrared and Raman data* (Ryan, 1971); *ESR data* (Edelstein *et al.*, 1974)

$[N(C_3H_7)_4]UCl_6$	yellow; air sensitive; soluble in $SOCl_2$, $MeNO_2$, MeCN, Me_2CO, Et_2O; IR data (cm^{-1}): $\nu_1 = 340$; $\nu_2 = 278$; $\nu_3 = 310$; $\nu_4 = 121$; $\nu_5 = 129$; $\nu_6 = 91$	*infrared and Raman data* (Shamir and Silberstein, 1975, Shamir *et al*., 1975)
$[As(C_6H_5)_4]UCl_6$	yellow cryst.; soluble in $MeNO_2$, MeCN, Me_2CO, Et_2O; $\mu_{eff.} = 2.14$ B.M.; $\theta = -280$ K; IR data (cm^{-1}): $\nu_1 = 340$; $\nu_2 = 276$; $\nu_3 = 319$; $\nu_4 = 124$; $\nu_5 = 124$	*infrared and Raman data* (Kolitsch and Müller, 1975)
other hexachloro complexes: $AgUCl_6$; $Ba(UCl_6)_2$; $[NH_2(CH_3)_2]UCl_6$; $[N(CH_3)_4]_3UCl_8$;		*general properties* (Brown, 1979)
$[(N(C_2H_5)_4]_2UOCl_5$	blue; assignment of electronic bands in D_4 symmetry: $\Gamma_7 \rightarrow \Gamma_6 = 1555$, $\Gamma_7 \rightarrow \Gamma_7 = 5050$, $\Gamma_7 \rightarrow \Gamma_7 = 6161$, $\Gamma_7 \rightarrow \Gamma_6 = 8584$, $\Gamma_7 \rightarrow \Gamma_7 = 10616$, $\Gamma_7 \rightarrow \Gamma_6 = 16835$; IR data ($cm^{-1}$): ν(U–O) = 913, 813; other observed bands: 296, 253, 197, and 120	*infrared* (Ryan, 1971) *and electronic spectral data* (Selbin *et al*., 1972a)
$UOCl_3$	brown; moisture sensitive, dissolves in alcohols and $MeNO_2$; sl. soluble in acetone and CCl_4; soluble. in water with decomposition; $UOCl_3$(cr): $\Delta_f G^o_m = -1045.6$ (8.3)†, $\Delta_f H^o_m = -1140.0$ (8.0)†, $S^o_m = 170.7$ (8.4)†; $C^o_{p,m} = 117.2$ (4.2)†. IR (cm^{-1}): 450, 615, 750, 845, 965	*synhthesis* (Brauer, 1981); *thermodynamic and infrared data* (Brown, 1979; Grenthe *et al.*, 1992; Guillaumont *et al*., 2003)

Table 5.28 (*Contd.*)

Formula	*Selected properties and physical constants*[b]	*Lattice symmetry, lattice constants* (Å), *polyhedron type and density* (g cm^{-3})[c]	*Remarks regarding information available and references*
UO_2Cl	violet brown or reddish grey; air sensitive; decomposes >600°C and in aqueous media; not soluble in organic solvents; UO_2Cl(cr): $\Delta_f G^o_m = -1095.2\ (8.4)^\dagger$, $\Delta_f H^o_m = -1171.1\ (8.0)^\dagger$, $S^o_m = 112.5\ (8.4)^\dagger$; $C^o_{p,m} = 88\ (5)^\dagger$. $\mu_{eff} = 1.86$ B.M., $\Theta = -95$ K		*thermal and magnetic properties data* (Brown, 1979; Grenthe *et al.*, 1992; Guillaumont *et al.*, 2003); *magnetic properties* (Levet, 1969); *photoelectron spectra* (Thibaut *et al.*, 1982)
$(UO_2)_2Cl_3$ (mixed valence)	black-brown; contains hexa- and pentavalent uranium; hygroscopic, forms $(UO_2)_2Cl_3 \cdot 7H_2O$ on exposure to air; dissolves slowly in H_2O and dilute mineral acids $\Delta_f G^o_m = -2234.8\ (2.9)^\dagger$, $\Delta_f H^o_m = -2404.5\ (1.7)^\dagger$, $S^o_m = 276\ (8)^\dagger$; $C^o_{p,m} = 203.6(5.0)^\dagger$	orthorhombic; $a = 5.833(2)$, $b = 20.978(2)$, $c = 11.9266(5)$; $Z = 8$, d(calc.) = 5.88, d(exp.) = 6.02	*crystallographic data* (Cordfunke *et al.*, 1977); *thermodynamic data* (Cordfunke *et al.*, 1977; Grenthe *et al.*, 1992; Guillaumont *et al.*, 2003)
$U_2O_2Cl_5$	$\Delta_f G^o_m = -2037.3\ (4.9)^\dagger$, $\Delta_f H^o_m = -2197.4\ (4.2)^\dagger$, $S^o_m = 326.3\ (8.4)^\dagger$; $C^o_{p,m} = 219.4(5.0)^\dagger$	orthorhombic; D^{19}_{2h}, *Cmmm*, No.65; $a = 8.431(3)$, $b = 13.663(3)$, $c = 4.106(2)$; $Z = 2$; $V = 472.98$; d(calc.) = 4.81	*crystallographic data* (Levet *et al.*, 1980); *thermodynamic data* (Cordfunke *et al.*, 1983; Grenthe *et al.*, 1992; Guillaumont *et al.*, 2003)
$U_5O_{12}Cl$	$\Delta_f G^o_m = -5518.0\ (12.4)^\dagger$, $\Delta_f H^o_m = -5854.4\ (8.6)^\dagger$, $S^o_m = 465\ (30)^\dagger$	orthorhombic; D^5_{2h}, *Pmma*, No.51; $a = 7.111(9)$, $b = 19.625(12)$, $c = 4.130(2)$; $Z = 2$; $V = 576.36$; d(calc.) = 8.17	*crystallographic data* (Cordfunke *et al.*, 1985); *thermodynamic data* (Cordfunke *et al.*, 1985; Grenthe *et al.*, 1992; Guillaumont *et al.*, 2003)

UBr_5	deep-brown, dec.. UBr_5(cr): $\Delta_f G^o_m$ = –769.3 (9.2)†, $\Delta_f H^o_m$ = –810.4 (8.4)†, S^o_m = 292.9 (12.6)†; $C^o_{p,m}$ = 160.7 (8.0)†. UBr_5(g): $\Delta_f G^o_m$ = –668.2 (15.3)†, $\Delta_f H^o_m$ = –648 (15)†, S^o_m = 498.7 (10.0)†; $C^o_{p,m}$ = 129.0 (5.0) $\mu_{eff.}$ = 1.42 B.M. (χ_g = 1.316×10^{-6} at 291 K), (11–291 K)	triclinic; C_1^1; $P\bar{1}$, No. 2; a = 7.449 (7), b = 10.127(14), c = 6.686(4); α = 89.25(12°), β = 117.56(4)°, γ = 108.87(9)°; Z = 2; V = 417.46; d(calc.) = 5.07; d(U–Br) = 2.81(7) and 2.94(7) for bridging atoms and 2.58(7) to 2.58(7) for terminal atoms	*crystallographic data* (Levy *et al.*, 1978); *magnetic susceptibility data* (Eichberger,, 1979); *photoelectron spectra* (Thibaut *et al.*, 1982); *thermodynamic data* (Grenthe *et al.*, 1992; Guillaumont *et al.*, 2003)
$P(C_6H_5)_4[UBr_6]$	brown crystals; extremely oxygen- and moisture-sensitive; soluble in CH_2Cl_2	monoclinic; C^6_{2h}, $C2/c$, No.15; a = 23.155(4), b = 6,950(3), c = 18.052 (3); β = 96.38(2)°; Z = 4; V = 2887; d(calc.) = 3.07 d(U–Br1 and U–Br2) = 2.669(3); d(U–Br3 or U–O) = 2.654(4); Br–U–Br = 89.9(11) and O–U–O = 88.8(1) or 89.9(1)	*synthesis and crystallographic data* (Bohrer *et al.*, 1988) *absorption spectra; ESR data* (Eichberger and Lux, 1980; Edelstein *et al.*, 1974); *infrared spectra* (Brown, 1979)
$P(C_6H_5)_4[UBr_6]\cdot2CCl_4$	almost black crystals; IR (cm^{-1}): ν(U–Br) = 215	monoclinic; C^5_{2h}, $P2_1/c$; No.14; a = 11.115(3), b = 21.142(5), c = 17.187(5), β = 95.42(3)°; Z = 4; V = 4021; d(calc.) = 2.25; d(U–Br) = 2.603(4) to 2.679(3); d(U–O) = 2.674(4); Br1–U–Br2 = 89.3(1) Br1–U–Br3 (or O) = 89.5(1) Br2–U–Br3 (or O) = 91.1(1)	*synthesis and crystallographic data* (Bohrer *et al.*, 1988)
$MUBr_6$ [M = (i) Na, K, Rb, (ii) Cs, NH_4, (iii) $N(C_2H_5)_4$, $N(C_4H_9)_4$, $As(C_6H_5)_4$,	brown to black; IR data (cm^{-1}) for $N(C_2H_5)_4UBr_6$: ν_3 = 215; ν_4 = 87; ν(lattice) = 62→68; ν_6 (IR and R inactive) = 61; (i) $\|g\|$ = 1.245; (ii) $\|g\|$ = 1.21; (iii) $\|g\|$ = 1.21		*absorption spectra; ESR data* (Eichberger and Lux, 1980; Edelstein *et al.*, 1974); *infrared spectra* (Brown, 1979); *crystal-field analysis for* $[N(C_2H_5)_4]UBr_6$ (Ryan, 1971, Eichberger and Lux, 1980)

Table 5.28 (*Contd.*)

Formula	*Selected properties and physical constants*[b]	*Lattice symmetry, lattice constants* (Å), *polyhedron type and density* (g cm^{-3})[c]	*Remarks regarding information available and references*
M_2UOB_5 (i) M = N $(C_2H_5)_4$ and (ii) As $(C_6H_5)_4$.	IR: 919, 817 (U–O, stetch.), 250, 190 and 80 cm^{-1}; for (i): green solid; $\varsigma_{5f} = 1750\ cm^{-1}$, $\Gamma_6 = 16194$, $\Gamma_7 = 10460$, $\Gamma_6 = 8163$, $\Gamma_7 = 6080$, $\Gamma_7 = 4865$, $\Gamma_7 = 1490$, $\Gamma_7 = 0$; $\|g\| = 1.24$; (ii) green solid		*absorption spectra; ESR data; infrared spec tra* (Selbin and Sherrill, 1974; Brown, 1979)
$[N(C_2H_5)_4]_2UBr_6 \cdot 2.5\ N(C_2H_5)_4Br$	green; IR data (cm^{-1}): ν(M–O) = 919, 817; ν(M–Br) = 190s, 80m.		*infrared data* (Ryan, 1971)
$UOBr_3$	brown; $UOBr_3$ (cr): $\Delta_f G^o_m$ = –901.5 (21.3)†, $\Delta_f H^o_m$ = –954(0)†, S^o_m = 205.0 (12.6)†; $C^o_{p,m}$ = 120.9 (4.2)†	monoclinic; C_2^3, *C*2, No.5; *a* = 16.24, *b* = 3.7, *c* = 9.0; $\beta = 110.5$	*crystallographic data* (Brown, 1973); *thermodynamic data* (Rand and Kubaschewski, 1963; Grenthe *et al*., 1992; Guillaumont *et al*., 2003)
UO_2Br	brown-black; $\mu_{eff} = 1.76$ B.M., $\Theta = -200$ K	orthorhombic; D_{2h}^{17}, *Cmcm*, No. 63; *a* = 4.106(1), *b* = 20.200 (5), *c* = 3.980(1); *d*(calc.) = 6.97. The coordination polyhedron is a pentagonal bipyramid with two Br and three U atoms; *d*(U–Br) = 2.939(3) in the base of the pentagon; *d*(U–O1) = 2.17(1)×2	*crystallographic data* (Levet *et al*., 1977); *magnetic susceptibility data* (Levet, 1969); *thermodynamic data* (Shchukarev *et al*., 1959); *photoelectron spectra* (Thibaut *et al*., 1982)

		and d(U–O'1) = 2.30(3) = 2.30(3) in the base of the pentagon; d(U–O2) = 2.054(1))×2 at the apices; d(Br–Br) = 3.870(6). The angles are: O(2)–U–(O2) = 176.8 (2); O(2)–U–O'(1) = 90.6(4); Br–U–Br = 85.2(2); Br–U–O(1) = 70.7(2)	
$[N(C_2H_5)_4]_2UOBr_5$; $[As(C_6H_5)_4]_2UOBr_5$; $[N(C_2H_5)_4]_2UOBr_5 \cdot 2.5N(C_2H_5)_4Br$	IR vibrations for $UOBr_5^{2-}$ species (cm^{-1}): 919, 817, 250, 190, and 80; ν(U–O, stretch.) = 919, 817		*absorption spectra; crystal-field analysis* (Selbin and Sherrill, 1974); *infrared spectra* (Ryan, 1971)

* Peritectic decomposition point.

† Values recommended by the Nuclear Energy Agency (Grenthe *et al.*, 1992; Guillaumont *et al.*, 2003).

* *R*, *rhombohedral* (*hexagonal parameters given*).

[a] Values have been selected in part from review articles (Brown, 1979; Bacher and Jacob, 1980; Freeman,1991; Grenthe *et al.*, 1992; Guillaumont *et al.*, 2003).

[b] m.p. = melting point (°C); b.p. = boiling point (°C); (cr) = crystalline; (g) = gaseous; thermodynamic values in kJ mol^{-1}, or J K^{-1} mol^{-1} at 298.15 K, unless otherwise mentioned; $\Delta_f G^o_m$ (kJ mol^{-1}), standard molar Gibbs energy of formation; $\Delta_f H^o_m$(kJ mol^{-1}), standard molar enthalpy of formation; S^o_m, standard olar entropy; $C^o_{p,m}$(J K^{-1} mol^{-1}), standard molar heat capacity; log p (mmHg) = $-AT^{-1} + B - C \log T$, vapor pressure equation for indicated temperature range; IR = infrared active; val. = valence vibrations; def. = deformation vibrations; stretch. = stretching; all values in cm^{-1}; s: strong; m: medium; w: weak; sh: shoulder; ς_{5f} = spin-orbit interaction parameter; B^k_2-crystal-field parameters; $\mu_{eff.}$ = effective magnetic moment; B.M. = Bohr magneton.

[c] All values are in Å and angles are in degrees; CN, coordination number; d = density [g cm^{-3}], V = molar volume [cm^3 mol^{-1}].

[d] Temperature range with linear relationship of χ_M^{-1} against T.

[e] Deduced from measurements in excited states spectra.

magnetic moments $\mu_{\text{eff}} = 2.84\sqrt{c}\mu_{\text{B}}$ along with some other physical constants are summarized in Table 5.28.

(*i*) *Uranium pentafluoride and uranium(v) complex fluorides*

Uranium pentafluoride

The pentafluoride exists in two crystalline modifications: a high-temperature α-UF_5 (over 150°C) and a low-temperature β-UF_5 form (below 125°C). The general preparation procedures involve either the oxidation of UF_4 or reduction of UF_6 (Bacher and Jacob, 1980). Halogen fluorides, some noble gas fluorides, and CoF_3, VF_3, and OF_2 may be used as oxidation reagents. The formation of α-UF_5 can be achieved by fluorine oxidation of UF_4 at 150°C, or the conversion of UCl_5 by gaseous HF at 300°C; the low-temperature form may be prepared by the reaction with anhydrous liquid HF (AHF) and UCl_6 or UCl_5. The β-form may be also obtained by reduction of UF_6 by silicium powder, NH_3, or $SOCl_2$. This compound is also formed in AHF in the presence of gold plates, by pyrolysis of NH_4UF_7, photolysis of UF_6 by UV light, and by reaction of $NOUF_6$ in a solution of AHF and BF_3. The reduction of UF_6 to UF_5 has also been achieved in hydrogen bromide and CF_3COOH. Some of the preparation methods are of little practical importance because of small yields, an impure product, or inconvenient starting materials. On laboratory scale the most convenient procedures involve photoreduction of UF_6 in the presence of H_2, CO, or SO_2. The reaction between UF_4 and UF_6 results in the formation of β-UF_5 below 125°C and α-UF_5 at 230–250°C. β-UF_5 is formed also in the following reaction at molar ratios 1.1 to 1 between UF_6 and $(CH_3)_3SiX$ (Brown *et al.*, 1983):

$$UF_6 + (CH_3)_3SiX \rightarrow (CH_3)_3SiF + 1/2X_2 + UF_5 \quad (X = \text{Cl or Br})$$

The pentafluoride is a hygroscopic crystalline solid, which disproportionates even in a humid atmosphere, according to reaction

$$2UF_5 + 3H_2O \rightarrow UF_4 + UO_2F_2 \cdot H_2O + 4HF$$

In aqueous solutions this reaction results in the precipitation of the hydrated tetrafluoride and the formation of a solution of uranyl fluoride. Above 150°C, UF_5 disproportionates slowly to U_2F_9(s) and UF_6(g). The disproportionation reaction can be limited by the presence of UF_6(g); the temperature dependence of the vapor pressure follows the equations (Wolf *et al.*, 1965):

$$\log p_{\text{solid}}(\text{mmHg}) = -8001\, T^{-1} + 13.99$$
$$\log p_{\text{liquid}}(\text{mmHg}) = -5388\, T^{-1} + 9.82$$

UF_5 can be reduced to UF_4 by H_2 or Ni (at 600°C) and by some covalent fluorides such as PF_3, AsF_3, or $AsCl_3$. Halide exchange reactions were observed with BCl_3, $TiCl_4$, and PCl_3, the products being respectively, BF_3, TiF_4, and PF_3, in addition to UF_4 and UCl_6.

Uranium pentafluoride dissolves without hydrolytic decomposition in 48–50% hydrofluoric acid, forming relatively stable blue solutions from which $(H_3O)UF_6 \cdot 1.5H_2O$ crystallizes; by addition of RbF or CsF, the blue MUF_6 salts (M = Rb or Cs) are formed. Uranium pentafluoride dissolves in acetonitrile and reacts with alkali fluorides and sodium ethoxide, NaOEt, to form $M[UF_4]$ and $U_2(OEt)_{10}$, respectively.

The structure of α-UF_5 consists of infinite chains of UF_6 octahedra, bridged by *trans*-fluorides to give a linear chain parallel to the *c*-axis. The remaining four fluorine atoms are single bonded to uranium. The low-temperature β-form is isostructural with PaF_5 and NpF_5 and consists of an eight-coordinate arrangement with a geometry intermediate between dodecahedral and square antiprismatic (Ryan *et al.*, 1976; Eller *et al.*, 1979). The crystal packing of β-UF_5 is shown on Fig. 5.43. Other crystallographic data are listed in Table 5.28.

Theoretical model calculations performed using the vibrational spectrum of monomeric UF_5 molecules isolated in an Ar-matrix indicate a square-pyramidal structure in which the U atoms are located above the equatorial plane formed by the fluorine atoms (Paine *et al.*, 1976).

In non-aqueous solvents such as nitriles, dimethyl sulfoxide, and dimethylformamide, uranium pentafluoride forms stable solutions containing UF_6^- anions and solvated UF_4^+ cations. From these solutions several adducts and complex

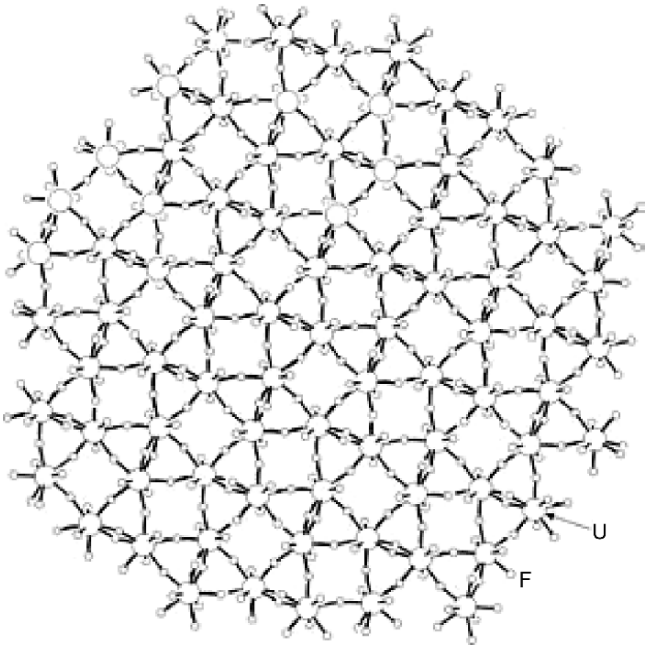

Fig. 5.43 *Crystal packing view of β-UF_5* (*from Ryan* et al., 1976).

fluorides have been isolated, for example, $UF_5 \cdot CH_3CN$, $[UF_4(Me_2SO)_3][UF_6]$, $[UF_4(DMF)_3][UF_6]$, $[(C_6H_5N(CH_3)_3][UF_6]$, $[(C_6H_5)_3PNP(C_6H_5)_3][UF_6]$, Na $[UF_6]$, and K$[UF_6]$ (Berry *et al*., 1977; Halstead *et al*., 1979). The compounds and their solutions have been characterized by electronic, infrared, Raman, and EPR spectra.

Complex uranium(v) fluoro compounds

A number of fluorouranates(v) have been characterized by determination of their crystallographic data and their chemical and thermodynamic properties (see Table 5.28). Additional information in the reviews of Chatalet (1967), Penneman *et al*. (1967), Ryan (1971), Brown (1972), Bacher and Jacob (1980), and Freestone and Holloway (1991). Complex compounds identified in a number of selected fused salt systems are listed in Table 5.29.

The compounds may be prepared by a variety of methods (Bacher and Jacob, 1980; Freestone and Holloway, 1991): (i) solid state reactions between UF_5 and the appropriate alkali fluorides in an inert atmosphere at 300°C constitute a general route to most of the fluoro complexes; (ii) melting of mixtures of hexa- and octafluoro complexes leads to the formation of the heptafluoro complex compounds; (iii) solid state reactions or reduction of UF_6 with NH_3 yield ammonium fluorouranates; (iv) treatment of equimolar mixtures of UF_5 and the appropriate alkali fluoride with anhydrous HF yields the hexafluorouranates(v); (v) oxidation of UF_4–alkli fluoride mixtures with fluorine also leads to the hexafluoruranates; and (vi) $RbUF_6$ may be also obtained by crystallization from solutions of RbF and UF_5 in concentrated HF.

The pentafluoro uranates may disproportionate into U(IV) and U(VI). However, they are relatively stable in the absence of substances that cause hydrolysis. Ohwada (1976) and Soulié (1978) suggest that the U–F bonds in the fluorouranates(v) are partly covalent (68 to 77% as compared to 46.3 and 35%, respectively, in UF_4 and β-K_2UF_5). The bonds in UF_5 are assumed to have

Table 5.29 *Uranium(v) complex fluorides identified in molten salt systems.*

System	*Complex fluorides*
$LiF\text{-}UF_5$	$LiUF_6$
$NaF\text{-}UF_5$	$NaUF_6$, Na_3UF_8
$KF\text{-}UF_5$	KUF_6, K_2UF_7, K_3UF_8
$RbF\text{-}UF_5$	$RbUF_6$, Rb_2UF_7, Rb_3UF_8
$CsF\text{-}UF_5$	$CsUF_6$, Cs_2UF_7, Cs_3UF_8
$NH_4F\text{-}UF_5$	NH_4UF_6, $(NH_4)_2UF_7$, $(NH_4)_3UF_8$
$N_2H_6F_2\text{-}UF_5$	$N_2H_6UF_7$, $N_2H_6(UF_6)_2$
$(NH_3OH)F\text{-}UF_5$	$(NH_3OH)UF_6$

a nearly 100% covalent character. The pentafluoro uranates of the M_2UF_7 type (M = K, Rb, Cs, or NH_4) have the same type of powder patterns ($P2_1/c$, C_{2h}^5, No. 14) as that of K_2NbF_7 where the coordination polyhedon is a monocapped trigonal prism (Brown and Walker, 1966). The analysis of the spectral data for $CsUF_6$ (Carnall and Crosswhite, 1985) made it possible to assign the electronic transitions from the Γ_7 ground state to the excited levels Γ_8, $\Gamma_{7'}$, $\Gamma_{8'}$ and Γ_6 of the $5f^1$ electronic configuration. The spin–orbit coupling parameter ς_{5f} and the B_0^2, B_0^4, and B_0^6 crystal-field parameters determined for the D_{3d} site symmetry are equal to 1910.2(13), 534.2(139), –14866(66) and 3305(78) cm^{-1}, respectively.

Pentavalent oxide fluorides and oxide fluoride complexes

White U_2OF_8 oxide fluoride has been obtained by heating of UF_4 in an intermittent oxygen flow at 850°C (Kirslis *et al.*, 1950; Freestone and Holloway, 1991). The compound disproportionates in vacuo at 300°C to form a mixture of uranyl fluoride and uranium hexa and tetrafluoride. The existence of this compound has not been confirmed by other authors (Ekstrom *et al.*, 1974). A series of uranium oxide fluoride phases, UO_xF_y, containing uranium in the oxidation state 5+ ($UO_{2.33}F_{0.33}$ to $UO_{2.00}F_{1.00}$), a mixture of 5+ and 6+ ($UO_{2.58}F_{0.17}$ to $UO_{2.17}F_{0.83}$) and a mixture of 4+ and 5+ ($UO_{2.00}F_{0.25}$) have been obtained by heating UF_4 with UO_3 or U_3O_8 at 400–500°C *in vacuo* (Kemmler-Sack, 1967, 1969). The possible structures of these phases have been discussed on the basis of X-ray powder, magnetic, and spectral data.

A number of complexes of the $M^IM^{II}U_2O_6F$-type (where M^I = Na, K, Rb, or Tl and M^{II} = Ba, Sr, or Pb) were obtained by heating appropriate mixtures of the component fluorides and oxide fluorides at 500–900°C *in vacuo*, e.g. (i) M^IF with $M^{II}UO_4$, and UO_2; (ii) $M^{II}F_2$ with $M_2{}^IUO_4$, $M^{II}UO_4$, and UO_2, and (iii) M^IUO_2 with $M^{II}O$, UO_3, UO_2, and UF_4 (Kemmler-Sack, 1968a). All complexes have cubic symmetry (Kemmler-Sack, 1968b,c) with similar lattice parameters (Table 5.28). Reflectance spectra of the compound have been analyzed on the basis of the $5f^1$ configuration of the U(v) ion in an octahedral field.

Two additional complex oxide fluoride compounds, $[N(C_2H_5)_4]_2UOF_5$ and $[N(C_2H_5)_4]_2UOF_5 \cdot 2H_2O$, have also been isolated. The hydrated compound is formed by hydrolysis of the corresponding UCl_6 salt in a saturated solution of $[N(C_2H_5)_4]F \cdot nH_2O$ in an ethanol–acetone mixture. The complex is easily dehydrated in vacuum (Ryan, 1971). Both compounds are pink colored and oxygen-sensitive. UOF_5^{2-} solutions may be stabilized by an excess of $[N(C_2H_5)_4]F$. Addition of water results in a rapid disproportionation of UOF_6^{2-} to U^{IV} and U^{VI} species. An analysis of the absorption spectra of $[N(C_2H_5)_4]_2UOF_5$ in solid state and in an acetonitrile solution made it possible to make an assignment of the six electronic transitions based on a D_4 ligand field model (Selbin and Sherrill, 1974).

(*ii*) *Uranium pentachloride and uranium*(*v*) *complex chlorides*

Uranium pentachloride

Uranium pentachloride may be prepared by a number of methods, but only a few of them result in high yields and high purity due to the instability of the compound towards thermal decomposition and disproportionation; these reactions take place below 100°C at pressures between 10^5 Pa (1 atm) and 133×10^{-4} Pa, respectively:

$$UCl_5 \xrightarrow{10^5 Pa} UCl_4 + 1/2Cl_2 \text{ and}$$

$$2UCl_5 \xrightarrow{133 \times 10^{-4} Pa} UCl_4 + UCl_6$$

At normal pressure, the disproportionation is complete in the range 100 to 175°C.

One of the most satisfactory preparative methods is to use liquid phase chlorination of UO_3 or U_3O_8 with carbon tetrachloride at 80–250°C under pressure and UCl_5 as catalyst (Brown, 1979). The most convenient laboratory method involves decomposition of UCl_6 at room temperatures in carbon tetrachloride, methylene dichloride, or 1,2-dichloroethane. Another relatively simple method is the reduction of UO_3 by silicon tetrachloride at 400°C followed by vacuum removal of the excess of reagent from the resulting solution of UCl_5 in $SiCl_4$ (Selbin *et al*., 1968).

Uranium pentachloride is obtained as dark brown crystals, which exist in two crystal modifications. The more often encountered α-UCl_5 is obtained by recrystallization from CCl_4 and the β-UCl_5 is formed by crystallization of UCl_6 from carbon tetrachloride or methylene dichloride (Kolitsch and Müller, 1974). UCl_5 is very hygroscopic and immediately disproportionates into U(IV) and U(VI) in aqueous solutions. It reacts instantly with a number of organic solvents such as alcohols, acetone, dimethyl ether, diethyl ether, ethyl acetate, formamide, or dioxane. In some anhydrous organic solvents such as carbon tetrachloride, carbon disulfide, and thionyl chloride, it forms relatively stable solutions; it is insoluble in benzene, xylene, or isopropyl ether. Impure samples may be recrystallized from carbon tetrachloride and separated from UCl_4 by dissolution and recrystallization from liquid chlorine. Hydrogen reduces UCl_5 to UCl_4 at 250–300°C. Anhydrous gaseous or liquid hydrogen fluoride converts it to UF_5 and fluorine oxidizes it to UF_6. The reactions of UCl_5 with some univalent chlorides yield $N(CH_3)_4UCl_6$, $As(C_6H_5)_4UCl_6$, or $N(CH_3)_2H_2UCl_6$ (Bagnall *et al*., 1964).

The structures of the monoclinic α-UCl_5 (space group $P2_1/n$) and triclinic β-UCl_5 (space group $P\bar{1}$) are based on a cubic or hexagonal close packing of the chlorine atoms. In the first one, the uranium atoms occupy one-fifth of the octahedral holes and two octahedra are forming a dimeric U_2Cl_{10} unit by sharing a common edge. The structure of the β phase contains the same

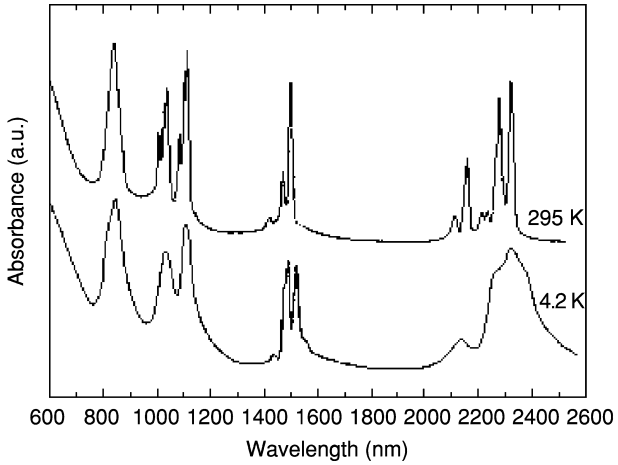

Fig. 5.44 *Absorption spectrum of UCl_5 single crystals at* 4.2 *and* 295 K (*partially adapted from Leung and Poon*, 1977). *Reproduced with the permission of Copyright Clearance on Government of Canada Works.*

U_2Cl_{10} units (Table 5.28). The following ligand-field parameters have been reported from an analysis of the UCl_5 spectrum: $\varsigma_{5f} = 1559(115)$, $B_0^4 = 13479$ (1125) and $B_0^6 = -158.6(745)$ (Leung and Poon, 1977). The electronic absorption spectra of the two UCl_5 crystal modifications (see Fig. 5.44) are identical and similar to those of the hexachlorouranates(v).

The magnetic susceptibility follows the Curie–Weiss law in the 14–300 K temperature range. Different effective magnetic moments were reported: according to Rüdorff and Menzer (1957), they range from 1.05 B.M. at 77 K to 1.42 B.M. at 398 K, while Handler and Hutchison (1956) report $\mu_{eff} = 2.00$ B. M. at 300 K with $\Theta = -99$ K.

Complex uranium(v) chloride compounds

The isolation of numerous pentavalent uranium complexes with ligands containing N, P, As, S, Se, and Te donor atoms has been reported (Selbin and Ortego, 1969; Brown,1972, 1979). Thus, complexes of UCl_5L-type are formed with triphenylphosphine oxide, thionyl chloride, phenazine, 2,2′-bipyridyl, ethylene bis(diphenylphosphine), triphenylphosphine, trioctylphosphine, diarsine, anthrone, benzanthrone, methyleneanthrone, triphenylbismuthine, diphenyldisulphide, Ph_2Se_2, and Ph_2Te_2; those of the $UCl_5{\cdot}2$L-type – with pyrazine, phthalazine, methyl cyanide, pyridine, 1,10-phenanthroline, 2-mercaptopyridine, ethylene bis-salicylaldiamine, 8-hydroxyquinoline, anthrone, benzil, benzanthrone, and triphenylphosphine oxide, while $UCl_5{\cdot}3$L complexes are formed with dioxane and tetramethyl amine.

The preparation of $[N(CH_3)_4]_3UCl_8$ and a number of $MUCl_6$ complexes (where M = $N(CH_3)_4$, $N(CH_3)_2H_2$, $N(C_2H_5)_4$, $N(C_3H_7)_4$, $N(C_3H_9)_4$,

$N(C_4H_9)_4$, $P(C_6H_5)_4$, $As(C_6H_5)_4$, NH_4, K, Rb, etc.) has been achieved by addition of carbon disulfide to thionyl chloride solutions of U(v) using the appropriate MCl compound (Bagnall *et al.*, 1964; Brown, 1979). A convenient alternative method to prepare $MUCl_6$ complexes (where M = $N(C_2H_5)_4$, As $(C_6H_5)_4$, or $N(CH_3)_4$) employs chlorine oxidation in nitromethane solutions (Ryan, 1974). UCl_5tcac (tcac is the acronym for $Cl_2C{=}CClCOCl$) has been reported (Fuji *et al.*, 1979) to be a useful starting material for the preparation of $RbUCl_5$, $(n\text{-}C_3H_7)_4NUCl_5$, and a number of UCl_5 adducts with different donor ligands. Other convenient routes to the U(v) complexes involve the addition of MCl (where M = NH_4, $As(C_6H_5)_4$, or $N(CH_3)_4$) to uranium hexachloride in methylene dichloride (Brown, 1979). The reactions between UO_3, $SOCl_2$, and MCl (M = Na, K, Rb, Cs, NH_4, Ag, Ba, or Tl) in sealed vessels at 180–200°C also lead to uranium(v) hexachloro complexes (Stumpp, 1969); the reaction between UO_3 and PCl_5 results in the formation of $UCl_5 \cdot PCl_5$. The last compound should be formulated as $[PCl_4]^+[UCl_6]^-$ (Brown, 1969). Gruen and McBeth (1969) have reported the formation of a uranium(v) chloro complexes in the vapor phase according to the reaction

$$UCl_4 + \frac{1}{2}Cl_2 + AlCl_3 \rightarrow UCl_5 \cdot AlCl_3$$

The analysis of the high-temperature electronic spectrum indicates that the compound should be formulated as $[AlCl_4]^+[UCl_6]^-$.

The hexachlorouranates(v) are very hygroscopic. On exposure to air they are hydrolyzed with disproportionation to U(IV) and U(VI). With the exception of those containing alkali metal cations, they are soluble in numerous organic solvents such as methyl cyanide, diethyl ether, acetone, nitromethane, or phosphorous oxytrichloride. $CsUCl_6$ is reported to react in inert solvents with oxygen donor ligands forming $UCl_5{\cdot}L$ adducts. Structure data and references to heats of formation determinations of several uranium(v) chloro-complexes are listed in Table 5.28. Spin–orbit and crystal field parameters, $\varsigma_{5f} = (1913)$, B_0^4 = 12209(710), and B_0^6 = –39(776), were determined for $N(C_2H_5)_4UCl_6$ by Edelstein *et al.* (1974). The magnetic susceptibility of $CsUCl_4$, $[(CH_3)_2H_2]$ UCl_6, $[N(CH_3)_4]UCl_6$, and $[As(C_2H_5)_4]UCl_6$ exhibits a Curie–Weiss dependence in two temperture ranges: 140–205 K and 210–310 K. The effective magnetic moments and Weiss constants (in brackets) range between 1.71 (161 K) and 2.14 B.M. (280 K) (Bagnall *et al.*, 1964; Brown, 1979). In the 250–310 K range $[N(CH_3)_4]_3UCl_8$ has a temperature-independent paramagnetism ($\chi_{mole} = 1100 \times 10^{-6}$ cm^3 mol^{-1}).

(*iii*) *Uranium*(*v*) *and mixed valence oxide chlorides*

The most convenient methods for the preparation of $UOCl_3$ involve heating of stoichiometric amounts of (i) UO_3 and $MoCl_5$ at 200–220°C *in vacuo*, (ii) UCl_4 and UO_2Cl_2 at about 370°C, or (iii) UO_2Cl_2 with WCl_5, $ReCl_5$, or $MoOCl_3$ at about 200°C (Brown, 1979). The mechanism of the first reaction is:

$$UO_3 + MoCl_5 \rightarrow UO_2Cl_2 + MoOCl_3$$
$$UO_2Cl_2 + MoOCl_3 \rightarrow UOCl_3 + \uparrow MoO_2Cl_2$$

The brown, moisture-sensitive solid is insoluble in non-polar organic solvents like carbon tetrachloride and benzene, but dissolves without decomposition in anhydrous ethanol. In the latter, it reacts with $C_6H_5N \cdot HCl$ to give $[C_6H_5NH]_2UOCl_5$. In other alcohols, acetone, and water, the compound dissolves with decomposition. Hydrolysis of $UOCl_3$ results in the formation of polymeric –U–O–U–O– chains. The reduction with $MoOCl_3$, $MoCl_5$, or $ReCl_5$ *in vacuo* around 200°C leads to UCl_4.

The preparation of UO_2Cl can be achieved by heating equimolar quantities of UO_2Cl_2 and UO_2 at 590°C *in vacuo* (Levet, 1969) or by reduction of UO_3 with $MoCl_3$ (Eliseev *et al.*, 1972). Uranium(v) dioxide monochloride is a brown-violet, air-sensitive solid. It is insoluble in organic solvents and decomposes to UO_2 and Cl_2 at 600°C in an inert atmosphere. UO_2Cl is reduced to UCl_4 by $MoCl_5$ at about 200°C and to $UOCl_2$ when heated with $MoOCl_3$. It exhibits Curie–Weiss dependence between 86 and 295 K with $\mu_{eff} = 1.86$ B.M. and $\Theta = -95$ K (Levet, 1969).

There is also a mixed valence state oxide chloride, $(UO_2)_2Cl_3$, which may be obtained by thermal decomposition of UO_2Cl_2 in high vacuum at 400–500°C, or by heating UO_2 and $UOCl_2$ in the molar ratio of 1:3 at 500°C; at higher temperature (500–650°C), UO_2Cl is formed. The black-brown solid has orthorhombic symmetry (Table 5.28) and dissolves slowly in water and in dilute mineral acids (Cordfunke *et al.*, 1977, Brown, 1979). On exposure to the atmosphere, the compound converts into the heptahydrate $(UO_2)_2Cl_3 \cdot 7H_2O$.

(*iv*) *Complex uranium*(v) *oxochlorides*

Brown (1979) has described methods for the preparation and characterization of a number of uranium(v) oxochloro-compounds, such as M_2UOCl_5 (where M = $N(C_2H_5)_4$, $N(C_2H_5)_3H$, $As(C_6H_5)_4$, or C_5H_5NH), $[N(C_2H_5)_4]UOCl_5 \cdot L$ (where L = phtalazine or 1,10-phenantroline), $[LH]_2UOCl_5 \cdot L$ (where L = pyridine, quinoline, isoquinoline, α- and β-picoline), and $[C_5H_5NH]_2UOCl_5 \cdot 2.5C_5H_5NHCl$. The complex $[C_5H_5NH]_2UOCl_5$ may be obtained by the addition of pyridine to an ethanolic solution of $UCl_5 \cdot SOCl_2$ saturated with hydrogen chloride; $[N(C_2H_5)_3H]_2UOCl_5$ by photolysis of $UO_2Cl_2 \cdot 2C_5H_5N$ in dry ethanol; and $[N(C_2H_5)_4]_2UOCl_5$ or $[As(C_2H_5)_4]_2UOCl_5$ by controlled hydrolysis in nitromethane of the corresponding hexachloro complexes. They are slightly soluble in nitromethane where they may react with other species to yield different uranium(IV), (V), or (VI) complexes. The oxopentachloro compounds are moisture-sensitive and undergo rapid disproportionation in water-containing solvents with the exception of $[N(C_2H_5)_4]_2UOCl_5$ and $[As(C_2H_5)_4]_2UOCl_5$ that are moderately stable on exposure to air. Reactions

between $[N(C_2H_5)_4]_2UOCl_5$ and nitrogen heterocyclic compounds in nitromethane or nitrobenzene yield complexes of uranyl(VI) or U(IV) (Selbin *et al.*, 1972b, 1973; Brown, 1979).

The electronic absorption spectra of $[UOCl_5]^{2-}$ in solid state and non-aqueous solvents are essentially identical (Ryan, 1971). A good agreement between observed and calculated energy levels of $[N(C_2H_5)_4]_2UOCl_5$ is obtained assuming D_4 symmetry and using the following crystal field parameters: $\tau = 700\ cm^{-1}$ and $\varsigma_{5f} = 1770\ cm^{-1}$, where τ is a parameter which depends on the radial function and ς_{5f} is the spin–orbit coupling parameter (Selbin *et al.*, 1972a).

(*v*) *Uranium pentabromide and uranium(v) complex bromides*

Uranium pentabromide

The most convenient method for the preparation of UBr_5 is bromination of either uranium metal or uranium tetrabromide at 55°C, or at room temperatures in the presence of catalytic amounts of methyl cyanide (Brown, 1979). The compound is a dark brown solid and is extremely sensitive to moisture. It disproportionates rapidly on dissolution in water and in various organic solvents like ethanol, acetone, dioxane, and ethylacetate. In chloroform and bromoform, the rate of disproportionation is much slower. Stable solutions may be obtained on dissolution in anhydrous, oxygen-free methyl cyanide and methylene dichloride. A number of stable $UBr_5{\cdot}L$ complexes with oxygen donors like $L = (C_6H_5)_3PO$ or $[(CH_3)_2N]_3PO$ have been prepared by bromine oxidation of UBr_4 in the presence of the ligand. Interactions with univalent bromides in thionyl bromide result in the formation of hexabromourantes(V), $MUBr_6$. Uranium pentabromide crystallizes with triclinic symmetry, space group $P\bar{1}$ and is isostructural with β-UCl_5 (see Table 5.28).

Ternary and polynary bromides and bromo compounds of uranium(v)

Hexabromouranates(V) of the formula $MUBr_6$ (where M = Na, K, Rb, Cs, NH_4, $N(CH_3)_4$, $N(C_2H_5)_4$, $N(C_4H_9)_4$, $As(C_6H_5)_4$, $P(C_6H_5)_4$, etc.) have been prepared by a variety of methods (Brown, 1979): (i) bromine oxidation of the appropriate tetravalent M_2UBr_6 compounds in non-aqueous solutions, e.g. nitromethane; (ii) halogen exchange reactions between the chloro complexes and an excess of liquid boron tribromide; (iii) reactions between thionyl bromide solutions of pentavalent uranium (prepared by dissolution of UO_3 in the solvent under refluxing) and the appropriate MBr; and (iv) reaction of UBr_6^{2-} and $UO_2Br_4^{2-}$ in nitromethane or methyl cyanide in the presence of anhydrous HBr according to the reaction

$$UBr_6^{2-} + UO_2Br_4^{2-} + 10HBr \rightarrow 2UBr_6^{-} + 2H_3O^{+} + 4HBr_2^{-}$$

The hexabromouranates have a brown-black color and are rapidly decomposed on dissolution in water or in the presence of moisture. $[As(C_6H_5)_4]UBr_6$ and $[N(C_2H_5)_4]UBr_6$ form stable solutions in anhydrous methylene dichloride

and nitromethane. In the last solvent, the presence of bromine is required to avoid reduction to uranium(IV). The complexes with M = $N(CH_3)_4$, $N(C_2H_5)_4$, and $N(C_4H_9)_4$ dissolve also in methylene dibromide and dibromoethane.

Vibronic side-bands dominate in the solid state and solution spectra of the bromo complexes, which indicates an octahedral or close to octahedral stereochemistry. An assignment of the electronic transitions in $[N(C_2H_5)_4]UBr_6$ from the Γ_7 ground level to the Γ_6, Γ_7, and Γ_8 excited levels of the $5f^1$ electronic configuration has been made (Edelstein *et al*., 1974). The spin–orbit coupling parameter ς_{5f} and the B_0^4 and B_0^6 crystal-field parameters determined from the fitting procedure are 1761(31), 10953(350) and –1058(274) cm^{-1}, respectively (Ryan, 1971; Eichberger and Lux, 1980). There are IR vibronic frequencies at 215 (ν_3) and 87 (ν_4) and at 61 cm^{-1} (ν_6); the identification of the infrared (IR) and Raman inactive (ν_6) vibration has been made by Brown *et al*. (1970). The first electron transfer band in a solution of anhydrous nitromethane has been registered at 17400 cm^{-1}, from which a value of 2.22 for the uncorrected optical electronegativity was deduced (Ryan, 1971).

(*vi*) *Uranium*(*V*) *oxide bromides*

Uranium(*V*) *oxide tribromide*

Uranium(V) oxide tribromide, $UOBr_3$, may be conveniently prepared by heating UO_3 in a stream of nitrogen and carbon tetrabromide vapour at 110°C. $UOBr_3$ is a moisture-sensitive and thermally unstable compound, slowly evolving bromine even at room temperatures. It is converted to UO_2Br_2 or UBr_4 by heating in oxygen at 148°C and with CBr_4 at 165°C, respectively. When heated at 200–300°C in a nitrogen atmosphere $UOBr_3$ converts to $UOBr_2$. In water and ethanol, acetone, ethyl acetate, and dioxan, it disproportionates to U(IV) and U(VI) species. The compound is insoluble in non-polar organic solvents like CCl_4 or CS_2.

Uranium(*V*) *dioxide monobromide*

The preparation of UO_2Br can be achieved by thermal decomposition of UO_2Br_2 in a sealed evacuated glass tube (Levet *et al*., 1977) or by heating the latter compound in a nitrogen–bromine mixture around 320°C (Gueguin, 1964). It may also be prepared by heating UO_3 at 250°C in a mixture of H_2 and HBr, or by treating UO_2Cl_2 with HBr (Levet, 1965). UO_2Br is a moisture-sensitive black-brown solid. When heated in an inert atmosphere (400–500°C), it decomposes to UO_2 and Br_2. It reacts with chorine (400°C) and oxygen (300°C) to yield UO_2Cl_2 and UO_3, respectively.

The compound has an orthorhombic symmetry in the space group *Cmcm* (No. 63). The coordination polyhedron is a pentagonal bipyramid with two bromine and three oxygen atoms in the equatorial plane and two oxygen atoms at the apices. The uranium atoms are linked in double chains by the sharing of three coordinated oxygen atoms. The structural arrangement is

similar to those in $PaOBr_3$, U_3O_8 and $PaCl_5$ and the compound is isostructural with PaO_2Br, NbO_2Br, TaO_2Br, NbO_2I and TaO_2I (Levet *et al.*, 1977). Crystallographic data are listed in Table 5.28. Magnetic susceptibility data are reported by Levet (1969) and the effective magnetic moment is 1.76 B.M. with $\Theta = -200$ K.

(*vii*) *Ternary and polynary uranium(v) oxide bromides and oxobromo compounds*

Green oxybromo complexes of the formulas $[As(C_6H_5)_4]_2UOBr_5$, $[N(C_2H_5)_4]_2UOBr_6 \cdot 2.5N(C_2H_5)_4Br$, etc. have been obtained by controlled hydrolysis of hexabromouranates(v) in acetone or acetone–nitromethane mixtures at –75°C (Ryan, 1971; Brown, 1979). The complexes are significantly less stable than their fluoro and chloro analogs. They are moisture-sensitive and rapidly disproportionate in numerous anhydrous solvents, such as nitromethane.

Selbin *et al.* (1972a) and Selbin and Sherrill (1974) have presented an interpretation of the electronic spectra of UBr_6^- and $UOBr_5^{2-}$ and have shown the effect of perturbing the $5f^1$ orbital energy levels successively by a tetragonal distortion of the octahedral field and spin–orbit coupling. Semi-empirical theoretical calculations of energy levels of UBr_6^- and $UOBr_5^{2-}$ have been performed in order to locate and assign all electronic transitions in these $5f^1$ species. The first electron transfer transition was observed at 26700 cm^{-1}. As compared with UBr_6^- species it is shifted by 9300 cm^{-1} to higher frequencies, equivalent to 0.3 eV. This change is reported to result from the pronounced anisotropic nature of the $UOBr_5^{2-}$ complex (Ryan, 1971).

(*viii*) *Intermediate uranium halides*

The reaction of solid UF_4 with gaseous UF_6 results in a gradual formation of intermediate fluorides with a composition between UF_4 and $UF_{4.5}$, depending on the temperature used and the partial pressure of uranium hexafluoride: U_2F_9 (= $UF_{4.5}$), U_4F_{17} (= $UF_{4.25}$), and U_5F_{22} (= $UF_{4.2}$) (Eller *et al.*, 1979; Bacher and Jacob, 1980).

$$3UF_4 + UF_6 \rightleftharpoons 2U_2F_9 \quad (200\,^\circ C)$$

$$7UF_4 + UF_6 \rightleftharpoons 2U_4F_{17} \quad (300\,^\circ C)$$

Agron (1958) has studied the chemical equilibria in these systems; the forward reactions take place at temperatures between 225–300 and 270–350°C, respectively. Agron (1958) has also reported the conditions of formation, equilibrium, dissociation, and the thermodynamics of the disproportionation reactions.

Intermediate uranium fluorides may also be prepared by reduction of UF_6 with HBr by a careful control of the reactant stoichiometry in reactions between

UF_3 and iodine, SiH_4 or PF_3. There are only two oxidation states, U(IV) and U(V), in U_2F_9 as shown by spectroscopic analyses. U_4F_{17} and U_2F_9 are slowly hydrolyzed, in water with the formation of $UF_4 \cdot nH_2O$, UO_2^{2+}, and F^-, and in moist air with the formation of $UO_2F_2 \cdot xHF \cdot yH_2O$. Organic solvents such as C_6H_6, $CHCl_3$, or CCl_4 react with U_2F_9 with reduction to UF_4.

U_4F_{17} has a monoclinic structure that is a distorted version of that of UF_4 (Chatalet, 1967). In U_2F_9 the uranium atoms are nine-coordinated with a tricapped trigonal prismatic arrangement (Zachariasen, 1949d; Taylor, 1976a,b).

Investigation of the UCl_3–UF_4 phase diagram identified mixed valence phases $2UCl_3 \cdot UF_4$ and $UCl_3 \cdot 7UF_4$ that melt incongruently at 625 and 760°C, respectively.

The preparation and characterization of a mixed-valence oxide chloride of the composition $(UO_2)_2Cl_3$ has been reported by Cordfunke *et al*. (1977). The compound is formed by thermal decomposition of anhydrous UO_2Cl_2 at 400–500°C in high vacuum, or by the reaction of UO_2 and UO_2Cl_2 in evacuated quartz tubes at temperatures between 400 and 800°C. On the basis of comparable uranium compounds, such as U_3O_8, the authors have assumed that uranium is present in both oxidation states 6+ and 5+. Structure data of the intermediate halides are given in Table 5.28.

(d) Hexavalent halides and complex halides

Uranium hexahalides and complex halides have been the most extensively investigated uranium compounds due to their commercial applications. The stability of the halides decreases with increasing atomic number of the halide anion, e.g. UCl_6 is much more prone to thermal decomposition than UF_6, and no simple halides are formed with iodine or bromine in this oxidation state. The hexahalides react violently with water at room temperatures to form soluble uranyl halides; they are also readily soluble in polar organic solvents, in many cases with formation of complexes. The uranyl ion (UO_2^{2+}) forms weak complexes with halide ions, with the exception of fluoride cf. Table 5.34, p.349. Hexavalent halides and complex halides are typically yellow and in a few cases colorless (e.g. UF_6) or green (e.g. UCl_6) (see Table 5.30).

Hexavalent uranium has the $[Rn]5f^0$ electronic configuration. The ground state is formally $^1S_0$. There are numerous reports on absorption and fluorescence spectra of hexavalent halides and uranyl halogeno complexes in the solid state, aqueous solutions, and organic solvents that are discussed in a review article by Carnall (1982). The spectra of UO_2^{2+} compounds exhibit a characteristic vibrational fine structure in the visible–ultraviolet region due to coupling with the stretch modes in the linear UO_2 unit. The absorption spectrum of UF_6 displays a similar complex vibronic structure, which is observed to be superimposed on broad and intense charge transfer bands centered near 26670 and 38460 cm^{-1}. An analysis of the spectrum (Lewis *et al*., 1976) has

Table 5.30 *Properties of selected uranium(VI) halides and complex halides.*[a]

Formula	*Selected properties and physical data*[b,c]	*Lattice symmetry, lattice constant* (Å), conformation and density (g cm^{-3})	*Remarks regarding information available and references*
UF_6	colorless; extremely hygroscopic; m.p. = 64.02 (1136 torr); reacts vigorously with water; soluble: liq. Cl_2, Br_2, CCl_4, CH_3Cl; gives dark red fuming solution with nitrobenzene. bond energies (kJ mol^{-1}): average bond: 523.4 first bond: 286; second bond: 422.9. ionization potential: 14.0 eV $\Delta_f H^o_m$(cr) = –2197.7(1.8)[†] $\Delta_f H^o_m$(g) = –2148.6(1.9)[†] S^o_m(g) = 376.3(1.0)[†] $C^o_{p,m}$(cr) = 166.8(0.2)[†] $C^o_{p,m}$(g) = 129.4(0.5[†] sublimation: $\Delta_{sub}H_m$(298.15K) = 49.1(5)[†] fusion: $\Delta_{fus}H_m$ (329.69K) = 18.8 vaporization: $\Delta_{vap}H_f$(337.202K) = 28.8 triple point : 337.20 K at p = 1522 mbar vapor pressure: solid (273.15–337.17K): log p (mmHg)[‡] = 6.38363 + 0.0075377t – [942.76/t+ 183.416)]; liquid (337.17–383.15K):	solid: orthorhombic; D^{16}_{2h}; *Pnma,* No.62; a = 9.900, b = 8.962, c = 5.207; [from neutron diffraction data a = 9.654(3), b = 8.776(4) c = 5.084(3); V = 430.73; d(calc.) = 5.43]; Z = 4; V = 462; d(calc.) = from 4.93 to 5.43, d(exp.) = 4.87; the molecule appears to have an undistorted octahedral structure; distances in the UF_6 octahedron: d(U–F1) = 1.981(4), d(U–F2) = 1.989(4), d(U–F3) (2×) = 1.979 (3), d(U–F4) (2×) = 1.978(3), d(F···F) = from 2.784 to 2.806; F–U–F = 89.78 to 90.20; F2–U–F1 = 179.9°; F4–U–F3 (2×) = 179.6; liquid: octahedral, space group O_h, a = 1.996; gaseous: octahedral, space group O_h, a = 1.996	*X-ray single crystal data* (Hoard and Stroupe, 1959; Levy *et al*., 1976; Rigny, 1965); *neutron diffraction data* (Taylor and Wilson 1975b; Levy *et al*., 1983)*; structure in liquid and gaseous states; NMR, IR, Raman, vis, UV, photoelectron and fluorescence spectra; physical constants* (Stoller and Richards, 1961 Lewis *et al*., 1976; Downs, 1986); *IR and Raman data* (McDowell *et al*., 1974); *mechanical and thermal properties, phase diagram, phase transformation, thermal conductivity, stability, diffusion coefficients, magnetic susceptibility; paramagnetic resonance; sorption on solids, thermal conductivity, dielectric polarization, transport phenomena, electrical properties, chemical properties; handling, reactions with UF_6, industrial applications* (Bacher and Jacob, 1980, 1986)

log p(mmHg)‡ = 6.99646 – [1126.288/(t+ 221.963)];
above 383.15K : log p(mmHg)‡ = 7.69069 – [1683.165/(t + 302.148)]
sublimation point: 56.54°C at 760 mmHg
vapor density(326–405K): may be considered ideal at 298K;
$P(1+1.2328 \times 10^{6}\, T^{-3}\, P)\cdot V = RT$.
critical constants:
temperature: 503.35(20)K
pressure: 45.5(5) atm
density: 1.39 g cm^{-3}
thermal conductivity:
liquid (345.15K):
$k = 16.02\times10^{-4}$ J cm^{-1}s^{-1}K^{-1}
gas‡ $k = (6.104 + 0.002568t)$ $\times10^{-5}$ J cm^{-1} s^{-1} K^{-1}
density (g cm^{-3}):
solid: 5.060 (at 298.15K); 4.87 (at 335.65K);
liquid‡ : $\rho = 3.630–5.805\times10^{-3}$ (t–64.0) –1.36 (t–64.0)^2 (at 333.15 to 436.15K)
viscosity, η (cP):
liquid: 0.731 at 340.35K; 0.663 at 348.15K.
gas‡ : (1.67–0.0044t) $\times10^{-2}$
surface tension, γ (N cm^{-1}):
16.8(3) $\times$ 10^{-5} at 343.15K;
13.1(3) 10^{-5}at 373.15K

Table 5.30 (*Contd.*)

Formula	*Selected properties and physical data*[b,c]	*Lattice symmetry, lattice constant* (Å), conformation and density ($g\ cm^{-3}$)	*Remarks regarding information available and references*
	refractive index: liquid (Na D line): $n_D = 1.3580$ (4) at 343.15K gas (5100 Å): $n-1 = 5.2\times10^{-4}$ pK^{-1} (p in mmHg) fundamental frequencies (IR and Raman, cm^{-1}): ν_1 (R) = 667.1 ; ν_2 (R) = 534.1; ν_3 (IR) = 625.5; ν_4 (IR) = 186.2; ν_5 (R) = 200.3; ν_6 (inact.) = 143 dielectric constants: liquid: $\varepsilon^{-1} = 2.18\cdot10^{-6}$ at 65°C and $p =$ 2745.9 kPa gaseous $\varepsilon^{-1} = 3815.4 \times 10^{-6}$ at 28.2°C $\varepsilon^{-1} = 3221.9 \times 10^{-6}$ at 83.1°C magnetic susceptibility: UF_6 exhibits temperature independent paramagnetism molar susceptibility: $\chi_M = (42.7\pm2.6) \times 10^{-6}\ cm^3 mol^{-1}$ molar polarization: $P_M = 31.453$ (25) $cm^3\ mol^{-1}$ (average value for 326–426 K) dipole moment: $\mu \approx 0$ ($\ll 10^{-18}$ Debye)		

$NaUF_7$	white to pale green; very hygroscopic; decomposes over 20°C to $Na_2UF_8 + UF_6$; Raman (solid): 636, 554, 540, 516, 463, 441, 430, 312, 305sh, 243, 218; (L): 111, 91, 57, 35; $\log p$ (mmHg) = $(11.06 \pm 0.02) - 3.48\times10^3 T^{-1}$ (T in K)	dimorphic; the high-temperature form is cubic, face centered, $a = 8.511$; $Z = 4$. The low-temperature form is monoclinic. The UF_7^- anion is octahedral with predominant covalent character	*crystallographic data* (Bougon *et al.*, 1976a); *IR, Raman, vis and UV spectra; physical constants, thermodynamic data, thermal decomposition; paramagnetic resonance; NMR* (Brown, 1968; Bacher and Jacob, 1980)
Na_2UF_8	yellow; very hygroscopic; decomposes to $UF_6 + NaF$; Raman (cm^{-1}): 607(10), 440(0.2), 410(0.6), 372(0.5), 343(.7) 303 (1.1), 284(1.1), 170(0.7), 141(0.3); $\log p$ (mmHg) = $(9.25 \pm 0.02) - 4.18\times10^3 T^{-1}$	tetragonal; space centered; D_{4h}^{17}; *I4/mmm*, No. 139; $a = 5.27$; $c = 11.20$; each U atom is surrounded by eight equidistant F atoms with d(U–F) = 2.29; d(F–F) = 2.63 and 2.97. Each Na atom is also surrounded by 8 F atoms with d(Na–F) = 2.37 and d(F–F) = 2.63 and 2.97	*crystallographic data* (Malm *et al.*, 1966); *IR, Raman, vis and UV spectra; physical constants, thermodynamic data, thermal decomposition* (Bougon *et al.*, 1976a; Katz, 1964); *magnetic susceptibility; paramagnetic resonance; NMR* (Brown, 1968; Bacher and Jacob, 1980).
KUF_7	extremely hygroscopic; decomposes at 100°C to $K_2UF_8 + UF_6$; IR(cm^{-1}): 626w,580sh, 540,s, 497s, 457w, 438w, 314w, 296sh, 256w, 234s, 202s, 140m, 100(L); Raman (solid): 623, 544, 517, 502, 455, 440, 311, 253, 232, 212, 201, 100L, 31L	dimorphic; the high-temperature form is cubic, $a = 5.22$	*crystallographic data* (Bougon *et al.*, 1976a); *IR and Raman spectra; thermal decomposition* (Brown, 1968; Bacher and Jacob, 1980)
K_2UF_8	extremely hygroscopic; decomposes at 300°C to $UF_6 + F_2 + K_2UF_7 + K_3UF_8$; IR: 598m, 510s,br, 460sh, 390sh, 294vw, 260s, 232s,br	orthorhombic; $a = 6.038$, $b = 12.899$, $c = 8.728$	*crystallographic data* (Bougon *et al.*, 1976a); *IR and Raman spectra; thermal decomposition* (Brown, 1968; Bacher and Jacob, 1980)
K_3UF_9		orthorhombic; $a = 6.974$, $b = 7.534$, $c = 9.768$	*crystallographic data* (Iwasaki *et al.*, 1981)

Table 5.30 (*Contd.*)

Formula	*Selected properties and physical data*[b,c]	*Lattice symmetry, lattice constant* (Å), conformation and density ($g\ cm^{-3}$)	*Remarks regarding information available and references*
$RbUF_7$	extremely hygroscopic: $4RbUF_7 + H_2O \rightarrow Rb_4UO_2F_6 + 3UO_2F_2 + 16HF$; decomposes in vacuum at 210°C to $UF_6 + Cs_2UF_8$; IR(cm^{-1}): 625w, 550, br, 482w, 457m, 442w, 230m, 210m; (L.): 100, 53, 35. at –170°C; Raman: 625(10), 520(0.1), 443 (0,9), 310(0.5), 248(0.5), 215(0.4)	dimorphic; the high temperature form is cubic; $a = 5.385(5)$	*crystallographic data* (Bougon *et al.*, 1976a); *IR and Raman spectra; thermal decomposition* (Brown, 1968; Bacher and Jacob, 1980)
Rb_2UF_8	very hygroscopic; decomposes over 350°C to $UF_6 + F_2 + Rb_2UF_7$ or Rb_3UF_8	orthorhombic; $a = 6.265(16)$, $b = 13.479(37)$, $c = 8.776(21)$	*crystallographic data* (Bougon *et al.*, 1976a); *IR and Raman spectra; thermal decomposition*; (Brown, 1968; Bacher and Jacob, 1980)
Rb_3UF_9		orthorhombic; $a = 8.121$, $b = 7.612$, $c = 9.614$	*crystallographic data* (Iwasaki *et al.*, 1981).
$CsUF_7$	yellow; hygroscopic; decomposes to $Cs_3UF_8 + UF_6$ at 210°C in vacuum; IR(cm^{-1}): 618vw, 605m, 540sh, 507s, 450sh, 200br, 170; Raman: 622, 462sh, 444, 312, 249, 211	the high-temperature form is cubic with $a = 5.517(5)$. At 15(1)°C it transforms to a tetragonal structure with $a = 5.30$ and $c = 5.37$	*crystallographic* data (Bougon *et al.*, 1976a); *IR and Raman spectra; thermal decomposition* (Bacher and Jacob, 1980)
Cs_2UF_8	very hygroscopic; decomposes to $Cs_3UF_8 + UF_6 + F_2$ over 400°C	orthorhombic; $a = 6.480(10)$, $b = 14.036(22)$, $c = 9.272(12)$	*crystallographic data* (Bougon *et al.*, 1976a); *IR and Raman spectra* (Brown, 1968; Bacher and Jacob, 1980)

NH_4UF_7	decomposes at 100–170°C to $UF_5 + NH_4F + HF + N_2$; IR(cm^{-1}): 625(10), 447(1.25), 314(0.55), 250 (0.76), 215(1.74), 195(1.53)	cubic; $a = 5.393(5)$	*crystallographic data* (Bougon *et al.*, 1976a); *IR and Raman spectra; thermal decomposition* (Bacher and Jacob, 1980)
$(NH_4)_2UF_8$	Raman (cm^{-1}): 592(10), 470(0.3), 420(0.3), 321(1.4), 286(1.5), 112 (L), 38(L)	orthorhombic; $a = 6.305(13)$; $b = 13.431(23)$, $c = 9.018(16)$	*crystallographic data* (Bougon *et al.*, 1976a); *IR, Raman spectra* (Bacher and Jacob, 1980).
$N_2H_5UF_7$	yellow		*synthesis* Bacher and Jacob (1980).
$NOUF_7$	hygroscopic; decomposes to $NOF + UF_6$ with reversible formation of $NOUF_7$. IR(cm^{-1}): 624vw, 604m, 540sh, 508s, 450sh, 420vw, 208vw, 188vw, 120(L); Raman (solid): 627, 446sh, 434, 310, 240, 210	cubic (high-temperature form); $a = 5.334(70)$; $Z = 1$; CN = 7; d(exp.) = 4.5. At room temperatures the lattice is composed of NO^+ cations and UF_7^- anions. Below –16°C exists β-$NOUF_7$ of lower symmetry.	*crystallographic data* (Geichman *et al.*, 1963; Bougon *et al.*, 1976a); *NMR, IR and Raman spectra* (Brown, 1968; Bacher and Jacob, 1980)
NO_2UF_7	hygroscopic; decomposes to $NO_2F + UF_6$ with reverse formation of NO_2UF_7	tetragonal; $a = 5.74$, $c = 2$	*crystallographic data* (Geichman *et al.*, 1963); *IR spectra and thermodynamic data* (Brown, 1968; Bacher and Jacob, 1980)
$(NO_2)_2UF_8$	IR (cm^{-1}): 590sh, 534sh, 510s, 498sh, 208w, 160m	orthorhombic; D_{2h}^{15}, *Pbca*, No.61; $a = 8.795(1)$, $b = 13.247(2)$, $c = 11.942(2)$; $Z = 8$; $V = 1391.33$; CN = 8. d(calc.) = 4.3 The lattice is composed of NO^+ cations and UF_8^{2-} anions. The coordination polyhedron around the uranium atom is a slightly distorted cube with an almost O_h symmetry	*crystallographic data* (Bougon *et al.*, 1976b; Seppelt and Hwang, 2000), *NMR, IR and Raman spectra* (Brown, 1968; Bacher and Jacob, 1980)
other fluorouranate (VI): $Na_3U_2F_{15}$, $K_3U_2F_{15}$, Rb_3UF_9, Cs_3UF_9,	$Na_3U_2F_{15}$ and $K_3U_2F_{15}$ are extremely hygroscopic		Bacher and Jacob (1980)

Table 5.30 (*Contd.*)

Formula	*Selected properties and physical data*[b,c]	*Lattice symmetry, lattice constant* (Å), conformation and density (g cm^{-3})	*Remarks regarding information available and references*
$NH_4(UO_2)F(SeO_4) \cdot H_2O$		orthorhombic; D_{2h}^{16}, *Pnma*, No.62; $a = 8.450(4)$, $b = 13.483(5)$, $c = 13.569(5)$; $V = 1545.93$; $Z = 8$; d(calc.) = 4.02	*crystallographic data* (Blatov *et al.*, 1989)
α-UOF_4	orange; hygroscopic; decomposes at 200 to 250°C into $UO_2F_2 + UF_4$; reacts with $H_2O \rightarrow UO_2F_2$. UOF_4(cr): $\Delta_f G_m^o = -1816.3$ (4.3)†, $\Delta_f H_m^o = -1924.6$ (4.0)†, $S_m^o = 195$ (5)†. UOF_4(g): $\Delta_f G_m^o = -1704.814$ (20.142)†, $\Delta_f H_m^o = -1763$ (20)†, $S_m^o = 363.2$ (8.0)†, $C_{p,m}^o = 108.1$ (5.0) IR ($U^{16}OF_4$) (cm^{-1}): ν(U–O, valence, terminal) = 893; ν(U–$F_{trans.}$, terminal) = 667s, ν(U–$F_{cis.}$, valence, terminal) = 558; 478m (L); 375s,br (L); Raman: ν(U–O stretch, terminal) = 890s; ν(U–$F_{trans.}$, stretch, terminal) = 660s, ν(U–$F_{cis.}$, stretch, terminal) = 552m	trigonal/rhombohedral; C_{3v}^5, *R3m*, No.160; $a = 13.095(6)$, $c = 5.658$ (2); $V = 840.24$; $Z = 9$, d(calc.) = 5.87; The idealized coordination sphere of the U atom consists of a pentagonal bipyramid formed by the light atoms; one O and one F atom occupy indistinguishable axial positions with d(U–O) = 1.870(16) and d(U–F1) = 1.884 (17), d(U–F2(a)) = 2.273, d(U–F2 (b)) = 2.270(11), d(U–F3) = 2.050 (5); O–U–F(1) = 179.2, U–F(2)–U = 153.2(7) (received from neutron diffraction analysis)	*crystallographic data* (Paine *et al.*, 1975); *neutron powder diffraction data* (Levy *et al.*, 1977), *electronic, IR and Raman spectra* (Jacob and Polligkeit, 1973; Paine *et al.*, 1975; Bacher and Jacob, 1980). *thermodynamic data* (Grenthe *et al.*, 1992; Guillaumont *et al.*, 2003)
$UOF_4(SbF_5)_2$		monoclinic; C_{2h}^5, $P2_1/c$, No.14; $a = 7.864(16)$, $b = 14.704(8)$, $c = 9.980$ (8); $\beta = 99.8(1)$; $Z = 4$; $V = 1137.17$; d(calc.) = 4.46	*crystallographic data; NMR-investigations* (Bougon, *et al.*, 1979)

$KUOF_5$	hygroscopic	orthorhombic; $a = 8.02(1)$, $b = 11.28(2)$, $c = 5.55(1)$. Each uranium atom is surrounded by eight light atoms forming a dodecahedron. The dodecahedra are linked together by fluorine atoms	*crystallographic data, IR and Raman spectra* (Joubert *et al.*, 1978a)
$RbUOF_5$	hygroscopic	orthorhombic; $a = 8.07(1)$, $b = 11.73(2)$, $c = 5.77(1)$. Each uranium atom is surrounded by eight light atoms forming a dodecahedron. The dodecahedra are linked together by fluorine atoms to form infinite chains	*crystallographic data, IR and Raman spectra* (Joubert *et al.*, 1978a)
$CsUOF_5$		rhombohedral; C_{3i}^2, $R\bar{3}$, No.148; $a = 5.41(1)$; $\alpha = 95.57(8)°$; $V = 155.9$; d(calc.) = 5.13, d(exp.) = 5.1(5). The unit cell is very close to that of $CsUF_6$	*neutron powder diffraction and, NMR data* (Joubert *et al.*, 1978b; Bougon *et al.*, 1978)
NH_4UOF_5	hygroscopic	orthorhombic; $a = 8.08(1)$, $b = 11.59(2)$, $c = 5.77(2)$. Each uranium atom is surrounded by eight light atoms forming a dodecahedron. The dodecahedra are linked together by fluorine atoms to form infinite chains.	*crystallographic data, IR and Raman spectra* (Joubert *et al.*, 1978a)
$AgUOF_5$		tetragonal; $a = 5.370$, $c = 8.043$	*crystallographic data* (Malm, 1980)
UO_2F_2	light yellow-green; decomposes in a He stream at 700–900°C to $UF_6 + U_3O_8 + O_2$; sublimes in the presence of HF over 550°C; may be transported with partial	rhombohedral; D_{3d}^5, $R\bar{3}m$, No = 166; $a = 5.755(1)$; $\alpha = 42{,}72(5)°$; $Z = 1$; CN = 8; d(calc.) = 6.37, d(exp.) = 5.8; d(U–O) = 1.91 (2×); d(U–F) = 2.50 (6×)	*synthesis* (Brauer, 1981); *X-ray and neutron powder diffraction data* (Atoji and McDermott, 1970); Zachariasen, 1948e); Bacher and Jacob, 1980) *IR and*

Table 5.30 (*Contd.*)

Formula	*Selected properties and physical data*[b,c]	*Lattice symmetry, lattice constant* (Å), conformation and density (g cm^{-3})	*Remarks regarding information available and references*
	decomposition in a He stream at 825°C. UO_2F_2(cr): $\Delta_f G_m^o$ = –1557.3 (1.3)†, $\Delta_f H_m^o$ = –1653.5 (1.3)†, S_m^o = 135.56 (0.42)†; $C_{p,m}^o$ = 103.22 (0.42)†. UO_2F_2(g): $\Delta_f G_m^o$ = –1318.1 (10.2)†, $\Delta_f H_m^o$ = –1352.5 (10.1)†, S_m^o = 342.7 (6.0)†; $C_{p,m}^o$ = 86.4 (3.0)†. IR ($U^{16}O_2F_2$)(cm^{-1}): ν_3 ($\nu_{asym.}UO_2$) = 1020vs; ν_4(L.) = inactive; ν_7 (L[$UF_{6/3}$]) = 260; ν_8($\delta_{asym.}UO_2$) = 238s. Raman (cm^{-1}): ν_1 ($\nu_{sym.}UO_2$) = 918vs; ν_2(L) = inactive (?); ν_5(L[$UF_{6/3}$]) = 444vw; ν_6 ($\delta_{sym.}$ UO_2) = 183m; ν_7	neutron powder diffraction data: a = 4.192; $c/3$ = 5.520; d(U–O) = 1.74(0.02) (2×); d(U–F) = 2.429 (0.002) (6×). The structure consists of layers of U atoms, which are 5.22 Å apart from each other. The axes of the UO_2 groups are perpendicular to the there planes. The fluorine atoms are 0.61 Å above and below the uranium planes, and weak O···O and O···F bonds holds the layer together	*Raman spectra, chemical properties, conversion of UO_2F_2 to UF_6.* (Bacher and Jacob, 1980); *photoelectron spectroscopy* (Thibaut *et al.*, 1982) *thermodynamic data* (Grenthe *et al.*, 1992; Guillaumont *et al.*, 2003)
$UO_2F_2{\cdot}nH_2O$ (n = 1,2,3,4) $UO_2FOH{\cdot}H_2O$; $UO_2FOH{\cdot}2H_2O$	monohydrate (yellow solid, soluble in H_2O, $\nu_{U=O}$ = 990 cm^{-1}); dihydrate (yellow solid, soluble in H_2O, $\nu_{U=O}$ = 966 cm^{-1}); formed when anhydrous compound is exposed to moist air. $UO_2F_2{\cdot}3H_2O$ (cr): $\Delta_f G_m^o$ = –2269.7 (6.9)†, $\Delta_f H_m^o$ = –2534.4 (4.4)†, S_m^o = 270 (18)†; $UO_2FOH{\cdot}H_2O$ (cr): $\Delta_f G_m^o$ = –1721.7 (7.5)†, $\Delta_f H_m^o$ = –1894.5 (8.4)†, S_m^o = 178 ($38UO_2F$ $OH{\cdot}2H_2O$ (cr): $\Delta_f G_m^o$ = – 1961.0 (8.4)†, $\Delta_f H_m^o$ = –2190.0 (9.4)†, S_m^o = 223 (38)†		*general properties* (Bacher and Jacob, 1980); *thermodynamic data* (Grenthe *et al.*, 1992; Guillaumont *et al.*, 2003)

$UO_2F_2(SbF_5)_3$		monoclinic; C_{2h}^5, $P2_1/c$, No.14; $a = 11.040(7)$; $b = 12.438(12)$; $c = 12.147(8)$; $\gamma = 111.16(20)$; $Z = 4$; $V = 1555.51$; d(calc.) = 4.09	*crystallographic data and characterization* (Fawcett *et al.*, 1982)
$[UO_2F_2\{CO(NH_2)_2\}_2]_2$		monoclinic; $P2_1/b$; $a = 10.240(1)$, $b = 10.983(1)$, $c = 8.254(1)$; $\beta = 98.65(1)$; $Z = 4$; d(U–F) = 2.23(2)–2.39(2); d(U–O) = 2.36(2) 2× and 1.72(2) 2×	*crystallographic data* (Mikhailov *et al.*, 1976a)
$Rb_2UO_2F_4 \cdot H_2O$		orthorhombic; C_{2h}^{15}, *Pbca*, No. = 61; $a = 8.881(3)$, $b = 14.547(6)$, $c = 11.975(4)$; $Z = 8$; d(calc.) = 4.59; $V = 1547.07$	*crystallographic data* (Brusset *et al.*, 1972)
$Cs_2UO_2F_4 \cdot H_2O$		monoclinic; C_{2h}^5, $P2_1/c$, No.14; $a = 8.06(1)$, $b = 12.18(1)$, $c = 9.29(1)$; $\beta = 109.12(4)$; $Z = 4$; $V = 861.7$, d(calc.) = 4.85	*crystallographic data* (Nguyen Quy Dao, 1972)
$K_3UO_2F_5$	yellow; $\nu_1(UO_2^{2+}) = 803\,cm^{-1}$, $\nu_3(UO_2^{2+}) = 863\,cm^{-1}$	tetragonal; C_{4h}^6, $I4_1/a$, No.88; $a = 9.159(4)$, $c = 18.170(8)$; $Z = 8$; $V = 1524.23$; d(calc.) = 4.2; pentagonal $UO_2F_5^{2-}$ units are held together by potassium ions	*crystallographic data* (Zachariasen, 1954d; Vodovatov *et al.*, 1984; Lychev *et al.*, 1986); *thermodynamic data* (Fuger *et al.*, 1983)
$Cs_3UO_2F_5$	yellow	cubic; T_h^3, $Fm3$, No.202; $a = 9.833(5)$; $Z = 4$; $V = 950.73$; d(calc.) = 5.33	*crystallographic data* (Rebenko *et al.*, 1968; Brusset and Nguyen Quy Dao, 1971); *thermodynamic data* (Fuger *et al.*, 1983).
$(NH_4)_3UO_2F_5$	yellow	monoclinic; C_s^3, Cm, No.8; $a = 29.22$, $b = 9.48$, $c = 13.51$; $\beta = 136.11^o$; $V = 2594.15$; d(calc.) = 3.22. Distorted pentagonal bipyramid	*crystallographic data* (Brusset *et al.*, 1969)

Table 5.30 (*Contd.*)

Formula	*Selected properties and physical data*[b,c]	*Lattice symmetry, lattice constant* (Å), conformation and density (g cm^{-3})	*Remarks regarding information available and references*
$K_2[UO_2F_2(C_2O_4)]$	yellow, stable in air, soluble in water; insoluble in common organic solvents. IR (cm^{-1}): ν_{as}(C=O) = 1650vs,b; ν_s(C–O) + ν(C–C) + δ(O–C=O) = 1355s, 1316s, 1480w, 1455m, 1415w, 1360m, 1315vs.; $\nu_{as}(UO_2)$ = 905. Other bands; 3610s, 3500s, 2920w, 845m, 800vs, 782w, 740w, 490s, 450s	triclinic; C_i^1, $P\bar{1}$, No. 2; $a = 10.981$, $b = 11.038$, $c = 12.629$; $\alpha = 108.00^o$, $\beta = 86.79^o$, $\gamma = 123.99^o$; $Z = 2$; d(calc.) = 1.31, d(exp.) = 1.36	*crystallographic data and IR spectral bands* (Chakravorti *et al.*, 1978)
$K_4[UO_2F_2(C_2O_4)_2]$	yellow, stable in air, soluble in water; insoluble in common organic solvents; ν_{as}(C=O) = 1720vs, 1655vs; ν_s(C–O)+ν(C–C)+δ(O–C=O) = 1410vs, 1295vs; $\nu_{as}(UO_2)$ = 890vs; Other bands: 3500s, 2910w, 830w, 790vs, 485s, 400s, in cm^{-1}	triclinic; C_i^1, $P\bar{1}$, No. 2; $a = 8.768$, $b = 8.777$, $c = 14.857$; $\alpha = 101.58^\circ$, $\beta = 114.27^o$, $\gamma = 85.27$; $Z = 4$; d(calc.) = 4.16, d(exp.) = 4.08	*crystallographic data and IR spectral bands* (Chakravorti *et al.*, 1978)
$K_2[(UO_2)_2F_4(C_2O_4)]$	yellow, stable in air, soluble in water; insoluble in common organic solvents; ν_{as}(C=O) = 1640, 1610vs; ν_s(C–O)+ν(C–C)+δ(O–C=O) = 1365m, 1318vs; $\nu_{as}(UO_2)$ = 920vs; Other bands: 3630s, 3460s, 3220w, 2920w, 855s, 795vs, in cm^{-1}	monoclinic; $a = 10.792$, $b = 12.028$, $c = 10.615$; $\beta = 136.88$; $Z = 2$; d(calc.) = 2.92, d(exp.) = 2.83	*crystallographic data and IR spectral bands* (Chakravorti *et al.*, 1978)

$Na_2(UO_2)_2\ (SiO_4)F_2$	The compound is structurally related to soddyite, and is formed during uranyl silicate synthesis in teflon-lined bombs	tetragonal; D_{4h}^{19}, $I4_1/amd$, No.141; $a = 6.975(8)$, $c = 18.31(2)$; $Z = 4$; $V = 890.79$	*crystallographic data* (Blaton *et al*., 1999)
$Cs_2[(UO_2)_2F_6(H_2O)_2]$		monoclinic; C_{2h}^5, $P2_1/c$, No.14; $a = 6.027(2)$, $b = 11.505(2)$, $c = 9.389(2)$; $\beta = 95.72(2)^\circ$; $Z = 2$; $V = 647.8$; d(calc.) = 4.9	*crystallographic data* (Mikhailov *et al*., 1979)
$[Na_3(UO_2)_2F_7](H_2O)_6$	yellow, transparent crystals: dehydration of the compound gives: $[Na_3(UO_2)_2F_7](H_2O)_2$ at 25–91°C : $[Na_3(UO_2)_2F_7]$ at 150–200°C; at higher temperatures (235–300°C) it decomposes to a mixture of $Na_3UO_2F_5$, UO_2F_2, $NaUO_2F_3$, and $Na(UO_2)_2F_5$	triclinic; C_i^1, $P\bar{1}$, No.2; $a = 6.997(1)$, $b = 7.176(1)$, $c = 8.630(1)$; $\alpha = 77.84(1)^o$, $\beta = 113.30(1)^o$, $\gamma = 104.95(1)^o$; $Z = 1$; $V = 381.62$; d(calc.) = 3.7; d(U–U)single bridge = 4.632(1) and 4.003(1) double bridge; d(U–O1) = 1.79(1), d(U–O2) = 1.77(1); d(U–F) = from 2.21 to 2.39; the structure consists of $[(UO_2)_2F_6{\cdot}F_{2/2}]^{3-}$ chains of complex ions formed by double and single F bridges alternatively	*crystallographic, thermogravimetric and IR data* (Nguyen Quy Dao *et al*., 1981)
$[K_3(UO_2)_2F_7](H_2O)_2$		triclinic; C_i^1, $P\bar{1}$, No.2; the structure consists of $(UO_2)_2F_7^{3-}$ chains of complex ions formed by double and single F bridges alternatively	*crystallographic data and physicochemical properties* (Mikhailov *et al.*, 1972a; Nguyen Quy Dao and Chourou, 1974)
$K_5(UO_2)_2F_9$		monoclinic; C_{2h}^6, $C2/c$, No. = 15; $a = 19.860(1)$, $b = 6.110(1)$, $c = 11.706(4)$; $\beta = 102.58(4)^\circ$; $V = 1386.36$; $Z = 4$; d(calc.) = 4.34	*crystallographic data* (Brusset *et al*., 1974; *Nguyen Quy Dao and Chourou,S.(1972)* Mikhailov *et al*., 1972b); *thermodynamic data* (Fuger *et al*., 1983)
$Cs_2(NH_4)[(UO_2)_2F_7]$		orthorhombic; D_{2h}^{25}, *Immm*, No.71; $a = 6.526(2)$, $b = 8.553(3)$, $c = 12.434(2)$; $Z = 2$; $V = 694.03$; d(calc.) = 4.58	*crystallographic data* (Ivanov *et al*., 1980)

Table 5.30 (*Contd.*)

Formula	*Selected properties and physical data*[b,c]	*Lattice symmetry, lattice constant* (Å), conformation and density (g cm^{-3})	*Remarks regarding information available and references*
$Rb_2[(UO_2)_3F_8(H_2O)]\cdot 3H_2O$		orthorhombic; C_{2v}^{16}, *Ama*2, No. = 40; $a = 8.4624(8)$, $b = 14.343(1)$, $c = 13.916(1)$; $V = 1689.07$; $Z = 4$; d(calc.) = 4.74	*crystallographic data* (Mikhailov *et al.*, 1976b)
$K_2[(UO_2)_3F_8(H_2O)]\cdot 3H_2O$		orthorhombic; C_{2v}^{16}, *Ama*2, No.40; $a = 8.39(5)$, $b = 14.12(8)$, $c = 13.66(8)$; $V = 1618.26$; $Z = 4$; d(calc.) = 4.56	*crystallographic data* (Nguyen Quy Dao., 1979)
$K_2(UO_2F_2)(SO_4)\cdot H_2O$		monoclinic; C_{2h}^5, $P2_1/c$, No. = 14; $a = 9.2634(18)$, $b = 8.6722(18)$, $c = 11.0195(15)$; $\beta = 101.60(1)^\circ$; d(calc.) = 3.83; $V = 867.16$; $Z = 4$	*crystallographic data* (Alcock *et al.*, 1980)
$Ni_2[(UO_2)F_4]_2\cdot 14H_2O$		monoclinic; C_{2h}^5, $P2_1/c$, No.14; $a = 10.141(1)$, $b = 11.901(1)$, $c = 9.510(1)$; $\beta = 96.80(1)$; $V = 1139.67$; $Z = 4$; d(calc.) = 3.09	*crystallographic data* (Ivanov *et al.*, 1982)
$Ni_3[(UO_2)_2F_7]_2\cdot 18H_2O$		monoclinic; C_{2h}^2, $P2_1/m$, No.11; $a = 9.132$, $b = 16.925$, $c = 12.500$; $\gamma = 114.62^o$	*crystallographic data* (Ivanov *et al.*, 1981)
$Cs_3UO_3F_5$		cubic; $a = 9.869$	*crystallographic data* (Rebenko *et al.*, 1968)
$U(OTeF_5)_6$		monoclinic; C_{2h}^3, $C/2m$, No. 12; d(calc) = 3.56; $a = 10.30(1)$, $b = 16.61(2)$, $c = 9.98(1)$; $\beta = 114.14(6)^\circ$; $Z = 2$; $V = 1558.09$; d(calc.) = 3.56	*crystallographic data* (Templeton *et al.*, 1976)

UCl_6	black to dark green crystalline material; extremely moisture sensitive; slightly soluble in some organic solvents: CCl_4, $CHCl_3$; hydrolyzes in moist air; reacts vigorously with water to form UCl_2O_2, m.p. = 177.5°C. UCl_6(cr): $\Delta_f G^o_m = -937.1$ (3.0)†, $\Delta_f H^o_m = -1066.5$ (3.0)†, $S^o_m = 285.5$ (1.7)†; $C^o_{p,m} = 175.7$ (4.2)†. UCl_6(g): $\Delta_f G^o_m = -901.6$ (5.2)†, $\Delta_f H^o_m = -985.5$ (5.0)†, $S^o_m = 438.0$ (5.0)†; $C^o_{p,m} = 147.2$ (3.0)†. vapour pressure: log p (mmHg) = $-4000T^{-1} + 10.20$ (298–450 K). IR and Raman (cm^{-1}): ν_1 (R) = 367, ν_2 (R) = 321, ν_3 (IR) = 343, ν_4 (IR) = 101, and ν_5 (R) = 133	hexagonal; D^3_{3d}, $P\bar{3}m1$, No. 164; $a = 10.95$, $c = 6.016(6)$; $Z = 3$; d(calc.) = 3.594, d(exp.) = 3.17–3.36. Chlorine atoms form an almost regular octahedron around U(1) with d(U–Cl) = 2.47 and Cl–U–Cl angles of 86.6 and 93.4°; the array around U(2) is slightly distorted; d(U–Cl) lie between 2.41(4) and 2.51(4); the Cl–U–Cl angles are of 79.7, 98.0 and 90.4	*synthesis* (Rediess and Sawodny, 1982), *crystallographic and neutron diffraction data* (Zachariasen, 1948c, Taylor and Wilson, 1974b); *thermodynamic data* (Brown, 1973, 1979; Grenthe *et al*., 1992; Guillaumont *et al*., 2003), *UV, vis, infrared and Raman spectra; magnetic susceptibility data* (Brown, 1979 and references therein)
$[P(C_6H_5)_4]UOCl_5$	deep orange-red moisture sensitive crystals. IR (cm^{-1}): ν(U–O) = 834, δ(U–O) = 231; Raman: ν(U–O) = 836, δ(U–O) = 229; . ν(U–Cl) = 345, 341(sh), 302, 298, 291 (IR); and 347, 341, 293 (R)	tetragonal; C^3_{4h}, *P4/n*, No. 85; $a = 13.264(5)$; $c = 7.621(5)$; $Z = 2$; d(calc.) = 1.924, d(exp.) = 1.916; d(U–O) = 1.76(1). The structure is composed of octahedral anions and cations with the $\bar{4}$ (S_4) symmetry. Both ions are forming linear stacks parallel to *c*. d(U–Cl) = 2.636(2) in the equatorial plane and 2.433(4) in the axial bond	*crystallographic data* (de Wet and du Preez, 1978); *infrared data* (Bagnall *et al*., 1975)
UO_2Cl_2	golden-yellow; very hygroscopic; m.p. = 570–578°C very volatile >775°C; soluble H_2O, acetone, alcohol, and common polar organic	orthorhombic; D^{16}_{2h}, *Pnma*, No. 62; $a = 5.725$, $b = 8.409$, $c = 8.720$; $Z = 4$; d(calc.) = 5.349; d(exp.) = 5.28; The U coordination polyhedron is a pentagonal	*crystallographic data* (Debets, 1968; Taylor and Wilson, 1973b); *thermodynamic data* (Cordfunke *et al*., 1976; Grenthe *et al*., 1992; Guillaumont *et al*., 2003)

Table 5.30 (*Contd.*)

Formula	*Selected properties and physical data*[b,c]	*Lattice symmetry, lattice constant* (Å), conformation and density (g cm^{-3})	*Remarks regarding information available and references*
	solvents. UO_2Cl_2 (cr): $\Delta_f G^o_m$ = –1145.9 (1.3)†, $\Delta_f H^o_m$ = –1243.6 (1.3)†, S^o_m = 150.54 (0.21)†; $C^o_{p,m}$ = 107.86 (0.17)†. UO_2Cl_2 (g): $\Delta_f G^o_m$ = –939.0 (15.1)†, $\Delta_f H^o_m$ = –970.3 (15.0)†, S^o_m = 373.4 (6.0)†; $C^o_{p,m}$ = 92.6 (3.0)†. IR (cm^{-1}): ($\nu_{as}(B_{1u}+B_{3u})$ = 958vs, 946vs; $\nu_s(B_{1u})$ = 832s; $\nu_s(B_{3u})$ = 781s; ν(U···O) = 320w; δ(O–U–O)(B_{1u}, B_{2u}, B_{3u}) = 727w, 258m, 200s; ν(U–Cl) = 97s, 80.5s; Raman: $\nu_{as}(A_g)$ = 940m; $\nu_s(B_{2g})$ = 848m; $\nu_s(A_g)$ = 767vs; ν(overtone or combination) = 750w; ν(U···O) = 340w; δ(O–U–O)(B_{1g}, B_{2g}, B_{3g}) = 270w; 255vw, 240w; δ(O–U–O) (A_g) = 197m; ν(U–Cl) = 178s, 105s	bipyramid with uranyl oxygen atoms at the apices: d(U–O, uranyl) = 1.78(2) and 1.73(1). Three Cl and one O atoms form the equatorial pentagon: d(U–Cl) = 2.73 and 2.75; d(U–O, pentagon) = 2.52(2); pentagonal angles in ring: ≈72; uranyl angle O–U–O = 178.8(8); angles in the bipyramid: ≈90°	*electronic absorption, luminescence and fluorescence spectra* (Brown, 1979); *IR and Raman data* (Bullock, 1969; Perrin and Caillet, 1976); *photoelectron spectroscopy* (Thibaut *et al.*, 1982)
$UO_2Cl_2 \cdot H_2O$	yellow powder; hygroscopic; soluble in H_2O, EtOH, Me_2CO; dec. > 300°C. $UO_2Cl_2 \cdot H_2O$(cr): $\Delta_f G^o_m$ = –1405.0 (3.3)†, $\Delta_f H^o_m$ = –1559.8 (2.1)†, S^o_m = 192.5 (8.4)†. IR (cm^{-1}): 150w, 182m, 208m, 240mw, 280m, 962vs, br, 1602vs, 3450ms. Raman: 52mw (sharp), 58w (sharp), 136w, 176m, 203m, br, 245ms, 869vs (sharp)	monoclinic system; C^2_{2h}, $P2_1/m$, No.11; a = 5.847(9), b = 8.596 (13), c = 5.543(9); β = 97.51(8); CN = 7; d(calc.) = 4.34; d(U–Cl) = 2.75(1) and 2.80(1); d(U–O) = 1.70 and 1.74(3); d(U–O)(water) = 2.46	*crystallographic and neutron diffraction data* (Taylor and Wilson, 1974c); *infrared and Raman data* (Gerding *et al.*, 1975); *thermodynamic data* (Grenthe *et al.*, 1992; Guillaumont *et al.*, 2003)

$UO_2Cl_2{\cdot}3H_2O$	yellow-green, fluorescent; deliquescent in air; extremely soluble in water, alcohol and ether $UO_2Cl_2{\cdot}3H_2O$(cr): $\Delta_f G_m^o$ = –1894.6 (3.0)†, $\Delta_f H_m^o$ = –2164.8 (1.7)†, S_m^o = 272.0 (8.4)†. IR (cm^{-1}): (B_{1u}, B_{2u}, B_{3u}): 93w,150m, 220sh, $\nu_2(UO_2^{2+})$ = 255s, ν(free H_2O) = 435br, 590br, $\nu_1(UO_2^{2+})$ = 879 (sharp), $\nu_3(UO_2^{2+})$ = 950s, 955s, $\nu_2(H_2O)$ = 1570sh, 1595m, 1610sh, $(\nu_1+\nu_3)(UO_2^{2+})$ = 1830w, 1835sh, ν(combination) = 2230w, $\nu_1+\nu_3(H_2O)$ = 3250vs,br	orthorhombic; C_{2v}^9, $Pn2_1a$, No.11; a = 12.738(5), b = 10.495(5), c = 5·47(2)	*crystallographic data* (Debets, 1968; Caville and Poulet, 1974; Brown, 1979); *infrared and Raman data* (Caville and Poulet, 1974); *thermodynamic data* (Brown, 1979; Grenthe *et al*., 1992; Guillaumont *et al*., 2003)
$[(UO_2)_4Cl_2O_2(OH)_2(H_2O)_6]\cdot(H_2O)_4$		monoclinic; C_{2h}^5, $P2_1/c$; No.14; a = 11.645(1), b = 10.101(1), c = 10.206(1); β = 105.77(1), Z = 2; V = 1155.31	*crystal structure* (Aberg, 1971, 1976)
$Li_2UO_2Cl_4$		monoclinic; C_{2h}^3, $C2/m$, No.12; a = 11.63, b = 7.56, c = 5.58; β = 95.7°	*crystallographic data* (Vorobei *et al*., 1971); *infrared and thermodynamic data* (Brown, 1979)
$Na_2UO_2Cl_4$		monoclinic; C_{2h}^3, $C2/m$, No.12; a = 11.53, b = 7.56, c = 5.60; β = 94.41	*crystallographic data* (Vorobei *et al*., 1971); *infrared and thermodynamic data* (Brown, 1979)
$Rb_2UO_2Cl_4$		monoclinic; C_{2h}^3, $C2/m$, No.12; a = 11.65, b = 7.42, c = 5.58; β = 98.6	*crystallographic data* (Vorobei *et al*., 1971); *infrared and thermodynamic data* (Brown, 1979)
$Rb_2UO_2Cl_4{\cdot}2H_2O$		triclinic; C_i^1, $P\bar{1}$, No.2; a = 6.795 (5); b = 6.929(5), c = 7.457(4),	*crystallographic data* (Anson *et al*., 1996)

Table 5.30 (*Contd.*)

Formula	*Selected properties and physical data*[b,c]	*Lattice symmetry, lattice constant* (Å), conformation and density (g cm^{-3})	*Remarks regarding information available and references*
		$\alpha = 91.96(5)$, $\beta = 102.13(5)$, $\gamma = 118.82(6)$; $Z = 1$; $V = 296.95$; d(calc.) = 3.46	
$Cs_2UO_2Cl_4$	IR and Raman (symmetry in D_{4h}) (cm^{-1}): A_{1g}(R) ν(O–U–O) sym. str. = 831; A_{2u}(IR) ν(O–U–O) asym. str. = 916; E_u(IR) ν(O–U–O) bend. = 252; A_{1g}(R) ν(U–Cl) sym.str. = 264; B_{2g}(R) ν(U–Cl) str. = 230; E_u(IR) ν(O–Cl) = 238; B_{1g}(R) ν(U–Cl) in plane bend. = 131; E_u(IR) ν(U–Cl) in plane bend. = 112; A_{2u}(IR) ν(U–Cl) out of plane bend. = 112; B_{1u} ν(U–Cl) out of plane bend. = 91****; E_g(R) ν(O–U–O) rock = 205–200; Lattice modes: 93(R), 73(R), 69(R), 56 (IR), 53(R), 48(R)	monoclinic; C_{2h}^3, *C2/m*, No.12; a = 11.92(2), b = 7.71(2), c = 5.83(1); $\beta = 99.66(3)$; d(calc.) = 4.26; d(U–O) = 1.81; d(U–Cl) = 2.62; O–U–O = 180; data from the neutron refinement: monoclinic; C_s^3, *Cm*, No.8; a = 12.005(8), b = 7.697(3), c = 5.850(3); $\beta = 100.00$ (4); $Z = 2$; $V = 532.34$; d(calc.) = 4.23	*crystallographic data* (Hall 1966; Vorobei *et al.*, 1971); *infrared and Raman data* (Denning *et al.*, 1976; Brown, 1979); *neutron diffraction refinement* (Tutov *et al.*, 1991) *thermodynamic data* (Brown, 1979; Fuger *et al.*, 1983)
$Cs(UO_2)_2Cl_5$		orthorhombic; a = 11.17(5), b = 12.80(5), c = 838(5); d(calc.) = 4.715	*crystallographic data* (Bevz *et al.*, 1970)
$[N(CH_3)_4]_2UO_2Cl_4$		tetragonal; D_{4h}^{14}, *P4$_2$/mmm*, No. 136; a = 9.175(5), c = 11.745(6); d(U–O) = 1.724(7); d(U–Cl) = 2.646(4) and 2.660(3); O–U–O = 180°	*crystallographic data* (Di Sipio *et al.*, 1974a); *infrared and Raman data*, *thermodynamic data* (Brown, 1979)

$[N(C_2H_5)_4]_2UO_2Cl_4$	triclinic; C_i^1, $P\bar{1}$, No. 2; $a = 9.997$ (5), $b = 10.064(5)$, $c = 12.914(5)$; $\alpha = 90.00(5)$, $\beta = 90.69(5)$, $\gamma = 90.00(5)$; d(U–O) = 1.76(2) and 1.77(3); d(U–Cl) = 2.65(1), 2.67(1) and 2.68(1)(2×); O–U–O = 180.0(1)	*crystallographic data* (Bois *et al.*, 1976a); *infrared and Raman data*, *thermodynamic data* (Brown, 1979)
$[N(C_2H_5)_3H]_2UO_2Cl_4$	tetragonal; C_{4h}^6, $I4_1/a$, No. 88; $a = 13.465(5)$, $c = 24.18(1)$; d(calc.) = 1.84; d(U–O) = 1.75(1); d(U–Cl) = 2.663(5) and 2.672(5); O–U–O = 179(1)	*crystallographic data* (Bois *et al.*, 1976b); *infrared and Raman, thermodynamic data* (Brown, 1979)
$[N(C_3H_7)_4N]_2UO_2Cl_4$	triclinic; C_i^1, $P\bar{1}$, No.2; $a = 10.890$ (5), $b = 17.257(7)$, $c = 11.076(5)$; $\alpha = 95.4(1)$, $\beta = 106.1(1)$, $\gamma = 114.9(13)$; $Z = 4$. The structure consists of tetrahedral $[CH_3CH_2CH_2]^+$ cations and bipyramidal $[UO_2Cl_4]^{2-}$ anions held together by Van der Waals forces. The U–O(2) bond distances [1.58(2)] are significantly shorter than the usual distances reported for uranyl U–O bonds (1.68–1.77) in hexacoordinated U (VI) compounds	*crystallographic data* (Di Sipio *et al.*, 1974b)
$[N(C_4H_9)_4]_2UO_2Cl_4$	monoclinic; C_{2h}^5, $P2_1/c$, No. 14; $a = 15.533(6)$, $b = 15.466(6)$, $c = 20.438(8)$; $\beta = 118.2(2)$; d(U–O) = 1.68(1) and 1.69(1); d(U–Cl) = 2.646(6), 2.648(5), 2.656(6) and 2.671(5); O–U–O = 178.1(5)°. The structure is built up of flattened $[UO_2Cl_4]^{2-}$ bipyramids and tetrahedral $[Bu_4N]^+$ ions held together by Van der Waals forces	*crystallographic data* (Di Sipio *et al.*, 1974c); *Infrared and Raman, thermodynamic data* (Brown, 1979)

Table 5.30 (*Contd.*)

Formula	*Selected properties and physical data*[b,c]	*Lattice symmetry, lattice constant* (Å), conformation and density ($g\ cm^{-3}$)	*Remarks regarding information available and references*
$[LH]_2UO_2Cl_4$[f]		monoclinic; C_{2h}^3, *C2/m*, No.12; ($P2_1/n$; No.14; non standard setting of P_21/c); $a = 11.199$, $b = 6.968$, $c = 23.675$; $\beta = 97.50$; d(U–O) = 1.78(1); d(U–Cl) = 2.66 (1) and 2.69(1); O–U–O = 180.0.	*crystallographic data* (Marzotto *et al.*, 1973; Clemente *et al.*, 1974)
$[L'H]_2UO_2Cl_4$ CH_3CN[g]		triclinic; C_i^1, $P\bar{1}$, No. 2; $a = 12.77$ (1), $b = 23.12(2)$, $c = 8.11(1)$; $\alpha = 94.33(3)$, $\beta = 89.43(3)$, $\gamma = 98.22$ (3); d(exp.) = 1.60; d(U–O) = 1.784(2) and 1.789(12); d(U–Cl) = 2.705(6), 2.706(4), 2.697(6) and 2.699(6); O–U–O = 179(1)	*crystallographic data* (Graziani *et al.*, 1975)
$UO_2(ClO_4)_2$	forms complexes with various donors ligands, e.g. DMSO and urea; soluble in H_2O; IR (cm^{-1}) (C_s): $\nu_8 = 1270$, 1234, $\nu_6 = 1116$, 1114; $\nu_1 = 1048$, $\nu_2 = 974$, $\nu_7 = 640$, $\nu_9 = 627$, $\nu_3 = 600$, $\nu_5 = 481$, $\nu_4 = 455$, $\nu_3(UO_{2(as)}^{2+}) = 996$, $\nu_3(UO_{2(sym)}^{2+}) = 900$		*infrared data* (Vdovenko *et al.*, 1964)
(i) $UO_2(ClO_4)_2{\cdot}H_2O$ (ii) $UO_2(ClO_4)_2{\cdot}3H_2O$ (iii) $UO_2(ClO_4)_2{\cdot}5H_2O$	(i) IR (cm^{-1})(C_s): $\nu_8 = 1250$, 1231, $\nu_6 = 1136$, 1114; $\nu_1 = 1075$, $\nu_2 = 996$, $\nu_7 = 646$, $\nu_9 = 633$, $\nu_3 = 613$, $\nu_5 = 470$, $\nu_4 = 450$, $\nu_3(UO_{2(as)}^{2+}) = 974$, $\nu_3(UO_{2(sym)}^{2+}) = 896$		*infrared data* (Vdovenko *et al.*, 1964)

	(ii) IR (cm^{-1}) (C_{3v}): $\nu_4 = 1192$, 1162, $\nu_1 = 1035$, 1017; $\nu_2 = 874$, $\nu_5 = 645$, $\nu_3 = 619$, $\nu_6 = 460$, $\nu_3(UO^{2+}_{2(as)}) = 967$, $\nu_3(UO^{2+}_{2(sym)}) = 892$. (iii) IR ($cm^{-1}$) ($T_d$): $\nu_3 = 1030$ to 1160, $\nu_1 = 930$; $\nu_4 = 624$, $\nu_3(UO^{2+}_{2(as)}) = 958$, $\nu_3(UO^{2+}_{2(sym)}) = 898$		
$UO_2(ClO_4)_2{\cdot}7H_2O$	soluble in: H_2O, EtOH, CH_3Cl, pyridine, DMSO etc.: loses H_2O at 270°C, dec. at 375°C; IR (cm^{-1}) (T_d): $\nu_3 = 1110$, $\nu_1 = 932$; $\nu_4 = 624$, $\nu_3(UO^{2+}_{2(as)}) = 958$, $\nu_3(UO^{2+}_{2(sym)}) = 888$	orthorhombic; C^5_{2v}, $Pca2_1$, No. 29; $a = 9.302(4)$, $b = 14.692(6)$, $c = 10.842(5)$; $Z = 4$; $d_{cal.} = 2.75$. The structure contains $[UO_2(OH_2)_5]^{2+}$ and ClO^-_4 ions and two H_2O molecules per U atom. The coordination polyhedron is a distorted bipyramid with d(U–O) = 1.62(7) and 1.80(3) in the uranyl group and 2.35 to 2.55 for the coordinated water molecules.	*crystallographic data* (Alcock and Esperäs, 1977); *Infrared data* (Vdovenko *et al.*, 1964); *absorption ,fluorescence and luminescence spectra* (Carnall, 1982)
$UO_2(HMPTA)_4(ClO_4)_2$; HMPTA = hexamethyl-phosphor-triamide = $[(CH_3)_2N]_3PO$.	$\nu_3(ClO^-_4) = 1095$, $\nu_4(ClO^-_4) = 624$, $\nu_{as}(UO^{2+}_2) = 917$	orthorhombic; D^{15}_{2h}, $Pbca$, No. 61; $a = 45,818(5)$, $b = 14.273(5)$, $c = 15.381(5)$; $V = 10056$	*crystallographic data* (Nassimbeni and Rodgers, 1976); *infrared spectra* (Gusev *et al.*, 1985)
(i) $K_xUO_3Cl_x$($x \approx 0.8$). (ii) $Rb_xUO_3Cl_x$ ($x \approx 0.8$). (iii) $Cs_xUO_3Cl_x$ ($x \approx 0.9$).		monoclinic; C^2_{2h}, $P2_1/m$, No.11. (i) $a = 8.55$, $b = 4.10$, $c = 7.00$; $\beta = 104.22$. (ii) $a = 8.734(2)$, $b = 4.118(2)$, $c = 7.718(2)$; $\beta = 105.34$. (iii) $a = 8.56$, $b = 4.11$, $c = 7.35$; $\beta = 104.56$; d(exp.) = 5.43. d(U–O) = 1.82(6); 1,85(9); 2.30(7); 2.17(7); d(U–Cl) = 2.98(2); O–U–O = 180.	*crystallographic data* (Allpress *et al.*, 1968)

Table 5.30 (*Contd.*)

Formula	*Selected properties and physical data*[b,c]	*Lattice symmetry, lattice constant* (Å), conformation and density ($g\ cm^{-3}$)	*Remarks regarding information available and references*
(i) $Rb_2U_2O_5Cl_4{\cdot}2H_2O$[d] (ii) $Cs_2U_2O_5Cl_4{\cdot}2H_2O$		monoclinic; C_{2h}^5, $P2_1/c$, No. 14; (i) $a = 8.540(11)$, $b = 8.096(8)$, $c = 21.735(32)$; $\beta = 111.74(11)^\circ$; d(U–O) = 1.78(2×), 2.203*, 2.268*, 2.289* and 2.509; d(U–Cl) = 2.743, 2.781, 2.800*, 2.804*, 2.825*, and 2.845*, O–U–O = 180.0 (ii) $a = 8.82(2)$, $b = 8.27(1)$, $c = 22.17(4)$; $\beta = 112.03(10)$; d(calc.) = 4.30	*crystallographic data* (Perrin, 1977a)
(i) $K_4U_5O_{16}Cl_2$ (ii) $Rb_4U_5O_{16}Cl_2$		monoclinic; C_{2h}^5, $P2_1/c$, No. 14; (i) $a = 9.96$, $b = 6.99$, $c = 19.60$; $\beta = 134.97^\circ$ (ii) $a = 10.21$, $b = 7.01$, $c = 19.64$; $\beta = 134.22$; d(calc.) = 6.13	*crystallographic data* (Allpress *et al*., 1968)
(i) $La_3(UO_6Cl_3)$ (ii) $Pr_3(UO_6Cl_3$ (iii) $Nd_3(UO_6Cl_3)$		hexagonal; C_{6h}^2, $P6_3/m$, No.176; (i) $a = 9.5155(16)$, $c = 5.6132(16)$; $Z = 2$; $V = 440.15$ (ii) $a = 9.3957(6)$, $c = 5.5470(5)$; $Z = 2$; $V = 424.08$ (iii) $a = 9.3668(5)$, $c = 5.5300(7)$; $Z = 2$; $V = 420.18$	*crystallographic data* (Henche *et al*., 1993)
$(NH_4)_2[(UO_2)_4O_2(OH)_2Cl_4(H_2O)_4]{\cdot}2H_2O$		triclinic; $a = 12.12(1)$, $b = 12.31(1)$, $c = 7.99(1)$; $\alpha = 111.2(1)$, $\beta = 95.1(1)$, $\gamma = 138.1(1)$	*crystallographic data* (Perrin, 1977b)

$K_2[(UO_2)_4O_2(OH)_2Cl_4(H_2O)_4] \cdot 2H_2O$[e]		triclinic; $a = 12.15(2)$, $b = 12.33(1)$, $c = 8.026(9)$; $\alpha = 110.5(1)$, $\beta = 96.3(1)$, $\gamma = 138.7(1)$; d[U(1)–O] = 1.767(6), 1.774(7), 2.205(2)*, 2.39(2)*, and 2.45(2)**; d[U(2)–O] = 1.795(6), 1.786(6), 2.246(19)*, 2.256(14)*, 2.39(2)*, and 2.41(1)**; d(U-Cl) = 2.873(9)*; O–U–O = 175.6(7)	*crystallographic data* (Perrin, 1977b; Perrin and Le Marouille, 1977)
$Rb_2[(UO_2)_4O_2(OH)_2Cl_4(H_2O)_4] \cdot 2H_2O$		triclinic; $a = 12.25(2)$, $b = 12.32(2)$, $c = 7.95(1)$; $\alpha = 110.4(1)$, $\beta = 95.6(1)$, $\gamma = 138.4(1)$	*crystallographic data* (Perrin, 1977b)
$Rb_4[(UO_2)_4O_2Cl_8(H_2O)_2] \cdot 2H_2O$		monoclinic; C_{2h}^5, $P2_1/c$, No.14; $a = 8.540(11)$, $b = 8.096(8)$, $c = 21.735(32)$; $\beta = 111.74(11)$; $Z = 2$; $V = 1395.87$; d(calc.) = 4.3	*crystallographic data* (Perrin, 1977a)
$Cs_3[(UO_2)_3O_2(OH)_3]_2Cl \cdot (H_2O)_3$		monoclinic; C_2^3, $C2$, No.5; $a = 19.6150(50)$, $b = 7.239(2)$, $c = 12.064(3)$; $\beta = 127.929(4)$; $Z = 2$; $V = 1351.17$; d(calc.) = 5.59	*synthesis and structural characterization* (Li *et al*., 2001)
$[N(C_6H_5CH_2)(CH_3)_3]_4 \cdot [UO_2Cl_3O]_2$[h]		monoclinic; C_{2h}^5, $P2_1/c$, No. 14; $a = 8.869(5)$, $b = 11.013(5)$, $c = 25.60(1)$; $\beta = 103.66(10)$; $Z = 4$; d(calc.) = 1.89; mean d(U–O, peroxy) = 2.30; the mean d(U–O, uranyl) = 1.78; mean d(U–Cl, uranyl) = 2.71; 1. O–U–O = 179.3 (1.0)	*crystallographyic data* (Boeyens and Haegele, 1976; Haegele and Boeyens, 1977)
UO_2Br_2	bright red; hygroscopic, thermally unstable; soluble in Me_2CO, Et_2O, EtOH, MeCN, H_2O; slowly loses Br_2 at room temp. UO_2Br_2 (cr): $\Delta_f G_m^o = -1066.4\ (1.8)^\dagger$, $\Delta_f H_m^o = -1137.4\ (1.3)^\dagger$, $S_m^o = 169.5\ (4.2)^\dagger$; $C_{p,m}^o = 116\ (8)^\dagger$. IR ($cm^{-1}$): 905s (stretching), 945, 930, and 825		*thermodynamic data* (Prins *et al*., 1978; Grenthe *et al*., 1992; Guillaumont *et al*., 2003); *IR spectra* (Prigent, 1958); *photoelectron spectroscopy* (Thibaut *et al*., 1982)

Table 5.30 (*Contd.*)

Formula	*Selected properties and physical data*[b,c]	*Lattice symmetry, lattice constant* (Å), conformation and density (g cm^{-3})	*Remarks regarding information available and references*
$UO_2Br_2{\cdot}H_2O$; $UO_2Br_2{\cdot}3H_2O$.	$UO_2Br_2{\cdot}H_2O$(cr): $\Delta_f G^o_m = -1328.6$ (2.5)†, $\Delta_f H^o_m = -1455.9$ (1.4)†, $S^o_m = 214$ (7)†. $UO_2Br_2{\cdot}3H_2O$(cr): $\Delta_f G^o_m = -1818.5$ (5.6)†, $\Delta_f H^o_m = -2058.0$ (1.5)†, $S^o_m = 304$ (18)†.		*thermodynamic data* (Grenthe *et al*., 1992; Guillaumont *et al*., 2003)
$(UO_2)_2(OH)_2Br_2(H_2O)_4]$	$UO_2OHBr(H_2O)_2$(cr): $\Delta_f G^o_m = -1744.2$ (4.4)†, $\Delta_f H^o_m = -1958.2$ (1.3)†, $S^o_m = 248$ (14)†	isostructural with the chloride analogue (monoclinic; C^5_{2h}, $P2_1/c$, No.14)	*X-ray powder diffraction data* (Peterson, 1961); *IR spectra* (Perrin, 1970); *thermodynamic data* (Prins *et al*., 1978; Grenthe *et al*., 1992; Guillaumont *et al*., 2003)
$[UO_2Br_2]{\cdot}3C_4H_8O$	light brown cryst.; soluble in THF	monoclinic; C^5_{2h}, $P2_1/c$, No.14; $a = 6.931(3)$, $b = 17.032(4)$, $c = 16.257(4)$; $\beta = 94.25(5)$; $V = 1914$ (2); $Z = 4$; d(calc.) = 2.242; the coordination polyhedron is a bipyramid with a non-planar pentagonal base made up of two Br^- anions three O atoms from the THF molecules. The two uranyl O atoms are in the apical positions; d(U–O) = 1.75(1), 1.77(1), 2.45(2), 2.47(1), 2.46(2); d(U–Br) = 2.845 (3), 2.856(3)	*crystallographic data* (Rebizant *et al*., 1987)
$Cs_2UO_2Br_4$	yellow; IR (cm^{-1}): ν(U–O, asym. stretch.) = 895–934; ν(O–U–O deformation) = 243–263; ν(U–Br	monoclinic; C^5_{2h}, $P2_1/a$, No.14; $a = 9.959(3)$, $b = 9.806(5)$, $c = 6.415$ (5); $\beta = 104.8(2)$; d(calc.) = 4.51;	*crystallographic data* (Mikhailov and Kuznetzov, 1971); *infrared and Raman data* (Brown, 1979);

	stretch.) = 160–180; Raman: ν(U–O sym. stretch.) = 826–835, ν(U–O–Br bend.) = 190–198, ν(U–Br stretch.) = 167–172, 81–83 ν(U–Br bending mode) = 81–83	d(U–O) = 1,70(5); d(U–Br) = 2.83 (1)(2×) and 2.80(1)(2×)	*thermodynamic data* (Fuger *et al.* (1983)
$(NH_4)_2UO_2Br_4(H_2O)_2$		triclinic; C_i^1, $P\bar{1}$, No.2; a = 6.8850 (9), b = 6.887(1), c = 7.7370(7); α = 94.44(1)°, β = 98.78(1), γ = 116.79(1); d(U-O) = 1.766(6); d(U–Br) = 2.813 (average); Z = 1; V = 319.17; d(calc.) = 3.44. The structure consists of $[UO_2Br_4]^{2-}$ and $[NH_4]^+$ ions. The U ions are octahedrally coordinated and the symmetry of $[UO_2Br_4]^{2-}$ is approx. D_{4h}	*crystallographic data* (Van den Bossche *et al.*, 1987)
$[N(CH_3)_4]_2UO_2Br_4$	yellow; IR (cm^{-1}): ν(U–O, asym. stretch.) = 895–934; ν(O–U–O, deformation) = 243–263; ν(U–Br, stetch.) = 160–180; Raman: ν(U–O, sym. stretch.) = 826–835, ν(U–O–Br, bend.) = 190–198, ν(U–Br, stretch.) = 167–172, 81–83; ν(U–Br, bending mode) = 81–83	tetragonal; D_{4h}^{14}, $P4_2/mmm$, No. 136; a = 9.350(5), c = 11.695(6); d(calc.) = 2.40; d(U–O) = 1,76(2); d(U–Br) = 2.783(6)(2×) and 2.828 (4) 2×	*crystallographic data* (Di Sipio *et al*. 1974a); *infrared and Raman data* (Brown, 1979)
$[N(C_3H_7)_4]_2UO_2Br_4$	yellow; IR (cm^{-1}): ν(U–O, asym. stretch.) = 895–934; ν(O–U–O, deformation) = 243–263; ν(U–Br, stetch.) = 160–180; Raman: ν(U–O, sym. stretch.) = 826–835, ν(U–O–Br, bend.) = 190–198, ν(U–Br, stretch.) = 167–172, 81–83 cm^{-1} ν(U–Br, bending mode) = 81–83.	monoclinic; $P2_1/n$; a = 13.706(6), b = 12.270(6), c = 10.758(5); β = 89.9(2); d(U–O) = 1,698(7); d(U–Br) = 2.837(2)(2×) and 2.829(6) 2×	*crystallographic data* (Di Sipio *et al*., 1974d); *Infrared and Raman data* (Brown, 1979)

Table 5.30 (*Contd.*)

Formula	*Selected properties and physical data*[b,c]	*Lattice symmetry, lattice constant* (Å), conformation and density ($g\ cm^{-3}$)	*Remarks regarding information available and references*
$[N(C_4H_9)_4]_2UO_2Br_4$		triclinic; C_i^1, $P\bar{1}$, No.2; $a = 18.62$ (2), $b = 11.52(1)$, $c = 11.50(1)$; $\alpha = 100.75(8)$, $\beta = 93.70(8)$, $\gamma = 115.96$ (8); $Z = 2$. The structure is built up of $[Bu_4N]^+$ and $[UO_2Br_4]^{2-}$ ions. The four Br anions are arranged around the linear UO_2 group to form a distorted to square bipyramidal octahedral coordination polyhedron. The U–Br moiety is strictly planar. The cations are tetrahedral. Alternating layers of anions and cations are linked by Van der Waals forces	*crystallographic data* (Di Sipio *et al.*, 1977)
$[P(C_6H_5)_4]_2$ $[UO_2\ Br_4]$ $\cdot 2CH_2Cl_2$	yellow	monoclinic; C_{2h}^6, $C2/c$, No.15; $a = 20.063(8)$, $b = 13.206(4)$, $c = 20.425(9)$; $\beta = 98.78(4)$; $V = 5348$; $Z = 4$; d(calc.) = 3.07 d(U–Br1) = 2.83.6(3); d(U–Br2) = 2.814(3); d(U–Br3 or U–O) = 1.72(2); Br–U–Br and O–U–O = 92.4(1) and 88.3(5)	*synthesis and crystallographic data* (Bohrer *et al.*, 1988)
$[C_7H_{16}NO_2]_2$ UO_2Br_4[i]	yellow; IR (cm^{-1}): ν(U–O, asym. stretch.) = 895–934; ν(O–U–O deformation) = 243–263; ν(U–Br	orthorhombic; D_{2h}^{16}, *Pnma*, No. 62; $a = 13.60(2)$, $b = 20.943)$, $c = 9.22$ (2); d(calc.) = 2.23; d(U–O) = 1,80	*crystallographic data* (Marzotto *et al.*, 1974); *Infrared and Raman data* (Brown, 1979)

	stetch.) = 160–180; Raman: ν(U–O sym. stretch.) = 826–835, ν(U–O–Br bend.) = 190–198, ν(U–Br stretch.) = 167–172 cm^{-1}, 81–83, ν(U–Br bending mode) = 81–83 cm^{-1}	(3); d(U–Br) = 2.804(4), 2.792 (4) and 2.859(2) 2×	
(i) $K_2[(UO_2)_4 O_2(OH)_2 Br_4(H_2O)_4] \cdot 2H_2O$ (ii) $Rb_2[(UO_2)_4O_2 (OH)_2Br_4(H_2O)_4] \cdot 2H_2O$		triclinic; C_i^1, $P\bar{1}$, No. 2. (i) $a = 12.42(2)$, $b = 12.46(1)$, $c = 8.08(1)$; $\alpha = 109.4(1)^o$, $\beta = 97.2(1)$, $\gamma = 139.0(1)$. (ii) $a = 12.47(2)$, $b = 12.34(2)$, $c = 8.07(3)$; $\alpha = 109.0(1)$, $\beta = 97.2(1)$, $\gamma = 138.6(1)$	*crystallographic data* (Perrin, 1977b)
$K_xUO_3Br_x$ ($x = 0.9$)		monoclinic; C_{2h}^2, $P2_1/m$, No.11; $a = 9.57$, $b = 4.14$, $c = 6.89$; $\beta = 11.77$	*crystallographic data* (Allpress *et al*., 1968)
$UO_2(HMPTA)_4 (BrO_4)_2$ HMPTA = hexamethyl-phosphor-triamide = $[(CH_3)_2N]_3PO$.	IR (cm^{-1}):$\nu_3(BrO_4^-)$ = 871, $\nu_{as}UO_{2(as)}^{2+}$ = 917	orthorhombic; D_{2h}^{15}, *Pbca*, No. 61; $a = 46.18(10)$, $b = 14.40(4)$, $c = 15.56(4)$; $V = 10347$	*crystallographic data and infrared spectra* (Gusev *et al*., 1985)
$K_2[(UO_2)_3 (IO_3)_4 O_2)]$		triclinic; C_i^1, $P\bar{1}$, No.2; $a = 7.0372(5)$, $b = 7.7727(5)$, $c = 8.9851(6)$; $\alpha = 93.386(1)$, $\beta = 105.668(1)$, $\gamma = 91.339(1)$; $Z = 1$; $V = 471.98$	*crystallographic data* (Bean *et al*., 2001b)
$Ba[(UO_2)_2(IO_3)_2 O_2)] H_2O$		monoclinic; C_{2h}^5, $P2_1/c$, No. 14; $a = 8.062(4)$, $b = 6.940(3)$,$c = 21.665(10)$; $\beta = 98.049(10)$; $Z = 4$; $V = 1200.22$	*crystallographic data* (Bean *et al*., 2001b)
$Ag_4(UO_2)_4 (IO_3)_2 (IO_4)_2 O_2$		monoclinic; C_{2h}^5, $P2_1/c$, No.14; $a = 15.040(7)$, $b = 8.051(4)$, $c = 18.3320(80)$; $\beta = 100.738(7)$; $V = 2180.9$; $Z = 4$	*crystallographic data* (Bean *et al*., 2001a)

Table 5.30 (*Contd.*)

Formula	*Selected properties and physical data*[b,c]	*Lattice symmetry, lattice constant* (Å), conformation and density (g cm^{-3})	*Remarks regarding information available and references*
(i) $UO_2(IO_3)_2$;. (ii)$UO_2(HMPTA)_4(IO_4)_2$ HMPTA = hexamethyl-phosphortriamide = $[(CH_3)_2N]_3PO$	(i) $UO_2(IO_3)_2$(cr): $\Delta_f G^o_m = -1250.2$ (2.4)†, $\Delta_f H^o_m = -1461.3$ (3.6)†, $S^o_m = 279$ (9)† (ii) IR (cm^{-1}):$\nu_3(IO_4^-) = 843$, $\nu_{as}(UO_2^{2+}) = 917$	orthorhombic; D^{15}_{2h}; *Pbca*, No. 61; $a = 46.52(10)$, $b = 14.50(4)$, $c = 15.66(4)$; $V = 10563$	*crystallographic data and infrared spectra* (Gusev *et al.*, 1985)

* Bridging oxygen or chlorine distances.
** U–O distances to the water molecule.
*** Estimated values.
**** Value obtained from a force constant calculation (IR inactive).
† Values recommended by the Nuclear Energy Agency (Grenthe *et al.*,1992; Guillaumont *et al.*, 2003).
‡ equation expressed in°C.
[a] Values have been selected in part from review articles (Brown, 1979; Bacher and Jacob 1980; Freeman,1991; Grenthe *et al.*, 1992; Guillaumont *et al.*, 2003.).
[b] m.p. = melting point; b.p(°C). = boiling point; (cr) = crystalline; (g) = gaseous; thermodynamic values in kJ mol^{-1}, or J K^{-1} mol^{-1} at 298.15 K, unless otherwise mentioned; $\Delta_f G^o_m$, - standard molar Gibbs energy of formation; $\Delta_f H^o_m$, standard molar enthalpy of formation; S^o_m (J K^{-1} mol^{-1}), standard molar entropy; $C^o_{p,m}$, standard molar heat capacity; log p (mmHg) = $-AT^{-1} + B - C \log T$: vapor pressure equation for indicated temperature range; R = Raman active; IR = infrared active; vs: very strong; s: strong; m: medium; ms: medium strong; w: weak; sh: shoulder; b: broad; L: lattice; all values are in cm^{-1}.
[c] All values are in Å and angles are in degrees; CN, coordination number; d, density [g cm^{-3}], V = molar volume [cm^3 mol^{-1}].
[d] The anion is $[(UO_2)_4O_2Cl_8(H_2O)_2]^4$.
[e] The anion is $[(UO_2)_4O_2(OH)_2Cl_4(H_2O)_4]^{2-}$.
[f] L = thiamine ($C_{12}H_{16}ClN_4OS$).
[g] L′ = 2,6-diacetylpyridine-bisphenyl hydrazone.
[h] The anion is $[(UO_2)_2Cl_6(\mu\text{-}O_2)]^{4-}$.
[i] Acetylcholine cation.

shown the existence of several progressions in the symmetric stretching frequency (ν_1) coupled with other modes. Two non-phonon transitions, originating at 24564 and 25265 cm^{-1}, are associated with the first band and four other with origins at 30331, 31032 (observed directly), 32120, and 32821 cm^{-1} with the second one; they could be located in the low-temperature spectra of the compound. The observed fine structure has been explained in terms of electric–dipole forbidden transitions from the t_{1u} ($\pi+\sigma$) orbitals of the fluorine atoms to the empty 5f orbitals of the uranium atoms. A strong absorption band without vibronic structure, observed at about 46730 cm^{-1}, has been assigned as a charge transfer transition.

Since the ground state of UO_2^{2+} does not contain unpaired electrons the uranyl compounds are either diamagnetic or weakly paramagnetic. The octahedral hexahalides exhibit a weak, almost temperature-independent, paramagnetism.

(*i*) *Uranium hexafluoride and uranium*(*VI*) *complex fluorides*

Uranium hexafluoride

Uranium hexafluoride is the only uranium compound that is readily volatilized and is therefore used for uranium isotope separation by gas diffusion, gas centrifugation, liquid thermal diffusion, or in mixtures with a light auxiliary gas like H_2 or He (separation nozzle). The uranium enrichment technologies have been surveyed by Becker (1979) and Ehrfeld and Ehrfeld (1980), for example. Due to the importance of UF_6, the physical and chemical properties of UF_6, including commercial syntheses, have been extensively studied. The literature is covered in a number of reviews (Caillat, 1961; Brown, 1968; Bacher and Jacob, 1980, 1982, 1986; Hellberg and Schneider, 1981; Freestone and Holloway, 1991). A scheme of reactions leading to UF_6 is shown in Fig. 5.45.

Some important preparative procedures are based on the following reagents (Bacher and Jacob, 1980; Freestone and Holloway, 1991):

(1) reaction of elemental fluorine with U, UF_4 (at 340°C), U_4F_{17}, U_2F_9 (at 300°C), UF_5 (at 270°C), $NaUF_5$ (at 340°C), UO_2 (at 500°C), UO_3 (at 400°C), U_3O_8 (at 360°C), UO_2F_2 (at 340°C), $Na_2U_2O_7$, CaU_2O_7, UCl_5 (at –20 to 30°C), UO_2HPO_4 (at 370°C), UC_2 (at 350°C); e.g.

$$U_3O_8 + 17F_2 \overset{360°C}{\rightarrow} 3UF_6 + 8F_2O$$

$$CaU_2O_7 + 7F_2 \rightarrow 2UF_6 + CaF_2 + 7/2O_2$$

(2) reaction of bromine trifluoride with U (at 50–125°C), U_2F_9 (at 170°C, leading to UF_4), UO_2, UO_3, U_3O_8, UO_2F_2; e.g.

$$U_3O_8 + 6BrF_3 \rightarrow 3UF_6 + 3Br_2 + 4O_2$$

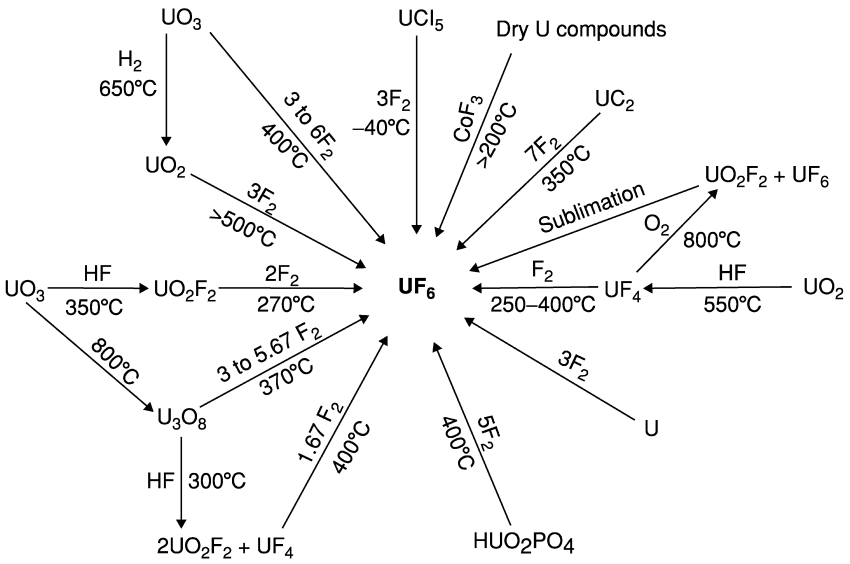

Fig. 5.45 *Reactions leading to UF_6 (adapted from Katz and Rabinowitch, 1951).*

(3) reaction of hydrogen fluoride with UO_2 (at 550°C), $Na_2U_2O_7$, UCl_5; e.g.

$$UCl_5 + 5HF \rightarrow UF_5 + 5HCl$$

followed by reactions (6b) and (6c) below;

(4) reaction with low temperature fluorinating agents: O_2F_2 with U_3O_8; KrF_2 with UF_4, and UO_2 and U_3O_8 in the gaseous phase or at room temperatures in HF solutions;

(5) reaction with other reagents:

(a) $O_2 + 2UF_4$ (at 660–800°C) $\rightarrow UF_6 + UO_2F_2$
(b) $3BrF_5 + U$ (at 50–125°C) $\rightarrow UF_6 + 3BrF_3$
(c) $3ClF_3 + U$ (at 25–75°C) $\rightarrow UF_6 + 3ClF$
(d) $2CoF_3 + UF_4$ (at 250°C) $\rightarrow UF_6 + 2CoF_2$

(6) decomposition reactions with disproportionation:

(a) $2U_4F_{17}$ (at 270–350°C) $\rightarrow 7UF_4 + UF_6$
(b) $3UF_5$ (at 170°C) $\rightarrow U_2F_9 + UF_6$
(c) $2U_2F_9$ (at >500°C) $\rightarrow 3UF_4 + UF_6$
(d) $9UO_2F_2$ (at >700°C) $\rightarrow 3UF_6 + 2U_3O_8 + O_2$.

As indicated above, the fluoride obtained by means of the reaction given in (3) can be converted to UF_6, using double decomposition with subsequent

disproportionation (reactions 6b and 6c). The separation from UF_4 and an excess of HF can be achieved by heating, followed by fractional distillation. The method based on reaction (5a) is also a convenient route, not involving the use of gaseous fluorine; UO_2F_2 is formed as a by-product, but can be converted to UF_4 by reduction and to UF_6 by hydrofluorination. An attractive method on laboratory scale uses reactions (5d) (Weigel, 1958). The by-product CoF_2 can easily be separated from UF_6 and regenerated with fluorine. The general route for purification of UF_6 employs trap-to-trap distillation followed by condensing the hexafluoride at about –80°C.

The production of UF_6 on an industrial scale is achieved mainly by oxidative fluorination of uranium oxides or lower fluorides by fluorine at elevated temperatures. A uranium ore concentrate is first purified by solvent extraction or by ion exchange methods. From this concentrate, $(NH_4)_2U_2O_7$ (ammonium diuranate, ADU, yellow cake) or $UO_2(NO_3)_2 \cdot 6H_2O$ (UNH) is then precipitated. ADU is converted to UO_2 by calcination in the presence of H_2 whereas UNH is first pyrolyzed to UO_3 and then reduced by H_2 to UO_2.

A detailed description of the commonly applied direct fluorination technology of UF_4

$$UF_4(s) + F_2(g) \rightarrow UF_6(g)$$

has been published by Smiley and Brater (1956) and Brater and Smiley (1958). In the conversion flow sheet shown in Fig. 5.46, the fluorination reactor used is either a flame reactor or a fluidized-bed reactor (Harrington and Ruehle, 1959). In the first one UF_4 is fed to the top of the reactor having a length of 3.60 m, diameter of 20 cm, and a capacity of 380 kg per hour. The highly exothermic fluorination reaction takes place over a length of ~1 m at the top of the reactor where a flame with temperatures up to 1100°C is formed. In order to suppress corrosion, the temperature of the reactor walls is maintained below 540°C. For a maximum yield of UF_6 a temperature limit of 450°C, which eliminates the formation of intermediate fluorides, is required. The off-gases contain ~75% UF_6 and have their outlet at the lower part of the reactor. All unreacted solids are collected, powdered, mixed with fresh UF_4 and transmitted again to the feed.

In the second method, UF_4 is fluorinated with F_2 at 500°C in a Monel fluidized-bed reactor with an annual production capacity of 4400 to 7400 tons of UF_6. The UF_4 feed material and fluorine gas are mixed continuously by means of a conveyor screw and a gas distributor (6–20 $cm^3\ s^{-1}$), respectively. For stabilization of the fluidized bed CaF_2 is added to the feed. It serves also to prevent sintering of UF_4 and as a heat transfer material. The product obtained in both types of reactors is passed through Monel filters in order to remove UF_4 dust and is then condensed, first at +4 to –15°C and finally at –40°C. The condensers are then heated to 80°C and UF_6, which liquefies at that temperature under its own pressure, is drained into transport cylinders, which have a volume of up to about 4 m^3, weigh around 2.36 tons, and have a capacity

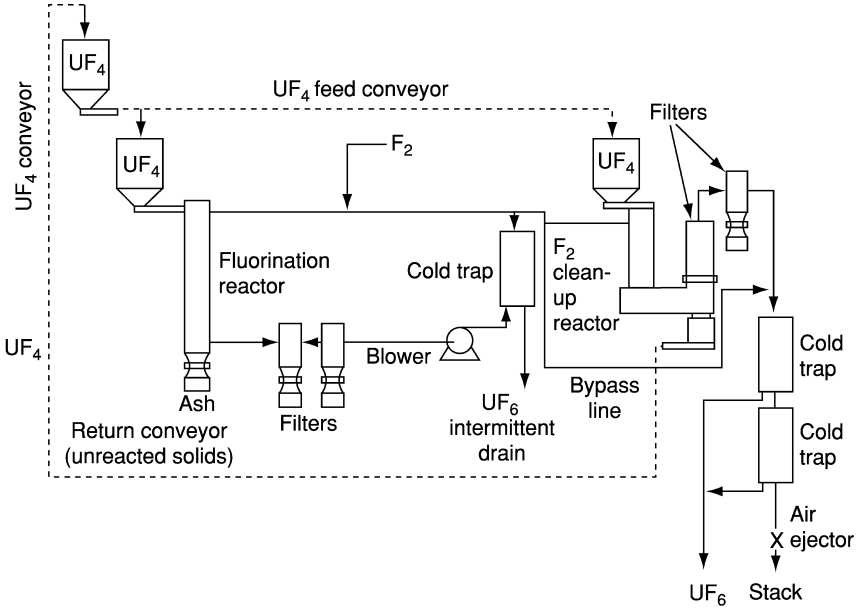

Fig. 5.46. *Schematic flow diagram for uranium hexafluoride production* (*Harrington and Ruehle*, 1959).

of 12.5–14 tons (Keller, 1956). The crude product usually contains numerous volatile impurities such as SiF_6, CF_4, SF_4, MoF_6, CrO_2F_2, or VF_5 as well as some less volatile compounds like MoF_4, VOF_3, and other transition metal fluorides. Since stringent purity specifications are required of commercial UF_6 for isotope separations, the impurities are removed by fractionation at temperatures and pressures above the triple point and by absorption–desorption techniques. At room temperature, UF_6 has a pressure of ca. 120 mmHg; it is thus possible to handle it as a gas in the separation of ^{235}U from natural uranium. For large-scale applications, solid UF_6 is delivered to isotope separation plants in containers, which are then placed into a steam-heated autoclave in which UF_6 builds up a high enough pressure to flow as a gas into the attached diffusion cascade for the separation process (Arendt *et al.*, 1957).

Uranium hexafluoride forms low-melting orthorhombic (space group *Pnma*) colorless crystals which sublime at 56.5°C at atmospheric pressure. The compound has a triple point at 64.02°C and a pressure of 1137 mmHg (Hoard and Stroupe, 1959; Rigny, 1965, 1966; Levy *et al.*, 1976). The structure of solid UF_6 was first determined by Hoard and Stroupe (1959) and later in a number of X-ray and neutron diffraction studies (Levy *et al.*, 1976; Jacob and Bacher, 1980). It consists of hexagonal close-packed fluorine ions with uranium atoms in octahedral holes. The crystallographic data of UF_6 are listed in Table 5.30 together with selected physical data.

The structure of UF_6 in the liquid and gaseous states is perfectly octahedral (point group O_h) with U–F bond lengths in solid UF_6 equal to 1.996 Å. The compound has a temperature-independent paramagnetism with a molar susceptibility of $\chi_{mole} = 43 \times 10^{-6}$ cm^3 mol^{-1}, after correction for a diamagnetic contribution of $\chi_{mole} = 106 \times 10^{-6}$ cm^3 mol^{-1}. Carnall (1982) has published extensive analyses of the absorption and fluorescence spectra of UF_6. The absorption spectrum of UF_6 in visible to the near-UV range is similar to that of the UO_2^{2+} ion; in the range 200–420 nm there is only one broad band at 375 nm.

The compound is highly reactive and extremely moisture-sensitive. It reacts with most elements but is relatively stable towards oxygen, chlorine, bromine, carbon dioxide, and noble gases even at elevated temperatures. UF_6 has a significant solubility in liquid chlorine and bromine. Thermodynamic calculations have shown that UF_6 is thermally stable below 1000 K; dissociation starts between 1100 and 1450 K. Since UF_6 is rapidly hydrolyzed by water with the formation of HF it is recommended to store the compound in teflon, Kel-F, nickel, or Monel containers.

$$UF_6 + 2\,H_2O \rightarrow UO_2F_2 + 4HF$$

It can be also stored in quartz or Pyrex tubes by using NaF and KF as HF 'getters'.

Uranium hexafluoride is a powerful fluorinating agent with a vapor pressure of 115 mm at 25°C. Bacher and Jacob (1982) have classified, as discussed below, a number of reactions of UF_6.

Oxidative fluorination results in a simultaneous formation of lower uranium fluorides. UF_6 oxidizes elements or their fluorides in low oxidation states to yields fluorides in higher oxidation state, e.g. with alkali, alkaline earth metals, B, Al, Ga, In, C, Si, Ge, Sn, Pb, As, Sb, S, Se, and Te binary fluorides are formed; lower fluorides such as PF_3, SF_4, MoF_5, or WF_4 are oxidized to higher fluorides:

$$nUF_6 + M(s) \rightarrow nUF_5(s) + MF_n$$

Lower oxides are converted to oxyfluorides whereas chlorides and bromides yield fluorides in presence of an excess of UF_6 with formation of Cl_2 and Br_2, respectively:

$$nUF_6 + 2MX_n \rightarrow nUF_4 + 2MF_n + nX_2 \quad (X = Cl \text{ or } Br)$$

The high fluorination efficiency of UF_6 is also demonstrated by interactions with SO_3 that leads to the formation of the peroxide $S_2O_6F_2$ (Wilson *et al.*, 1977; Masson *et al.*, 1978). The effective first bond dissociation energy of UF_6, according to the the reaction scheme

$$UF_6 \rightarrow (UF_5)_{solid} + F$$

is equal to (134.0 ± 29.3) kJ mol^{-1}, and is of the same order of magnitude as the bond energy of elemental F_2 (153.2 kJ mol^{-1}, Jacob and Bacher, 1986).

Reaction of UF_6 with other highly electronegative groups may lead to a total or partial substitution of the fluorine atoms with retained oxidation state of uranium as in the vapor phase hydrolysis:

$$UF_6 + 3H_2O \rightarrow UO_2F_2 \cdot H_2O + 4HF$$

and the hydrolysis in liquid HF:

$$UF_6 + nH_2O \rightarrow UO_nF_{(6-2n)} + 2nHF \quad (\text{where } n = 1 \text{ or } 2)$$

or in exchange reactions where fluorine is replaced by groups such as Cl, OCH_3, and $OTeF_5$:

$UF_6 + 6BCl_3 \rightarrow UCl_6 + 6BCl_2F$ (with excess of BCl_3) (O'Donnell *et al.*, 1966)
$UF_6 + 6Si(OCH_3)_4 \rightarrow U(OCH_3)_6 + 6SiF(OCH_3)_3$ (with excess of $Si(OCH_3)_4$) (Jacob, 1982).

UF_6 is a strong Lewis acid that can bind fluoride from Lewis bases such as MF (where M = Na, K, Cs, Rb, NH_4, N_2H_5, NO, and NO_2) under the formation of the corresponding heptafluorouranates(VI), MUF_7 and octafluorouranates(VI), M_2UF_8. UF_6 can oxidize various metals, as well as NO, NO_2, and I_2 in other less common reactions. These reactions are due to the high electron affinity of UF_6 (5.2 eV) and to a favorable lattice energy when fluorouranates(V) are formed, e.g.:

$$NO \rightarrow NO^+ + e \quad + 9.2 \text{ eV}$$

$$UF_6 + e \rightarrow UF_6^- \quad - 5.2 \text{ eV}$$

$$NO^+ + UF_6^- \rightarrow NOUF_6 \quad - \text{lattice energy}$$

The hexafluoride is reduced to the tetravalent state by a number of reagents, e.g. HCl (250°C), PF_3, HBr (80°C), CCl_4, CS_2, H_2S, amorphous carbon as well as $SiCl_4$, $AsCl_3$, $SbCl_3$, PBr_5, and BBr_3, with the formation of the appropriate free halogen. Reduction with H_2 is slow and may be carried out at 650°C, or in pressurized systems at 300°C. Exposure of UF_6 to UV light or photocatalytic reduction with HBr, SO_2, or CO yield β-UF_5:

$$2UF_6 \xrightarrow{h\nu} (UF_5)_{\text{solid}} + 1/2F_2$$

$$2UF_6 + X \xrightarrow{h\nu} 2\beta\text{-}(UF_5)_{\text{solid}} + XF_2 \quad (X = H_2, CO, \text{or } SO_2).$$

Alpha radiation from hexafluoride enriched with ^{235}U or ^{234}U results in significant reduction to lower fluorides.

A number of binary phase diagrams of uranium hexafluoride with fluorine and elements of the 7th main group have been reported (Bacher and Jacob, 1980). Simple eutectic types were observed in the UF_6–BrF_3, UF_6–BrF_5, and UF_6–BrF_2 systems. Some deviation from ideality was found for the UF_6–BrF_3, UF_6–BrF_5, UF_6–ClF_3, and UF_6–BrF_3 systems. In all of these systems, the solid

phases are pure stoichiometric compounds. The UF_6–HF phase diagram investigated by Rutledge *et al.* (1953) has practical importance due to the common presence of HF in UF_6. In the phase diagram shown in Fig. 5.47 there is a complete miscibility above 100°C and above a pressure of 10 atm.

The system possesses an eutectic point at –85°C with less than 0.5 mol% of UF_6. The separation of HF from UF_6–HF solutions by distillation is limited due to the appearance of azeotropes.

Complex uranium(VI) fluorides

Bacher and Jacob (1980) and Freestone and Holloway (1991) have compiled data on the synthesis and characterisation of numerous fluorouranate(VI) compounds listed below in Table 5.31; some of their physical data are presented in Table 5.30.

NaF has found practical application in nuclear processing. It absorbs UF_6 quickly and has the largest absorption capacity of all alkali metal fluorides. The sodium fluorouranates(VI) formed in the process can easily be thermally dissociated to UF_6 (Bacher and Jacob, 1986).

Several methods have been applied for the preparation of the fluoro complexes (Bacher and Jacob, 1980; Freestone and Holloway, 1991), e.g.: (i) most of

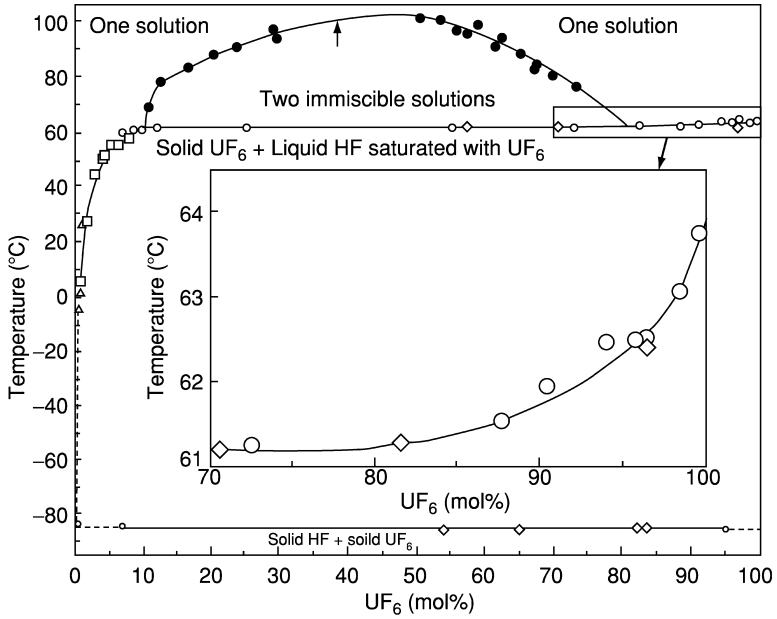

Fig. 5.47 *Phase diagram of the binary system UF_6-HF* (*Rutledge* et al., 1953). •, *Visual observation of disappearance of two liquid layers;* □, *visual observation of precipitation of solid UF_6;* Δ, *filter cell;* ○, *freezing point cell–K2 potentiometer;* ◇, *freezing point cell–white potentiometer. The thin arrow indicates rupture of polyethylene tube.*

Table 5.31 *Identified uranium(VI) complex fluorides.*

System	*Complex fluorides*
$NaF–UF_6$	$NaUF_7$, Na_2UF_8, Na_3UF_9, $Na_3U_2F_{15}$
$KF–UF_6$	KUF_7, K_2UF_8, K_3UF_9, $K_3U_2F_{15}$
$RbF–UF_6$	$RbUF_7$, Rb_2UF_8, Rb_3UF_9
$CsF–UF_6$	$CsUF_7$, Cs_2UF_8, Cs_3UF_9
$NH_4F–UF_6$	NH_4UF_7, $(NH_4)_2UF_8$
$N_2H_5F–UF_6$	$N_2H_5UF_7$, $N_2H_6(UF_6)_2$
$NO_xF–UF_6$	$NOUF_7$, NO_2UF_7, $(NO)_2UF_8$

the compounds can be obtained by the reaction of gaseous UF_6 with solid MF (where M = Na, K, Rb, Cs, or NH_4). In some cases, the reactions are carried out at higher temperatures and pressures. The products may be however contaminated by unreacted solid fluorides; (ii) the interaction of a large excess of liquid UF_6 with solid MF yields MUF_7 (M = K, Rb, or Cs); (iii) complex fluorides of the formula MUF_7 or M_2UF_8 are formed by interaction of UF_6 with NaF, KF, RbF, CsF, AgF, or TlF_3 by using appropriate solutions or suspensions in perfluoroheptane, C_7F_{16}, C_8F_{16}, ClF_3, or anhydrous HF; (iv) fluorination of a M_2UF_6 (M = Rb or Cs) or a $NaF–UF_4$ mixture with F_2 results in the formation of M_2UF_8 and $NaUF_7$, respectively; (v) the M_2UF_8 octafluoro uranate(VI) may also be prepared by thermal decomposition of the corresponding sodium (at 60–145°C), potassium (at 130°C), rubidium (at 150°C), and cesium (180–200°C) heptafluoro uranates; (vi) the reaction between UF_6 and liquid or gaseous ammonia yields NH_4UF_5 and NH_4UF_6, respectively. In the latter case also, a mixture of NH_4UF_5 and UF_5 may be obtained; (vii) the condensing of UF_6 in a suspension of NH_4F in tetrachloroethane yields NH_4UF_7; (viii) the corresponding hydrazinium $N_2H_5UF_7$, nitrosonium $NOUF_7$, and nitronium NO_2UF_7 salts are prepared by direct reaction of the component fluorides, the former in anhydrous hydrofluoric acid.

The fluoro uranates(VI) are extremely moisture-sensitive solids, very susceptible to hydrolysis. With some exception (e.g. NH_4UF_7, which decomposes to UF_5 or UF_4, depending of the applied temperature) they decompose to UF_6 when heated. The UF_6–bromine fluorides and the UF_6–HF systems (HF removal) have also found application in the fluorination reactions in nuclear reprocessing.

(*ii*) *Uranium(VI) oxide fluorides and complex oxide fluorides*

Uranium(VI) oxide tetrafluoride, UOF_4

UOF_4 can most conveniently be prepared either by the interaction of an excess of UF_6 with quartz wool in liquid HF

$$3UF_6 + SiO_2 \overset{\text{HF (liquid)}}{\rightarrow} 3UOF_4 + SiF_4$$

or by reaction with an excess of B_2O_3

$$3UF_6 + B_2O_3 \rightarrow 3UOF_4 + 2BF_3$$

Uranium oxide tetrafluoride is an orange solid with a shade of red. It is non-volatile and decomposes at 200–250°C without melting. At 250°C in vacuum UOF_4 decomposes spontaneously in an exothermic reaction to UF_6 and UO_2F_2. The reaction proceeds quantitatively and may be used for purity checking. UOF_4-hydrate is formed after some time in moist air, but liquid water results in a rapid hydrolysis. UOF_4 reacts with KF and NH_4F in liquid HF to form $MUOF_5$ type of salts. Fluorination of UOF_4 by ClF_5, ClF_3, or $ClOF_3$ at room temperature yields UF_6:

$$ClF_5 + 2UOF_4 \rightarrow ClO_2F + 2UF_6$$

UOF_4(cr) has trigonal symmetry in the space group $R3m$ and a pentagonal bipyramidal coordination geometry formed by the O and F atoms. Some physical data are given in Table 5.30.

Uranium(*VI*) *oxide difluoride* (*uranyl fluoride*), UO_2F_2

One of the simplest methods to prepare UO_2F_2 is by heating of UO_3 in gaseous HF at 300–500°C. Other satisfactory routes employ fluorination of uranium oxides at 350°C and oxidation of UF_4 with O_2 at 600–800°C. The compound is a pale yellow solid with a green hue, slightly soluble in water, methanol, and ethanol. Recrystallization from water results in the formation of $UO_2F_2 \cdot 2H_2O$. Controlled action of H_2O in a closed vessel yields hydrates $UO_2F_2 \cdot nH_2O$ ($n = 1$ to 4). The reaction of an excess of UF_6 with water vapour at 60°C leads to the formation of $UO_2F_2 \cdot 1.53H_2O$. Adducts of the $UO_2F_2 \cdot L(H_2O)$ and $UO_2F_2 \cdot nL$ ($n = 1$ to 4) type are formed by interactions with oxygen or nitrogen donor ligands (L) such as NH_3, pyridine (py), tributylphosphine oxide (tbpo), dimethylsulfoxide (dmso), antipyrine (antypy), 2,2′-dipyridyl (dipy), dimethylformamide (dmf), acetamide (aa), dimethylacetamide (dma), urea (ur), dimethylurea (dmur), and tetramethylurea (tmur) (Shchelokov *et al.*, 1977; Bagnall, 1979, 1987; Mass, 1979). IR and Raman data are available for most of the compounds. The nature of the uranium–oxygen bonds in UO_2^{2+} depends on the electron donor properties of the ligands, which result in variations of the UO_2^{2+} ν_1 and ν_2 frequencies that provide valuable structural information. The k_{UO} force constants, determined from both of these frequencies, decrease in the series (Shchelokov *et al.*, 1977) $H_2O >$ aa $>$ dma $>$ dmur $>$ dmso $>$ dmf $>$ tmur$\sim$antipy $>$ ur.

The total energy, molar entropy, heat capacity, and vibration frequencies of the compound in the gas phase have been calculated by *ab initio* methods to obtain thermodynamic data for reactions. They agree well with experimental values and previous results (Privalov *et al.*, 2002).

UOF_2 is converted to UF_6 by gaseous fluorides such as XeF_6 (25°C), BrF_3 (25°C), ClF_3 (50–160°C), ClF (64–150°C), ClO_2F (100–150°C), ClF_5 (>120°C)

F_2 (>300°C), BrF_5 (250°C), SF_4 (>300°C), and VF_5 (100°C). The reactions proceed with much greater difficulty than oxidative fluorination of UF_4 or UF_5 (Bacher and Jacob, 1980). The compound crystallizes with a rhombohedric structure in the space group $R\bar{3}m$. Selected crystallographic data are given in Table 5.30. Besides, Otey and LeDoux (1967) have identified an oxide fluoride of the composition $U_3O_5F_8$ and suggested the existence of an intermediate, $U_2O_3F_6$ compound.

Hexavalent oxide fluoride complexes

There is a large variability in the stoichiometry of the very large number of reported hexavalent oxide fluorides: M^IUOF_5, $M^I(UO_2)_2F_5$, $M^IUO_2F_3$, $M^I_2UO_2F_4$, $M^I_3UO_2F_5$, $M^I_3(UO_2)F_3$, $M^I_3(UO_2)_2F_7$, $M^I_4(UO_2)_2F_8$, $M^I_5(UO_2)F_9$ (where M^I is usually an alkali metal ion), $M^{II}(UO_2)F_4$ (where M^{II} = Ca, Pb, Cu, Zn, or Cd) and $M^{II}(UO_2)_2F_6$ (where M^{II} = Sr, Ba, or Mg) (Freestone and Holloway, 1991). Many of the compounds were identified from phase diagram investigations. The complexes of the M^IUOF_5-type (M = K, Rb, Cs, NH_4) have been prepared by interaction of UOF_4 with the appropriate MF fluoride in liquid sulfur dioxide or anhydrous HF (Joubert and Bougon, 1975; Joubert *et al.*, 1978a,b). Hydrated complexes of the $M^{II}(UO_2)F_4 \cdot 4H_2O$ (M^{II} = Zn, Cd, Cu, Mn, Co, or Ni) were obtained by crystallization from aqueous solutions. A number of fluoro-oxalato compounds of the $[UO_2F(C_2O_4)_2(H_2O)]^{3-}$ and $[UO_2F_3(C_2O_4)(H_2O)]^{3-}$ types with alkali metals, ammonium, and guanidinium have been reported by Chernyayev (1966) and Shchelokov and Belomestnykh (1968a,b). Fluoro-oxalato compounds of the types $M_2[UO_2F_2(C_2O_4)]$, $M_4[UO_2F_2(C_2O_4)_2]$, and $M_2[(UO_2)_2F_4(C_2O_4)]$ (where M = Rb or K) are obtained by mixing of saturated solutions of $H[UO_2F_3] \cdot H_2O$ with alkali metal oxalates in different mole ratios (Chakravorti *et al.*, 1978). Some crystallographic data and IR spectral bands are collected in Table 5.30.

Numerous hydrated and anhydrous uranyl fluoro compounds have been obtained from aqueous solutions by varying the preparation conditions with a given alkali metal or organic base cation (Brown, 1968; Bacher and Jacob, 1980), e.g. $CsUO_2F_3$, $CsUO_2F_3 \cdot H_2O$, $NaUO_2F_3 \cdot xH_2O$ (x = 2 and 4), $CsUO_2F_4 \cdot H_2O$, $M_3UO_2F_5$ (M = Na, K, Rb, Cs, NH_4), $M_4(UO)_2F_5 \cdot 2H_2O$ (M = K, R, Cs), $M^I(UO_2)_2F_5 \cdot xH_2O$, $M^IUO_2F_3 \cdot xH_2O$ and $M^I(UO_2)_3F_7 \cdot xH_2O$ (where M^I is an organic base and x varies from 0 to 6). The MF/UO_2F_2 ratio in aqueous solutions has a significant influence on the stoichiometry of the complexes obtained. With a large excess of MF one usually obtains the $M_3UO_2F_5$ type of complexes. When the ratio is less than 3 one obtains di- or polynuclear complexes. The compounds obtained using the preparative methods described above can be rationalized from information on the equilibrium constants of the complexes present (cf. Section 5.9).

In $CsUOF_5$, the fluorine and oxygen atoms form a pseudo-octahedral surrounding of the uranium atom. In the other $MUOF_5$ (M = NH_4, K or Rb) oxide fluorides, uranium is eight coordinated with dodecahedral coordination geometry. The structure consists of chains formed by surface sharing of individual

dodecahedra through bridging fluoride ligands. (Joubert *et al.*, 1978a,b). Some structural details are also available for other hexavalent oxide fluoride complexes (see Table 5.30).

(*iii*) *Uranium hexachloride*

Uranium hexachloride may be obtained by thermal decomposition of UCl_5 at 120–150°C *in vacuo*. The green UCl_6 crystals are collected on a cold finger and purified from contaminating UCl_5 by sublimation in vacuum at 75–100°C or distillation in a stream of an inert gas at a low pressure. On laboratory scale it is best prepared by condensing an excess of BCl_3 onto UF_6 at –196°C and allowing the vessel with the compounds to warm up slowly. It is not necessary to purify the product by sublimation since the by-products are volatile at room temperatures (Brown, 1979).

UCl_6 is an extremely moisture-sensitive, black to dark green crystalline solid. The compound is reported to melt at (177.5 ± 2.5)°C, but it readily liberates chlorine at temperatures higher than ≈120°C. It reacts violently with water to form uranyl(VI) solutions. Hydrogen reduces UCl_6 to UCl_4 at 250°C. Reaction of UCl_6 with anhydrous liquid hydrogen fluoride or UF_6 converts it to UF_4 and UF_5, respectively. The hexachloride is slightly soluble in carbon tetrachloride, liquid chlorine, methyl chloride, isobutyl bromide, and thionyl chloride. On prolonged storage in carbon tetrachloride, it decomposes forming crystalline red-brown, volatile U_2Cl_{10}. The decomposition reaction proceeds much faster in 1,2-dichloroethane and methylene dichloride. The reduction in the last solvent appears to be photochemically mediated. Interaction with chlorides such as NH_4Cl, $(C_6H_5)_4AsCl$, and $(CH_3)_4NCl$ yields the appropriate $MUCl_6$ hexachloorouranate(v) compounds.

UCl_6 has hexagonal symmetry, space group D_{3d}^3; $P\bar{3}m1$ (Zachariasen, 1948f). The structure has been refined with neutron and X-ray powder diffraction data by Taylor and Wilson (1974b) and can be described as a hexagonal close packing of chlorine atoms with uranium atoms in one-sixth of the octahedral holes. The chlorine atoms form an almost regular octahedron around the U(1) located at 0,0,0 while the geometry around U(2) at 1/3, 2/3, 0.518 is slightly distorted (Fig. 5.48).

The absorption spectra for UCl_6 in the solid state, vapor phase, and solutions in perfluoroheptane in the UV–Vis range have been reported and analyzed (Brown, 1979). Charge transfer bands were observed at 17000 and 20800 cm^{-1} for solid UCl_6 and at 21000 and 20800 cm^{-1} in the vapor phase. Some X-ray and physical data of the compound are summarized in Table 5.30.

(*iv*) *Uranium(VI) dioxide dichloride, UO_2Cl_2, and related compounds*

Uranium(VI) dioxide dichloride (*uranyl chloride*)

Since the literature on uranium(VI) dioxide dichloride is very extensive (Brown, 1979), the results of investigations presented in this section must necessarily be incomplete. The most attractive methods for the preparation of UO_2Cl_2 involve

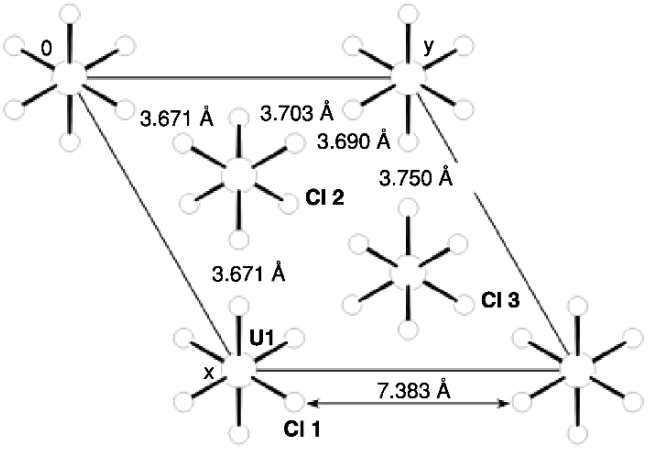

Fig. 5.48 *View of the crystal packing of* UCl_6 (*distances are taken from Taylor and Wilson*, 1974*b*).

the oxidation of UCl_4 at temperatures between 300 to about 350°C or the dehydration of $UO_2Cl_2 \cdot H_2O$. The last method may readily be performed by heating in a stream of gaseous HCl or HCl + Cl_2 mixtures at 400–450°C. UO_2Cl_2 may be also obtained by electrochemical oxidation of uranium in an acetonitrile solution of Cl_2 in the presence of oxygen. This solution of UO_2Cl_2 may be used for the preparation of numerous adducts, e.g. $(Et_4N)_2UO_2Cl_4$ (Kumar and Tuck, 1984).

The anhydrous compound is a yellow, hygroscopic solid, readily soluble in a number of organic solvents, in many cases with complex formation. It is not soluble in non-polar organic solvents. Thermal decomposition in air leads to formation of a mixture of α-UO_3 and $UO_{2.9}$ at 460°C and to U_3O_8 at higher temperature. The compound decomposes to UO_2 and Cl_2 on heating in a nitrogen atmosphere. Vacuum thermal decomposition results first in the formation of an intermediate state $(UO_2)_2Cl_3$ and next, at 450°C, of a mixture of UO_3 and U_3O_8. UO_2Cl_2 may be converted to $UOCl_3$ by reaction with UCl_4 *in vacuo* at 370°C.

The reaction of UO_2Cl_2 solutions with a variety of ligands in both aqueous and non-aqueous media results in the formation of a large number of stable compounds of different UO_2Cl_2:ligand stoichiometry, e.g.:

- (1:1): with methyl cyanide, methylmalonamide, benzophenone; acetyl chloride, 1,10-phenantroline and *N*,*N*,*N*′,*N*′- teramethyl-α,α-dimethylmalonamide;
- (1:1,5): with *N*,*N*,*N*′,*N*′-tetramethylmalonamide, *N*,*N*,*N*′,*N*′-tetramethylglutaramide;
- (1:2): aniline, pyridine, ethanol, acetic anhydride, diethyl ether, acet-*p*-phenetidine, 1,10-phenantroline, dimethylurea, tetramethylurea,

trialkyl-phosphine, triaryl-phosphine, 2,2′-bipyridine, and 4-methoxoy-pyridine-*N*-oxide;
- (1:3): with 4-methylpyridine-*N*-oxide, *N*,*N*-dimethylformamide, ethylurea, diethylurea;
- (1:4): hydrazine, urea, 1,3-dimethylurea and 4-chloropyridine-*N*-oxide etc.

A number of uranyl chloro-complexes have been identified during investigations of the $MCl–UO_2Cl_2$, $CuCl_2–UO_2Cl_2$, and $NaCl–KCl–UO_2Cl_2$ phase diagrams (where M = Li, Na, K, Rb, or Cs) (Brown, 1979).

UO_2Cl_2 has orthorhombic symmetry, space group *Pnma* (see Table 5.30). Uranium has pentagonal bipyramidal coordination geometry with two uranyl oxygen atoms at the apices; there are four chlorine atoms and one oxygen atom in the equatorial plane, the latter an "yl" oxygen atom from neighbouring uranium. The pentagons form chains parallel to the *b* axis by sharing Cl–Cl edges (Taylor and Wilson, 1973b). Electronic absorption spectra in the solid state and solutions in non-aqueous media and luminescence spectra have been discussed in numerous papers (Brown, 1979; Wells, 1990). Some physical data are listed in Table 5.30.

Uranyl(VI) chloride hydrates and hydroxide chlorides

The following compounds have been identified $UO_2Cl_2 \cdot 3H_2O$, $UO_2Cl_2 \cdot H_2O$, $[(UO_2)_2(OH)_2Cl_2(H_2O)_4]$, $[(UO_2)_4O_2(OH)_2Cl_2(H_2O)_6]$, and $4UO_3 \cdot HCl \cdot 8H_2O$ (Brown, 1979). The tri- and monohydrate are most conveniently prepared by slow evaporation from concentrated uranyl(VI) hydrochloric acid solutions over KOH and P_2O_5, or from an aqueous solution in dry air at room temperature; they form yellow hygroscopic powders. The hydrates are readily soluble in water and in various organic solvents such as ether, acetone, ethyl acetate, and a number of alcohols. The trihydrate may be dehydrated to $UO_2Cl_2 \cdot H_2O$ and then readily converted to the anhydrous salt by heating in a stream of dry hydrogen chloride or a $HCl + Cl_2$ mixture. When heated in an inert atmosphere, it is converted at about 220°C to impure UO_2Cl_2 and at temperatures above 400°C to U_3O_8 (Brown, 1979). $UO_2Cl_2 \cdot H_2O$ reacts with $P(C_6H_5)_4Cl$ by refluxing in a thionyl chloride solution to give $[P(C_6H_5)_4]UOCl_5$ on cooling. With smaller cations reductive chlorination to hexachlorouranates(V) occurs.

$UO_2Cl_2 \cdot H_2O$ and $UO_2Cl_2 \cdot 3H_2O$ have monoclinic ($P2_1/m$) and orthorhombic ($Pn2_1a$) symmetry, respectively. Neutron diffraction studies of $UO_2Cl_2 \cdot H_2O$ (Taylor and Wilson, 1974c) show that uranium has the common pentagonal bipyramidal coordination geometry with four chlorine and one water oxygen atoms in the equatorial plane. Infinite chains similar to those in UO_2Cl_2 are formed by sharing two Cl–Cl edges (Table 5.30).

Three basic hydroxide chlorides are observed in the $UO_3–HCl–H_2O$ phase diagram at 25°C, but only one, $[(UO_2)_2(OH)_2Cl_2(H_2O)_4]$, is reported to be congruently soluble (Prins and Cordfunke, 1975). The compound may be easily obtained as hydrolysis product of a UO_2Cl_2 solution prepared by dissolution of

UO_3 in concentrated HCl (Åberg, 1969). Thermal decomposition of the compound in air leads first to the hemi-hydrate $UO_2(OH)Cl \cdot 0.5H_2O$ at 80–120°C, from which the nearly anhydrous salt, $UO_2(OH)Cl$ is formed at about 250°C. The compound crystallizes with monoclinic symmetry (see Table 5.30) and has a structure in which two linear uranyl units are linked through a double OH bridge, the remaining coordination sites are occupied by one Cl atom and four O atoms from two H_2O molecules, resulting in an irregular planar pentagon (Åberg, 1969).

(*v*) *Uranium*(VI) *oxochloro complexes*

The typical representatives of this group have the composition: $M^{I}UOCl_5$ (e.g. M = $P(C_6H_5)_4$, $M^{I}_2UO_2Cl_4$ (e.g. M = Li, Na, K, Rb Cs, NH_4, $P(C_6H_5)_4$, $N(C_2H_5)_4$, and others), $M^{I}_2UO_2Cl_4 \cdot 2H_2O$ (M = Li, Na, K, Rb, or NH_4), $M^{II}UO_2Cl_4 \cdot 2H_2O$ (M = Mg, Ca, Sr, Ba, Zn, Zn, Cd, and others), $M^{I}UO_2Cl_3$ (e.g. M = $P(C_6H_5)_4$, $N(C_{10}H_{21})_4$, and others), $M^{I}(UO_2)_2Cl_5$ (e.g. M = Na, K, Rb, Cs, or NH_4), $M^{I}_2U_2O_5Cl_4$ (M = Na, K, Rb, or Cs), $M^{I}_2U_2O_5Cl_4 \cdot xH_2O$ (M = Na, K, Rb or Cs), $KNa_2(UO_2)_2Cl_7$, KUO_3Cl, $K_2U_3O_8Cl_4$, and $K_2(UO_2)_xCl_{2x+2}$ ($x = 2$, 3, or 4). The compounds have been prepared by variety of methods (Brown, 1979), most commonly by crystallization from organic solvents (methyl cyanide or ethanol solutions) or aqueous hydrochloric acid solutions of the corresponding chlorides, as well as by solid-state reactions. Some of them are air-sensitive (e.g. $[P(C_6H_5)_4]UOCl_6$) or are hydrated on exposure to moist air ($M^{I}_2UO_2Cl_4$ where M = Li to Rb and NH_4); they are soluble in some organic solvents.

Structure data (Brown, 1979) are available for a number of the compounds (see Table 5.30). In $M^{I}_2UO_2Cl_4$ there are discrete $UO_2Cl_4^{2-}$ units with linear O–U–O groups. The structure of $M_2U_2O_5Cl_4 \cdot 2H_2O$ (M = Rb or Cs) consists of discrete planar tetranuclear anions, $[(UO_2)_4O_2Cl_8(H_2O)_2]^{4-}$, in which the uranyl groups in the equatorial plane are linked by oxygen and chloride bridges. In the structure of $[N(C_6H_5CH_2)(CH_3)_3]_4[UO_2Cl_3O]_2$ there are puckered sheets of binuclear $[Cl_3O_2U\text{-}(\mu\text{-}O_2)\text{-}UO_2Cl_3]^{4-}$ anions parallel to (001), which are interleaved by the cations. The anion is built of two identical, distorted pentagonal bipyramides sharing the peroxo-group as a common edge. Oxochlorouranates of the formula $Ln_3UO_6Cl_3$ (Ln = La, Pr, or Nd) were prepared by heating stoichiometric amounts of $LnOCl/Ln_2O_3/U_3O_8$ (Ln = La or Nd) or $PrOCl/Pr_6O_{11}/U_3O_8$ in silica ampoules at 800–1000°C in an excess of chlorine (Henche *et al*., 1993). The crystals were investigated by X-ray diffraction methods (see Table 5.30) and high-resolution electron microscopy.

(*vi*) *Uranium*(VI) *perchlorates and related compounds*

The synthesis and characterization of uranyl(VI) perchlorate, $UO_2(ClO_4)_2$ and its hydrates $UO_2(ClO_4)_2 \cdot xH_2O$ ($x = 0$, 1, 3, 5, or 7) have been investigated by a number of authors (Brown, 1979). The heptahydrate has been obtained by

crystallization from aqueous solution at room temperatures. Vacuum drying of the compound at that temperature leads to the pentahydrate, and vacuum dehydration over sulfuric acid to the trihydrate. Further vacuum drying converts the latter to the monohydrate; in the temperature range 100–140°C anhydrous perchlorate $UO_2(ClO_4)_2$ is formed (Vdovenko *et al.*, 1963). All of the compounds are readily soluble in water and polar organic solvents, in many cases with the formation of stable uranyl(VI) perchlorate complexes. The interaction with oxygen and nitrogen donor ligands leads to the formation of the following types of complexes:

$UO_2(ClO_4)_2$5L: where L = pyridine, pyridine-*N*-oxide, antipyrene, dimethylsulfoxide, dimethylselenoxide, dimethylformamide, diphenylsulfoxide, thioxane oxide, urea, 1,3-dimethylurea, 1,3-diethylurea, hexamethylphosphoramide.

$UO_2(ClO_4)_2$4L: where L = trimethylphosphine oxide, triphenylphosphine oxide, tripropylphosphine oxide.

$UO_2(ClO_4)_2$3L: where L = octamethylphosphoramide, camphor, methyl cyanide, nonamethylimido-diphosphoramide.

$UO_2(ClO_4)_2$2L: where L = tributylphosphate, tributylphosphine oxide, nitromethane, dibutyl ether.

$UO_2(ClO_4)_4 \cdot 7H_2O$ crystallizes in the orthorhombic space group $Pca2_1$ The structure consists of $[UO_2(OH_2)_5]^{2+}$ and ClO_4^- ions, with two additional water of solvation. The crystal structure is held together by an extensive network of hydrogen bonds.The coordination polyhedron is a distorted pentagonal bipyramid (Alcock and Esperas, 1977). Some crystallographic and infrared data are are listed in Table 5.30.

(*vii*) *Uranium*(VI) *oxide bromides and complex oxobromo compounds*

Uranyl(VI) *bromide and related complexes*

One of the most convenient methods for the preparation of UO_2Br_2 is the reaction of anhydrous UBr_4 with oxygen at a carefully controlled temperature in the range 150–160°C; at higher temperature, U_3O_8 is formed (Brown, 1979). An alternative method involves the electrochemical anodic oxidation of uranium in CH_3CN/Br_2 solution in the presence of dry oxygen. The resulting solution of UO_2Br_2 may also be used for the preparation of adducts by adding a two-fold excess of the appropriate ligand (Kumar and Tuck, 1984).

The compound is a bright red, hygroscopic solid which turns yellow on exposure to moisture. It is thermally unstable and appears to lose bromine slowly even at room temperature. The decomposition is complete within 48 h in an inert atmosphere at 350°C. UO_2Br_2 is extremely soluble in water and polar organic solvents. Numerous complex compounds have been prepared by reactions with a variety of ligands in anhydrous solvents, for example, of the following types: UO_2Br_2L (L = methyl cyanide), $UO_2Br_2$2L (L = acetic anhydride, ether, *N*,*N*–dimethylacetamide, antipyrine, *N*-methylacetanilide,

$(CH_3)_3PO$, $(C_2H_5)_3PO$, $(C_6H_5)_3PO$, etc), $UO_2Br_2 3L$ (L = dimethylformamide), $UO_2Br_2 4L$ (L = dimethylsulfoxide) $UO_2Br_2 \cdot xNH_3$ (x = 2, 3, and 4), $UO_2Br_4 \cdot (LH)_2$ (L = 2,2′-dipyridine,1,10-phenanthroline) and $(Et_4N)_2UO_2Br_4$. In addition, a number of oxo-tetrabromo complexes of the $M_2UO_2Br_4$ (M = Cs, $P(C_6H_5)_3CH_3$, $P(C_6H_5)_3H$, $P(CH_3)_3H$, $P(C_6H_5)_3C_6H_5CH_2$, etc.) and $M_2UO_2Br_4 \cdot 2H_2O$ (M = NH_4, K, or Rb) types have been obtained by reaction of UO_2Br_2 with the appropriate ligands in HBr or in anhydrous organic solvents (Brown, 1979, Kumar and Tuck, 1984).

Uranyl(VI) hydroxide bromide and bromide hydrates

A stable hydrate of the formula $UO_2Br_2 \cdot 3H_2O$ is obtained in the form of dark yellow needles by crystallization from an aqueous solution of HBr and UO_2Br_2, followed by vacuum drying (Peterson, 1961). The dehydration of the trihydrate over phosphoric acid leads to the formation of the monohydrate $UO_2Br_2 \cdot H_2O$. The hydrates may be also obtained by other methods (Brown, 1979). Crystallization of UO_2Br_2 from acid-deficient solutions leads to the formation of $UO_2(OH)Br \cdot 2H_2O$ (alternative formulations are: $[U_2O_5(H_2O)]Br_2 \cdot 4H_2O$ or $[UO_2(OH)_2UO_2]Br_2 \cdot 4H_2O$). The compound is isostructural with its chloride analog $[UO_2(OH)_2UO_2]Cl_2 \cdot 4H_2O$; it is converted to $UO_2(OH)Br$ when heated at 200°C.

The hydrates are readily soluble in water and numerous organic solvents like ethanol, ether, amyl alcohol, etc. $M_2UO_3Br_2$ (M = NH_3 or K) is formed by reacting the monohydrate with ammonia gas or a stiochiometric quantity of KOH (Brown, 1979). According to Peterson (1961) the trihydrate is stable in dry air and may lose one molecule of water at 60°C without decomposition.

Uranium(VI) oxobromo complexes

The synthesis and characterization of a large number of complex oxobromo compounds containing uranium(VI) have been summarized by Brown (1979). Oxo-tetrabromo complexes of the $M_2UO_2Br_4 \cdot 2H_2O$ type (M = NH_4, Na, K, or Rb) were prepared from aqueous or alcoholic HBr solutions of uranyl bromide by precipitation with appropriate MBr. The anhydrous analogs were obtained by heating at 120°C in an inert atmosphere. With large cations, for example Cs^+ or pyridinium, only anhydrous complexes of the $M_2UO_2Br_4$-type are formed.

Other anhydrous complexes of this type were prepared by reactions of uranyl bromide solutions in ethanol or methyl cyanide with various phosphonium bromides (e.g. $P(C_6H_5)_3C_4H_9Br$, $P(C_6H_5)_3HBr$, $P(C_6H_5)_3C_6H_5CH_2)Br$, $P(C_2H_5)_3HBr$, and $P(C_3H_7)_3HBr$) as well as with $N(C_2H_5)_4Br$ (in ethanol), $N(CH_3)_4Br$ (in a C_2H_5OH–HBr mixture), choline bromide, $(C_5H_{14}NO)Br$ (in methanol), and acetylcholine bromide, $(C_7H_{16}NO_2)Br$ (in methanol). The reaction of UO_2Br_2 with tetradecylammonium bromide in anhydrous benzene results in the formation of a viscous liquid of the $[N(C_{10}H_{21})_4]UO_2Br_3$. In the presence of traces of water in benzene compound converts into the oxo-tetrabromo complex.

The oxobromo complexes are yellow and readily soluble in aqueous solutions; those with organic cations also in anhydrous solvents such as acetone, benzene, methyl cyanide, and nitromethane. Structure investigations reveal a distorted octahedral geometry in complexes with M = Cs, $N(CH_3)_4$, $N(C_3H_7)_4$, and $C_7H_{16}NO_2$, where the U–O and U–Br bond distances range from 1.70 to 1.90 and 2.78 to 2.86 Å, respectively. For structural data, see Table 5.30. Extensive information on the infrared and Raman spectra is also available (Brown, 1979). On the basis of these data the observed frequencies for various oxotetrabromo complexes can be assigned as follows:

IR (cm^{-1}): ν(U–O, asym. stretch.) = 895–934; ν(O–U–O deformation) = 243–263; ν(U–Br stetch.) = 160–180; Raman (cm^{-1}): ν(U–O sym. stretch.) = 826–835, ν(U–O–Br bend.) = 190–198, ν(U–Br stretch.) = 167–172 ν(U–Br bending mode) = 81–83. The fluorescence spectrum of $Cs_2UO_2Br_4$ measured at 14.3 K reveals the existence of two sites of different symmetry, which has been supported by the observed differences in the fluorescence relaxation time. The solution spectra of $[N(C_{10}H_{21})_4]UO_2Br_3$ and $[N(C_{10}H_{21})_4]UO_2Br_4$ in anhydrous benzene have absorption bands at 508, 491, 483, 447, and 431 nm and at 497, 480, 464, and 449 nm, respectively. For $[P(C_6H_5)_3H]_2 \cdot UO_2Br_3$ in methyl cyanide solution these bands appear at 19800, 20080, 20790, 21550, 20220, and 22880 cm^{-1}. As one should expect, the absorption bands of the solid state reflectance spectra of $[C_5H_{14}NO]_2UO_2Br_4$ and $[C_7H_{16}NO_2]UO_2Br_4$ are somewhat shifted towards longer wavelengths as compared to their chloro analogs.

The reactions of uranyl bromide with various metal bromides in aqueous HBr lead to the formation of the following hydrated bromo compounds:

$MUO_2Br_4 \cdot xH_2O$ (M = Sr, $x = 3$; M = Zn, Mg, $x = 4$; M = Ca, $x = 8$);
$MUO_2Br_5 \cdot xH_2O$ (M = La, $x = 3$; M = Y, $x = 5$);
$MUO_2Br_6 \cdot 4H_2O$ (M = Ce or Th);
$MU_3O_8Br_5 \cdot xH_2O$ (M = Co, $x = 12$; M = Sc, $x = 8$), and
$Be_2UO_2Br_6 \cdot 8H_2O$, $Mn_3UO_2Br_8 \cdot 11H_2O$, and $HgU_3O_8Br_4 \cdot 4H_2O$

The complexes may be dehydrated in an oxygen atmosphere at about 200°C. $LaUO_2Br_5$, YUO_2Br_5, and $CeUO_2Br_5$ are converted to $LaUO_2(O_2)Br$, $YUO_2(O_2)Br$, and $LaUO_2(O_2)Br$, respectively, at 290–305°C. Decomposition at high temperature results in the formation of appropriate uranates, $CaUO_4$, Mn_3UO_6, $Co_2U_6O_{21}$, and HgU_3O_{10}, etc. The heating of $K_2UO_2Br_4$ at 250°C and $(NH_4)_2K_2UO_2Br_4$ at 250–350°C in an oxygen atmosphere results in the formation of $K_2UO_3Br_2$ and $(NH_4)_2UO_3Br_2$, respectively. $K_2UO_3Br_2$ may be also prepared by interaction of uranyl bromide monohydrate with KOH, or by heating K_2UO_4 with gaseous hydrogen bromide, whereas $(NH_4)_2UO_3Br_2$ is obtained by action of gaseous NH_3 on $UO_2Br_2 \cdot H_2O$. Compounds of the composition $K_2U_2O_6Br_2$ and $K_2U_3O_9Br_2$ have been prepared by heating K_2UO_4 or $K_2U_3O_{10}$ with gaseous HBr, respectively. A phase of the composition $K_xUO_3Br_x$ ($x = 0.9$) is obtained when UO_3 and KBr are heated

at 300–550°C *in vacuo*. The compound is isostructural with $K_xUO_3Cl_x$ (see Table 5.30).

The interaction of $M_2UO_2Br_4 \cdot 2H_2O$ (M = K or Rb) with $UO_2(OH)_2$ results in the formation of compounds containing the tetranuclear unit $M_2[(UO_2)_4O_2(OH)_2Br_4(H_2O)_4] \cdot 2H_2O$. The complexes lose four H_2O molecules in an inert atmosphere at 60°C and form $M_2U_4O_{11}Br_4$ at ≈200°C. The compounds are triclinic ($P\bar{1}$) and isostructural with the chloro analogs (see Table 5.30).

(*viii*) *Uranium*(VI) *compounds with iodine*

$UI_4 \cdot 4$dmf is obtained by electrochemical oxidation of uranium anodes in *N*,*N*-dimethylformamide (dmf) (Kumar and Tuck, 1984). The preparation of an extremely unstable UO_2I_2 has been reported in a number of papers (Brown, 1979; du Preez and Zeelie, 1989). The compound has not been obtained in a pure form but relatively stable compounds, such as $UO_2I_2 \cdot 4$dmf (yellow, m.p. = 156°C; dmf = dimethylformamide), $UO_2I_2 \cdot 2$tppo (orange red, m.p. = 268°C; tppo = triphenylphosphine oxide), $UO_2I_2 \cdot 2$tmu (orange, tmu = *N*,*N*,*N*′,*N*′-tetramethylurea), $UO_2I_2 \cdot 5CO(NH_2)_2 \cdot H_2O$ (orange-red), $UO_2I_2 \cdot 2$hmpa (orange, hmpa = hexamethylphosphoric triamide), $UO_2I_2 \cdot xNH_3$ ($x = 2$ or 3), $UO_2I_2 \cdot 2$tbso (yellow-green, tbso = di-*tert*-butyl sulfoxide), $UO_2I_2 \cdot 2$dmeu (dmeu = *N*,*N*′-dimethylethylene urea), $(PPh_4)_2UO_2I_4$ (black), $UO_2I_2 \cdot 2Et_2O$ (decomposes at room temperature by evolving iodine), may be separated from solutions in water and various organic solvents (for example, ether, methanol, ethanol, amyl alcohol, methyl acetate, ethyl acetate, pyridine) (Brown, 1989; du Preez and Zeelie, 1989). A red uranyl(VI) iodo compound, $[P(C_6H_5)_3C_4H_9]_2UO_2I_4$, has been obtained by interaction of uranyl(VI) iodide with phosphonium iodide in a methyl cyanide solution (Day and Venanzi, 1966).

The addition of soluble iodides to uranyl nitrate solutions at room temperatures results in the formation of the uranyl(VI) iodide dihydrate, $UO_2(IO_3)_2 \cdot 2H_2O$. The compound is converted to α-$UO_2(IO_3)_2 \cdot H_2O$ when UO_2NO_3 and iodic acid are mixed in boiling nitric acid. β-$UO_2(IO_3)_2 \cdot H_2O$ is formed by recrystallization from water in the absence of acid. The compound $(UO_2)_2I_2O_9$ has been obtained by addition of potassium periodate to a cold solution of $UO_2(NO)_2$. The preparation of a number of uranium(VI) iodato and periodato complexes has also been reported: $KUO_2(IO_3)_3 \cdot 3H_2O$, $(KIO_4)_2(UO_2)_2O_2 \cdot 5H_2O$, $[Co(NH_3)_6][(UO_2)_2(IO_3)_7] \cdot 10H_2O$, $K_2I_2O_5(UO_2)_2$, $H(UO_2)_2IO_6 \cdot 8H_2O$, $NaH_2UO_2IO_6 \cdot 7H_2O$, $Ba(H_2UO_2IO_6)_2 \cdot xH_2O$ (Brown, 1979).

(*ix*) *Mixed halogeno-complexes*

Mixed uranyl(VI) halogeno-compounds $M^I_2UO_2Cl_2Br_2$ (M^I = NH_4, Na, K, or Cs), $Cs_2UO_2X_3Y$ (X and Y = Cl or Br), $[N(C_{10}H_{21})_4]_2[UO_2X_3I]$ (where X = Cl or Br), and $[P(C_6H_5)_3C_4H_9]_2[UO_2Cl_2Br_2]$, $[P(C_6H_5)_3C_4H_9]_2[UO_2Br_2I_2]$ have

been obtained by interaction of uranyl halides with appropriate univalent bromides or iodides in aqueous HBr solutions, or in anhydrous organic solvents such as benzene and methyl cyanide. Alternative routes to these and similar mixed halogeno complexes have been also reported (Brown, 1968, 1979). $Cs_2UO_2BrCl_3$ and $Cs_2UO_2Br_3Cl$ (Ellert *et al*., 1965) have been obtained by varying the HBr concentration in the interaction between CsBr and $UO_2Cl_2 \cdot H_2O$ The preparation of the dihydrate $K_2UO_2Br_2Cl_2 \cdot 2H_2O$ has been achieved by crystallization from 20% HCl containing KBr and UO_2Cl. Dehydration of the compound in an inert atmosphere at 110°C leads to $K_2UO_2Br_2Cl_2$ (Lucas, 1964). Dihydrates of the composition $M_2UO_2Br_{4-x}Cl_x$ (M = NH_4 or Rb; x = 1, 2, or 3) have also been isolated (Kharitonov *et al*., 1967).

Complexes containing alkali metal cations are soluble in water and aqueous acetic acid solution; those containing phosphonium or tetralkylammonium cations are soluble in numerous non-aqueous solvents like methyl cyanide, benzene, and ethanol. In water, hydrolysis takes place. Dehydration of the compound in an inert atmosphere at ≈110°C leads to the anhydrous complexes (Lucas, 1964).

X-ray powder diffraction data are available for $Cs_2UO_2Cl_2Br_2$, $Cs_2UO_2BrCl_3$, $Cs_2UO_2Br_3Cl$ (Ellert *et al*., 1965), $K_2UO_2Cl_2Br_2$, $K_2UO_2Br_2Cl_2 \cdot 2H_2O$, and $K_2U_2O_5Cl_2Br_2$ (Lucas, 1964). The ν(U–O) asymmetric stretching vibrations occur at 905–910 cm^{-1} for $M_2UO_2Br_{4-x}Cl_x \cdot 2H_2O$ (M = NH_4, K or Rb) and at 907–922 cm^{-1} for various anhydrous complexes. In the IR spectrum of $[P(C_6H_5)_4]UOBr_4Cl$, they appear at 838 cm^{-1}.

The metal–halogen stretching frequencies have been reported for: $[P(C_6H_5)_3C_4H_9]_2UO_2Br_2Cl_2$, ν(U–Cl) = 260 cm^{-1}; $[N(C_{10}H_{21})_4]_2UO_2BrCl_3$, ν(U–Cl) = 255 cm^{-1}, ν(U–Br) = 165 cm^{-1}; $[N(C_{10}H_{21})_4]_2UO_2Cl_3I$, ν(U–Cl) = 236 cm^{-1}, and ν(U–I) = 135 cm^{-1}, with the uranyl deformation mode at 261 cm^{-1} (Brown, 1979). The first high-intensity bands in the visible spectra of $[N(C_{10}H_{21})_4]_2UO_2Cl_3I$, and $[N(C_{10}H_{21})_4]_2UO_2BrCl_2I$ in benzene solutions, were recorded at about 20000 cm^{-1} (Vdovenko *et al*., 1969).

5.8 CHEMICAL BONDING IN URANIUM COMPOUNDS

5.8.1 U(III) and U(IV) compounds

In general, the discussion of chemical bonding in U(III) and U(IV) compounds is related to metal–organic complexes as discussed in Chapters 25 and 26. A recent review of the organometallic chemistry of lanthanides and actinides has been given by Hyeon *et al*. (2005). An early example is given in a study by Bursten and Strittmatter (1987) that discussed the bonding in $[Cp_3UCO]$ and $[Cp_3UCO]^+$, where Cp is cyclopentadiene, η^5-C_5H_5. They suggested an extensive U(III) 5f–CO π-back-bonding, an effect that decreases significantly on oxidation to U(IV). The coordination of dinitrogen in $[\{U(NN'_3)\}_2(\mu_2{-}\eta^2{:}\eta^2{-}N_2)]$, where NN'_3 is $N(CH_2CH_2NSiBu^tMe_2)_3$, was studied by Roussel and Scott (1998). The end-on

coordination is consistent with U → N back-bonding, but the authors suggest that the effect is minor. The role of the 5f orbitals in back-bonding has also been studied by comparison with the bonding in lanthanide compounds in oxidation states 3+ and 4+. A typical example is given in a study by Berthet *et al.* (2002) of the selective complexation of U(III) over Ce(III) and Nd(III) in 2,2′:6,2″-terpyridine complexes. This ligand forms much stronger complexes with uranium than cerium in solution. The authors probed the possible reasons behind this by determination of the X-ray crystal structure of the complexes $[MI_2(terpy)_2]I$, M = Ce, Nd, $[CeI_2(terpy)_2(H_2O)]I$, and $[UI_2(terpy)_2(pyridine)]I$. They suggest that the shortening of the average M–N distance by 0.05 Å in the uranium complex as compared to that of cerium might be a result of a stronger π back-bonding interaction between uranium and the terpyridyl ligand. The evidence for back-bonding is indirect and more direct information is necessary to draw definite conclusions, e.g. Di Bella *et al.* (1996) point out, based on electronic structure calculations and photoelectron spectroscopic data, that the bonding in isoleptic 4f and 5f M(III) bis-(cyclopentadienyl) is very similar. Experimental data and quantum chemical calculations on different model systems indicate 5f orbital participation in chemical bonding, but the extent of this and its chemical effects are far from clear. A detailed discussion of the quantum chemistry of uranium and other actinides is given in Chapter 17.

Roos and Gagliardi have used quantum chemical methods to explore the stability and possible existence of compounds with U–U bonds, similar to those found for some d-transition elements, e.g. Cr, Mo, W, Tc and Re. They predicted stable diatomic U_2 with a quintuple U–U bond and a bond distance of 2.43 Å (Gagliardi and Roos, 2005a). Gagliardi *et al.*, (2005) found that also U_2^{2+} is a stable ion with several low-lying electronic states, all with U–U bond distances around 2.30 Å.

Compounds containing U–U bonds have been identified by matrix isolation techniques; H_2U–UH_2 by Souter *et al.* (1997) and O-U–U-O by Gorokhov *et al.* (1974). In their most recent paper Gagliardi and Roos (2005b) have studied the stability and chemical bonding in U_2Cl_6, $U_2Cl_6^{2-}$, $U_2(OCHO)_4$, $U_2(OCHO)_6^{2-}$, and $U_2(OCHO)_4Cl_2^{2-}$. It seems unlikely that compounds where the formal oxidation state of uranium is +2 can be prepared, but those with the oxidation state of +3 seem more probable. $U_2Cl_6^{2-}$, has a similar structure and bonding as $Re_2Cl_6^{2-}$, with the eclipsed conformation as the most stable one. The weakest bond is found in $U_2(OCHO)_4Cl_2^{2-}$, where the U–U distance is 2.80 Å.

5.8.2 UF_5 and UF_6 compounds

The bonding in these compounds has been discussed by Rosén and Fricke (1979), Wadt and Hay, (1979), and Onoe *et al.* (1993, 1997); these compounds can presumably be used as models for the bonding also in other uranium(V) and uranium(VI) halides. The authors point out that there is extensive involvement of 5f, 6p, and 6d orbitals in the U–F bonds, the orbital population in the 7s and 7p orbitals is smaller, and relativistic effects are of great importance for the

chemical bonding. The participation of the 5f orbitals in the bonding explains the fluxional geometry of UF_5 between C_{4v} and D_{3h} (Onoe *et al.*, 1997).

5.8.3 Uranyl(V) and uranyl(VI) compounds

The linear "yl"-ions in aqueous systems are unique for the actinide elements; in other "yl"-ions, such as VO_2^+, MoO_2^{2+}, and WO_2^{2+}, the oxygen atoms are mutually *cis*, thereby maximizing $(p_\pi) \rightarrow M(d_\pi)$ bonding. A linear MO_2^{2+} group is known in compounds of technetium, rhenium, ruthenium, and osmium, but the corresponding aqua-ions are unknown (a recent discussion of the electronic structure of these *trans*-dioxometal complexes is found in Hummel *et al.*, 2006). The short U(VI)–O_{yl} bond distance, approximately 1.75 Å, indicates a strong multiple uranium–oxygen bonding, one of σ and two of π character. The uranium–"yl" distance in UO_2^+ is somewhat longer due to the smaller effective charge of uranium (Vallet *et al.*, 2004a). The orbitals involved in the uranium–"yl"-oxygen bonds have been extensively discussed (see Denning, 1992; Kaltsyoannis, 2000; Matsika *et al.*, 2001 for a review); the MO diagram in Fig. 5.49 illustrates the bonding.

The bonding molecular orbitals are $\sigma_g^2\ \sigma_u^2\ \pi_g^4\ \pi_g^4$ with 5fδ and 5fφ as the lowest unoccupied orbitals. The bonding orbitals have mainly O 2p character and the uranyl(VI) ion can therefore be described as $O^{2-}{\equiv}U^{6+}{\equiv}O^{2-}$.

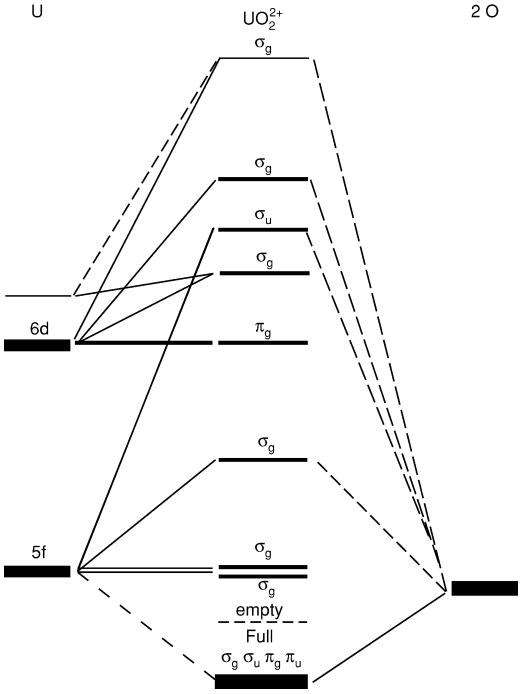

Fig. 5.49 *Schematic molecular orbital diagram for the uranyl(VI) ion.*

The nonbonding and antibonding orbitals have 5f and 6d character. The ordering of the bonding orbitals and the HOMO in UO_2^{2+} is not straightforward (de Jong *et al.*, 1999); Denning (1992) and later Kaltsyoannis (2000) suggested the order $\pi_g < \pi_u < \sigma_g << \sigma_u$, where σ_u is the highest occupied orbital. The significant energy gap between the σ_g and σ_u orbitals is traced to the filled–filled interactions between the semi-core 6p orbitals and the σ_u valence level, the 'pushing from below' mechanism. Triatomic UN_2 and UON^+ are isoelectronic with UO_2^{2+} and Pyykkö *et al.* (1994) suggested that these and other triatomic groups could have a significant stability. This was confirmed in experimental studies by Brown and Denning (1996) who prepared a number of stable compounds containing the linear –N≡U=N– and O=U=N– groups and discussed their chemical bonding. Kaltsyoannis (2000) made a more detailed study using density functional methods and concluded that the U–N bond is significantly more covalent than the U–O bond in UON^+ and UO_2^{2+} and that the uranium f-orbitals play a more important role than the d-orbitals in the metal to ligand bonding. He also pointed out that the U–N bond in iminato complexes is best described as a triple bond.

The previous correlation diagram can also be used to describe the bonding in UO_2^+, where the single 5f electron is located in one of the nonbonding 5fδ or 5fφ orbitals.

Tatsumi and Hoffmann (1980) and Wadt (1981) have discussed the electronic reasons for the change from the linear geometry in UO_2^{2+} to the *cis*-geometry in MoO_2^{2+}. Dyall (1999) and Straka *et al.* (2001) have discussed the bonding in actinyl ions and showed that the 5f character in the M–O bond increases steadily through the actinide series, while the 6d population remains nearly constant. The nonlinear O–M–O bonds are a result of an increased 6d population. As a result of the strong covalent $U–O_{yl}$ bonding, the formal charge of uranium is much lower than +6, +2.43 for $UO_2(H_2O)_5^{2+}$ in gas phase (Vallet *et al.*, 2004a); the charge of the 'yl' oxygen atoms is –0.43. Because of their negative charge, the 'yl' oxygen atoms in UO_2^{2+} and UO_2^+ are Lewis bases, resulting in the formation of 'cation–cation' complexes of type O=U=O- - - M (Section 5.10.2f). The negative charge on the 'yl'-oxygen atoms varies with the nature of the ligands in the equatorial plane and by proper ligand choice, the Lewis basicity of the 'yl'-oxygen atoms can be significantly increased, resulting in coordination of strong Lewis acids such as $B(C_6F_5)_3$ (Sarsfield and Helliwell, 2003). The charges on U and oxygen in $UO_2(H_2O)_5^+$ are 2.19 and –0.66, respectively (Vallet *et al.*, 2004a), making the uranyl(v) oxygen atoms even stronger Lewis bases than in uranyl(vi). A more detailed discussion of the electronic structure and energy levels of the other oxidation states of uranium is given in Chapter 16. The slight variations in the effective charge of uranium in different compounds result in small differences in the $U–O_{yl}$ bond distance and the effect is also noticeable as small changes in the vibrational stretch frequencies of the UO_2 group in infrared and Raman spectra. In the same way the 'yl'-stretch frequency is lower in UO_2^+ than in UO_2^{2+}, indicating a weaker bond in the former ion.

5.9 STRUCTURE AND COORDINATION CHEMISTRY OF URANIUM COMPLEXES IN SOLUTION AND THE SOLID STATE

The structure of complexes in solution is characterized by their coordination geometry, coordination number, and bond distances. The coordination geometry in solid-state structures is also influenced by additional factors, such as the efficiency of packing, the charge distribution in the structure, and the formation of hydrogen bond networks. The solid-state structures are often good models for bond distances and coordination geometry in solution. The structure in solution refers to discrete ions and molecules, more or less solvated, depending on the nature of the solvent and the charge of the complex. In some cases solid-state structures may contain discrete ions and molecules, but in general, the solid is better regarded as a 'polymer'. For example, UO_2CO_3(s) is a layer structure that does not contain isolated UO_2CO_3 units (see Fig. 5.54), while $Na_4UO_2(CO_3)_3$(s) contains discrete complexes of $UO_2(CO_3)_3^{4-}$ (Fig. 5.53).

The three-dimensional structures can be described using polyhedra and nets, and for simple structures, using packing of spheres (Chapters 3 and 4 in Wells, 1990). Polynuclear complexes are more common in the solid state than in solution, presumably as a result of the stronger electrostatic interactions in the solid phase. The water solvent with its high dielectric constant and strong hydrogen bond donor/acceptor properties reduces the stability of polynuclear complexes, except those involving hydroxide and oxide donors. Polynuclear fluoride complexes are very common in the solid state (Allen *et al.*, 2000), but are not formed in significant amounts in aqueous solution. This is presumably a result of the strong hydrogen bond acceptor properties of fluoride that makes hydrogen bonding to the water more favored than fluoride bridge formation between uranium atoms.

The stoichiometry, coordination number, and the number of available donor atoms per uranium atom indicate whether a certain compound contains isolated complexes, or if chains, layer structures, or three-dimensional networks are formed. Networks are common in oxide, uranate, phosphate, arsenate, and silicate compounds where they are a result of the sharing of oxygen donor atoms between two or more metal ions. These compounds are sparingly soluble and have a variable stoichiometry, (*cf.* Section 5.7.2).

The structure principles are demonstrated in the structure models of uranium compounds in oxidation states 3+, 4+, and 6+ described in the following sections. The largest number of structures are found for uranium(VI) compounds, many of which can be prepared from aqueous solution. In these compounds, the linear UO_2 unit is inert and the additional ligands in the coordination sphere are located in, or close to the plane through uranium and perpendicular to the UO_2 axis; the number of coordinated ligands in the plane varies between four and six; in solution, these ligands are labile, i.e. they can rapidly exchange with free ligand or in ligand substitution reactions as discussed in Section 5.10.3.

5.9.1 Uranyl(VI) compounds

The coordination chemistry of U(VI) differs from that of the d-transition and main-group elements. The common coordination geometry in UO_2^{2+} complexes with small ligands is a pentagonal bipyramid, with all labile ligands in the plane perpendicular to the linear UO_2 unit. Other coordination geometries are possible; a number of oxides and uranates have distorted octahedral or pentagonal bipyramidal structure, (Section 5.7.2.2, Fig. 5.25). Isolated ions of $UO_2(OH)_4^{2-}$ are found in the compound $[Co(NH_3)_6]_2[UO_2(OH)_4]_3 \cdot xH_2O$, the X-ray structure of which was determined by Clark *et al.* (1999) (Fig. 5.50), $UO_2(OH)_4^{2-}$ has a square bipyramidal geometry also in solution (Clark *et al.*, 1999; Wahlgren *et al.*, 1999; Moll *et al.*, 2000a); this geometry may also occur in complexes where there is a strong steric interference between coordinated organic ligands. The tetra-hydroxide complex has also been studied using quantum chemical methods (Schreckenbach *et al.*, 1998; Wahlgren *et al.*, 1999; Vallet *et al.*, 2001).

The structure of $K_2UO_2(SO_4)_2 \cdot 2H_2O$ is an example of pentagonal bipyramidal coordination consisting of uranium(VI) bipyramids linked in three dimensions by bridging sulfate groups (Niinistö *et al.*, 1979). Each sulfate acts as a bridge between two uranium atoms, leaving two non-coordinated sulfate oxygen atoms. The remaining coordination site on uranium is occupied by one of the two water molecules (Fig. 5.51).

A different structure (Burns and Hayden, 2002) still with pentagonal bipyramidal coordination is found in $Na_{10}[UO_2(SO_4)_4](SO_4)_2 \cdot 3H_2O$, shown in Fig. 5.52. This structure contains discrete complexes where the five-coordination in the equatorial plane is achieved by one chelating and three monodentate sulfate ions.

A hexagonal bipyramidal geometry with six ligands in the equatorial plane is in general obtained with ligands that can form chelates that have a small distance between their donor atoms. Examples are nitrates, $M[UO_2(NO_3)_3]$, where $M = NH_4$, K, Rb, Cs, and Tl (Zalkin *et al.*, 1989), carbonates such as $K_4UO_2(CO_3)_3$ (Anderson *et al.*, 1980), and acetates (Navaza *et al.*, 1991); these

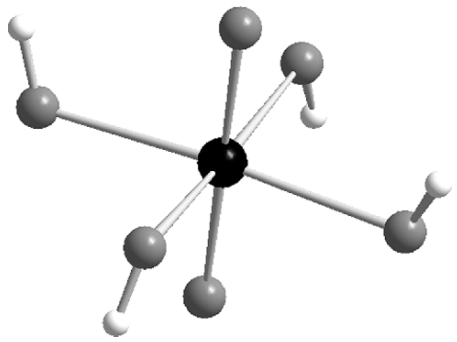

Fig. 5.50 *The structure of* $UO_2(OH)_4^{2-}$ (*from Clark* et al., 1999).

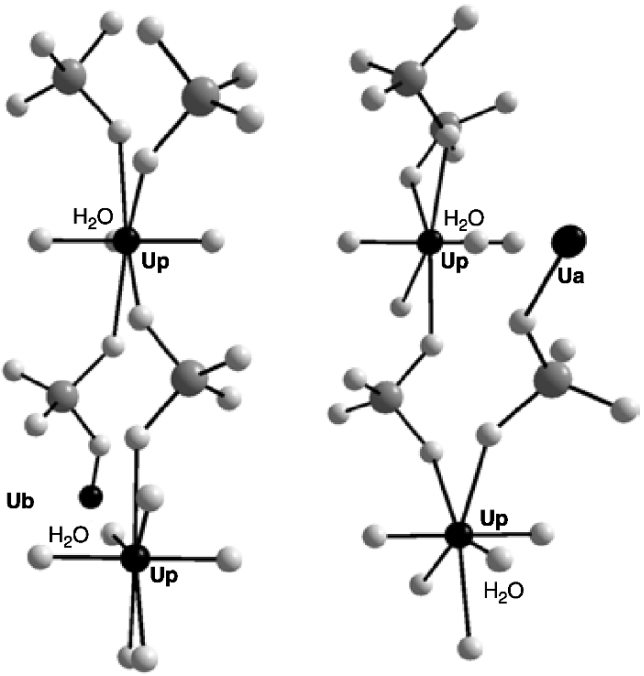

Fig. 5.51 *Coordination geometry and the three-dimensional linking in* $K_2UO_2(SO_4)_2 \cdot 2H_2O$ (*from Niinistö* et al., 1979). *The uranium atoms denoted* U_p *are located in the same plane and those denoted* U_a *and* U_b *in planes above and below this. The potassium atoms and one of the water molecules* (*not shown in the figure*) *provide additional links between the coordination polyhedra through coordination to the back end of the sulfate ions and through hydrogen bonding.*

compounds contain nine oxygen donors per uranium and from the geometry of the ligand, it is obvious that at most two per ligand can be coordinated to the same uranium atom. The donor atoms form hexagonal bipyramidal coordination together with the 'yl'-oxygen atoms. This results in structures that are composed of discrete complexes (Fig. 5.53). However, it is also feasible to have isomers; isolated pentagonal bipyramidal geometry is obtained if one of the ligands is coordinated through a single oxygen atom as in $UO_2(\text{oxalate})_3^{4-}$, discussed by Vallet *et al*. (2003). The only way to distinguish between these alternatives is through a structure determination or by using quantum chemical methods.

In UO_2CO_3(s), there are three oxygen donors per uranium and therefore the structure cannot contain isolated complexes; it turns out to be a layer structure where each oxygen donor is shared between two adjacent uranium atoms giving rise to hexagonal bipyramidal coordination (Fig. 5.54). This coordination geometry is very similar to that in the tris-carbonato complex (Fig. 5.53), but the three-dimensional structure of the latter is very different.

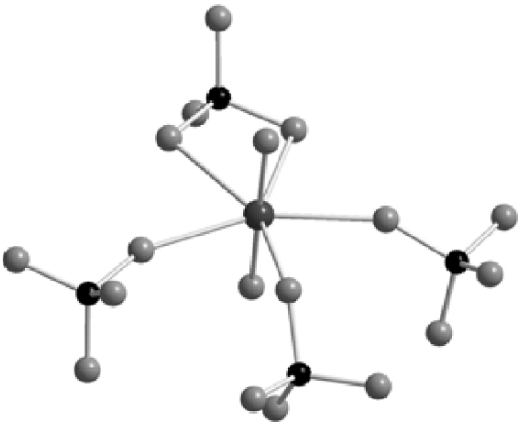

Fig. 5.52 *The coordination geometry of the* $UO_2(SO_4)_4^{6-}$ *ion in* $Na_{10}[UO_2(SO_4)_4](SO_4)_2 \cdot 3H_2O$ (*Burns and Hayden,* 2002). *One sulfate ion forms a chelate while the other three sulfate ions are monodentate.*

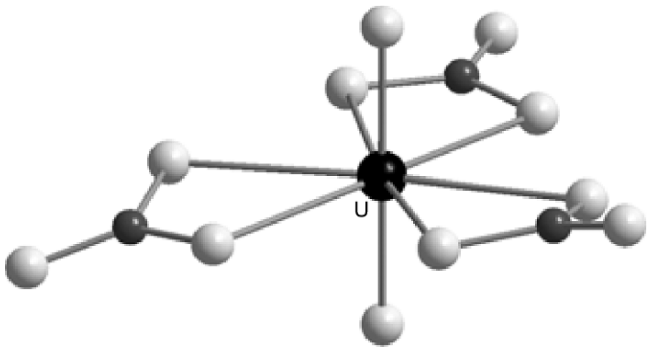

Fig. 5.53 *The coordination geometry, a hexagonal bipyramid, in* $K_4UO_2(CO_3)_3$ (*from the X-ray structure of Anderson* et al., 1980). *The ion* $[UO_2(CO_3)_3]^{4-}$ *occurs as discrete units in the structure; these units are linked through coordination to the counter ion* K^+.

Rare examples of six-coordination are also known in compounds containing organic ligands, e.g. $[UO_2(OTf)_2(bipy)_2]$ and $[UO_2(phen)_3][OTf]_2$, where bpy and phen denote bipyridine and phenantroline, respectively, and OTf^- the weakly coordinating triflate ion. Berthet *et al.* (2003) have determined the structure (Fig. 5.55) of these compounds, where the six nitrogen donors in the ligands are separated into two parallel and staggered equilateral triangles, (N2, N4, N6) and (N1, N3, N5) with the UO_2-axis perpendicular to the triangles. The uranium atom is equidistant, about 0.6 Å from these planes. The distortion is a result of geometric constraints in the chelating ligands.

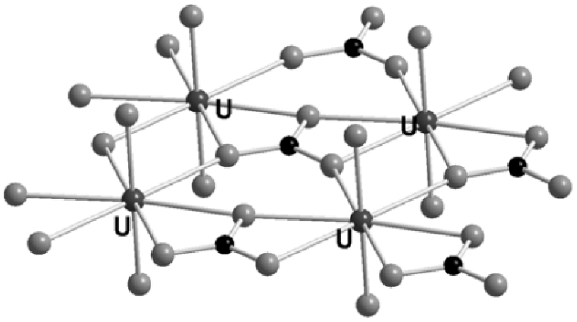

Fig. 5.54 *Part of the layer structure in $UO_2CO_3(s)$ showing the hexagonal bipyramidal coordination geometry of U(VI). By sharing each of the carbonate oxygens between two adjacent uranium atoms, six coordination in the plane perpendicular to the linear UO_2^{2+} ion is achieved. The structure is based on the X-ray study of Christ* et al. (1955).

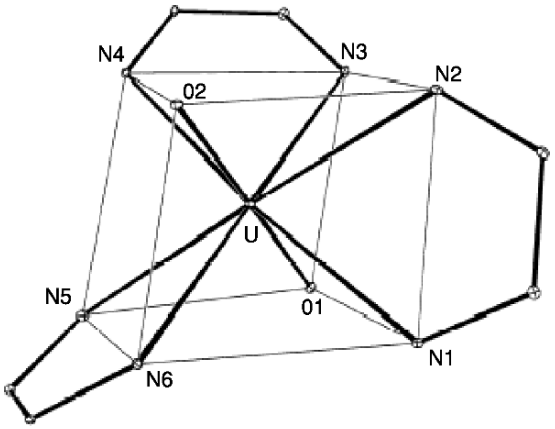

Fig. 5.55 *The coordination geometry for the six-coordinated U(VI) in $[UO_2(OTf)_2(bipy)_2]$ and $[UO_2(phen)_3][OTf]_2$; bpy denotes bipyridine, phen denotes phenantroline, and OTf the weakly coordinating triflate ion* (*from Berthet* et al., 2003, *reproduced by the permission of Royal Society of Chemistry*).

Uranium(VI) forms a number of peroxide complexes both in solution and in the solid state where the peroxide ligand is bonded 'side-on' to uranium as shown in Fig. 5.56a and b. The first one is the very rare mineral studtite, $UO_2(O_2)(H_2O)_2$ (Burns *et al.*, 2003); this compound has also been identified as a corrosion product on $UO_2(s)$ formed as a result of α-radiolysis (Sattonnay *et al.*, 2001); the second one is the structure of $Na_4[UO_2(O_3)_2](H_2O)_9$ from Alcock (1968). A number of other peroxide compounds and complexes in solution have been prepared by adding hydrogen peroxide to uranyl(VI) solutions; the sulfate and malonate systems were studied by Gurevich *et al.* (1971a,b);

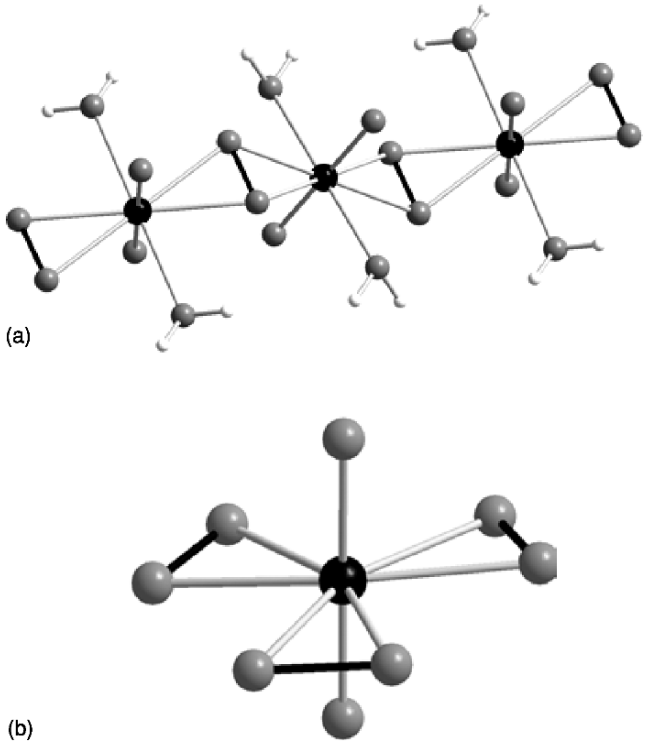

Fig. 5.56 (*a*) *The structure of studtite* (*from Burns* et al., 2003). *The peroxide group* (*black bond*) *is bridging two uranyl*(VI) *ions and forms a hexagonal bipyramidal coordination geometry around uranium together with two coordinated water molecules.* (*b*) *The structure of* $Na_4[UO_2(O_2)_3](H_2O)_9$ (*from Alcock,* 1968). *The structure contains discrete complexes with hexagonal bipyramidal coordination geometry*.

the oxalate system by Moskvin (1968); the uranyl(VI)-monoperoxo species was characterized by Djogic and Branica (1992). Self-assembled uranyl peroxide nanosphere clusters of 24, 28, and 32 polyhedra (some containing neptunyl) that crystallize from alkaline solution have been characterized (Burns *et al*., 2005).

5.9.2 Uranium(III) compounds

The structures of U(III) complexes are expected to be very similar to those of the other trivalent actinides; the coordination chemistry of which has been extensively studied as they are chemically more stable than the corresponding U(III) compounds. A point of interest is if there are differences in bonding between trivalent lanthanides and their actinide homologs. A comparison of equilibrium constants indicates that the actinide complexes are somewhat more stable, but the difference is not large. In the same way there are no large differences in bond distances and coordination geometry; the differences that

do exist may be due to the larger ionic radius of the actinide homologs as compared to the corresponding lanthanides. Uranium(III) compounds are characterized by high coordination numbers, eight and nine coordination are predominating as in the corresponding lanthanide(III) compounds. There are no structure determinations of uranium(III) complexes of simple inorganic ligands in solution, but it is reasonable to assume that their coordination geometry is similar to those of the trivalent lanthanides and transuranium elements (Allen *et al*., 2000). Examples of solid uranium(III) compounds are given by Chernyayev (1966) and Mehdoui *et al*. (2004), the latter also provides comparisons between U(III) and lanthanide(III) compounds.

Fig. 5.57 shows the structure of $K_3U(SO_4)_3 \cdot 3H_2O$ from Barnard *et al*. (1972a); it contains nine-coordinated U(III) through two chelating and two mono-dentate sulfate ions and three coordinated water molecules that form a strongly distorted trigonal prism around uranium.

5.9.3 Uranium(IV) compounds

Uranium(IV) forms both normal and basic salts with most inorganic ligands. The formation of basic salts is the result of the strong hydrolysis of U(IV) and these compounds contain coordinated hydroxide and/or oxide in addition to donor atoms from the other ligand. The relatively large ionic radius, 0.93 Å (eight coordination), and the high charge of U^{4+} results in high and often variable coordination numbers in different compounds, eight, nine and ten are

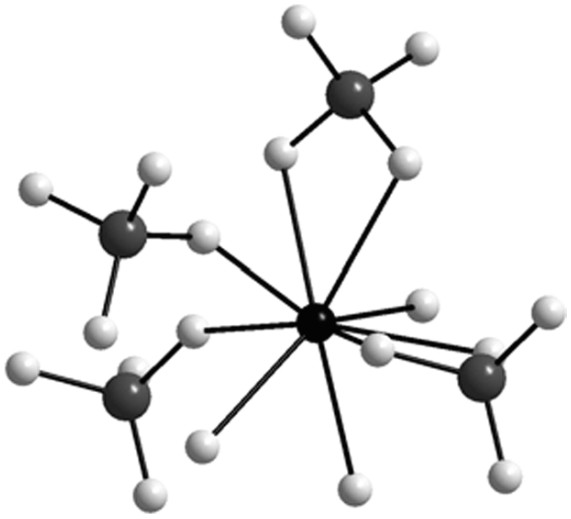

Fig. 5.57 *The coordination geometry of U(III) in* $K_3U(SO_4)_3 \cdot 3H_2O$ (*Barnard* et al., 1972*a*)*; uranium is nine-coordinated through two chelating and two monodentate sulfate ligands and three coordinated water molecules. The coordination polyhedron is strongly distorted from all the ideal geometries.*

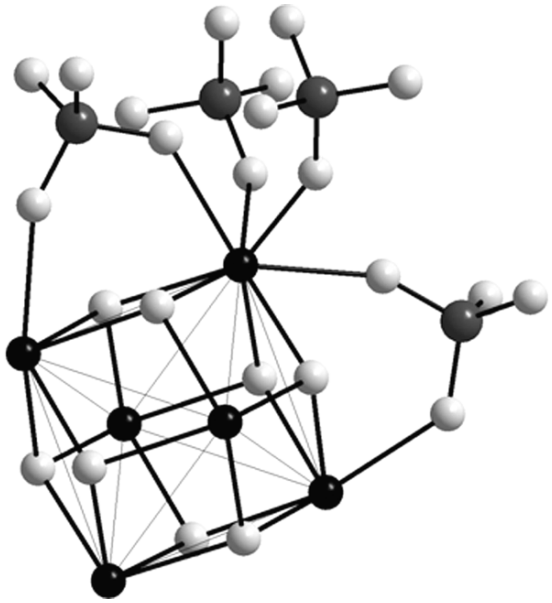

Fig. 5.58 *Structure of* $U_6(SO_4)_6O_4(OH)_4(s)$. *The characteristic structure element is an octahedron of six uranium*(IV) *ions* (*black*) *shown in the lower part of the figure. The oxide and hydroxide ions* (*light gray*) *are placed outside the eight triangular faces of this octahedron. The sulfate ions* (*sulfur is dark gray*) *are coordinated outside the octahedron and act as bridges between the U*(IV) *ions within the octahedron and between adjacent octahedra* (*not shown in the figure*). *Uranium*(IV) *is eight-coordinated in this compound. The structure is based on the X-ray study of Lundgren* (1952).

the most common ones. Uranium(IV) is in this respect similar to the elements in the lanthanide group, notably Ce(IV). Two examples of the coordination geometry of uranium(IV) in solid compounds are given in Figs. 5.58 and 5.59.

Fig. 5.59, based on an X-ray study of Fuchs and Gebert (1958), shows the structure of the mineral coffinite, $USiO_4$. A coordination number of eight can only be achieved by sharing all oxygen atoms in the silicate between two U(IV) atoms. The coordination geometry is best described as a triangular dodecahedron (Kepert, 1982, p. 153), the two 'arms' of which are indicated by the black full drawn lines.

The coordination number of the U(IV) and Th(IV) aqua ions in solution has been discussed based on data from Large-Angle X-ray Scattering (LAXS) and Extended X-ray Absorption Fine structure Spectroscopy (EXAFS). These methods provide accurate bond distances, while the determination of the coordination number is more uncertain, (9 ± 1). The high coordination number is retained in UF^{3+}(aq), as indicated by EXAFS data (Moll *et al.*, 1999); these data demonstrate a pronounced difference in bond distance between coordinated fluoride and water; the U–F distance is 2.15 Å and the U–H_2O distance 2.45 Å. The large variability of the coordination geometry in complexes of tetravalent actinides is demonstrated also by the structure of

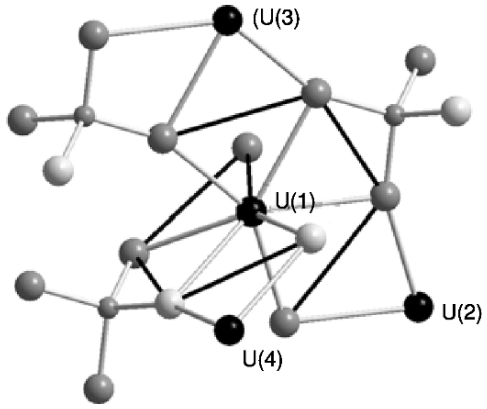

Fig. 5.59 *The structure of $USiO_4$ from Fuchs and Gebert* (1958). *The silicate group forms both a chelate and acts as a bridge between adjacent uranium atoms U*(2–4). *The chelate bonding is shown in the figure; the two remaining oxygen atoms in the silicate group are coordinated to adjacent uranium*(IV) *atoms not shown in the figure. The black full-drawn lines connect the atoms in the 'arms' of the dodecahedral coordination polyhedron. Each arm is approximately planar and the two planes are perpendicular.*

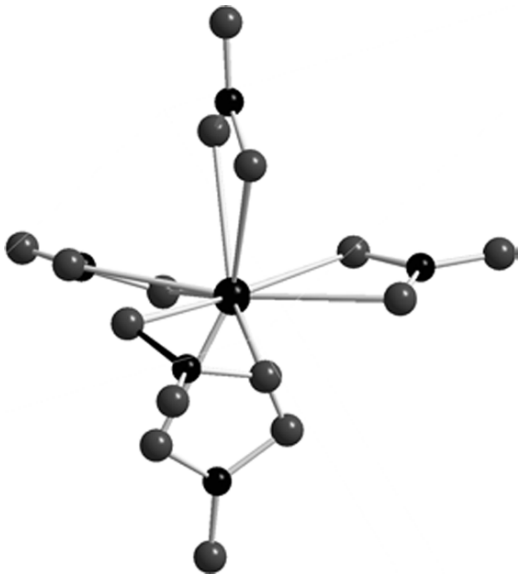

Fig. 5.60 *The structure of $Th(CO_3)_5^{6-}$ and the isostructural $U(CO_3)_5^{6-}$ from Voliotis and Rimsky* (1975).

$Na_6[Th(CO_3)_5] \cdot 12H_2O$ from Voliotis and Rimsky (1975), shown in Fig. 5.60; the corresponding uranium compound is isostructural. The carbonate ligands are arranged in an approximately trigonal bipyramidal arrangement around the central actinide ion; this geometry is very different from the common ones for ten-coordination, as discussed by Kepert (1982, p. 188). We may describe each carbonate ligand with one 'effective' charge because of its small ligand bite, resulting in a trigonal bipyramidal charge distribution in a geometry that minimizes the electrostatic repulsion between the ligands.

Another example of the variable coordination geometry is given by the structure of tetra(glycolato)uranium(IV) dihydrate, $[U(HOCH_2COO)_4] \cdot 2H_2O$ where uranium is ten-coordinated as indicated by Fig. 5.61, based on the structure data of Alcock *et al*. (1980). A recent example of the variable coordination geometry of U(IV) is the structure of the azide complex $U(N_3)_7^{3-}$, with an approximately pentagonal bipyramidal coordination geometry (Crawford *et al*., 2005). The azide ion is linear, but the angle U–N–N–N is highly variable (from 120° to 180°).

5.9.4 Uranyl(v) compounds

There are few experimental data on the structure and bonding of uranyl(v) complexes, the only example is the structure of the uranyl(v) triscarbonate complex studied in solution using EXAFS (Docrat *et al*., 1999). The complex has

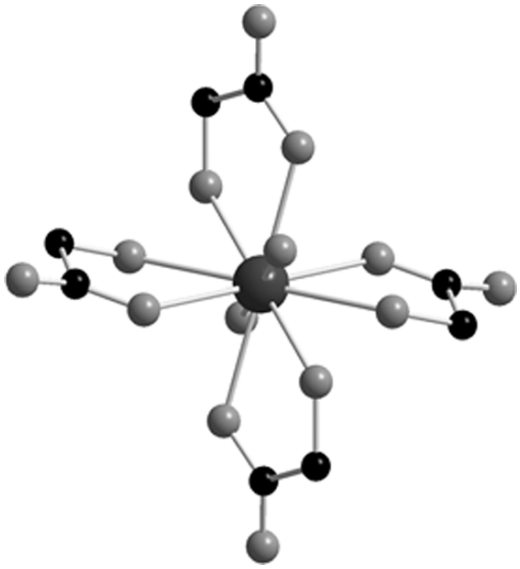

Fig. 5.61 *The coordination geometry in tetra(glycolato)uranium(IV) dihydrate from Alcock* et al. (1980). *The structure contains discrete ten-coordinated complexes* $[U(HOCH_2COO)_4(OH_2)_2]$ *with zero charge.*

hexagonal bipyramidal geometry similar to that of the uranyl(VI) triscarbonate complex, *cf*. Fig. 5.53. The corresponding information on neptunyl(V) complexes should provide good models also for the corresponding U(V) species. The geometry of the uranyl(V) and -(VI) carbonate complexes are supported by quantum chemical calculations by Gagliardi *et al*. (2001). The predominant coordination geometry is presumably a pentagonal or hexagonal bipyramid, with the labile ligands in the plane perpendicular to the linear UO_2 unit. The lower charge of the central atom results in the formation of weaker complexes and somewhat longer U–L distances than for the corresponding U(VI) complexes.

5.9.5 Uranium compounds of organic ligands

There is an abundance of organic ligands that form solid uranium complexes and we will restrict the examples to simple carboxylates, α-hydroxy and amino carboxylates.

The same structural principles as observed with the inorganic ligands are found also among the organic ones; the main difference between the two groups is that the geometry of the organic ligands puts additional constraints on the availability of the various donor atoms for bonding to uranium. In addition, the larger versatility of many organic ligands also opens up the possibility to form structural and bonding isomers.

Stoichiometric information on the constitution of complexes in solution can be obtained by an array of experimental methods (Rossotti and Rossotti, 1961), but this rarely gives information on structure and bonding. As is the case of inorganic ligands, the important methods to obtain structural information from solution are LAXS or EXAFS methods. However, both of them provide only limited structural information in the form of radial distribution functions, i.e. the distance from the central uranium atom to the atoms in the first and second coordination spheres and the number of such distances. In the case of LAXS one can also obtain information on the distances between the coordinated donor atoms. Allen *et al*. (1996b) give examples of the use of EXAFS for the deduction of structure models of uranyl(VI) tartrate, citrate, and malate complexes. Jiang *et al*. (2002) have investigated the structure and bonding of uranyl(VI) imino- and oxy-diacetate compounds and identified different modes of coordination of the ligands, an example that the stoichiometry of a complex does not provide sufficient information to identify the mode of coordination. In order to obtain more precise structure data it is often necessary to obtain additional structural information, such as provided by NMR spectroscopy (Szabó *et al*., 1997, 2000; Moll *et al*., 2000a,b) or by quantum chemical methods (Schreckenbach *et al*., 1998; Tsushima *et al*., 2001; Vallet *et al*., 2001, 2004b; Yang *et al*., 2003). The uranyl(VI) oxalate system provides a good example of different modes of bonding of the oxalate ligand in solid compounds and the structure of $UO_2(\text{oxalate})_3^{4-}$ complex in solution (Vallet *et al*., 2003). The ground state structure predicted by the quantum chemical methods is the one that is found experimentally (Fig. 5.62a–c).

The stoichiometry and the value of the stability constants of the complexes given in Tables 5.33–5.37 give some indications of the mode of bonding of the ligands, in particular whether a certain ligand forms a chelate or not. A comparison between acetate and glycolate is instructive: acetate can only coordinate through the carboxylate group, either using one oxygen donor or both. In the latter case a four-membered chelate ring is formed. Glycolate can bind in the same way if only the carboxylate group is involved and one then expects a stability constant of the same magnitude for both ligands. However, glycolate can also form a chelate by using one donor atom from each of the carboxylate and the α-OH groups, in which case a five-membered chelate ring is formed. Chelate formation results in a large increase in the stability constant, *cf.* the $\log\beta_n$ values for the acetate and glycolate complexes of U(IV) in Table 5.36. The stability constants, with the exception of $\log\beta_1$, are slightly larger for the U(VI) acetate than those for the glycolate complexes, which strongly indicates the same mode of bonding of acetate and glycolate in the U(VI) complexes (Beck and Nagypál, 1990; Grenthe *et al.*, 1997). The stepwise equilibrium constants for the formation of $UO_2(ox)$ ($\log\beta_1 = 5.99$), $UO_2(ox)_2^{2-}$ ($\log K_2 = 4.65$ for the reaction $UO_2(ox) + ox^{2-} \rightleftharpoons UO_2(ox)_2^{2-}$) are large compared to the value for the formation of $UO_2(ox)_3^{4-}$ ($\log K_3 = 0.36$ for the reaction $UO_2(ox)_2^{2-} + ox^{2-} \rightleftharpoons UO_2(ox)_3^{4-}$), indicating that the third oxalate does not form a chelate. This assumption has been verified both by experimental EXAFS data from solution and by quantum chemical calculations (Vallet *et al.*, 2003) as shown in Fig. 5.62a–c. These data also illustrate the possible occurrence of isomers.

5.10 URANIUM CHEMISTRY IN SOLUTION

5.10.1 The uranium aqua ions

The most stable oxidation state of uranium in aqueous solution is 6+, with the linear uranyl(VI) ion, UO_2^{2+}, as the stable entity. The only known uranium ion in the 5+ oxidation state in aqueous solution is the linear dioxouranium(V) ion, UO_2^+. Aqueous solutions containing U^{4+} are stable in the absence of oxidation agents like dissolved oxygen. Aqueous solutions containing U^{3+} are rapidly oxidized under evolution of hydrogen. The relative stability of the various oxidation states is strongly depending on the pH of the solution and on the presence of complexing ligands as indicated in Fig. 5.63. The rate of the redox transformations between the different oxidation states of uranium is rapid when there is no change in chemical composition between the oxidized and reduced forms, otherwise it is very slow. This means that the reactions $UO_2^{2+} + e^- \rightleftharpoons UO_2^+$ and $U^{4+} + e^- \rightleftharpoons U^{3+}$ are fast, while $UO_2^{2+} + 4H^+ + 2e^- \rightleftharpoons U^{4+} + 2H_2O$ is slow.

The kinetics of the redox transformations in aqueous actinide systems has been described in a report by Newton (1975) (Section 5.10.3i). The structures and chemical properties of actinide aqua ions are discussed and compared in

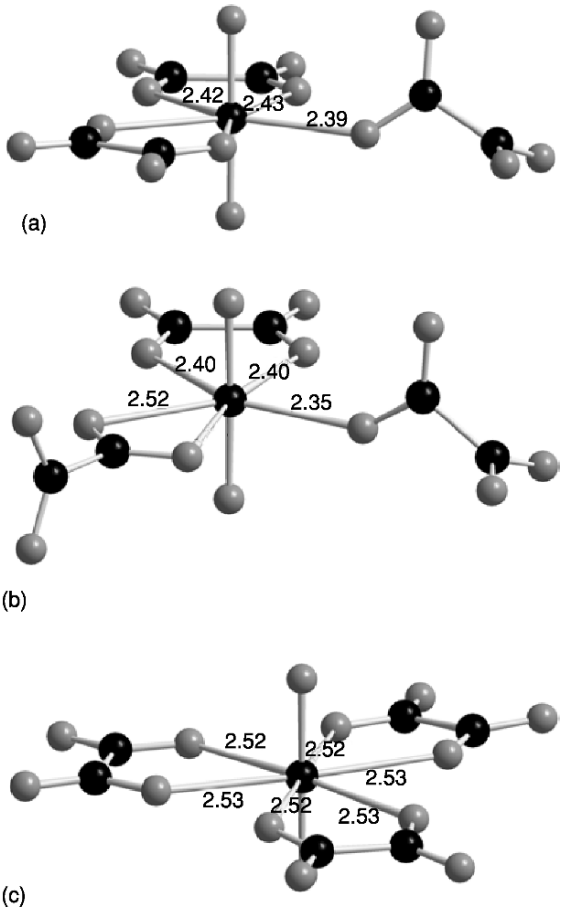

Fig. 5.62 (*a–c*) *Perspective views of three* $[UO_2(oxalate)_3]^{4-}$ *isomers, where* (*a*) *is the most stable one from Vallet* et al. (2003). *By using quantum chemical methods one can estimate the relative stability of the different isomers. The uranium atom and the carbon atoms are black and the oxygen atoms gray; distances are in ångströms. The bond distances for the ground state isomer a obtained from quantum chemical calculations agree with those obtained from EXAFS data in solution within* 0.03 Å. *The same mode of bonding has also been found in solid-state structures, but here there are no discrete complexes as the oxalate ligands act as bridges between adjacent uranium atoms.*

Chapter 23, section 2; a comparison of the complex formation properties of actinides is given in Chapter 23, sections 3–8. The kinetics of actinide reactions are compared and discussed in Chapter 23, sections 10 and 11.

Aqueous solutions of UO_2^+ are prone to disproportionation and the range of stability of U(v) is therefore small, a fact that makes it difficult to study its solution chemistry.

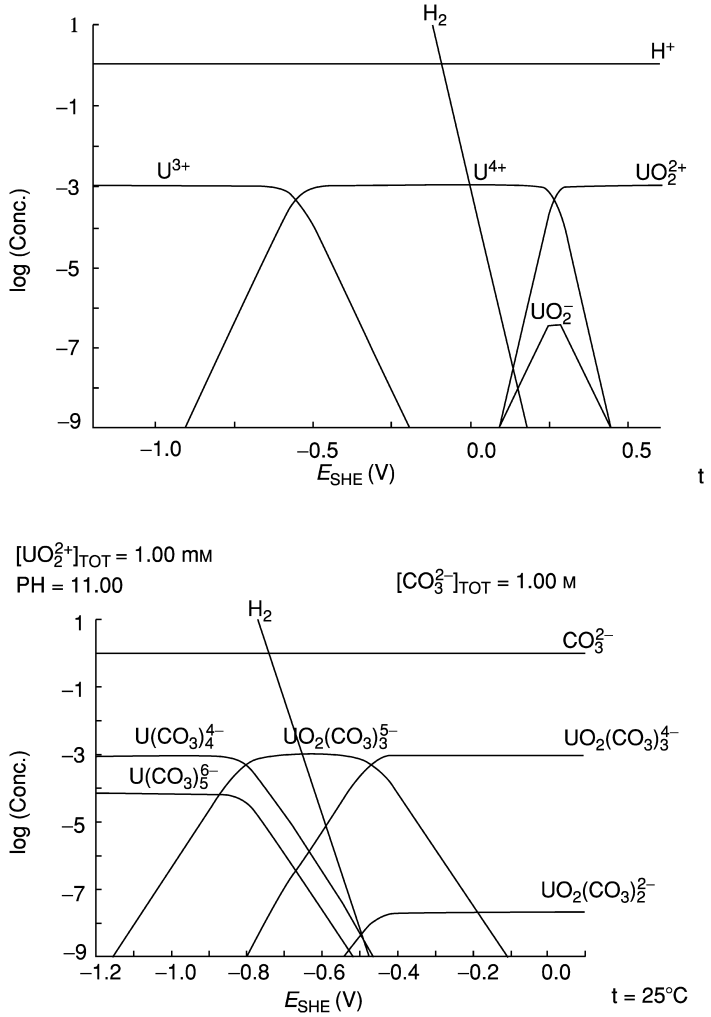

Fig. 5.63 *Logarithmic diagrams showing the distribution of* U^{3+}, U^{4+}, UO_2^+ *and* UO_2^{2+} *as a function of the redox potential in* 1 M *perchloric acid* (*the first diagram*), *and in* 1 M Na_2CO_3 (*the second diagram*). *U*(*V*) *is predominant between* –0.7 *and* –0.4 V *in the second diagram.*

The oxygen atoms in UO_2^{2+} and UO_2^+ are kinetically inert and their rate of exchange with oxygen from water is slow, with a half-life of approximately 5×10^4 h in 1 M perchloric acid for the former (Gordon and Taube, 1961a), but much faster for the latter as indicated by the fact that UO_2^+ catalyzes the oxygen exchange between UO_2^{2+} and water (Gordon and Taube, 1961b).

However no exchange rate has been determined for UO_2^+ alone. The rate of exchange of the 'yl' oxygen atoms with the water solvent is strongly catalyzed by light in the near UV/visible region and varies with the chemical composition of the complexes present in solution as discussed in Section 5.10.3, where also some spectroscopic characteristics of the various species are described.

Solutions of U^{3+}, U^{4+}, and UO_2^{2+} can be used to prepare complexes in solution and various solid compounds using standard techniques. A treatise by Chernyayev (1966) gives an excellent account of the compounds prepared from aqueous media.

(a) Tripositive uranium, U^{3+}

Aqueous solutions of U^{3+} can be prepared by dissolving uranium trichloride in water. Alternatively, solutions of U(IV) or U(VI) can be reduced by electrolysis at a mercury cathode (Barnard *et al.*, 1967, 1972b; Weigel, 1958). The course of the reduction can conveniently be observed by the colour of the solutions in *incandescent* light: Solutions of U(VI) are yellow, while those of U(IV) and U(III) are green and wine red, respectively. These colors cannot be observed in fluorescent light. There are only few studies of the chemical properties of U^{3+} and its complexes in solution (Section 5.8.6); however the properties can often be estimated from those of the trivalent lanthanides. The standard redox potential of the U^{4+}/U^{3+} redox couple and the Gibbs energy and enthalpy of formation, entropy and heat capacity of U^{3+}(aq) have been reviewed by Grenthe *et al.* (1992) and Guillaumont *et al.* (2003). These data are reported in Table 5.32.

There is no structural information available on the U^{3+}(aq) ion, however the structure of Pu^{3+}(aq) has been determined (Matonic *et al.*, 2001) by a single-crystal X-ray diffraction study of $[Pu(H_2O)_9][CF_3SO_3]_3$. In addition, the structures of trivalent lanthanides and Am(III) and Cm(III) have been determined in solution using EXAFS (Allen *et al.*, 2000). The solid Pu(III) compound contains discrete nine-coordinated complexes that are very similar to those found among the trivalent lanthanides, in the same way the bond distances and coordination number determined from the EXAFS data are close to those in lanthanide(III) and actinide(III) complexes, indicating an aqua-ion of the composition $U(H_2O)_9^{3+}$ for trivalent uranium.

(b) Tetrapositive uranium, U^{4+}

U(IV) in the form of U^{4+}(aq) is a very strong acid and accordingly hydrolyzed except in solutions with a hydrogen ion concentration larger than 0.5 M. The hydrolysis will be discussed in Section 5.10.2b. Uranium(IV) species can be prepared by electrolysis of corresponding uranium(VI) solutions at low pH using a two-compartment cell and a mercury cathode, U(III) is formed simultaneously, but is rapidly oxidized by blowing air through the cathode

Table 5.32 *The redox potentials, Gibbs energy and enthalpy of formation, molar entropy, and heat capacity for the different uranium aqua ions under standard state conditions* (298.15 K, 0.1 MPa) *in pure water solvent at zero ionic strength* (*Grenthe* et al., 1992; *Guillaumont* et al., 2003).

Species and redox reaction	E° (V)	$\Delta_f G^\circ_m$ (kJ mol^{-1})	$\Delta_f H^\circ_m$(kJ mol^{-1})	S°_m (J K^{-1} mol^{-1})	$C^\circ_{p,m}$ (J K^{-1} mol^{-1})
$U^{3+}(aq)$		–(476.5 ± 1.8)	–(489.1 ± 3.7)	–(188 ± 14)	–(150 ± 50)
$U^{4+} + e^- \rightleftharpoons U^{3+}$	–(0.553 ± 0.004)				
$U^{4+}(aq)$		–(529.9 ± 1.8)	–(591.2 ± 3.3)	–(417 ± 13)	–(220 ± 50)
$UO_2^+(aq)$		–(961.0 ± 1.8)	–(1025.1 ± 3.0)	–(25 ± 8)	–
$UO_2^{2+} + e^- \rightleftharpoons UO_2^+$	(0.0878 ± 0.0013)				
$UO_2^{2+}(aq)$		–(952.6 ± 1.7)	–(1019.0 ± 1.5)	–(98.2 ± 3.0)	(42.4 ± 3.0)
$UO_2^{2+} + 4H^+ + 2e^- \rightleftharpoons U^{4+} + 2H_2O$	(0.2673 ± 0.0012)				

compartment. Acid solutions of U(IV) are only slowly oxidized by oxygen but the situation is very different in the presence of strong complexing agents where the oxidation is very rapid and great experimental care has to be taken in order to keep the 4+ oxidation state. Uranium(IV) in acid solution can also be obtained by reduction of U(VI) with hydrogen using platinum black as a catalyst. The coordination number of the $U^{4+}(aq)$ in solution has been studied by LAXS (Johansson, 1992) and by EXAFS (Moll *et al.*, 1999); the U–O distance is (2.42 ± 0.01) Å and the coordination number (9 ± 1). The coordination number is not well defined and the energy difference between isomers with different geometries is probably small (Kepert, 1982), an assumption supported by quantum chemical data on $Th^{4+}(aq)$ by Yang *et al.* (2001, 2003). The rate constant for the exchange between coordinated and bulk water has been determined using ^{17}O NMR spectroscopy as discussed in section 5.10.3 (b). Experimental data for the redox potential and other thermodynamic quantities for $U^{4+}(aq)$ have been reviewed (Grenthe *et al.*, 1992; Guillaumont *et al.*, 2003) and selected values are given in Table 5.32.

(c) Dioxouranium(v), UO_2^+

The 5+ oxidation state of uranium has a very narrow range of existence in aqueous solution, (Fig. 5.63). Millimolar solutions of UO_2^+ can be prepared by reduction of UO_2^{2+} with zinc amalgam or hydrogen, or by dissolving UCl_5 in water. A more convenient method is to irradiate a 0.5 M 2-propanol–0.2 M $LiClO_4$ solution of uranium(VI) at a pH between 1.7 and 2.7, with UV radiation from a Hg lamp (Howes *et al.*, 1988). The uranium(V) solution formed is not thermodynamically stable, but the rate of oxidation is so slow that there is little decomposition during 1 h.

There is no experimental information on the structure of $UO_2^+(aq)$ and the number of coordinated water molecules. However, as judged by the chemical similarity between U(V) and Np(V) complexes, it is reasonable to assume that they also have a similar coordination geometry, as exemplified by the coordination geometry of different Np(V) carbonate complexes in solution is given by Clark *et al.* (1996); these structures are also very similar to those of the corresponding U(VI) system (Docrat *et al.*, 1999; Gagliardi *et al.*, 2001). Vallet *et al.* (2004a) have used quantum chemical models to predict that the most probable constitution of $UO_2^+(aq)$ is $UO_2(H_2O)_5^+$, with pentagonal bipyramidal geometry. The thermodynamics of $UO_2^+(aq)$ has been reviewed (Grenthe *et al.*, 1992; Guillaumont *et al.*, 2003) and the redox potential for the reaction: $UO_2^{2+}(aq) + e^- \rightleftharpoons UO_2^+(aq)$, and other thermodynamic data for $UO_2^+(aq)$ from these reviews are given in Table 5.32. U(V) is an intermediate in the photochemical reduction of uranium(VI) (Heidt and Moon, 1953).

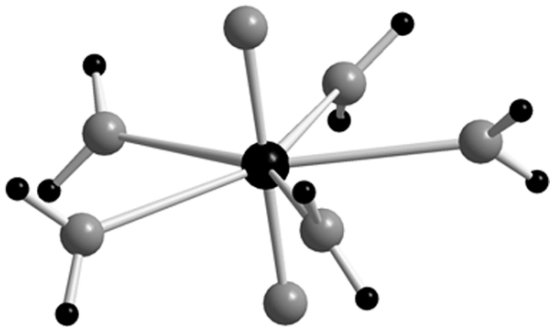

Fig. 5.64 *The coordination geometry of* $UO_2(H_2O)_5^{2+}$ *and* $UO_2(H_2O)_5^{+}$*, deduced from quantum chemical calculations using a solvent model as discussed by Vallet* et al. (2001, 2004). *Only the bond distances differ between the two structures; the U–O water distances are* 2.47 Å *in the uranyl(*VI*) aqua ion and* 2.63 Å *in the corresponding uranyl(*V*) species. The* $U–O_{yl}$ *distance is* 0.1 Å *longer in the uranyl(*V*) compound than in the corresponding uranyl (*VI*) compound.*

(d) Dioxouranium(VI), UO_2^{2+}

The 6+ state is the most stable of the oxidation states of uranium and has accordingly been extensively studied. A large number of different compounds have been prepared from aqueous solution both by simple crystallization, by using hydrothermal techniques and other methods; numerous examples are given in other parts of this chapter. Under certain circumstances, the oxo ligands can undergo ligand exchange, scrambling, and substitution reactions; the ligand exchange reactions are in general slow but are strongly photo-catalyzed and these reactions are discussed in Section 5.10.3. The structure of the aqua ion $UO_2(H_2O)_5^{2+}$ in solution has been determined using LAXS (Åberg *et al.*, 1983) and EXAFS techniques (Wahlgren *et al.*, 1999; Sémon *et al.*, 2001; Neuefeind *et al.*, 2004b); more detailed studies have been made using quantum chemical methods (Spencer *et al.*, 1999; Wahlgren *et al.*, 1999; Hay *et al.*, 2000; Vallet *et al.*, 2001). Guilbaud and Wipff (1993), Hagberg *et al.* (2005) have determined the structure by using molecular dynamics simulations, a method that also gives some information on the structure of the second hydration sphere. The structure of the aqua ion is shown in Fig. 5.64. The redox potentials for reactions involving $UO_2^{2+}(aq)$, and the standard Gibbs energy and enthalpy of formation, the molar entropy, and heat capacity of $UO_2^{2+}(aq)$ from the reviews by Grenthe *et al.* (1992) and Guillaumont *et al.* (2003) are given in Table 5.32. The rate of exchange between coordinated water and the pure water solvent has been studied using ^{17}O NMR (Farkas *et al.*, 2000a), and these data are discussed in section 5.10.3(b).

5.10.2 Aqueous uranium complexes

Uranium is a very strong Lewis acid and a hard electron acceptor in all its different oxidation states. This means that the donor–acceptor interactions follow the sequences:

$$F^- \gg Cl^- > Br^- \approx I^-; O \gg S > Se; N \gg P \approx As$$

where the donors are either simple ions like fluoride, or part of a larger ion/molecule like carbonate. These sequences are expected if the donor–acceptor interactions are dominated by electrostatic forces. There is extensive information in the literature on the chemical thermodynamics of uranium complexes. Most of these data are compiled in *Stability Constants, Special Publications* No. 6 (Bjerrum *et al*., 1957), No. 7 (Bjerrum *et al*., 1958), No. 17 (Sillén and Martell, 1964), No. 25 (Sillén and Martell, 1971), and in the International Union of Physical and Applied Chemistry (IUPAC) Chemical Data Series, *Stability Constants of Metal-Ion Complexes, Part A* (Högfeldt, 1982) and *Part B* (Perrin, 1979). There are several critical evaluations of the compiled data; the series *Critical Stability Constants*, Vols 1–6, by Martell and Smith, is now available in a computer database that also includes the necessary software, *NIST Standard Reference Database* 46 (NIST, 2004). Grenthe *et al*. (1992) and Guillaumont *et al*. (2003) have given a more detailed critical evaluation of thermodynamic data for uranium, including a discussion of many of the experimental investigations on which the selected data are based.

The high Lewis acidity results in extensive hydrolysis of uranium that decreases in the order U(IV) > U(VI) >> U(III) > U(V). Another effect of the high Lewis acidity is that coordinated uranium exerts a very strong inductive effect on coordinated ligands, e.g. the dissociation constant of the proton in the α-hydroxy group of coordinated α-hydroxy carboxylic acids can increase by more than 13 orders of magnitude (Szabó and Grenthe, 2000) on coordination to uranium(VI); a similar effect is also found in some Th(IV) complexes (Toraishi *et al*., 2002) and therefore most likely also in U(IV) complexes:

$$HOCH_2COO^- \rightleftharpoons {}^-OCH_2COO^- + H^+; pK \approx 17$$
$$UO_2(HOCH_2COO^-) \rightleftharpoons UO_2({}^-OCH_2COO^-) + H^+; pK = 3.6.$$

A similar example is found in the structure of the complex $[UO_2L(MeO)(MeOH)]_2$ where L is a thiosemicarbazone (Santos and Abram, 2004); this complex contains one coordinated (MeOH) and one deprotonated (MeO^-) methanol ligand. The 'inductive effect' is an electron redistribution in the coordinated ligand; if this is an organic species it will result in a changed ligand reactivity, a fact that has been used in preparative chemistry (van Axeel Castelli *et al*., 2000).

(a) Uranium(III) and uranyl(V) complexes

Uranium(III) is a very strong reducing agent that is oxidized by water, hence no stable complexes can be maintained in aqueous solution. However, the chemical properties of uranium(III) are expected to be very similar to those of trivalent lanthanides, actinium(III) and the transuranium elements in oxidation state 3+. Guidance on the magnitude of equilibrium constants for U(III) species can therefore be obtained from databases for lanthanide(III) and actinide(III) elements: examples are given in Tables 5.34 and 5.36. The differences in chemical properties between U(III) and other An(III) ions and the corresponding Ln(III) species can be exploited by proper choice of ligand. This is a useful strategy for the design of An(III)/Ln(III) separation processes (Karmazin *et al.*, 2002). The narrow range of existence of uranium(V) in aqueous solution results in very little quantitative information on equilibrium constants. In view of the large chemical similarity between actinides in the same oxidation state, one may use the equilibrium constants for Np(V) complexes as estimates for the corresponding U(V) complexes (Chapter 6, section 9).

(b) Hydrolysis of uranium

A summary of the stoichiometry and equilibrium constants of the various hydroxide complexes are given in Table 5.33: they refer to reactions of the type

$$pM + qH_2O \rightleftharpoons M_p(OH)_q + qH^+$$

where all charges except for H^+ have been omitted for simplicity, and where M denotes, UO_2^{2+} UO_2^+, U^{4+}, or U^{3+}; the equilibrium constants are taken from Grenthe *et al.* (1992), Guillaumont *et al.* (2003) and Baes and Mesmer (1976).

In most of the experimental determinations of hydrolytic equilibria it is not possible to decide if the species formed contain coordinated hydroxide and/or oxide; the reason being that $2OH^- \equiv O^{2-}$ in experiments where the equilibrium constants and the stoichiometry are deduced from measurements of the free hydrogen ion concentration; this is an example of the so-called 'proton ambiguity' (Rossotti and Rossotti, 1961). The following example illustrates the point:

$$3UO_2^{2+} + 5H_2O \rightleftharpoons (UO_2)_3(OH)_5^+ + 5H^+$$
$$3UO_2^{2+} + 5H_2O \rightleftharpoons (UO_2)_3(O)(OH)_3^+ + 5H^+ + H_2O$$

Both reactions result in the formation of five H^+ and can therefore not be distinguished. As the activity of water is a constant, the stability constant is the same for both stoichiometric formulations. This tri-nuclear complex was originally formulated as $(UO_2)_3(OH)_5^+$, but when structural data became available the actual composition turned out to be $(UO_2)_3(O)(OH)_3^+$, with the structure given in Fig. 5.65 (Åberg, 1978).

Table 5.33 *Stoichiometry and stability constants for the hydrolysis complexes of uranium. The stability constants refer to zero ionic strength and a temperature of* 25°C*; data from Grenthe* et al. (1992), *Guillaumont* et al. (2003), *and Baes and Mesmer* (1976).

Uranium(VI) Chemical reaction	$log^*\beta_{p,q}$	*Uranium(IV) Chemical reaction*	$log^*\beta_{p,q}$
$UO_2^{2+} + H_2O \rightleftharpoons UO_2OH^+ + H^+$	–5.25	$U^{4+} + H_2O \rightleftharpoons UOH^{3+} + H^+$	–0.54
$UO_2^{2+} + 2H_2O \rightleftharpoons UO_2(OH)_2(aq) + 2H^+$	–12.15	$U^{4+} + 2H_2O \rightleftharpoons U(OH)_2^{2+} + 2H^+$	–2.6[a]
$UO_2^{2+} + 3H_2O \rightleftharpoons UO_2(OH)_3^- + 3H^+$	–20.25	$U^{4+}3H_2O \rightleftharpoons U(OH)_3^+ + 3H^+$	–5.8[a]
$UO_2^{2+} + 4H_2O \rightleftharpoons UO2(OH)_4^{2-} + 4H^+$	–32.40	$U^{4+} + 4H_2O \rightleftharpoons U(OH)_4(aq) + 4H^+$	–10.3[a]
$2UO_2^{2+} + H_2O \rightleftharpoons (UO_2)_2OH^{3+} + H^+$	–2.7	$6U^{4+} + 15H_2O \rightleftharpoons U_6(OH)_{15}^9 + 15H^+$	–16.9
$2UO_2^{2+} + 2H_2O \rightleftharpoons (UO_2)_2(OH)^{2+} + 2H^+$	–5.62	Uranium(v): Estimates from Np(v) data	
$3UO_2^{2+} + 5H_2O \rightleftharpoons (UO_2)_3(OH)_5^+ + 5H^+$	–15.55	$UO_2^+ + H_2O \rightleftharpoons UO_2OH(aq) + H^+$	≈–11.3
$3UO_2^{2+} + 7H_2O \rightleftharpoons (UO_2)_3(OH)_7^+ + 7H^+$	–32.7	$UO_2^+ + 2H_2O \rightleftharpoons UO_2(OH)_2^- + 2H^+$	≈–23.6
$4UO_2^{2+} + 7H_2O \rightleftharpoons (UO_2)_4(OH)_7^+ + 7H$	–21.9	Uranium(III): Estimates from Cm(III) data	
		$U^{3+} + H_2O \rightleftharpoons UOH^{2+}$	–7.6
		$U^{3+} + 2H_2O \rightleftharpoons U(OH)_2^{2+}$	–15.7

[a] Estimates from Baes and Mesmer (1976).

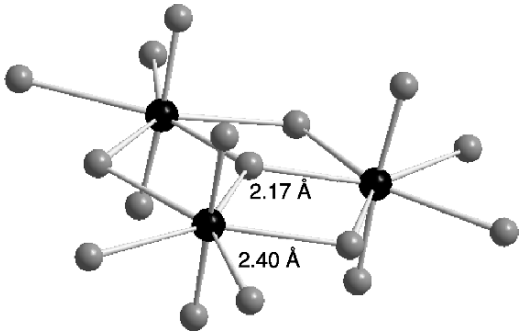

Fig. 5.65 *The structure of* $(UO_2)_3(O)(OH)_3^+$ (*from Åberg,* 1978). *The bond distance between uranium and the bridging oxide and hydroxide groups are* 2.17 Å *and* 2.40 Å, *respectively.*

Except at very low total concentrations of uranium, the polynuclear hydroxide complexes are predominant for all oxidation states, with the possible exception of U(v). There are no experimental data for U(iii), but its behavior can be estimated from the chemically analogous Cm(iii) ion, for which precise data are available.

The coordination chemistry of $U(OH)_4(aq)$ and $UF_4(aq)$ (Section 5.10.2c) deserves a comment. Because of the strong inductive effect of uranium on the dissociation of H^+ from coordinated water one would have expected the formation of anionic hydroxide complexes according to

$$U(OH)_4(H_2O)_n \rightleftharpoons U(OH)_5(H_2O)_{n-1}^- + H^+$$

if water is present in the first coordination sphere. However, there is no experimental indication of the formation of negatively charged hydroxide complexes even in 1 M hydroxide solutions. A coordination number of four is unlikely in view of the large ionic radius of U^{4+}. A possible resolution of this dilemma might be that the complex formulated as $U(OH)_4(aq)$ is a polymer, e.g. a tetramer $U_4(OH)_{16}$ with one of the A_4X_{16}-type structures (Wells, 1990, p. 201), where the coordination number of A, in this case uranium(iv), is six. Hydroxide and fluoride ions have similar size and often replace one another in solid-state structures. One might therefore expect that their coordination geometry is similar also in aqueous solution. However, $UF_4(aq)$ is not the limiting stoichiometry in aqueous solution where two negatively charged fluoride complexes UF_5^- and UF_6^{2-} have been identified (Table 5.34). This indicates a coordination number of at least six in the U(iv)–fluoride system, the same as the coordination number for $U(OH)_4(aq)$ if this has an $U_4(OH)_{16}$ structure. Polynuclear complexes, e.g. $U_4F_{16}(aq)$ do not form because of the poor bridging ability of fluoride in aqueous solution.

Table 5.34 *Stoichiometry and stability constants of uranium complexes of some common inorganic ligands at zero ionic strength and a temperature of* 25°C. *Data from Grenthe* et al. (1992) *and Guillaumont* et al. (2003). *The stability constants for U(III) have been estimated from the corresponding constants for Cm(III). Charges of the complexes have been deleted, to simplify notations.*

	$log\,\beta_n$			
Chemical reaction	$M \equiv UO_2^{2+}$	$M \equiv UO_2^{+}$	$M \equiv U^{4+}$	$M \equiv U^{3+}$
$M + F^- \rightleftharpoons MF$	5.1		9.3	~3.4
$M + 2F^- \rightleftharpoons MF_2$	8.6		16.2	
$M + 3F^- \rightleftharpoons MF_3$	10.9		21.6	
$M + 4F^- \rightleftharpoons MF_4$	11.7		25.6	
$M + 5F^- \rightleftharpoons MF_5$	11.5		27.0	
$M + 6F^- \rightleftharpoons MF_6$	–		29.1	
$M + Cl^- \rightleftharpoons MCl$	0.17		1.7	~0.24
$M + 2Cl^- \rightleftharpoons MCl_2$	–1.1			~–0.74
$M + NO_3^- \rightleftharpoons MNO_3$	0.3		1.5	
$M + SO_4^{2-} \rightleftharpoons MSO_4$	3.15		6.6	~3.3
$M + 2SO_4^{2-} \rightleftharpoons M(SO_4)_2$	4.14		10.5	~3.7
$M + PO_4^{3-} \rightleftharpoons MPO_4$	13.2			
$M + HPO_4^{2-} \rightleftharpoons MHPO_4$	7.2			
$M + H_2PO_4^- \rightleftharpoons MH_2PO_4$	1.12			
$M + CO_3^{2-} \rightleftharpoons MCO_3$	9.68			
$M + 2CO_3^{2-} \rightleftharpoons M(CO_3)_2$	16.9			
$M + 3CO_3^{2-} \rightleftharpoons M(CO_3)_3$	21.6	12.7		
$M + 4CO_3^{2-} \rightleftharpoons M(CO_3)_4$			35.1	
$M + 5CO_3^{2-} \rightleftharpoons M(CO_3)_5^{6-}$			34.0	

(c) Complexes between uranium and other inorganic ligands

Uranium(IV) and uranium(VI) form very strong fluoride complexes, while those formed with Cl^-, Br^-, and I^- are weak. There are no experimental data for halide complexes of U(V) and U(III); however, data from the chemically analogous Np(V) and Cm(III) indicate that they are all weak, the strongest being the fluoride complexes. The strength of complexes containing ligands with oxygen donors, such as sulfate, sulfite, phosphate, carbonate, silicate, and nitrate increases strongly with the charge and base strength of the ligand. However, complexes of the strongest bases such as $HSiO_4^{3-}$ and SiO_4^{4-} are difficult to study in aqueous solution because of competition from OH^- (and the formation of sparingly soluble hydrous oxides) at the high pH where these ions are present in significant amounts.

Strong complexes are also formed between UO_2^{2+} and the peroxide ion and the mode of coordination of the ligand is known from solid state structures (Fig. 5.56a and b). Examples of uranyl(VI) peroxide complex formation in solution have been given by Djogic and Branica (1992), Gurevich *et al.* (1971a,b), and

Moskvin (1968). However, most of the stability constants are uncertain (Sillén and Martell, 1971; NIST, 2004).

Ternary complexes of the type MA_qH_r may be formed when the ligand is the anion of a polyprotic acid.

The stoichiometry and equilibrium constants of uranium complexes of inorganic ligands are given in Table 5.34 where the data are taken from Grenthe *et al.* (1992) and Guillaumont *et al.* (2003). The structure of the complexes may be inferred from the known coordination geometry of the central uranium atom and from the structure of the ligand. However, quantitative information requires other methods, either X-ray or neutron diffraction data from solid compounds containing the ligands, or from EXAFS spectroscopy of solutions. It is interesting to note that the tetrahedral sulfate (Moll *et al.*, 2000b) and phosphate ions (Dusausoy *et al.*, 1996) rarely form chelates in solid compounds. In most cases the ligands are bonded either through a single oxygen donor, or act as a bridge between different uranium atoms (Figs. 5.51, 5.52, 5.57, and 5.58). In solution, however, EXAFS data indicate that the sulfate ion forms a bidentate chelate in $UO_2(SO_4)_2^{2-}$ and in ternary hydroxide–sulfate complexes (Moll *et al.*, 2000b) but not in UO_2SO_4(aq) (Neuefeind *et al.*, 2004a). On the other hand, carbonate invariably forms complexes where the ligand is chelate-bonded to uranium via two oxygen atoms (Fig. 5.66).

The data in Table 5.34 provide the experimental basis for describing uranium as a strong Lewis acid, or as a hard acceptor. Uranium also forms complexes of moderate stability with inorganic nitrogen donors like azide, N_3^-, and thiocyanate, SCN^- (Table 5.35). Uranium does not form ammine complexes in aqueous solution; ammines are strong bases and under the conditions where complexes might form the pH is so high that the stronger uranium hydroxide complexes predominate. However, N-donor complexes are found in organic ligands of various types, some examples are given in Table 5.36.

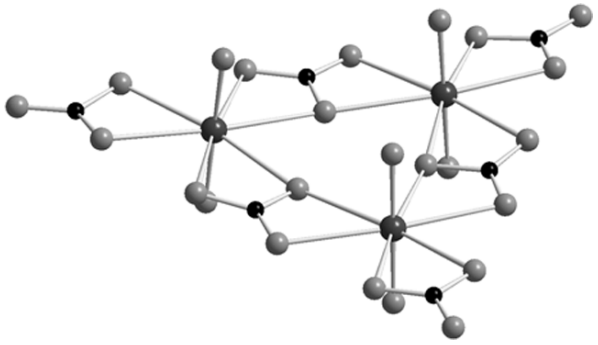

Fig. 5.66 *The structure of* $(UO_2)_3(CO_3)_6^{6-}$ *from Allen* et al. (1995). *Three terminal carbonate ligands form bidentate chelates and the remaining three act as bridges between the uranium atoms. The structure is closely related to that of* $UO_2(CO_3)_3^{4-}$ *containing three bidentate carbonate ligands.*

Table 5.35 *Equilibrium constants for uranium azide and thiocyanate complexes at zero ionic strength and a temperature of* 25°C. *Data from Grenthe* et al. (1992) *and Guillaumont* et al. (2003).

Chemical reaction	$log\,\beta_n$ $U(VI)$	*Chemical reaction*	$log\,\beta_n$ $M^{n+} \equiv U^{4+}$	$log\,\beta_n$ $M^{n+} \equiv UO_2^{2+}$
$UO_2^{2+} + N_3^- \rightleftharpoons UO_2N_3^+$	2.58	$M^{n+} + SCN^- \rightleftharpoons MSCN^{(n-1)+}$	1.4	2.97
$UO_2^{2+} + 2N_3^- \rightleftharpoons UO_2(N_3)_2$	4.3	$M^{n+} + 2SCN^- \rightleftharpoons M(SCN)_2^{(n-2)+}$	1.2	4.3
$UO_2^{2+} + 3N_3^- \rightleftharpoons UO_2(N_3)_3^-$	5.7	$M^{n+} + 3SCN^- \rightleftharpoons M(SCN)_3^{(n-3)+}$	2.1	–
$UO_2^{2+} + 4N_3^- \rightleftharpoons UO_2(N_3)_4^{2-}$	4.9			

(d) Complexes between uranium and some important organic ligands

Two groups of ligands will be discussed, those containing carboxylate functional groups alone and those containing in addition one or more hydroxy or amino/imino groups; the first group is exemplified by acetate and oxalate, and the second by glycolate, glycine, iminodiacetate, and ethylenediaminetetraacetate ($EDTA^{4-}$). The stoichiometry and stability constants for the corresponding UO_2^{2+} and U^{4+} complexes are listed in Table 5.36. There is no experimental information available for U(III) and the equilibrium constants have been estimated from corresponding data for trivalent lanthanides and other trivalent actinides. The first chemical issue to be discussed is the mode of bonding of the ligand; the stoichiometry and the magnitude of the stability constants provide some insight, but more precise information requires direct structure information, either from X-ray or neutron diffraction, EXAFS spectroscopy, or from quantum chemistry. The relative magnitude of the stepwise stability constants often gives indication of changes in the mode of bonding of the ligand and structural changes of the complexes. An example is the stepwise stability constants of oxalate complexes of U(VI) (Table 5.36). It is also tempting to relate the very small equilibrium constant for the reaction $U(CO_3)_4^{4-} + CO_3^{2-} \rightleftharpoons U(CO_3)_5^{6-}$ (Table 5.34) to a structural rearrangement from a trigonal bipyramid arrangement of the carbonate ligands in $U(CO_3)_5^{6-}$ with CN = 10, (Fig. 5.60), to a tetrahedral arrangement with CN = 8 in $U(CO_3)_4^{4-}$ (the carbonate ligand is modelled with a single point change). The small stability constant for $UO_2(Hgly)^{2+}$, where Hgly is the "zwitter-ion" form of glycine, $^+H_3NCH_2COO^-$ indicates that the ligand is bonded only at the carboxylate end.

The equilibrium constants for the glycine complexes also deserve a comment. The predominant form of glycine at pH < 8 is the zwitter-ion; this means that one has to take the possible formation of complex with the formally uncharged zwitter-ion into account, which has not always been done in the

Table 5.36 *Stability constants for complexes between U(VI), U(IV), and U(III), and some organic ligands; acetate (ac^-); glycolate/α-hydroxyactate (α-ac^-), oxalate (ox^{2-}), glycinate ($glyc^-$), iminodiacetate ($IMDA^{2-}$), ethylenediamine-tetraacetate ($EDTA^{4-}$). The equilibrium constants are taken from Smith and Martell* (1989). *For some of the reactions, we have tabulated the equilibrium constant for the corresponding Th(IV) and Ce(III) complexes that should be good models for U(IV) and U(III).*

Chemical reaction	$\log \beta_n$ $U(VI)$	*Chemical reaction*	$\log \beta_n$ $M^{n+} \equiv U^{4+}$	$\log \beta_n$ $M^{n+} \equiv U^{3+}$
$UO_2^{2+} + ac^- \rightleftharpoons UO_2(ac)^+$	2.44	$M^{n+} + ac^- \rightleftharpoons M(ac)^{n-1}$	3.9	1.9
$UO_2^{2+} + 2ac^- \rightleftharpoons UO_2(ac)_{22}$	4.42	$M^{n+} + 2ac^- \rightleftharpoons M(ac)_2^{n-2}$	6.9	3.1
$UO_2^{2+} + 3ac^- \rightleftharpoons UO_2(ac)_3^-$	6.43	$M^{n+} + 3ac^- \rightleftharpoons M(ac)_3^{n-3}$	9.0	3.7
$UO_2^{2+} + \alpha{-}ac^- \rightleftharpoons UO_2(\alpha{-}ac)^+$	2.72	$M^{n+} + 4ac^- \rightleftharpoons M(ac)_4^{n-4}$	10.3	
$UO_2^{2+} + 2\alpha{-}ac^- \rightleftharpoons UO_2(\alpha{-}ac)_2$	4.45	$M^{n+} + 5ac^- \rightleftharpoons M(ac)_5^{n-5}$	11.0	
$UO_2^{2+} + 3\alpha{-}ac^- \rightleftharpoons UO_2(\alpha{-}ac)_3^-$	5.70	$M^{n+} + \alpha - ac^- \rightleftharpoons M(\alpha - ac)^{n-1}$	4.4	2.7
$UO_2^{2+} + ox^{2-} \rightleftharpoons UO_2(ox)$	5.99	$M^{n+} + 2\alpha - ac^- \rightleftharpoons M(\alpha - ac)_2^{n-2}$	8.3	4.5
$UO_2^{2+} + 2ox^{2-} \rightleftharpoons UO_2(ox)_2^{2-}$	10.64	$M^{n+} + 3\alpha - ac^- \rightleftharpoons M(\alpha - ac)_3^{n-3}$	11.8	5.3
$UO_2^{2+} + 3ox^{2-} \rightleftharpoons UO_2(ox)_3^{4-}$	11.0	$M^{n+} + ox^{2-} \rightleftharpoons M(ox)^{n-2}$	8.8	4.9
$UO_2^{2+} + Hgly \rightleftharpoons UO_2(Hgly)^{2+}$	1.16	$M^{n+} + 2ox^{2-} \rightleftharpoons M(ox)_2^{n-4}$	16.8	8.3
$UO_2^{2+} + 2gly^- \rightleftharpoons UO_2(gly)_2^a$	13.0			
$UO_2^{2+} + IMDA^{2-} \rightleftharpoons UO_2(IMDA)$	8.75	$M^{n+} + 3ox^{2-} \rightleftharpoons M(ox)_3^{n-6}$	22.8	10.2
$UO_2^{2+} + HIMDA^- \rightleftharpoons UO_2(HIMDA)$	2.41	$M^{n+} + 4ox^{2-} \rightleftharpoons M(ox)^{n-8}$	27.2	11.7
$UO_2^{2+} + HEDTA^{3-} \rightleftharpoons UO_2(HEDTA)^-$	6.35	$M^{n+} + IMDA^{2-} \rightleftharpoons M(IMDA)^{n-2}$	9.7	6.2
		$M^{n+} + EDTA^{4-} \rightleftharpoons M(EDTA)^{n-4}$	25.7	15.9

[a] From Szabó and Grenthe (2000).

published studies. The corresponding complexes with gly^- are strong as indicated by $\log k = 13.0$ for the reaction $UO_2^{2+} + 2gly^- \rightleftharpoons UO_2(gly)_2(aq)$ (Szabó and Grenthe, 2000). Aliphatic nitrogen donors are strong bases and the competition between H^+ prevents coordination to uranium unless the pH is above 6. The interpretation of experimental results is then complicated by the possible formation of binary and ternary complexes containing hydroxide. Sessler *et al.* (2001) have reviewed complex formation between uranium and macrocyclic ligands; these complexes together with organometallic complexes of uranium are discussed in Chapter 25.

(e) Ternary uranium complexes

Most experimental studies of uranium complexes in aqueous solution have been made in two-component systems (metal ion and ligand). Accordingly, most of the published equilibrium constant data refer to binary M_pL_q complexes. However, in experimental studies performed in water one must also take the possibility of the formation of ternary $M_pL_q(OH)_r$ complexes into account. When the ligand is a polyprotic acid also species of the type $M_pL_qH_r$ may form (the phosphate complexes in Table 5.34). The 'proton ambiguity' referred to in the case of hydroxide complexes, cf. $(UO_2)_3(OH)_5^+$ vs. $(UO_2)_3(O)(OH)_3^+$), is also found in other cases, notably for polyprotic ligands. An example is the UO_2^{2+}–glycolate system where there is a large difference in the dissociation constants of the carboxylate and α-hydroxy group. When studying the complex formation with this ligand using potentiometric methods, it is not possible to distinguish between the following two reactions:

$$UO_2^{2+}(aq) + HOCH_2COO^- \rightleftharpoons UO_2(OCH_2COO) + H^+$$

and

$$UO_2^{2+}(aq) + HOCH_2COO^- + H_2O \rightleftharpoons UO_2(HOCH_2COO)(OH) + H^+$$

To decide on the stoichiometry of the complex formed, it is necessary to use other methods, e.g. NMR spectroscopy as discussed by Szabó *et al.* (2000) and Toraishi *et al.* (2003).

It is possible to use coordination chemical data to decide on the conditions where ternary complexes containing different ligands (except OH^- and protonated ligands) may form; Beck and Nagypál (1990) and Grenthe *et al.* (1997) have discussed this issue and point out that the strength of a ternary complex MA_qB_r depends strongly on the strength of the binary complexes MA_q and MB_r and the steric constraints imposed by metal ion and ligands. Hence, ternary complexes are not common even in multicomponent systems; most of them contain fluoride or hydroxide, both strong donors that do not impose large steric constraints on the second ligand. Table 5.37 gives examples of some ternary uranium(VI) complexes. Note that the presence of the strongly binding oxalate and carbonate ligands has only a moderate influence on the strength of

Table 5.37 *Stoichiometry and stepwise equilibrium constants for reactions of the type* $UO_2AF_r + F^- \rightleftharpoons UO_2AF_{r+1}$. *Charges have been omitted for simplicity. The data are from Aas* et al. (1998) *and refer to a* 1 M $NaClO_4$ *ionic medium at* 25°C. *For comparison* $\log K_q$ *for the stepwise formation of the binary complexes* $UO_2F_q^{2-q}$ *are* 4.54, 3.44, *and* 2.43, *respectively*.

	log K		
A	$UO_2A + F^- \rightleftharpoons UO_2AF$	$UO_2AF + F^- \rightleftharpoons UO_2AF_2$	$UO_2AF_2 + F^- \rightleftharpoons UO_2AF_3$
Oxalate	3.93	2.55	1.72
Carbonate	4.08	2.30	1.91

bonding of fluoride as compared to that in the binary fluoride system. Ternary uranium(IV) complexes containing hydroxide/oxide ligands are abundant both in solid state structures and in solution. An example of the latter is U(EDTA)$(OH)^-$, where the equilibrium constant for the reaction U(EDTA)(aq)+ $H_2O \rightleftharpoons$ U(EDTA)$(OH)^- + H^+$ is equal to $\log^* K = -9.3$ (Smith and Martell, 1989), indicating a very large decrease in the acid strength of coordinated water from that in U^{4+}(aq), where $\log^* K$ is equal to –0.54 (see Table 5.33).

(f) Complex formation between UO_2^+ and other cations

The lower effective nuclear charge on uranium (V) as compared to uranium(VI) in uranyl ions results in a correspondingly larger negative charge of the 'yl' oxygen atoms (Vallet *et al.* (2004a). Electrostatic interactions between the 'yl' oxygen in MO_2^+ and the high positive effective charge of M(VI) in MO_2^{2+} is probably the reason for the formation of weak cation–cation complexes between the two. Newton and Baker (1965) were first to identify these species for UO_2^+ and UO_2^{2+} and Sullivan *et al.* (1961) for NpO_2^+ and UO_2^{2+}; Frolov and Rykov (1979) have reviewed the field.

5.10.3 Reaction mechanisms of ligand substitution reactions

The analysis of the rate and mechanism of chemical reactions requires information on the experimental rate equation and the thermodynamics of the reaction studied; in addition the structure and coordination geometry of reactants, intermediates, and products provide important clues on the microscopic details of the reaction. The rate equation describes how the rate of reaction depends on the concentration of different chemical species in the reacting system, some of them may appear as reactants/products in the total (stoichiometric) reaction, but this is not always the case. The rate equation may be simple or complex depending on the mechanism; details on the analysis of rate equations are given in standard texts on chemical kinetics, e.g. Katakis and Gordon (1987), Wilkins (1991) and Espenson (1995). 'Mechanism' is defined as the sequence of

elementary reactions that transform the reactant(s) to product(s); these different steps can rarely be studied in isolation, but have to be inferred from the experimental rate equation and the activation parameters $\Delta H^{\neq}$, $\Delta S^{\neq}$, and $\Delta V^{\neq}$ of the reaction. The rate equation rarely provides a unique mechanistic model for a certain reaction: one reason is that it contains only stoichiometric information on the rate determining step and the fast equilibria preceding this, but no information on the fast reactions following the rate-determining step. The mechanism deduced from the rate equation is usually referred to as the *stoichiometric mechanism* of the reaction; the *intimate mechanism* describes the molecular details of a certain reaction, e.g. the timing of bond breaking and bond formation.

The information on rates and mechanisms of ligand substitution reactions in uranium complexes is limited and in general only includes information on rate equations, while the mechanistic discussions are much more speculative. Most experimental data refer to uranyl(VI) complexes where three reviews provide some details. Lincoln (1979) and Tomiyasu and Fukutomi (1982) have reviewed reactions that mostly take place in non-aqueous solvents, while Nash and Sullivan (1998) have reviewed the kinetics and mechanism of actinide redox and complexation reactions in aqueous solution. Vallet *et al.* (2004b) have discussed the combination of experimental and quantum chemical methods for the elucidation of the intimate mechanism of solvent exchange and ligand substitution in uranyl(VI) complexes.

Substitution reactions of simple unidentate ligands in uranium complexes are in general very fast and require special experimental methods (stopped-flow, temperature jump and other relaxation methods; NMR spectroscopy). Only the uranyl(VI) fluoride system has been studied in detail (Szabó *et al.*, 1996).

Most of the experimental studies of ligand substitution have been made using multidentate ligands. These reactions involve several elementary reactions, chelate ring opening/ring closure, and ligand dissociation/association steps. In addition, the ligands are often protolytes and the rate equation therefore depends on the hydrogen ion concentration. All these factors result in complicated rate equations from which it is difficult to deduce the reaction mechanism. The activation parameters, $\Delta H^{\neq}$, $\Delta S^{\neq}$, and $\Delta V^{\neq}$ (of which only the first two are known for reactions involving uranium) provide additional mechanistic information that in some cases can be corroborated by quantum chemical methods as will be described later. The ligand substitution reactions with multidentate ligands are conveniently followed using conventional stopped-flow spectrophotometric methods. Experiments of this type start from a system that is not in equilibrium and its evolution is then followed until equilibrium has been attained. In many cases the reaction has to be followed by using a color indicator and this introduces additional complications when deducing the reaction mechanism (Friese *et al.*, 2001).

A more direct method to obtain mechanistic information on ligand exchange reactions is to use NMR equilibrium dynamics with ^{1}H, ^{13}C, ^{17}O, and ^{19}F as the NMR-active nuclei. The use of ^{17}O-enriched UO_2^{2+} and ternary complexes

containing fluoride have been particularly useful as the high sensitivity and wide chemical shift scales of these nuclei makes it possible to study a very large range of exchange rates. A typical example is the exchange reaction

$$UO_2(H_2O)_5^{2+} + H_2O^* \rightleftharpoons UO_2(H_2O^*)_5^{2+} + H_2O$$

that was studied using proton-NMR in mixed water–acetone media by Ikeda *et al*. (1979a) and Bardin *et al*. (1998) and by ^{17}O-NMR in water by Farkas *et al*. (2000a). An analogous example is the exchange between dimethyl sulfoxide (DMSO) and $UO_2(DMSO)_5^{2+}$ in DMSO solvent that was studied by Ikeda *et al*. (1979b). It should be noted that the NMR methods give information on all reactions that contribute to the dynamics at the reaction center. Hence one can use one NMR-active ligand as a probe to provide information on the dynamics of other ligands that are not easily studied using NMR, an example is the use of ^{19}F-NMR to estimate of the rate of water exchange in $UO_2(oxalate)F(H_2O)_2^-$ and $UO_2(oxalate)F_2(H_2O)^{2-}$ (Szabó *et al*., 1997).

The range of rates that can be studied using NMR depends on the magnitude of the chemical shift between the NMR-active nuclei located in different exchanging sites, the larger the chemical shift the faster processes can be studied. The NMR method can be used in different ways: (a) as an analytical tool where the concentration is measured as a function of time. This method can only be used if the rate of exchange is slow in comparison with the time for measurement; (b) using magnetization transfer, which is a method appropriate for reactions with half-lives of a few seconds; (c) by measurement of the line-broadening which is the method for study of the fastest reactions. The NMR-active nuclei may be located in different chemical surroundings in the same complex allowing studies of intramolecular exchange, or located in different species, e.g. a complex and free ligand, making studies of intermolecular exchange possible. In order to provide accurate data the different sites must have similar concentrations.

It is often difficult, or impossible to use the NMR method to study the rate and mechanism of the formation of the first complex in systems where strong complexes are formed (Szabó *et al*., 1996) because the free ligand concentration is here very small. In these cases stopped-flow technique is a useful alternative; on the other hand, NMR spectroscopy is superior when studying the rate and mechanism of limiting complexes (Ikeda *et al*., 1984; Szabó *et al*., 1997). A summary of experimental kinetic data is given in Tables 5.38 and 5.39, and a general discussion of the mechanistic conclusions in the following section.

(a) Reaction mechanisms

The Eigen–Wilkins mechanism describes the stoichiometric mechanism for many ligand substitution reactions; it includes the following two steps where N denotes the coordination number:

$$[(H_2O)_N M]^{n+} + [(H_2O)L^-] \rightleftharpoons [(H_2O)_N M \ldots L]^{(n-1)} + H_2O \quad (1)$$

$$[(H_2O)_N M \ldots L]^{(n-1)+} \rightarrow [M(H_2O)_{N-1}L]^{(n-1)+} + H_2O \quad (2)$$

Table 5.38 *Rate constants at* 25°C *and activation enthalpies for water exchange in* $U^{3+}(aq)$, $U^{4+}(aq)$, *and* UO_2^{2+} (aq). *The rate constant for* U(III) *has been estimated from data on the trivalent lanthanides* (*Helm and Merbach,* 1999). *There is no experimental information on ligand exchange mechanisms in any actinide*(*V*) *species.*

Exchange reaction	k_{ex} (s^{-1})	*Activation enthalpy*, ($\Delta H^{\neq}$) (kJ mol^{-1})	*Activation entropy*, ($\Delta S^{\neq}$) (J K^{-1} mol^{-1})	*References*
$U(H_2O)_9^{3+} + H_2O^* \rightleftharpoons U(H_2O^*)_9^{3+} + H_2O$	$\approx 10^8$	–	–	Helm and Merbach (1999)
$U(H_2O)_9^{4+} + H_2O^* \rightleftharpoons U(H_2O^*)_9^{4+} + H_2O$	5.4×10^6	34	–16	Farkas *et al.* (2000b)
$UO_2(H_2O)_5^{2+} + H_2O^* \rightleftharpoons UO_2(H_2O^*)_5^{2+} + H_2O$; in water at 25°C	1.3×10^6	26	–40	Farkas *et al.* (2000a)
in water–acetone 1/4.38 at –70°C and at 25°C	3.6×10^2 9×10^5	42	12	Ikeda *et al.* (1979a)
In water–acetone 1/1.86 at –70°C and at 25°C	8×10^2 4.6×10^5	32	–30	Bardin *et al.* (1998)

Reaction (1) describes the formation of an outer-sphere ion pair; this is a fast diffusion controlled equilibrium reaction with equilibrium constants K_{os}. The second reaction is rate-determining with the rate constant k_2 (unit s^{-1}); it involves the substitution of water in the first coordination sphere of the metal ion with a ligand from the second coordination sphere. This situation may arise when L is a unidentate ligand, but also for polydentate ligands, when the rate of chelate ring-closure is fast. The rate equation deduced from the two elementary reactions is often approximated by the expression

$$\frac{-\mathrm{d}[M(H_2O)]}{\mathrm{d}t} = \frac{k_2 K_{os}[M(H_2O)][L]}{1 + K_{os}[L]} \cong k_2 K_{os}[M(H_2O)][L]$$

K_{os} is usually estimated using the Fuoss equation (Fuoss, 1958).

For reactions where the experimental rate equation has the form

$$\frac{-\mathrm{d}[M(H_2O)]}{\mathrm{d}t} = k_{obs}[M(H_2O)][L]$$

we have $k_{obs} = k_2 K_{os}$. The analysis of experimental rate data using the Eigen–Wilkins mechanism is described by Katakis and Gordon (1987) and Wilkins (1991). The intimate mechanism of the water–ligand exchange can be associative, A, dissociative, D, or of interchange type, I. The assignment is based on the identification of intermediates (A and D); if no intermediates are identified the reaction is classified as interchange (I) (Langford and Gray, 1965). The A intermediate has a higher and the D intermediate a lower coordination number

than that of the reactant; in both cases there are two transition states along the reaction pathway. As no intermediate is formed in the interchange mechanism there is only one transition state. A rate constant k_{obs}, that is largely independent on the chemical nature of the entering ligand, indicates that the reaction mechanism is of dissociative type; the rate constant that depends strongly on the entering ligand is a characteristic of an associative mechanism. Szabó *et al.* (1996) have discussed fluoride exchange reactions in $UO_2F_n^{2-n}$ complexes using the Eigen–Wilkins mechanism.

The accessible coordination number at the metal center is often an important indicator when selecting the reaction mechanism. The characteristic coordination number for U(VI) and U(V) is five, but complexes with coordination numbers four and six are not uncommon; also U(IV) and U(III) have variable coordination numbers (9 ± 1). Hence, the coordination number is of little value as a mechanistic indicator in these cases, as neither associative nor dissociative mechanisms can be excluded. The size and charge of the metal ion and the ligand are also important for the mechanism; large ligands cannot enter the first coordination sphere until room is available through the dissociation of water. If water dissociation is rate determining, the intimate mechanism of the ligand exchange is dissociative; if the entry of the ligand from the second coordination sphere is rate determining the mechanism is associative.The simplest and most fundamental of the exchange reactions takes place between the aqua ions and the water solvent and this rate is often an important indicator for the mechanism of ligand substitution reactions of the Eigen–Wilkins type.

(b) Rates and mechanism of water exchange

The rate of water exchange has been studied both by proton NMR line-broadening at low temperature in mixed water–acetone solvents and in water containing 1 M $NaClO_4$. A complicating factor in experiments of this type is that it is not possible to vary the concentration of water in a pure water solvent; this is possible in the mixed water–acetone solvent. In the latter case, however, the concentration changes are often so large that the interpretation of the experimental data is ambiguous. Rate constants and activation parameters for the water exchange reactions are given in Table 5.38.

Because of the fast rate of exchange it is not possible to identify intermediates in these reactions and the rate equation alone is not sufficient to make a mechanistic assignment. This can be obtained by comparing the experimental activation energy with those for the D, A, and I mechanisms (Scheme 5.1), obtained using quantum chemical methods to identify the pathway of lowest activation energy; this value can then can be compared with the experimental data (Vallet *et al.*, 2001, 2004b). The theoretical activation energy of the pathways D, A, and I are 74, 19, and 21 kJ mol^{-1}, respectively; the dissociative pathway can be ruled out because of its high activation energy, while both the A and I mechanisms are consistent with the experimental value,

Table 5.39 *Experimental rate constants and activation parameters for some ligand substitution and ligand exchange reactions in aqueous uranyl(VI) systems studied by NMR and stopped-flow methods. The NMR experiments have been made in equilibrium systems where the rates of the forward reaction and the reverse reaction are equal. The stopped-flow experiments have been made under non-equilibrium conditions. The reactions in the table are in some cases elementary reactions; in other cases the mechanism is more complex and involves consecutive and/or parallel reactions. The ligand notation is: acetate ≡ ac; oxalate ≡ ox; picolinate ≡ pic; i-pentyl- picolinate ≡ i-pent-pic; 5-nitro-picolinate ≡ NO_2-pic; dipicolinate ≡ dipic; oxydiacetate ≡ oda. The following notation is used for the different fluoride ligands:* [a] *central fluoride,* [b,c] *edge fluorides. The rate constant in the forward and reverse directions is denoted +1 and –1, respectively; k_{ex} denotes an exchange reaction without net chemical change.*

Reaction	k_{obs} (s^{-1})	$\Delta H^{\neq}$ (kJ mol^{-1})	$\Delta S^{\neq}$ (J K^{-1} mol^{-1})	*References*
	NMR data at –5°C			
$UO_2(ac)F_3^{2-} + ac^{-*} \rightleftharpoons$ $UO_2(ac^*)F_3^{2-} + ac^-$	$k_1 = 2 \times 10^3$ s^{-1} $k_{-1} = 2.5 \times 10^4$ $M^{-1}s^{-1}$	–	–	Aas *et al.* (1999)
$UO_2(ac)_3^- \rightleftharpoons UO_2(ac)_2 + ac^-$	$k_1 = 2.7 \times 10^3$ s^{-1} $k_{-1} = 3.8 \times 10^5$ M^{-1} s^{-1}	22 ± 3	-61 ± 9	Aas *et al.* (1999)
$UO_2CO_3F_3^{3-} + F^{-*} \rightleftharpoons$ $UO_2CO_3F_3^{*3-} + F^-$	$k_{ex} = 14.2 \pm 2.1$[a,b,c] s^{-1}	53.7 ± 1.6	-15.7 ± 0.8	Szabó and Grenthe (1998)
$UO_2CO_3F_3^{3-} + C^*O_3^{2-} \rightleftharpoons$ $UOC^*O_3F_3^{3-} + CO_3^{2-}$	$k_{ex} = 8$ s^{-1} at pH 8.5	–	–	
$UO_2(pic)F_3^{3-} + F^{-*} \rightleftharpoons$ $UO_2(pic)F^{*3-}_3 + F^-$	$k_{ex} = 24.4 \pm 0.6$[a] s^{-1}; $k_{ex} = 12.8 \pm 0.3$[b,c] s^{-1}	61.4 ± 1.6	14.6 ± 0.5	Szabó and Grenthe (1998)
$UO_2(i\text{-pent-pic})F_3^{3-} + F^{-*} \rightleftharpoons$ $UO_2(i\text{-pent-pic})F^{*3-}_3 + F^-$	$k_{ex} = 18.2 \pm 1.8$[a] s^{-1} ; $k_{ex} = 13.9 \pm 1.1$[b,c] s^{-1}	59.7 ± 1.2	10.4 ± 0.8	
$UO_2(NO_2\text{-pic})F_3^{3-} + F^{-*} \rightleftharpoons$ $UO_2(NO_2\text{-pic})F^{*3-}_3 + F^-$	$k_{ex} = 16.0 \pm 1.2$[a,b,c] s^{-1}	60.3 ± 2.6	14.6 ± 0.6	
$UO_2(pic)F_3^{3-} + pic^{-*} \rightleftharpoons$ $UO_2(pic*)F_3^{3-} + pic^-$	$k_{ex} = 4.7 \pm 0.2$ s^{-1}	56.2 ± 4.2	-16.3 ± 1.2	
$UO_2(NO_2\text{-pic})F_3^{3-} + NO_{2-}$ $pic^{-*} \rightleftharpoons UO_2(NO_2\text{-}pic^*)F_3^{3-}$ $+NO_2\text{-}pic^-$	$k_{ex} = 55$ s^{-1}	59.4	11.3 ± 0.4	

	picolinate ring rotation			
pic	k_{ex}=300 s^{-1}	40.1 ± 2.4	–46.7 ± 2.8	Szabó and Grenthe (1998)
i-pent- pic	k_{ex} = 90 s^{-1}	46.8 ± 1.5	–32.8 ± 1.0	
NO_2-pic	k_{ex} = 2060 s^{-1}	49.6 ± 3.4	3.3 ± 1.2	
$UO_2(ox)F_3^{4-} + F^{-*} \rightleftharpoons$ $UO_2(ox)F^{*4-}_3 + F^-$	$k_{ex} = 21.6 \pm 2.4^{a,b,c}$ s^{-1}	58.9 ± 3.4	12.4 ± 1.0	Szabó and Grenthe (1998)
(In D_2O)	$k_{ex} = 14.1 \pm 0.8^{a,b,c}$ s^{-1}	60.4 ± 2.0	18.9 ± 0.6	
$UO_2(ox)F_3^{4-} + ox^{2-*} \rightleftharpoons$ $UO_2(ox^*)F_3^{4-} + ox^{2-}$	k_{ex} = 6.2 ± 0.2 s^{-1}	70.2 ± 5.6	23.1 ± 1.8	
$UO_2(ox)F(H_2O)_2^- + H_2O^* \rightleftharpoons$ $UO_2(ox)F(H_2O^*)_2^- + H_2O$	$k_{ex} = 1.6 \times 10^4$ s^{-1}	45.4 ± 3.8	–11.3 ± 0.5	Szabó *et al*. (1997) Farkas *et al*. (2000)
$UO_2(ox)F_2(H_2O)_2^- + H_2O^* \rightleftharpoons$ $UO_2(ox)F_2(H_2O^*)^{2-} + H_2O$	$k_{ex} = 1.6 \times 10^3$ s^{-1}			Szabó *et al*. (1997)
$UO_2(ox)_2F_3^- + F^{-*} \rightleftharpoons$ $UO_2(ox)_2F^{*3-} + F^-$	k_{ex} = 12.3 ± 1.0 s^{-1}	40.8 ± 2.0	–74.8 ± 3.6	Szabó and Grenthe (1998)
		47.1 ± 2.6	–56.3 ± 3.2	
(In D_2O)	8.7 ± 1.5 s^{-1}	42.0 ± 3.4	–73.3 ± 5.8	
$UO_2(ox)_2F^{3-} + ox^{2-*} \rightleftharpoons$ $UO_2(ox^*)_2F^{3-} + ox^{2-}$				
$UO_2(ox)_2(H_2O)^{2-} + ox^{2-*} \rightleftharpoons$ $UO_2(ox^*)_2(H_2O)^{2-} + ox^{2-*}$	$k_{ex} = 1.6 \times 10^3$ s^{-1}	31 ± 2	–56 ± 5	Aas *et al*. (1999)
$UO_2^{2+} + SO_4^{2-} \rightleftharpoons UO_2SO_4$	$k_1 = 3.4 \times 10^3$ M^{-1} s^{-1} $k_{-1} =$ 80 s^{-1}			Moll *et al*. (2000b)
$UO_2F_4(H_2O)^{2-} + F^- \rightleftharpoons UO_2F_5^{3-}$	$k_1 \approx 4 \times 10^3$ M^{-1} s^{-1} $k_{-1} = 6.5 \times 10^3$ s^{-1}			Vallet *et al*. (2002)
	stopped-flow data at 25°C μ = 0.10 M			
$UO_2^{2+} + dipic^{2-} \rightleftharpoons UO_2(dipic)$;		47.3 ± 2.6	–39 ± 9	Friese *et al*. (2001)
pH = 1.0	$k_1 = 0.94 \times 10^3$ M^{-1} s^{-1} $k_{-1} = 0.74$ s^{-1}	62.4 ± 1.6	–41 ± 6	
pH = 3.0	$k_1 = 3.21 \times 10^3$ M^{-1} s^{-1}	55.3 ± 1.3	6 ± 4	
	$k_{-1} = 0.38$ s^{-1}	57.1 ± 9.1	–61 ± 31	
$UO_2^{2+} + oda^{2-} \rightleftharpoons UO_2(oda)$;	$k_1 = 3.4$ M^{-1} s^{-1}	62.1 ± 2.8	–27 ± 9	Friese *et al*. (1998)
pH = 3.0	$k_{-1} = 0.43$ s^{-1}	58.0 ± 1.2	–57 ± 4	

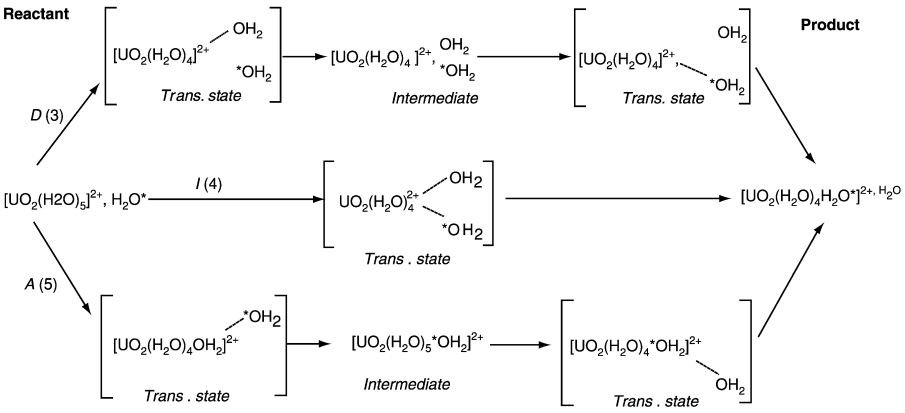

Scheme 5.1 *The scheme shows the dissociative* (*D*), *associative* (*A*) *and interchange* (*I*) *pathways for the water exchange between* $UO_2(OH_2)_5^{2+}$ *and water solvent from Vallet* et al. (2001) (*by permission of the American Chemical Society*).

$\Delta H^{\neq} = 26$ kJ mol^{-1}. The small difference in activation energy between these two pathways is understandable from the very similar structures of their transition states (Fig. 5.67a and b).

There are no experimental water exchange data for

$$UO_2(H_2O)_5^+ + H_2O^* \rightleftharpoons UO_2(H_2O^*)_5^+ + H_2O$$

However, the reaction has been studied using quantum chemical methods (Vallet *et al.* 2004a). In this system no stable intermediate $UO_2(H_2O)_6^+$ was found, hence the reaction cannot be associative. It was only possible to identify the reaction pathway for the dissociative mechanism with the electronic activation energy $\Delta E^{\neq} = 36.4$ kJ mol^{-1}. As judged by the activation energy one would expect the rate of water exchange to be slower in the uranyl(v) aquo-ion than that for the A/I mechanisms of the uranyl(vi) ion. However, the rate of reaction is determined by the Gibbs energy of activation, $\Delta G^{\neq} = \Delta H^{\neq} (\approx \Delta E^{\neq}) - T\,\Delta S^{\neq}$, where the activation entropy is larger for the D than for the A/I reactions (Wilkins, 1991, p. 202). Hence it is a reasonable assumption that the rate of water exchange in $UO_2(H_2O)_5^+$ is not too different from that in $UO_2(H_2O)_5^{2+}$.

The rate of water exchange and the activation energy for the reaction

$$U(H_2O)_n^{4+} + H_2O^* \rightleftharpoons U(H_2O^*)_n^{4+} + H_2O$$

has been determined experimentally (Farkas *et al.*, 2000b). The coordination number n is probably (9 ± 1), the rate constant 5.4×10^6 s^{-1} at 298 K and the activation enthalpy 34 kJ mol^{-1}. From the experimental data alone, it is not possible to determine the reaction mechanism. However, a quantum chemical study by Yang *et al.* (2003) of the water exchange in the corresponding thorium system indicates that the water exchange between $Th(H_2O)_9^{4+}$ and the water

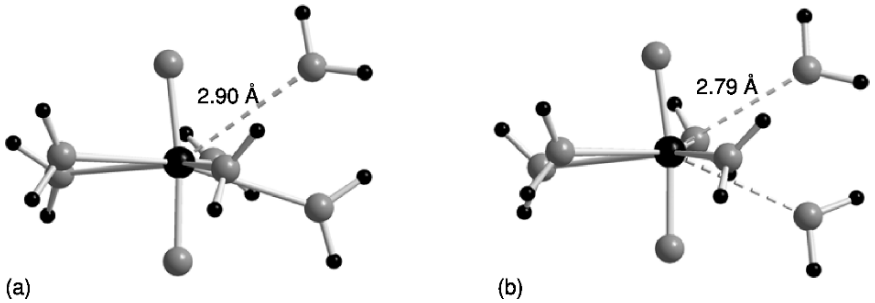

Fig. 5.67 (*a*) *Transition state in the A mechanism for the water exchange in the uranyl(VI) aqua ion. The geometry of the intermediate is very close to that of the I transition state*; *the bond distance in the entering and leaving water molecules are both* 2.65 Å. (*b*) *Transition state in the I mechanism. The U–H_2O distance for the two ligands above and below the equatorial plane in the I transition state is* 2.79 Å.

solvent takes place through an associative mechanism; from this we suggest that the mechanism is the same also for $U(H_2O)_9^{4+}$.

There are no experimental data for ligand exchange reactions in U(III) complexes, but Helm and Mehrbach (1999) have made extensive studies of the water exchange reactions of the trivalent lanthanides that are chemically very similar to the trivalent actinides. Based on these data, one expects the substitution mechanisms on U(III) to be similar to the nine-coordinated early lanthanides and to follow a dissociative mechanism.

(c) Water exchange in uranyl(VI) and uranium(IV) complexes

It is often assumed that the rate of water exchange at metal complexes is larger than that of the corresponding aqua ions. This does not seem to be the case for uranyl(VI) complexes as shown by the rate constant of water exchange in $UO_2(oxalate)F(H_2O)_2^-$ and $UO_2(oxalate)F_2(H_2O)^{2-}$, that are approximately 2×10^3 s^{-1} (Table 5.39); this is much smaller than that of $UO_2(H_2O)_5^{2+}$ ($k_{ex} = 1.3 \times 10^6$ s^{-1}; Szabó *et al.*, 1997). The rate constant of water exchange in $UF(H_2O)_8^{3+}$ is not significantly different from that in $U(H_2O)_9^{4+}$ (Farkas *et al.*, 2000b).

(d) Rates and mechanisms of complex formation reactions with inorganic and organic ligands

The rates and mechanisms of complex formation reactions have been studied both in equilibrium systems using NMR methods and in non-equilibrium systems using mainly stopped-flow and relaxation methods. In the former case the reactions are typically

$$ML_n + L^* \rightleftharpoons ML_n^* + L;$$

The rate constants in the forward and reverse directions are denoted k_1 and k_{-1}, respectively; as the system is in equilibrium the *rates* in the forward and reverse directions are the same. This is not the case in the non-equilibrium reactions where one often can arrange the experimental conditions so that the reverse reaction can be neglected; that is the reactions studied are of the type

$$ML_n + L \rightarrow ML_{n+1}$$

Some examples of experimental data, rate constants, and activation parameters are given in Table 5.39. The rate equations and reaction mechanisms have been deduced by investigating how the reaction rate depends on the concentration of reactants, products, and catalysts like H^+. The mechanistic deductions are complicated for multidentate ligands that in general are moderately strong bases; the rate of reaction is therefore often strongly dependent on the pH. Hines *et al*. (1993), Ekstrom and Johnson (1974), and Pippin and Sullivan (1989) give examples of such systems using the ligands diphosphonic acids and 4-(2-pyridylazo) resorcinol. However, the mechanisms of these reactions are far from clear. The rates of exchange for the ligands in Table 5.39 have been studied in more detail and some general comments about rate constants and mechanisms can therefore be made.

The rate of dissociation of coordinatively saturated complexes varies strongly with the strength of the complexes, e.g. from 2.7×10^3 s^{-1} for the acetate exchange in $UO_2(acetate)_3^-$ to 0.38 s^{-1} for the rate of dissociation of UO_2(dipicolinate); the latter ligand forms a very strong three-dentate chelate complex. The rate of formation and dissociation of UO_2(dipicolinate) and $UO_2(CO_3)F_3^{3-}$ are proton-catalyzed; the same is certainly the case for UO_2(oxydiacetate), but here there is only experimental data at one pH.

For multidentate ligands the mode of coordination is not always known and it is also unlikely that the formation or dissociation of such complexes takes place in one step. Hence, the experimental rate equation does not provide information on the rate-determining step. Some information may be obtained using the Eigen–Wilkins mechanism as exemplified by the rate constant for the formation of UO_2(dipicolinate) and UO_2SO_4. Both rate constants have nearly the same value (Table 5.39) indicating that the reaction is not strongly dependent on the entering ligand; this is a typical feature of dissociative reactions where the rate of water dissociation from the first coordination sphere is rate-determining. However, in the Eigen–Wilkins mechanism the experimental rate constant is a product of the rate of water exchange and the equilibrium constant for the formation of an outer-sphere complex with the entering ligand. A crude estimate of K_{os} for sulfate and dipicolinate is 5–50 M^{-1}, which would correspond to a rate constant for the water dissociation equal to $(0.7–0.07) \times 10^3$ s^{-1}. This is very different from the experimental value for the water exchange, indicating that the mechanism is more complex, suggesting that the rate of chelate ring closure/ring opening might have a significant effect on the rate of

formation/dissociation of the complexes. Hurwitz and Kustin (1967) have studied the rate and mechanism of reactions between UO_2^{2+} and SO_4^{2-}, SCN^-, CH_3COO^-, and $ClCH_2COO^-$ using the temperature jump method. The rate of complex formation with sulphate is 180 M^{-1} s^{-1} at 20°C, very different from the value obtained by Moll *et al.* (2000b) using NMR. This is not an ionic strength effect that would result in a larger rate constant at lower ionic strength (Wilkins, 1991, p. 110). The bimolecular rate constants for the formation of the 1:1 complex between UO_2^{2+} and actate and monochloracetate are 1050 and 110 M^{-1} s^{-1}. Hurwitz and Kustin (1967) note that the most significant feature of their observations is the relative slowness of the substitution reactions and their strong ligand dependence. This indicates that the substitution reactions are associative.

Jung *et al.* (1988) have determined the rate and mechanism of the formation and decomposition of the binuclear hydroxide complex $[(UO_2)_2(OH)_2]^{2+}$. The rate is sufficiently slow so that NMR line broadening of $U^{17}O_2^{2+}$ can be used. The rate equation is

$$\text{Rate} = k_2[UO_2^{2+}][UO_2OH^+] - k_{-2}K_a[H^+][(UO_2)_2(OH)_2^{2+}]/2$$

where K_a is the equilibrium constant for the reaction $(UO_2)_2(OH)_2^{2+} + H^+ \rightleftharpoons (UO_2)_2(OH)^{3+} + H_2O$. The suggested mechanism consists of two steps:

$$UO_2^{2+}UO_2OH^+ \rightleftharpoons (UO_2^{2+} \ldots UO_2(OH^+) \rightarrow [UO_2 - (OH) - UO_2]^{3+}$$

that are followed by the fast reaction

$$(UO_2)_2(OH)^{3+} + H_2O \rightleftharpoons (UO_2)_2(OH)_2^{2+} + H^+.$$

The first step is the formation of an outer-sphere ion pair and the second is rate determining. The estimated rate constant for this step is 7.6×10^5 s^{-1}, close to the rate of water exchange in the aqua ion. Frei and Wendt (1970) have studied the rate of dissociation of the binuclear complex using the stopped-flow method and also they suggested a mechanism where a single OH-bridged intermediate is formed.

Ligand exchange between a limiting complex (the complex with the largest number of coordinated ligands) and free ligand is most conveniently studied by using NMR methods. A typical example is the rate of ligand exchange for the reaction

$$UO_2F_5^{3-} + {}^*F^- \rightleftharpoons UO_2{}^*F_5^{3-} + F^-$$

As one reactant is a coordinatively saturated complex it is unlikely that the ligand exchange takes place according to an associative mechanism. It also turns out that the rate of ligand exchange for the above and many other reactions involving limiting complexes is independent on the concentration of free ligand, confirming that the exchange mechanism is dissociative (Vallet *et al.*, 2002). This result is supported by quantum chemical calculations, which

demonstrate that there is no stable intermediate $UO_2F_6^{4-}$ (Ikeda *et al.*, 1984; Szabó *et al.*, 1997; Vallet *et al.*, 2002).

(e) Mechanisms of intramolecular reactions

Important examples within this group are chelate ring opening/ring closure reactions, exemplified by the complex UO_2(picolinate)F_3^{2-}, (Fig. 5.68) (Szabó *et al.*, 1997; Vallet *et al.*, 2004b) and the experimental data in Table 5.39. In this complex there are three non-equivalent fluoride ligands, F_A, F_B and F_C, as shown in the ^{19}F NMR spectrum. The central peak, F_C, is narrow, indicating a slow exchange on the NMR time-scale while the other two peaks are broad, corresponding to a rate constant of 300 s^{-1} for the exchange between the F_A and F_B sites. This exchange is a result of an intramolecular process as the intermolecular exchange between coordinated and free fluoride is much slower, k_{obs} = 13 s^{-1} for F_A and F_B and 24 s^{-1} for F_C. The intramolecular exchange between F_A and F_B is the result of a a chelate ring opening/closure reaction that results in a rotation of the picolinate ligand and an exchange of the F_A and F_B sites The rate of exchange for the intermolecular exchange of picolinate is much slower, 4.7 s^{-1}.

The exchange between the different isomers of UO_2(picolinate)$_2F^-$ (Fig. 5.69) probably also takes place through a ring opening/ring closure reaction; a similar reaction mechanism has also been proposed for the kinetics of intra- and

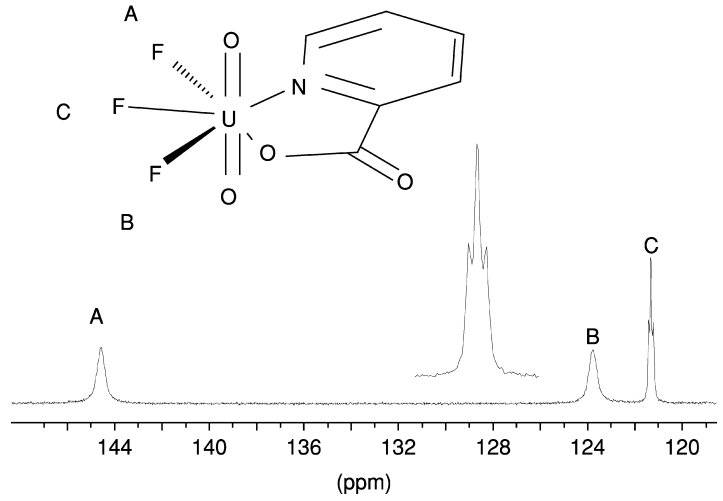

Fig. 5.68 *The ^{19}F NMR spectrum of UO_2(picolinate)F_3^{2-} at –5°C showing peaks for the three different fluorides (from Szabó* et al. *(1997), reproduced by the permission of American Chemical Society). There is no visible spin–spin coupling in the exchanged broadened peaks for fluorides A and B. Spin–spin coupling, a collapsed doublet of doublets, is evident in the narrow peak C, cf. the insert.*

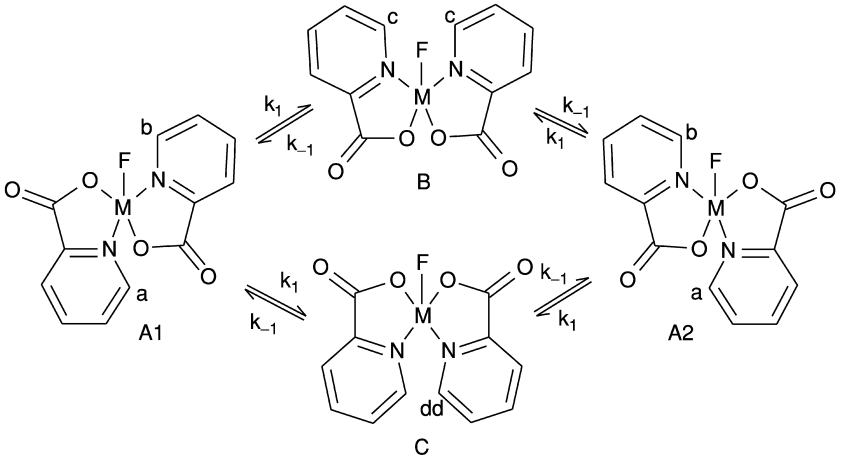

Fig. 5.69 *Different isomers of the complex* $UO_2(picolinate)_2^{F-}$ *and the possible exchange pathways between them* (*from Szabó* et al. (1997), *reproduced by the permission of American Chemical Society*). *The exchange presumably takes place through chelate ring opening/ring closure reactions.*

intermolecular exchange reactions of nonamethyl-imidodiphosphoramide (NIPA) in $UO_2(NIPA)_3^{2+}$ (Bokolo *et al.*, 1981).

Intramolecular reactions of the type encountered in $UO_2(picolinate)_2F^-$ do not necessarily proceed through chelate ring opening/ring closure as exemplified by $UO_2(acac)_2L$, in Fig. 5.70, where acac is a β-diketonate like acetylacetonate or dibenzoylmethanate and L an uncharged ligand such as dimethylsulfoxide (DMSO) (Ikeda *et al.*, 1984). The two methyl groups in the acetylacetone ^{13}C NMR spectrum are equivalent at room temperature due to fast exchange, but not at low temperature. The rate of intermolecular exchange between coordinated and free acac is slow and the fast exchange between the two methyl groups is therefore not the result of chelate ring opening/ring closure but of the fast dissociation/reentry of the ligand L that also results in exchange between the methyl groups (Fig. 5.70); the chelate ring opening is a very slow reaction.

Kramer and Maas (1981) have studied the fluxionality in U(VI) complexes of trifluoroacetylacetonate and various uncharged bases and suggest that the fluxionality of the complexes is a result of an intramolecular base migration; however, it is difficult to envisage that such a reaction is geometrically feasible.

(f) Rate and mechanism of ligand exchange in non-aqueous systems

The proposed mechanisms and activation parameters for ligand exchange in uranyl(VI) complexes between a number of uncharged ligands in non-aqueous systems are given in Table 5.40. The experimental rate constant k_{obs} for many of the reactions is given by

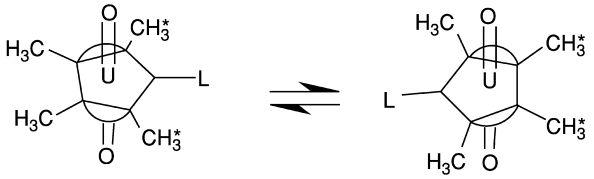

Fig. 5.70 *Ligand exchange in acetylacetonato complex $UO_2(acac)_2L$. The methyl groups in the coordinated acetylacetonate are non-equivalent as a result of their different chemical surroundings. The two sites are in fast exchange at room temperature as a result of the fast dissociation/re-entry of the ligand L.*

$$k_{obs} = k_1 + k_2[L],$$

where [L] is the free ligand concentration. In most systems k_2 is equal to zero, indicating a dissociative mechanism as seen in Table 5.40. When $k_2 \neq 0$ the rate of exchange depends on the ligand concentration, indicating an associative pathway. The difference in exchange mechanism for water (associative or associative interchange mechanism) and the dissociative pathway for the ligands in Table 5.40 is probably due to the larger steric constraints for the latter ligands. The occurrence of two parallel pathways, e.g. for DMSO indicates that the energy difference between complexes with four-, five-, and six-coordinated DMSO ligands is small. It is worth noting that there is no connection between the suggested mechanisms and the activation entropy for these reactions that all involve an uncharged ligand.

(g) Rate and mechanism of 'yl'-oxygen exchange in uranyl(VI) and uranyl(V) complexes: isotope exchange reactions

The rate of exchange between the 'yl'-oxygen atoms in $UO_2^{2+}(aq)$ and the water solvent is very slow, the half-life is 5000 to 10000 h as demonstrated by Gordon and Taube (1961a) using ^{18}O-enriched uranyl(VI). They noticed that the rate of exchange depends on the hydrogen ion concentration and that the reaction was photo-catalyzed. The fact that the exchange is very fast in the photo-excited state of the uranyl(VI) aqua ion (Bell and Buxton, 1974) has been used to prepare uranyl(VI) complexes where the 'yl'-oxygens are isotope-enriched in ^{17}O or ^{18}O (Howes *et al.*, 1988). The rate of exchange of the 'yl'-oxygens and the water solvent is strongly catalyzed by $UO_2^+(aq)$ (Gordon and Taube, 1961b). These two observations indicate that the exchange is related to the weakening of the $U–O_{yl}$ bond. In the photo-excited state, this is the result of transfer of a bonding electron to an empty f-orbital, and in $UO_2^+(aq)$ from the f-electron that is localized in a nonbonding f-orbital (Vallet *et al.*, 2004a). There are few precise and reproducible experimental observations and the mechanism for the exchange reaction has therefore not yet been clarified. Gordon and Taube (1961b) suggested that the rate law for the UO_2^+-catalyzed exchange

Table 5.40 *Mechanisms and activation parameters for the exchange of monodentate uncharged ligands, L, in the uranyl(VI) complexes $UO_2L_5^{2+}$ and $UO_2L_4^{2+}$. The solvent is deuterated acetone or dichloromethane. The ligands are: dimethylsulfoxide (DMSO), N,N,-dimethylacetamide (DMA), trimethylphosphate (TMP), triethylphosphate (TEP), N-methylacetamide (NMA), diethylphosphate (DEP), tetramethylurea (TMU), and hexamethylphosphoramide (HMPA).*

Complex	*Solvent*	*Mechanism*	$\Delta H^{\neq}$ (kJ mol^{-1})	$\Delta S^{\neq}$ (J K^{-1} mol^{-1})	*References*
$UO_2(DMSO)_5^{2+}$	CD_3COCD_3	D	39	–48	Honan *et al.* (1978); Ikeda *et al.* (1979b)
		D	54	6	
		A	39	–28	
$UO_2(DMA)_5^{2+}$	CD_2Cl_2	D	43	–44	Bowen *et al.* (1976)
$UO_2(TMP)_5^{2+}$	"	D or I_d	25	–110	Crea *et al.* (1977)
$UO_2(TEP)_5^{2+}$	"	D or I_d	44	–48	Crea *et al.* (1977)
$UO_2(NMA)_5^{2+}$	"	D	67	45	Honan *et al.* (1979)
$UO_2(DEP)_5^{2+}$	"	D	32	–54	Bowen *et al.* (1979)
$UO_2(TMU)_5^{2+}$	"	D	80	85	Ikeda *et al.* (1979b)
$UO_2(HMPA)_5^{2+}$	"	D	14	–172	Honan *et al.* (1978)
		A	22	–120	

$U^*O_2^{2+} + H_2O \rightleftharpoons UO_2^{2+} + H_2{}^*O$ is first order in $[UO_2^+]$ and suggest the mechanism

$$UO_2^+ + H_2{}^*O \rightleftharpoons U^*O_2^+ + H_2O$$

$$U^*O_2^+ + UO_2^{2+} \rightleftharpoons U^*O_2^{2+} + UO_2^+$$

where the first reaction is assumed to be fast, but the details of the oxygen exchange are not known and quantum chemical studies, similar to those of Schreckenbach *et al.* (1998) and Clark *et al.* (1999) on UO_2^{2+}, have not been made to our knowledge. Howes *et al.* (1988) have studied the second reaction and use the experimental data, in combination with the Marcus' cross-relations, to estimate the rate constant for the outer-sphere self-exchange to be in the range 1–15 M^{-1} s^{-1}, a value that is in good agreement with quantum chemical estimates by Privalov *et al.* (2004).

There are a number of other experimental studies of exchange between uranyl (VI) complexes and water, using ^{17}O-enriched uranyl(VI). This exchange is pH-dependent and much faster than in the $UO_2^{2+}(aq)$. The half-life is less than 1 h in the pH range where polynuclear complexes containing hydroxide/oxide bridges are present (Moll *et al.*, 2000b); the rate of exchange is much slower in $UO_2(OH)_4^{2-}$ and $UO_2(OH)_5^{3-}$ and very slow in limiting complexes that do not contain water or hydroxide in the first coordination sphere. Schreckenbach *et al.* (1998) and Clark *et al.* (1999) have discussed the mechanism, however the estimated activation energy seems large (160 kJ mol^{-1}).

(h) Isotopic exchange reactions involving uranium

Isotopic exchange using ^{233}U as a probe has been used to study the rate and mechanism of exchange reactions between UO_2^{2+}, UO_2^{+}, and U^{4+}. These studies have been made in acid solutions where the degree of hydrolysis is known. The exchange can take place either through bond breaking/bond formation or through electron transfer. The following exchange reaction is a typical example (Rona, 1950; Masters and Schwartz, 1961):

$$U^{4+}(aq) + {}^{*}UO_2^{2+}(aq) + 2H_2O \underset{k_r}{\overset{k_f}{\rightleftharpoons}} 2{}^{*}UO_2^{+}(aq) + 4H^{+}$$

where *U denotes uranium enriched in ^{233}U. The reaction follows two parallel pathways where the rate of exchange for the forward reaction at [U(IV)] < 0.01 M is equal to

$$\text{Rate} = k_f[U^{4+}][UO_2^{2+}][H^{+}]^{-3} \quad \text{with } k_f = 2.1 \times 10^{-7}\ \text{M}^{-1}\ \text{s}^{-1} \text{ at } 25^{\circ}\text{C}$$

Imai (1957) studied the rate for the reverse reaction and found

$$\text{Rate} = k_r[UO_2^{+}]^2[H^{+}] \quad \text{with } k_r = 436\ \text{M}^{-2}\ \text{s}^{-1} \text{ at } 25^{\circ}\text{C}$$

The ratio $k_r/k_f = 2 \times 10^9\ \text{M}^4$ is in good agreement with the experimental equilibrium constant $1 \times 10^9\ \text{M}^4$, indicating that both reactions have the same transition state. A slightly lower value of $k_r \approx 130$, was determined by Kern and Orleman (1949). The rate of exchange of the forward reaction is slow because it goes thermodynamically 'uphill', a result of the extensive bond breaking/bond formation during the exchange. The reverse reaction is fast because the reaction is now thermodynamically favored.

The intimate mechanism for most isotope exchange reactions is not known; for the U(IV)–U(V)–U(VI) reaction there is only information on the stoichiometry of the activated complex, $[HOUOUO_2^{3+}]^{\neq}$ and the activation energy 157 kJ mol^{-1}. At U(IV) concentrations higher than 0.01 M, there is a significant contribution from a second reaction pathway and the rate of exchange is now

$$\text{Rate} = k[U^{4+}]^2[UO_2^{2+}][H^{+}]^{-2}$$

but the mechanistic implications are not clear.

It is often difficult to decide if isotope exchange takes place through bond breaking/bond formation, or as a result of electron transfer; the isotope exchange between uranyl(VI) and uranyl(V) and other actinyl ions are typical examples. Kato *et al.* (1970) studied the exchange between UO_2^{2+} and U^{4+} by measuring the transfer of ^{18}O-enriched 'yl' oxygen to water. The rate constant was 6.5×10^{-4} M^{-1} s^{-1}, is very different from that of Masters and Schwartz (1961) that used different experimental conditions. Kato *et al.* suggested that the activated complex has the composition $[U(IV)U(VI)]^{\neq}$ and that the rate of oxygen exchange and electron exchange are of the same order of magnitude.

A number of the redox reactions to be discussed in the following section have been investigated experimentally using isotope exchange technique.

(i) Rate and mechanism of redox reactions

These reactions are in general studied using isotope exchange as exemplified by

$$U^*O_2^{2+}(aq) + UO_2^+(aq) \rightleftharpoons UO_2^{2+}(aq) + U^*O_2^+(aq)$$

The rate of exchange has been studied using ^{18}O-enriched UO_2^{2+} by following the isotope distribution using mass spectroscopy after separation of U(VI) and U(V) (Gordon and Taube, 1961b; Masters and Schwartz, 1961). The experimental rate of exchange is equal to

$$\text{Rate} = k_{obs}[UO_2^{2+}][UO_2^+]$$

with $k_{obs} \approx 50$ M^{-1} s^{-1} (Gordon and Taube, 1961b), close to the more accurate determination of the corresponding exchange reaction between Np(VI) and Np(V), $k_{obs} \approx 110$ M^{-1} s^{-1}, determined by Cohen *et al.* (1954). Howes *et al.* (1988) report rate constants in the range 1–15 M^{-1} s^{-1}. Privalov *et al.* (2004) have discussed the mechanism for the U(V)–U(VI) electron exchange between the aqua-ions, the fluoride, and the carbonate complexes using quantum chemical methods. Both outer-sphere and inner-sphere mechanisms were studied; the former for the aqua ions using the Marcus model and the latter using an inner-sphere model for binuclear complexes containing hydroxide, fluoride, and carbonate bridges. The calculated rate constant for the homogeneous electron exchange (outer-sphere) between $UO_2^{2+}(aq)$ and $UO_2^+(aq)$ is 26 M^{-1} s^{-1} in fair agreement with experimental data. The rate of electron transfer for the inner-sphere reactions is much faster, but here there are no experimental data that can be used for comparison. This study provides a model for the intimate reaction mechanisms as exemplified by the following structure of the precursor and transition state structures (Fig. 5.71).

The kinetics of redox reactions is also discussed in Chapter 23.

Rate constants and reaction mechanisms for a number of redox reactions involving uranium have been reported by Newton (1975) and in the second edition of this book (Katz *et al.*, 1986). It is not possible to discuss all this

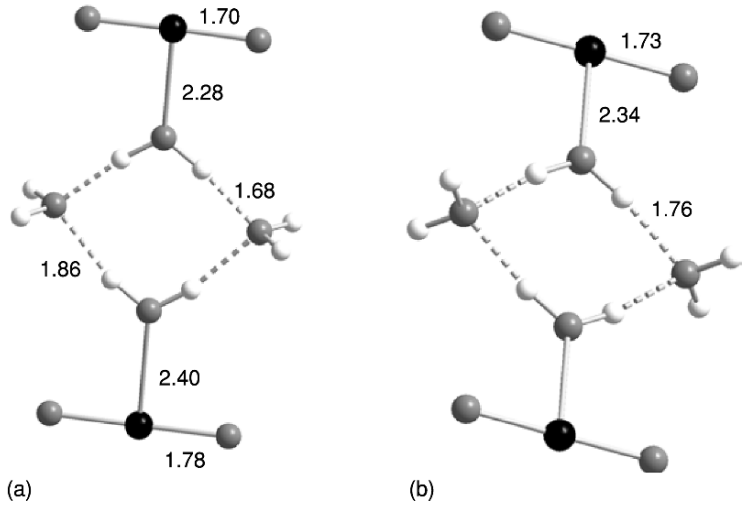

Fig. 5.71 *Quantum chemical model of the precursor* $[UO_2^{2+}\ldots UO_2^{+}]$ *in the outer-sphere electron transfer reaction* $U^*O_2^{2+}(aq) + UO_2^{+}(aq) \rightleftharpoons UO_2^{2+}(aq) + U^*O_2^{+}(aq)$ *from Privalov* et al. (2004). *The model is focused on the bridge between the two uranyl ions and their complete coordination spheres are therefore modeled using a continuum model.* (*a*) *shows the precursor with uranyl*(*v*) *and uranyl*(*vi*) *ions and* (*b*) *the transition state where the two uranyl ions are equivalent.*

information and we have accordingly selected a few examples that illustrate the interpretation of the experimental rate laws. A prerequisite for the mechanistic discussion is information on the equilibrium system, i.e. the complexes present in the test solutions under different experimental conditions. When determining the experimental rate law, care must be taken to identify possible parallel reaction pathways and possible catalysts. We will discuss the oxidation of U(IV) with Pu(VI) as this reaction is not only of scientific interest, but also important in nuclear reprocessing (Newton, 1958). In acid solutions of moderate concentration of the reactants, there is a complete reduction of Pu(VI) to Pu(III). When the reactant concentrations are about 10^{-4} M 96% of the U(IV) reacts according to

$$2\mathrm{Pu(VI)} + \mathrm{U(IV)} \rightleftharpoons 2\mathrm{Pu(V)} + \mathrm{U(VI)}$$

and the remaining 4% react according to

$$2/3\mathrm{Pu(VI)} + \mathrm{U(IV)} \rightleftharpoons 2/3\mathrm{Pu(III)} + \mathrm{U(VI)}$$

The latter two equations only represent the change in oxidation states of the actinides but do not account for the overall stoichiometry. At constant hydrogen ion concentration, the experimental rate law is

$$-\frac{\mathrm{d}[\mathrm{Pu(VI)}]}{\mathrm{d}t} = 2k''[\mathrm{Pu(VI)}][\mathrm{U(IV)}]$$

This rate equation requires that the activated complex has the composition $[\mathrm{Pu(VI)}^{\cdots}\mathrm{U(IV)}]^{\neq}$; as the hydrogen ion concentration is constant, there is no information of the hydrogen ion concentration dependence of the reaction rate. Based on this limited information, a possible reaction mechanism that involves the following two elementary reactions has been suggested (charges have been omitted):

$$\mathrm{Pu(VI)} + \mathrm{U(IV)} \rightleftharpoons \mathrm{Pu(V)} + \mathrm{U(V)}$$

$$\mathrm{Pu(VI)} + \mathrm{U(V)} \rightleftharpoons \mathrm{Pu(V)} + \mathrm{U(VI)}$$

The first reaction is rate-determining as it involves a major rearrangement between the coordination spheres of reactants and products, while the second is fast because these rearrangements are minor.

Additional mechanistic information is obtained by investigating how the rate of reaction depends in the hydrogen ion concentration. One finds that the rate is

$$-\frac{\mathrm{d}[\mathrm{Pu(VI)}]}{\mathrm{d}t} = 2k''\left(1 + \frac{K}{[\mathrm{H}^+]}\right)\left[\mathrm{PuO_2^{2+}}\right]\left[\mathrm{U^{4+}}\right]$$

This rate law suggests that there are two parallel pathways according to the following elementary reactions:

$\mathrm{U^{4+}} + \mathrm{H_2O} = \mathrm{UOH^{3+}} + \mathrm{H^+}$ (a fast equilibrium prior to the rate-determining step);

$\mathrm{UOH^{3+}} + \mathrm{PuO_2^{2+}} \rightleftharpoons \mathrm{HOUOPuO^{5+}}$ (rate-determining step in a reversible reaction);

$\mathrm{HOUOPuO^{5+}} = \mathrm{OUOPuO^{4+}} + \mathrm{H^+}$ (a fast equilibrium reaction);

$\mathrm{OUOPuO^{4+}} + \mathrm{H_2O} \rightleftharpoons \mathrm{UO_2^+} + \mathrm{PuO_2^+} + 2\mathrm{H^+}$ (a slow equilibrium reaction).

The elementary reactions above provide information on the stoichiometric mechanism, but not the details at the microscopic level, as that exemplified in Fig. 5.71 for the electron transfer reaction

$$\mathrm{U^*O_2^{2+}(aq)} + \mathrm{UO_2^+(aq)} \rightleftharpoons \mathrm{UO_2^{2+}(aq)} + \mathrm{U^*O_2^+(aq)}.$$

5.10.4 Fluorescence properties and photochemistry of uranyl(VI) complexes

Only light that is absorbed by a substance is effective in producing a photochemical change; Grotthuss and Draper stated this principle of photochemical activation in 1818, long before the quantum theory. According to quantum theory, the primary step of a photochemical reaction is the activation of *one* molecule by *one* absorbed quantum of radiation. The absorption of a photon leads to a transition from a singlet ground state to a singlet excited state; this is followed by a number of very fast processes with lifetimes in the picosecond

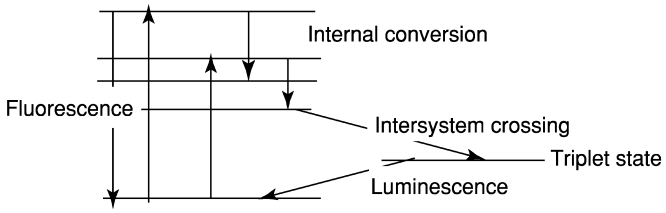

Fig. 5.72 *Molecular energy levels where the arrows denote the corresponding process for energy loss of the excited states. The ground state is a singlet, the excitation takes place without change of spin. The excited states can lose energy by fluorescence back to the ground state, via internal conversion from higher to lower excited states and by intersystem crossing to the triplet state. The typical fluorescence lifetime in the excited state is* 10^{-8} *to* 10^{-9} s *and for internal conversion* 10^{-12} s. *The energy loss from the triplet state to the ground state takes place either by luminescence/phosphorescence or thermally. In addition energy dissipation can take place through non-radiative decay and collisional quenching.*

range that take place before any photochemical reaction can occur. *Fluorescence* takes place from an excited singlet to the ground state, *internal conversion* between the excited singlet states, and *intersystem crossing* from the lowest excited singlet state to the triplet state (Fig. 5.72). The lifetime of the triplet state is long (micro to milliseconds) in comparison with that of the singlet states; the radiative emission from triplet to singlet is called phosphorescence. The long lifetime of the triplet also makes thermal energy dissipation possible.

There are other energy dissipation pathways than fluorescence from the excited states such as non-radiative transfer of the excitation energy to vibrational excitation in the coordinated ligands and the solvent and in collisional pathways, so called dynamic quenching; a more detailed discussion is given by Szabó *et al*. (2006). The intensity of fluorescence or phosphorescence depends on the competition between these physical and chemical processes. The quantum yield, Q_Y, is defined as the ratio between the number of photons emitted and absorbed and this quantity is accordingly strongly dependent on the different quenching mechanisms

$$Q_Y = \frac{1/\tau_n}{1/\tau_n + k_{nr}} = \frac{\tau}{\tau_n}$$

where τ_n is the lifetime in the absence of non-radiative processes and k_{nr} the rate constant for non-radiative decay; τ is the lifetime in the presence of non-radiative processes. In systems with dynamic quenching it is $1/\tau = 1/(1/\tau_n + k_{nr} + k_q)$, where k_q is the rate constant for collision quenching.

In addition to these quenching processes, the fluorescence intensity may also depend on static quenching that is the result of the formation of a non-fluorescent complex with a ligand, L, in the ground state. In order to understand and use information of fluorescence intensity and fluorescence lifetimes, it is essential to be able to distinguish and quantify all these mechanisms. Static and dynamic quenching can be distinguished by lifetime analysis (Toraishi *et al*., 2004).

In steady-state excitation the concentration of excited molecules and therefore the fluorescence intensity is constant. Hence, we have the following relations in the absence and presence of quenching:

$$\frac{\mathrm{d}I^*}{\mathrm{d}t} = f - (1/\tau_0)[I^*] = 0;$$

and

$$\frac{\mathrm{d}I^*}{\mathrm{d}t} = f - \left(1/\tau_0 + k_\mathrm{q}[L][I^*]\right) = 0$$

where f is the light flux, I^* is the concentration of the fluorescent species with a lifetime τ_0 in the absence of the quencher L. k_q is the rate constant for fluorescence decay in the presence of L. Hence

$$\left(\frac{I}{I_0}\right)^{-1} = \frac{1/\tau_0 + k_\mathrm{q}[\mathrm{L}]}{1/\tau_0} = 1 + k_\mathrm{q}\tau_0[\mathrm{L}]$$

where I and I_0 represent the measured fluorescence intensity in the presence and absence of L; this is the Stern–Volmer equation. The fraction of excited fluorophores relative to the total is equal to

$$\left(\frac{I}{I_0}\right) = \left(\frac{\tau}{\tau_0}\right)$$

which for the case of only static quenching in the ground state reduces to $(I/I_0) = 1$ because then $\tau = \tau_0$.

In uranyl(VI) systems where the ligand is a strong quencher, the rate constant k_q is very large; it is then not possible to detect the fluorescence spectrum for the complexes (e.g. Moll *et al*., 2003).

The photochemistry of uranium compounds is a 'classical' field of research that dates back to the Becquerels more than 100 years ago. The experimental quantities are the excitation and emission spectra and the lifetime(s) of the excited state(s) as a function of chemical parameters. The chemistry of photo-excited UO_2^{2+} has been extensively studied, both as a tool for synthesis, as a method to determine equilibrium constants in ground and excited states, and for elucidation of luminescence quenching mechanisms. Recent reviews by Baird and Kemp (1997), Fazekas *et al*. (1998), and Yusov and Shilov (2000) provide an introduction to the literature.

The photo-oxidation of oxalic acid was used in the first chemical actinometers to measure photon flux based on the reactions

$$UO_2^{2+} + h\nu \rightarrow (UO_2^{2+})^*;$$
$$(UO_2^{2+})^* + (COOH)_2 \rightarrow UO_2^{2+} + CO_2 + CO + H_2O$$

The actinometer must be calibrated to determine the quantum efficiency at the wavelength used.

The excited states responsible for luminescence emission have a charge-transfer character as a result of excitations from the σ_u or σ_g bonding U–O orbitals to an empty f-orbital via internal conversion and intersystem crossing as outlined in Fig. 5.72. The resulting triplet state is $^3\Delta_g$, or to be more precise the $\Omega = 1_g$ component of the relativistic $^3\Delta_g$ state (Zhang and Pitzer, 1999; Matsika *et al.*, 2001) and the transition to the ground state is accordingly spin forbidden, which accounts for the long lifetime. The very long lifetime in comparison with those from electronically excited states of organic molecules is the basis for the photo-reactivity of $(UO_2^{2+})^*$. The photo-excited state is a very strong oxidant with an estimated oxidation potential of 2.6 V. The probable deactivation pathways are (Fazekas *et al.*, 1998):

- intra-molecular radiationless deactivation via O-H stretch modes of coordinated water;
- intra-molecular energy transfer to vibrational modes of the water solvent as in rare-earth metal ions;
- electron transfer and radical formation

$$(UO_2^{2+})^* + H_2O \rightarrow UO_2^+ + (H_2O^+)^*;$$

or hydrogen abstraction

$$(UO_2^{2+})^* + H_2O \rightarrow UO_2H^+ + OH^*$$

The experimental basis for photochemical studies is provided by fluorescence spectroscopy and measurements of the decay of the fluorescence as a function of chemical parameters. The terminology is often misleading, the majority of the experimental 'fluorescence' spectra of uranyl(VI) systems refer to phosphorescence, often denoted luminescence. In the following we will use the luminescence terminology. Despite all experimental efforts there is no consensus about the primary deactivation processes. The luminescence properties of the uranyl(VI) ion in water solution can be used as an example. When the pH is increased in the UO_2^{2+}–water system, the peaks of the emission spectrum are displaced towards longer wavelength. At the same time, the luminescence lifetime is no longer mono-exponential; this is presumably a result of the formation of hydroxide complexes (Fazekas *et al.*, 1998). Moriyasu *et al.* (1977) made similar observations on other uranyl(VI) systems where complexes with fluoride and phosphate were formed, in particular they observed a strong enhancement of both the luminescence intensity and its lifetime that is the basis for an analytical method to determine uranium in low concentration. The increase of the lifetime of the triplet state is assumed to be a result of shielding of the uranyl ion from water that is an efficient quencher. Some authors explain the non-exponential luminescence decay by exciplex formation (Deschaux and Marcantanatos, 1979), other by a reversible crossing between two different excited uranyl states (Formosinho and Da Graca Miguel, 1984; Formosinho *et al.*, 1984). Billard and Lützenkirchen (2003) have discussed the problems encountered when analyzing experimental luminescence data in terms of elementary reactions as discussed below.

Laser-induced fluorescence spectroscopy is extensively used as a tool for the analytical determination of trace amounts of uranium as described in Chapter 30. The technique is also used to determine equilibrium constants and the speciation of uranium(VI) in aqueous solution both in laboratory and environmental systems. This raises the question if the measured equilibrium constant, K_{app}, refers to the ground or the excited state, a problem that has been discussed by Billard and Lützenkirchen (2003). Their starting point is the following mechanistic scheme (Scheme 5.2): where K is the equilibrium constant

$$\begin{array}{ccc} & \overset{k_1,\, k_{-1}}{} & \\ M^* + L & \rightleftharpoons & (ML)^* \\ \uparrow\downarrow \lambda_1 & & \uparrow\downarrow \lambda_2 \\ M + L & \rightleftharpoons & ML \\ & \underset{K}{} & \end{array}$$

Scheme 5.2 *Mechanistic scheme for the complex formation between M and L in ground and excited state. The notation is explained in the text.*

in the ground state, k_1 and k_{-1} the rate constants for the formation and dissociation of ML*, and λ_1 and λ_2 the rate constants for decay of M* and ML*.

In the experimental studies, time-resolved spectra are measured at different total concentrations of M and L, where the former is the fluorescence probe and the latter is assumed to be non-absorbing at the excitation wavelength. Scheme 5.2 has been used to deduce rate constants k_1 and k_{-1} and information on ground state and excited state chemistry from the amplitude of the emission spectra and ground state concentrations. In the case where there is no interac-

$$\begin{array}{ccc} M^* + L & & (ML)^* \\ \uparrow\downarrow \lambda_1 & & \uparrow\downarrow \lambda_2 \\ M + L & \rightleftharpoons & ML \\ & \underset{K}{} & \end{array}$$

Scheme 5.3 *Mechanistic scheme for reactions where the complex formation in the excited state can be neglected.*

tion between M* and L, or when the rate constants k_1 and $k_{-1} \ll \lambda_1$ and λ_2, Scheme 5.2 is reduced to Scheme 5.3 as follows:
where the measured lifetimes now represent M* and ML*. Billard and Lützenkirchen (2003) discuss the conditions under which K_{app} is a satisfactory approximation for the equilibrium constant K in the ground state. In their Model A, k_1 and $k_{-1} \ll \lambda_1$ and λ_2 and $K_{app} = K$ is then a good approximation. When k_1 and $k_{-1} \gg \lambda_1$, the chemistry in the excited state is dominating and the apparent equilibrium constant, K_{app} is then equal to

$$K_{app} = K^* \frac{\alpha\tau_1}{\beta\tau_2}$$

where α and β are the molar absorption coefficients and τ_1 and τ_2 the lifetimes of M* and ML* (Model C). In systems where k_1 and $k_{-1} \approx \lambda_1$ and λ_2, one has to use numerical simulations to deduce the rate constants from the experimental data (Model B). K^* is the equilibrium constant for the formation of ML*.

Billard and Lützenkirchen (2003) discuss a number of time-resolved laser fluorescence studies of uranyl complexes using the model outlined above. For example, in the uranyl–hydroxide system can be described by either Model A or B. Lopez and Birch (1997) observed two decay times that were independent of pH in the range 2.5–4.5, indicating that $K_{app} = K$.

(a) Quenching mechanisms of the uranyl ion

Quenching is in general described by the Stern–Volmer mechanism as described previously; it can proceed through a number of different reactions as outlined by Baird and Kemp (1997). Quenching by halide ions most likely takes place by electron transfer as indicated by the fact that the quenching efficiency depends on the oxidation potential, and decreases in the order $I^- > Br^- > Cl^- > F^-$; metal ions in low oxidation states like Ag^+, Fe^{2+}, and Mn^{2+} are also efficient quenchers that also act through an electron transfer mechanism.

Many organic compounds are very efficient quenchers and the mechanism involves either a process where the quencher forms a short-lived exciplex with the excited uranyl, or an electron transfer. In the latter case, the relative quenching rate depends on the ionization potential of the quencher (as for the halide ions). Burrows and Kemp (1974) have reviewed quenching reactions with different alcohols where hydrogen abstraction may be an important quenching mechanism as indicated by large primary hydrogen isotope effects.

The lifetime of the excited uranyl ion, $(UO_2^{2+})^*$ depends strongly on the total concentration of uranium (self-quenching), an observation that has been described by Deschaux and Marcantonatos (1979) and others as due to the formation of the binuclear exciplex

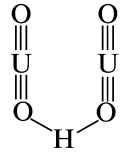

(b) Photochemistry of the uranyl(VI) ion

Rabinowitch and Belford (1964), Balzani and Carassiti (1970), and Güsten (1983) have reviewed the photochemistry of uranyl(VI) with organic substrates. The reactions involve oxidation of the substrate and reduction to uranyl(V); in

the absence of oxygen, a subsequent fast reaction leads to formation of uranyl (VI) and uranium(IV). In the presence of oxygen, uranyl(V) is rapidly oxidized to uranyl(VI) and accordingly the uranyl(VI) ion acts as a photo-catalyst, e.g. for the oxidation of alkanes, alkenes, alcohols, and aldehydes. The uranyl ion has also been used as a photo-catalyst for DNA footprinting as described in Section 5.11. All these reactions seem to take place by hydrogen abstraction from a C–H bond, followed by uranium-mediated product formation (Wang *et al.*, 1995). The mechanism can schematically be described by the following reactions, where SH_2 is the organic substrate, and S_{ox} the final oxidation product, an aldehyde or carboxylic acid.

$$SH_2 + (UO_2^{2+})^* \rightarrow SH^+ + UO_2^+ + H^+;$$
$$2SH^+ \rightarrow SH_2 + S_{ox};$$
$$2UO_2^+ \rightarrow UO_2^{2+} + U(IV).$$

5.11 ORGANOMETALLIC AND BIOCHEMISTRY OF URANIUM

There is an extensive organometallic chemistry for uranium(III) and uranium (IV); in fact, most of the organometallic chemistry as described in Chapters 25 and 26 deals with uranium and a detailed description of the synthesis and properties of organometallic uranium compounds can be found there. For historical reasons, we will here mention a few examples; the field was started by Wilkinson with the preparation of $(\eta^5\text{-cyclopentadienyl})_3UCl$ (Reynolds and Wilkinson, 1956), followed by reports from Fischer and Hristidu (1962) of additional cyclopentadienyl compounds, e.g. tetrakis(η^5-cyclopentadienyl)uranium(IV) (Fischer and Hristidu, 1962). The 'sandwich' compound uranocene, bis(π-cyclooctatetraene) uranium(IV), $U(C_5H_5)_2$ was prepared by Streitweiser and Müller-Westerhoff (1968). These compounds are π-complexes where uranium is coordinated by the cyclic ligands through their delocalized π-orbitals. Other complexes with the cyclopentadienyl ion $C_5H_5^-$ are $U(\eta^5\text{-}C_5H_5)_3$, $U(\eta^5\text{-}C_5H_5)_4X$, where X is an alkyl group, an alkoxy group, or BH_4. For description of these and other metal organic compounds the reader is referred to Chapter 25.

The biochemistry of uranium is totally dominated by investigations of the coordination of the uranyl(VI) ion to proteins, DNA/RNA and polysaccharide coatings in cell walls. In the proteins, the bonding takes place at the carboxylate and amino groups, in DNA/RNA at the phosphate groups, and in the polysaccharides at deprotonated OH groups. The strong binding of uranium has been used to make heavy-atom derivatives in protein crystallography (Tame, 2000) and as staining reagent in electron microscopy (Gray, 1994, 2001).

Photochemical oxidation of polydeoxynucleotides by UO_2^{2+} has been used for footprinting of DNA (Nielsen *et al.*, 1988). This is a technique used to identify the DNA region where a particular protein is bonded. It involves labeling of one

end of a DNA chain with ^{32}P; addition of UO_2^{2+} that binds to the phosphate groups and then irradiation with near-UV light to obtain photo-excited uranyl(VI) that abstracts a hydrogen from a nearby C–H group, resulting in cleavage of the DNA backbone diester chain both in single- and double-stranded DNA. The cleavage is random and not sensitive to the base sequence; it results in ^{32}P fragments of different lengths that can be identified through gel electrophoresis. When a protein is bonded to certain base sequences of DNA, these regions are not accessible to UO_2^{2+} and are therefore protected from cleavage; this results in a different fragmentation pattern and the base sequence where protein bonding takes place can therefore be identified. For details, see Stryer (1988). An important advantage of this method, as compared to the use of DNA-se enzymes as 'scissor', is the small size of the uranyl(VI) ion compared to the enzymes.

The uranyl ion has been used as a very efficient regioselective and stereoselective catalyst for the synthesis of oligonucleotides in solution (Sawai *et al.*, 1989, 1990, 1992, 1996; Shimazu *et al.*, 1993).

Uranium in the form of uranyl(VI) compounds is taken up by living organisms. In mammals the uranium is bonded to proteins, e.g. transferrin, with a residence time of several hours during which it is gradually transported and incorporated into bone tissue. The residence time is long and removal requires an extensive treatment with different sequestering agents (Scapolan, 1998). A detailed discussion of the behavior of uranium and other actinides is given in Chapter 31.

5.12 ANALYTICAL CHEMISTRY

There is wide array of options available for the determination of uranium including both classical wet chemical and instrument-based spectrometric techniques. The purpose of this section is to provide an overview of the analytical techniques and methods applicable to the determination of uranium in a variety of matrices with an emphasis on those techniques and methods useful for samples with uranium concentrations larger than 1 μg per gram of sample. An extensive review of the techniques and methods that are used for the determination of uranium at trace and ultra-trace (less than 1 μg per gram of sample) concentrations in geological, environmental, and biological matrices is given in Chapter 30.

5.12.1 Chemical techniques

(a) Sample preparation

Most bulk analytical techniques require that a stable, aqueous solution be prepared prior to analysis and element determination. The dissolution of uranium containing compounds and materials is typically performed either by fluxed fusion decomposition or acid dissolution. Fluxed fusion decomposition is the first step in many standard classical wet chemical procedures used for the determination of uranium at major and minor concentrations in uranium

containing ores. Ingamells and Pitard (1986) describe a chemical method for the determination of uranium in silicate minerals. In this method a several-gram quantity of silicate material is decomposed via fusion with Na_2O_2 in a platinum crucible. The fusion mass is dissolved in dilute HNO_3 and uranium is precipitated with a mixture of Na_2CO_3 and K_2CO_3 (Sandell, 1959). This precipitate is evaporated and redissolved in dilute HNO_3 before further purification or direct determination of uranium. Other fluxes that can be used for the fusion of uranium containing materials include hydroxides, carbonates, bisulfates, hydrosulfates, pyrosulfates, tetraborates, and metaborates (Dean, 1995).

Nearly all uranium compounds and uranium containing alloys can be dissolved in HNO_3. As briefly discussed in Section 5.6.4, uranium metal dissolves very rapidly in HCl, but a voluminous black residue is left unless a small amount of fluosilicate ion is present. uranium containing minerals, such as autunite, carnallite, gummite, phosphuranylite, torbernite, tyuyammite, uraninite, and uranophane will dissolve via open vessel digestion with HNO_3, HCl, and H_2SO_4 (Meites, 1963). Acid leaching with HNO_3, HCl, or H_2SO_4 has been used for industrial scale recovery of uranium from its ores. The various leaching processes for uranium ores are discussed in more detail in Section 5.4.3. A mixture of HF and HNO_3 can be employed when dissolution of silicates is required. When this mixture is used, complete recovery of uranium requires conversion of UF_4 to a soluble form by fuming with $HClO_4$ or H_2SO_4 or by complexation of F^- with H_3BO_3.

Separation and preconcentration of uranium can be achieved by most of the common chemical and physical separation methods: precipitation, coprecipitation, volatilization, electrolysis, liquid–liquid extraction, and ion-exchange chromatography. The simplest methods for the separation of uranium from solution are by precipitation or coprecipitation. Precipitation of uranium can be accomplished using inorganic and organic precipitants (Gindler, 1962). The formation of many precipitates in uranium containing solutions that also contain other anions and cations typically yields a group separation of uranium along with other elements. Uranium will coprecipitate from a carbonate-free solution with Fe(III) and Al(III) hydroxides. Carbonate is removed by heating the solution. Coprecipitation is accomplished by adding a macroscopic amount of Fe(III) or Al(III) to an acidified solution and adjusting the solution pH to basic with the addition of NH_4OH. Separation of uranium can also be accomplished by coprecipitation with $Ca(OH)_2$, $(NH_4)_2CO_3$, and $(NH_4)_2S$ (Rodden and Warf, 1950). Precipitation of uranium from acidic solutions can be performed fairly selectively as a peroxide or oxalate.

Electrochemical separation of uranium can be accomplished via Hg-cathode electrolysis and electrolytic deposition on a variety of solid metal electrodes (Casto, 1950) as well as electrodialysis and pyrometallurgical processes (Gindler, 1962). Electrodeposition from an electrolyte matrix adjusted to pH 3.5 onto a metal planchet is the most common method for the preparation of a thin sample for high-resolution alpha-spectrometric determination (Kressin, 1977

and references therein). Further discussion on sample preparation by electrodeposition for alpha spectrometry is given in Chapter 30, section 3.1.

Liquid–liquid extraction of uranium can be accomplished using organic acids, ketones, ethers, esters, alcohols, and phosphoric acid derivatives (Lally, 1992). In many cases, extraction of uranium can be greatly enhanced with the addition of nitrate salts to the solution (Gindler, 1962). Uranium(IV) can be extracted with ethyl acetate after treatment of an acidified solution with $Al(NO_3)_3 \cdot 9H_2O$ (Guest and Zimmerman, 1955). Uranium(VI) can be extracted with 25% TBP in toluene (Mair and Savage, 1986). Methyl isobutyl ketone has been used in large-scale uranium-separation processes. Recently, several uranium-specific exchange resins have been developed for the separation of uranium from acidic matrices. While these resins function by passing uranium-containing solution down an exchange column containing the material, the separation is based on liquid–liquid extraction. One of these extraction chromatographic resins, TRU Spec resin, consists of octyl(phenyl)-*N*,*N*-diisobutylcarbamoylmethylphosphine oxide in tri(*n*-butyl)phosphate supported by an inert polymeric substrate, Amberlite XAD-7 (Horwitz *et al.*, 1993). The second extraction chromatographic resin, U/TEVA Spec resin consists of diamylphosphonate sorbed on Amberlite XAD-7. This resin possesses tetravalent ion specificity.

Cation exchange is not a commonly used method for the separation of uranium due to the lack of selectivity of the UO_2^{2+} cation over other divalent metal ions. UO_2^{2+} forms strong anionic sulfate and weaker chloride complexes that can be the basis for uranium separation from other metals in solution via anion exchange. Uranium separations can be performed by use of basic anion-exchange resins such as Dowex-1, Dowex-2, Amberlite IRA-400, Amberlite IRA-410, and Bio-Rad AG1X8 from solutions of HCl, HF, HNO_3, H_2SO_4, $(NH_4)_2CO_3$, and H_3PO_4 (Gindler, 1962).

(b) Sample analysis

Total analysis techniques (also known as classical techniques) are the most accurate of all the available methods for uranium determination. Because these techniques provide definitive results, they are typically used as the basis for establishing primary uranium standards and are used extensively in the areas of material control, accountability, and safeguards. Volumetric and gravimetric techniques have both been applied for high accuracy determination of macroscopic quantities of uranium.

Volumetric techniques provide the highest precision and accuracy for uranium determination. Volumetric determination of uranium can be performed via complexation titration with ethylenediaminetetraacetic acid (EDTA). However, the most widely used method is a redox titration where U(VI) is first reduced (e.g. in a Jones reductor) and then back-titrated via oxidation with $KMnO_4$ or Ce(IV) using 1,10-phenanthroline as an indicator (Dean, 1995). The method of Davies and Gray (1964) utilizes excess Fe(II) to reduce U(VI) to U(IV) in a concentrated

H_3PO_4 solution containing H_2NSO_3H. The Fe(II) is selectively oxidized with the addition of HNO_3 in the presence of a Mo(IV) catalyst. After addition of H_2SO_4, U(IV) is titrated with standard Cr(VI) with Ba-diphenylaminesulfonate as an indicator. A modified version of this method has been developed in which the end point is determined potentiometrically (American Society for Testing and Materials, 1994, ASTM C1267–94). This method is exceptionally accurate (relative bias –0.042% and within laboratory variation 0.042%), but requires milligrams of uranium in the sample aliquot.

The necessity for the preparation of redox standard solutions can be circumvented by electrochemical titrations. Coulometric titration of uranium can be performed in both constant-current and controlled-potential titration. Procedures for oxidative coulometric titration of U(IV) and reductive coulometric titration of U(VI) in constant-current mode have been developed. Oxidative coulometric titration of U(IV) is performed via the electrogeneration of Ce(IV) subsequent to preparation of U(IV) by reduction with cadmium amalgam (Furman *et al.*, 1953). Reductive coulometric titration of U(VI) is performed with electrogenerated Ti(III) at a platinum cathode with amperometric endpoint detection (Kennedy and Lingane, 1958). Errors are as low as $\pm 0.3\%$. An improved version of this method has been developed that is capable of a precision of 0.008% (Marinenko *et al.*, 1983). Methods for oxidative controlled-potential titration of U(IV) and reductive controlled-potential titration of U(VI) have been developed. Oxidative controlled-potential titration of U(IV) can be performed in 1 M $HClO_4$ at a platinum electrode (Boyd and Menis, 1961). The most established controlled-potential coulometric titration of uranium utilizes a mercury pool for reduction of U(VI) (McEwen and DeVries, 1959). Experimental conditions have been established which enable uranium to be determined via controlled-potential coulometric titration at a platinum electrode (Davies *et al.*, 1970). Use of the platinum electrode has several advantages including the possibility of simultaneous consecutive determinations of Fe(III) and U(VI), or Pu(IV) and U(VI) in the same cell.

Gravimetric determination of the uranium content of uranium ores can be performed via the sulfide–carbonate–hydroxide method. In this method, the solid U-containing ore sample is dissolved with HNO_3 and H_2SO_4. Arsenic is first removed via addition of HBr. A treatment of the acidic solution with H_2S precipitates a large number of cations as sulfides; Co and Ni are precipitated with H_2S at low acidity; Al, Cr, and Fe are removed with subsequent addition of NH_4OH and $(NH_4)_2CO_3$;. The solution is then reacidified with HCl and U is precipitated with NH_4OH. The precipitate is filtered, washed, ignited, and determined gravimetrically as U_3O_8. Alternatively, the sample can be decomposed via fluxed fusion followed by dissolution in HCl and precipitation of U(IV) on the addition of 6% cupferron solution. The precipitate is filtered, washed, ignited, and determined gravimetrically as U_3O_8. This separation effectively removes Al, Cr, Mn, Zn, and PO_4^{3-} but the presence of Fe, Ti, V(V), and Zr would interfere with the uranium determination

(Dean, 1995). In general, the use of gravimetric methods is limited due to lack of specificity.

5.12.2 Nuclear techniques

The natural radioactivity inherent to uranium isotopes provides the means for their direct analysis by radiometric analytical techniques. While several radiometric techniques are amenable to the determination of uranium at concentrations higher than 1 μg per gram of sample, the most frequently used are high-resolution alpha and gamma spectrometries. Complete isotopic analysis of the naturally occurring isotopes ^{238}U, ^{235}U, and ^{234}U can be performed via high-resolution alpha spectrometry. Alpha-spectrometric determination requires complete sample dissolution, chemical separation of uranium, followed by preparation of a thin source, typically via electrodeposition or precipitation (Kressin, 1977 and references therein). Either ^{232}U or ^{236}U can be used as isotopic recovery spikes. Backgrounds and efficiencies of typical alpha spectrometers equipped with a 450-mm^2 ion-implanted Si detector would require a total of 0.4 μg of natural uranium to achieve 10% counting statistics for a 24-h sample count. Examples of several applications of alpha spectrometry for the determination of uranium and the measurement of U-series disequilibria are given in Ivanovich and Murray (1992).

High-resolution high-purity germanium (HPGe) detectors are capable of high-specificity measurement of individual radionuclide γ-rays and virtually eliminates the need for chemical treatment of samples. Due to its long half-life, the quantification of ^{238}U is usually based on the measurement of the 92.5 keV or the 63.3 keV γ-ray doublets produced by the short-lived daughter ^{234}Th provided secular equilibrium has been achieved (Harbottle and Evans, 1997). Determination of ^{238}U can also be performed by measurement of the 1001 keV γ-ray from the decay of ^{234m}Pa ($t_{1/2} = 1.175$ minutes). The low branching ratio for this γ-ray precludes its use for samples with uranium concentrations smaller than 10 μg per gram of sample. In the case of ^{235}U, direct quantification can be performed using its 185.7-keV γ-ray. A correction for interference from the 186.1 keV γ-ray, ^{226}Ra ($t_{1/2} = 1600$ years), is required for samples in secular equilibrium.

Radiometric determination of uranium can also be performed utilizing scintillation detection after chemical separation of uranium from interfering radionuclides. A standard test method for the determination of uranium in water by high-resolution alpha liquid-scintillation spectrometry utilizes a selective extractive scintillator solution containing dialkyl phosphoric acid (ASTM D6239–98, 1998).

Activation analysis of uranium is typically performed subsequent to irradiation with thermal neutrons. Uranium is essentially unique among naturally occurring elements in that neutron activation analysis (NAA) can be performed by detection of delayed neutrons (Parry, 1991). This method is highly

specific for uranium and has been used for many years in the exploration of uranium ores. NAA with delayed-neutron detection can be automated for online and unattended determination of uranium content in solid and liquid samples.

The coupling of NAA with high-resolution gamma spectrometric detection (instrumental neutron activation analysis, or INAA) yields a highly specific and sensitive method for the determination of uranium. At high concentrations, uranium can be determined by INAA via measurement of the 74 keV γ-ray photo peak from the decay of ^{239}U ($t_{1/2}$ = 23.5 minutes). Minor and trace quantities of uranium are typically determined by INAA via the $^{238}U(n,\gamma)^{239}U(\beta^-,$ 23.5 minutes$)^{239}Np$ reaction with measurement of the 105 keV γ-ray photo peak from the decay of ^{239}Np (Parry, 1991). Enhanced sensitivity can be achieved by performing post-irradiation chemical separations (radiochemical neutron activation analysis, or RNAA) (Anders *et al.*, 1988). Both INAA and RNAA are applicable to the determination of trace and ultra trace concentrations of uranium and are further discussed in Chapter 30, section 3.3.

5.12.3 Spectrometric techniques

Uranium is amenable to determination by several fundamentally different spectrometric techniques including spectrophotometry, atomic absorption spectrometry (AAS), atomic emission spectrometry (AES), fluorometry, phosphorimetry, X-ray fluorescence (XRF), and mass spectrometry.

Spectrophotometric determination of uranium can be performed subsequent to sample dissolution, separation of uranium, complexation with an appropriate chromophore, and colorometric determination by comparison with prepared standards. For example, uranium can be determined colorimetrically in the aqueous phase after complexation with 4-(2-pyridylazo)recorcinol (PAR) (Pollard *et al.*, 1959) or as an organic-miscible complex with 4-(2- pyridylazo) napthol (PAN) (Pollock, 1977).

Selectivity of uranium spectrometric determination can be improved using techniques based on atomic absorption and emission. The determination of uranium via AAS techniques can be performed using flame sources (FAAS) or graphite furnace sources (GFAAS). FAAS determination of uranium is performed via the 358.5 nm absorption line using a nitrous oxide/acetylene flame. The detection limit for AAS is 40 $\mu g\ mL^{-1}$ for uranium in solution (Dean, 1995). GFAAS can achieve detection limits of 30 $ng\ mL^{-1}$ in much smaller sample volumes (20 μL). Both AAS and GFAAS are single-element methods that can achieve accuracies greater than $\pm 1\%$ if uranium concentrations are significantly higher than the detection limits.

Sensitivity of atomic spectrometric techniques can be improved via excitation in a high-temperature inductively coupled plasma (ICP) source followed by atomic emission spectrometric (AES) determination. The emission spectrum of U consists of thousands of resolvable lines. ICPAES determination of uranium

based on the 385.96 nm emission line can achieve detection limits of 20 ng mL^{-1} with accuracies of $\pm 1\%$ if concentrations are significantly higher than the detection limits (Dean, 1995). While all atomic spectrometric techniques generally determine total uranium concentration without isotopic selectivity, a high-resolution ICPAES has been developed for the determination of uranium isotopic ratios (Edelson, 1992).

Uranium is unique among most elements in that it can be determined directly via fluorometry without the addition of a fluorescent chelating agent. The fluorometric technique can determine uranium concentrations as low as 5 ng mL^{-1} (ASTM D2907–91, 1991a). Superior detection limits can be achieved by utilizing the ability of uranyl ions to phosphoresce when excited to a triplet state. The uranyl ion can be directly determined phosphorometrically in a H_3PO_4 or H_2SO_4 solution. The pulsed-laser phosphorometric technique can determine uranium concentrations as low as 50 pg mL^{-1} (ASTM D5174–91, 1991b). Further discussion of the fluorometric and phosphorometric techniques is given in Chapter 30 (Sections 30.4.1 and 30.4.2, respectively).

X-ray fluorescence (XRF) can provide qualitative identification and quantitative determination of uranium in a variety of matrices. A procedure for the determination of uranium in soils can be found in ASTM C1255-93 (1993). This procedure can be used to determine as little as 20 μg per gram of uranium.

Mass spectrometry is the most sensitive method for the determination of uranium. In contrast to most of the atomic spectrometric techniques outlined previously, mass spectrometry also provides the means for the determination of uranium isotopic composition. As such, mass spectrometry is an essential tool for the determination of uranium in nuclear fuel cycle applications, material control and accountability, environmental chemistry, geochemistry, and cosmo-chemistry. While a variety of mass spectrometric methodologies have been applied to the determination of uranium (Section 30.5; Wolf, 1999 and references therein), the most commonly used mass spectrometric methods for the determination of uranium are electron-impact gas source mass spectrometry, thermal ionization mass spectrometry (TIMS), and inductively coupled plasma mass spectrometry (ICPMS).

Electron-impact gas source mass spectrometry is used specifically for uranium isotopic analysis to monitor U-enrichment processes. Typically, UF_6 is analyzed in ultracentrifuge and thermal diffusion processes and uranium vapor is analyzed in laser enrichment processes (Platzner, 1997). Measurement by gas source mass spectrometry requires approximately 100 mg of sample. Such instruments are used in production line applications and can achieve a precision of $\pm 0.40\%$ for UF_6 with $>1\%$ ^{235}U enrichment (Nagatoro *et al.*, 1980). Highly portable quadrupole mass analyzers have been designed for UF_6 isotopic analysis in nuclear safeguard applications (Depaus *et al.*, 1987). A standard method for the isotopic analysis of UF_6 with an electron-impact gas source mass spectrometer utilizing a single standard has been developed for nuclear fuel cycle applications (ASTM C1344-97, 1997).

TIMS is one of the most precise and accurate methods for single element isotope ratio determination and is used when small masses of uranium are analyzed. Instruments configured with multiple Faraday detectors can routinely determine major uranium isotope ratios to a precision better than 0.05% (Walder, 1997) and require less than 1 μg of U. TIMS is a commonly used method in nuclear fuel cycle applications including the isotopic analysis of hydrolyzed UF_6 and uranyl nitrate solutions (ASTM C1413–99, 1999) and for the determination of atom percent fission in irradiated nuclear fuels (ASTM E244-80, 1980). Determination of uranium concentrations is performed via isotope dilution (ID) analysis typically using ^{233}U as an isotopic spike. The high sensitivity of TIMS makes this method suitable for the determination of uranium concentrations and isotopic composition at trace and ultra-trace concentrations such as in geological and cosmo-chemical materials. Procedures and applications of TIMS to uranium measurements in geological samples are summarized in Chen *et al*. (1992) and references therein. The TIMS methodology is capable of determining $^{234}U/^{238}U$ ratios with a precision of 0.5% (2σ) for a sample size of 5×10^9 ^{234}U atoms. The primary disadvantage of TIMS is that extensive sample preparation is required and only one element can be determined in a given prepared sample. Further discussion of the application of TIMS to trace and ultratrace analysis is given in Chapter 30, section 5.1.

A review of the trends of the techniques used for elemental determination indicates that ICPMS is one of the most commonly used methods today (Lipschutz *et al*., 2001). ICPMS has found applications for the determination of uranium in waters, soils, sludges, wastes, nuclear materials, biological, geological, and cosmo-chemical materials (Chapter 30, section 5.4 and references therein). The strength of ICPMS resides in its high sensitivity, multielement, high sample throughput capabilities. Quantification is typically performed based on external calibration using the most abundant uranium isotope ^{238}U. Solutions can be analyzed with minimal or no sample pre-treatment. Considering the sensitivities of modern state-of-the-art instruments, a minimum detection limit (MDL) of less than 100 fg in a 1 mL sample is readily attainable for uranium determination by ICPMS (Brenner *et al*., 1998). The combination of an ICP source with a high-precision, double-focusing, mass spectrometer in a single detector configuration (HR-ICPMS) results in an instrument capable of determining less than 1 fg uranium in 1mL solution (Wolf, 1999). This corresponds to a detection limit of approximately 3×10^6 atoms of uranium. Moens and Jakubowski (1998) have published a review of HR-ICPMS instrumentation and applications. Configuration of HR-ICPMS with multiple detectors (MC-ICPMS) yields a method possessing all the attributes of HR-ICPMS with enhanced precision. The routine use of MC-ICPMS in nuclear fuel cycle applications has the potential to dramatically decrease the cost of sample analysis by means of increased sample throughput while maintaining the high precision required for fuel fabrication. A five-fold improvement in sample throughput has been demonstrated for the analysis of

hydrolyzed UF_6 with accuracy and precision comparable to TIMS (Walder and Hodgeson, 1994). High sensitivity makes MC-ICPMS particularly attractive for uranium isotope determination in geo-chronological applications. A review of MC-ICPMS instrumentation and applications to uranium isotopic analysis in geological samples has been reported (Halliday *et al*., 1998). This paper reviews results of replicate analysis of NIST SRM-906 measured by TIMS and MC-ICPMS. Precisions comparable to the best achievable TIMS precisions were achieved. The external reproducibility of MC-ICPMS was superior to TIMS. Further discussion of the application of MC-ICPMS techniques to trace and ultratrace uranium analysis is given in Chapter 30, section 5.4, of this book.

REFERENCES

Aas, W., Moukhamet-Galeev, A., and Grenthe, I. (1998) *Radiochim. Acta*, **82**, 77–82.

Abazli, H., Cousson, A., Tabuteau, A., and Pagès, M. (1980) *Acta Cryst. B*, **36**, 2765–6.

Åberg, M. (1969) *Acta Chem. Scand.*, **23**, 791–810.

Åberg, M. (1971) *Acta Chem. Scand.*, **25**, 368–9.

Åberg, M. (1976) *Acta Chem. Scand. Series A*, **30**, 507–14.

Åberg, M. (1978) *Acta Chem. Scand.*, **A32**, 101–7.

Åberg, M., Ferri, D., Glaser, J., and Grenthe, I. (1983) *Inorg. Chem.*, **32**, 3986–9.

Abraham, B. M. Flotow, H. E. (1955) *J. Am. Chem. Soc.*, **77**, 1446–8.

Abraham, B. M., Osborne, D. W., Flotow, H. E., and Marcus, R. B. (1960) *J. Am. Chem. Soc.*, **82**, 1064–8.

Ackermann, R. J., Gilles, P. W., and Thorn, R. J. (1956) *J. Chem. Phys.*, **25**, 1089–97.

Ackermann, R. J., Thorn, R. J., Alexander, C., and Tetenbaum, M. (1960) *J. Phys. Chem.*, **64**, 350–5.

Ackermann, R. J. and Rauh, E. G. (1969) *J. Phys. Chem.*, **73**, 769–78.

Ackermann, R. J., Rauh, E. G., and Chandrasekharaiah, M. S. (1969) *J. Phys. Chem.*, **73**, 762–9.

Ackermann, R. J. and Rauh, E. G. (1972) *High Temp. Sci.*, **4**, 496–505.

Ackermann, R. J. and Chang, A. T. (1973) *J. Chem. Thermodyn.*, **5**, 873–90.

Ackermann, R. J. and Rauh, E. G. (1973) *J. Inorg. Nucl. Chem.*, **35**, 3787–94.

Ackermann, R. J., Rauh, E. G., and Rand, M. H. (1979) in *Thermodynamics of Nuclear Materials,* Proc. Symp. 1979, International Atomic Energy Agency, Vienna, pp. 11–27.

Addison, C. C. and Hodge, N. (1961) *J. Chem. Soc.*, 2490–6.

Addison, C. C. (1969) *J. Chem. Soc. A*, 2457–9.

Agron, P. A. (1958) in *The Chemistry of Uranium, Collected Papers* (eds. J. J. Katz and E. Rabinowitch), USAEC Technical Information Extension, Oak Ridge, TID-5290 Book 2, pp. 610–26.

Aitken, E. A., Bartram, S. F., and Juenke, E. F. (1964) *Inorg. Chem.*, **3**, 949–54.

Aitken, E. A. and Joseph, R. A. (1966) *J. Phys. Chem.*, **70**, 1090–7.

Akin, G. A., Kackenmaster, H. P., Schrader, R. J., and Strohecker, J. W., Tate, R. E. (1950) *Chemical Processing Plant Equipment: Electromagnetic Separation Process*, Nat. Nucl. En. Ser., Div. I, 12, TID-5232, Oak Ridge, TN.

Alberman, K. B., Blakey, R. C., and Anderson, J. S. (1951) *J. Chem. Soc.*, 1352–6.
Albrecht-Schmitt, T. E., Almond, P. M., Illies, A. J., Raymond, C. C., and Talley, C. E. (2000) *J. Solid State Chem.*, **46**, 87–100.
Alcock, C. B. and Grieveson, P. (1962) *J. Inst. Method.*, **90**, 304–10.
Alcock, C. B. and Grieveson, P. (1963) *Proc. Symp. Thermodyn. Nucl. Mater.*, 1962, International Atomic Energy Agency, Vienna, STI/PUB/58, pp. 563–79.
Alcock, N. W. (1968) *J. Chem. Soc.*, 1588–94.
Alcock, N. W. and Esperas, S. (1997) *J. Chem. Soc. Dalton Trans.*, 893–6.
Alcock, N. W., Kemp, T. J., Sostero, S., and Traverso, O. (1980) *J. Chem. Soc. Dalton Trans.*, 1182–5.
Alcock, N. W., Roberts, M. M., and Chakravorti, M. C. (1980) *Acta Cryst. B*, **36**, 687–90.
Aléonard, K. B., Le Fur, Y., Champarnaud-Mesjard, J. C., Frit, B., and Roux, M. T. (1983) *J. Cryst. Growth*, **217**, 250–4.
Alexander, C. A., and Ogden, J. S., Cunningham, G. C. (1967) Battelle Memorial Institute Report, BMI-1789.
Alibegoff, G. (1886) *Liebig's Ann.*, **233**, 117–43.
Allen, A. L., Anderson, R. W., and McGill, R. M., Powell, F. W. (1950) *Electrochemical Preparation of Uranium Tetrafluoride*, part I, Low Temperature Cell, K-680.
Allen, G. C. and Griffiths, G. C. (1977) *J. Chem. Soc. Dalton Trans.*, 1144–8.
Allen, G. C. Griffiths, A. J., and Suckling, C.W. (1978) *Chem. Phys. Lett.*, **53**, 309–12.
Allen, G. C., Tempest, P. A., and Tyler, J. W. (1982) *Nature*, **295**, 48–9.
Allen, G. C. and Tyler, J. W. (1986) *J. Chem. Soc., Faraday Trans. 1*, **82**, 1367–79.
Allen, G. C. and Holmes, N. R. (1995) *J. Nucl. Mater.*, **223**, 231–7.
Allen, P. G., Bucher, J. J., Clark, D. L., Edelstein, N. M., Ekberg, S. A., Gohdes, J. W., Hudson, E. A., Kaltsyoannis, N., Lukens, W. W., Neu, M. P., Palmer, P. P., Reich, T., Shuh, D. K., Tait, C. D., and Zwick, B. D. (1995) *Inorg. Chem.*, **34**, 4797–807.
Allen, P. G., Shuh, D. K., Bucher, J. J., Edelstein, N. M., Palmer, C. E. A., Silva, R. J., Nguyen, S. N., Marquez, L. N., and Hudson, E. A. (1996a) *Radiochim. Acta*, **75**, 47–53.
Allen, P. G., Shuh, D. K., Bucher, J. J., Edelstein, N. M., Reich, T., Denecke, M. A., and Nitsche, H. (1996b) *Inorg. Chem.*, **35**, 784–7.
Allen, P. G., Bucher, J. J., Shuh, D. K., and Edelstein, N. M. (2000) *Inorg. Chem.*, **39**, 595–601.
Allen, S., Barlow, S., Halasyamani, P. S., Mosselmans, J. F. W., O'Hare, D., Walker, S., and Walton, R. I. (2000) *Inorg. Chem.*, **39**, 3791–8.
Allpress, J. G. (1964) *J. Inorg. Nucl. Chem.*, **26**, 1847–51.
Allpress, J. G. and Wadsley, A. D. (1964) *Acta Cryst.*, **17**, 41–6.
Allpress, J. G. (1965) *J. Inorg. Nucl. Chem.*, **27**, 1521–7.
Allpress, J. G., Anderson, J. S., and Hambly, A. N. (1968) *J. Inorg. Nucl. Chem.*, **30**, 1195–208.
Almond, P. M. and Albrecht-Schmitt, T. E. (2002) *Inorg. Chem.*, **41**, 1177–83.
Almond, P. M., Peper, S. M., Bakker, E., and Albrecht-Schmitt, T. E. (2002) *J. Solid State Chem.*, **168**, 358–66.
Almond, P. M. and Albrecht-Schmitt, T. E. (2004) *Am. Miner.*, **89**, 976–80.
Amberger, H.-D., Grape, W., and Stumpp, E. (1983) *J. Less Common Metals*, **95**, 181–90.

American Society for Testing and Materials (1980) ASTM E244-80, Annual Book of ASTM Standards, vol. 12.01.
American Society for Testing and Materials (1991a) ASTM D2907-91, Annual Book of ASTM Standards, vol. 11.02.
American Society for Testing and Materials (1991b) ASTM D5174-91, Annual Book of ASTM Standards, vol. 11.02.
American Society for Testing and Materials (1993) ASTM C1255-93, Annual Book of ASTM Standards, vol. 12.01.
American Society for Testing and Materials (1994) ASTM D1267-94, Annual Book of ASTM Standards, vol. 12.01.
American Society for Testing and Materials (1997) ASTM C1344-97, Annual Book of ASTM Standards, vol. 12.01.
American Society for Testing and Materials (1998) ASTM D6239-98, Annual Book of ASTM Standards, vol. 11.02.
American Society for Testing and Materials (1999) ASTM C1413-99, Annual Book of ASTM Standards, vol. 12.01.
Amme, M. (2002) *Radiochim. Acta*, **90**, 399–406.
Anders, E., Wolf, R., Morgan, J. W., Ebihara, M., Woodrow, A. B., and Janssens, M.-J., Hertogen, J. (1988) NAS-NS-3117, Office of Scientific and Technical Information, USDOE.
Andersen, R. A. (1979) *Inorg. Chem.*, **18**, 1507–9.
Anderson, A., Chieh, C., Irish, D. E., and Tong, J. P. K. (1980) *Can. J. Chem.*, **58**, 1651–8.
Anderson, R. W., and Allen, A. L., Powell, E. W. (1950) *Electrochemical Preparation of Uranium Tetrafluoride*, Part II, High Temperature Cell, K-681.
Anderson, J. S. and Johnson, K. D. B. (1953) *J. Chem. Soc.*, 1731–7.
Anderson, J. S., Edgington, D. N., Roberts, L. E. J., and Wait, E. (1954) *J. Chem. Soc.*, 3324–31.
Anderson, J. S. and Barraclough, C. G. (1963) *Trans. Faraday Soc.*, **59**, 1572–9.
Anderson, J. S. (1969) *Chimia*, **23**, 438–44.
Anderson, J. S. (1970) in *Modern Aspects of Solid State Chemistry* (ed. C. N. R. Rao), Plenum Press, New York, pp. 29–105.
Andreev, A. V., Bartashevich, M. I., Deryagin, A. V., Havela, L., and Sechovský, V. (1986) *Phys. Status Solidi. A*, **98**, K47–K51.
Andreev, A. V., Zadvorkin, S. M., Bartashevich, M. I., Goto, T., Kamarád, J., Arnold, Z., and Drulis, H. (1998) *J. Alloys Compds*, **267**, 32–6.
Andres, H. P., Krämer, K., and Güdel, H.-U. (1996) *Phys. Rev B*, **54** (6), 3830–40.
Andresen, A. F. (1958) *Acta Crystallogr.*, **11**, 612–14.
Andrieux, L. (1948) *Rev. Met.*, **45**, 49–59.
Andrieux, L. and Blum, P. (1949) *C. R. Acad. Sci.*, **229**, 210–12.
Anonymous (1955) *Purex Technical Manual*, Chemical Development Subsection, Separations Technology Section, Engineering Department, Hanford Atomic Products Operation, declassified with deletion as HW-31000 DEL, ch.II, p. 202, fig. II-1.
Anson, C. E., Al-Jowder, O., Upali, A., Jayasooriya, U. A., and Powell, A. K. (1996) *Acta Cryst. C*, **52**, 279–81.
Anthony, A. M., Kiyoura, R., and Sata, T. (1963) *J. Nucl. Mater.*, **10**, 8–14.

Antill, J. E., Barnes, E., and Gardner, M. (1961) *Prog. Nucl. Energy, Div. V, Metallurgy and Fuels* (eds. H. H. Finniston and J. P. Howe), Pergamon Press, Oxford, vol. 1. pp. 9–18.
Appleman, D. E. and Evans, H. T. (1965) *Am. Miner.*, **50**, 825–42.
Arajs, S. and Colvin, R. V. (1964) *J. Less Common Metals*, 7, 54–66.
Arendt, J., Powell, E. W., and Saylor, H. (1957) A brief guide to UF_6-Handling, K-1323.
Arko, A. J. and Schirber, J. E. (1979) *J. Physique*, Suppl. 40, Coll. C4, 9–14.
Aronson, S. and Belle, J. (1958) *J. Chem. Phys.*, **29**, 151–8.
Aronson, S. and Clayton, J. C. (1960) *J. Chem. Phys.*, **32**, 749–54.
Aronson, S. and Clayton, J. C. (1961) *J. Chem. Phys.*, **35**, 1055–8.
Aronson, S., Rulli, J. E., and Schaner, B. E. (1961) *J. Chem. Phys.*, **35**, 1382–8.
Asami, N., Nishikawa, M., and Taguchi, M. (1975)in *Thermodynamics of Nuclear Materials,* Proc. Symp. 1974, vol. I, International Atomic Energy Agency, Vienna, pp. 287–94.
Atencio, D., Neumann, R., and Silva, A. J. G. C. (1991) *Can. Miner.*, **29**, 95–105.
Atencio, D., Carvalho, F. M. S., and Matioli, P. A. (2004) *Am. Miner.*, **89**, 721–4.
Atoji, M. and McDermott, M. J. (1970) *Acta Crysallogr. B*, **26**, 1540–4.
Aukrust, E., Førland, T., and Hagemark, K. (1962) in *Thermodynamics of Nuclear Materials,* Proc. Symp. 1962, International Atomic Energy Agency, Vienna, pp. 713–22.
Aurov, N. A. and Chirkst, D. E. (1983) *Radiokhimiya*, **25**, 468–73.
Aurov, N. A., Volkov, V. A., and Chirkst, D. E. (1983) *Radiokhimiya*, **25**, 366–72.
Auzel, F. and Malta, O. (1983) *J. Phys.(Paris)*, **44**, 201–6.
Avens, L. R., Bott, S. G., Clark, D. L., Sattelberger, A. P., Watkin, J. G., and Zwick, B. D. (1994) *Inorg. Chem.*, **33**, 2248–56.
Avignant, D. and Cousseins, J.-C. (1971) *Compt. Rend. C*, **272**, 2151–3.
Avignant, D., Vedrine, A., and Cousseins, J.-C. (1977) *Compt. Rend. C*, **284**, 651–4.
Avignant, D., Mansouri, I., Sabatier, R., and Cousseins, J.-C. (1980) *Acta Crystallogr. B*, **36**, 664–6.
Avignant, D., Mansouri, I., Sabatier, R., and Cousseins, J.-C. (1982) *Acta Crystallogr. B*, **24**, 1968–38.
Babelot, J. F., Brumme, G. D., Kinsman, P. R., and Ohse, R. W. (1977) *Atomwirtsch. Atomtech.*, **22**, 387–9.
Bacher, W. and Jacob, E. (1980) Verbindungen mit Fluor, in *Gmelin Handbuch der Anorganischen Chemie,* (1980) System no. 55, Uranium, Suppl. vol. C8, Springer, Berlin.
Bacher, W. and Jacob, E. (1982) *Chemiker-Zeitung*, **106** (3), 117–36.
Bacher, W. and Jacob, E (1986) Uranium hexafluoride, its chemistry related to its major applications, in *Handbook on the Physics and Chemistry of the Actinides* (eds. A. J. Freeman and C. Keller), Elsevier, Amsterdam, vol. 4, ch. 1, 1–38.
Bacmann, M. (1973) *Acta Crystallogr.*, **B29**, 1570–2.
Baes, C. F. Jr, Zingeno, R. A., and Coleman, C. F. (1958) *J. Phys. Chem.*, **62**, 129–35.
Baes, C. F. Jr and Mesmer, R. E. (1976) *The Hydrolysis of Cations,* John Wiley, New York.
Baer, Y. (1984) Electronic spectroscopy studies, in *Handbook on the Physics and Chemistry of the Actinides,* vol. 1, ch. 4, (eds. J. P. Desclaux and A. J. Freeman), Elsevier, Amsterdam, 271–340.

Bagnall, K. W., Brown, D., and Deane, A. M. (1962) *J. Chem. Soc.*, 1655–7.
Bagnall, K. W., Brown, D., and du Preez, J. G. H. (1964) *J. Chem. Soc.*, 2603–8.
Bagnall, K. W., Brown, D., Jones, P. J., and du Preez, J. G. H. (1965) *J. Chem. Soc.*, 350–3.
Bagnall, K. W. (1967) in *Halogen Chemistry of the Actinides,* (ed. V. Gutman), Academic Press, London, vol. 3, ch. 7.
Bagnall, K. W., Brown D., and Easey, J. F. (1968) *J. Chem. Soc. A*, 288–92.
Bagnall, K. W. and Wakerley, M. W. (1974) *J. Less Common Metals*, **35**, 267–74.
Bagnall, K. W., du Preez. J. G. H., Gellatly, B. J., and Holloway, J. H. (1975) *J. Chem. Soc. Dalton Trans.*, 1963–8.
Bagnall, K. W. (1979) Complex compounds of uranium, in *Gmelin Handbook of Inorganic Chemistry*, E 1 Suppl., 1–223.
Bagnall, K. W. (1987) The actinides, in *Comprehensive Coordination Chemistry* vol. 3, ch. 40 (eds. G. Wilkinson, R. D. Gillard, and J. A. McCleverty), Pergamon Press, New York, 1129–228.
Baïchi, M., Chattillon, C., and Guéneau, Le Ny, J. (2002) *J. Nucl. Mater.*, **303**, 196–9.
Baird, C. P. and Kemp, T. J. (1997) *Prog. Reaction Kinetics*, **22**, 87–139.
Bakakin, V. V. (1965) *Zh. Strukt. Khim.*, **6**, 563–6; *J. Struct. Chem.* (*USSR*), **6**, 536–9.
Baker, R. D., Hayward, B. R., Hull, G., Raich, B., and Weiss, A. R. (1946) *Preparation of Uranium Metal by the Bomb Method*, LA-472.
Balzani, V. and Carassiti, V. (1970) *Photochemistry of Coordination Compounds,* Academic Press, London, ch. 15.
Bannister, M. J. (1967) *J. Nucl. Mater.*, **24**, 340–2.
Bannister, M. J. and Taylor, J. C. (1970) *Acta Crystallogr.*, **B26**, 1775–81.
Bannister, M. J. and Buykx, W. J. (1974) *J. Nucl. Mater.*, **55**, 345–51.
Barash, Y. B., Barak, J., and Mintz, M. H. (1984) *Phys. Rev. B*, **29**, 6096–104.
Bard, A. J. and Parsons, R. (1985) *Standard Potentials in Aqueous Solution,* Marcel Dekker, New York.
Bardin, N., Rubini, P., and Madic, C. (1998) *Radiochim. Acta*, **83**, 189–94.
Barnard, R., Bullock, J. I., and Larkworthy, L. F. (1967) *Chem. Comm.*, 1270–2.
Barnard, R., Bullock, J. I., and Larkworthy, L. F. (1972a) *J. Chem. Soc. Dalton Trans.*, 964–70.
Barnard, R., Bullock, J. I., Gellatly, B. J., and Larkworthy, L. F. (1972b) *J. Chem. Soc. Dalton Trans.*, 1932–8.
Barnard, R., Bullock, J. I., Gellatly, B. J., and Larkworthy, L. F. (1973) *J. Chem. Soc. Dalton Trans.*, **6**, 604–7.
Barrett, C. S., Mueller, M. H., Hitterman, R. L. (1963) *Phys. Rev.* **129**, 625–9.
Barton, C. J., Friedman, H. A., Grimes, W. R., Insley, H., Moore, R. E., and Thoma, R. E. (1958) *J. Am. Ceram. Soc.*, **41**, 63–9.
Bartram, S. F., Juenke, E. F., and Aitken, E. A. (1964) *J. Am. Ceram. Soc.*, **47**, 171–5.
Bartram, S. F. (1966) *Inorg. Chem.*, **5**, 749–54.
Bartram, S. F. and Fryxell, R. E. (1970) *J. Inorg. Nucl. Chem.*, **32**, 3701–6.
Bartscher, W. and Sari, C. (1983) *J. Nucl. Mater.*, **118**, 220–3.
Bartscher, W., Boeuf, A., Caciuffo, R., Fournier, J. M., Kuhs, W. F., Rebizant, J., and Rustichelli, F. (1985) *Solid State Commun.*, **53**, 423–6.
Baskin, Y. and Shalek, P. D. (1964) *J. Inorg. Nucl. Chem.*, **26**, 1679–84.
Baskin, Y. (1969) *J. Inorg. Nucl. Chem.*, **29**, 2480–2.

Basnakova, G., Spencer, A. J., Palsgard, E., Grime, G. W., and Macaskie, L. E. (1998) *Environ. Sci. Technol.*, **32**, 760–5.
Bates, J. L. (1964) USAEC Hanford Report, HW-81603.
Bates, J. L. (1966) *J. Am. Ceram. Soc.*, **49**, 395–6.
Bates, J. L., Hinman, C. A., and Kawada, K. (1967) *J. Am. Ceram. Soc.*, **50**, 652–6.
Bates, J. K., Bradley, J. P., Teetsov, A., Bradley, C. R., and Buchholtz ten Brink, M. (1992) *Science*, **256**, 469–71.
Battles, J. E., Shinn, W. A., and Blackburn, P. E. (1972) *J. Chem. Thermodyn.*, **4**, 425–39.
Bayliss, P., Mazzi, F., Munno, R., and White, T. J. (1989) *Miner. Mag.*, **53**, 565–9.
Bayovlu, A. S. and Lorenzelli, R. (1984) *Solid State Ionics*, **12**, 53–66.
Beals, R. J. and Handwerk, J. H. (1965) *J. Am. Ceram. Soc.*, **48**, 271–4.
Bean, A. C., Campana, C. F., Kwon, O., and Albrecht-Schmitt, T. E. (2001a) *J. Am. Chem. Soc.*, **123**, 8806–10.
Bean, A. C., Ruf, M., and Albrecht-Schmitt, T. E. (2001b) *Inorg. Chem.*, **40**, 3959–63.
Beaudry, B. J. and Daane, A. H. (1959) *Trans. Met. Soc. (AIME)*, **215**, 199–203.
Beck, H. P. and Kuehn, F. (1995) *Z. Anorg. Allg. Chem.*, **621**, 1659–62.
Beck, M. T. and Nagypál, I. (1990) *Chemistry of Complex Equilibria,* Harwood Ltd. Publishers, New York.
Becker, E. W. (1979) in *Uranium Enrichment* (ed. S. Villani), Springer, Berlin, p. 245.
Becker, J. S. and Dietze, H.-J. (1998) *Spectrochim. Acta*, **52B**, 177–87.
Becquerel, H. (1896) *C.R. Acad. Sci.*, **122**, 501–3.
Belbeoch, B., Boivineau, J. C., and Pério, P. (1967) *J. Phys. Chem. Solids*, **28**, 1267–75.
Bell, J. T. (1969) *J. Inorg. Nucl. Chem.*, **31**, 703–10.
Bell, J. T. and Buxton, S. R. (1974) *J. Inorg. Nucl. Chem.*, **36**, 1575–9.
Bellamy, R. G. and Hill, N. A. (1963) *The Extraction and Metallurgy of Uranium, Thorium, and Beryllium,* Pergamon Press, Oxford.
Belle, J. (1961) *Uranium Dioxide, Properties and Nuclear Applications,* U.S. Atomic Energy Commission Division of Reactors, U.S. Government Printing Office, Washington, DC.
Belle, J. (1969) *J. Nucl. Mater.*, **30**, 3–15.
Benard-Rocherulle, P., Louer, M., Louer, D., Dacheux, N., Brandel, V., and Genet, M. (1997) *J. Solid State Chem.*, **132**, 315–22.
Bendall, P. J., Fitch, A. N., and Fender, B. E. F. (1983) *J. Appl. Cryst.* **16**, 164–70.
Benedict, U. (1987) *J. Less Common Metals*, **128**, 7–45.
Ben Salem, A., Meerschaut, A., and Rouxel, J. (1984) *Compt. Rend. Hebd. Séances. Acad. Sci. Ser. 2*, **299**, 617–19.
Benson, D. A. (1977) Sandia National Laboratories Report, SAND-77–0429.
Benz, R., Douglas, R. M., Kruse, F. H., and Penneman, R. A. (1963) *Inorg. Chem.*, **2**, 799–803.
Bereznikova, I. A., Ippolitova, E. A., Simanov, Yu. P., and Kovba, L. M. (1961) Argonne National Laboratory Report, ANL-trans-33, p. 176.
Berger, M. and Sienko, M. J. (1967) *Inorg. Chem.*, **6**, 324–6.
Berlincourt, T. G. (1959) *Phys. Rev.*, **114**, 969–77.
Berndt, U. and Erdman, B. (1973) *Radiochim. Acta*, **19**, 45–6.
Berndt, U., Tanamas, R., and Keller, C. (1976) *J. Solid State Chem.*, **17**, 113–20.
Bernstein, E. R., Keiderling, T. A., Lippard, S. J., and Mayerle, J. J. (1972a) *J. Am. Chem. Soc.*, **94**, 2552–3.

Bernstein, E. R., Hamilton, W. C., Keiderling, T. A., LaPlaca, S. J., Lippard, S. J., and Mayerle, J. J. (1972b). *Inorg. Chem.*, **11**, 3009–16.
Bernstein, E. R. and Keiderling, T. A. (1973) *J. Chem. Phys.*, **59**, 2105–22.
Berry, J. A., Poole, R. T., Prescott, A., Sharp, D. W. A., and Winfield, J. M. (1976) *J. Chem. Soc. Dalton Trans.*, 272–4.
Berry, J. A., Prescott, A., Sharp, D. W. A., and Winfield, J. M. (1977) *J. Fluorine Chem.*, **10**, 247–54.
Berthet J.-C., Rivière, C., Miquel, Y., Nierlich, M., Madic, C., and Ephritikhine, M. (2002) *Eur. J. Inorg. Chem.*, 14390–46.
Berthet, J.-C., Nierlich, M., and Ephritikhine, M. (2003) *Chem. Commun.*, 1660–1.
Berthold, H. J., Hien, H. G., and Reuter, H. (1957) *Ber. Dtsch. Keram. Ges.*, **50**, 111–14.
Berthold, H. J. and Knecht, H. (1965a) *Angew. Chem.*, **77**, 428.
Berthold, H. J. and Knecht, H. (1965b) *Angew. Chem.*, **72**, 453.
Berthold, H. J. and Delliehausen, C. (1966) *Angew. Chem.*, **78**, 750–1.
Berthold, H. J. and Knecht, H. (1966) *Z. Anorg. Allg. Chem.*, **348**, 50–7.
Berthold, H. J. and Knecht, H. (1968) *Z. Anorg. Allg. Chem.*, **356**, 151–62.
Bertino, J. P. and Kirchner, J. A. (1945) *U^{233} Purification and Metal Production*, LA-245.
Bertsch, P. M., Hunter, D. B., Sutton, S. R., Bajt, S., and Rivers, M. L. (1994) *Environ. Sci. Technol.*, **28**, 980–4.
Besson, J. and Chevallier, J. (1964) *Compt. Rend. Hebd. Séances Acad. Sci.*, **258**, 5888–91.
Bevan, D. J. M., Grey, I. E., and Willis, B. T. M. (1986) *J. Solid State Chem.*, **61**, 1–7.
Bevz, A. S., Kapshukov, I. I., Vorobei, M. P., and Skiba, O. V. (1970) *Zh. Strukt. Khim.*, **11**, 936; *J. Struct. Chem.* (*USSR*), **11**, 872.
Biennewies, M. and Schäfer, H. (1974) *Z. Anorg. Allg. Chem.*, **407**, 7–44.
Billard, I. and Lützenkirchen, K. (2003) *Radiochim. Acta*, **91**, 285–94.
Birch, W. D., Mumme, W. G., and Segnit, E. R. (1988) *Aust. Miner.*, **3**, 125–31.
Bittel, J. T., Sjodahl, L. H., and White, J. F. (1969) *J. Am. Ceram. Soc.*, **52**, 446–51.
Bjerrum, J., Schwarzenbach, G., and Sillén, L. G. (1956) *Stability Constants. Part I Organic Ligands,* The Chemical Society, London.
Bjerrum, J., Schwarzenbach, G., and Sillén, L. G. (1957) *Stability Constants. Part II Inorganic Ligands,* The Chemical Society, London.
Blackburn, P. E. (1958) *J. Phys. Chem.*, **62**, 897–902.
Blake, C. A., Baes, C. F. Jr, Brown, K. B., Coleman, C. F., and White, J. C. (1958) *Proc. Second Int. Conf. on Peaceful Uses of Atomic Energy*, **vol. 28**, pp. 289–98. Geneva, 1958,
Blank, H. and Ronchi, C. (1968) *Acta Crystallogr.*, **A24**, 657–66.
Blasse, G. (1964) *Z. Anorg. Allg. Chem.*, **331**, 44–50.
Blaton, N., Vochten, R., Peters, O. M., and van Springel, K. (1999) *Neues Jahrb. Miner. Monatsschr.*, pp. 253–64.
Blatov, V. A., Serezhkina, L. B., Serezhkin, V. N., and Trunov, V. K. (1989) *Zh. Neorg. Khim.*, **34**, 162–4; *Russian J. Inorg. Chem.*, **34**, 91–2.
Blum, P. L., Guinet, P., and Vaugoyeau, H. (1963) *C.R. Acad. Sci.(Paris)*, **257**, 3401–3.
Blumenthal, B. and Noland, R. A. (1956) *Progress in Nuclear Energy, Div. V, Metallurgy and Fuels* (eds. H. H. Finniston and J. P. Howe), Pergamon Press, Oxford, vol. 1 pp. 62–80.
Bober, M., Karow, H. U., and Schretzmann, K. (1975) in *Thermodynamics of Nuclear Materials,* Proc. Symp. 1974, vol. I, , International Atomic Energy Agency, Vienna, pp. 295–305.

Boehme, D. R., Nichols, M. C., Snyder, R. L., and Matheis, D. P. (1992) *J. Alloys Compds*, **179**, 37–59.
Boeyens, J. C. A. and Haegele, R. (1976) *Inorg. Chim. Acta*, **20**, L7.
Bogacz, A., Bros, J. P., Gaune-Escard, M., Hewat, A. W., and Taylor, J. C. (1980) *J. Phys. C*, **13**, 5273–8.
Bohrer, R., Conradi, E., and Müller, U. (1988) *Z. Anorg. Allg. Chem.*, **558**, 119–27.
Bohres, E. W., Krasser, W., Schenk, H.-J., and Schwochau, K. (1974) *J. Inorg. Nucl. Chem.*, **36**, 809–13.
Bois, C., Dao, N. Q., and Rodier, N. (1976a) *Acta Crystallogr. B*, **32**, 1541–9.
Bois, C., Dao, N. Q., and Rodier, N. (1976b) *J. Inorg. Nucl. Chem.*, **38**, 755–7.
Bokolo, K., Delpuech, J.-J., Rodehüser, L. R., and Rubini, P. R. (1981) *Inorg. Chem.*, **20**, 992–7.
Bommer, H. (1941) *Z. Anorg. Allg. Chem.*, **247**, 249–58.
Boraopkova, M. N., Kanetsova, G. N., and Novoselova, A. B. (1971) *Izvestia A.N. SSSR, Ser. Neorgan. Mater.*, **7**, 242.
Borène, J. and Cesbron, F. (1971) *Bull. Soc. Fr. Minér. Crystallogr.*, **94**, 8–14.
Borisov, S. K. and Zadneporovskii, G. M. (1971) *At. Energy (USSR)*, **31**, 63–5; Sov. At. Energy, **31**, 761–73.
Boroujerdi, A. (1971) Research Center Karlsruhe Report, KFK-1330.
Bougon, R. and Plurien, P. (1965) *Compt. Rend.*, **260**, 4217–18.
Bougon, R., Charpin, P., Desmoulin, J. P., and Malm, J. G. (1976a) *Inorg. Chem.*, **15**, 2532–40.
Bougon, R., Costes, R. M., Desmoulin, J. P., and Michel, J., Person, J. L. (1976b) *J. Inorg. Nucl. Chem.*, Suppl., 99–105.
Bougon, R., Joubert, P., Weulersse, J.-M., and Gaudreau, B. (1978) *Can. J. Chem.*, **56**, 2546–9.
Bougon, R., Fawcett, J., Holloway, J. H., and Russell, D. R. (1979) *J. Chem. Soc. Dalton Trans.*, 1881–5.
Boulet, P., Daoudi, A., Potel, M., Noël, H., Gross, G. M., Andre, G., and Bouree, F. (1997a) *J. Alloys Compds*, **247**, 104–8.
Boulet, P., Daoudi, A., Potel, M., and Noël, H. (1997b) *J. Solid State Chem.*, **129**, 113–16.
Boulet, P., Potel, M., Levet, J. C., and Noël, H. (1997c) *J. Alloys Compds*, **262–3**, 229–34.
Bowen, R. B., Lincoln, S. F., and Williams, E. H. (1976) *Inorg. Chem.*, **15**, 2126–9.
Bowen, R. B., Honan, G. J., Lincoln, S. F., Spotswood, T. M., and Williams, E. H. (1979) *Inorg. Chim. Acta*, **33**, 235–9.
Boyd, C. M. and Menis, O. (1961) *Anal. Chem.*, **33**, 1016–18.
Bradley, M. J. and Ferris, L. M. (1962) *Inorg. Chem.*, **1**, 683–7.
Bradley, M. J. and Ferris, L. M. (1964) *Inorg. Chem.*, **3**, 189–95.
Brandel, V., Dacheux, N., and Genet, M. (1996) *J. Solid State Chem.*, **121**, 467–72.
Branstätter, F. (1981) *Tschermaks Miner. Petrogr. Mitt.*, **29**, 1–8.
Brater, D. C. and Smiley, S. H. (1958) Structural transitions in UCl_4 anticipating melting, in *Progress in Nuclear Chemistry,* Ser. III, *Process Chemistry* vol. 2 (eds. F. R. Bruce, J. M. Fletcher, and H. H. Hyman), Pergamon Press, London, pp. 136–48.
Brauer, G. (1981) *Handbuch der Präparativen Anorganischen Chemie*, 3rd edn, Ferdinand Elke Verlag, Stuttgart.

Braun, R., Kemmler-Sack, S., Roller, H., Seemann, I., and Wall, I. (1975) *Z. Anorg. Allg. Chem.*, **415**, 133–55.
Bredig, M. A. (1972) in *Proc. CNRS Conf. in Odeillo, 1971*, CNRS, Paris, p. 183.
Breeze, E. W., Brett, N. H., and White, J. (1971) *J. Nucl. Mater.*, **39**, 157–65.
Breeze, E. W. and Brett, N. H. (1971) *J. Nucl. Mater.*, **40**, 113–15.
Breeze, E. W. and Brett, N. H. (1972) volume date1972/1973, *J. Nucl. Mater.*, **45**, 131–8.
Breitung, W. (1978) *J. Nucl. Mater.*, **74**, 10–18.
Brendt, U. and Erdman, B. (1973) *Radiochim. Acta*, **19**, 45–6.
Brenner, I. B., Liezers, M., Godfrey, J., Nelms, S., and Cantle, J. (1998) *Spectrochim. Acta*, **53**, 1087–107.
Brisi, C. (1960) *Ric. Sci.*, **30**, 2376–81.
Brisi, C. (1969) *Ann. Chim. (Rome)*, **59**, 400–11.
Brisi, C. (1971) *Rev. Int. Hautes Temp. Réfract.*, **8**, 37–41.
Brisi, C., Montorsi, M., and Burlando, G. A. (1972) *Atti. Acad. Sci. Torino, Cl. Sci. Fis. Mater. Nat.*, **106**, 257.
Brit, D. W. and Anderson, H. J. (1962) USAEC Technical Information Service, TID-7637, p. 408.
Brochu, R. and Lucas, J. (1967) *Bull. Soc. Chim. France*, 4764–7.
Brodsky, M. B., Griffin, N. J., and Odie, M. D. (1969) *J. Appl. Phys.*, **8**, 895–7.
Brookins, D. G. (1990) *Waste Manage.*, **10**, 285–96.
Bros, J. P., Gaune-Escard, M., Szczepaniak, W., Bogacz, A., and Hewat, A. W. (1987) *Acta Crystallogr. B*, **43**, 113–16.
Brown, D. (1966) *J. Chem. Soc.* (*A*), 766–9.
Brown, D. (1968) *The Halides of the Lanthanides and Actinides,* Wiley Interscience, New York.
Brown, D., Fletcher, S., and Holah, D. G. (1968) *J. Chem. Soc. A*, 1889–94.
Brown, D., Hill, J., and Rickard, C. E. F. (1970) *J. Chem. Soc. A*, 476–80.
Brown, D. (1972) The actinide halides and their complexes, in MTP (*Med. Tech. Publ. Co.*) *Intern. Rev. Sci. Inorg. Chem. Ser. One*, 7, 87–137.
Brown, D. and Edwards, J. (1972) *J. Chem. Soc. Dalton Trans.*, 1757–62.
Brown, D. (1973) in *Comprehensive Inorganic Chemistry,* vol. 5, Pergamon Press, Oxford, pp. 151–208.
Brown, D., Whittaker, B., and Lidster, P. E. (1975) Atomic Energy Research Establishment (UK) Report, AERE-R-8035, p. 16.
Brown, D., Lidster, P., Whittaker, B., and Edelstein, N. (1976) *Inorg. Chem.*, **15**, 511–51.
Brown, D. (1979) Compounds of Uranium with Chlorine, Bromine and Iodine, in *Gmelin Handbook of Inorganic Chemistry,* System no. 55, Uranium, Suppl., vol. C9, Springer, Berlin, pp. 1–186.
Brown, D., Berry, J. A., Holloway, J. H., Holland, R. F., and Staunton, G. M. (1983) *J. Less Common Metals*, **92**, 149–53.
Brown, D. R. and Denning, R. G. (1996) *Inorg. Chem.*, **35**, 6158–63.
Brown, G. M. and Walker, L. A. (1966) *Acta Crystallogr.*, **20**, 220–9.
Brown, K. B., Coleman, C. F., Crouse, D. J., Blake, C. A., and Ryan, A. D. (1958) *Proc. Second Int. Conf. on Peaceful Uses of Atomic Energy*, Geneva, 1958, vol. 3, pp. 472–87.
Browning, P., Gillan, M. J., and Potter, P. E. (1978) *Rev. Int. Hautes Tempér. Réfract. Fr.*, **15**, 333–46.

Browning, P. (1981) *J. Nucl. Mater.*, **98**, 345–56.
Browning, P., Hyland, G. J., and Ralph, J. (1983) Oak Ridge National Laboratory Report, *High Temp.-High Press.*, **15**, 169–78.
Brugger, J., Burns, P. C., and Meisser, N. (2003) *Am. Miner.*, **88**, 676–85.
Brugger, J., Krivovichev, S. V., Berlepsch, P., Meisser, N., Ansermet, S., and Armbruster, T. (2004) *Am. Mineral.*, **89**, 339–47.
Brunton, G. D. (1965) Oak Ridge National Laboratory Report, ORNL-3913, p. 10.
Brunton, G. D., Insley, H., and McVay, T. N., Thoma, R. E. (1965) Oak Ridge National Laboratory Report, ORNL-3761, p. 212; (1965) N.S.A. 19, no. 15416.
Brunton, G. D. (1966) *Acta Crystallogr.*, **21**, 814–17.
Brunton, G. D. (1967) *J. Inorg. Nucl. Chem.*, **29**, 1631–6; Oak Ridge National Laboratory Report, ORNL-4076; (1967) N.S.A. 21.
Brunton, G. D. (1969a) *Acta Crystallogr. B*, **25**, 2163–4; **26B**, 2519.
Brunton, G. D. (1969b) *Acta Crystallogr. B*, **25**, 1919–21.
Brunton, G. D. (1971) *Acta Crystallogr. B*, **27**, 245–7.
Brusset, H., Gillier-Pandraut, H., and Dao, N. Q. (1969) *Acta Crystallogr.*, **25B**, 67–73.
Brusset, H. and Dao, N. Q. (1971) *J. Inorg. Nucl. Chem.*, **33**, 1365–72.
Brusset, H., Dao, N. Q., and Rubinstein-Auban, A. (1972) *Acta Cryst. B*, **28**, 2617–19.
Brusset, H., Dao, N. Q., and Chourou, S. (1974) *Acta Cryst.*, **30B**, 768–73.
Buck, E. C., Brown, N. R., and Dietz, N. L. (1996) *Environ. Sci. Technol.*, **30**, 81–8.
Buck, E. C., Wronkiewicz, D. J., Finn, P. A., and Bates, J. K. (1997) *J. Nucl. Mater.*, **249**, 70–6.
Buck, E. C. and Bates, J. K. (1999) *Appl. Geochem.*, **14**, 635–53.
Buck, E. C., Finn, P. A., and Bates, J. K. (2004) *Micron*, **35**, 235–43.
Budnikov, P. P., Tresvyatsky, S. G., and Kushakovsky, V. I. (1958) in *Proc. Second Int. Conf. on Peaceful Uses of Atomic Energy*, Geneva, 1958, vol. 6, United Nations, Geneva, pp. 124–31.
Bugl, J. and Bauer, A. A. (1964) in Waber *et al.* (1964), pp. 215–24.
Buhrer, C. F. (1969) *J. Phys. Chem. Solids*, **30**, 1273–6.
Bullock, J. I. (1969) *J. Chem. Soc. A*, 781– 4.
Bunnell, L. R., Chikalla, T. D., and Woodley, R. E. (1975) *Hydrolysis of Uranium Carbide Fuel Beads*, BNWL-SA-5513.
Burk, W. (1967) *Z. Anorg. Allg. Chem.*, **350**, 92–6.
Burk, W. and Naumann, D. (1969) *Z. Chem. (Leipzig)*, **9**, 189.
Burns, J. H., Osborne, D. W., and Westrum, E. F. Jr (1960) *J. Chem. Phys.*, **33**, 387–94.
Burns, J. H. and Duchamp, D. J. (1962) Oak Ridge National Laboratory Report, ORNL-3262, pp. 14–16; N.S.A. 16, no. 17553.
Burns, J. H., Ellison, R. D., and Levy, H. A. (1968) *Acta Crystallogr. B*, **24**, 230–7.
Burns, P. C., Miller, M. L., and Ewing, R. C. (1996) *Can. Miner.*, **34**, 845–80.
Burns, P. C. (1997) *Am. Miner.*, **82**, 1176–86.
Burns, P. C., Ewing, R. C., and Miller, M. L. (1997a) *J. Nucl. Mater.*, **245**, 1–9.
Burns, P. C., Finch, R. J., Hawthorne, F. C., Miller, M. L., and Ewing, R. C. (1997b) *J. Nucl. Mater.*, **249**, 199–206.
Burns, P. C. (1998a) *Can. Miner.*, **36**, 847–53.
Burns, P. C. (1998b) *Can. Miner.*, **36**, 187–99.
Burns, P. C. (1998c) *Can. Miner.*, **36**, 1061–7.
Burns, P. C. (1998d) *Can. Miner.*, **36**, 1069–75.

Burns, P. C. (1999a) *Rev. Miner.*, **38**, 23–90.
Burns, P. C. (1999b) *Am. Miner.*, **84**, 1661–73.
Burns, P. C. and Finch, R. J. (1999) *Am. Miner.*, **84**, 1456–60.
Burns, P. C. and Hanchar, J. M. (1999) *Can. Miner.*, **37**, 1483–91.
Burns, P. C. (2000) *Am. Miner.*, **85**, 801–5.
Burns, P. C. and Hill, F. C. (2000a) *Can. Miner.*, **38**, 163–73.
Burns, P. C. and Hill, F. C. (2000b) *Can. Miner.*, **38**, 175–82.
Burns, P. C., Olson, R. A., Finch, R. J., Hanchar, J. M., and Thibault, Y. (2000) *J. Nucl. Mater.*, **278**, 290–300.
Burns, P. C. (2001a) *Can. Miner.*, **39**, 1139–46.
Burns, P. C. (2001b) *Can. Miner.*, **39**, 1153–60.
Burns, P. C. and Hayden, L. A. (2002) *Acta Crystallogr. C*, **58**, 121–2.
Burns, P. C. and Li, Y. (2002) *Am. Miner.*, **87**, 550–7.
Burns, P. C. and Hughes, K.-A. (2003) *Am. Mineralogist*, **88**, 1165–8.
Burns, P. C., Deely, K. M., and Hayden, L. A. (2003) *Can. Miner.*, **41**, 687–706.
Burns, P. C., Deely, K. M., and Skanthakumar, S. (2004a) *Radiochim. Acta*, **92**, 151–60.
Burns, C. J., Neu, M. P., Boukhalfa, H., Gutowski, K. E., Bridges, N. J., and Rogers, R. D. (2004) *The Actinides* in *Comprehensive Coordination Chemistry II*, vol. 3, 3.3, 189–345, Elsevier Ltd, Amsterdam.
Burns, P. C., Kubatko, K.-A., Sigmon, G., Fryer, B. J., Gagnon, J. E. Antonio, M. R. and Soderholm, L. (2005) *Angew. Chem. Int. Ed.,* **44**, 2135.
Burrows, H. D. and Kemp, T. J. (1974) *Chem. Soc. Rev.*, **3**, 139–65.
Bursten, B. E. and Strittmatter, R. J. (1987) *J. Am. Chem. Soc.*, **109**, 6606–9.
Busch, G., Hulliger, F., and Vogt, O. (1979a) *J. Physique Colloq.*, **40**, C4 62–3.
Busch, G., Vogt, O., and Bartolin, H. (1979b) *J. Physique Colloq.*, **40**, C4 64–5.
Cahill, C. L. and Burns, P. C. (2000) *Am. Miner.*, **85**, 1294–7.
Caillat, R., Coriou, H., and Perio, P. (1953) *Compt. Rend. Hebd. Séances Acad. Sci.*, **237**, 812–13.
Caillat, R. (1961) in *P. Pascal, Nouveau Traité de Chimie Minérale, Masson et Cie., Paris 1967*, vol. **XV** (2), 59–121; (1967) vol. **XV** (4), 497–517.
Caira, M. R., de Wet, J. F., du Preez, J. G. H., and Gellatly, B. J. (1978) *Acta Crystallogr. B*, **34**, 1116–20.
Caley, E. R. (1948) *Isis*, **38**, 190–3.
Caneiro, A. and Abriata, J. P. (1984) *J. Nucl. Mater.*, **126**, 255–67.
Carbajo, J. J., Yoder, G. L., Popov, S. G., and Ivanov, V. K. (2001) *J. Nucl. Mater.*, **299**, 181–98.
Carlson, E. H. (1969) *Phys. Lett.*, **29A**, 696–7.
Carlson, R. S. (1975) in *Proc. Int. Conf. on Radiation Effects and Tritium Technology for Fusion Reactors*, Gatlinburg, TN, 1975, vol. 4, p. 361.
Carnall, W. T., Neufeldt, S. J., and Walker, A. (1965) *Inorg. Chem.*, **4**, 1808–13.
Carnall, W. T., Walker, A., and Neufeldt, S. J. (1966) *Inorg. Chem.*, **5**, 2135–40.
Carnall, W. T. (1970) Unpublished results.
Carnall, W. T. (1982) in *Gmelin Handbuch der Anorganischen Chemie,* 8th edn, Uranium Suppl., vol. A5, , Springer Verlag, New York, pp. 69–161.
Carnall, W. T. and Crosswhite, H. M. (1985) Argonne National Laboratory Report, ANL 84–90.
Carnall, W. T. (1989) Argonne National Laboratory Report, ANL-89/39.

Carnall, W. T., Liu, G. K., Williams, C. W., and Reid, M. F. (1991) *J. Chem. Phys.*, **95**, 7194–203.
Carter, R. E. and Lay, K. W. (1970) *J. Nucl. Mater.*, **36**, 77–86.
Casto, C. C. (1950) in *Analytical Chemistry of the Manhattan Project* (ed. C. J. Rodden), McGraw-Hill, New York, pp. 511–36.
Catalano, J. G. and Brown, G. E. (2004) *Am. Miner.*, **89**, 1004–21.
Catlow, C. R. A. and Pyper, N. C. (1979) *J. Nucl. Mater.*, **80**, 110–14.
Caville, C. and Poulet, H. (1974) *J. Inorg. Nucl. Chem.*, **36**, 1581–7.
Čejka, J. (1999) *Rev. Miner.*, **38**, 521–622.
Cesbron, F., Ildefonse, P., and Sichere, M.-C. (1993) *Miner. Mag.*, **57**, 301–8.
Chakravorti, M. C., Bharadwaj, P. K., Pandit, S. C., and Mathur, B. K. (1978) *J. Inorg. Nucl. Chem.*, **40**, 1365–7.
Champarnaud-Mesjard, J.-C. and Gaudreau, B. (1976) *Comp. Rend. C*, **282**, 745–7.
Chapman, A. T. and Clark, G. W. (1965) *J. Am. Ceram. Soc.*, **48**, 494–5.
Charpin, P. (1965) *Compt. Rend.*, **260**, 1914–16.
Charpin, P., Montoloy, F., and Nierlich, M. (1968) *Compt. Rend. C*, **266**, 1685–7.
Charpin, P., Montoloy, F., and Nierlich, M. (1969) *Compt. Rend. C*, **268**, 156–8.
Charvillat, J. P., Baud, G., and Besse, J. P. (1970) *Mater. Res. Bull.*, **5**, 933–8.
Chatalet, J. (1967) in *P. Pascal, Nouveau Traité de Chimie Minérale, Masson et Cie.,* Paris (1967) vol. 4, 508–13.
Chen, F., Burns. P. C., and Ewing, R. C. (1999) *J. Nucl. Mater.*, **275**, 81–94.
Chen, F., Burns. P. C., and Ewing, R. C. (2000) *J. Nucl. Mater.*, **278**, 225–32.
Chen, J. H., Edwards, R. L., and Wasserburg, G. J. (1992) in *Uranium Series Disequilibrium Applications to Earth, Marine, and Environmental Sciences* (eds. M. Ivanovich and R. S. Harmon), Clarendon Press, Oxford, pp. 174–206.
Chen, Z., Luo, K., Tan, F., Zhang, Y., and Gu, X. (1986) *Kexue Tongbao*, **31**, 396–401.
Chernyayev, I. I. (1966) *Complex Compounds of Uranium* (translated from Russian by L. Mandel, eds. M. Govre and IPST staff), Israel Program for Scientific Translation, Jerusalem.
Chervet, J. (1960) *Nouveau Traité de Chimie Minérale* (ed. P. Pascal), XV (1), Masson et Cie, Paris., 52–94,
Chevalier, P.-Y., Fischer, E., and Cheynet, B. (2002) *J. Nucl. Mater.*, **303**, 1–28.
Chilton, J. M. (1963) *Proc. First Protactinium Chemistry Symp*., Gatlinburg, TN, April 25–26, TID-7675, p. 157.
Chiotti, P. (1980) *Bull. Alloy Phase Diagrams*, **1**, 99.
Chiotti, P., Akhachinskij, V. V., Ansara, I., and Rand, M. H. (1981) *The Chemical Thermodynamics of Actinide Elements and Compounds*, part 5, *The Actinide Binary Alloys*, IAEA, Vienna, STI/PUB/424/5.
Chirkst, D. E. (1981) *Koord. Khimiya*, **7**, 3–17.
Chisholm-Brause, C. J., Berg, J. M., Matzner, R. A., and Morris, D. E. (2001) *J. Colloid Interface Sci.*, **233**, 38–49.
Chodos, S. L. (1972) *J. Chem. Phys.*, **57**, 2712–14.
Choppin, G. R., Bokelund, H., and Valkiers, S. (1983) *Radiochim. Acta*, **33**, 229–32.
Christ, C. L., Clark, J. R., and Evans, H. T. Jr (1955) *Science*, **121**, 472–2.
Chukanov, N. V., Pushcharovsky, D. Y., Pasero, M., Merlino, S., Barinova, A. V., Mockel, S., Pekov, I. V., Zadov, A. E., and Dubinchuk, V. T. (2004) *Eur. J. Miner.*, **16**, 367–74.
Cinader, G., Peretz, M., Damir, D., and Hadari, Z. (1973) *Phys. Rev. B*, **8**, 4063–8.

Clark, D. L., Conradson, S. D., Ekberg, S. A., Hess, N. J., Neu, M. P., Palmer, P. D., Runde, W., and Tait, C. D. (1996) *J. Am. Chem. Soc.*, **118**, 2089–90.
Clark, D. L., Conradson, S. D., Donohue, R. J., Keogh, W. D., Morris, D. E., Palmer, P. D., Rogers, R. D., and Tait, C. D. (1999) *Inorg. Chem.*, **38**, 1456–66.
Clausen, K., Hayes, W., Hutchings, M. T., Kjems, J. K., Macdonald, J. E., and Osborn, R. (1985) *High Temp. Sci.*, **19**, 189–96.
Cleaves, H. E., Cron, M. M., and Sterling, J. T. (1945) AEC Report CT2–618.
Clegg, J. W. and Foley, D. D. (1958) *Uranium Ore Processing,* Addison-Wesley, Reading, MA.
Clemente, D. A., Bandoli, G., Benetollo, F., and Marzotto, A. (1974) *J. Cryst. Mol. Struct.*, **4**, 1–14.
Clifton, J. R., Gruen, D. M., and Ron, A. (1969) *J. Chem. Phys.*, **51**, 224–32.
Clusius, K. and Dickel, G. (1938) *Naturwissenschaften*, **26**, 546.
Cody, J. A. and Ibers, J. A. (1995) *Inorg. Chem.*, **34**, 3165–72.
Cody, J. A., Mansuetto, M. F., Pell, M. A., Chien, S., and Ibers, J. A. (1995) *J. Alloys Compds*, **219**, 1239–45.
Cohen, D. and Carnall, W. T. (1960) *J. Phys. Chem.*, **64**, 1933.
Cohen, I. and Schaner, B. E. (1963) *J. Nucl. Mater.*, **9**, 18–52.
Cohen, I. and Berman, R. M. (1966) *J. Nucl. Mater.*, **18**, 77–107.
Colella, M., Lumpkin, G. R., Zhang, Z., Buck, E. C., and Smith, K. L. (2005) *J. Phys. Chem. Miner.*, **32**, 52–64.
Condon, J. B. and Larson, E. A. (1973) *J. Chem. Phys.*, **59**, 855–65.
Contamin, P., Bacmann, J. J., and Marin, J. F. (1972) *J. Nucl. Mater.*, **42**, 54–64.
Conway, J. G. (1959) *J. Chem. Phys.*, **31**, 1002–4.
Cooper, M. A. and Hawthorne, F. C. (1995) *Can. Miner.*, **33**, 1103–9.
Cooper, M. A. and Hawthorne, F. C. (2001) *Can. Miner.*, **39**, 797–807.
Cordfunke, E. H. P. (1961) *J. Inorg. Nucl. Chem.*, **23**, 285–6.
Cordfunke, E. H. P. and Debets, P. C. (1964) *J. Inorg. Nucl. Chem.*, **26**, 1671.
Cordfunke, E. H. P. and Aling, P. (1965) *Trans. Faraday Soc.*, **61**, 50–3.
Cordfunke, E. H. P. and Loopstra, B. O. (1967) *J. Inorg. Nucl. Chem.*, **29**, 51–7.
Cordfunke, E. H. P. (1969) *The Chemistry of Uranium,* Elsevier, Amsterdam.
Cordfunke, E. H. P. and Loopstra, B. O. (1971) *J. Inorg. Nucl. Chem.*, **33**, 2427–36.
Cordfunke, E. H. P. (1975) in *Thermodynamics of Nuclear Materials,* Proc. Symp. 1974, vol. II, International Atomic Energy Agency, Vienna, pp. 185–92.
Cordfunke, E. H. P., van Egmond, A. B., and van Voorst, G. (1975) *J. Inorg. Nucl. Chem.*, **37**, 1433–6.
Cordfunke, E. H. P., Oweltjes, W., and Prins, G. (1976) *J. Chem. Thermodyn.*, **8**, 241–50.
Cordfunke, E. H. P., Prins, G., and van Vlaanderen, P. (1977) *J. Inorg. Nucl. Chem.*, **39**, 2189–90.
Cordfunke, E. H. P. and Westrum, E. F. Jr. (1979) in *Thermodynamics of Nuclear Materials,* Proc. Symp. 1979, vol. II, International Atomic Energy Agency, Vienna, pp. 125–41.
Cordfunke, E. H. P., Oweltjes, W., and van Vlaanderen, P. (1983) *J. Chem. Thermodyn.*, **15**, 237–43.
Cordfunke, E. H. P., van Vlaanderen, P., Goubitz, K., and Loopstra, B. O. (1985) *J. Solid State Chem.*, **56**, 166–70.
Cordier, S., Perrin, C., and Sergent, M. (1997) *Mater. Res. Bull.*, **32**, 25–33.

Cotton, F. A., Marler, D. O., and Schwotzer, W. (1984) *Acta Crystallogr.*, **40C**, 1186–8.
Cousson, A., Pagès, M., Cousseins, J.-C., and Vedrine, A. (1977) *J. Crystal Growth*, **40**, 157–60.
Cousson, A., Tabuteau, A., Pagès, M., and Gasperin, M. (1979) *Acta Crystallogr. B*, **35**, 1198–2000.
Cox, J. D., Wagman, D. D., and Medvedev, V. A. (1989) *CODATA Key Values for Thermodynamics,* Hemisphere, New York.
Crawford, M.-J., Ellern, A., and Mayer, P. (2005) *Angew. Chem. Int. Ed.* 1–5.
Crea, J., Diguisto, R., Lincoln, S. F., and Williams, E. H. (1977) *Inorg. Chem.*, **16**, 2825.
Crosswhite, H. M., Crosswhite, H., Carnall, W. T., and Paszek, A. P. (1980) *J. Chem. Phys.*, **72**, 5103–17.
Cunningham, J. E. and Adams, R. E. (1957) *Fuel Elements Conference*, Paris, November 18–23, TID-7546, Book 1, pp.102–19.
Dao, N. Q. (1972) *Acta Crystallogr. B*, **288**, 2011–15.
Dao, N. Q. and Chourou, S. (1972) *C. R. Acad. Sci. (Paris)*, **275C**, 745–8.
Dao, N. Q. and Chourou, S. (1974) *C. R. Acad. Sci. (Paris)*, **278C**, 879–81.
Dao, N. Q., Chourou, S., Rodier, N., and Bastein, P. (1979) *Compt. Rend. Serie C, Sciences Chimiques*, **289**, 405–8.
Dao, N. Q., Chourou, S., and Heckly, J. (1981) *J. Inorg. Nucl. Chem.*, **43**, 1835–9.
Daoudi, A., Levet, J. C., Potel, M., and Noël, H. (1996) *Mater. Res. Bull.*, **31**, 1213–18.
Davies, W. and Gray, W (1964) *Talanta*, **11**, 1203–11.
Davies, W., Gray, W., and McLeod, K. C. (1970) *Talanta*, **17**, 937–44.
Dawson, J. K. (1951) *J. Chem. Soc.*, 429–31.
Dawson, J. K., D'Eye, R. W. M., and Truswell, A. E. (1954) *J. Chem. Soc.*, 3922–9.
Dawson, J. K., Wait, E., Alcock, K., and Chilton, D. R. (1956) *J. Chem. Soc.*, 3531.
Day, J. P. and Venanzi, L. M. (1966) *J. Chem. Soc. A*, 1365–7.
D'Eye, R. W. M. and Martin, F. S. (1957) N.S.A. 11, no. 3372.
de Alleluia, I. B., Hoshi, M., Jocher, W. G., and Keller, C. (1981) *J. Inorg. Nucl. Chem.*, **43**, 1831–4.
Dean, J. A. (1995) *Analytical Chemistry Handbook,* McGraw-Hill, New York.
Debets, P. C. and Loopstra, B. O. (1963) *J. Inorg. Nucl. Chem.*, **25**, 945–53.
Debets, P. C. (1966) *Acta Crystallogr.*, **21**, 589–93.
Debets, P. C. (1968) *Acta Crystallogr.*, **24B**, 400–2.
de Coninck, R. and Devreese, J. (1969) *Phys. Status Solidi*, **32**, 823–9.
De Jong, W. A., Visscher, L., and Nieupoort, W. C. (1999) *Theochemistry*, **458**, 41–52.
Delamoye, P., Rajnak, K., Genet, M., and Edelstein, N. (1983) *Phys. Rev. B*, **28**, 4923–30.
Deleon, A. and Lazarević, M. (1971) in *The Recovery of Uranium,* Proc. Symp. Sao Paulo, Brazil, August 17–21, 1970, International Atomic Energy Agency, Vienna, STI/PUB/262, pp. 351–61.
Deliens, M. and Piret, P. (1981) *Can. Miner.*, **19**, 553–7.
Deliens, M. and Piret, P. (1982) *Can. Miner.*, **20**, 231–8.
Deliens, M. and Piret, P. (1983a) *Am. Miner.*, **68**, 456–8.
Deliens, M. and Piret, P. (1983b) *Bull. Minér.*, **106**, 305–8.
Deliens, M. and Piret, P. (1984a) *Bull. Minér.*, **107**, 21–4.
Deliens, M. and Piret, P. (1984b) *Bull. Minér.*, **107**, 15–19.
Deliens, M. and Piret, P. (1990a) *Eur. J. Miner.*, **1**, 85–8.
Deliens, M. and Piret, P. (1990b) *Eur. J. Miner.*, **2**, 407–11.

Dell, R. M. and Wheeler, V. I. (1963) *Trans. Faraday Soc.*, **59**, 485.
Della Ventura, G., Bonazzi, P., Oberti, R., and Ottolini, L. (2002) *Am. Miner.*, **87**, 739–44.
Demartin, F., Diella, V., Donzelli, S., Gramaccioli, C. M., and Pilati, T. (1991) *Acta Crystallogr.*, **B47**, 439–46.
Demartin, F., Gramaccioli, C. M., and Pilati, T. (1992) *Acta Crystallogr.*, **C48**, 1–4.
Dempster, A. J. (1935) *Nature*, **136**, 180.
Denes, G., Fonteneau, G., and Lucas, J. (1973) *Compt. Rend. C.*, **276**, 1553–6.
Denning, R. G., Snellgrove, T. R., and Woodwark, D. R. (1976) *Mol. Phys.*, **31**, 419–42.
Dent, A. J., Ramsey, J. D. F., and Swanton, S. W. (1992) *J. Colloid Interface Sci.*, **150**, 45–60.
Depaus, R., Guzzi, G., and Federico, A. (1987) *Proc. Int. Symp. Nuclear Material Safeguards*, Vienna, Austria, IAEA, vol. 2, p. 116.
Dereń, P., Karbowiak, M., Krupa, J. P., and Drożdżyński, J. (1998) *J. Alloys Compds*, **275–7**, 863–6.
Deschaux, M. and Marcantonatos, M. D. (1979) *Chem. Phys. Lett.*, **63**, 283–8.
Destriau, M. and Sériot, J. (1962) *Compt. Rend. Hebd. Séances Acad. Sci.*, **254**, 2982–4.
Deutsch, W. J., Krupka, K. M., Lindberg, M. J., Cantrell, K. J., Brown, C. F., and Schaef, H. F. (2004) *Hanford Tanks 241-C-203 and 241-C-204: Residual Waste Contaminant Release Model and Supporting Data,* PNNL-14903, Pacific Northwest National Laboratory, Richland, Washington.
de Wet, J. F., Caira, M. R., and Gellatly, B. J. (1978) *Acta Crystallogr. B*, **34**, 1121–4.
de Wet, J. F. and du Preez, J. G. H. (1978) *J. Chem. Soc., Dalton Trans.*, 592–7.
Dhar, S. K., Kimura, Y., Kouzaki, M., Sugiyama, K., Settai, R., Onuki, Y., Takeuchi, T., Kindo, K., Manfrinetti, P., and Palenzona, A. (1998) *Physica B* (*Amsterdam, Neth*), **245**, 210–18.
Dharwadkar, S. R., Chandrasekharaiah, M. S., and Karkhanavala, M. D. (1975) *J. Thermal Anal.*, **7**, 219–21.
Dharwadkar, S. R., Chandrasekharaiah, M. S., and Karkhanavala, M. D. (1978) *J. Nucl. Mater.*, **71**, 268–76.
Di Bella, S., Lanza, G., Fragalà, I. L., and Marks, T. J. (1996) *Organometallics*, **15**, 205–7.
Dickens, P. G., Stuttard, G. P., Dueber, R. E., Woodall, M. J., and Patat, S. (1993) *Solid State Ionics*, **63–5**, 417–23.
Diehl, H. G. and Keller, C. (1971) *J. Solid State Chem.*, **3**, 621–36.
Dion, C., Obbade, S., Raekelboom, E., Abraham, F., and Saadi, M. (2000) *J. Solid State Chem.*, **155**, 342–53.
Di Sipio, L., Tondello, E., Pellizzi, G., Ingletto, G., and Montenero, A. (1974a) *Crystal Struct. Commun.*, **3**, 297–300.
Di Sipio, L., Tondello, E., Pellizzi, G., Ingletto, G., and Montenero, A. (1974b) *Crystal Struct. Commun.*, **3**, 731–4.
Di Sipio, L., Tondello, E., Pellizzi, G., Ingletto, G., and Montenero, A. (1974c) *Crystal Struct. Commun.*, **3**, 527–30.
Di Sipio, L., Tondello, E., Pellizzi, G., Ingletto, G., and Montenero, A. (1974d) *Crystal Struct. Commun.*, **3**, 301–3.
Di Sipio, L., Tondello, E., Pellizzi, G., Ingletto, G., and Montenero, A. (1977) *Crystal Struct. Commun.*, **6**, 723–6.

Djogic, R. and Branica, M. (1992) *Electroanalysis*, **4**, 151–9.
Docrat, T. I., Mosselmans, J. F. W., Charnock, J. M., Whitley, M. W., Collison, D., Livens, F. R., Jones, C., and Edmiston, M. J. (1999) *Inorg. Chem.*, **38**, 1879–82.
Dodé, M. and Touzelin, B. (1972) *Rev. Chim. Minér.*, **9**, 139.
Donohue, J. and Einspahr, H. (1971) *Acta Crystallogr. B*, **27**, 1740–3.
Douglas, R. M. and Staritzky, E. (1957) *Anal. Chem.*, **29**, 459.
Douglass, R. M. (1962) *Acta Crystallogr.*, **15**, 505–6.
Downs, A. J. and Gardner, C. J. (1986) *J. Chem. Soc. Dalton Trans.*, 1289–96.
Doyle, G. A., Goodgame, D. M. L., Sinden, A., and Williams, D. L. (1993) *J. Chem. Soc. Chem. Commun.*, 1170–2.
Drożdżyński, J. and Conway, J. G. (1972) *J. Chem. Phys.*, **56**, 883–91.
Drożdżyński, J. (1978) *J. Inorg. Nucl. Chem.*, **40**, 319–23.
Drożdżynski, J. and Kamenskaya, A. N. (1978) *Chem. Phys. Lett.*, **56**, 549–53.
Drożdżyński, J. and Miernik, D. (1978) *Inorg. Chim. Acta*, **30**, 185–8.
Drożdżyński, J. (1979) *Inorg. Chim. Acta.*, **32**, L83–5.
Drożdżyński, J. (1984) *J. Mol. Struct.*, **114**, 449–56.
Drożdżyński, J. (1985) *Inorg. Chim. Acta*, **109**, 79–81.
Drożdżyński, J. (1988a) *Polyhedron*, **7**, 167–8.
Drożdżyński, J. (1988b) *J. Less Common Metals*, **138**, 271–9.
Drożdżyński, J. (1991) Chemistry of tervalent uranium, in *Handbook on the Physics and Chemistry of the Actinides* vol. 6, ch. 5 (eds. A. J. Freeman and C. Keller), North-Holland, Amsterdam, pp. 281–336.
Drożdżyński, J. and du Preez, J. G. H. (1994) *Inorg. Chim. Acta*, **218**, 203–5. no.1–2,
Drożdżyński, J., and Karbowiak, M. (2005) unpublished results.
Drulis, H., Petryński, W., Staliński, B., and Zigmunt, A. (1982) *J. Less Common Metals*, **83**, 87–93.
Ducroux, R. and Baptiste, Ph. J. (1981) *J. Nucl. Mater.*, **97**, 333–6.
Dudney, N. J., Coble, R. L., and Tuller, H. L. (1981) *J. Am. Ceram. Soc.*, **64**, 627–31.
Duff, M. C., Amrhein, C., Bertsch, P. M., and Hunter, D. B. (1997) *Geochim. Cosmochim. Acta*, **61**, 73–81.
Duff, M. C., Coughlin, J. U., and Hunter, D. B. (2002) *Geochim Cosmochim. Acta*, **66**, 3533–47.
du Preez, J. G. H., Gonsalves, J. W., and Steenkamp, P. J. (1977a) *Inorg. Chim. Acta*, **21**, 167–72.
du Preez, J. G. H., Gellatly, B. J., and Gibson, M. L. (1977b) *J. Chem. Soc. Dalton Trans.*, 1062–8.
du Preez, J. G. H. and Zeelie, B. (1987) *Inorg. Chim. Acta*, **134**, 303–8.
du Preez, J. G. H. and Zeelie, B. (1989) *Inorg. Chim. Acta*, **161**, 187–92.
Dusausoy, Y., Ghermain, N.-E., Podor, R., and Chuney, M. (1996) *Eur. J. Miner.*, **8**, 667–73.
Dyall, K. G. (1999) *Mol. Phys.*, **96**, 511–18.
Eastman, E. D., Brewer, L., Bromley, L. A., Gilles, P. W., and Lofgren, N. A. (1950) *J. Am. Chem. Soc.*, **72**, 2248–850; 4019–23.
Eastman, E. D. and Fontana, B. I. (1958) in *Chemistry of Uranium* (*TID –5290*), *Paper 30* (eds. J. Katz and E. Rabinowitch), Oak Ridge, TN, pp. 206–13.
Eastman, M. P., Eller, P. G., and Halstead, G. W. (1981) *J. Inorg. Nucl. Chem.*, **43**, 2839–42.

Ebert, W. L., Bates, J. K., and Bourcier, W. L. (1991) *Waste Manage.*, **11**, 205–21.
Edelson, M. C. (1992) in *Inductively Coupled Plasmas in Analytical Atomic Spectrometry,* 2nd edn (eds. A. Montaser and D. W. Golightly), VCH Publishers, New York, pp. 341–72.
Edelstein, N., Brown, D., and Whittaker, B. (1974) *Inorg. Chem.*, **13**, 563–7.
Edghill, R. (1991) *Radiochim. Acta*, **32**, 381–6.
Eding, H. J. and Carr, E. M. (1961) *High-Purity Uranium Compounds – Final Report*, ANL-6339.
Edwards, R. K. and Martin, A. E. (1966) in *Thermodynamics,* Proc. Symp. 1965, vol. 2, International Atomic Energy Agency, Vienna, pp. 423–9.
Edwards, R. K., Chandrasekharaiah, M. S., and Danielson, P. M. (1969) *High Temp. Sci.*, **1**, 98–113.
Efremova, K. M., Ippolitova, E. A., Simanov, Yu. P., and Spitsyn, V. I. (1959) *Dokl. Akad. Nauk. SSSR*, **124**, 1057–60.
Efremova, K. M., Ippolitova, E. A., and Simanov, Yu. P. (1961a) Argonne National Laboratory Report, ANL-trans-33, p. 44.
Efremova, K. M., Ippolitova, E. A., and Simanov, Yu. P. (1961b) Argonne National Laboratory Report, ANL-trans-33, p. 59.
Efremova, K. M., Ippolitova, E. A., and Simanov, Yu. P. (1961c) Argonne National Laboratory Report, ANL-trans-33, p. 65.
Ehrfeld, W. and Ehrfeld, U. (1980) in *Gmelin Handbuch der Anorganischen Chemie,* Uranium Suppl., vol. A2, Springer, Berlin, p. 57.
Eichberger, K. (1979) *Dissertation,* T.U. Munich, Germany.
Eichberger, K. and Lux, F. (1980) *Ber. Bunsenges. Phys. Chem.*, **84**, 800–7.
Eick, H. A. (1994) Lanthanide and actinide halides, in *Handbook on the Physics and Chemistry of Rare Earths* (eds. K. A. Gschneidner Jr, L. Eyring, G. R. Choppin, and G. H. Lander), Elsevier Science B. V., vol. 18, ch. 124, 365–411.
Ekeroth, E. and Jonsson, M. (2003) *J. Nucl. Mater.*, **322**, 242–8.
Ekstrom, A., Batley, G. E., and Johnson, D. A. (1974) *J. Catalysis*, **34**, 106–16.
Ekstrom, A. and Johnson, D. A. (1974) *J. Inorg. Nucl. Chem.*, **36**, 2549–56.
Eliseev, S. S., Glukhov, I. A., and Vozhdaeva, E. E. (1972) *Zh. Neorg. Khim.*, **17**, 1203–8; *Russ. J. Inorg. Chem.*, **17**, 627–9.
Ellens, A., Krämer, K., and Güdel, H. U. (1998) *J. Lumin.*, **76/77**, 548.
Eller, P. G., Larson, A. C., Peterson, J. R., Ensor, D. D., and Young, J. P. (1979) *Inorg. Chim. Acta*, **37**, 129–33.
Ellert, G. V., Tsapkin, V. V., Mikhailov, Yu. N., and Kuznetsov, V. G. (1965) *Zh. Neorg. Khim.*, **10**, 1572–80; (1965) *Russ. J. Inorg. Chem.*, **10**, 858–62.
Ellert, G. V., Eliseev, A. A., and Slovyanskikh, V. K. (1971) *Zh. Neorg. Khim.*, **16**, 1451; *Russ. J. Inorg. Chem.*, **16**, 768.
Ellert, G. V., Sevast'yanov, V. G., and Slovyanskikh, V. K. (1975) *Zh. Neorg. Khim.*, **20**, 221–7; *Russ. J. Inorg. Chem.*, **20**, 120–3.
Elliot, R. P. (1965) *Constitution of Binary Alloys,* 1st Suppl., McGraw-Hill, New York.
Ellison, A. J. G., Mazer, J. J., and Ebert, W. L. (1994) *Effect of Glass Composition on Waste Form Durability: A Critical Review*, Argonne National Laboratory Report, ANL-94/28, Argonne, IL, USA.
Engmann, R. and de Wolff, P. W. (1963) *Acta Crystallogr.*, **16**, 993–6.
Esch, U. and Schneider, A. (1948) *Z. Anorg. Allg. Chem.*, **257**, 254–66.

Espenson, J. H. (ed.) (1995) *Chemical Kinetics and Reaction Mechanisms,* McGraw-Hill, New York.
Evers, E. C. and Reynolds, M. B. (1954) U.S. Patent 2674518.
Ewing, R. C. (1999) *Proc. Nat. Acad. Sci.*, **96**, 3432–29.
Faber, J. Jr. and Lander, G. H. (1976) *Phys. Rev.*, **B14**, 1151–64.
Faile, S. P. (1978) *J. Crystal Growth*, **43**, 133–4.
Farges, F., Ponader, C. W., Calas, G., and Brown, G. E. (1992) *Geochim. Cosmochim. Acta*, **56**, 4205–20.
Farkas, I., Bányai, I., Szabó, Z., Wahlgren, U., and Grenthe, I. (2000a) *Inorg. Chem.*, **39**, 799–805.
Farkas, I., Grenthe, I., and Bányai, I. (2000b) *J. Phys. Chem. A*, **104**, 1201–6.
Faucher, M. D., Moune, O. K., Garcia, D., and Tanner, P. (1996) *Phys. Rev. B*, **53**, 9501–4.
Fawcett, J., Holloway, J. H., Laycock, D., and Russell, D. R. (1982) *J. Chem. Soc. Dalton Trans.*, 1355–60.
Fazekas, Z., Tomiyasu, H., Park, I.-L., Yamamura, T., and Harada, M. (1998) *Models in Chemistry*, **135** (5), 783–97, Akademiai,Kiadó, Budapest.
Fee, D. C. and Johnson, C. E. (1978) *J. Inorg. Nucl. Chem.*, **40**, 1375–81.
Feng, X., Buck, E. C., Mertz, C., Bates, J. K., Cunnane, J. C., and Chaiko, D. J. (1994) *Radiochim. Acta*, **66/67**, 197–205.
Ferguson, I. F. and Fogg, P. G. T. (1957) *J. Chem. Soc.*, 3679–81.
Ferguson, I. F. and Street, R. S. (1963) AERE Harwell Report, AERE-M 1192.
Fernandes, J. C., Continentino, M. A., and Guimarães, A. P. (1985) *Solid State Commun.*, **55**, 1011–15.
Figgins, P. E. and Bernardinelli, R. J. (1966) *J. Inorg. Nucl. Chem.*, **28**, 2193.
Finch, R. J. and Ewing, R. C. (1992) *J. Nucl. Mater.*, **190**, 133–56.
Finch, R. J., Suksi, J., Rasilainen, K., and Ewing, R. C. (1995) *Mater. Res. Soc. Symp. Proc.*, **353**, 647–52.
Finch, W. I. (1996) *Uranium Provinces of North America – Their Definition, Distribution, and Models*, U.S. Geological Survey Bulletin, 2141.
Finch, R. J., Cooper, M. A., Hawthorne, F. C., and Ewing, R. C. (1996a) *Can. Miner.*, **34**, 1071–88.
Finch, R. J., Suksi, J., Rasilainen, K., and Ewing, R. C. (1996b) *Mater. Res. Soc. Symp. Proc.*, **412**, 823–30.
Finch, R. J. and Ewing, R. C. (1997) *Am. Miner.*, **82**, 607–19.
Finch, R. J., Hawthorne, F. C., and Ewing, R. C. (1998) *Can. Miner.*, **36**, 831–45.
Finch, R. J. and Murakami, T. (1999) *Rev. Miner.*, **38**, 91–180.
Finch, R. J., Buck, E. C., Finn, P. A., and Bates, J. K. (1999a) *Mater. Res. Soc. Symp. Proc.*, **556**, 431–8.
Finch, R. J., Cooper, M. A., Hawthorne, F. C., and Ewing, R. C. (1999b) *Can. Miner.*, **37**, 929–38.
Findley, J. R., Gregory, J. N., and Weldrick, G. (1955) AERE Report, AERE-C/M-265.
Fine, M. A., Mendelson, A., and Schwartz, D. F. (1945) *Purification of Tuballoy by the Thermal Decomposition of Tuballoy Iodide*, CT-2695.
Fink, J. K. (2001) *World Wide Web, INSC Materials Properties Database*, http://www.insc.anl.gov/matprop/

Finnie, K. S., Zhang, Z., Vance, E. R., and Carter. M. L. (2003) *J. Nucl. Mater.*, **317**, 46–53.
Fischer, E. A., Kinsman, P. R., and Ohse, R. W. (1976) *J. Nucl. Mater.*, **59**, 125–36.
Fischer, E. O. and Hristidu, Y. (1962) *Z. Naturforsch.*, **17b**, 275–6.
Fisk, Z., Moreno, N. O., and Thompson, J. D. (2003) *J. Phys. Condensed Matter*, **15**, S1917–21.
Fitzmaurice, J. C. and Parkin, I. P. (1994) *New J. Chem.*, **18**, 825–32.
Flotow, H. E. and Abraham, B. M. (1951) Argonne National Laboratory, IL, Report AEDP-3074.
Flotow, H. E., Lohr, H. R., Abraham, B. M., and Osborne, D. W. (1959) *J. Am. Chem. Soc.*, **81**, 3529–33.
Flotow, H. E. and Osborne, D. W. (1967) *Phys. Rev.*, **164**, 755–8.
Flotow, H. E., Haschke, J. M., and Yamauchi, S. (1984) in *The Chemical Thermodynamics of Actinide Elements and Compounds, part 9, The Actinide Hydrides* (ed. F. L. Oetting), International Atomic Energy Agency, Vienna, pp. 32–44.
Fonteneau, G. and Lucas, J. (1974) *J. Inorg. Nucl. Chem.*, **36**, 1515–19.
Foote, F. (1956) *Proc. Int. Conf. on Peaceful Uses of Atomic Energy*, Geneva, 1955, vol. 9, p. 33.
Formosinho, S. J., Da Graca, M., and Miguel, M. (1984) *J. Chem. Soc., Faraday Trans. I*, **80**, 1745–56.
Formosinho, S. J., Da Graca, M., Miguel, M., and Burrows, H. D. (1984) *J. Chem. Soc., Faraday Trans. I*, **80**, 1717–33.
Fortner, J. A., Kropf, A. J., Finch, R. J., Bakel, A. J., Hash, M. C., and Chamberlain, D. B. (2002) *J. Nucl. Mater.*, **304**, 56–62.
Fournier, J.-M. and Troć, R. (1985) in *Handbook on the Physics and Chemistry of the Actinides* (eds. A. J. Freeman and G. H. Lander), vol. 2, North-Holland, Amsterdam, pp. 29–173.
Fredrickson, D. R. and Chasanov, M. G. (1970) *J. Chem. Thermodyn.*, **2**, 623–9.
Fredrickson, D. R. and Chasanov, M. G. (1972) *J. Chem. Thermodyn.*, **4**, 419–23.
Fredrickson, J. K., Zachara, J. M., Kennedy, D. W., Liu, C., Duff, M. C., Hunter, D. B., and Dohnalkova, A. (2002) *Geochim. Cosmochim. Acta*, **66**, 3247–62.
Freeman, A. J. and Darby, J. B. Jr (1974) *The Actinides: Electronic Structure and Related Properties,* Academic Press, New York.
Freestone, N. P. and Holloway, J. H. (1991) Actinide fluorides, in *Synthesis of Lanthanide and Actinide Compounds* (eds. G. Meyer and L. R. Morss), Kluwer, Dordrecht, pp. 67–133.
Frei, V. and Wendt, H. (1970) *Ber. Bunsenges. Phys. Chem.*, **74**, 593.
Friedman, H. A., Weaver, C. F., and Grimes, W. R. (1970) *J. Inorg. Nucl. Chem.*, **32**, 3131–3.
Friese, J. I., Nash, K. L., Jensen, M. P., and Sullivan, J. C. (1998) *Radiochim. Acta*, **83**, 175–81.
Friese, J. I., Nash, K. L., Jensen, M. P., and Sullivan, J. C. (2001) *Radiochim. Acta*, **89**, 35–41.
Frlec, B., Brčič, B. S., and Slivnik, J. (1966) *Inorg. Chem.*, **5**, 542–6.
Frlec, B. and Hyman, H. H. (1967) *Inorg. Chem.*, **6**, 2233–9.
Frolov, A. A. and Rykov, A. G. (1979) *Radiokhimiya*, **21**, 329–42; *Sov. Radiochem.*, **21**, 281–92.

Frondel, C. (1951a) *Am. Miner.*, **36**, 671–9.
Frondel, C. (1951b) *Am. Miner.*, **36**, 680–6.
Fuchs, L. H. and Gebert, E. (1958) *Am. Miner.*, **43**, 243–8.
Fuger, J. and Brown, D. (1973) *J. Chem. Soc. Dalton Trans.*, 428–34.
Fuger, J., Parker, V. B., Hubbard, W. N., and Oetting, F. L. (1983) *The Chemical Thermodynamics of Actinide Elements and Compounds,* part 8, The Actinide Halides, IAEA, Vienna, STI/PUB/424–8.
Fuji, K., Miyake, C., and Imoto, S. (1979) *J. Nucl. Sci. Technol.*, **16**, 207–13.
Fujino, T. and Naito, K. (1969) *J. Am. Ceram. Soc.*, **52**, 574–7.
Fujino, T. and Naito, K. (1970) *J. Inorg. Nucl. Chem.*, **32**, 627–36.
Fujino, T. (1972) *J. Inorg. Nucl. Chem.*, **34**, 1563–74.
Fujino, T., Masaki, N., and Tagawa, H. (1977) *Z. Kristallogr.*, **145**, 299–309.
Fujino, T., Tateno, J., and Tagawa, H. (1978a) *J. Solid State Chem.*, **24**, 11–19.
Fujino, T., Tagawa, H., Adachi, T., and Hashitani, H. (1978b) *Anal. Chim. Acta*, **98**, 373–83.
Fujino, T., Tagawa, H., and Adachi, T. (1981) *J. Nucl. Mater.*, **97**, 93–103.
Fujino, T., Ouchi, K., Yamashita, T., and Natsume, H. (1983) *J. Nucl. Mater.*, **116**, 157–65.
Fujino, T., Yamashita, T., and Tagawa, H. (1988) *J. Solid State Chem.*, **73**, 544–55.
Fujino, T. and Miyake, C. (1991) in *Handbook on the Physics and Chemistry of the Actinides* vol. 6 (eds. A. J. Freeman and C. Keller), North-Holland, Amsterdam, pp. 155–240.
Fujino, T., Ouchi, K., Mozumi, Y., Ueda, R., and Tagawa, H. (1990) *J. Nucl. Mater.*, **174**, 92–101.
Fujino, T. and Sato, N. (1992) *J. Nucl. Mater.*, **189**, 103–15.
Fujino, T., Sato, N., and Yamada, K. (1995) *J. Nucl. Mater.*, **223**, 6–19.
Fujino, T., Nakama, S., Sato, N., Yamada, K., Fukuda, K., Serizawa, H., and Shiratori, T. (1997a) *J. Nucl. Mater.*, **246**, 150–7.
Fujino, T., Sato, N., and Yamada, K. (1997b) *J. Nucl. Mater.*, **247**, 265–72.
Fujino, T., Sato, N., Yamada, K., Nakama, S., Fukuda, K., Serizawa, H., and Shiratori, T. (1999) *J. Nucl. Mater.*, **265**, 154–60.
Fujino, T., Sato, N., Yamada, K., Okazaki, M., Fukuda, K., Serizawa, H., and Shiratori, T. (2001a) *J. Nucl. Mater.*, **289**, 270–80.
Fujino, T., Park, K., Sato, N., and Yamada, M. (2001b) *J. Nucl. Mater.*, **294**, 104–11.
Fukushima, S., Ohmichi, T., Maeda, A., and Watanabe, H. (1981) *J. Nucl. Mater.*, **102**, 30–9.
Fukushima, S., Ohmichi, T., Maeda, A., and Watanabe, H (1982) *J. Nucl. Mater.*, **105**, 201–10.
Fukushima, S., Ohmichi, T., Maeda, A., and Handa, M. (1983) *J. Nucl. Mater.*, **114**, 312–25.
Fuoss, R. M. (1958) *J. Am. Chem. Soc.*, **80**, 5059–61.
Furman, N. H., Bricker, C. E., and Ditts, R. V. (1953) *Anal. Chem.*, **25**, 482–6.
Furman, S. C. (1957) Knolls Atomic Power Laboratory Report, KAPL-1664.
Gabuda, S. P., Matsutsin, A. A., and Zadneprovskii, G. M. (1969) *Zh. Strukt. Khimii*, **10**, 1115–16; (1969) *J. Struct. Chem.* (*USSR*), **10**, 996–8.
Gagarinskii, Yu. V., Khanaev, E. I., Galkin, N. P., Ananeva, L. A., and Gabuda, S. P. (1965) *At. Energy* (*USSR*)*, 18, 40–5;* (*1965*) *Sov. At. Energy*, **31**, 43–8.

Gagliardi, L., Grenthe, I., and Roos, B. O. (2001) *Inorg. Chem.*, **40**, 2976–8.
Gagliardi, L., Pyykkö, I., and Roos, B. O. (2005) *Phys. Chem. Chem. Phys.* **17**, 2415–17.
Gagliardi, L. and Roos, B. O. (2005a) *Nature*, **433**, 848–51.
Gagliardi, L. and Roos, B. O. (2005b) *Inorg. Chem. Prepublication, ASAP*, Dec. 15.
Gaines, R. V., Skinner, C. W., Foord, E. E., Mason, B., and Rosenzweig, A. (1997) *Dana's New Mineralogy: The System of Mineralogy of James Dwight Dana and Edward Salisbury Dana,* 8th edn, John Wiley, New York.
Gale, W. F. and Totemeier, T. C. (2003) *Smithells Metals Reference Book,* 8th edn, Elsevier, Amsterdam.
Galkin, N. P. and Sudarikov, B. N. (eds.) (1966) *Technology of Uranium*, Israel Program for Scientific Translations, Jerusalem; translated from Tekhnologiya Urana, Atomizdat, Moscow (1964).
Gamp, E., Edelstein, N., Khan Malek, C., Hubert, S., and Genet, M. (1983) *J. Chem. Phys.*, **79**, 2023–6.
Garg, S. P. and Ackermann, R. J. (1977) *Met. Trans.*, **8A**, 239–44.
Garg, S. P. and Ackermann, R. J. (1980) *J. Nucl. Mater.*, **88**, 309–11.
Garrido, F., Ibberson, R. M., Nowicki, L., and Willis, B. T. M. (2003) *J. Nucl. Mater.*, **322**, 87–9.
Gatehouse, B. M., Grey, I. E., and Kelly, P. R. (1979) *Am. Miner.*, **64**, 1010–17.
Gebert, E., Hoekstra, H. R., Reis, A. H. Jr, and Peterson, S. W. (1978) *J. Inorg. Nucl. Chem.*, **40**, 65–8.
Geichman, J. R., Smith, E. A. Trond, S. S., and Ogle, P. R. (1962) *Inorg. Chem.*, **2**, 1012–15.
Geichman, J. R., Smith, E. A., and Ogle, P. R. (1963) *Inorg. Chem.*, **1**, 661–5.
George, A. M. and Karkhanavala, M. D. (1963) *J. Phys. Chem. Solids*, **24**, 1207–12.
Gerdanian, P. (1964) CEA Report, CEA-R 2438.
Gerdanian, P. and Dodé, M. (1965) *J. Chim. Phys. Phys. Chim. Biol.*, **62**, 171–84.
Gerdanian, P. and Dodé, M. (1968) in *Thermodynamics of Nuclear Materials,* Proc. Symp. 1967, International Atomic Energy Agency, Vienna, pp. 41–54.
Gerdanian, P. (1974) *J. Phys. Chem. Solids*, **35**, 163–70.
Gerding, H., Prins, G., and Gabes, W. (1975) *Rev. Chim. Miner.*, **12**, 303–15.
Gesing, T. M. and Jeitschko, W. (1995) *Z. Naturforsch. B: Chem. Sci.*, **50**, 196–200.
Giammar, D. E. and Hering, J. G. (2002) *Geochim. Cosmochim. Acta.*, **66**, 3235–45.
Gibson, G. and Katz, J. J. (1951) *J. Am. Chem. Soc.*, **73**, 5436–8.
Gibson, G., Beintema, C. D., and Katz, J. J. (1960) *J. Inorg. Nucl. Chem.*, **15**, 110–14.
Gieré, R., Williams, C. T., and Lumpkin, G. R. (1998) *Schweiz Miner. Petrogr. Mitt.*, **78**, 433–59.
Gieré, R., Hatcher, C., Reusser, E., and Buck, E. C. (2002) *Mater. Res. Soc. Symp. Proc.*, **713**, 303–10.
Gillan, M. J. (1975) in *Thermodynamics of Nuclear Materials,* Proc. Symp. 1974, vol. I, International Atomic Energy Agency, Vienna, pp. 269.
Gilpatrick, L. O., Stone, H. H., and Secoy, C. H. (1964) Oak Ridge National Laboratory Report, ORNL-3591.
Ginderow, D. and Cesbron, F. (1983a) *Acta Crystallogr.*, **C39**, 1605–7.
Ginderow, D. and Cesbron, F. (1983b) *Acta Crystallogr.*, **C39**, 824–7.
Ginderow, D. and Cesbron, F. (1985) *Acta Crystallogr.*, **C41**, 654–7.

Ginderow, D. (1988) *Acta Crystallogr.*, **C44**, 421–4.
Gindler, G. E. (1962) *Radiochemistry of Uranium*, NAS-NS-3050, Technical Information Center, USAEC.
Gingerich, K. A. (1970) *J. Chem. Phys.*, **53**, 746–8.
Girdhar, H. L. and Westrum, E. F. Jr (1968) *J. Chem. Eng. Data*, **13**, 531–3.
Gittus, J. H. (1963) *Uranium,* Butterworths, Washington.
Gleichman, J. R., Ogle, P. R., and Swaney, L. R. (1961) *Reactions of Molybdenium, Tungsten and Uranium Hexafluoride with Nitrogen Compounds,* III, *Reactions with Nitrogen Dioxide and Nitrogen Oxyhalides*, GAT-T-809.
Gmelin, Handbook of Inorganic, chemistry, System no. 55, *Uran und Isotope mit einem Anhang über Transurane.* (1936) *Main volume,* Verlag Chemie, Berlin.
Gmelin Handbook of Inorganic Chemistry, Suppl. Ser., *Uranium*, Springer-Verlag, Berlin, Heidelberg, and New York.
(1979a) vol. Al, Uranium Deposits.
(1979b) vol. C9, Compounds with Chlorine, Bromine, and Iodine.
(1979c) vol. E1, Coordination Compounds.
(1980a) vol. A2, Isotopes.
(1980b) vol. C8, Compounds with Fluorine.
(1980c) vol. E2, Coordination Compounds (including Organouranium Compounds).
(1981a) vol. A3, Technology Uses.
(1981b) vol. C7, Compounds with Nitrogen.
(1981c) vol. C11, Compounds with Selenium, Tellurium, and Boron.
vol. C12, Carbides.
(1981d) vol. C14, Compounds with P, As, Sb, Bi, Ge.
(1982a) vol. A4, Irradiated Fuel Reprocessing.
(1982b) vol. A5, Spectra.
(1982c) vol. A7, Analytical Chemistry. Determination of the Isotope Composition. Biological Behavior. Health Protection and Safety Control.
vol. B2, Alloys with Alkali metals, Alkaline Earths, and Elements of Main Groups III and IV.
vol. B3, Alloys with Transition Metals of Groups IB to IVB.
(1983a) vol. A6, General Properties – Criticality.
(1983b) vol. C13, Carbonates, Cyanides, Thiocyanates, Alkoxides, Carboxylates, Compounds with Si.
(1983c) vol. D4, Cation Exchange and Chromatography.
(1984a) vol. C4, Uranium Dioxide. Preparation and Crystallographic Properties.
vol. C5, Uranium Dioxide. Physical Properties. Electrochemical Behavior.
(1984b) vol. C10, Compounds with Sulfur.
(1984c) vol. D1, Properties of U ions in Solutions and Melts.
(1982d) vol. D2, Solvent Extraction.
(1982e) vol. D3, Anion Exchange.
(1995a) vol. B4, Alloys with Transition Metals of Groups VB to VIIB.
vol. C1, Compounds with Rare Gases, and Hydrogen.System Uranium-Oxygen.
vol. C2, Oxides U_3O_8 and UO_3. Hydroxides. Oxide Hydrides. Peroxides.
vol. C3, Ternary and Polynary Oxides.
(1995b) vol. D5, Chemistry in Nonaqueous Solutions (Conductivity, Molecular weight, Solubility)

(1996a) vol. C6, Uranium Dioxide. Chemical Behavior.
(1996b) vol. D6, Chemistry in Nonaqueous Solutions (Formation of Complexes and Redox Reactions).
Gnandi, K. and Tobschall, H. J. (2003) *J. African Earth Sci.*, **37**, 1–10.
Gonsalves, J. W., Steenkamp, P. J., and du Preez, J. G. H. (1977) *Inorg. Chim. Acta*, **21**, 167–72.
Gorban, Yu. A., Pavlinov, L. V., and Bykov, V. N. (1967) *Sov. At. Energy*, **22**, 580–4.
Gordon, G. and Taube, H. (1961a) *J. Inorg. Nucl. Chem.*, **16**, 189–91.
Gordon, G. and Taube, H. (1961b) *J. Inorg. Nucl. Chem.*, **16**, 272–8.
Gorokhov, L. N., Emelyanov, A. M., and Khodeev, Y. S. (1974) *Teplofiz. Vyz. Temp.,* **12**, 1307–09.
Gotoo, K. and Naito, K. (1965) *J. Phys. Chem. Solids*, **26**, 1673–7.
Gray, C. W. (1994) *Methods Mol. Biol.*, **22**, 1–12.
Gray, C. W. (2001) *Methods Mol. Biol.*, **148**, 579–87.
Graziani, R., Bombieri, G., Forsellini, E., and Paolucci, G. (1975) *J. Crystal Mol. Struct.*, **5**, 1–14.
Greaves, C. and Fender, B. E. F. (1972) *Acta Crystallogr.*, **B28**, 3609–14.
Greaves, C., Cheetham, A. K., and Fender, B. E. F. (1973) *Inorg. Chem.*, **12**, 3003–7.
Greegor, R. B., Lytle, F. W., Chakoumakos, B. C., Lumpkin, G. R., Warner, J. K., and Ewing, R. C. (1989) *Mater. Res. Soc. Symp. Proc.*, **127**, 261–8.
Greek, B. F., Allen, O. W., and Tynan, D. E. (1957) *Ind. Eng. Chem.*, **49**, 628.
Greenberg, E. and Westrum, E. F. Jr (1956) *J. Am. Chem.Soc.*, **78**, 5144–7.
Gregory, N. W. (1958) in *The Chemistry of Uranium, Collected Papers.* TID-5290 (eds. J. J. Katz and E. Rabinowitch), USA EC Technical Information Extension, Oak Ridge, TN, pp. 465–510.
Grenthe, I., Ferri, D., Salvatore, F., and Diego, F. (1984) *J. Chem. Soc. Dalton Trans.*, 2439–43.
Grenthe, I., Fuger, J., Konings, R. J. M., Lemire, R. J., Muller, A. B., Nguyen-Trung, C., and Wanner, H. (1992) *Chemical Thermodynamics of Uranium,* NEA/OECD, North Holland.
Grenthe, I., Sandino, M. C. A., Puigdomenech, L., and Rand, M. H. (1995) *Corrections to the Uranium NEA-TDB Review. Appendix D in vol. 2. Chemical Thermodynamics of Americium*. By R. J. Silva *et al*. Nuclear Energy Agency, OECD, p. 347–74. Elsevier, Amsterdam.
Grenthe, I., Hummel, W., and Puigdomenech, I. (1997) in *Modelling in Aquatic Chemistry* (eds. I. Grenthe and I. Puigdomenech), Nuclear Energy Agency, OECD, Paris, ch. III.
Griffiths, T. R. and Volkovich, V. A. (1999) *J. Nucl. Mater.*, **274**, 229–51.
Grimes, W. R. (1978) Report CONF-780571-1; *Energy Res. Abstr.*, **3** (22), no. 52726.
Grimes, W. R. and Cuneo, D. R. (1960) in *Reactor Handbook,* vol. 1 (ed. R. Tripton), Interscience Publishers, New York.
Grønvold, F. (1955) *J. Inorg. Nucl. Chem.*, **1**, 357–70.
Grønvold, F., Kveseth, N. J., Sveen, A., and Tichý, J. (1970) *J. Chem. Thermodyn.*, **2**, 665–79.
Gross, E. B., Corey, A. S., Mitchell, R. S., and Walenta, K. (1958) *Am. Miner.*, **43**, 1134–43.
Grossman, L. N. and Priceman, S. (1954) *Nucleonics*, **12 (6)**, 68–9.

Grossman, L. N., Lewis, J. E., and Rooney, D. M. (1967) *J. Nucl. Mater.*, **21**, 302–9.
Gruen, D. M., Koehler, W. C., and Katz, J. J. (1951) *J. Am. Chem. Soc.*, **73**, 1475–9.
Gruen, D. M. (1955) *J. Chem. Phys.*, **23**, 1708–10.
Gruen, D. M. and McBeth, R. L. (1968) *Inorg. Nucl. Chem. Letters*, **4**, 294–8.
Gruen, D. M. and McBeth, R. L. (1969) *Inorg. Chem.*, **8**, 2625–33.
Grunzweig-Genossar, J., Kuznietz, M., and Meerovici, B. (1970) *Phys. Rev. B*, **1**, 1958–77.
Gueguin, M. M. (1964) *Bull. Soc. Chim. France*, 1184–7.
Guéneau, C., Dauvois, V., Pérodeaud, P., Gonella, C., and Dugne, O. (1998) *J. Nucl. Mater.*, **254**, 158–74.
Guéneau, C., Baichi, M., Labroche, D., Chatillon, C., and Sundman, B. (2002) *J. Nucl. Mater.*, **304**, 161–75.
Guest, R. J. and Zimmerman, J. B. (1955) *Anal. Chem.*, **27**, 931–6.
Guilbaud, P. and Wipff, G. (1993) *J. Phys. Chem. A*, **97**, 5685–92.
Guillaumont, R., Fanghänel, T., Fuger, J., Grenthe, I., Palmer, D., Rand, M., and Neck, V. (2003) *Chemical Thermodynamics of Uranium, Neptunium, Plutonium, Americium and Technetium,* NEA/OECD, North Holland.
Guinet, P., Vaugoyeau, H., and Blum, P. L. (1966) *C.R. Acad. Sci.* (*Paris*), **C263**, 17–20.
Gurevich, A. M., Polozhenskaya, L. P., Osicheva, N. P., and Solntseva, L. F. (1971a) *Radiokhimiya*, **13**, 688–692; *Sov. Radiochem.*, **13**, 706–9.
Gurevich, A. M., Polozhenskaya, L. P., and Osicheva, N. P. (1971b) *Radiokhimiya*, **13**, 588–92; *Sov. Radiochem.*, **13**, 604–7.
Gusev, Yu. K., Lychev, A. A., Mashirov, L. G., and Suglobov, D. N. (1985) *Radiokhimiya*, **27**, 412–15.
Güsten, H. (1983) in *Gmelin Handbook of Inorganic Chemistry,* Suppl., vol. A6, Springer-Verlag, Berlin-Heidelberg. ch. 3,
Haas, W. O. Jr and Smith, D. J. (1956) *Thorex Process Development at KAPL,* KAPL-1306 (declassified with deletions).
Habenschuss, A. and Spedding, F. H. (1980) *Crystal Struct. Commun.*, **9**, 71–6.
Haegele, R. and Boeyens, J. C. A. (1977) Nat. Inst. Met. Repub. S. Africa Res. Rep. no 1856.
Hagberg, D., Karlström, G., Roos, B. O., and Gagliardi, L. (2005) *J. Am. Chem. Soc.* **127**, 14250–6.
Hagemark, K. and Broli, M. (1966) *J. Inorg. Nucl. Chem.*, **28**, 2837–50.
Hagemark, K. and Broli, M. (1967) *J. Am. Ceram. Soc.*, **50**, 563–7.
Hagrman, D. T. (1995) SCADAP/RELAP5/MOD 3.1 Code Manual vol. 4, MATPRO, NUREG/CR-6150.
Hahn, O. (1925) *Z. Anorg. Chem.*, **147**, 16–23.
Hahn, O., Meitner, L., and Strassmann, F. (1937) *Ber. Dtsch. Chem. Ges.*, **70**, 1374–92.
Hahn, O. and Strassmann, F. (1939) *Naturwissenschaften*, **27**, 11–12.
Hall, D. A., Rae, A. D., and Waters, T. N. (1966) *Acta Crystallogr.*, **20**, 160–2.
Halliday, A. N., Lee, D.-C., Christensen, J. N., Rehkämper, M., Yi, W., Luo, X., Hall, C. M., Ballentine, C. J., Pettke, T., and Stirling, C. (1998) *Geochim. Cosmochim. Acta*, **62**, 919–40.
Halstead, G. W., Eller, P. G., and Eastman, P. (1979) *Inorg. Chem.*, **18**, 2867–72.
Handler, P. and Hutchison, C. A. (1956) *J. Chem. Phys.*, **25**, 1210–15.

Hansen, M. and Anderko, K. (1958) *Constitution of Binary Alloys,* McGraw-Hill, New York.
Hanson, S. L., Simmons, W. B., Falster, A. U., Foord, E. E., and Lichte, F. E. (1999) *Min. Mag.*, **63**, 27–36.
Hanuza, J., Hermanowicz, K., Macalik, L., Drożdżyński, J., Zych, E., and Meyer, G. (1999) *Vibrational Spectrosc.*, **21**, 111–26.
Harbottle, G. and Evans, C. V. (1997) *Radioact. Radiochem.*, **8**, 38–46.
Harrington, C. D. and Ruehle, A. E. (1959) *Uranium Production Technology,* Van Nostrand, Princeton, p. 461.
Harris, L. A. and Taylor, A. J. (1962) *J. Am. Ceram. Soc.*, **45**, 25.
Hart, F. A. and Tajik, M. (1983) *Inorg. Chim. Acta*, **71**, 169–73.
Haschke, J. M. (1991) in *Synthesis of Lanthanide and Actinide Compounds* (eds. G. Meyer and L. R. Morss), Kluwer Academic Publishers, Dordrecht, pp. 1–53.
Hauck, J. (1969) *Z. Naturforsch.*, **24b**, 1067–8.
Hauck, J. (1973) *Z. Naturforsch.*, **28b**, 215–16.
Hauck, J. (1974) *J. Inorg. Nucl. Chem.*, **36**, 2291–8.
Haug, H. and Weigel, F. (1963) *J. Nucl. Mater.*, **9**, 355–9.
Hay, P. J., Martin, R. L., and Schreckenbach, G. (2000) *J. Phys. Chem. A*, **104**, 6259–70.
Hayden, L. A. and Burns, P. C. (2002) *J. Solid State Chem.*, **163**, 313–18.
Hecht, H. G. and Gruber, J. B. (1974) *J. Chem. Phys.*, **60**, 4872–9.
Hecht, H. G., Malm, J. G., Foropoulos, J., and Carnall, W. T. (1986a) *J. Chem. Phys.*, **84**, 3653–62.
Hecht, H. G., Malm, J. G., and Carnall, W. T. (1986b) *J. Less Common Metals*, **115**, 79–89.
Heckers, U., Jacobs, H., and Kockelmann, W. (2003) *Z. Anorg. Allg. Chem.*, **629**, 2431–2.
Heidt, L. J. and Moon, K. A. (1953) *J. Am. Chem. Soc.*, **75**, 5808–9.
Hein, R. A. and Flagella, P. N. (1968) General Electric Report, GEMP-578.
Hein, R. A., Sjodahl, L. H., and Szwarc, R. (1968) *J. Nucl. Mater.*, **25**, 99–102.
Hellberg, K.-H. and Schneider, H. (1981) in *Gmelin Handbuch der Anorganischen Chemie*, System no. 55, Uranium, Suppl., vol. A3, Springer, Berlin, *Technology*, pp. 121–47.
Helm, L. and Mehrbach, A. E. (1999) *Coord. Chem. Rev.*, **187**, 151–81.
Helm, L. and Mehrbach, A. E. (2002) *J. Chem. Soc. Dalton Trans.*, 633–41.
Henche, G., Fiedler, K., and Gruehn, R. (1993) *Z. Anorg. Allg. Chem.*, **619**, 77–87.
Hendricks, M. E. (1971) DP-MS-71-46, p. 195.
Hendricks, M. E., Jones, E.R. Jr, Stone, J. A., and Karraker, D. G. (1971) *J. Chem. Phys.*, **55**, 2993–7.
Hendricks, M. E., Jones, E. R. Jr, Stone, J. A., and Karraker, D. G. (1974) *J. Chem. Phys.*, **60**, 2095–103.
Henkie, Z., Johanson, W. R., Crabtree, G. W., Dye, D. H., and Arko, A. J., Bazan, C. (1981) *Actinides*, Abstracts of September 1981 Asilomar Conf., Pacific Grove, CA, LBL-12441, pp. 176–8.
Henry, W. E. (1958) *Phys. Rev.*, **109**, 1976–80.
Hermann, J. A. and Suttle, J. F. (1957) *Inorg. Synth.*, **5**, 143–5.
Herrmann, H. (1861) *Uber verschiedene Uranverbindungen,* Dissertation, Göttingen.
Hidaka, H. and Holliger, P. (1998) *Geochim. Cosmochim. Acta*, **62**, 89–108.

Hiernaut, J. P., Hyland, G. J., and Ronchi, C. (1993) *Int. J. Thermophys.*, **14**, 259–83.
Higgins, L. R. and Roberts, J. T. (1956) *Development of the EXCER Process*, Part I, ORNL-1696.
Hildenbrand, D. (1977) *J. Chem. Phys.*, **66**, 4788.
Hill, D. C., Handwerk, J. H., and Beals, R. J. (1963) Argonne National Laboratory Report, ANL-6711.
Hill, F. C. (1999) *Rev. Miner.*, **38**, 635–79.
Hill, F. C. and Burns, P.C. (1999) *Can. Miner.*, **37**, 1283–8.
Hinatsu, Y. and Fujino, T. (1985) *J. Solid State Chem.*, **60**, 244–51.
Hinatsu, Y. and Fujino, T. (1986) *J. Solid State Chem.*, **62**, 342–50.
Hinatsu, Y. and Fujino, T. (1987) *J. Solid State Chem.*, **68**, 255–65.
Hinatsu, Y. and Fujino, T. (1988a) *J. Solid State Chem.*, **73**, 348–55.
Hinatsu, Y. and Fujino, T. (1988b) *J. Solid State Chem.*, **73**, 388–97.
Hinatsu, Y. and Fujino, T. (1988c) *J. Solid State Chem.*, **74**, 163–70.
Hinatsu, Y. and Fujino, T. (1988d) *J. Solid State Chem.*, **74**, 393–400.
Hinatsu, Y., Masaki, N., and Fujino, T. (1988) *J. Solid State Chem.*, **73**, 567–71.
Hinatsu, Y., Fujino, T., and Edelstein, N. (1992a) *J. Solid State Chem.*, **99**, 95–102.
Hinatsu, Y., Fujino, T., and Edelstein, N. (1992b) *J. Solid State Chem.*, **99**, 182–8.
Hines, M. A., Sullivan, J. C., and Nash, K. L. (1993) *Inorg Chem.*, **32**, 1820–3.
Ho, C. I., Powell, R. W., and Liley, P. E. (1972) *J. Phys. Chem. Ref. Data*, **1**, 279–421.
Hoard, J. L. and Stroupe, J. D. (1959) in *The Chemistry of Uranium – Collected Papers*, TID-5290, vol. 1, 325–49.
Hoch, M. and Furman, F. J. (1966) in *Thermodynamics*, Proc. Symp. 1965, International Atomic Energy Agency, Vienna, vol. 2, pp. 517–32.
Hodge, M. (l960) *Advances in Inorganic Chemistry and Radiochemistry,* vol. 2, Academic Press, New York, ch. 7.
Hoekstra, H. R. and Katz, J. J. (1952) *J. Am. Chem. Soc.*, **74**, 1683–90.
Hoekstra, H. R., Siegel, S., Fuchs, L. H., and Katz, J. J. (1955) *J. Phys. Chem.*, **59**, 136–8.
Hoekstra, H. and Siegel, S. (1956) in *Proc. First Int. Conf. on Peaceful Uses of Atomic Energy*, Geneva, vol. 7, P/737, 394–400.
Hoekstra, H. R. and Siegel, S. (1958) in *Proc. Second Int. Conf. on Peaceful Uses of Atomic Energy*, Geneva, paper 15/P/1548.
Hoekstra, H. R., Santoro, A., and Siegel, S. (1961) *J. Inorg. Nucl. Chem.*, **18**, 166–78.
Hoekstra, H. R. and Siegel, S. (1961) *J. Inorg. Nucl. Chem.*, **18**, 154–65.
Hoekstra, H. R. and Siegel, S. (1964) *J. Inorg. Nucl. Chem.*, **26**, 693–700.
Hoekstra, H. R. (1965) *J. Inorg. Nucl. Chem.*, **27**, 801–8.
Hoekstra, H. R. and Marshall, R. H. (1967) in *Lanthanide/Actinide Chemistry* (eds. P. Fields and T. Moeller), (ACS Advan. Chem. Ser. 71), American Chemical Society, Washington, DC, ch. 16, pp. 211–27.
Hoekstra, H. R., Siegel, S., and Charpin, P. (1968) *J. Inorg. Nucl. Chem.*, **30**, 519–23.
Hoekstra, H. R., Siegel, S., and Gallagher, F. X. (1970) *J. Inorg. Nucl. Chem.*, **32**, 3237–48.
Hoekstra, H. R. and Siegel, S. (1973) *J. Inorg. Nucl. Chem.*, **35**, 761–79.
Högfeldt, E. (1982) *Stability Constants of Metal-Ion Complexes. Part A Inorganic Ligands,* IUPAC Chemical Data Series no. 21, Pergamon Press, New York.
Holc, J. and Kolar, D. (1983) *J. Solid State Chem.*, **47**, 98–102.
Holden, A. N. (1958) *Physical Metallurgy of Uranium,* Addison-Wesley, London.

Holden, N. E. (1977) *Isotopic Composition of the Elements and Their Variation in Nature – A Preliminary Report, BNL-NCS-50605; (1979) Pure Appl. Chem.*, **52**, 2371.
Horwitz, E. P., Dietz, M. L., Chiarizia, R., Diamond, H., and Nelson, D. M. (1993) *Anal. Chim. Acta*, **281**, 361–72.
Hoskins, P. W. O. and Burns, P. C. (2003) *Miner. Mag.*, **67**, 689–96.
Howard, C. J., Taylor, J. C., and Waugh, A. B. (1982) *J. Solid State Chem.*, **45**, 396–8.
Howes, K. R., Bakac, A., and Espenson, J. H. (1988) *Inorg. Chem.*, **27**, 791–4.
Howlett, B. (1959/1960) *J. Inst. Met.*, **88**, 91–2.
Hsini, S., Caignol, E., Metin, J., Avignant, D., and Cousseins, J. C. (1986) *Rev. Chim. Minér.*, **23**, 35–47.
Hughes, K.-A. and Burns, P. C. (2003) *Am. Miner.*, **88**, 962–6.
Hughes, K.-A., Burns, P. C., and Kolitsch, U. (2003) *Can. Miner.*, **41**, 677–85.
Hughes-Kubatko, K.-A., Helean, K., Navrotsky, A., and Burns, P. C. (2003) *Science*, **302**, 1191–3.
Hughes-Kubatko, K. A., Helean, K., Navrotsky, A., and Burns, P. C. (2005) *Am. Miner.*, **90**, 1284–90.
Huie, R. E., Clifton, C. L., and Neta, P. (1991) *Radiat. Phys. Chem.*, **38**, 477–81.
Hummel, P., Winkler, J. R., and Gray, H. B. (2006) *J. Chem. Soc. Dalton Trans*. 168–71.
Hund, F., Peetz, U., and Kottenhahn, G. (1965) *Z. Anorg. Allg. Chem.*, **278**, 184–91.
Huntzicker, J. J. and Westrum, E. F. Jr (1971) *J. Chem. Thermodyn.*, **3**, 67–76.
Hutchings, M. T., Clausen, K., Dickens, M. H., Hayes, W., Kjems, J. K., Schnabel, P. G., and Smith, C. (1984) *J. Phys. C*, **17**, 3903–40.
Hutchings, M. T., Clausen, K., Hayes, W., Macdonald, J. E., Osborn, R., and Schnabel, P. (1985) *High Temp. Sci.*, **20**, 97–108.
Hyeon, J.-Y., Gottfriedsen, J., and Edelman, F. T. (2005) *Coord. Chem. Rev.* **249(24)** 2787–844.
Hyman, H. H., Sheft, I., and Katz, J. J. (1955) *Nuclear Engineering and Science Congress,* Cleveland, OH, Preprint 1997.
IAEA (1965) *Thermodynamic and Transport Properties of Uranium Dioxide and Related Phases*, Technical Report Series 39, IAEA, Vienna, STI/DOC/10/39 (1965).
IAEA (1966) *Processing of Low Grade Uranium Ores*, Proc. Panel convened by the International Atomic Energy Agency, Vienna, June 27–July 1, 1966, IAEA, Vienna, STI/PUB/146.
IAEA (1970) *The Recovery of Uranium*, Proc. Symp. Sao Paulo, Brazil, August 17–21, 1970, International Atomic Energy Agency, Vienna, STI/PUB/262.
IAEA (1978) *IWGFR Meeting on Equation of State of Materials of Relevance to the Analysis of Hypothetical Fast Breeder Reactor Accidents*, Harwell, UK, International Atomic Energy Agency,Vienna.
IAEA (1980) *Production of Yellow Cake and Uranium Fluorides*, Proc. Advisory Group Meeting organized by the IAEA, Paris, June 5–8, 1979, International Atomic Energy Agency, Vienna, STI/PUB/553.
Iandelli, A. (1952) *Atti Acad. Lincei, Class. Sci. Fiz. Mat. Nat. Rend.*, **13**, 138–44.
Ifill, R. O., Cooper, W. C., and Clark, A. H. (1996) *CIM Bull.*, **89**, 93–103.
Ikeda, Y., Soya, S., Fukutomi, H., and Tomiyasu, H. (1979a) *J. Inorg. Nucl. Chem.*, **41**, 1333–7.
Ikeda, Y., Tomiyasu, H., and Fukutomi, H. (1979b) *Bull. Res. Lab. Nucl. Reactors*, **4**, 47–59.

Ikeda, Y., Tomiyasu, H., and Fukutomi, H. (1984) *Inorg. Chem.*, **23**, 1356–60.
Imai, H. (1957) *Bull. Chem. Soc. Japan*, **30**, 873.
Inaba, H. and Naito, K. (1973) *J. Nucl. Mater.*, **49**, 181–8.
Inaba, H., Shimizu, H., and Naito, K. (1977) *J. Nucl. Mater.*, **64**, 66–70.
Inada, Y., Wisniewski, P., Murakawa, M., Aoki, D., Miyake, K., Watanabe, N., Haga, Y., Yamamoto, E., and Onuki, Y. (2001) *J. Phys. Soc. Japan*, **70**, 558–68.
Ingamells, C. O. and Pitard, F. (1986) *Applied Geochemical Analysis,* John Wiley, New York.
Ippolitova, E. A., Simanov, Yu. P., Kovba, L. M., Polunina, G. P., and Berznikova, N. A. (1959) *Radiokhimiya*, **1**, 660–4.
Ippolitova, E. A. and Kovba, L. M. (1961) *Dokl. Akad. Nauk. SSSR*, **138**, 377–80.
Ippolitova, E. A., Efremova, K. M., Orlinkova, O. L., and Simanov, Yu. P. (1961a) Argonne National Laboratory Report, ANL-trans-33, p. 52.
Ippolitova, E. A., Bereznikova, I. A., Kosynkin, V. D., Simanov, Yu. P., and Kovba, L. M. (1961b) Argonne National Laboratory Report, ANL-trans-33, p. 180.
Ippolitova, E. A., Bereznikova, I. A., Leonidov, V. Y., and Kovba, L. M. (1961c) Argonne National Laboratory Report, ANL-trans-33, p. 186.
Ippolitova, E. A., Simanov, Yu. P., Kovba, L. M., Murav'eva, I. A., and Krasnoyarskaya, A. A. (1961d) Argonne National Laboratory Report, ANL-trans-33, p. 153.
Ippolitova, E. A., Polunina, G. P., Kovba, L. M., and Simanov, Yu. P. (1961e) Argonne National Laboratory Report, ANL-trans-33, p. 213.
Ishii, T., Naito, K., and Oshima, K. (1970a) *J. Solid State Chem.*, **8**, 677–83.
Ishii, T., Naito, K., and Oshima, K. (1970b) *J. Nucl. Mater.*, **35**, 335–44.
Ishii, T., Naito, K., and Oshima, K. (1970c) *J. Nucl. Mater.*, **36**, 288–96.
Ivanov, V. E., Krugich, A. A., Pavlov, V. C., Kovtun, G. P., and Amonenko, V. M. (1962) in *Thermodynamics of Nuclear Materials,* Proc. Symp. 1962, International Atomic Energy Agency, Vienna, pp. 735–47.
Ivanov, S. B., Mikhailov, Yu. N., Kuznetsov, V. G., and Davidovich, R. L. (1980) *Koord. Khim.* [*Coord. Chem. (USSR)*], **6**, 1746–50.
Ivanov, S. B., Mikhailov, Yu. N., Kusnetsov, V. G., and Davidovich, R. L. (1981) *Zh. Strukt. Khim.*, **22**, 188–91.
Ivanov, S. B., Mikhailov, Yu. N., and Davidovich, R. L. (1982) *Koord. Khim.* (*Coord. Chemistry, USSR*), **8**, 1250–5.
Ivanovich, M. and Murray, A. (1992) in *Uranium Series Disequilibrium Applications to Earth, Marine, and Environmental Sciences* (eds. M. Ivanovich and R. S. Harmon), Clarendon Press, Oxford, pp. 127–73.
Iwasaki, M., Ishikawa, N., Ohwada, K., and Fujino, T. (1981) *Inorg. Chim. Acta*, **54**, L193–4.
Jackson, J. M. and Burns, P. C. (2001) *Can. Miner.*, **39**, 187–95.
Jackson, R. A., Murray, A. D., Harding, J. H., and Catlow, C. R. A. (1986) *Phil. Mag.*, **A53**, 27–50.
Jacob, I., Hadari, Z., and Reilly, J. J. (1984) *J. Less Common Metals*, **103**, 123–7.
Jacobs, H., Heckers, U., Zachwieja, U., and Kockelmann, W. (2003) *Z. Anorg. Allg. Chem.*, **629**, 2240–3.
Jakeš, D., Moravec, J., Křivý, I., and Sedláková, L. (1966) *Z. Anorg. Allg. Chem.*, **347**, 218–22.
Jakeš, D. and Schauer, V. (1967) *Proc. Brit. Ceram. Soc.*, **8**, 123–5.

Jakeš, D. (1973) *Colloq. Czech. Chem. Commun.*, **38**, 1–6.
Jakeš, D. and Křivý, I. (1974) *J. Inorg. Nucl. Chem.*, **36**, pp. 3885.
Jacob, E. and Polligkeit, W. (1973) *Z. Naturforsch.*, **28b**, 120–4.
Jacob, E. (1982) *Angew. Chem. Int. Ed. Engl.*, **21**, 142–3; (1982) *Angew. Chem.*, Suppl., 317.
Janeczek, J. and Ewing, R. C. (1991) *J. Nucl. Mater.*, **185**, 66–77.
Janeczek, J. and Ewing, R. C. (1992) *J. Nucl. Mater.*, **190**, 128–32.
Janeczek, J. (1999) *Rev. Miner.*, **38**, 321–92.
Jayadevan, N. G., Singh Mudher, K. D., and Chackraburtty, D. M. (1974) Bhabha Atomic Research Center Report, BARC-726.
Jensen, K. A., Palenik, C. S., and Ewing, R. C. (2002) *Radiochim. Acta*, **90**, 761–70.
Jerden, J. L. and Sinha, A. K. (2003) *Appl. Geochem.*, **18**, 823–43.
Jiang, J., Sarsfield, M. J., Renshaw, J. C., Livens, F. R., Collison, D., Charnock, J. M., Helliwell, M., and Eccles, H. (2002) *Inorg. Chem.*, **41**, 2799–806.
Jocher, W. G. (1978) Research Center Karlsruhe Report, KFK-2518.
Johansson, G. (1992) Structures of complexes in solution derived from X-ray diffraction measurements, in *Advances in Inorganic Chemistry* (ed. A. G. Sykes), Academic Press, Londonvol. 39.
Johnson, O., Powell, T., and Nottorf, R. (1974) *A Summary, of the Properties, Preparation and Purification of the Anhydrous Chlorides and Bromides of Uranium*, part A, Uranium Chlorides, part B, Uranium Bromides, CC-1974.
Johnson, Q., Biel, T. J., and Leider, H. R. (1976) *J. Nucl. Mater.*, **60**, 231–3.
Johnston, D. R., Satten, R. A., Schreiber, C. L., and Wong. E. (1966) *J. Chem. Phys.*, **44**, 3141–3.
Jones, E. R. Jr, Hendricks, M. E., Stone, J. A., and Karraker, D. G. (1974) *J. Chem. Phys.*, **60**, 2088–94.
Jones, L. H. (1958) *Spectrochim. Acta*, **10**, 395–403.
Jones, L. H. (1959) *Spectrochim. Acta*, **15**, 409–11.
Jones, L. V., Etter, D. E., Hudgens, C. R., Huffman, A. A., Rhinehammer, T. B., Rogers, N. E., and Wittenberg, L. J. (1959) Phase Equilibria in the LiF-BeF_2-UF_4 Ternary Fused Salt System, MLM-1080.
Jones, W. M., Gordon, J., and Long, E. A. (1952) *J. Chem. Phys.*, **20**, 695–9.
Joubert, P. and Bougon, R. (1975) *Compt. Rend.*, **C280**, 193–5.
Joubert, P., Bougon, R., and Gandreau, B. (1978a) *Can. J. Chem.*, **56**, 1874–80.
Joubert, P., Weulersse, J. M., Bougon, R., and Gaudreau, B. (1978b) *Can. J. Chem.*, **56**, 2546–9.
Jove, J. and Cousson, A. (1977) *Radiochim. Acta*, **24**, 73–5.
Jung, W.-S. and Juza, R. (1973) *Z. Anorg. Allg. Chem.*, **399**, 148–62.
Jung, W.-S., Harada, M., Tomiyasu, H., and Fukutomi, H. (1988) *Bull. Chem. Soc. Jpn.*, **61**, 3895–900.
Juza, R. and Sievers, R. (1965) *Naturwissenschaften*, **52**, 538–8.
Juza, R. and Meyer, W. (1966) *Naturwissenschaften*, **53**, 552.
Juza, R. and Meyer, W. (1969) *Z. Anorg. Allg. Chem.*, **366**, 43–50.
Kaltsyoannis, N. (2000) *Inorg. Chem.*, **39**, 6009–17.
Kanellakopulos, B., Henrich, E., Keller, C., Baumgärtner, F., König, E., and Desai, V. P. (1980) *Chem. Phys.*, **53**, 197–213.

Kanellakopulos, B. (1983) Electron paramagnetic resonance, in *Gmelin Handbook of Inorganic Chemistry*, System no. 55, Uranium, Suppl., vol. A6, Springer, Berlin, pp. 241–50.
Karabulut, M., Marasinghe, G. K., Ray, C. S., Day, D. E., Waddill, G. D., Allen, P. G., Booth, C. H., Bucher, J. J., Caulder, D. L., Shuh, D. K., Grimsditch, M., and Saboungi, M.-L. (2000) *J. Mater. Res.*, **15**, 1972–84.
Karbowiak, M. and Drożdżyński, J. (1990) *J.Less Common Metals*, **164**, 159–64.
Karbowiak, M. and Drożdżyński, J. (1993) *J. Alloys Compds*, **190**, 291–4.
Karbowiak, M., Drożdżyński, J., and Hanuza, J. (1996a) *Eur. J. Solid State Inorg. Chem.*, **33**, 1071–8.
Karbowiak, M., Hanuza, J., Drożdżyński, J., and Hermanowicz, K. (1996b) *J. Solid State Chem.*, **121**, 312–18.
Karbowiak, M., Drożdżyński, J., and Janczak, J. (1996c) *Polyhedron*, **15 (2)**, 241–4.
Karbowiak, M., Murdoch, K., Drożdżyński, J., Edelstein, N., and Hubert, S. (1996d) *Acta Phys. Polon.*, **90 (2)**, 371–6.
Karbowiak, M., Simoni, E., Drożdżyński, J., and Hubert, S. (1996e) *Acta Phys. Polon.*, **90 (2)**, 367–70.
Karbowiak, M., Drożdżyński, J., Murdoch, K. M., Edelstein, N. M., and Hubert, S. (1997) *J. Chem. Phys.*, **106**, 3067–77.
Karbowiak, M. and Drożdżyński, J. (1998a) *J. Alloys Compds*, **275–7**, 848–51.
Karbowiak, M. and Drożdżyński, J. (1998b) *J. Alloys Compds*, **271–3**, 863–6.
Karbowiak, M., Edelstein, N., Gajek, Z., and Drożdżyński, J. (1998a) *Spectrochim. Acta A*, **54**, 2035–44.
Karbowiak, M., Drożdżyński, J., Hubert, S., Simoni, E., and Streçk, W. (1998b) *J. Chem. Phys.*, **108**, 10181–8.
Karbowiak, M., Edelstein, N., Gajek, Z., and Drożdżyński, J. (1998c) *Spectrochim. Acta A*, **54**, 2035–44.
Karbowiak, M., Drożdżyński, J., Hubert, S., Simoni, E., and Stręk, W. (1998d) *J. Chem. Phys.*, **108**, 10181–8.
Karbowiak, M., Gajek, Z., and Drożdżyński, J. (2000) *Chem. Phys.*, **261**, 301–15.
Karbowiak, M., Drożdżyński, J., and Gajek, Z. (2001) *J. Alloys.Compds*, **323–4**, 678–82.
Karbowiak, M., Drożdżyński, J., and Sobczyk, M. (2002a) *J. Chem. Phys.*, **117**, 2800–8.
Karbowiak, M. A., Mech, A., Drożdżyński, J., Gajek, Z., and Edelstein, N. M. (2002b) *New. J. Chem.*, **26**, 1651–7.
Karbowiak, M. and Drożdżyński, J. (2003) *Mol. Phys.*, **101**, 971–5.
Karbowiak, M., Zych, E., Dereń, P., and Drożdżyński, J. (2003a) *Chem. Phys.*, **287**, 365–75.
Karbowiak, M., Mech, A., Drożdżyński, J., Edelstein, N. M., and Hubert, S. (2003b) *J. Phys. Chem. B*, **108**, 160–70.
Karbowiak, M., Sobczyk, M., and Drożdżynski, J. (2003c) *J. Solid State Chem.*, **173**, 59–68.
Karbowiak, M., Mech, A., Drożdżyński, J., and Edelstein, N. M. (2003d) *Phys. Rev. B*, **67**, 195108 (1–17).
Karbowiak, M., and Drożdżyński, J. (2004) *J. Phys. Chem. A.* **108**, 6397–406.
Karbowiak, M. (2005a) *J. Phys. chem. A*., **109**, 3569–77.
Karbowiak, M. (2005b) *Chem. Phys*., **314**, 189–97.

Karbowiak, M., Mech, A., Drozdzynski, J., Ryba-Romanowski, W., and Reid, M. F. (2005a) *J. Phys. Chem. B*, **109**, 155–66.
Karbowiak, M., Mech, A., and Drożdźński, J. (2005b) *Chem. Phys*., **308**, 135–45.
Karchevskĭ, A. I. and Buryak, E. M. (1962) *Sov. Phys. JETP*, **15**, 260–5.
Karmazin, L., Mazzanti, M., Gateau, C., Hill, C., and Pecaut, J. (2002) *Chem. Commun.* (*Cambridge, UK*), **23**, 2892–3.
Karraker, D. G. (1964) *Inorg. Chem.*, **3**, 1618–22.
Katakis, D. and Gordon, G. (1987) *Mechanism of Inorganic Reactions,* Wiley-Interscience, New York.
Kato, Y., Suzuki, K., Fukutomi, H., Tomiyasu, H., and Gordon, G. (1970) *Bull. Tokyo Inst Technol.*, **96**, 133–6.
Katz, J. J. and Rabinowitch, E. (1951) *The Chemistry of Uranium,* Natl. Nucl. En. Ser., Div. VIII, vol. 5, McGraw-Hill, New York.
Katz, J. J. and Rabinowitch, E. (1958) *The Chemistry of Uranium – Collected Papers*, TID-5290, Books I and 2, USAEC Technical Information Service, Oak Ridge, TN.
Katz, J. J. and Sheft, I. (l960) *Advances in Inorganic Chemistry and Radiochemistry,* vol. 2, Academic Press, New York, ch. 5.
Katz, J. J., Seaborg, G. T., and Morss, L. R. (1986) *The Chemistry of the Actinide Elements,* 2nd edn, vol. 1, Chapman and Hall, London, Table 5.68.
Katz, S. (1964) *Inorg. Chem.*, **3**, 1598–600.
Katzin, L. 1. (1952) *Production and Separation of* U^{233} *– Collected Papers*, Natl Nucl. En. Ser., Div. IV, 17B, Books 1 and 2, USAEC Technical Information Service, Oak Ridge, TN (declassified with deletions as TID-5223, Books 1 and 2).
Katzin, L. I. (1958) *J. Am. Chem. Soc.*, **80**, 5908–10.
Katzin, L. I., Kaplan, L., and Steitz, T. (1962) *Inorg. Chem.*, **1**, 963–4.
Kaufman, A. R., Cullity, B., and Brisianes, G. (1957) *Trans. AIME, J. Met.*, **209**, 23.
Keenan, T. K. (1966) *Inorg. Nucl Chem. Lett.*, **2**, 153–6.
Keenan, T. K. and Asprey, L. B. (1969) *Inorg. Chem.*, **8**, 235–8.
Keller, C. (1962a) *Nukleonik*, **4**, 271–7.
Keller, C. (1962b) *Z. Anorg. Allg. Chem.*, **317**, 241–4.
Keller, C. (1964) KFK Reports, KFK-225.
Keller, C., Koch, L., and Walter, K. H. (1965) *J. Inorg. Nucl. Chem.*, **27**, 1225–32.
Keller, C. and Salzer, M. (1967) *J. Inorg. Nucl. Chem.*, **29**, 2925–34.
Keller, C., Engerer, H., Leitner, L., and Sriyotha, U. (1969) *J. Inorg. Nucl. Chem.*, **31**, 965–80.
Keller, C. (1972) in *MTP International Review of Science, Inorganic Chemistry*, ser. 1, vol. 7 (ed. K. W. Bagnall), Butterworths, London; University Park Press, Baltimore, ch. 2, pp. 47–85.
Keller, C., Berndt, U., Debbabi, M., and Engerer, H. (1972) *J. Nucl. Mater.*, **42**, 23–31.
Keller, C. and Boroujerdi, A. (1972) *J. Inorg. Nucl. Chem.*, **34**, 1187–93.
Keller, C. (1975) in *Gmelin Handbuch der Anorganischen Chemie*, Suppl. Ser., Uranium, part C3, System no. 55, Springer-Verlag, Berlin, Heidelberg, and New York; *Ternäre und Polynäre Oxide des Urans*, pp. 295–359.
Keller, C. (1985) Heptavalent actinides, in *Handbook on the Physics and Chemistry of the Actinides* vol. 3, ch. 3 (eds. A. J. Freeman and G. H. Lander), North-Holland, Amsterdam, 143.

Keller, E. L. (compiler.) (1956) Uranium Hexafluoride Handling Procedures and Container Criteria, ORO-651; Revised Edition, ORO-651.
Keller, E. L., Furrer, A., Fischer, P., Allemspach, P., Krämer, K., Güdel, H. U., Doni, A., and Suzuki, T. (1995) *Phys. Rev. B*, **51** (5), 2881–90.
Kelley, W. E. (1955) *Nucleonics* **13**, 68–71.
Kelly, S. D., Newville, M. G., Cheng, L., Kemner, K. M., Sutton, S. R., Fenter, P., Sturchio, N. C., and Spötl, C. (2003) *Environ. Sci. Technol.*, **37**, 1284–7.
Kemmler-Sack, S. (1965) *Z. Anorg. Allg. Chem.*, **338**, 9–14.
Kemmler-Sack, S. and Rüdorff, W. (1966) *Z. Anorg. Allg. Chem.*, **344**, 23–40.
Kemmler-Sack, S. (1967) *Z. Naturforsch.*, **22B**, 597–79.
Kemmler-Sack, S. and Rüdorff, W. (1967) *Z. Anorg. Allg. Chem.*, **354**, 255–72.
Kemmler-Sack, S., Stumpp, E., Rüdorff, W., and Erfurth, H. (1967) *Z. Anorg. Allg. Chem.*, **354**, 287–300.
Kemmler-Sack, S. (1968a) *Z. Naturforsch. B*, **23**, 1260.
Kemmler-Sack, S. (1968b) *Z. Anorg. Allg. Chem.*, **363**, 295–304.
Kemmler-Sack, S. (1968c) *Z. Anorg. Allg. Chem.*, **363**, 282–94.
Kemmler-Sack, S. (1969) *Z. Anorg. Allg. Chem.*, **364**, 88–99.
Kemmler-Sack, S. and Wall, I. (1971) *Z. Naturforsch.*, **26b**, 1229–31.
Kemmler-Sack, S. (1973) *Z. Anorg. Allg. Chem.*, **402**, 255–78.
Kemmler-Sack, S. and Seemann, I. (1974) *Z. Anorg. Allg. Chem.*, **409**, 23–34.
Kemmler-Sack, S. and Seemann, I. (1975) *Z. Anorg. Allg. Chem.*, **411**, 61–78.
Kennedy, J. H. and Lingane, J. J. (1958) *Anal. Chim. Acta*, **18**, 240–4.
Kepert, D. L. (1982) *Inorganic Stereochemistry,* Springer-Verlag, Berlin.
Kern, D. M. H. and Orleman, E. F. (1949) *J. Am. Chem. Soc.*, **71**, 2102–6.
Kern, S., Hayward, J., Roberts, S., Richardson, J. W. Jr, Rotella, F. J., Soderholm, L., Cort, B., Tinkle, M., West, M., Hoisington, D., and Lander, G. H. (1994) *J. Chem. Phys.*, **101**, 9333–7.
Khanaev, E. I., Teterin, E. G., and Lukyanova, L. A. (1967) *Zh. Prikl. Spektrosk.*, **6**, 789–96; *J. Appl. Spectrosc.* (USSR), **6**, 533–8.
Kharitonov, Yu. Ya., Knyazeva, N. A., Tsapkin, V. V., and Ellert, G. V. (1967) *Radiokhimiya*, **9**, 322–30; (1967) *Sov. Radiochem.*, **9**, 316–23.
Khodadad, P. (1959) *C.R. Acad. Sci.*, **249**, 694–46.
Khodadad, P. (1960) *C.R. Acad. Sci.*, **250**, 3998–4000.
Khodadad, P. (1961) *Bull. Soc. Chim. Fr.*, 133–6.
Khosrawan-Sazedj, F. (1982) *Tschermaks Miner. Petrogr. Mitt.*, **30**, 111–15.
Killeen, J. C. (1980) *J. Nucl. Mater.*, **88**, 185–92.
Kim, K. C. and Olander, D. R. (1981) *J. Nucl. Mater.*, **102**, 192–9.
King, E. G. (1971) Quat. Met. Progr. Rep., no. 51.
Kirslis, S. S., McMillan, T. S., and Bernhardt, H. A. (1950) U.S. Report K-567, 1–36; (1956) N.S.A. Report **10**, no. 7198.
Kiukkola, K. (1962) *Acta Chem. Scand.*, **16**, 327–45.
Kjaerheim, G. and Rolstad, E. (1969) Halden Report, HPR-107.
Klaproth, M. H. (1789) *Chem. Ann.* (*Crell*), **11**, 387–403.
Klein-Haneveld, A. J. and Jellinek, F. (1964) *J. Inorg. Nucl. Chem.*, **26**, 1127–8.
Klein-Haneveld, A. J. and Jellinek, F. (1969) *J. Less Common Metals*, **18**, 123–9.
Klein-Haneveld, A. J. and Jellinek, F. (1970) *J. Less Common Metals*, **21**, 45–9.

Klepfer, H. H. and Chiotti, P. (1957) *Characteristics of the Solid State Transformations in Uranium*, ISC-893.
Kleykamp, H. (1985) *J. Nucl. Mater.*, **131**, 221–46.
Klíma, J., Jakeš, D., and Moravec, J. (1966) *J. Inorg. Nucl. Chem.*, **28**, 1861–9.
Koch, F. and Cohen, J. B. (1969) *Acta Crystallogr.*, **B25**, 275–87.
Kohlmann, H. and Beck, H. P. (1997) *Z. Anorg. Allg. Chem.*, **623**, 785–90.
Kohlmann, H. and Beck, H. P. (2000) *J. Solid State Chem.*, **150**, 336–41.
Kolitsch, U. and Giester, G. (2001) *Min. Mag.*, **65**, 717–24.
Kolitsch, W. and Müller, U. (1974) *Z. Anorg. Allg. Chem.*, **410**, 21–31.
Kolitsch, W. and Müller, U. (1975) *Z. Anorg. Allg. Chem.*, **418**, 235–42.
Kolomiets, A. V., Havela, L., Rafaja, D., Bordallo, H. N., Nakotte, H., Yartys, V. A., Hauback, B. C., Drulis, H., Iwasieczko, W., and De Long, L. E. (2000) *J. Appl. Phys.*, **87**, 6815–17.
Konrad, T. and Jeitschko, W. (1996) *J. Alloys Compds*, **233**, L3–7.
Korba, V. M. (1983) *Zh. Strukt. Khim.*, **24**, 172.
Kotlar, A., Gerdanian, P., and Dodé, M. (1967a) *J. Chim. Phys. Phys. Chim. Biol.*, **64**, 862–8.
Kotlar, A., Gerdanian, P., and Dodé, M. (1967b) *J. Chim. Phys. Phys. Chim. Biol.*, **64**, 1135–44.
Kotlar, A., Gerdanian, P., and Dodé, M. (1968) *J. Chim. Phys. Phys. Chim. Biol.*, **65**, 687–91.
Kovba, L. M., Ippolitova, E. A., Simanov, Yu . P., and Spitsyn, V. I. (1958) *Dokl. Akad. Nauk. SSSR*, **120**, 1042–4.
Kovba, L. M. (1960) *Zh. Strukt. Khim.*, **1**, 390.
Kovba, L. M. (1961) *Zh. Strukt. Khim.*, **2**, 585.
Kovba, L. M., Polunina, G. P., Simanov, Yu. P., and Ippolitova, E. A. (1961a) Argonne National Laboratory Report, ANL-trans-33, p. 17.
Kovba, L. M., Simanov, Yu. P., Ippolitova, E. A., and Spitsyn, V. I. (1961b) Argonne National Laboratory Report, ANL.trans-33, p. 24.
Kovba, L. M. (1962) *Zh. Strukt. Khim.*, **3**, 159.
Kovba, L. M., Vidanskii, L. M., and Lavut, E. G. (1963) *Zh. Strukt. Khim.*, **4**, 627.
Kovba, L. M. (1970) *Sov. Radiochem.*, **12**, 486–7.
Kovba, L. M. (1971a) *Sov. Radiochem.*, **13**, 319–20.
Kovba, L. M. (1971b) *Zh. Neorg. Khim.*, **16**, 3089–91.
Kovba, L. M. and Trunova, V. I. (1971) *Sov. Radiochem.*, **13**, 796–7.
Kovba, L. M. (1972a) *Sov. Radiochem.*, **14**, 746–9.
Kovba, L. M. (1972b) *Zh. Strukt. Khim.*, **13**, 256–9.
Kovba, L. M. (1972c) *Zh. Strukt. Khim.*, **13**, 458–60.
Kovba, L. M., Tsigunov, A. N., Kuz'micheva, E. U., and Kamaratseva, N. I. (1972) *Radiokhimiya*, **14**, 921–3.
Kovba, L. M., Murav'eva, I. A., and Orlova, A. S. (1974) *Sov. Radiochem.*, **16**, 638–9.
Krämer, K. and Meyer, G. (1989) (unpublished results).
Krämer, K., Meyer, G., Karbowiak, M., and Drożdżyński, J. (1991) *J. Less Common Metals*, **175**, 347–52.
Krämer, K., Keller, L., Fischer, P., Jung, B., Edelstein, N. M., Güdel, H. U., and Meyer, G. (1993) *J. Solid State Chem.*, **103**, 152–9.

Krämer, K., Güdel, H. U., Meyer, G., Heuer, T., Edelstein, N., Jung, B., Keller, L., Fischer, P., Zych, E., and Drożdżyński, J. (1994) *Z. Anorg. Allg. Chem.*, **620**, 1339–45.
Kramer, G. M. and Maas, E. T. Jr (1981) *Inorg. Chem.*, **20**, 3514–16.
Krause, W., Effenberger, H., and Brandstätter, F. (1995) *Eur. J. Miner.*, **7**, 1313–24.
Kressin, I. K. (1977) *Anal. Chem.*, **49**, 842–5.
Krol, D. M. (1981) *J. Chem. Soc., Dalton Trans.*, 687–93.
Krivovichev, S. V. and Burns, P. C. (2000a) *Can. Miner.*, **38**, 847–51.
Krivovichev, S. V. and Burns, P. C. (2000b) *Can. Miner.*, **38**, 717–26.
Krivovichev, S. V. and Burns, P. C. (2002a) *J. Solid State Chem.*, **168**, 245–58.
Krivovichev, S. V. and Burns, P. C. (2002b) *Can. Miner.*, **40**, 201–9.
Krivovichev, S. V. and Burns, P. C. (2002c) *Inorg. Chem.*, **41**, 4108–10.
Krivovichev, S. V. and Burns, P. C. (2003) *Can. Miner.*, **41**, 707–19.
Kruger, O. L. and Moser, J. B. (1967) *J. Phys. Chem. Solids*, **28**, 2321–5.
Krupa, J .C. (1987) *Inorg. Chim. Acta*, **139**, 223–41.
Kruse, F. H. (1962) *Inorg. Chem.*, **1**, 137–9.
Kruse, F. H. and Asprey, L. B. (1962a) *J. Inorg. Nucl. Chem.*, **33**, 1625–27.
Kruse, F. H. and Asprey, L. B. (1962b) *Inorg. Chem.*, **1**, 137–9.
Kruse, F. H. (1971) *J. Inorg. Nucl. Chem.*, **33**, 1625–7.
Kubaschewski, O. and Alcock, C. B. (1979) *International Series of Material Science and Technology*, Metallurgical Thermochemistry, vol. 24, 5th edn, Pergamon Press, Oxford.
Kudryashov, V. L., Suglobova, I. G., and Chirkst, D. E. (1978) *Radiokhimiya*, **20**, 366–72.
Kumar, N. and Tuck, D. G. (1984) *Inorg. Chim. Acta*, **95**, 211–15.
Labroche, D., Dugne, O., and Chatillon, C. (2003a) *J. Nucl. Mater.*, **312**, 21–49.
Labroche, D., Dugne, O., and Chatillon, C. (2003b) *J. Nucl. Mater.*, **312**, 50–66.
Lakner, J. F. (1978) University of California, Livermore, Lawrence Livermore National Laboratory, Report UCRL-52518.
Lally, A. E. (1992) in *Uranium Series Disequilibrium Applications to Earth, Marine, and Environmental Sciences* (eds. M. Ivanovich and R. S. Harmon), Clarendon Press, Oxford., pp. 94–126.
Lambertson, W. H. and Mueller, M. H. (1954) Argonne National Laboratory Report, ANL-5312.
Lander, G. H. and Müller, M. H. (1970) *Acta Crystallogr. B*, **26**, 129–36.
Lander, G. H., Fisher, E. S., and Bader, S. D. (1994) *Adv. Phys.*, **43**, 1–111.
Lang, S. M., Knudsen, F. P., Fillmore, C. L., and Roth, R. S. (1956) NBS Circ., no. 568, 32 pp.
Langford, C. H. and Gray, H. B. (1965) *Ligand Substitution Processes*, W. A. Benjamin, New York.
Larson, A. C., Roof, R. B., and Cromer, D. T. (1964) *Acta Crystallogr.*, **17**, 555.
Latta, R. E. and Fryxell, R. E. (1970) *J. Nucl. Mater.*, **35**, 195–210.
Lau, K. H. and Hildenbrand, D. L. (1982) *J. Chem. Phys.*, **76**, 2646.
Lau, K. H. and Hildenbrand, D. L. (1984) *J. Chem. Phys.*, **80**, 1312–17.
Laugier, J., Blum, P. L., and Detourminé, R. J. (1971) *J. Nucl. Mater.*, **41**, 106–8.
Laval, J. P., Mikou, A., Frit, B., Roult, G., and Pannetier, J. (1987) *Rev. Chim. Minér.*, **24**, 165–82.

Laveissière, J. (1967) *Bull. Soc. Franc. Minér. Crist.*, **90**, 308–10.
Lawson, A. C., Severing, A., Ward, J. W., Olsen, C. E., Goldstone, J. A., and Williams, A. (1990) *J. Less Common Metals*, **158**, 267–74.
Lawson, A. C., Goldstone, J. A., Huber, J. G., Giorgi, A. L., Conant, J. W., Severing, A., Cort, B., and Robinson, R. A. (1991) *J. Appl. Phys.*, **69**, 5112–16.
Lay, K. W. (1970) *J. Am. Ceram. Soc.*, **53**, 369–73.
Leask, M. J. M., Roberts, L. E. J., Walker, A. J., and Wolf, W. P. (1963) *J. Chem. Soc.*, 4788–94.
Lebeau, P. and Damien, A. (1913) *C.R. Acad. Sci.*, **156**, 1987–9.
Le Bihan, T., Rogl, P., and Noël, H. (2000) *J. Nucl. Mater.*, **277**, 82–90.
Lederer, C. M. and Shirley, V. S. (1978) *Table of Isotopes*, 7th edn, John Wiley, New York.
Lee, H. M. (1974) *J. Nucl. Mater.*, **50**, 25–30.
Leibowitz, L., Mishler, L. W., and Chasanov, M. G. (1969) *J. Nucl. Mater.*, **29**, 356–8.
Leonidov, V. Y. (1960) *Zh. Fiz. Khim.*, **34**, 1862.
Leroy, J. M. and Tridot, G. (1966) *C.R. Acad. Sci.* (*Paris*), **C262**, 1376–9.
Leslie, B. W., Pearcy, E. C., and Prikryl, J. D. (1993) *Mater. Res. Soc. Symp. Proc.*, **294**, 505–12.
Leung, A. F. and Poon, Y.-M. (1977) *Can. J. Phys.*, **55**, 937–42.
Leuze, R. E., Clinton, S. O., Chilton, J. M. and Vaughen, V. C. A. (1962) in *Transuranium Quarterly Progress Report for period ending Feb. 28, 1962* (compiler D. E. Ferguson), ORNL-3290, p. 79.
Leuze, R. E., Clinton, S. D., Chilton, J. M., and Vaughen, V. C. A. (1963) in *Transuranium Quarterly Progress Report for period ending Aug. 31, 1962* (compiler D. E. Ferguson), ORNL-3375, p. 51.
Levet, J. C. (1965) *Compt. Rend. C*, **260**, 4775–6.
Levet, J. C. (1969) *Compt. Rend. C*, **268**, 703–5.
Levet, J. C., Potel, M., and Le Marouille, J. Y. (1977) *Acta Crystallogr. B*, **33**, 2542–6.
Levet, J. C. and Noël, H. (1979) *J. Solid State Chem.*, **28**, 67–73.
Levet, J. C., Potel, M., and Le Marouille, J. Y. (1980) *J. Solid State Chem.*, **32**, 297–301.
Levet, J. C. and Noël, H. (1981) *J. Inorg. Nucl. Chem.*, **43**, 1841–3.
Levy, J. H., Taylor, J. C., and Wilson, P. W. (1975) *J. Less Common Metals*, **39**, 265–70.
Levy, J. H., Taylor, J. C., and Wilson, P. W. (1976) *J. Chem. Soc. Dalton Trans.*, 219–24.
Levy, J. H., Taylor, J. C., and Wilson, P. W. (1977) *J. Inorg. Nucl. Chem.*, **39**, 1989–91.
Levy, J. H., Taylor, J. C., and Wilson, P. W. (1978) *J Inorg. Nucl. Chem.*, **40**, 1055–7.
Levy, J. H., Taylor, J. C., and Waugh, A. B. (1980) *Inorg. Chem.*, **19**, 672–4.
Levy, J. H., Taylor, J. C., and Waugh, A. B. (1983) *J. Fluorine Chem.*, **23**, 29–36.
Lewis, W. B., Asprey, L. B., Jones, L. H., McDowell, R. S., Rabideau, S. W. Zeltman, A. H., and Levet, J. C. (1965) *Compt. Rend. C*, **260**, 4775–6.
Lewis, W. B., Hecht, H. G., and Eastman, M. P. (1973) *Inorg. Chem.*, **12**, 1634–9.
Lewis, W. B., Asprey, L. B., Jones, L. H., McDowell, R. S., Rabideau, S. W., Zeltman, A. H., and Paine, R. T. (1976) *J. Chem. Phys.*, **65**, 2707–14.
Li, J., Bursten, B. E., Liang, B., and Andrews, L. (2002) *Science*, **295**, 2242–5.
Li, Y.-P. and Burns, P. C. (2000a) *Can. Miner.*, **38**, 737–49.
Li, Y.-P. and Burns, P. C. (2000b) *Can. Miner.*, **38**, 727–35.
Li, Y.-P., Burns, P. C., and Gault, R. A. (2000) *Can. Miner.*, **38**, 153–62.
Li, Y.-P. and Burns, P. C. (2001a) *J. Nucl. Mater.*, **299**, 219–26.

Li, Y.-P. and Burns, P. C. (2001b) *Can. Miner.*, **39**, 1147–51.
Li, Y.-P., Krivovichev, S. V., and Burns, P. C. (2001a) *Miner. Mag.*, **65**, 285–92.
Li, Y.-P., Cahill, C. L., and Burns, P. C. (2001b) *Chem. Mater.*, **13**, 4026–31.
Libowitz, G. G. and Gibb, T. R. P. Jr (1957) *J. Phys. Chem.*, **61**, 793–5.
Libowitz, G. G. (1968) in *Metal Hydrides* (eds. W. Mueller, J. P. Blackledge, and G. G. Libowitz), Academic Press, New York., ch. 11
Lin, S. T. and Kaufmann, A. R. (1956) *Phys. Rev.*, **102**, 640–6.
Lincoln, S. F. (1979) *Pure Appl. Chem.*, **51**, 2059–65.
Lindemann, F. and Aston, F. W. (1919) *Phil. Mag.*, **6(37)**, 523.
Lindemer, T. B. and Besmann, T. M. (1985) *J. Nucl. Mater.*, **130**, 473–88.
Lindemer, T. B. and Brynestad, J. (1986) *J. Am Ceram. Soc.*, **69**, 867–76.
Lindemer, T. B. and Sutton, A. L. Jr (1988) *J. Am. Ceram. Soc.*, **71**, 553–61.
Lipschutz, M. E., Wolf, S. F., Hanchar, J. M., and Culp, F. B. (2001) *Anal. Chem.*, **73**, 2687–700.
Litz, L. M. (1948) *Uranium Carbides – Preparation, Structure and Hydrolysis*, Thesis, Ohio State University, NP-1453.
Litz, L. M., Garrett, A. B., and Croxton, E. C. (1948) *J. Am. Chem. Soc.*, **70**, 1718–22.
Locock, A. J. and Burns, P. C. (2003a) *Am. Miner.*, **88**, 240–4.
Locock, A. J. and Burns, P. C. (2003b) *Min. Mag.*, **67**, 1109–20.
Locock, A. J. and Burns, P. C. (2003c) *Can. Miner.*, **41**, 91–101.
Locock, A. J. and Burns, P. C. (2003d) *Can. Miner.*, **41**, 489–502.
Locock, A. J., Burns, P. C., and Flynn, T. M. (2005a) *Am. Miner.*, **90**, 240–6.
Locock, A. J., Burns, P. C., Flynn, T. M. (2005b) *Can. Miner*., **43**, 721–33.
Locock, A. J., Kinman, W. S., and Burns, P. C. (2005c) *Can. Miner.* **43**, 989–1003.
Lopez, M. and Birch, D. S. J. (1997) *Chem. Phys. Lett.*, **268**, 125–32.
Loopstra, B. O. (1962) *Acta Crystallogr.*, **17**, 651–4.
Loopstra, B. O. and Cordfunke, E. H. P. (1966) *Rec. Trav. Chim. Pays-Bas*, **58**, 135–42.
Loopstra, B. O. and Rietveld, H. M. (1969) *Acta Crystallogr.*, **B25**, 787–91.
Loopstra, B. O. (1970a) *J. Appl. Crystallogr.*, **3**, 94–6.
Loopstra, B. O. (1970b) *Acta Crystallogr.*, **B26**, 656–7.
Lorenzelli, R. and Touzelin, B. (1980) *J. Nucl. Mater.*, **95**, 290–302.
Lu, W. C., Ree, T., Gerard, V., and Eyring, H. (1968) *J. Chem. Phys.*, **49**, 797.
Lucas, J. (1964) *Rev. Chim. Minér.*, **1**, 479–517.
Lumpkin, G. R., Eyal, Y., and Ewing, R. C. (1988) *J. Mater. Res.*, **3**, 357–68.
Lumpkin, G. R. and Ewing, R. C. (1995) *Am. Miner.*, **80**, 732–43.
Lumpkin, G. R., Hart, K. P., McGlinn, P., Gieré, R., and Williams, C. T. (1995) *Radiochim. Acta*, 469–74.
Lumpkin, G. R., Payne, T. E., Fenton, B. R., and Waite, T. D. (1999) *Mater. Res. Soc. Symp. Proc.*, **556**, 1067–74.
Lundgren, G. (1952) *Arkiv Kemi*, 421–8.
Lupinetti, A. J., Fife, J. L., Garcia, E., Dorhout, P. K., and Abney, K. D. (2002) *Inorg. Chem.*, **41**, 2316–18.
Lychev, A. A., Mashirov, L. G., Smolin, Yu. I., and Shepelev, Yu. F. (1986) *Radiokhimiya*, **28**, 682–5.
Lyon, W. G., Osborne, D. W., Flotow, H. E., and Hoekstra, H. R. (1977) *J. Chem. Thermodyn.*, **9**, 201–10.
Lynch, E. D. (1965) Argonne National Laboratory Report, ANL-6894.

Łyżwa, R. and Erdös, P. (1987) *Phys. Rev. B*, **36**, 8570.
Macaskie, L. E., Bonthrone, K. M., Yong, P., and Goddard, D. T. (2000) *Microbiology*, **146**, 1855–67.
Mac Cordick, J. and Brun, C. (1970) *Compt. Rend. Acad. Sci. Ser. C.*, **270**, 620–3.
Mac Leod, A. C. (1972) *J. Chem. Thermodyn.*, **4**, 699–708.
Mac Wood, G. E. (1958) TID-5290, pp. 543–609.
Maglic, K. and Herak, R. (1970) *Rev. Int. Hautes Tempér. Réfract. Fr.*, **7**, 247.
Mair, M. A. and Savage, D. J. (1986) UK Atomic Energy Agency Report, ND-R-134.
Malek, C. K., Krupa, J.-C., Delamoye, P., and Genet, M. (1986a) *J. Phys.* (*Paris*), **47**, 1763–73.
Malek, C. K., Krupa, J.-C., and Genet, M. (1986b) *Spectrochim. Acta* part A, **42**, 907–12.
Malek, C. K. and Krupa, J.-C. (1994) *J. Chem. Phys.*, **84**, 6584–90.
Maletka, K., Fischer, P., Murasik, A., and Szczepaniak, W. (1992) *J. Appl. Cryst.*, **25**, 1–5.
Maletka, K., Murasik, A., Szczepaniak, W., Rundloef, H., and Tellgren, R. (1995) *Solid State Ionics*, **76**, 115–20.
Maletka, K., Tellgren, R., Rundloef, H., Szczepaniak, W., and Rycerz, L. (1996a) *Solid State Ionics*, **90**, 67–74.
Maletka, K., Ressouche, E., Szczepaniak, W., Rycerz, L., and Murasik, A. (1996b) *Mater. Sci. Forum*, **228**, 711–16.
Maletka, K., Ressouche, E., Rundloef, H., Tellgren, R., Delaplane, R., Szczepaniak, W., and Zablocka-Malicka, M. (1998) *Solid State Ionics*, **106**, 55–69.
Mallett, M. W., Gerds, A. F., and Nelson, H. R. (1952) *J. Electrochem. Soc.*, **99**, 197–204.
Mallett, M. W. and Gerds, A. F. (1955) *J. Electrochem. Soc.*, **102**, 292–6.
Mallett, M. W., Trzeciak, M. J., and Griffith, C. B. (1955) *Nuclear Engineering and Science Congress*, Cleveland, OH, Preprint 334.
Mallett, M. W. and Trzeciak, M. J. (1958) *Trans. Am. Soc. Met.*, **50**, 981–93.
Malm, J. G., Selig, H., and Siegel, S. (1966) *Inorg. Chem.*, **5**, 130–2.
Malm, J. G. (1980) *J. Inorg. Nucl. Chem.*, **42**, 993–4.
Manes, L. (ed.) (1985) *Struct. Bonding*, **59/60**; *Actinide-Chemistry and Physical Properties*, Springer Verlag, New York.
Marakov, E. S. and Bykov, V. N. (1959) *Kristallographica*, **4**, 183–5.
Marchidan, D. I. and Matei-Tanasescu, S. (1972) *Rev. Roum. Chim.*, **17**, 195–202.
Marchidan, D. I. and Matei-Tanasescu, S. (1974) *Rev. Roum. Chim.*, **19**, 1435.
Marchidan, D. I. and Matei-Tanasescu, S. (1975) *Rev. Roum. Chim.*, **20**, 1365.
Marcon, J.-P. (1969) *Contribution à l'Etude des Sulfures d'Actinides*, Thesis, University of Paris, CEA-3919.
Marcon, J. P. (1972) *Rev. Int. Hautes Temp. Réfract.*, **9**, 193.
Marin, J. F. (1968) CEA Report, CEA-N-883.
Marin, J. F. and Contamin, P. (1969) *J. Nucl. Mater.*, **30**, 16–25.
Marinenko, G., Koch, W. F., and Etz, E. S. (1983) *J. Res. Natl. Bur. Stand.*, **88**, 117–24.
Marinsky, J. A. (1956) Development of the EXCER Process, part II, ORNL-1979.
Markin, T. L. and Bones, R. J. (1962a) UKAEA Harwell Report, AERE-R 4178.
Markin, T. L. and Bones, R. J. (1962b) UKAEA Report, AERE-R 4042.
Markin, T. L. and Crough, E. C. (1970) *J. Inorg. Nucl. Chem.*, **32**, 77–82.
Markin, T. L., Street, R. S., and Crough, E. C. (1970) *J. Inorg. Nucl. Chem.*, **32**, 59–75.

Marples, J. A. C. (1976) in *Plutonium 1975 and Other Actinides*, Proc. Fifth Int. Conf. on Plutonium and Other Actinides, Baden-Baden, Germany (eds. H. Blank and R. Lindner), North-Holland, Amsterdam, pp. 353–9.
Martin, A. E. and Edwards, R. K. (1965) *J. Phys. Chem.*, **69**, 1788.
Martin, A. E. and Shinn, W. A. (1971) Argonne National Laboratory Report, ANL-7877.
Martin, P., Ripert, M., Petit, T., Reich, T., Hennig, C., D'Acapito, F., Hazemann, J. L., and Proux, O. (2003) *J. Nucl. Mater.*, **312**, 103–10.
Martinot, L. (1984) Uranium in molten in molten salts and melts, in *Gmelin Handbook of Inorganic Chemistry*, Uranium Suppl., vol. D1, 332–78.
Martinot, L. (1991) Molten-salt chemistry of the actinides, in *Handbook on the Physics and Chemistry of the Actinides* , vol. 6, ch. 4 (eds. A. J. Freeman and C. Keller), North-Holland, Amsterdam, 241–79.
Marzotto, A., Bandoli, G., Clemente, D. A., Benetollo, F., and Galzigna, L. (1973) *J. Inorg. Nucl. Chem.*, **35**, 2769–74.
Marzotto, A., Grazotto, R., Bombieri, G., and Forsellini, E. (1974) *J. Cryst. Mol. Struct.*, **4**, 253–62.
Masaki, N. and Tagawa, H. (1975) *J. Nucl. Mater.*, **58**, 241–3.
Mass, E. T. (1979) *J. Inorg. Nucl. Chem.*, **41**, 991.
Masson, J. P., Desmoulin, R., Charpin, P., and Bougon, R. (1976) *Inorg. Chem.*, **15**, 2529–31.
Masson, J. P., Naulin, C., Charpin, P., and Bougon, R. (1978) *Inorg. Chem.*, **17**, 1858–61.
Masters, B. J. and Schwartz, L. L. (1961) *J. Am. Chem. Soc.*, **83**, 2620–24.
Matonic, J. H., Scott, B. L., and Neu, M. P. (2001) *Inorg. Chem.*, **40**, 2638–9.
Matsika, S., Zhang, Z., Brozell, S. R., Bladeau, J.-P., Wang, Q., and Pitzer, R. M. (2001) *J. Phys. Chem. A*, **105**, 3825–8.
Matson, L. K., Moody, J. W., and Himes, R. C. (1963) *J. Inorg. Nucl. Chem.*, **25**, 795–800.
Matsui, T., Tsuji, T., and Naito, K. (1974) *J. Nucl. Sci. Technol.*, **11**, 216–22.
Matsui, T. and Naito, K. (1975) *J. Nucl. Mater.*, **56**, 327–35.
Matsui, T. and Naito, K. (1985a) *J. Nucl. Mater.*, **132**, 212–21.
Matsui, T. and Naito, K. (1985b) *J. Nucl. Mater.*, **136**, 59–68.
Matsui, T. and Naito, K. (1986) *J. Nucl. Mater.*, **138**, 19–26.
Matzke, Hj. (1981) in *Non-Stoichiometric Oxides* (ed. O. T. Sørensen), Academic Press, New York, ch. 4, pp. 156–232.
Matzke, Hj. (1987) *J. Chem. Soc., Faraday Trans. 2*, **83**, 1121–42.
Maximov, V. (compiler.) (1963) *Uranium Carbides, Nitrides, and Silicides*, vol. I (1961/1963), IAEA Bibliographical Series 14, International Atomic Energy Agency, Vienna, STI/PUB/21/14.
Maximov, V. (compiler.) (1965) *Uranium Carbides, Nitrides, and Silicides*, vol. II (1963/1965), IAEA Bibliographical Series 21, International Atomic Energy Agency, Vienna, STI/PUB/21/21.
Maximov, V. (compiler.) (1967) *Uranium Carbides, Nitrides, and Silicides*, vol. III (1965/1967), IAEA Bibliographical Series 33, International Atomic Energy Agency, Vienna, STI/PUB/21/33.
Mayer, H. and Mereiter, K. (1986) *Tschermaks Miner. Petrogr. Mitt.*, **35**, 133–46.
Mazurak, M., Drożdżyński, J., and Hanuza, J. (1988) *J.Mol. Struct.*, **174**, 443–8.

Mazzi, F. and Munno, R. (1983) *Am. Miner.*, **68**, 262–76.
McDowell, R. S., Asprey, L. B., and Paine, R. T. (1974) *J. Chem. Phys.*, **61**, 3571–80.
McEachern, R. J. and Taylor, P. (1998) *J. Nucl. Mater.*, **254**, 87–121.
McEwen, D. J. and De Vries, T. (1959) *Anal. Chem.*, **31**, 1672–2.
McLaughlin, R. (1962) *J. Chem. Phys.*, **36**, 2699–705.
McNamara, B. K., Buck, E. C., and Hanson, B. D. (2003) *Mater. Res. Soc. Symp. Proc.*, **757**, 401–6.
Mech, A., Karbowiak, M., Lis, T., and Drożdżyński, J. (2005) Polyhedron, in press.
Meinrath, G., Lis, S., Stryla, S., and Noubactep, C. (2000) *J. Alloys Compds.*, **300/301**, 107–12.
Meites, L. (ed.) (1963) *Handbook of Analytical Chemistry*, McGraw-Hill, New York.
Meitner, L., Hahn, O., and Strassmann, F. (1937) *Z. Phys.*, **106**, 249–70.
Mellor, J. W. (1932) *Comprehensive Treatise on Inorganic and Theoretical Chemistry*, vol. XII, , Longmans, Green and Co., London.
Mentink, S. A. M., Mason, T. E., Buyers, W. J. L., and Clausen, K. N. (1998) *Physica B.* (*Amsterdam, Neth.*), **241–243**, 669–71.
Menzies, C. (1966) UKAEA Report, TRG-1119(D).
Mereiter, K. (1982a) *Tschermaks Miner. Petrogr. Mitt.*, **30**, 277–88.
Mereiter, K. (1982b) *Tschermaks Miner. Petrogr. Mitt.*, **30**, 129–39.
Mereiter, K. (1982c) *Tschermaks Miner. Petrogr. Mitt.*, **30**, 47–51.
Mereiter, K. (1984) *Acta Crystallogr.*, **A40**, Suppl. C-247.
Mereiter, K. (1986) *Tschermaks Miner. Petrogr. Mitt.*, **35**, 1–18.
Merritt, R. C. (1971) *The Extractive Metallurgy of Uranium*, Colorado School of Mines Research Institute and USAEC, Golden, CO.
Meunier, G. and Galy, J. (1973) *Acta Crystallogr.*, **B29**, 1251–5.
Meusemann, H. and von Erichsen, L. (1973) *Bundesministerium für Forschung und Technologie*, Report no. BMFT-FBK-73–18.
Meyer, G., Gaebell, H.-Chr., and Hoppe, R. (1983) *J. Less Common. Metals*, **93**, 347–51.
Meyer, H. C., McDonald, P. F., and Settler, J. D. (1967) *Phys. Lett.*, **24A**, 569.
Meyer, R. A. and Wolfe, B. E. (1964) *Trans. Am. Nucl. Soc.*, **7**, 111–12.
Mighell, A. D. and Ondik, H. M. (1977) *J. Phys. Chem. Ref. Data*, **6**, 675–829.
Mignanelli, M. A. and Potter, P. E. (1983) *J. Nucl. Mater.*, **118**, 150–8.
Mignanelli, M. A. and Potter, P. E. (1986) *J. Less Common Metals*, **121**, 605–13.
Miguta, A. K. (1997) *Geol. Ore Deposits*, **39**, 275–93.
Mikhailov, Yu. N. and Kuznetsov, V. G. (1971) *Russ. J. Inorg. Chem.*, **16**, 1340–2.
Mikhailov, Yu. N., Udovenko, A. A., Kuznetsov, V. G., and Davidovich, R. L. (1972a) *Zh. Strukt. Khim.*, **13**, 942–3; (1972) *J. Strukt. Chem.* (*USSR*), **13**, 879–80.
Mikhailov, Yu. N., Udovenko, A. A., Kuznetsov, V. G., and Davidovich, R. L. (1972b) *Zh. Strukt. Khim.*, **13**, 741.
Mikhailov, Yu. N., Ivanov, S. B., Orlova, I. M., Podnebesnova, G. V., Kuznetsov, V. G., and Shchelokov, R. N. (1976a) *Koord. Khim.* [*Coord. Chem.* (*USSR*)], **2**, 1570–3.
Mikhailov, Yu. N., Ivanov, S. B., Kuznetsov, V. G., and Davidovich, R. L. (1976b) *Koord. Khim.* [*Coord. Chem.* (*USSR*)], **2**, 95–8.
Mikhailov, Yu. N., Ivanov, S. B., and Sadikov, G. G. (1979) *Koord. Khim.* [*Coord. Chem.* (*USSR*)], **5**, 1702–5.
Miller, D. (1965) Argonne National Laboratory Report, ANL-7120, p. 641.

Miller, M. L., Finch, R. J., Burns, P. C., and Ewing, R. C. (1996) *J. Mater. Res.*, **11**, 3048–56.
Miller, S. A. and Taylor, J. C. (1986) *Z. Kristallogr.*, **177**, 247–53.
Mills, K. C. (1974) *Thermodynamic Data for Inorganic Sulphides, Selenides, and Tellurides*, Butterworths, London.
Misaelides, P., Godelitsas, A., Filippidis, A., Charistos, D., and Anousis, I. (1995) *Sci. Total Environ.*, **173–174**, 237–46.
Miyake, C., Fuji, K., and Imoto, S. (1977) *Chem. Phys. Lett.*, **46**, 349–51.
Miyake, C., Fuji, K., and Imoto, S. (1979) *Chem. Phys. Lett.*, **61**, 124–6.
Miyake, C., Takeuchi, H., Ohya-Nishiguchi, H., and Imoto, S. (1982) *Phys. Status Solidi*, **A74**, 173–80.
Miyake, C., Kanamaru, M., Imoto, S., and Taniguchi, K. (1986) *J. Nucl. Mater.*, **138**, 36–9.
Miyake, C. (1991) Magnetochemistry of U(V) complexes and compounds, in *Handbook on the Physics and Chemistry of the Actinides* (eds. A. J. Freeman and C. Keller), Elsevier, vol. 6, ch. 5, 337–66.
Miyake, C., Kawasaki, O., Gotoh, K., and Nakatani, A. (1993) *J. Alloys Compds*, **200**, 187–90.
Miyake, C. and Fujino, T. (1998) *J. Alloys Compds*, **271–273**, 479–81.
Moens, L. and Jakubowski, N. (1998) *Anal. Chem.*, **70**, 251A–6A.
Moll, H., Denecke, M. A., Jalilehvand, F., Sandström, M., and Grenthe, I. (1999) *Inorg. Chem.*, **38**, 1795–99.
Moll, H., Reich, T., and Szabó, Z. (2000a) *Radiochim. Acta*, **88**, 411–15.
Moll, H., Reich, T., Hennig, C., Rossberg, A., Szabó, Z., and Grenthe, I. (2000b) *Radiochim. Acta*, **88**, 559–66.
Moll, H., Geipel, G., Reich, T., Bernhard, D., and Grenthe, I. (2003) *Radiochim. Acta*, **91**, 11–20.
Montignie, E. (1947) *Bull. Soc. Chim. Fr.*, 748–49.
Montoloy, F. and Plurien, P. (1968) *C. R. Acad. Sci.*, **267**, 1036.
Moody, D. C. and Odom, J. D. (1979) *J. Inorg. Nucl. Chem.*, **41**, 533–5.
Moody, D. C., Penneman, R. A., and Salazar, K. V. (1979) *Inorg. Chem.*, **18**, 208–9.
Moody, D. C., Zozulin, A. J., and Salazar, K. V. (1982) *Inorg. Chem.*, **21**, 3856–7.
Moore, G. E. and Kelley, K. K. (1947) *J. Am. Chem. Soc.*, **69**, 2105–7.
Morris, D. E., Allen, P. G., Berg, J. M., Chisolm-Brause, C. J., Conradson, S. D., Hess, N. J., Musgrave, J. A., and Tait, C. D. (1996) *Environ. Sci. Technol.*, **30**, 2322–31.
Morss, L. R. (1982) in *Actinides in Perspective* (ed. N. M. Edelstein), Pergamon Press, Oxford, pp. 381–407.
Morss, L. R. (1991) in *Synthesis of Lanthanide and Actinide Compounds* (eds. G. Meyer and L. R. Morss), Kluwer Academic Publishers, Dordrecht., pp. 237–58.
Moriyasu, M., Yokoyama, Y., and Ikeda, S. (1977) *J. Inorg. Nucl. Chem.*, **39**, 2199–203.
Moskvin, A. I. and Zaitseva, V. P. (1962) *Radiokhimiya*, **4**, 73–82; *Sov. Radiochem.*, **4**, 63–9.
Moskvin, A. I. (1968) *Radiokhimiya*, **10**, 13–21; *Sov. Radiochem*, **10**, 10–13.
Mucke, A. and Strunz, H. (1978) *Am. Miner.*, **63**, 941–6.
Mulak, J. and Żołnierek, Z. (1972) *Bull. Acad. Pol. Sci. Ser. Sci. Chim.*, **20**, 1081.
Mulak, J. and Żołnierek, Z. (1977) *Proc. Second Int. Conf. Electron. Struct. Actinides*, Wrocław, Poland., 1976, pp. 125–31.

Mulford, R. N. R., Ellinger, F. H., and Zachariasen, W. H. (1954) *J. Am. Chem. Soc.*, **76**, 297–8.
Müller, U. and Kolitsch, W. (1974) *Z. Anorg. Allgem. Chem.*, **410**, 32–8.
Murakami, T., Ohnuki, T., Isobe, H., and Sato, T. (1997) *Am. Miner.*, **82**, 888–99.
Murasik, A., Suski, W., Troć, R., and Leciewicz, L. (1968) *Phys. Status Solidi*, **30**, 61–6.
Murasik, A., Furrer, A., and Szczepaniak, W. (1980) *Solid State Commun.*, **33**, 1217.
Murasik, A., Fischer, P., and Szczepaniak, W. (1981) *J. Phys. C., Solid State Phys.*, **14**, 1847.
Murasik, A., Fischer, P., Furrer, A., and Szczepaniak, W. (1985) *J. Phys. C, Solid State Phys.*, **18**, 2909–21.
Murasik, A., Fischer, P., Furrer, A., Schmid, B., and Szczepaniak, W. (1986) *J. Less Common Metals*, **121**, 151–5.
Murch, G. E. and Catlow, C. R. A. (1987) *J. Chem. Soc., Faraday Trans. 2*, **83**, 1157–69.
Nagarajan, K., Saha, R., Yadav, R. B., Rajagopalan, S., Kutty, K. V. G., Saibaba, M., Rao, P. R. V., and Matthews, C. K. (1985) *J. Nucl. Mater.*, **130**, 242–9.
Nagatoro, Y., Ochiai, K., and Kaya, A. (1980) *J. Nucl. Sci. Technol.*, **17**, 687–93.
Nagels, P., Devreese, J., and Denayer, M. (1964) *J. Appl. Phys.*, **35**, 1175–80.
Naito, K., Ishii, T., Hamaguchi, Y., and Oshima, K. (1967) *Solid State Commun.*, **5**, 349–52.
Naito, K., Kamagashira, N., and Nomura, Y. (1971) *J. Crystal Growth*, **8**, 219–20.
Naito, K., Tsuji, T., and Matsui, T. (1973) *J. Nucl. Mater.*, **48**, 58–66.
Naito, K. and Kamegashira, N. (1976) in *Advances in Nuclear Science and Technology*, vol. 9, pp. 99–180.
Naito, K., Inaba, H., and Takahashi, S. (1982) *J. Nucl. Mater.*, **110**, 317–23.
Naito, K., Tsuji, T., and Ohya, F. (1983) *J. Nucl. Mater.*, **114**, 136–42.
Naito, K. (1989) *J. Nucl. Mater.*, **167**, 30–5.
Nakagawa, T., Matsuoka, H., Sawa, M., Hirota, M., Miyake, M., and Katsura, M. (1997) *J. Nucl. Mater.*, **247**, 127–30.
Nakajima, K., Ohmichi, T., and Arai, Y. (2002) *J. Nucl. Mater.*, **304**, 176–81.
Nakamura, A. and Fujino, T. (1986) *J. Nucl. Mater.*, **140**, 113–30.
Nakamura, A. and Fujino, T. (1987) *J. Nucl. Mater.*, **149**, 80–100.
Narducci, A. A. and Ibers, J. A. (1998) *Chem. Mater.*, **10**, 2811–23.
Nash, K. L. and Sullivan, J. C. (1998) *J. Alloys Compds*, **271–273**, 712–18.
Nassimbeni, L. R. and Rodgers, A. L. (1976) *Crystal Struct. Commun.*, **5**, 301–8.
Nasu, S. (1964) *Japan. J. Appl. Phys.*, **3**, 664–5.
Navaza, A., Charpin, P., Vigner, D., and Heger, G. (1991) *Acta Crystallogr. C*, **47**, 1842–5.
Neuefeind, J., Skanthakumar, S., and Soderholm, L. (2004a) *Inorg. Chem.*, **43**, 2422–6.
Neuefeind, J., Soderholm, L., and Skanthakumar, S. (2004b) *J. Phys. Chem. A*, **108**, 2733–9.
Neuhaus, A. (1958) *Fortschr. Miner.*, **35**, 151–4.
Neuhaus, A. and Recker, K. (1959) *Z. Elektrochem.*, **63**, 89–97.
Newton, A. S., Warf, J. C., Spedding, F. H., Johnson, O., Johns, I. B., Nottorf, R. W., Ayres, J. A., Fisher, R. W., and Kant, A. (1949) *Nucleonics*, **4** (2), 17–25.
Newton, T. W. and Baker, F. B. (1965) *Inorg. Chem.*, **4**, 1166–70.
Newton, T. W. (1975) *The Kinetics of the Oxidation-Reduction Reactions of Uranium, Neptunium, Plutonium and Americium in Aqueous Solution*, Report TID-26506,

Technical Information Center, Office of Public Affairs, US Energy and Development Administration.
Nguyen-Nghi, H., Dianoux, A.-J., and Marquet-Ellis, H. (1964) *Compt. Rend. Acad. Sci.* (*Paris*), **259**, 4683.
Nguyen-Nghi, H., Dianoux, A.-J., Marquet-Ellis, H., and Plurien, P. (1965) *Compt. Rend. Acad. Sci.* (*Paris*), **260**, Group 8, 1963–6.
Niedrach, C. W. and Glamm, A. (1954) *Electrorefining of Uranium – A New Approach*, KAPL-1154.
Nielsen, P. E., Jeppesen, C., and Buchardt, O. (1988) *FEBS Lett.*, **235**, 122–4.
Niinistö, L., Toivonen, J., and Valkonen, J. (1979) *Acta Chem. Scand.*, **33**, 621–4.
Nishioka, T., Motoyama, G., Nakamura, S., Kadoya, H., and Sato, N. K. (2002) *Phys. Rev. Lett.*, **88**, 237203/1–237203/4.
NIST (2004) *NIST Critically Selected Stability Constants of Metal Complexes: version 8.0. NIST Standard Reference Database 46,* National Institute of Standards and Technology, Gaithersburg, MD.
Noël, H. and Prigent, J. (1980) *Physica B+C: Phys. Condensed Matter + Atom Mol. Plasma Phys., Optics*, **102**, 372–9.
Noël, H. and Le Marouille, J. Y. (1984) *J. Solid State Chem.*, **52**, 197–202.
Noël, H. (1985a) *Inorg. Chim. Acta*, **109**, 205–7.
Noël, H. (1985b) *Physica B and C*, **130**, 499–500.
Noël, H. and Levet, J. C. (1989) *J. Solid State Chem.*, **79**, 28–33.
Noël, H., Potel, M., Troć, R., and Shlyk, L. (1996) *J. Solid State Chem.*, **126**, 22–6.
Noland, R. A. and Marzano, C. (1953) *The Electrolytic Refining of Uranium*, ANL-5102.
Norris, D. I. R. and Kay, P. (1983) *J. Nucl. Mater.*, **116**, 184–94.
Northrup, C. J. M. Jr (1975) *J. Phys. Chem.*, **79**, 726–31.
Nowicki, L., Garrido, F., Turos, A., and Thomé, L. (2000) *J. Phys. Chem. Solids*, **61**, 1789–804.
Nriagu, J. O. (1984) Formation and stability of base metal phosphates in soils and sediments, in *Phosphate Minerals* (eds. J. O. Nriagu and P. B. Moore), Springer Verlag, London, pp. 318–29.
Obbade, S., Dion, C., Saadi, M., and Abraham, F. (2004) *J. Solid State Chem.*, **177**, 1567–74.
O'Donnell, T. A., Stewart, D. F., and Wilson, P. W. (1966) *Inorg. Chem.*, **5**, 1438–41.
O'Donnell, T. A. (1983) *J. Fluorine Chem.*, **23**, 97.
OECD-NEA (1982) *Uranium–Resources, Production and Demand*, Paris.
Oetting, F. H., Rand, M. H., and Ackerman, R. J. (1976) *The Chemical Thermodynamics of Actinide Elements and Compounds*, part 1, The Actinide Elements, IAEA, Vienna, STI/PUB/421/1.
Ogard, A. E. and Leary, J. A. (1968) in *Thermodynamics of Nuclear Materials*, Proc. Symp. 1967, International Atomic Energy Agency, Vienna, pp. 651–65.
Ogliaro, F., Cordier, S., Halet, J.-F., Perrin, C., Saillard, J.-Y., and Sergent, M. (1998) *Inorg. Chem.*, **37**, 6199–207.
O'Hare, P. A. G., Shinn, W. A., Mrazek, F. C., and Martin, A. E. (1972) *J. Chem. Thermodyn.*, **4**, 401–9.
O'Hare, P. A. G. and Hoekstra, H. R. (1973) *J. Chem. Thermodyn.*, **5**, 769–75.
O'Hare, P. A. G. and Hoekstra, H. R. (1974a) *J. Chem. Thermodyn.*, **6**, 251–8.
O'Hare, P. A. G. and Hoekstra, H. R. (1974b) *J. Chem. Thermodyn.*, **6**, 1161–9.

O'Hare, P. A. G., Boerio, J., Fredrickson, D. R., and Hoekstra, H. R. (1977) *J. Chem. Thermodyn.*, **9**, 963–72.
Ohmichi, T., Fukushima, S., Maeda, A., and Watanabe, H. (1981) *J. Nucl. Mater.*, **102**, 40–6.
Ohnuki, T., Kozai, N., Samadfam, M., Yasuda, R., Yamamato, S., Narumi, K., Naramoto, H., and Murakami, T. (2004) *Chem. Geol.*, **211**, 1–14.
Ohse, R.W. (1966) *J. Chem. Phys.*, **44**, 1375–8.
Ohse, R. W., Babelot, J. F., Cercignani, C., Kinsman, P. R., Long, K. A., Magill, J., and Scotti, A. (1979) *J. Nucl. Mater.*, **80**, 232–48.
Ohwada, K. (1970a) *J. Inorg. Nucl. Chem.*, **32**, 1209–18.
Ohwada, K. (1970b) *Spectochim. Acta*, **26A**, 1723–30.
Ohwada, K. (1971) *Inorg. Chem.*, **10**, 2281–5.
Ohwada, K. (1972) *J. Chem. Phys.*, **56**, 4951–6.
Ohwada, K., Soga, T., and Iwasaki, M. (1972) *J. Inorg. Nucl. Chem.*, **34**, 363–5.
Ohwada, K. (1976) *J. Inorg. Nucl. Chem.*, **38**, 741–5.
Oikawa, K., Kamiyama, T., Asano, H., Onuki, Y., and Kohgi, M. (1996) *J. Phys. Soc. Japan*, **65**, 3229–32.
Ollier, N., Guittet, M.-J., Gautier-Soyer, M., Panczer, G., Champagnon, B., and Jollivet, P. (2003) *Opt. Mater.*, **24**, 63–8.
Olsen, T., Gerwald, L., and Benedict, U. (1985) *J. Appl. Crystallogr.*, **18**, 37–41.
Olsen, T., Gerwald, L., Benedict, U., Dabos, S., and Vogt, O. (1988) *Phys. Rev. B*, **37**, 8713–8.
Ondruš, P., Veslovský, F., and Rybka, R. (1990) *Neues Jahrb. Miner., Monatsschr.*, **9**, 393–400.
Ondruš, P., Skála, P., Veselovský, F., Sejkora, J., and Vitti, C. (2003) *Am. Miner.*, **88**, 686–93.
Onoe, J., Takeuchi, K., Nakamatsu, H., Mukoyama, T., Sekine, R., Kim, B.-I., and Adachi, H. (1993) *J. Chem. Phys.*, **99**, 6810–17.
Onoe, J., Nakamatsu, H., Mukoyama, T., Sekine, R., Adachi, H., and Takeuchi, K. (1997) *Inorg. Chem.*, **36**, 1934–8.
Onuki, Y., Ukon, I., Komatsubara, T., Takayanagi, S., Wada, N., and Watanabe, T. (1990) *Physica B* (*Amsterdam, Neth.*), **163**, 368–70.
Onuki, Y., Ukon, I., Yun, S. W., Umehara, I., Satoh, K., Fukuhara, T., Sato, H., Takayanagi, S., Shikama, M., and Ochiai, A. (1992) *J. Phys. Soc. Japan*, **61**, 293–9.
Orlandi, P., Pasero, M., Duchi, G., and Olmi, F. (1997) *Am. Miner.*, **82**, 807–11.
Osborne, D. W., Westrum, E. F. Jr, and Lohr, H. R. (1955) *J. Am. Chem. Soc.*, **77**, 2737–9.
Osborne, D. W. and Flotow, H. E. (1972) *J. Chem. Thermodyn.*, **4**, 411–18.
Osborne, D. W., Flotow, H. E., Dallinger, R. P., and Hoekstra, H. R. (1974) *J. Chem. Thermodyn.*, **6**, 751–6.
Otey, M. G. and Le Doux, R. A. (1967) *J. Inorg. Nucl. Chem.*, **29**, 2249–56.
Outebridge, W. F., Staatz, M. H., Meyrowitz, R., and Pommer, A. M. (1960) *Am. Miner.*, **45**, 39–52.
Pabalan, R. T., Prikryl, J. D., Muller, P. M., and Dietrich, T. B. (1993) *Mater. Res. Soc. Symp. Proc.*, **294**, 777–82.
Pabst, A. (1954) *Am. Miner.*, **37**, 137–57.
Pagoaga, M. K., Appleman, D. E., and Stewart, J. M. (1987) *Am. Miner.*, **72**, 1230–8.

Paine, R. T., Ryan, R. R., and Asprey, L. B. (1975) *Inorg. Chem.*, **14**, 1113–17.
Paine, R. T., McDowell, R. S., Asprey, L. B., and Jones, L. H. (1976) *J. Chem. Phys.*, **64**, 3081–3.
Paixão, J. A., Rebizant, J., Blaise, A., Delapalme, A., Sanchez, J. P., Lander, G. H., Nakotte, H., Burlet, P., and Bonnet, M. (1994) *Physica B* (*Amsterdam, Neth.*), **203**, 137–46.
Palenzona, A. and Manfrinetti, P. (1995) *J. Alloys Compds*, **221**, 157–60.
Panlener, R. J., Blumenthal, R. N., and Garnier, J. E. (1975) *J. Phys. Chem. Solids*, **36**, 1213–22.
Papiernik, R., Mercurio, D., and Frit, B. (1980) *Acta Crystallogr. B*, **36**, 1769–74.
Papiernik, R., Mercurio, D., Frit, B., and Baernighausen, H. (1983) *Acta Cryst. C*, **39**, 667–8.
Parks, S. I. and Moulton, W. G. (1968) *Phys. Rev.*, **1973**, 333–7.
Parry, S. J. (1991) in *Activation Spectrometry in Chemical Analysis* (eds. J. D. Winefordner, and I. M. Kolthoff), John Wiley, New York, pp. 206–7.
Partington, J. R. (1949) in *Treatise on Physical Chemistry*, vol. I, Longman, Green, p. 639.
Pascal, P. (ed.) (1962–1970) *Nouveau, Traité de Chimie, Minérale*, vols. VII (1962), IX (1963), XV (2) (1961), XV (3) (1962), XV (4) (1967), and XV (5) (1970), Masson et Cie, Paris.
Pascal, J., Morin, J., and Lacombe, P. (1964) *J. Nucl. Mater.*, **13**, 28–32.
Paszek, A. P. (1978) Ph.D. Dissertation, The John Hopkins University, Baltimore.
Patton, F. S., Googin, J. M., and Griffith, W. L. (1963) *Enriched Uranium Processing*, Int. Ser. Monogr. Nucl. En. Div. IX, vol. 2, Pergamon Press, New York.
Pattoret, A., Drowart, J., and Smoes, S. (1964) *Trans. Faraday Soc.*, **65**, 98.
Pattoret, A., Drowart, J., and Smoes, S. (1968) in *Thermodynamics of Nuclear Materials*, Proc. Symp. 1967, International Atomic Energy Agency, Vienna, pp. 613–36.
Paul, R. (1970) Research Center Karlsruhe Report, KFK-1297.
Paul, R. and Keller, C. (1971) *J. Nucl. Mater.*, **41**, 133–42.
Pearcy, E. C., Prokryl, J. D., Murphy, W. M., and Leslie, B. W. (1994) *Appl. Geochem.*, **9**, 713–32.
Pé1igot, E. (1841a) *J. Prakt. Chem.*, **1** (24), 442–51.
Pé1igot, E. (1841b) *C. R. Acad. Sci.*, **12**, 735–7; **13**, 417–26.
Péligot, E. (1842) *Ann. Chim. Phys.*, Series 3, **5**, 5–47.
Péligot, E. (1844) *Ann. Chim. Phys.*, Series 3, **12**, 549–74.
Penneman, R. A., Kruse, F. H., George, R. S., and Coleman, J. S. (1964a) *Inorg. Chem.*, **3**, 309–15.
Penneman, R. A., Sturgeon, G. D., and Asprey, L. B. (1964b) *Inorg. Chem.*, **3**, 126–9.
Penneman, R. A., Keenan, K., and Asprey, L. B. (1967) *Adv. Chem. Ser.*, **71**, 248–55.
Penneman, R. A., Ryan, R. R., and Rosenzweig, A. (1973) *Struct. Bonding*, Berlin, Heidelberg, New York, **13**, 1–52.
Penneman, R. A., Ryan, R. R., and Rosenzweig, A. (1974) *Acta Crystallogr.*, **B30**, 1966–70.
Pepper, R. T. (1964) *Appl. Mater. Res.*, **3**, 203.
Pério, P. (1953a) *Bull. Soc. Chim. Fr*, 256–63.
Pério, P. (1953b) *Bull. Soc. Chim. Fr*, 840–1.
Perrin, A. (1970) *Compt. Rend. C*, **270**, 319–22.

Perrin, A. and Caillet, P. (1976) *Compt. Rend. C*, **282**, 721–4.
Perrin, A. (1977a) *J. Inorg. Nucl. Chem.*, **39**, 1169–72.
Perrin, A. (1977b) *J. Appl. Crystallogr.*, **10**, 359–60.
Perrin, A. and Le Marouille, J. Y. (1977) *Acta Crystallogr. B*, **33**, 2477–81.
Perrin, D. D. (1979) *Stability Constants of Metal-Ion Complexes. Part B Organic Ligands*, IUPAC Chemical Data Series no. 22, , Pergamon Press, New York.
Perron, P. O. (1968) Atomic Energy of Canada Ltd Report, AECL-3072.
Peterson, S. (1961) *J. Inorg. Nucl. Chem.*, **17**, 135–7.
Pfeil, P. C. L. (1956) *Proc. Int. Conf. on Peaceful Uses of Atomic Energy*, Geneva 1955, vol. 9, p. 117.
Picard, C. and Gerdanian, P. (1981) *J. Nucl. Mater.*, **99**, 184–9.
Picon, M. and Flahaut, J. (1968) *Bull. Soc. Chim. Fr.*, 772–80.
Piekarski, C. and Morfeld, P. (1997) *Appl. Occup. Environ. Hyg.*, **12**, 915–18.
Pippin, C. G. and Sullivan, J. C. (1989) *Radiochim. Acta*, **48**, 37–8.
Piret, P., Declerq, J.-P., and Piret-Meunier, J. (1979) *Acta. Crystallogr.*, **B35**, 1880–2.
Piret, P., Declerq, J.-P., and Wauters-Stoop, D. (1980) *Bull. Minér.*, **103**, 176–8.
Piret, P. and Deliens, M. (1982) *Bull. Minér.*, **105**, 125–8.
Piret, P. and Declerq, J.-P. (1983) *Bull. Minér.*, **106**, 383–9.
Piret, P., Deliens, M., Piret-Meunier, J., and Germain, G. (1983) *Bull. Minér.*, **106**, 299–304.
Piret, P. (1985) *Bull. Minér.*, **108**, 659–66.
Piret, P. and Deliens, M. (1987) *Bull. Minér.*, **110**, 65–7.
Piret, P., Deliens, M., Piret-Meunier, J., and Germain, G. (1988) *Bull. Minér.*, **111**, 443–9.
Piret, P., Piret-Meunier, J., and Deliens, M. (1990) *Eur. J. Miner.*, **2**, 399–405.
Plaine, R. T., Ryan, R. R., and Asprey, L. B. (1975) *Inorg. Chem.*, **14**, 1113–17.
Plant, J., Simpson, P. R., Smith, B., and Windley, B. F. (1999) *Rev. Miner.*, **38**, 255–319.
Platzner, I. T. (1997) in *Modern Isotope Ratio Mass Spectrometry* (ed. I. T. Platzner), John Wiley, New York, pp. 363–77.
Plesko, E. P., Scheetz, B. E., and White, W. B. (1992) *Am. Miner.*, **77**, 431–7.
Plumer, M. L. and Caillé, A. (1989) *Phys. Rev. B*, **40**, 396–8.
Pollard, F. H., Hanson, P., and Geary, W. J. (1959) *Anal. Chim. Acta*, **20**, 26–31.
Pollock, E. N. (1977) *Anal. Chim. Acta*, **88**, 399–401.
Polunina, G. P., Kovba, L. M., and Ippolitova, E. A. (1961) Argonne National Laboratory Report, ANL-trans-33, p. 224.
Potol, M., Brochu, R., Padiou, J., and Grandjean, D. (1972) *C.R. Acad. Sci. C*, **275**, 1419–21.
Prescott, C. H., Reynolds, F. L., and Holmes, J. A. (1946) *The Preparation of Uranium Metal by Thermal Dissociation of the Iodide*, MDDC-437.
Prigent, J. (1958) *Compt. Rend. Hebd. Séances Acad. Sci.*, **247**, 1737–9.
Prigent, J. and Lucas, J. (1965) *Bull. Soc. Chim. Fr.*, **4**, 1129–31.
Prins, G. and Cordfunke, E. P. H. (1975) *J. Inorg. Nucl. Chem.*, **37**, 119–27.
Prins, G., Cordfunke, E. P. H., and Ouweltjes, W. (1978) *J. Chem. Thermodyn.*, **10**, 1003–10.
Prins, G. and Cordfunke, E. H. P. (1983) *J. Less Common Metals*, **91**, 177–80.
Privalov, T., Schimmelpfennig, B., Wahlgren, U., and Grenthe, I. (2002) *J. Phys. Chem.*, **106**, 11277–82.

Privalov, T., Macak, P., Schimmelpfennig, B., Fromager, E., Grenthe, I., and Wahlgren, U. (2004) *J. Am. Chem. Soc.*, **124**, 9801–8.
Proceedings (1960a) *Proc. Uranium Carbide Meeting*, Oak Ridge National Laboratory, December 1–2, 1960, TID-7603.
Proceedings (1960b) *Prog. Carbide Fuels, Notes from the Second AEC Uranium Carbide Meeting*, Battelle Memorial Institute, March 22 and 23, 1960, TID-7589.
Proceedings (1961) *Proc. Symp. on Uranium Carbides as Reactor Fuel Materials*, USAEC, April 4, 1961, AEC Headquarters, Germantown, MD, TID-7614.
Proceedings (1963) *Proc. Fourth Uranium Carbide Conf.*, East Hartfield, CT, May 20–21, 1963, TID-7676.
Proceedings (1966) *Proc. Second Int. Thorium Fuel Cycle Symp.*, Gatlinburg, TN, May 3–6, 1966, CONF-660524.
Pushcharovsky, D. Y., Rastsvetaeva, R. K., and Sarp, H. (1996) *J. Alloys Compds.*, **239**, 23–6.
Pyykkö, P., Li, J., and Runeberg, N. J. (1994) *J. Phys. Chem.*, **98**, 4809–13.
Rabinovich, D., Schimek, G. L., Pennington, W. T., Nielsen, J. B., and Abney, K. D. (1998) *Acta Crystallogr. C*, **54**, 1740–2.
Rabinowitch., E. and Belford, R. L. (1964) *Spectroscopy and Photochemistry of Uranyl Compounds*, Pergamon Press, Oxford.
Raetsky, V. M. (1967) *J. Nucl. Mater.*, **21**, 105–8.
Raj, P., Sathyamoorthy, A., Shashikala, K., Kumar, N. H., Rao, C. R. V., and Malik, S. K. (2000) *J. Alloys Compds.*, **296**, 20–6.
Rajnak, K., Gamp, E., Shinomoto, R., and Edelstein, N. M. (1998) *J. Chem. Phys.*, **80**, 5942–50.
Ralph, J. and Hyland, G. J. (1985) *J. Nucl. Mater.*, **132**, 76–9.
Rand, M. H. and Kubaschewski, O. (1963) *The Thermochemical Properties of Uranium Compounds*, Olivier&Boyd, Edinbourgh.
Rand, M. H., Ackermann, R. J., Grønvold, F., Oetting, F. L., and Pattoret, A. (1978) *Rev. Int. Hautes Tempér. Réfract. Fr.*, **15**, 355–65.
Ratho, T. and Patel, T. (1968) *Indian J. Phys.*, **42**, 240–2.
Ratho, T., Patel, T., and Sahoo, B. (1969) *Indian J. Phys.*, **43**, 164–6.
Rebenko, A. N., Brusentsev, F. A., and Opalovskii, A. A. (1968) *Izv. Sib. Otd. Nauk. SSSR, Ser. Khim. Nauk*, **1**, 136–8.
Rebizant, J., Van den Bossche, G., Spirlet, M. R., and Goffart, J. (1987) *Acta Crystallogr.*, **C43**, 1298–300.
Rediess, K. and Sawodny, W. (1982) *Z. Naturforsch.*, **37B**, 524–5.
Reeder, R. J., Nugent, M., Lamble, G. M., Tait, C. D., and Morris, D. E. (2000) *Environ. Sci. Technol.*, **34**, 638–44.
Reeder, R. J., Nugent, M., Drew Tait, C., Morris, D. E., Heald, S. M., Beck, K. M., Hess, W. P., and Lanzirotti. A. (2001) *Geochim. Cosmochim. Acta*, **65**, 3491–503.
Reedy, G. T. and Chasanov, M. G. (1972) *J. Nucl. Mater.*, **42**, 341–4.
Reis, A. H. Jr, Hoekstra, H. R., Gebert, E., and Peterson, S. W. (1976) *J. Inorg. Nucl. Chem.*, **38**, 1481–5.
Reshetov, K. V. and Kovba, L. M. (1966) *Zh. Strukt. Khim.*, **7**, 625–6.
Reynolds, L. T. and Wilkinson, G. (1956) *J. Inorg. Nucl. Chem.*, **2**, 246–53.
Rietveld, H. M. (1966) *Acta Crystallogr.*, **20**, 508–13.
Rigny, P. (1965) CEA Report CEA-R2827, pp. 1–30.

Rigny, P. (1966) N.S.A. 20, no. 1807.
Rigny, P. and Plurien, P. (1967) *J. Phys. Chem. Solids*, **28**, 2589–95.
Rigny, P., Dianoux, A.-J., and Plurien, P. (1971) *J. Chem. Phys. Solids*, **32**, 1175–80.
Rizzo da Rocha, S. M., Rodrigues de Aquino, A., and Abrao, A. (1995) *An. Assoc. Brasil. Quimica*, **44**, 33–40.
Roberts, L. E. J. and Walter, A. J. (1961) *J. Inorg. Nucl. Chem.*, **22**, 213–29.
Roberts, L. E. J. and Walter, A. J. (1966) in *Physico-Chimie du Protactinium* (eds. G. Bouissières and R. Muxart), Colloq. Int. 154, Centre National de la Recherche Scientifique, Paris, pp. 51–9.
Roberts, W. L., Campbell, T. J., and Rapp, G. R. (1990) in *Encyclopedia of Minerals*, Kluwer Academic Publishers, 2nd edn, February 1990.
Robins, R. G. (1961) *J. Nucl. Mater.*, **3**, 294–301.
Rodden, C. J. and Warf, J. C. (1950) in *Analytical Chemistry of the Manhattan Project* (ed. C. J. Rodden), McGraw-Hill, New York, pp. 3–159.
Rodriguez de Sastre, M. S., Philippot, J., and Moreau, C. (1967) CEA Report, CEA-R 3218.
Rogova, V. P., Belova, L. N., Kiziyarov, G. P., Kuznetsova, N. N. (1973) *Zap. Uses. Miner. Obshch.*, **102**, 75–81.
Rona, E. (1950) *J. Am. Chem. Soc.*, **72**, 4339–43.
Ronchi, C. and Hyland, G. J. (1994) *J. Alloys Compds.*, **213/214**, 159–68.
Ronchi, C., Sheindlin, M., Musella, M., and Hyland, G. J. (1999) *J. Appl. Phys.*, **85**, 776–89.
Rosén, A. and Fricke, B. (1979) *Chem. Phys. Lett.*, **61**, 75–8.
Rosenthal, M. W., Briggs, R. B., and Kasten, P. R. (1969) *Molten Salt Reactor Program Semiannual Progress Report for Period Ending August 31, 1968*, ORNL-4344, p. IX.
Rosenthal, M. W., Haubenreich, P. N., and Briggs, R. B. (1972) ORNL-4812, pp. 1–416.
Rosenzweig, A. and Cromer, D. T. (1970) *Acta Crystallogr.*, **B26**, 38–44.
Rosenzweig, A., Ryan, R. R., and Cromer, D. T. (1973) *Acta Crystallogr.*, **B29**, 460–2.
Rosenzweig, A. and Ryan, R. R. (1975) *Am. Miner.*, **60**, 448–53.
Rosenzweig, A. and Ryan, R. R. (1977) *Crystal Struct. Commun.*, **6**, 53–6.
Ross, M. and Evans, H. T. (1964) *Am. Miner.*, **49**, 1578–602.
Ross, J. W. and Lam, D. W. (1968) *Phys. Rev.*, **165**, 617.
Rossetto, G., Zanella, P., Paolucci, G., and de Paoli, G. (1982) *Inorg. Chim. Acta*, **61**, 39–42.
Rossotti, F. J. R. and Rossotti, H. (1961) *The Determination of Stability Constants and Other Equilibrium Constants in Solution*, McGraw-Hill, New York.
Roth, W. L. (1960) *Acta Crystallogr.*, **13**, 140–9.
Rough, F. A. and Bauer, A. A. (1958) *Constitution of Uranium and Thorium Alloys*, BMI-1300.
Roussel, P. and Scott, P. (1998) *J. Am. Chem. Soc.*, **1998**, 1070–1.
Ruch, W. C., Peterson, D. A., Gaskill, E. A., and Tepp, H. G. (1959) *Nuclear Engineering and Science Conf.*, Am. Inst. Chem. Eng., April 6–9, 1959, Cleveland, OH, Preprint V-52.
Rundle, R. E. (1947) *J. Am. Chem. Soc.*, **69**, 1719–23.
Rundle, R. E., Baenziger, N. C., Wilson, A. S., and McDonald, R. A. (1948) *J. Am. Chem. Soc.*, **70**, 99–105.
Rundle, R. E. (1951) *J. Am. Chem. Soc.*, **78**, 4172–4.

Runnals, O. J. C. (1953) *Can. J. Chem.*, **3**, 694.
Rutledge, G. P., Jarry, R. L., and Davis, W. Jr (1953) *J. Phys. Chem.*, **57**, 541–4.
Rüdorff, W. and Pfitzer, F. (1954) *Z. Naturforsch.*, **9b**, 568–9.
Rüdorff, W. and Leutner, H. (1957) *Z. Anorg. Allg. Chem.*, **292**, 193–6.
Rüdorff, W. and Menzer, W. (1957) *Z. Anorg. Allg. Chem.*, **292**, 197–202.
Rüdorff, W., Kemmler, S., and Leutner, H. (1962) *Angew. Chem.*, **74**, p. 429.
Rüdorff, W., Erfurth, H., and Kemmler-Sack, S. (1967) *Z. Anorg. Allg. Chem.*, **354**, 273–85.
Ryan, J. L. (1962) *Proc. Seventh Int. Conf. Coordination Chemistry*, pp. 367–9; and Ryan, J. L. and Keder, W. E., unpublished work.
Ryan, R. R. (1971) *J. Inorg. Nucl.Chem.*, **33**, 153–77.
Ryan, R. R. (1972) *Med. Tech. Pub. Co. Int. Rev. Sci. Inorg. Chem., Ser.1*, **7**, 323–67.
Ryan, R. R. (1974) *Inorg. Synth.*, **15**, 235–43.
Ryan, R. R., Cleveland, J. M., and Bryan, G. H. (1974) *Inorg. Chem.*, **13**, 214–18.
Ryan, R. R., Penneman, R. A., Asprey, L. B., and Paine, R. T. (1976) *Acta Crystallogr. B*, **32**, 3311–13.
Ryan, R. R. and Rosenzweig, A. (1977) *Crystal Struct. Commun.*, **6**, 611–15.
Saito, Y. (1974) *J. Nucl. Mater.*, **51**, 112–25.
Sakurai, T., Kameda, O., and Ishigame, M. (1968) *J. Crystal Growth*, **2**, 236–7.
Saller, H. A. and Rough, F. A. (1954) *Chem. Eng. Prog. Symp. Ser.* 11, **50**, 63–7.
Saller, H. A. and Rough, F. H. (1955) *Compilation of U.S. and U.K. Uranium and Thorium Constitutional Diagrams*, 1st edn, BMI-1000.
Samson, S. and Sillén, L. G. (1947) *Ark. Kemi. Min. Geol.*, **25A** (21), 1–16.
Samsonov, G. V. (1968) *Handbook of the Physicochemical Properties of the Elements*, IFI/Plenum, New York-Washington, p. 437.
Sandell, E. B. (1959) *Colorimetric Determination of Traces of Metals*, 3rd edn, Interscience, New York.
Sandino, A. and Bruno, J. (1992) *Geochim. Cosmochim. Acta.*, **56**, 4135–45.
Santini, P., Lémanski, R., and Erdös, P. (1999) *Adv. Phys.*, **48** (5), 538–653.
Santos, I. G. and Abram, U. (2004) *Inorg. Chem. Commun.*, **7**, 440–2.
Sara, K. H. (1970) *J. Indian Chem. Soc.*, **47**, 88.
Sarp, H., Bertrand, J., and Deferne, J. (1983) *Neues Jahrb. Miner., Monatsschr.*, **6**, 417–23.
Sarsfield, M. J. and Helliwell, M. (2003) *J. Am. Chem. Soc.*, **126**, 1036–7.
Satonnay, G., Ardois, C., Corbel, C., Lucchini, J. F., Barthe, M. F., Garrido, F., and Gosset, D. (2001) *J. Nucl. Mater.*, **288**, 11–19.
Satten, R. A., Schreiber, C. L., and Wong, E. Y. (1983) *J. Chem. Phys.*, **78**, 79–87.
Savage, A. W. (1956) *J. Am. Chem. Soc.*, **78**, 2700–2.
Sawai, H., Kuroda, K., and Hojo, T. (1989) *Bull. Chem. Soc. Japan*, **62**, 2018–23.
Sawai, H., Shibusawa, T., and Kuroda, K. (1990) *Bull. Chem. Soc. Japan*, **63**, 1776–80.
Sawai, H., Higa, K., and Kuroda, K. (1992) *J. Chem. Soc. Dalton Trans.*, 505–8.
Sawai, H., Ito, T., Kokaji, K., Shimazu, M., Shinozuka, K., and Taira, H. (1996) *Biorg Med. Chem. Lett.*, **6**, 1785–90.
Sawodny, W., Rediess, K., and Thewalt, U. (1980) *Z. Anorg. Allg. Chem.*, **469**, 81–6.
Sawodny, W., Rediess, K., and Thewalt, U. (1983) *Z. Anorg. Allg. Chem.*, **499**, 81–8.
Sawyer, J. O. (1963) *J. Inorg. Nucl. Chem.*, **25**, 899–902.
Sawyer, J. O. (1972) *J. Inorg. Nucl. Chem.*, **34**, 3268–71.

Saxena, S. S., Agarwal, P., Ahilan, K., Grosche, F. M., Haselwimmer, R. K. W., Steiner, J. J., Pugh, E., Walker, I. R., Julian, S. R., Monthoux, P., Lonzarich, G. G., Huxley, A., and Shalek, P. D. (1963) *J. Am. Ceram. Soc.*, **46**, 155–61.
Scapolan, S. (1998) *Mise au Point et Evaluation de Techniques de Spéciation pour L'Etudes des Especes Biologiques Circulantes de L'Uranium* (*VI*), Thesis, Université de Paris Sud.
Schaner, B. E. (1960) *J. Nucl. Mater.*, **2**, 110–20.
Schäfer, H. (1975) *Z. Anorg. Allg. Chem.*, **414**, 151–9.
Schindler, M. and Hawthorne, F. C. (2004) *Can. Miner.*, **42**, 1601–27.
Schindler, M., Mutter, A., Hawthorne, F. C., and Putnis, A. (2004) *Can. Miner.*, **42**, 1651–66.
Schirber, J. E., Arko, A. J., and Fischer, E. S. (1975) *Solid State Commun.*, **17**, 553.
Schleid, T., Meyer, G., and Morss, L. R. (1987) *J. Less Common Metals*, **132**, 69–77; Schleid, T. and Meyer, G. (1988) unpublished results.
Schleid, T. and Meyer, G. (1989) *Naturwissenschaften*, **76**, 118.
Schlesinger, H. I. and Brown, H. C. (1953) *J. Am. Chem. Soc.*, **75**, 219–21.
Schlyter, K. (1953) *Ark. Khemi*, **5**, 73.
Schmieder, H., Dornberger, E., and Kanelakopulos, B. (1970) *Appl. Spectrosc.*, **24**, 499.
Schmitz-Dumont, O., Füchtenbusch, F., and Schneiders, H. (1954) *Z. Anorg. Allg. Chem.*, **277**, 315–28.
Schmitz, F., Dean, G., and Halachmy, M. (1971) *J. Nucl. Mater.*, **40**, 325–37.
Schoebrechts, J.-P., Gens, R., Fuger, J., and Morss, L. R. (1989) *Thermochim. Acta*, **139**, 49–66.
Scholder, R. and Brixner, L. (1955) *Z. Naturforsch.*, **10b**, 178–9.
Scholder, R. (1958) *Angew. Chem.*, **70**, 583–94.
Scholder, R. (1960) *Angew. Chem.*, **72**, pp. 120.
Scholder, R. and Gläser, H. (1964) *Z. Anorg. Allg. Chem.*, **327**, 15–27.
Schreckenbach, G., Hay, P. J., and Martin, R. L. (1998) *Inorg. Chem.*, **37**, 4442–51.
Seaborg, G. T. and Katzin, L. 1. (1951) *Production and Separation of U^{233} – Survey*, Natl. Nucl. En. Ser. Div. IV, 17A, USAEC Technical Information Service, Oak Ridge, TN (declassified as TID-5222).
Seijo, L. and Barandiaran, Z. (2001) *J. Chem. Phys.*, **115**, 5554.
Sejkora, J., Čejka, J., Hloušek, J., Novák, M., and Šrein, V. (2004) *Can. Miner.*, **42**, 963–72.
Selbin, J. and Ortego, J. (1969) *Chem. Rev.*, **69**, 657–71.
Selbin, J., Ortego, J. D., and Gritzner, N. (1968) *Inorg. Chem.*, **7**, 976–82.
Selbin, J., Ballhausen, C. J., and Durrett, D. G. (1972a) *Inorg. Chem.*, **11**, 510–15.
Selbin, J., Durret, D. G., Sherrill, H. J., Newkome, G. R., and Wharton, J. H. (1972b) *J. Chem. Soc. Chem. Comm.*, 380–1.
Selbin, J., Durret, D. G., Sherrill, H. J., Newkome, G. R., and Collins, M. (1973) *J. Inorg. Nucl. Chem.*, **35**, 3467–80.
Selbin, J. and Sherrill, H. J. (1974) *Inorg. Chem.*, **13**, 1235–9.
Sémon, L., Boeme, C., Billard, I., Hennig, C., Lützenkirchen, K., Reich, T., Rossberg, A., Rossini, I., and Wipff, G. (2001) *Chem. Phys. Chem.*, **2**, 591–8.
Seppelt, K. and Hwang, I.-C. (2000) *J. Fluorine Chem.*, **102**, 69–72.

Sessler, J. L., Vivian, A. E., Seidel, D., Burrel, A. K., Hoehner, M., Mody, T. D., Gebauer, A., Weghorn, S. J., and Lynch, V. (2001) *Coord. Chem. Rev.*, **216–217**, 411–34.
Seta, K., Matsui, T., Inaba, H., and Naito, K. (1982) *J. Nucl. Mater.*, **110**, 47–54.
Shamir, J. and Silberstein, A. (1975) *J. Inorg. Nucl. Chem.*, **37**, 1173–5.
Shamir, J., Silberstein, A., Ferraro, J. B., and Choca, M. (1975) *J. Inorg. Nucl. Chem.*, **37**, 1429–32.
Shchelokov, R. N. and Belomestnykh, V. I. (1968a) *Zh. Neorg. Khim.*, **13**, 1398–1403; *Russ. J. Inorg. Chem.*, **13**, 733–6.
Shchelokov, R. N. and Belomestnykh, V. I. (1968b) *Zhur. Neorg. Khim.*, **13**, 3386–891; *Russ. J. Inorg. Chem.*, **13**, 1744–7.
Shchelokov, R. N., Tsivadze, A. Yu., Orlova, I. M., and Podnebesnova, G. V. (1977) *Inorg. Nucl. Chem. Lett.*, **13**, 367–74.
Shchukarev, S. A., Vasil'kova, I. V., Drozdova, V. M., and Frantseva, K. E. (1959a) *Zh. Neorg. Khim.*, **4**, 39–41; (1959) *Russ. J. Inorg. Chem.*, **4**, 15–16.
Shchukarev, S. A., Vasilkova, I. V., Drozdova, V. M., and Martynova, N. S. (1959b) *Zh. Neorg. Khim.*, **4**, 33–8; (1959) *Russ. J. Inorg. Chem.*, **4**, 13–15.
Sheikin, I., Braithwaite, D., and Flouquet, J. (2000) *Nature*, **406**, 587–92.
Shen, J. and Peny, Z. (1981) *Acta Crystallogr.*, **A37**, Suppl. C-186.
Shimazu, M., Shinozuka, K., and Sawai, H. (1993) *Angew. Chem. Int. Ed. Engl.*, **32**, 870–2.
Shoesmith, D. W. and Sunder, S. (1994) in *The Electrochemistry of Novel Materials* (eds. J. Lipkowski and P. N. Ross), VCH, New York, p. 297.
Shull, C. G. and Wilkinson, M. K. (1955) *Oak Ridge National Laboratory Report*, *ORNL*-1879, p. 24.
Shunk, F. A. (1969) *Constitution of Binary Alloys*, 2nd Suppl., McGraw-Hill, New York.
Siegel, S. (1956) *Acta Crystallogr.*, **9**, 827.
Siegel, S., Hoekstra, H. R., and Sherry, E. (1966) *Acta Crystallogr.*, **20**, 292–5.
Siegel, S. and Hoekstra, H. R. (1968) *Acta Crystallogr.*, **B24**, 967–70.
Siegel, S. and Hoekstra, H. R. (1971a) *Inorg. Nucl. Chem. Lett.*, **7**, 497–504.
Siegel, S. and Hoekstra, H. R. (1971b) *Inorg. Nucl. Chem. Lett.*, **7**, 455–9.
Siegel, S., Viste, A., Hoekstra, H. R., and Tani, B. (1972) *Acta Crystallogr.*, **B28**, 117.
Silberstein, A. (1972) INIS-mf-36, p. 46.
Sillén, L. G. and Martell, A. E. (1964) *Stability Constants of Metal-Ion Complexes*, The Chemical Society, London.
Sillén, L. G. and Martell, A. E. (1971) *Stability Constants of Metal-Ion Complexes*, Suppl. no. 1, The Chemical Society, London.
Silverman, L. and Sallach, R. A. (1961) *J. Phys. Chem.*, **65**, 370.
Simoni, E., Hubert, S., and Genet, M. (1988) *J. Phys.* (*France*), **49**, 1425–34.
Simoni, E., Louis, M., Gesland, J. Y., and Hubert, S. (1995) *J. Lumin.*, **65**, 153–61.
Simpson, K. A. and Wood, P. (1983) in *Proc. NRC Workshop on Spent Fuel/Cladding Reaction during Dry Storage*, Gaithersburg, MD, NUREG/CP-0049, p. 70.
Singh, R. N. and Coble, R. L. (1974) *J. Crystal Growth*, **21**, 261–6.
Sjkora, J., Čejka, J., Hloušek, J., Šrein, V., Novotná M. (2002) *Neu. Jahr. Miner. Monat.*, **8**, 353–67.
Slain, H. (1950) *Production of Uranium by Electrolysis of Fused Salts*, LA-1056.
Sleight, A. W. and Ward, R. (1962) *Inorg. Chem.*, **1**, 790–3.

Slovyanskikh, V. K., Ellert, G. V., and Yarembash, E. L. (1967) *Izv. Akad. Nauk SSSR, Neorg. Mater.*, **3**, 1088–90; *Inorg. Mater.* (*USSR*), **3**, 969–71.
Slovyanskikh, V. K., Rozanov, I. A., and Gracheva, N. V. (1977) *Zh. Neorg. Khim.*, **22**, 1645–50; *Russ. J. Inorg. Chem.*, **22**, 893–6.
Smiley, S. H. and Brater, D. C. (1956) Current Commission Methods for producing UO_3, UF_4 and UF_6, TID-5295, pp. 245–89.
Smiley, S. H. and Brater, D. C. (1958) K-1379 Del., pp. 1–18.
Smiley, S. H. and Brater, D. C. (1960) N.S.A, **16**, no.1573.
Smith, G. S., Johnson, O., and Elson, R. E. (1967) *Acta Crystallogr.*, **22**, 300–3.
Smith, R. M. and Martell, A. E. (1989) *Critical Stability Constants*, vol. 6, Second Suppl., Plenum Press, New York.
Sobczyk, M., Karbowiak, M., and Drożdżyński, J. (2003) *J. Solid State Chem.*, **170**, 443–9.
Sobczyk, M., Drożdżyński, J., and Karbowiak, M. (2005) *J. Solid. State Chem.*, **178/2**, 536–44.
Soga, T., Ohwada, K., and Iwasaki, M. (1972) *Appl. Spectrosc.*, **26**, 482–3.
Soga, T., Ohwada, K., and Iwasaki, M. (1973) *J. Inorg. Nucl. Chem.*, **35**, 2069–74.
Soulié, E. (1978) *J. Inorg. Nucl. Chem.*, **40**, 351–2.
Souter, P. F., Kushto, G. P., Andrews, L., and Neurock, M. J. (1997) *J. Am. Chem. Soc.*, **119**, 1682–87.
Spedding, F. H., Newton, A. S., Warf, J. C., Johnson, O., Nottorf, R. W., Johns, I. B., and Daane, A. H. (1949) *Nucleonics*, **4** (1), 4–15.
Speer, J. A. (1982) *Rev. Miner.*, **5**, 113–35.
Spencer, S., Gagliardi, L., Handy, N. C., Ioannou, A. G., Skylaris, C.-K., and Willets, A. (1999) *J. Phys. Chem. A*, **103**, 1831–7.
Spirlet, J. C. (1979) *J. Phys. Colloq.*, C4, **40**, 87–94.
Spirlet, J. C., Bednarczyk, E., and Müller, W. (1979) *J. Phys. Colloq.*, **40**, C4, 108–10.
Spirlet, M. R., Rebizant, J., Fuger, J., and Schoebrechts, J. P. (1988) *Acta Crystallogr. C*, **44**, 1300.
Spitsyn, V. I., Ippolitova, E. A., Simanov, Yu. P., and Kovba, L. M. (1961a) Argonne National Laboratory Report, ANL-trans-33, p. 4.
Spitsyn, V. I., Ippolitova, E. A., Efremova, K. M., and Simanov, Yu. P. (1961b) Argonne National Laboratory Report, ANL-trans-33, p. 142.
Spitsyn, V. I., Ippolitova, E. A., Efremova, K. M., and Simanov, Yu. P. (1961c) Argonne National Laboratory Report, ANL-trans-33, p. 148.
Spitsyn, V. I., Tshigunov, A. N., Kovba, L. M., and Kuz'micheva, E. U. (1972) *Dokl. Akad. Nauk SSSR*, **204**, 604–43.
Srirama Murti, P., Yadav, R. B., Nawada, H. P., Vasudeva Rao, P. R., and Mathews, C. K. (1989) *Thermochim. Acta*, **140**, 299–303.
Stadlbauer, E., Wichmann, U., Lott, U., and Keller, C. (1974) *J. Solid State Chem.*, **10**, 341–50.
Staritzky, E. and Singer, J. (1952) *Acta Crystallogr.*, **5**, 536–40.
Staritzky, E., and Douglass, R. M. (1956) *Anal. Chem.*, **28**, 1210–11.
Steinitz, M. O., Burleson, C. E., and Marcus, J. A. (1970) *J. Appl. Phys.*, **41**, 5057.
Stephens, F. M. Jr and McDonald, R. O. (1956) *Proc. First Int. Conf. on Peaceful Uses of Atomic Energy*, Geneva, 1955, vol. 8, pp. 18–25.
Sterns, M. (1967) *Acta Crystallogr.*, **23**, 264–72.

Stoewe, K. (1996a) *Z. Anorg. Allg. Chem.*, **622**, 1419–22.
Stoewe, K. (1996b) *Z. Anorg. Allg. Chem.*, **622**, 1423–7.
Stoewe, K. (1997a) *Z. Anorg. Allg. Chem.*, **623**, 749–54.
Stoewe, K. (1997b) *J. Alloys Compds*, **246**, 111–23.
Stohl, F. V. and Smith, D. K. (1981) *Am. Miner.*, **66**, 610–25.
Stoller, S. M. and Richards, R. B. (1961) *Reactor Handbook*, 2nd edn, vol. II, Fuel Processing, Interscience, New York.
Storms, E. K. (1985) *J. Nucl. Mater.*, **132**, 231–43.
Straka, M., Dyall, K. G., and Pyykkö, P. (2001) *Theor. Chem. Acc.*, **106**, 393–403.
Streitweiser, A. and Müller-Westerhoff, U. (1968) *J. Am. Chem. Soc.*, **90**, 7364.
Strotzer, E. F., Schneider, O., and Biltz, W. (1943) *Z. Anorg. Allg. Chem.*, **243**, 307–21.
Stryer, L. (1988) *Biochemistry*, 3rd edn, W. H. Freeman and Co, New York, p. 705.
Stumpp, E. (1969) *Naturwissenschaften*, **56**, 370.
Stumpp, E. and Piltz, G. (1974) *Z. Anorg Allg. Chem.*, **409**, 53–9.
Sturchio, N. C., Antonio, M. R., Soderholm, L., Sutton, S. R., and Brannon, J. C. (1998) *Science*, **281**, 971–3.
Sugisaki, M., Hirashima, K., Yoshihara, S., and Oishi, Y. (1973) *J. Nucl. Sci. Technol.*, **10**, 387–9.
Sugisaki, M. and Sueyoshi, T. (1978) *J. Inorg. Nucl. Chem.*, **40**, 1543–9.
Sugiyama, K. and Onuki, Y. (2003) *High Magn. Fields*, **2**, 139–70.
Suglobova, I. G. and Chirkst, D. E. (1978a) *Radiokhimiya*, **20**, 361–5; *Sov. Radiochem.*, **20**, 310–14.
Suglobova, I. G. and Chirkst, D. E. (1978b) *Radiokhimiya*, **20**, 352–60; (1978) *Sov. Radiochem.*, **20**, 302–9.
Suglobova, I. G. and Chirkst, D. E. (1981) *Koord. Khimiya*, **7**, 97–102.
Sullivan, J. C., Hindman, J. C., and Zielen, A. J. (1961) *J. Am. Chem. Soc.*, **83**, 3373–8.
Sunder, S., Cramer, J. J., and Miller, N. H. (1996) *Radiochim. Acta*, **74**, 303–7.
Sunder, S., Miller, N. H., and Shoesmith, D. W. (2004) *Corrosion Sci.*, **46**, 1095–111.
Suski, W., Gibifiski, T., Wojakowski, A., and Czaynik, A. (1972) *Phys. Status Solidi*, **9**, 653–8.
Suski, W., Wojakowski, A., Blaise, A., Salmon, P., Fournier, J., and Mydlarz, T. (1976) *J. Magn. Mater.*, **3**, 195–200.
Sutton, S. (1955) *J. Inorg. Nucl. Chem.*, **1**, 68–74.
Swihart, G. H., Sen Gupta, P. K., Schlemper, E. O., Bach, M. E., and Gaines, R. V. (1993) *Am. Miner.*, **78**, 835–9.
Sylwester, E. R., Hudson, E. A., and Allen, P. G. (2000) *Geochim. Cosmochim. Acta*, **64**, 2431–8.
Szabó, Z., Glaser, J., and Grenthe, I. (1996) *Inorg. Chem.*, **35**, 2036–44.
Szabó, Z., Aas, W., and Grenthe, I. (1997) *Inorg. Chem.*, **36**, 5369–75.
Szabó, Z., Moll, H., and Grenthe, I. (2000) *J. Chem. Soc., Dalton Trans.*, 3158–161.
Szabó, Z. and Grenthe, I. (2000) *Inorg. Chem.*, **39**, 5036–43.
Szabó, Z. (2002) *J. Chem. Soc., Dalton Trans.*, 4242–7.
Szabó, Z. Toraishi, T., Vallet, V., and Grenthe, I. (2006) *Coord. Chem. Rev.*, In print.
Szwarc, R. and Latta, R. E. (1968) *J. Am. Ceram. Soc.*, **51**, 264–8.
Tabuteau, A., Jové, J., Pagès, M., and de Novion, C. H. (1984) *Solid State Commun.*, **50**, 357–61.

Tachibana, T., Ohmori, T., Yamanouchi, S., and Itaki, T. (1985) *J. Nucl. Sci. Technol.*, **22**, 155–7.
Tagawa, H. (1975) *J. Inorg. Nucl. Chem.*, **37**, 731–3.
Tagawa, H., Fujino, T., and Tateno, J. (1975) Japan Atomic Research Institute Report, JAERI-M 6180.
Tagawa, H. and Fujino, T. (1977) *Inorg. Nucl. Chem. Lett.*, **13**, 489–93.
Tagawa, H., Fujino, T., and Tateno, J. (1977) *Bull. Chem. Soc. Japan*, **50**, 2940–4.
Tagawa, H. and Fujino, T. (1978) *J. Inorg. Nucl. Chem.*, **40**, 2033–6.
Tagawa, H. and Fujino, T. (1980) *Inorg. Nucl. Chem. Lett.*, **16**, 91–6.
Tagawa, H., Fujino, T., Watanabe, K., Nakagawa, Y., and Saita, K. (1981a) *Bull. Chem. Soc. Japan*, **54**, 138–42.
Tagawa, H., Fujino, T., Ouchi, K., Watanabe, K., and Morimoto, T. (1981b) *J. Nucl Sci. Technol.*, **18**, 811–16.
Tagawa, H., Fujino, T., Ouchi, K., Watanabe, K., Saita, K., and Morimoto, T. (1983) *J. Nucl. Sci. Technol.*, **20**, 467–74.
Takano, Y. (1961) *Am. Miner.*, **46**, 812–22.
Tame, J. R. H. (2000) *Acta Crystallogr.*, **D56**, 1554–9.
Tanaka, H., Kimura, E., Yamaguchi, A., and Moriyama, J. (1972) *J. Jpn. Inst. Metals*, **36**, 633–7.
Tanamas, R. (1974) Research Center Karlsruhe Report, KFK-1910.
Tanner, P. A., Hung, S.-T., Mak, T. C. W., and Wang, R.-J. (1992) *Polyhedron*, **11**, 817–22.
Tanner, P. A., Silvestre, J. P. F., and Dao, N. Q. (1993) *New J. Chem.*, **17**, 263–6.
Tasker, I. R., O'Hare, P. A. G., Lewis, B. M., Johnson, G. K., and Cordfunke, E. H. P. (1988) *Can. J. Chem.*, **66**, 620–5.
Tateno, J., Fujino, T., and Tagawa, H. (1979) *J. Solid State Chem.*, **30**, 265–73.
Tatsumi, K. and Hoffmann, R. (1980) *Inorg. Chem.*, **19**, 2656–8.
Taylor, J. C. (1971) *Acta Crystallogr.*, **B27**, 1088–91.
Taylor, J. C. and Wilson, P. W. (1973a) *Acta Crystallogr. B*, **29**, 1942–4.
Taylor, J. C. and Wilson, P. W. (1973b) *Acta Crystallogr. B*, **29**, 1073–6.
Taylor, J. C. and Wilson, P. W. (1974a) *Acta Crystallogr. B*, **30**, 175–7.
Taylor, J. C. and Wilson, P. W. (1974b) *Acta Crystallogr. B*, **30**, 1481–4.
Taylor, J. C. and Wilson, P. W. (1974c) *Acta Crystallogr. B*, **30**, 169–75.
Taylor, J. C. and Wilson, P. W. (1974d) *J. Chem. Soc. Chem. Commun.*, pp. 598–5.
Taylor, J. C. and Wilson, P. W. (1974e) *Acta Crystallogr. B*, **30**, 2664–7.
Taylor, J. C. and Wilson, P. W. (1974f) *Acta Crystallogr. B*, **30**, 2803–5.
Taylor, J. C. and Wilson, P. W. (1975a) *J. Inorg. Nucl. Chem.*, **39**, 1989–91.
Taylor, J. C., and Wilson, P. W. (1975b) *J. Solid State Chem.*, **14**, 378–82.
Taylor, J. C. (1976a) *Coord. Chem. Rev.*, **20**, 197–273.
Taylor, J. C. (1976b) *Inorg. Nucl. Chem. Lett.*, **12**, 725–8.
Taylor, J. C. and Waugh, A. B. (1980) *J. Solid State Chem.*, **35**, 137–40.
Taylor, J. C., Stuart, W. I., and Mumme, I. A., (1981) *J. Inorg. Nucl. Chem.*, **43**, 2719–23.
Taylor, J. C. and Waugh, A. B. (1983) *Polyhedron*, **2**, 211–16.
Taylor, J. C. (1987) *Z. Kristallogr.*, **181**, 151–60.
Tempest, P. A., Tucker, P. M., and Tyler, J. W. (1988) *J. Nucl. Mater.*, **151**, 251–68.
Templeton, L. K., Templeton, D. H., Bartlett, N., and Seppelt, K. (1976) *Inorg. Chem.*, **15**, 2720–2.

Tetenbaum, M. and Hunt, P. D. (1968) *J. Chem. Phys.*, **49**, 4739–44.
Tetenbaum, M. and Hunt, P. D. (1970) *J. Nucl. Mater.*, **34**, 86–91.
Thibaut, E., Boutique, J.-P., Verbist, J. J., Levet, J.-C., and Noël, H. (1982) *J. Am. Chem. Soc.*, **104**, 5266–73.
Thoma, R. E. and Grimes, W. R. (1957) Phase Equilibria Diagrams for Fused Salt Systems, ORNL-2295.
Thoma, R. E., Insley, H., Landau, B. S., Friedman, H. A., and Grimes, W. R. (1958) *J. Am. Ceram. Soc.*, **41**, 538–44.
Thoma, R.E. (1959) Phase diagrams of Nuclear Reactor Materials, ORNL-2548.
Thoma, R. E. and Penneman, R. A. (1965) ORNL-3789, 33–35; (1965) N.S.A. 19, no. 30066.
Thoma, R. E., Insley, H., Hebert, G. M., Friedman, H. A., and Weaver, C. F. (1963) *J. Am. Ceram. Soc.*, **46**, 37–42.
Thoma, R. E., Friedman, H. A., and Penneman, R. A. (1966) *J. Am. Chem. Soc.*, **88**, 2046–7.
Thoma, R. E. (1971) ORNL-4812, pp. 1–416.
Thoma, R. E. (1972) N.S.A. 26, no. 24796.
Tomiyasu, H. and Fukutomi, H. (1982) *Bull. Res. Lab. Nucl. Reactors*, **7**, 57–80.
Tougait, O., Potel, M., Padiou, J., and Noël, H. (1997) *J. Alloys Compds*, **262**, 320–4.
Tougait, O., Potel, M., and Noël, H. (1998a) *J. Solid State Chem.*, **139**, 356–61.
Tougait, O., Potel, M., Levet, J. C., and Noël, H. (1998b) *Eur. J. Solid State Inorg. Chem.*, **35**, 67–76.
Tougait, O., Potel, M., and Noël, H. (1998c) *Inorg. Chem.*, **37**, 5088–91.
Toussaint, C. J. and Avogadro, A. (1974) *J. Inorg. Nucl. Chem.*, **36**, 781–4.
Toraishi, T., Farkas, I., Szabó, Z., and Grenthe, I. (2002) *J. Chem. Soc. Dalton Trans.*, 3805–12.
Toraishi, T., Aoyagi, N., Nagasaki, S., and Tanaka, S. (2004) *J. Chem. Soc. Dalton Trans.*, 3495–502.
Totemeier, T. C. (1995) *A Review of the Corrosion and Pyrophoricity Behavior of Uranium and Plutonium*, ANL/ED/95–2.
Traverso, O., Portanova, R., and Carassiti, V. (1974) *Inorg. Nucl. Chem. Lett.*, **10**, 771–5.
Troć, R. (1992) *Proc. 22èmes Journées des Actinides*, Méribel, France, p. 97.
Troć, R. and Suski, W. (1995) *J. Alloys Compds*, **219**, 1–5.
Trzebiatowski, W., Śliwa, A., and Staliński, B. (1954) *Rocz. Chem.*, **28**, 12–20.
Trzebiatowski, W. and Jabloński, A. (1960) *Nukleonika*, **5**, 587–96.
Trzebiatowski, W. and Mulak, J. (1970) *Bull. Acad., Polon. Sci. Ser. Sci. Chim.*, **18**, 121–6.
Tsai, H. C., Corington, A., and Olander, D. R. (1975) Lawrence Berkeley Laboratory Report, LBL-6016, p. 188.
Tso, T. C., Brown, D., Judge, A. I., Holloway, J. H., and Fuger, J. (1985) *J. Chem. Soc. Dalton Trans.*, 1853–8.
Tsushima, S., Yang, T., and Suzuki, A. (2001) *Chem. Phys. Lett.*, **334**, 365–73.
Tuller, H. L. (1981) in *Nonstoichiometric Oxides* (ed. O. T. Sørensen), Academic Press, New York, ch. 6. pp. 271–335.
Tutov, A. G., Plakhtii, V. P., Usov, O. A., Bublyaev, R. A., and Chernenkov, Yu. P. (1991) *Kristallografiya*, **36**, 1135–8.
Ugajin, M. (1982) *J. Nucl. Mater.*, **110**, 140–6.

Ugajin, M. (1983) *J. Nucl. Sci. Technol.*, **20**, 228–36.
Ugajin, M., Shiratori, T., and Shiba, K. (1983) *J. Nucl. Mater.*, **116**, 172–7.
Une, K. and Oguma, M. (1982) *J. Nucl. Mater.*, **110**, 215–22.
Une, K. and Oguma, M. (1983a) *J. Am. Ceram. Soc.*, **66**, C179–80.
Une, K. and Oguma, M. (1983b) *J. Nucl. Mater.*, **115**, 84–90.
Une, K. and Oguma, M. (1983c) *J. Nucl. Mater.*, **118**, 189–94.
United Nations, (1955) *Proc. First Int. Conf. on Peaceful Uses of Atomic Energy*, Geneva, 1955, vol. 8, pp. 3–145.
United Nations, (1958) *Proc. Second Int. Conf. on Peaceful Uses of Atomic Energy*, Geneva, 1958, vol. 4, pp. 3–68.
United Nations, (1964) *Proc. Third Int. Conf. on Peaceful Uses of Atomic Energy*, Geneva, 1964, vol. 12, pp. 119–325.
Uvarova, Y. A., Sokolova, E., Hawthorne, F. C., Agakhanov, A. A., and Pautov, L. A. (2004) *Can. Miner.*, **42**, 1005–11.
Vallet, V., Maron, L., Schimmelpfennig, B., Leininger, T., Teichteil, C., Gropen, O., Grenthe, I., and Wahlgren, U. (1999) *J. Phys. Chem. A*, **103**, 9285–9.
Vallet, V., Wahlgren, U., Schimmelpfennig, B., Szabó, Z., and Grenthe, I. (2001) *J. Am. Chem. Soc.*, **123**, 11999–2008.
Vallet, V., Wahlgren, U., Szabó, Z., and Grenthe, I. (2002) *Inorg. Chem.*, **41**, 5626–33.
Vallet, V., Moll, H., Wahlgren, U., Szabó, Z., and Grenthe, I. (2003) *Inorg. Chem.*, **42**, 1982–93.
Vallet, V., Privalov, T., Wahlgren, U., and Grenthe, I. (2004a) *J. Am. Chem. Soc.*, **124**, 7766–7.
Vallet, V., Szabó, Z., and Grenthe, I. (2004b) *J. Chem. Soc. Dalton Trans.*, 3799–807.
Van Axeel Castelli, V., Dalla Cort, A., Mandolini, L., Reinhoudt, D. N., and Schiaffino, L. (2000) *Chem. Eur. J.*, **7**, 1193–8.
Van den Bossche, G., Rebizant, J. G., Spirlet, M. R., and Goffart, J. (1986) *Acta Crystallogr. C*, **42**, 1478–80.
Van den Bossche, G., Spirlet, M. R., Rebizant, J., and Goffart, J. (1987) *Acta Crystallogr. C*, **43**, 383–4.
van Egmond, A. B. (1975) *J. Inorg. Nucl. Chem.*, **37**, 1929–31.
van Egmond, A. B. (1976a) *J. Inorg. Nucl. Chem.*, **38**, 1645–7.
van Egmond, A. B. (1976b) *J. Inorg. Nucl. Chem.*, **38**, 1649–51.
van Egmond, A. B. (1976c) *J. Inorg. Nucl. Chem.*, **38**, 2105–7.
Van Impe, J. (1954) *Chem. Eng. Prog.*, **50**, 230–4.
van Lierde, W., Strumane, R., Smets, E., and Amelinckx, S. (1962) *J. Nucl. Mater.*, **5**, 250–3.
van Lierde, W., Pelsmaekers, J., and Lecocq-Robert, A. (1970) *J. Nucl. Mater.*, **37**, 276–85.
Vance, E. R., Watson, J. N., Carter, M. L., Day, R. A., and Begg, B. D. (2001) *J. Am. Ceram. Soc.*, **84**, 141–4.
Vance, J. E. and Warner, J. C. (1951) *Uranium Technology-General Survey*, Natl. Nucl. En. Ser., Div. VII, 2A, TID-5231, USAEC Technical Information Service, Oak Ridge, TN.
Vaugoyeau, H., Lombard, L., and Morterat, J. P. (1971) *J. Nucl. Mater.*, **39**, 323–9.
Vdovenko, V. M., Mashirov, L. G., Blokhima, V. K., Suglobova, I. G., and Suglobov, D. N. (1963) *Sov. Radiochem.*, **5**, 67–75.

Vdovenko, V. M., Mashirov, L. G., and Suglobov, D. N. (1964) *Radiokhimiya*, **6**, 299–305; *Sov. Radiochem.*, **6**, 289–94.
Vdovenko, V. M., Skoblo, A. I., Suglobov, D. N., Shcherbakova, L. L., and Scherbakov, V. A. (1969) *Zh. Neorg. Khim.*, **12**, 2863–5; *Russ. J. Inorg. Chem.*, **12**, 1513–15.
Vdovenko, V. M., Volkov, V. A., Kozhina, I. I., and Suglobova, I. G. (1972a) *Sov. Radiochem.*, **14**, 492–3.
Vdovenko, V. M., Volkov, V. A., Kozhina, I. I., and Suglobova, I. G. (1972b) *Sov. Radiochem.*, **14**, 489–91.
Vdovenko, V. M., Suglobova, I. G., and Chirkst, D. E. (1973a) *Radiokhimiya*, **15**, 58–61; (1973a) *Sov. Radiochem.*, **15**, 53–5.
Vdovenko, V. M., Kozhina, I. I., Suglobova, I. G., and Chirkst, D. E. (1973b) *Radiokhimiya*, **15**, 172–127; *Soviet Radiochem.*, **15**, 168–72.
Vdovenko, V. M., Kozhina, I. I., Suglobova, I. G., and Chirkst, D. E. (1974a) *Radiokhimiya*, **16**, 369–77; (1974) *Sov. Radiochem.*, **16**, 369–76.
Vdovenko, V. M., Volkov, V. A., and Suglobova, I. G. (1974b) *Radiokhimiya*, **16**, 363–8.
Vdovenko, V. M., Suglobova, I. G., and Chirkst, D. E. (1974c) *Radiokhimiya*, **16**, 203–8.
Védrine, A., Baraduc, L., and Cousseins, J.-C. (1973) *Mater. Res. Bull.*, **8**, 581–8.
Védrine, A., Trottier, D., Cousseins, J.-C., and Chevalier, R. (1979) *Mater. Res. Bull.*, **14**, 583–7.
Vilcu, R. and Misdolea, C. (1967) *J. Chem. Phys.*, **46**, 906.
Viswanathan, K. and Harnett, O. (1986) *Am. Miner.*, **71**, 1489–93.
Vita, O. A., Walker, C. R., and Litteral, E. (1973) *Anal. Chim. Acta*, **64**, 249–57.
Vochten, R. and Deliens, M. (1980) *Phys. Chem. Miner.*, **6**, 129–43.
Vochten, R., Blaton, N., Peeters, O., and Deliens, M. (1996) *Can. Miner.*, **34**, 1317–22.
Vochten, R., Blaton, N., and Peeters. O. (1997) *Can. Miner.*, **35**, 1021–5.
Vochten, R. and Deliens, M. (1998) *Can. Miner.*, **36**, 1077–81.
Vochten, R., Deliens, M., and Medenbach, O. (2001) *Can. Miner.*, **39**, 1685–9.
Vodovatov, V. A., Gorshkov, N. G., Lychev, A. A., Mashirov, L. G., and Leikena, E. V. (1984) *Radiokhimiya*, **26**, 261–4.
Vogt, O. (1982) *Actinides in Perspective* (ed. N. M. Edelstein), Pergamon Press, Oxford, pp. 289–307.
Voliotis, S. and Rimsky, A. (1975) *Acta Crystalogr. B*, **34**, 2612–15.
Volkov, V. A., Suglobova, I. G., and Chirkst, D. E. (1979) *At. Energy.*, **47** (2), 110–12.
Volkov, V. A., Suglobova, I. G., and Chirkst, D. E. (1987) *Radiokhimiya*, **29** (3), 273–6.
Volkovich, V. A., Griffiths, T. R., Fray, D. J., and Fields, M. (1998) *Vibr. Spectrosc.*, **17**, 83–91.
Vorobei, M. P., Siba, O. V., Bevz, A. S., and Kapshukov, I. I. (1971) *Zh. Fiz. Khim.*, **45**, 22–5.
Voronov, N. M., Danilin, A. S., and Kovalev, I. T. (1962) in *Thermodynamics of Nuclear Materials*, Proc. Symp. 1962, International Atomic Energy Agency, Vienna, pp. 789–800.
Voronov, N. M. and Sofronova, R. M. (1972) in *Physical Chemistry of Alloys and Refractory Compounds of Thorium and Uranium* (ed. O. S. Ivanov), Academy of Sciences of the USSR, Israel Program for Scientific Translations, Ltd., Jerusalem, pp. 204–14.
Voronov, N. M., Sofrononova, R. M., and Voitekhova, E. A. (1972) in *Physical Chemistry of Alloys and Refractory Compounds of Thorium and Uranium* (ed. O. S. Ivanov),

Academy of Sciences of the USSR, Israel Program for Scientific Translations, Ltd., Jerusalem, pp. 222–8.
Waber, J. T., Chiotti, P., and Miner, W. N. (1964) *Compounds of Interest to Reactor Technology*, IMD Special Report 13, Metallurgical Society of AIME.
Wachter, P. (ed.) (1980) *Proc. Int. Conf. on the Physics of Actinides and Related 4f Materials*, North-Holland, Amsterdam; *Physica*, 102B and 102C.
Wadier, J. F. (1973) CEA Report, CEA-R 4507.
Wadt, W. R. and Hay, P. J. (1979) *J. Am. Chem. Soc.*, **101**, 5198–206.
Wadt, W. R. (1981) *J. Am. Chem. Soc.*, **103**, 6053–7.
Wagner, W., Edelstein, N. M., Whittaker, B., and Brown, D. (1977) *Inorg. Chem.*, **16**, 1021–6.
Wahlgren, U., Moll, H., Grenthe, I., Schimmelpfennig, B., Maron, L., Vallet, V., and Gropen, O. (1999) *J. Phys. Chem. A*, **103**, 8257–64.
Wait, E. (1955) *J. Inorg. Nucl. Chem.*, **1**, 309–12.
Walder, A. J. and Hodgeson, T. (1994) in *DOE-ORNL 1994 Conf. Analytical Chemistry in Energy Technology* (eds. R. W. Morrow and J. S. Crain), ASTM Spec. Tech. Publ. 1291.
Walder, A. J. (1997) in *Modern Isotope Ratio Mass Spectrometry* (ed. I. T. Platzner), John Wiley, New York, pp. 83–108.
Walenta, K. (1965) *Am. Miner.*, **50**, 1143–57.
Walenta, K. (1974) *Am. Miner.*, **59**, 166–71.
Walenta, K. (1976) *Schweiz. Miner. Petrogr. Mitt.*, **56**, 167–85.
Walenta, K. (1983) *Neues Jahrb. Miner. Monatsschr.*, **6**, 259–69.
Walenta, K. (1985) *Tschermaks Miner. Petrogr. Mitt.*, **34**, 25–34.
Walenta, K. (1998) *Aufschluss*, **49**, 253–7.
Wang, W.-D., Bakac, A., and Espenson, J. H. (1995) *Inorg. Chem.*, **34**, 6034–9.
Ward, J. W., Cox, L. E., Smith, J. L., Stewart, G. R., and Wood, J. H. (1979) *J. Phys.* (*Paris*), **40**, C4, 15–17.
Ward, J. W. (1985) in *Handbook on the Physics and Chemistry of the Actinides,* vol. 3 (eds. A. J. Freeman and C. Keller) Elsevier, Amsterdam, pp, 1–74.
Wardman, P. (1989) *J. Phys. Chem. Ref. Data*, **18**, 1637.
Warf, J. C. (1958) in *The Chemistry of Uranium, Collected Papers*, TID-5290 (eds. J. J. Katz and E. Rabinowitch), Oak Ridge, TN, p. 81.
Warner, J. C. (1953) *Metallurgy of Uranium*, Natl Nucl. En. Ser., Div. IV, 12A, , USAEC Technical Information Service, Oak Ridge, TN.
Warner, J. K. and Ewing, R. C. (1993) *Am. Miner.*, **62**, 403–10.
Watkin, D. J., Denning, R. G., and Prout, K. (1991) *Acta Crystallogr. C*, **47**, 2517–19.
Watt, G. W., Baugh, D. W., and Gadd, K. F. (1974) *Inorg Nucl. Chem. Lett.*, **10**, 987–9.
Wedekind, E. and Jochem, O. (1913) *Ber. Dtsch. Chem. Ges.*, **46**, 1204–5.
Wedermeyer, H. (1984) in *Gmelin Handbuch der Anorganischen Chemie*, Suppl. Ser. Uranium, C4, pp. 1–64.
Weeks, J. L. (1955) *AIME, J. Metals*, **203**, 192.
Weigel, F. (1958) in *Handbuch der Präparativen Anorganischen Chemie* (ed. G. Brauer), Enke, Stutttgart, pp. 1197–203.
Weigel, F. and Neufeldt, S. (1961) *Angew. Chem.*, **73**, 468.
Weitzel, H. and Keller, C. (1975) *J. Solid State Chem.*, **13**, 136–41.

Weller, M. T., Light, M. E., and Gelbrich, T. (2000) *Acta Crystallogr.*, **B56**, 577–83.
Wells, A. F. (1990) in *Structural Inorganic Chemistry*, Oxford University Press.
Westrum, E. F. Jr and Grønvold, F. (1959) *J. Am. Chem. Soc.*, **81**, 1777–80.
Westrum, E. F. Jr and Grønvold, F. (1962) in *Thermodynamics of Nuclear Materials*, Proc. Symp. 1962, International Atomic Energy Agency, Vienna, pp. 3–37.
Westrum, E. F. Jr, Takahashi, Y., and Grønvold, F. (1965) *J. Phys. Chem.*, **69**, 3192–3.
White, T. J. (1984) *Am. Miner.*, **69**, 1156–72.
Whitman, C. I., Compton, V., and Holden, R. B. (1955) *Zone Melting of Uranium*, TID-10098.
Wicke, E. and Otto, K. (1962) *Z. Phys. Chem.* (NF), **31**, 222–48.
Wilhelm, H. A., Chiotti, P., Snow, A. I., and Daane, A. H. (1949) *J. Chem. Soc.*, Suppl. 2, 318–21.
Wilhelm, H. A. (1956) *Proc. First Int. Conf. on Peaceful Uses of Atomic Energy*, Geneva, 1955, vol. 8, pp. 162–74.
Wilkins, R. G. (1991) *Kinetics and Mechanism of Reactions of Transition Metal Complexes*, 2nd edn, VCH Publishers, Weinheim, Germany.
Wilkinson, M. K., Shull, C. G., and Rundle, R. E. (1955) *Phys. Rev.*, **99**, 627.
Wilkinson, W. D. and Murphy, W. F. (1958) *Nuclear Reactor Metallurgy*, van Nostrand.
Wilkinson, W. D. (1962) *Uranium Metallurgy*, vol. I, *Uranium Process Metallurgy*, vol. II, *Uranium Corrosion and Alloys*, Interscience, New York.
Williams, C. W., Morss, L. R., and Choi, I.-K. (1984) in *Geochemical Behavior of Disposed Radiochemical Waste* (eds. G. S. Barney, J. D. Navratil, and W. W. Schulz), Am. Chem. Soc. Symp. Ser. 246, American Chemical Society, Washington, DC, pp. 323–34.
Willis, B. T. M. (1964a) *J. Phys.* (*Paris*), **29**, 431–40.
Willis, B. T. M. (1964b) *Proc. Brit. Ceram. Soc.*, **1**, 9–19.
Willis, B. T. M. (1978) *Acta Crystallogr.*, **A34**, 88–90.
Willis, B. T. M. (1987) *J. Chem. Soc., Faraday Trans. 2*, **83**, 1073–81.
Wilmarth, W. R. and Peterson, J. R. (1981) Characterization of selected solid-state actinide (and related) compounds via Raman and absorption spectroscopy, in *Handbook on the Physics and Chemistry of the Actinides*, vol. 6 (eds. A. J. Freeman and C. Keller), North-Holland, Amsterdam, pp. 1–39.
Wilson, W. B., Alexander, C. A., and Gerds, A. F. (1961) *J. Inorg. Nucl. Chem.*, **20**, 242–51.
Wilson, W. W., Naulin, C., and Bougon, R. (1977) *Inorg. Chem.*, **16**, 2252–7.
Winslow, G. H. (1971) *High Temp. Sci.*, **3**, 361–80.
Winslow, G. H. (1973) *High Temp. Sci.*, **5**, 176–91.
Winter, P. W. (1989) *J. Nucl. Mater.*, **161**, 38–43.
Wisnyi, L. G. and Pijunowski, S. W. (1957) USAEC Technical Information Service, TID-7530.
Wolf, A. S., Posey, J. C., and Rapp, K. E. (1965) *Inorg. Chem.*, **4**, 751–4.
Wolf, S. F. (1999) in *Reviews in Mineralogy*, vol. 38 (eds. P. C. Burns and R. Finch), Mineralogical Society of America, Washington, DC, pp. 623–53.
Woodley, R. E. (1981) *J. Nucl. Mater.*, **96**, 5–14.
Woodward, L. A. and Ware, M. J. (1968) *Spectrochim. Acta A*, **24**, 921–5.
Woody, R. J. and George, D. R. (1955) *Nucl. Eng. Sci. Congr.*, Cleveland, OH, Preprint 329.

Wronkiewicz, D. J., Bates, J. K., Gerding, T. J., Veleckis, E., and Tani, B. S. (1992) *J. Nucl. Mater.*, **190**, 107–27.
Wronkiewicz, D. J., Bates, J. K., Wolf. S. F., and Buck, E. C. (1996) *J. Nucl. Mater.*, **238**, 78–95.
Wronkiewicz, D. J. and Buck, E. C. (1999) *Rev. Miner.*, **38**, 475–97.
Yamamoto, T., Kayano, H., Sinaga, S., Ono, S., Tanaka, S., and Yamawaki, M. (1991) *J. Less Common Metals*, **172–174**, 71–8.
Yamamoto, T., Kayano, H., and Yamawaki, M. (1994) *J. Alloys Compds*, **213–214**, 533–5.
Yamamoto, T., Teshigawara, M., Kayano, H., Minakawa, N., and Funahashi, S. (1995) *J. Alloys Compds*, **224**, 36–8.
Yamamoto, T., Ishii, Y., and Kayano, H. (1998) *J. Alloys Compds*, **269**, 162–5.
Yamanaka, S., Iguchi, T., Fujita, Y., Uno, M., Katsura, M., Hoshino, Y., and Saiki, W. (1999) *J. Alloys Compds*, **293–295**, 52–6.
Yamashita, T. and Fujino, T. (1985) *J. Nucl. Mater.*, **136**, 117–23.
Yamashita, T., Fujino, T., and Tagawa, H. (1985) *J. Nucl. Mater.*, **132**, 192–201.
Yang, T., Tsushima, S., and Suzuki, A. (2003) *J. Solid State Chem.*, **171**, 235–41.
Yoshihara, K., Yamagami, S., Kanno, M., and Mukaibo, T. (1971) *J. Inorg. Nucl. Chem.*, **33**, 3323–9.
Young, A. P. and Schwartz, C. M. (1962) Battelle Memorial Institute Report, BMI-1585.
Young, A. P. and Schwartz, C. M. (1963) *J. Inorg. Nucl. Chem.*, **25**, 1133–7.
Young, E. J., Weeks, A. D., and Meyrowitz, R. (1966) *Am. Miner.*, **51**, 651–63.
Young, G. A. (1955) *Feed Materials. A Bibliography of Classified Report Literature*, TID-3081.
Yusov, A. B. and Shilov, V. P. (2000) *Russ. Chem. Bull. Int. Ed.* **49**, 1925–53.
Zachariasen, W. H. (1945) Manhattan Project Report, CP-2611, p. 14.
Zachariasen, W. H. (1946) University of Chicago Metallurgical Laboratory Report, MDDC-1152.
Zachariasen, W. H. (1948a) *Acta Crystallogr.*, **1**, 265–8.
Zachariasen, W. H. (1948b) *Acta Crystallogr.*, **1**, 281–5.
Zachariasen, W. H. (1948c) *J. Chem. Phys.*, **16**, 254.
Zachariasen, W. H. (1948d) *J. Am. Chem. Soc.*, **70**, 2147–51.
Zachariasen, W. H. (1948e) *Acta Crystallogr.*, **1**, 277–81.
Zachariasen, W. H. (1948f) *Acta Crystallogr.*, **1**, 285–7.
Zachariasen, W. H. (1949a) *Acta Crystallogr.*, **2**, 94–9.
Zachariasen, W. H. (1949b) *Acta Crystallogr.*, **2**, 291–6.
Zachariasen, W. H. (1949c) *Acta Crystallogr.*, **2**, 296–8.
Zachariasen, W. H. (1949d) *Acta Crystallogr.*, **2**, 390–3.
Zachariasen, W. H. (1954a) *Acta Crystallogr.*, **7**, 788–91.
Zachariasen, W. H. (1954b) *Acta Crystallogr.*, **7**, 795–9.
Zachariasen, W. H. (1954c) *Acta Crystallogr.*, **7**, 783–7; 792–4.
Zachariasen, W. H. (1954d) *Acta Crystallogr.*, **7**, 783–7.
Zachariasen, W. H. (1975) LA-UR-75–1364, 1977, INIS Atomindex 8, no. 283142.
Zadneporovskii, G. M. and Borisov, S. V. (1971) *Zh. Strukt. Khim.*, **12**, 831–9; *J. Strukt. Chem.*, **12**, 761–9.
Zalkin, A., Templeton, D. H., and Hopkins, T. E. (1967) *Inorg. Chem.*, **5**, 1466–70.
Zalkin, A., Templeton, L. K., and Templeton, D. H. (1989) *Acta Cryst. C*, **45**, 810–11.

Zhang, J., Wan, A., and Gong, W. (1992) *Acta Petrol. Miner.*, **11**, 178–84. (in Chinese).
Zhang, Z. and Pitzer, R. M. (1999) *J. Phys. Chem. A*, **103**, 6880–6.
Zhangru, C., Keding, L., Falan, T., Yi, Z., and Xiaofa, G. (1986) *Kexue Tongbao* (*Chinese Science Bulletin*), **31**, 396–401.
Zhao, D. and Ewing, R. C. (2000) *Radiochim. Acta.*, **88**, 739–49.
Zimmermann, J. I. C. (1882) *Ber. Dtsch. Chem. Ges.*, **15**, 847–51; *Liebig's Ann. Chem.*, **213**, 285–319.
Zogal, O. J., Lam, D. J., Zygmunt, A., Drulis, H., Petryński, W., and Staliński, S. (1984) *Phys. Rev. B*, **29**, 4837–42.
Żołnierek, Z., Gajek, Z., and Khan Malek, Ch. (1984) *Physica B+C* (*Amsterdam, Neth.*), **125**, 199–214.
Zych, E. and Drożdżyński, J. (1986) *Inorg. Chim. Acta, f-Block Elements*, **115**, 219–22.
Zych, E. and Drożdżyński, J. (1990a) *Polyhedron*, **9** (17), 2175–6.
Zych, E. and Drożdżyński, J. (1990b) *J. Less Common Metals*, **164**, 233–8.
Zych, E. and Drożdżyński, J. (1991) *Eur. J. Solid State Inorg. Chem.*, **28**, 575–80.
Zych, E., Starynowicz, P., Lis, T., and Drożdżyński, J. (1993) *Polyhedron*, **12** (13), 1661–6.